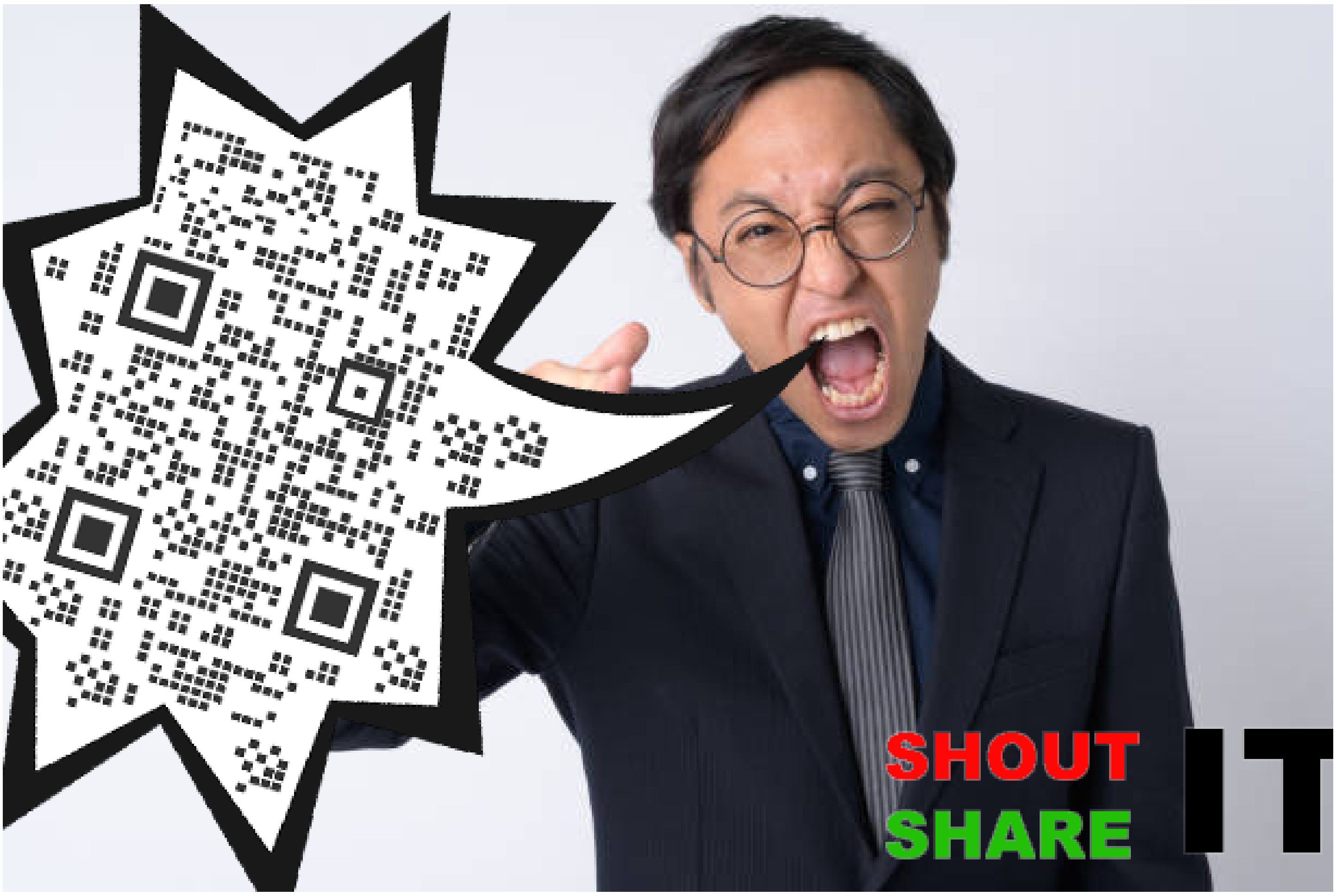
SHOUT
SHARE
IT

1.6.77

J. B. M.
1020

THE ORNITHISCHIAN DINOSAUR *HYPSILOPHODON* FROM THE WEALDEN OF THE ISLE OF WIGHT

P. M. GALTON

BULLETIN OF
THE BRITISH MUSEUM (NATURAL HISTORY)
GEOLOGY Vol. 25 No. 1
LONDON: 1974

22 JUL 19
NATURAL HIST

THE ORNITHISCHIAN DINOSAUR *HYPSILOPHODON* FROM THE WEALDEN OF THE ISLE OF WIGHT

BY
PETER MALCOLM GALTON
Department of Biology
University of Bridgeport, Bridgeport
Connecticut 06602 U.S.A.

Pp. 1–152 ; 2 *Plates* ; 64 *Text-figures*

BULLETIN OF
THE BRITISH MUSEUM (NATURAL HISTORY)
GEOLOGY Vol. 25 No. 1
LONDON: 1974

THE BULLETIN OF THE BRITISH MUSEUM (NATURAL HISTORY), *instituted in* 1949, *is issued in five series corresponding to the Departments of the Museum, and an Historical series.*

Parts will appear at irregular intervals as they become ready. Volumes will contain about three or four hundred pages, and will not necessarily be completed within one calendar year.

In 1965 *a separate supplementary series of longer papers was instituted, numbered serially for each Department.*

This paper is Vol. 25, *No.* 1, *of the Geological (Palaeontological) series. The abbreviated titles of periodicals cited follow those of the World List of Scientific Periodicals.*

World List abbreviation :
Bull. Br. Mus. nat. Hist. (Geol.)

© Trustees of the British Museum (Natural History), 1974

TRUSTEES OF
THE BRITISH MUSEUM (NATURAL HISTORY)

Issued 16 *May,* 1974 *Price* £7·35

S. SBM.P.

BRITISH
GENERAL
31 OCT
LIBRARY
NATURAL

BULLETIN OF THE BRITISH MUSEUM (NATURAL HISTORY)

GEOLOGY

VOL. 25

1974–1975

TRUSTEES OF
THE BRITISH MUSEUM (NATURAL HISTORY)
LONDON : 1975

DATES OF PUBLICATION OF THE PARTS

No. 1	16 May 1974
No. 2	23 May 1974
No. 3	26 July 1974
No. 4	3 January 1975
No. 5	19 May 1975

ISSN 0007–1471

PRINTED IN GREAT BRITAIN
BY JOHN WRIGHT & SONS LIMITED, AT
THE STONEBRIDGE PRESS, BRISTOL BS4 5NU

CONTENTS

GEOLOGY VOLUME 25

PAGE

No. 1. The Ornithischian dinosaur *Hypsilophodon* from the Wealden of the Isle of Wight. P. M. GALTON 1

No. 2. The taxonomy and morphology of *Puppigerus camperi* (Gray), an Eocene sea-turtle from northern Europe. R. T. J. MOODY 153

No. 3. The shell structure of Spiriferide Brachiopoda. D. I. MACKINNON 187

No. 4. Cretaceous faunas from Zululand and Natal, South Africa. Introduction, Stratigraphy. W. J. KENNEDY & H. C. KLINGER 263

No. 5. A revision of Sahni's types of the brachiopod subfamily Carneithyridinae. U. ASGAARD 317

An index is provided for each part.

THE ORNITHISCHIAN DINOSAUR *HYPSILOPHODON* FROM THE WEALDEN OF THE ISLE OF WIGHT

By PETER MALCOLM GALTON

CONTENTS

Page

I. INTRODUCTION 5
II. MATERIALS AND METHODS 6
  a) Preparation 6
  b) Material 6
  c) British Museum numbers of previously figured specimens 10
  d) Measurements 12
III. THE *Hypsilophodon* BED 15
  a) Stratigraphy 15
  b) *Hypsilophodon* localities 17
  c) Fauna 17
IV. OSTEOLOGY OF *Hypsilophodon foxii* 18
  a) The skull and lower jaw 21
    i) INDIVIDUAL BONES 21
    ii) TEETH AND TOOTH REPLACEMENT 41
      Dental formula 41
      Premaxillary teeth 41
      Maxillary and dentary teeth 42
      Special foramina and replacement teeth . 44
      Sequence of tooth replacement 45
    iii) ACCESSORY ELEMENTS 46
      Hyoid apparatus 46
      Sclerotic ring 46
      Stapes 47
  b) The vertebral column and ribs 48
    i) PROATLAS, ATLAS AND AXIS 48
    ii) CERVICAL VERTEBRAE 3 TO 9 51
    iii) DORSAL VERTEBRAE 56
    iv) SACRAL VERTEBRAE 57
    v) SACRAL RIBS 60
    vi) THE HEXAPLEURAL TYPE OF SACRUM 60
    vii) OTHER VARIATIONS IN THE SACRUM 61
    viii) CAUDAL VERTEBRAE AND CHEVRONS 63
  c) Ossified tendons 71
  d) The appendicular skeleton 72
    i) THE PECTORAL GIRDLE 72
    ii) THE FORELIMB 75
    iii) THE PELVIC GIRDLE 83
    iv) THE HINDLIMB 95
  e) Dermal armour 102
V. *Camptosaurus valdensis*, A LARGE *Hypsilophodon foxii* . . 102

Page
VI. Aspects of cranial anatomy 103
  a) The foramina of the braincase 103
  b) The paroccipital process and the post-temporal fenestra . 105
  c) The eye 106
  d) Jaw musculature 110
    i) ADDUCTOR MANDIBULAE GROUP 110
    ii) CONSTRICTOR DORSALIS GROUP 112
    iii) CONSTRICTOR VENTRALIS GROUP 114
    iv) M. DEPRESSOR MANDIBULAE 114
  e) Kinetism 114
  f) Streptostyly 116
  g) The antorbital fenestra 117
  h) Jaw action 119
VII. Aspects of post-cranial anatomy 122
  a) Individual variation 122
  b) The first sacral rib 123
  c) Articulation and posture 124
    i) FORELIMB 124
    ii) HINDLIMB 126
    iii) QUADRUPEDAL OR BIPEDAL POSE AND THE POSTURE OF THE VERTEBRAL COLUMN 127
VIII. Was *Hypsilophodon* arboreal? 130
  a) Historical survey 130
  b) Summary of the purported anatomical evidence that *Hypsilophodon* was arboreal 133
  c) Discussion of this evidence 133
    i) GRASPING CAPABILITIES OF THE PES . . . 133
    ii) GRASPING CAPABILITIES OF THE MANUS . . 135
    iii) WIDER RANGE OF BRACHIAL MOVEMENTS POSSIBLE 135
    iv) LARGE FORE-ARM SPACE 136
    v) RIGID TAIL AS A BALANCING ORGAN . . . 136
    vi) DERMAL ARMOUR 136
    vii) LIMITED RUNNING CAPABILITIES 136
IX. Generalized features of *Hypsilophodon* 137
X. Summary 142
XI. Acknowledgements 144
XII. References 144
XIII. Note 149

SYNOPSIS

The anatomy of the primitive ornithopod *Hypsilophodon* is described. The femur described as *Camptosaurus valdensis* is referred to *Hypsilophodon foxii*. The skull was possibly mesokinetic, metakinetic and amphistylic. The large antorbital fenestra was enclosed to a varying extent in lower ornithopods to form a fossa for the M. pterygoideus. The jaw musculature was typically sauropsid, the coronoid process is large and the jaw articulation offset. The mouth was probably small with a cheek pouch lateral to the tooth rows. The teeth had sharp and serrated leading edges and oblique but parallel occlusal surfaces with a high shear component between them. There is a large amount of individual variation and the sacral count varies. The massive first sacral rib strengthened the slender pubic peduncle of the ilium and keyed the pubis to it. *Hypsilophodon* was definitely bipedal but probably ran with the vertebral column held horizontally. The structure of the phalanges of the pes is not unique and the hallux was

not opposable. *Hypsilophodon* was the most cursorial of the known post-Triassic ornithopods and it was not arboreal. *Hypsilophodon* was probably not directly ancestral to any Cretaceous ornithischian but structurally it is quite similar to the hypothetical Triassic ancestor of most ornithischians other than *Fabrosaurus*.

I. INTRODUCTION

A slab of sandstone containing the partial skeleton of a reptile was discovered in 1849 at the top of the Wealden Marls near Cowleaze Chine, on the south-west coast of the Isle of Wight, England. Mantell (1849) figured and described three cervical vertebrae from this specimen as those of a very young *Iguanodon.* Owen (1855) illustrated the complete block and described it as belonging to a young *Iguanodon mantelli.* Fox exhibited more material from this same Wealden bed at the British Association meeting at Norwich in 1868. This included a skull and various post-cranial remains, which he identified as a new species of *Iguanodon* (Fox 1869). Huxley (1870, abstract 1869) described and figured this skull, making it the type of a new genus and species, *Hypsilophodon foxii.* He showed that a centrum from a dorsal vertebra on this specimen was identical to those described by Owen, and he therefore suggested that Owen's skeleton too belonged to *Hypsilophodon.* Huxley separated *Hypsilophodon* from *Iguanodon* by differences in the teeth, vertebrae and femur and in the number of metatarsals. He showed the parallel position of the pubis and ischium and the obtuse angle between these two bones and the anterior part of the ilium, the first time that this typically ornithischian condition had been shown.

In 1873 Hulke collected some additional material that formed the basis of two papers (1873, 1874) ; the first dealt mainly with the teeth and appendicular skeleton and the second with the skull. He noted that *Hypsilophodon* differed from *Iguanodon* in having four metatarsals, in the shape of the unguals, in having longer phalanges in the hind foot, a tibia longer than the femur and in the more proximal position of the inner (fourth) trochanter of the femur. In the discussion following Hulke (1873), Owen denied the generic separation of *Hypsilophodon* and referred to it as *Iguanodon foxii.* He stated that generic identity was shown by the similarity in tooth shape and wear, with the enamel layer on opposite sides in the upper and lower jaws, and by the peculiar spout-like form of the edentulous anterior end of the mandible. Owen (1874) elaborated these points when he described the skull of *Hypsilophodon* as that of *Iguanodon foxii.* Hulke (1882), in his attempt at a complete osteology, figured most of the important material and described the individual elements.

Lydekker (1888) catalogued the material of *Hypsilophodon* in the British Museum (Natural History). Nopcsa (1905) discussed certain aspects of the anatomy while von Huene (1907) figured the ilium and ischium. Abel in 1911 reconstructed the forearm and hand, and the foot in 1912. He argued (1912, 1922, 1925, 1927) that *Hypsilophodon* was arboreal, a conclusion that was followed and expanded by Heilmann (1916) and Swinton (1934, 1936*a*, *b*) although Heilmann later (1926) disagreed.

Reconstructions and restorations of *Hypsilophodon* are given by Hulke (1882), Smit (in Hutchinson 1894), Marsh (1895, 1896*a*, *b*), Heilmann (1916), Abel (1922 and later), von Huene (1956), Wilson (in Oakley & Muir-Wood 1959), Ostrom (1964) and Colbert (1965). General accounts are given in Swinton (1934, 1936*a*, *b*, 1954, 1962) and with one exception (1936*b*) these are accompanied by restorations. He also (1936) described the maxilla, teeth, pectoral girdle and limbs from two fairly complete skeletons in the Hooley Collection acquired by the British Museum (Natural History). Mounts were made of these two skeletons, photographs of which were published by Swinton (1934, 1936*a*).

Because of its primitive structure and supposedly arboreal mode of life, *Hypsilophodon* is an especially interesting dinosaur and, as indicated above, it has been the subject of numerous papers. However, the available account of its anatomy is still far from complete despite the fact that it is the best represented British dinosaur. This paper is the result of further preparation and study of the specimens available ; there are twenty individuals represented by articulated bones, including one almost complete skeleton and two good skulls. The study of the pelvic musculature of *Hypsilophodon*, with a consideration of the functional significance of the prepubic process of ornithischians, has already been published (Galton 1969). The mode of life of *Hypsilophodon* has also been discussed elsewhere (see p. 149).

II. MATERIAL AND METHODS

a) *Preparation*

Apart from the material noted on page 10 all the remains of *Hypsilophodon* are in the British Museum (Natural History) and the appropriate specimen numbers are used in this paper. With the exception of R5829 and R5830 all articulated remains were in blocks with the bones exposed on the surface. The slab (28707) figured by Owen (1855) has been left unprepared to show the original appearance of these blocks. Hulke (1882) figured all the other important blocks ; these were developed further so that now, in most cases, the bones are completely free of matrix. Mechanical preparation was used on most of the material. The matrix of blocks with articulated remains was a hard sandstone which prepared well in 10 per cent acetic acid, following the methods developed by Toombs (1948) and Rixon (1949). Polybutyl methacrylate dissolved in methylethyl ketone was used to strengthen and harden the bone, with Glyptal as an adhesive. Acid preparation was used on R193, R195, R196, R197, R198, R200 and R2477.

b) *Material*

There are many isolated bones of *Hypsilophodon* in the British Museum (Natural History) collection but most are incomplete and badly preserved. Details of all the material are listed by Galton (1967). Diagrams showing the amount of each bone preserved in specimens 28707, R192, R193, R195, R196, R200, R2466–76, R2477, S.M. 4127, R5829 and R5830 are given as well as a table listing all the skull bones in the collection (Galton 1967, figs. 5–18). The following list contains only specimens referred to in the literature or in this paper and the author and plate or figure numbers are given. For details of the actual bones figured reference should be made to Section (c) in which all previous figures are listed with the relevant specimen numbers (not given in papers prior to 1936) and an indication of the bones concerned.

Mantell Collection, purchased 1853

28707, 39560–1. This specimen will be referred to as 28707 and is the paratype (Huxley 1869). Slab of sandstone with an articulated skeleton consisting of a partial vertebral column, pelvic region and hindlimbs. Found in cliff about 100 yd west of Cowleaze Chine, Isle of Wight (Owen 1855 : 2). Figured by Mantell (1849, pl. 29, fig. 9*), Owen (1855, pl. 1 – complete block ; pl. 15, fig. 8), Huxley (1870, pl. 1, figs. 6–8 ; pl. 2) and Hulke (1882, pl. 74, figs. 1–4).

36509. Distal end of right femur, matrix a soft red sandstone, from Cuckfield, Sussex. This specimen was referred to *Hypsilophodon* by Lydekker (1888) and was the only specimen not from the Isle of Wight. However, this femur has a deep anterior intercondylar groove, and is therefore not referable to *Hypsilophodon* (see Text-fig. 54) ; this means that the genus has not been found outside the Isle of Wight.

Fox Collection, purchased 1882

R167. Large left femur, ends imperfect (Pl. 2, fig. 4), referred by Lydekker (1888) to *Hypsilophodon* but subsequently (1889) made the type of *Camptosaurus valdensis*. The generic position of this specimen is discussed in Section V.

R170. Left tibia, listed by Lydekker (1888) as right but corrected later (1891). The 1888 catalogue also lists under *Iguanodon* for this number 'Three specimens of the distal extremity of the humerus of very young individuals'. Material actually consists of a distal end of a left tibia, two proximal and two distal ends of femora, distal end of a humerus and a distal end of the third metatarsal – all *Hypsilophodon*.

R183. An ulna of *Hypsilophodon* according to Lydekker (1888) ; but actually the fourth right metatarsal of an ornithopod.

R184, R185. Associated pair of femora listed by Lydekker (1888). These are ornithopod but not *Hypsilophodon*.

R186. Right tibia, listed by Lydekker (1888) as a left tibia which was apparently associated with the femora R184 and R185. Corrected to right tibia when Lydekker (1891) referred it to the coelurosaur *Calamospondylus foxi* ; R186 was obviously not from the same animal as the femora !

R189. Part of right ramus of mandible found about 210 yd east of Barnes High (Fox in letter quoted by Owen 1874 : 13). Figured by Owen (1874 : 2, figs. 8–11).

R190. Right mandibular ramus, two caudal vertebrae and parts of ribs on a sandstone slab. Found about 150 yd east of Barnes High (Fox, letter quoted by Owen 1874 : 13). Figured by Owen (1874, figs. 1–2).

R191. Tooth from R190 figured by Owen (1874, pl. 2, figs. 12–17).

R192. Block with articulated bones of pectoral girdle, forelimbs, neck and jaws with various disarticulated skull bones of a large individual. Also other blocks with parts of pelvis and hind limbs ; all the bones are poorly preserved. From *Hypsilophodon* Bed (Fox MS) ; main block figured by Hulke (1882, pl. 73).

R192a. Large left femur that does not belong to same individual as R192 because latter already includes two femora. From *Hypsilophodon* Bed (Fox MS) ; figured by Hulke (1882, pl. 78, figs. 1–5).

R192b. Ilium and prepubic process from an extremely young individual.

R193. Block with articulated bones of pelvis, hindlimb and tail. From *Hypsilophodon* Bed ; figured by Hulke (1882, pl. 77), Galton (1969, figs. 4, 6–11, 13, 15) and Text-figs. 24, 25D, 26B, C, 30, 31, 49, 50, 53A, B and 55.

R194. Block with skull elements, right humerus and radius. From *Hypsilophodon* Bed (Fox MS) ; incorrectly listed by Lydekker (1888 : 194) as 'an imperfect pelvis and bones of the hind limb'. Figured by Hulke (1882, pl. 72, fig. 1) as an eroded internal aspect of skull but actually the external aspect. Partial basis for Text-fig. 9.

R195. Block with pelvic region from *Hypsilophodon* Bed (Fox MS). Figured by Hulke (1882, pl. 76) and Text-figs. 25A, B, E, F, 26A, 27, 46, 47 and 52.

R196, R196a. Two blocks (for photographs taken before preparation see Galton 1967, figs. 19–21) which together contained a practically complete articulated skeleton (R196) plus the posterior half of a tail from a larger individual (R196a) ; from *Hypsilophodon* Bed (Fox MS). R196 figured by Hulke (1882, pl. 72, fig. 2 ; pl. 74, fig. 13 ; pl. 75 and pl. 79, figs. 2–3), Nopcsa (1905, fig. 1), Abel (1911, fig. 12 ; 1912, fig. 12), Galton (1970, fig. 5B ; in press *a*, figs. 5A, B) and Text-figs. 12, 13, 19–23, 25C, 26D, 28, 29, 33–35, 37, 38, 40, 41, 48A, 51, 53C, D, 58 and Pl. 2, fig. 3 ; R196a by Hulke (1882, pl. 74, fig. 13) and in text-fig. 62.

R197. The holotype, a skull of a small individual plus a partial atlas, a cervical vertebra and a dorsal centrum. Found about 210 yd east of Barnes High (Fox in letter quoted by Owen 1874 : 13). Figured by Huxley (1870, figs. 1–5), Owen (1874, pl. 1, figs. 9–10 ; pl. 2, figs. 1, 5), Hulke (1882, pl. 71, figs. 2–4) and in Text-fig. 2.

R199. Left tibia of large individual, listed as right by Lydekker (1888) but later corrected (1891). From *Hypsilophodon* Bed (Fox MS) ; figured by Hulke (1882, pl. 80, fig. 2 ; pl. 81, fig. 1).

R200. Left and right hind-feet of large animal(s) from *Hypsilophodon* Bed (Fox MS). These two feet are about the same size and the matrix is very similar but they may be from different animals as they were given separate find numbers – IJ (right) and IL in Fox (MS) ; figured by Hulke (1882, pl. 81, figs. 2–3).

R202a. Imperfect dorsal vertebra listed by Lydekker (1888).

R752. Right tibia, listed by Lydekker (1888) as a left tibia but later (1891) corrected.

R8422. Sacral centra 1, 2 and 3 from a large individual, damaged, no data.

Hulke Collection, purchased 1895

R2466–R2476. Parts of one small individual in soft grey marl. Found in cliff about 100 yd west of Cowleaze Chine (Hulke MS : 40), not the west end of the Bed as stated by Hulke (1874 : 18). All this material was described by Hulke (1873) who figured some of it in that work (pl. 18, figs. 1–8) and again in 1882 (pl. 72, figs. 3–9 ; pl. 79, figs. 1, 4) ; Nopcsa (1905, fig. 3) figured the only known predentary, which is also shown in Text-fig. 11.

R2477. Block which contained a skull with atlas and axis, dermal armour and two vertebral series (a, b) each consisting of the posterior dorsals and the anterior sacrals. Found on the beach between Barnes High and Cowleaze Chine after it had been rolling about for some time (Hulke 1874). Figured by Hulke in 1874 (pl. 3, figs. 1, 2) and 1882 (pl. 71, fig. 1 ; pl. 76, fig. 2) as well as by Nopcsa (1905, figs. 2, 4). Photographs showing the complete block before preparation plus the lateral and dorsal views of the skull in the round are given by Galton (1967, figs. 22–25). The skull is shown in Text-figs. 4–8, 12, 17, 60, 61, Pl. 1, and Pl. 2, figs. 1, 2 ; the atlas and axis in Text-fig. 18 ; skull also in Galton (in press figs. 6–8).

R2481. Twelve centra and one complete cervical vertebra found near Cowleaze Chine (Hulke MS). Figured by Hulke (1882, pl. 74, figs. 5–8).

Hooley Collection, purchased 1924

R5829. Nearly complete mounted skeleton (see Swinton 1936*a*, fig. 2) of a large individual ; bones slightly crushed. Found near Cowleaze Chine (Register B.M. (N.H.) Collection and on card with Hooley Collection) and not from the Chine itself as stated by Swinton (1936), who gives measurements and descriptions of some of these bones.

R5830. Nearly complete mounted skeleton (see Swinton 1934, pl. 23 ; 1936*a*, fig. 2) of a small individual ; bones show practically no distortion, articular surfaces are well preserved. Locality data as for R5829 ; bones figured by Swinton (1936, figs. 4–7) and in Text-figs. 32, 36, 39, 42–45, 53E, 54, 56 and 57.

The manus as mounted contained phalanges of a pes but, because the hind-feet are already complete, these extra pedal elements must belong to a second individual. In the Hooley Collection there are several bones from a small individual (see Galton 1967, fig. 17) of which the state of preservation closely resembles that of R5830 ; some of these correspond to elements which are missing from the mounted skeleton and probably belong to it, others duplicate elements from the mounted skeleton (see Galton 1967, fig. 16) and must belong to other individuals. All this material is numbered R5830.

R5862. Left maxilla from near Cowleaze Chine (Register B.M. (N.H.) Collection), figured by Swinton (1936, fig. 1).

R5863. Part of left mandible from near Cowleaze Chine (Register B.M. (N.H.) Collection) ; teeth figured by Swinton (1936, figs. 2, 3).

R6372. Intercentrum of atlas described by Swinton (1936) and five jaw fragments ; from Cowleaze Chine (Register B.M. (N.H.) Collection).

R8367. Isolated skull bones, no data ; isolated teeth, see Text-figs. 14–16.

R8419. Right exoccipital and paroccipital process, no data, see Text-fig. 9.

Other material

R8352. Distal part of large right femur with fourth trochanter, found near Cowleaze Chine in the early 1960's.

R8366. Many isolated bones from at least two individuals, one small and the other medium-sized ; discovered about 100 m west of Cowleaze Chine in September, 1965 by a field party from the 13th Symposium on Vertebrate Palaeontology and Comparative Anatomy.

R8418. Skull elements and teeth from the above find, partial basis for Text-fig. 9.

Museum of the Geology of the Isle of Wight, Sandown, I.o.W. : Poole Collection, donated 1938 – **S.M. 4127.** Part of tail and hind-limb from Cowleaze Chine, basis for metatarsal V in Text-fig. 58 and for identification of distal tarsals in Text-fig. 57.

Department of Zoology, University College London : material found by a party led by Dr P. L. Robinson.

Vertebrae and limb bones from at least three small animals all found in a few cubic feet of the *Hypsilophodon* Bed. This material is badly preserved though much is in natural articulation. Photographs show that the locality was about 100 metres west of Cowleaze Chine in practically the same position as where R8366 was found.

c) *British Museum (Natural History) numbers of previously figured specimens*

Mantell, 1849	pl. 29, fig. 9*	28707	three cervical vertebrae
Owen, 1855	pl. 1,	28707	complete block
	pl. 15, fig. 8	28707	dermal armour (as integument)
Huxley, 1870	pl. 1, figs. 1–5	R197	skull and vertebra
	figs. 6–8	28707	caudal vertebra
	pl. 2	28707	pelvic region
Hulke, 1873	pl. 18, fig. 1	R2470	front part of dentary
	fig. 2	R2467	right scapula and coracoid
	fig. 3	R2473	part of manus
	fig. 4–7	R2471	teeth
	fig. 8	R2466	right foot
Hulke, 1874	pl. 3, fig. 1	R2477	skull and dermal armour
	fig. 2	R2477	two vertebral series a and b
Owen, 1874	pl. 1, figs. 9, 9a, 10	R197	skull
	pl. 2, figs. 1, 5	R197	skull
	figs. 8–11	R189	part of mandible

Owen, 1874	pl. 2,	figs. 12–17	R191	tooth
		text-fig. 1	R190	mandibular ramus
		fig. 2	R190	caudal vertebra
Hulke, 1882	pl. 71,	fig. 1	R2477	skull, palate
		figs. 2–4	R197	skull
	pl. 72,	fig. 1	R194	eroded skull
		fig. 2	R196	part of left mandible
		figs. 3–5	R2471	teeth
	pl. 73		R192	block with pectoral girdle, neck, jaws
	pl. 74,	figs. 1–4	28707	three cervical vertebrae
		figs. 5–8	R2481	cervical vertebra
		figs. 9–12		from Fox Collection but originals could not be found
		fig. 13	R196a	three caudal vertebrae
	pl. 75		R196	pelvic region
	pl. 76,	fig. 1	R195	pelvic region
		fig. 2	R2477	sacrum b
	pl. 77		R193	right pelvic bones and foot
	pl. 78,	figs. 1–5	R192a	left femur
		figs. 6–7		from Hulke Collection but originals could not be found
	pl. 79,	fig. 1	R2467	right scapula, coracoid, humerus
		figs. 2–3	R196	right fore-arm, left humerus
		fig. 4	R2466	left foot
	pl. 80,	fig. 1		from Hulke Collection but original could not be found
		fig. 2	R199	right tibia
		figs. 3–8		originals could not be found
	pl. 81,	fig. 1	R199	right tibia
		figs. 2–3	R200	right and left foot
Nopcsa, 1905		fig. 1	R196	braincase, occiput
		figs. 2, 4	R2477	occiput
		fig. 3	R2470	right dentary with predentary
von Huene, 1907		fig. 330	? R196	reconstruction of ilium
		fig. 331	R193	right ischium
Swinton, 1934	pl. 23		R5830	photograph of mounted skeleton
Swinton, 1936		fig. 1	R5862	left maxilla
		figs. 2–3	R5863	maxillary teeth

Swinton, 1936	figs. 4–7	R5830	scapula, coracoid, humerus, radius, ulna, tibia, fibula, astragalus, calcaneum
Swinton, 1936*a*	fig. 2	R5829 and R5830	photograph of the mounted skeletons
Galton, 1969	figs. 4, 6–11, 13, 15	all R193	figures and stereo-photographs of pelvic girdle and femur to show areas of muscle attachment
Galton, in press	figs. 6–8	R2477	skull

Outline figures of the skull (R2477) and limb bones (R196) are given in Galton (1970*a*, 1971*a*, *b*, 1973, in press *a* ; see page 149).

d) *Measurements*

The proximal part of the femur gives the best indication of the relative size of important specimens. In Table I the measurement given is the minimum distance between the proximal end and the distal side of the base of the fourth trochanter (Text-fig. 1f). In specimens where no femur was available this distance was calculated by comparing other bones with specimens which have a femur ; the calculated values are given in parentheses. The total length of R5830 was about ·9 m, R196 about 1·36 m, R5829 about 1·8 m and R167 about 2·3 m. To facilitate comparison of the sizes of different bones from the same specimen all the measurements are given together in Tables II and III. Unless indicated to the contrary by a diagram in Text-fig. 1, L = greatest length, M_w = minimum width of shaft, W_d and W_p maximum width of distal and proximal ends. All measurements are in millimetres.

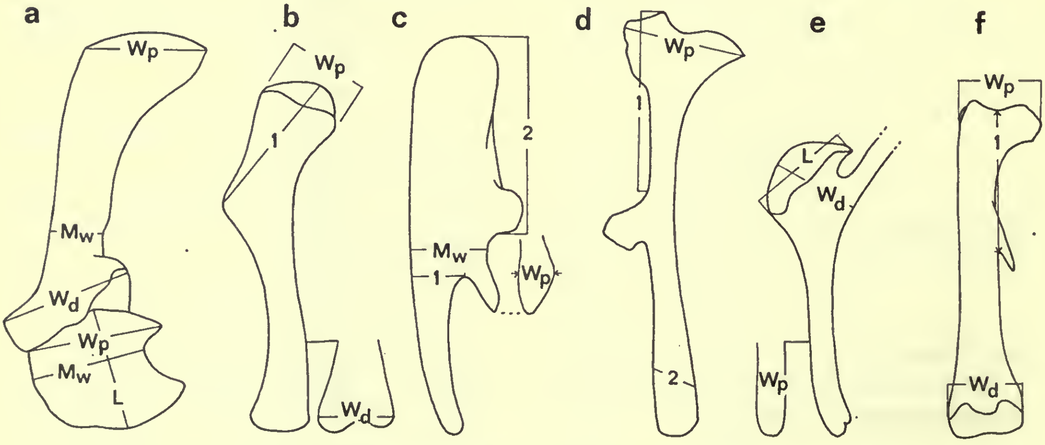

FIG. 1. Diagram to show the basis for some of the measurements in Tables I and II : a. scapula and coracoid ; b. humerus ; c. ilium ; d. ischium ; e. pubis ; f. femur.

TABLE I

To show the relative size of the specimens of *Hypsilophodon* – measurements in mm of fourth trochanter index of the femur, see Text-fig. 1f.

R5830	43	R196	65
R197	(49)	R192a	76
R2466-76	(55)	R200	(81)
S.M. 4127	(57)	R192	± 82
R2477 skull	(57)	R193	86
R2477a	± 60	R5829	87
R195	62	R167	108
28707	64		

TABLE II

Measurements of the bones of the girdles and the long limb bones
(All measurements in mm)

Bone	Spec. No.	L/R	L	Wp	Wd	Mw	1	2
Scapula	R5830	L	70·5	–	–	10	–	
(Text-fig. 1a)		R	(67·5)	24·5	25	–	–	
	R2467	R	88	32	26·5	12·5	–	
	R196	R	105	45	41	15	–	
	R192	R	+ 144	47	53	22	–	
	R5829	R	–	–	–	21	–	
Coracoid	R5830	R	20·5	–	–	–	–	
(Text-fig. 1a)	R2467	R	26	30	–	–	–	
	R196	L	35·5	43	–	35	–	
	R192	R	43	–	–	–	–	
Humerus	R5830	L	(74)	17	15	–	26	
(Text-fig. 1b)		R	69	16·5	14	6	–	
	R196	L	105	26·5	25	9·5	45·5	
		R	105	28	–	–	45·5	
	R192	L	147	+ 39	–	18	72	
	R5829	L	(159)	41	–	–	(64)	
		R	151	–	33	–	(68·5)	
Radius	R5830	L	–	9·5	–	4	–	
	R196	L	82·5	15(R)	13	6	–	
	R192	L	+ 111	–	–	8	–	
	R5829	R	114	–	–	–	–	
Ulna	R5830	L	–	8	–	–	9·5	–
	R196	L	88	11·5	14·5	6	19	–
	R192	L	± 125	–	–	11	25	–
Ilium	R195	R	–	11·5	–	21	15	–
(Text-fig. 1c)	R196	L	142	9	14	22	16	67
	R2477a	R	–	–	–	23	–	–
	R193	R	–	16	–	32	21	89(L)

TABLE II (*cont.*)

Bone	Spec. No.	L/R	L	Wp	Wd	Mw	1	2
Ischium (Text-fig. 1d)	R5830	L	102	25·5	8·5	5·5	± 40	–
	R195	L	–	36	–	8	60	14
	R196		–	46	–	9	–	21
	R193	R	–	49	–	14	79	28
	R5829	R	197	53	21	13·5	72	27
Pubis (Text-fig. 1e)	R195	L	–	8	15	21·5	–	–
	R196	R	–	10	–	–	–	–
	R193	R	38	14	–	–	–	–
	R5829	L	36	12	–	–	–	–
Femur (Text-fig. 1f)	R5830	L	101	26·5	25	10·5	43	–
	28707	L	± 150	–	–	–	64	–
	R196	L	± 150	–	–	14	65	–
	R192a	L	173	–	–	–	76	–
	R5829	R	202	–	56	–	–	–
		L	198	52	–	–	87	–
Tibia	R5830	R	117	26·5(L)	25·5	9		
	R196	R	–	–	40	–		
	SM4127	R	170	33	36	12		
	R193		–	58(L)	56·5(R)			
	R5829	L	238	(62)	45	17		
		R	(242)	(42)	–	–		

TABLE III

Measurements of Manus and Pes
(All measurements in mm)

		R5830 L	R5830 R	R2466 L	SM4127 R	R196 L	R196 R	R200	Manus R196 R
First metatarsal	L	–	–	–	–	–	46	± 56	13
	Wp	–	–	–	–	–	10	12	8
	Wd	7	7	6	14	12	13	15	6
Phalanx	I	18·5	–	–	–	28	29	–	8
	ungual	–	–	± 15	–	23	–	–	+ 8
Second metatarsal	L	55	54	± 65	69	–	66	± 83	21
	Wp	–	8	–	8	–	12	–	11
	Wd	9	9	–	13	–	15	19	11
Phalanx	I	–	–	25	–	29	28	–	12
	II	–	–	± 19	–	21	–	–	8·5
	ungual	–	–	22	–	–	–	–	–
Third metatarsal	L	62·5	63	± 70	77	–	84	106	24
	Wp	8	7·5	–	9	–	10	15	9·5
	Wd	11·5	–	14	15	–	18	22	8·5

Table III (*cont.*)

		R5830	R5830	R2466	SM4127	R196	R196	R200	Manus R196
		L	R	L	R	L	R		R
Phalanx	I	–	–	25	–	28	25	–	10
	II	–	–	19	–	23	21	–	7
	III	–	–	16	–	–	–	–	5
	ungual	–	–	± 23	–	–	–	–	app. 8
Fourth metatarsal	L	55·5	53	± 59	72	–	69	± 90	15
	Wp	9	9	–	13	–	15	–	7
	Wd	9·5	9	± 10	14	–	14	20	6
Phalanx	I	–	–	± 17	–	19	18	–	5
	II	–	–	15	–	15	17	–	3·5
	III	–	–	13	–	14	–	–	–
	IV	–	–	12	–	12	12	–	?
	ungual	–	–	17	–	–	–	–	–
Fifth metatarsal	L	–	–	–	23	–	24	35	10
	Wp	–	–	–	6	–	9	8	6·5
	Wd	–	–	–	3	–	–	5	5

III. THE *HYPSILOPHODON* BED

a) *Stratigraphy*

Casey (1963) showed that the onset of the Cretaceous period in Southern England is indicated by the marine invasion that formed the Cinder Bed at the base of the Durlston Beds in the Middle Purbeck Series. The rest of the Durlston Beds and the succeeding Wealden Series consist mainly of lagoon and deltaic deposits. The Lower Greensand, Gault and Upper Greensand beds are marine and represent the remainder of the Lower Cretaceous in this region (B.M. (N.H.) Handbook 1962, Hughes 1958), although Kirkaldy (1939, 1963) has included the last two in the Upper Cretaceous with the Chalk. On the Isle of Wight there is no exposure of the equivalents of the Hastings Beds of the Weald but only of the younger beds of the Weald Clay, here represented by the Weald Marls with the overlying Shales. Remains of *Hypsilophodon*, which occur next to the contact between the Marls and the Shales, have been found only in Brightstone (= Brixton) Bay, although this contact is also exposed in the cliffs of Compton Bay and Sandown Bay (White 1921). The absence of ostracods in the Marls and the lower part of the Shales makes it difficult to determine accurately the age of the *Hypsilophodon* Bed. It is probably Barremian (Allen 1955, B.M. (N.H.) Handbook 1962, Hughes 1958) but it might possibly be Early Aptian (Hughes 1958) (see Text-fig 64).

The *Hypsilophodon* Bed is exposed in the cliff at beach level about 100 yd west of Cowleaze Chine and rises in the cliff to end about ¾ mile further west just beyond Barnes High (White 1921, fig. 1b, c; Chatwin 1960, fig. 17b, c). A detailed succession of these marls and shales was given by Strahan (1889) who gave two descending sections of the beds at the junction region. He noted that the first (page 13), between Cowleaze and Barnes Chine, was taken from various points in the cliffs :

'. . .

Grey and black shales, the upper part interlaminated with much sand in Cowleaze Chine ; a band crowded with *Paludina* and *Unio* near the top, and another with *Cyrena* and *Paludina* near the bottom	19′ 0″
White sand and clay, with lignite	2′ 6″
Current-bedded white rock	2′ 6″
Reddish-blue sand and clay, with bone fragments (*Hypsilophodon* Bed)	3′ 0″
Red and variegated marls	44′ 0″

. . .'

while the second (pages 14–16), from Atherfield to near Brook, gave the succession at Cowleaze Chine :

'. . . about 144′ . . .

Wealden shales	Blue shales, with *Unio* and *Paludina* in the top, and *Cyrena* and *Paludina* near the bottom	19′ 0″
	White sand and clay	2′ 6″
	White rock	2′ 6″
	Red sand, with bones (*Hypsilophodon* Bed)	3′ 0″
Wealden marls	Red and mottled marls, rocky and ripple-marked at the top	44′ 0″

. . . about 510′ . . .'

Judging on the lithology of these localities today, Strahan interchanged the two sections – it will be noted that 'sand in Cowleaze Chine' is mentioned in the section which purports to relate to the cliff-section rather than to the beds at Cowleaze Chine.

White (1921 : 16) noted that near Cowleaze Chine the white rock 'is a pale, calcareous, silty stone, indistinctly shaly in places, and having an uneven base [see Galton 1967, fig. 3A]. It contains *Unio* and water-worn bones'. The articulated material found by Dr P. L. Robinson was in this shaly portion as well as in the *Hypsilophodon* Bed below. Hooley, as noted by White (1921), found remains of *Hypsilophodon* in the Marls a little below the *Hypsilophodon* Bed but not in the Shales above.

White (1921 : 16) reproduced the second succession of Strahan (1889) and noted that the *Hypsilophodon* Bed, although included with the shales, 'is lithologically and stratigraphically more nearly allied to the marls'. As noted by Hulke (1882), the *Hypsilophodon* Bed is extremely variable, even within the space of a few yards. This is certainly true of the first hundred metres exposed in the cliff near Cowleaze Chine. Here the bed consists of reddish-blue marls which are indistinguishable from the Marls below. In the lower part of the Bed there are, in addition, several rocky bands of varying thickness which also occur near the top of the Marls (see Galton 1967, figs. 3B, C). About 160 m west of Cowleaze Chine there are well-developed desiccation cracks in the marls (see Galton 1967, fig. 3C). These cracks, which are about 45 cm deep and 4 cm wide, are filled with sand continuous with that of the overlying rocky band. It is difficult to determine whether this band is at the top of the Marls or at the base of the *Hypsilophodon* Bed.

b) *Hypsilophodon* localities

Lydekker (1888) listed specimens of *Hypsilophodon* and in each instance the locality, where given, was Cowleaze Chine. Swinton (1936*b* : 213) stated that 'almost every specimen comes from Cowleaze Chine' while, in connection with the two skeletons from the Hooley Collection, he stated (1936 : 555) that 'these two specimens, like the type, are from the Wealden of Cowleaze Chine'. The *Hypsilophodon* Bed where it crosses the mouth of Cowleaze Chine is buried underneath 12 ft of shingle. If all the specimens actually came from the Chine then this productive site is now very rarely accessible.

Owen (1855 : 2) stated that 28707 'was discovered . . . about one hundred yards west of Cowleaze Chine . . . the mass of Wealden stone . . . was broken into two parts in its extraction from the bed'. Owen (1874 : 12, 13) quoted from a letter written by Fox in 1870 as follows (specimen numbers have been added) : 'This jaw [R189] was found within a yard of the skull [R197 – the holotype]. They were both in a mass of mud that had slided down from the cliff . . .', and '. . . you will find one very small tooth [R191], quite perfect, that came out of this slab [R190] in dressing. This slab [R190] was found in the fallen cliff, about 150 yards east of Barnes High. . . . The skull [R197 – holotype] and broken jaw [R189] were found about 60 yards further eastward.' All these specimens were listed by Lydekker (1888) as from Cowleaze Chine, whereas the actual site is at the opposite end of the bed, a little over half a mile further west. Consequently the entry 'Cowleaze Chine' is equivalent to *Hypsilophodon* Bed ; this is all the data we have for specimens R192–R196 and R200 (Fox MS).

Hulke (MS) gave nearly all his localities as near Cowleaze Chine and exact details were given only for R2466–R2476 which was found about 100 yd west of the Chine (not the west end of the bed as stated by Hulke, 1874 : 18). In a memorandum dated Oct. 1894, Hulke (MS, opposite find no. 260) wrote that 'I do not suppose the Cowleaze end of this bed richer than the other parts of it, but its waste is greater and fresh exposures are frequent'. The locality for R5829 and R5830 was near Cowleaze Chine and the two recent finds of *Hypsilophodon* were both about 100 m west of the Chine. Consequently more material may be found in the productive region about 100 m west of the Chine.

c) *Fauna*

The Wealden of the Isle of Wight is famous for its dinosaurs but most of these are represented by very fragmentary remains (for details see Swinton 1936*b*). Apart from the *Hypsilophodon* material, only two other reasonably complete skeletons have been found – those of *Iguanodon atherfieldensis* and *Polacanthus foxii*. Both represent large animals (about 5 m) whose cadavers were probably carried some distance by water. The fragmentary and broken nature of the other dinosaurian remains indicates that they were transported quite a long distance.

In marked contrast to this is the *Hypsilophodon* Bed, from which well preserved and naturally articulated bones representing 20 individuals of this relatively small dinosaur have been found. Three of these (R196, R5829, R5830) are reasonably complete skeletons. The incomplete nature of the remainder reflects faults of discovery rather than of preservation because, in most instances, the edges of the blocks cut across articulated bones. The skeleton of R196 is almost complete and nearly all the bones were in natural articulation. It is unlikely that this individual was carried very far, if at all, from where it died. The same is true of the two skulls of young individuals (R197, R2477) in which the fragile bones are excellently preserved and only slightly disarticulated. In a few instances (R196, R2477, U.C.L.) two or three skeletons have been preserved very close to each other in the same small block.

The 'fauna' represented in the *Hypsilophodon* Bed is very restricted. Apart from *Hypsilophodon*, Hulke (1882 : 1036) recorded the presence of 'a small scuted crocodile (*Goniopholis*?) and a chelonian (*Trionyx*?)'. He also noted that neither Fox nor he had found any remains of *Iguanodon mantelli* in this bed. In the Hooley collection there is a cervical vertebra that is probably *Goniopholis* and a phalanx that might be from *Iguanodon*, but it is not certain that these came from the *Hypsilophodon* Bed. The same is true of the proximal end of a small femur, possibly of *Iguanodon*, which is catalogued with several odd femora of *Hypsilophodon* (R170). The coelurosaur *Calamospondylus foxi* may not have come from the *Hypsilophodon* Bed, because the tibia is not listed as such by Fox (MS). Why *Hypsilophodon*, which is represented by such excellent material, is the only dinosaur found in the Bed is a mystery. This, however, is certainly the case, because Fox, Hulke and Hooley collected much material from this Bed (full list in Galton 1967), all referable to *Hypsilophodon*.

IV. OSTEOLOGY OF *HYPSILOPHODON FOXII*

Order ORNITHISCHIA

Suborder ORNITHOPODA

Family **HYPSILOPHODONTIDAE** Dollo 1882 (page 175)

Genus ***HYPSILOPHODON*** Huxley 1869 (page 3)

Emended diagnosis. Five premaxillary teeth separated by step from maxillary row with 10 or 11 teeth, 13 or 14 on dentary ; enamelled medial surface of a dentary tooth has a strong central ridge that is absent on the lateral surface of a maxillary tooth. Narial openings completely separated by anterior process of premaxillae ; large antorbital recess or depression plus row of large foramina in maxilla ; jugal does not contact quadrate ; large fenestrated quadratojugal borders lower temporal opening. Five or six sacral ribs, the additional one borne on the anterior part of the first sacral vertebra. Scapula same length as humerus ; obturator process on middle of ischium. Femur with following combination of characters: fourth trochanter on proximal half, lesser trochanter triangular in cross-section with a shallow cleft separating it from the greater trochanter, practically no anterior condylar groove and posteriorly outer condyle almost as large as inner. The type-species, *H. foxii*, is the only species known.

Holotype. British Museum (Natural History) No. R197.

Paratype. British Museum (Natural History) No. 28707.

Huxley read his paper on *Hypsilophodon* on 10 November 1869; this was published in 1870 and citations are given as *Hypsilophodon* Huxley 1870. However, later authors have overlooked a summary of this paper published in 1869; the year of publication is confirmed by a reference in abstract in the *Proceedings of the Geological Society* No. **205** p. 4 to the papers which were to be given at the next meeting on 24 November 1869. This summary provides an adequate diagnosis of *Hypsilophodon foxii* which is certainly more detailed than that given by Boulenger (1881) for *Iguanodon bernissartensis.*

Specimens used for osteology and reconstructions

The individual skull bones of R2477 were stuck together with Carbowax (polyethylene glycol 4000) and their spatial relationships are maintained in all the figures of this specimen. The description of the skull is mostly based on this specimen as is the reconstruction of the complete skull (Text-fig. 3). Certain details are from other specimens: the anterior end of the premaxilla is from R196, the premaxillary teeth and the quadratojugal are from R197, the supraorbital is from R194 and R197 and the predentary is from R2470. The mandibular ramus is based on R196 with supplementary details from specimen R192, R197, R2470, R2477 and R8418. The restored lengths of the dentary and of its tooth row are probably not absolutely accurate because the jaw is reconstructed from several incomplete specimens of different size. The size of the predentary is approximate because the only specimen is of a small individual. The spatial relationship between the articular head of the quadrate and the end of the tooth row is accurate as this is based on the lower jaw of R2477. The jugal is adapted from R197 and R2477 but the resulting quadratojugal (Text-fig. 3) is proportionally rather longer ventrally than that of R197 (Text-fig. 2). In the reconstruction the basipterygoid processes are separated by about 7 mm from their original contact with the pterygoid. This indicates that the braincase should be situated some 7 mm more anteroventrally. However, if the parietal, squamosal and quadrate are also moved by the same amount the posterior teeth of the lower jaw fail to engage the corresponding teeth of the maxilla.

The reconstruction of the postcranial skeleton (Text-fig. 62) and the osteology of the individual elements (apart from the femur, tibia and fibula, for which R5830 is used) are based on the nearly complete skeleton of R196 and the tail R196a. Individual variations exhibited by specimens other than R2477, R196 and R5830 are noted after the description of the element concerned. In the Text-figures all bones are drawn from the left side unless otherwise stated.

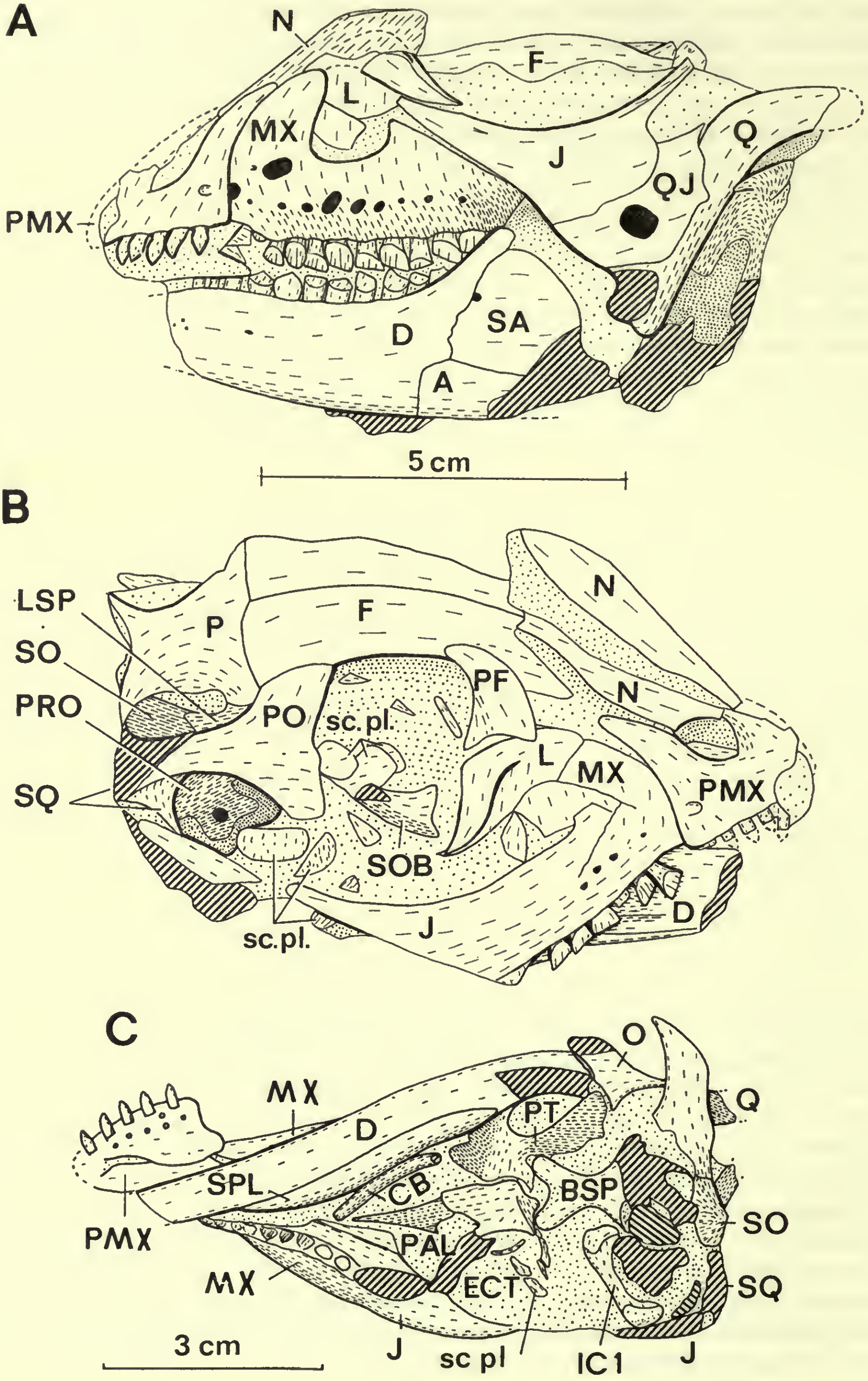
A
N
F
L
MX
J
Q
QJ
PMX
SA
D
A
5 cm
B
LSP
SO
PRO
SQ
P
F
N
PF
N
PO
sc. pl.
L
MX
PMX
SOB
D
J
sc.pl.
C
O
MX
D
PT
Q
SPL
CB
BSP
SO
PMX
PAL
MX
ECT
SQ
3 cm
J
sc pl
IC1
J

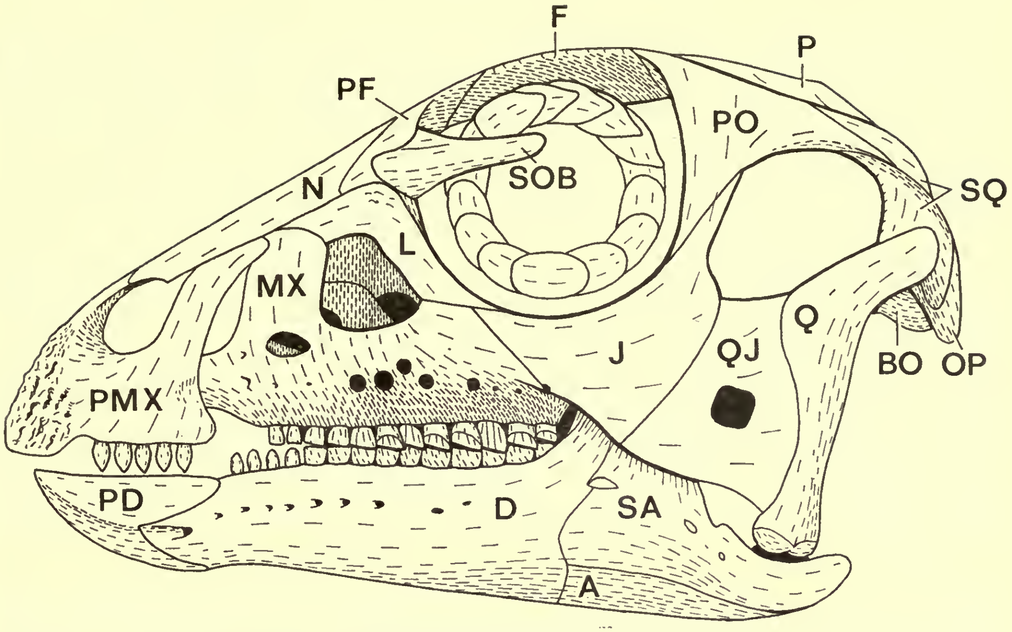

FIG. 3. *Hypsilophodon foxii.* Skull reconstruction, mainly R2477 × 1. For abbreviations see below; for specimens used see page 19.

a) *The skull and lower jaw*

i) INDIVIDUAL BONES

Supraoccipital (SO). This bone forms the dorsal boundary of the foramen magnum. The posterior surface (Text-fig. 8) which is inclined forwards at an angle of about 55 degrees to the skull axis (Text-fig. 5A), is flat ventrally but bears a median ridge dorsally. The surface on either side of this ridge is concave and sweeps obliquely outwards, forming a dorso-lateral corner with the lateral part of the bone. This forms part of the side-wall of the braincase and is concave antero-posteriorly and to a lesser extent dorso-ventrally (Text-fig. 5C). Apart from the median ridge the dorsal and medial parts of the bone are quite thin. The ventro-lateral part, especially more posteriorly, is very thick. The ventral surface is gently convex antero-posteriorly but strongly concave transversely.

FIG. 2. *Hypsilophodon foxii.* Holotype, R197. Skull × 1. A, left side; B, right side; C, ventral view. Abbreviations used in Text-figs. 2–16

A	angular	F	frontal	PSP	parasphenoid	QJ	quadratojugal
ART	articular	J	jugal	PA	prearticular	sc.pl.	sclerotic plate
BO	basioccipital	L	lachrymal	PD	predentary	SPL	splenial
BSP	basisphenoid	LSP	laterosphenoid	PF	prefrontal	SQ	squamosal
CB	ceratobranchial	MX	maxilla	PMX	premaxilla	SO	supraoccipital
CO	coronoid	N	nasal	PO	postorbital	SOB	supraorbital
D	dentary	OP	opisthotic	PRO	prootic	SA	surangular
ECT	ectopterygoid	P	parietal	PT	pterygoid	V	vomer
EO	exoccipital	PAL	palatine	Q	quadrate		

The end part of the dorso-lateral corner has suture markings (Text-fig. 5C, Pl. 2, fig. 1) while anteriorly there is a lateral groove that becomes wider as it runs diagonally across the side-wall. From the central part of this groove a ventral groove arises that passes through the floor of the lateral groove. The vena capitis dorsalis probably ran in the anterior part of the lateral groove and then into the ventral groove. Anteriorly it was bounded laterally by the parietal that enclosed the dorsal part of the supraoccipital (Text-fig. 5A) and fitted against the side-wall adjacent to the groove. In passing ventrally the vena capitis dorsalis passed medially to the edge of the parietal. More posteriorly the edge of the parietal fitted into the tapering posterior part of the lateral groove and on to the sutural surface of the dorso-lateral corner. The opisthotic is sutured to the obliquely truncated postero-lateral corner of the supraoccipital which has a large and almost square sutural surface. The prootic is sutured to a triangular surface on the ventral edge and, like the surface for the opisthotic (both visible in R8418), it has well-developed sutural ridges. The sutural junction with the prootic is excavated medially to form a large tapering tunnel, the fossa subarcuata (Text-fig. 9B, C), which was probably for the floccular lobe.

Exoccipital (EO). The suture between the exoccipital and the opisthotic is not visible in R2477. In R8418 on the medial surface there is a sutural line (Text-fig. 9B) but unfortunately this cannot be followed on to the other surfaces. The exoccipital forms the ventro-lateral border of the foramen magnum while the round posterior surface forms part of the occipital condyle. The ventral surface has strong sutural ridges for the basioccipital.

Basioccipital (BO). This forms most of the sub-spherical occipital condyle whose smooth articular surface is well developed ventrally (Text-fig. 6A) as well as posteriorly (Text-fig. 8). Anteriorly from the condyle there is a tapering median ventral ridge (Text-fig. 6A) with well-developed insertion markings. In R5830 the anterior surface, which is more or less vertical, has two subcircular areas for the buttress oi the basisphenoid. On each side there are two obliquely inclined lateral surfaces, with well-developed sutural ridges, which are set at an angle of about 135 degrees to each other. The smaller anterior surface is for the basisphenoid while the larger surface is for the opisthotic and also, more posteriorly, for the exoccipital.

Opisthotic (OP). This forms the lateral wall of the foramen magnum (Text-figs. 4B, 9A). The paroccipital processes of R2477 are missing but have been restored with reference to specimens R194 and R196. The proximal end of the bone is thick, roughly triangular in cross-section, with a ventrally directed part that continues the side-wall of the braincase (Text-fig. 9A). The bone tapers laterally, with the anterior edge gradually disappearing, to form a flattened paroccipital process (Text-fig. 9A). The anterior edge is flat, forming a sutural surface for the prootic. Dorsal to this the surface of the proximal half is laterally concave as it is ventrally where this curve is much more strongly developed. The ventral edge is thick and rounded proximally but becomes thinner laterally. The dorsal edge is thin and moderately sharp along all its length.

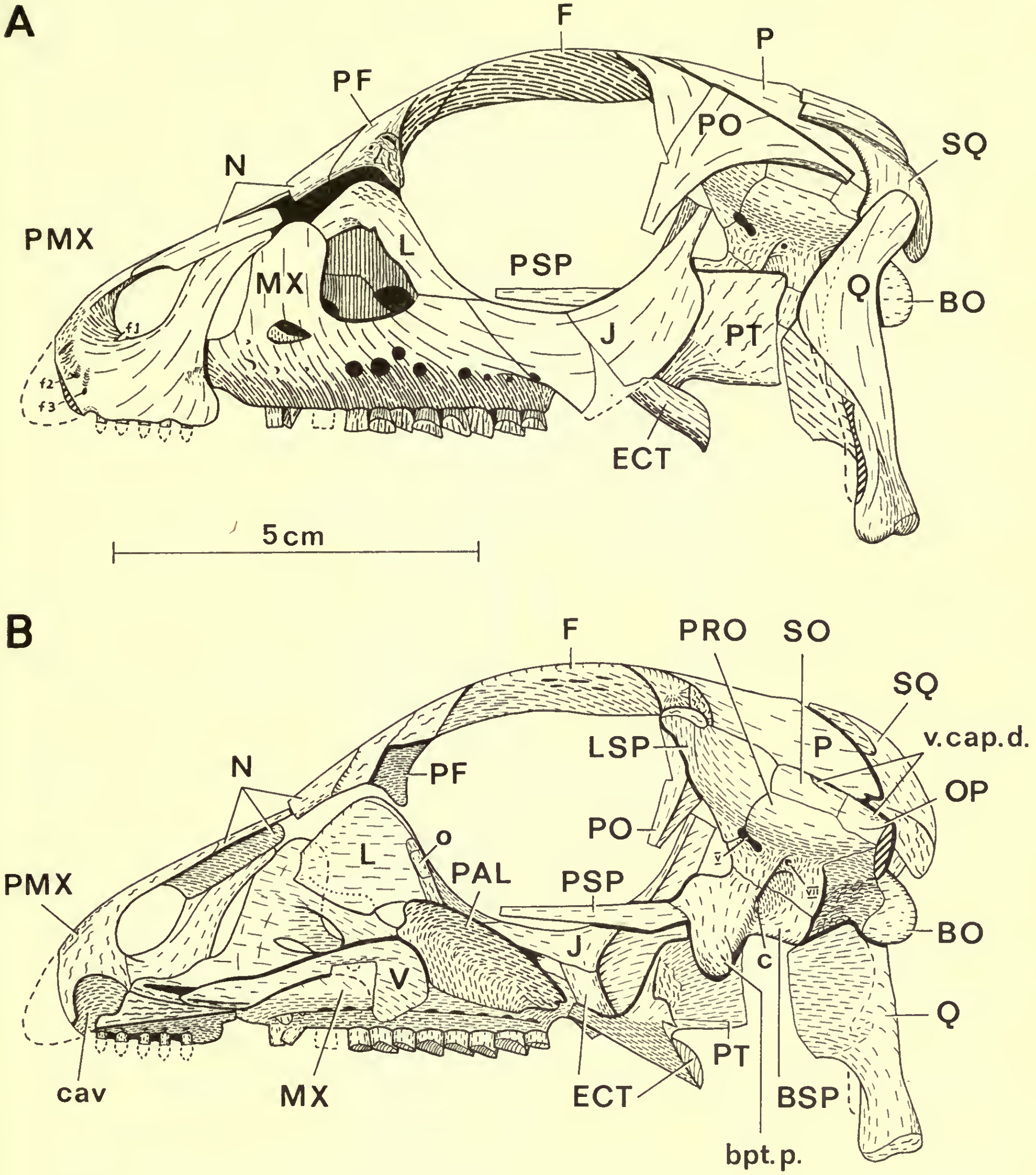
A
F
P
PF
PO
SQ
N
PMX
MX
L
PSP
Q
BO
f1
f2
f3
J
PT
ECT
5 cm
B
F
PRO
SO
SQ
LSP
P
v.cap.d.
N
PF
OP
PO
o
PMX
L
PAL
PSP
V
VII
BO
J
c
Q
PT
cav
MX
ECT
BSP
bpt. p.

FIG. 4. *Hypsilophodon foxii.* Skull R2477 × 1. A, lateral view, compare with Pl 1, figs. 3, 4; B, medial view, as A but with lateral bones of the left side removed, compare with Pl. 2, fig. 2. Abbreviations: bpt p., basipterygoid process; c, foramen for internal carotid artery; cav, cavity in the premaxilla; o, bony element; v. cap. d., vena capitis dorsalis; V, trigeminal foramen; VII, facial foramen. For other abbreviations see page 21.

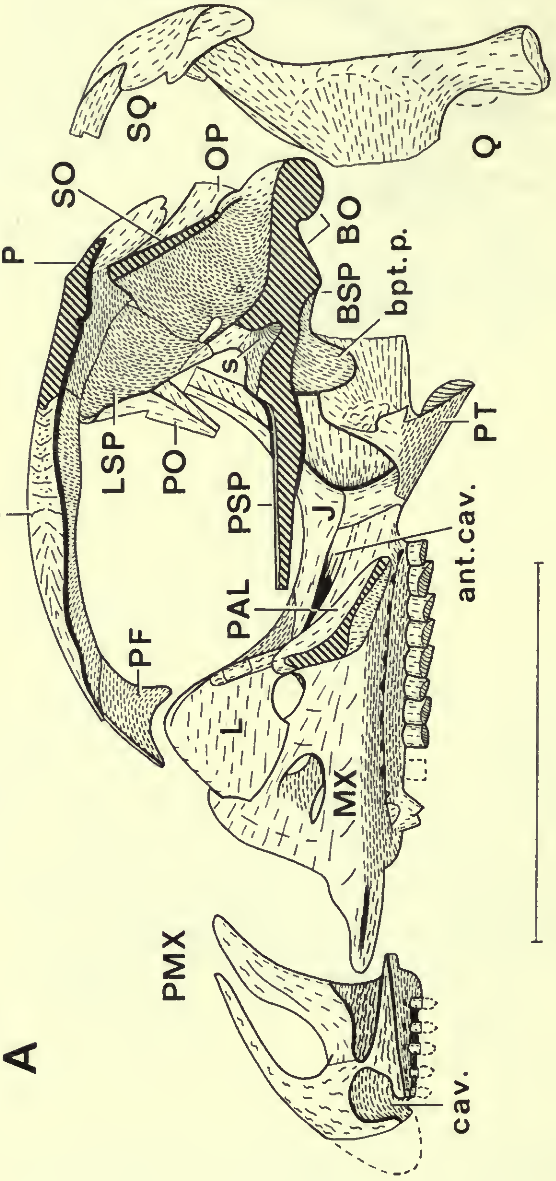
A
SQ
Q
OP
SO
BO
P
BSP
bpt.p.
s
PT
F
LSP
PO
PSP
J
ant.cav.
PAL
PF
L
MX
PMX
cav.

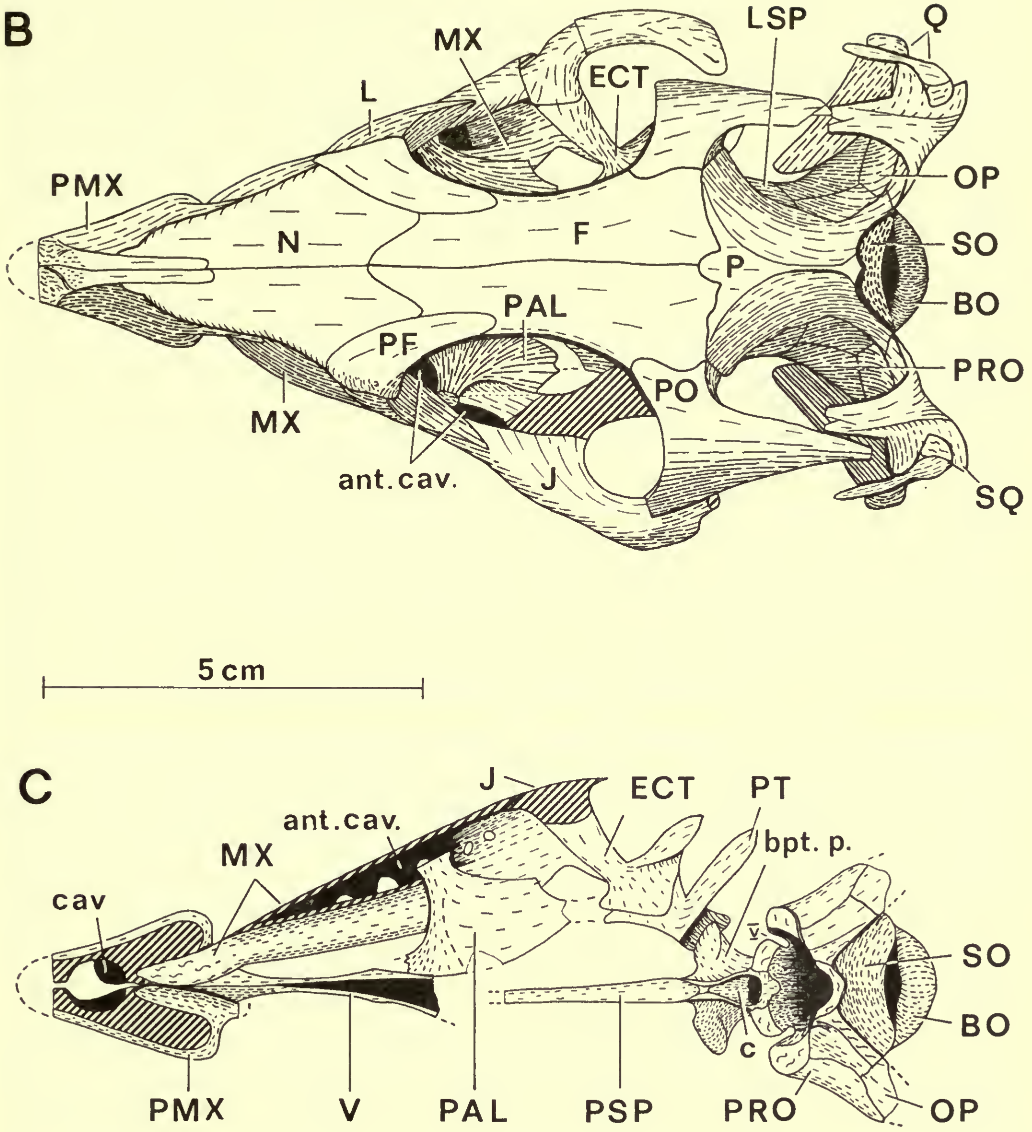
B
MX
L
ECT
LSP
Q
PMX
N
F
P
OP
SO
BO
PAL
PF
PO
PRO
MX
ant.cav.
J
SQ
5 cm
C
J
ECT
PT
ant.cav.
bpt. p.
MX
cav
V
SO
BO
c
PMX
V
PAL
PSP
PRO
OP

Fig. 5. *Hypsilophodon foxii*. Skull R2477. × 1. A, medial view as Text-fig. 4B but with braincase and palatine sectioned, nasals and vomer removed, premaxilla, squamosal and quadrate displaced; B, dorsal view, compare with Pl. 1, fig. 1; C, dorsal view of the palate and braincase, as B but with bones of the skull roof and most of the left side removed, premaxillae, maxilla and jugal sectioned, compare with Pl. 2, fig. 1. Abbreviations: ant. cav., antorbital cavity or fossa; bpt.p., basipterygoid process; cav., cavity in premaxilla; s, sella turcica; V, trigeminal foramen. For other abbreviations see page 21.

The ventral surface of the braincase side-wall forms a rectangular surface with well-developed sutural ridges (visible in R8418) for the basioccipital. The anterior part of this wall forms an irregularly shaped sutural surface with well-developed sutural ridges for the prootic. The fenestra ovalis, middle ear cavity, internal auditory meatus and the jugular foramen are situated between the opisthotic and the prootic (Text-fig. 9). The tapering postero-dorsal part of the prootic also sutures to the flat-topped anterior edge of the opisthotic. The surface for the supraoccipital (Text-fig. 9B) has strong sutural ridges. The adjacent dorsal edge contacted the squamosal which is overlapped by the paroccipital process (Text-fig. 8).

Prootic (PRO). This is an irregularly shaped bone (Text-fig. 9) which forms part of the lateral wall of the braincase. The dorsal part of the bone continues the dorso-ventrally convex curve from the adjacent laterosphenoid (Text-fig. 4B). This curve becomes more acute passing posteriorly where the prootic tapers to a point which overlaps the paroccipital process (Text-fig. 9A). The ventral part is concave dorso-ventrally but this curve is complicated by three foramina (Text-fig. 9A). Posterior and ventral to the foramen ovale (V) the surface slopes gently away from the foramen but dorsally the slope is steeper, as it is around the facial foramen (VII), while the posterior edge is vertical. The sides of VII spiral slightly so that the steeper anterior surface forms a step above the ventral edge. This step is continued antero-ventrally where it becomes more pronounced as there is a well-developed depression at this point. Dorsally the depression is overhung by a thin and sharp edge. The prootic is sutured to the laterosphenoid, supraoccipital, opisthotic and basioccipital.

Basisphenoid (BSP). This median bone forms a thick floor to the anterior part of the braincase (Text-fig. 5A). In ventral view (Text-fig. 6A) the posterior part forms two buttresses which abut against the basioccipital and slightly overlap this vertical suture. The two buttresses, which are separated by a median depression, taper anteriorly with the lateral edges becoming thinner and sharper. The diverging pterygoid processes have, on the anterior part of their base, a well-developed depression which is continued on to the base of the parasphenoid. Adjacent to this depression the anterior edge is thin and sharp but more distally it is much thicker and rounded.

In lateral view (Text-fig. 4B) the distal part of the basipterygoid process has a rough surface which, with its continuation on to the rounded anterior edge and a smaller but similar surface on the medial surface, articulated with the pterygoid. The posterior edge of the process is thick and rounded and it continues postero-dorsally across the side of the basisphenoid. There is a deep excavation of the side of the bone postero-ventral to this edge so that there is only a thin median sheet. This thickens considerably postero-laterally and the excavation becomes progressively shallower. The ventral edge is formed by the buttress which is latero-ventrally flattened. The excavation and its bordering diagonal edge are continued on to the adjacent surface of the prootic. Anterior to this diagonal edge the surface of the basisphenoid is rough textured. The dorso-median part of the bone is deeply excavated to form the pituitary fossa (Text-figs. 5A, C) from which paired foramina for the carotid arteries pass postero-laterally, one on each side of the thin median sheet (Text-fig. 6A).

Parasphenoid (PSP). This arises from the basal region of the basipterygoid processes, anterior to the pituitary fossa, and runs forward to bisect the posterior part of the palatal vacuity (Text-fig. 6A). This tapering process is triangular in cross-section, with a concave dorsal surface, and the edges are thin and sharp. Its anterior limit cannot be determined in R2477.

Laterosphenoid (LSP). The lateral surface (Text-fig. 4B) is gently concave antero-posteriorly and convex dorso-ventrally ; there is a well-developed depression on the ventral part running antero-dorsally from the foramen ovale (V). The dorsal end of the bone is expanded laterally (Text-fig. 7B) to form a head, the rounded dorsal surface of which fits into a cavity formed by the frontal and postorbital (Text-fig. 6B). The anterior surface is flat and tapers ventrally (Text-fig. 7B). The medial surface (Text-fig. 5A) is dorso-ventrally concave while antero-posteriorly it consists of two very gently concave areas separated by a very gently convex ridge.

The dorsal surface for the parietal is thin and flat with a few minor ridges. The thin dorsal part of the posterior edge is gently rounded for the supraoccipital. More ventrally this edge is much thicker and formed the sutural surface for the prootic. The suture is obliquely inclined with the laterosphenoid overlapping the prootic (Text-figs. 9A, C). Just above the foramen ovale (Text-fig. 9A) there is a notch in the margin to receive a process of the prootic. Ventrally the second surface for the prootic is vertical, flat and triangular in outline.

Orbitosphenoid. This is not represented by the ossified plate present in *Parksosaurus* (see Galton, in press) and *Camptosaurus* (see Gilmore 1909). Anteriorly on the medial part of the laterosphenoid head there is a slight step, continuous with the straight antero-medial edge (Text-figs. 6B, 7B), while on the adjacent edge of the frontal there is a groove (Text-fig. 6B). These probably represent two of the contact surfaces of the orbitosphenoid which may not have been ossified.

Premaxilla (PMX). Each premaxilla has an anterior and a posterior process (Text-fig. 4A) while medially there is a ventral sheet (Text-fig. 6A). The narial opening is bordered by the anterior process which, together with its fellow on the other side, wedges between the nasals (Text-figs. 5B, 6B) so that they overlap very slightly. This process, triangular in cross-section, has a lateral edge which continues on to the main body of the bone (Text-fig. 4A). The surface in front of this edge is covered with large knobs while more ventrally there are two foramina (f_2, f_3, Text-fig. 4A). The rough and knobbly anterior end of the premaxilla was probably covered by horn to form a beak. Behind this edge the surface is concave and it is more obliquely inclined on the process, at the base of which there is another foramen (f_1). The posterior half of the lateral surface is gently convex antero-posteriorly (Text-fig. 5B) and concave dorso-ventrally (Text-fig. 7A). Anteriorly the posterior process is gently rounded while posteriorly the edge is thin and sharp. More ventrally the bone is thicker with a well rounded edge (Text-fig. 7A).

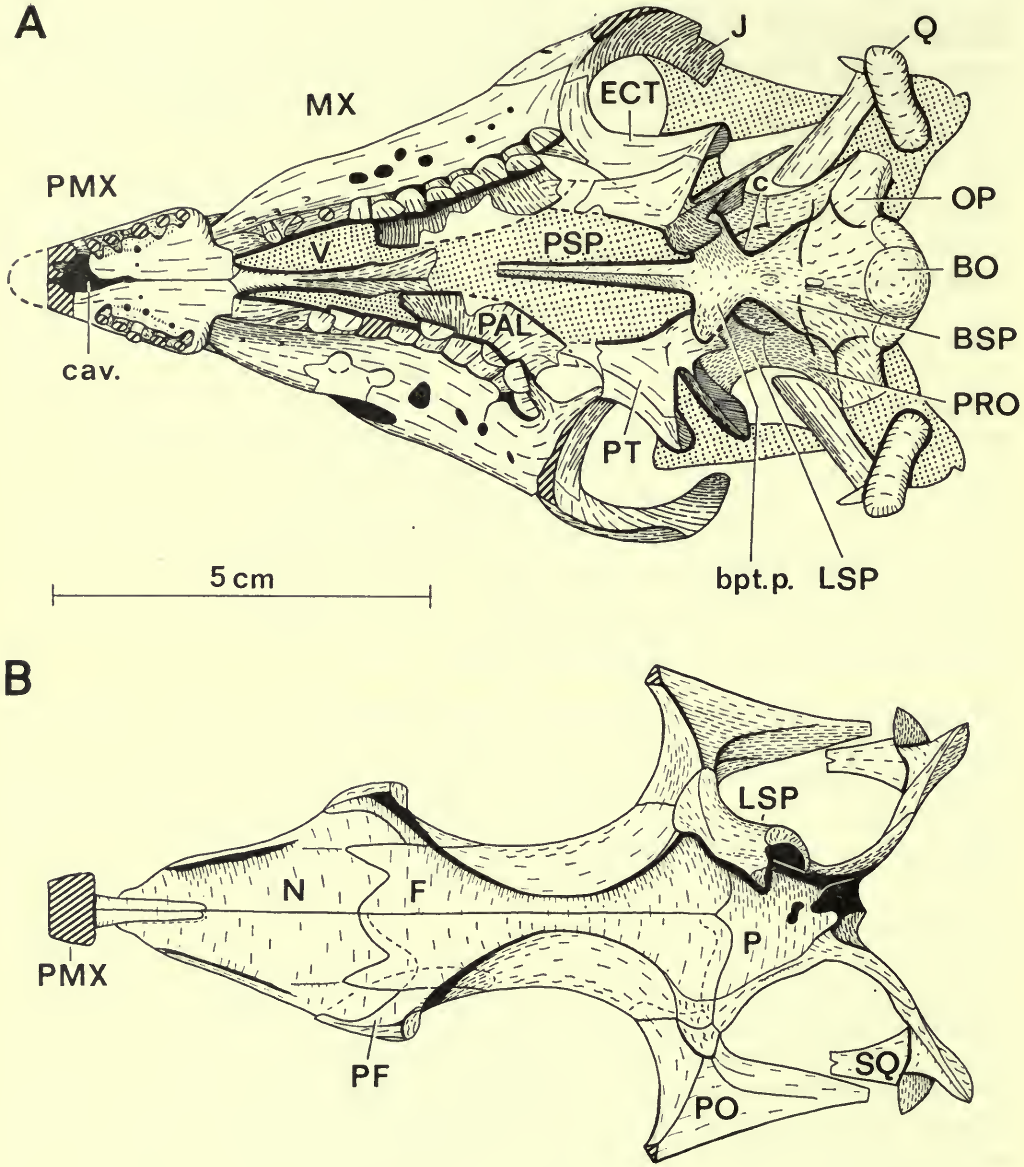
A
J
Q
MX
ECT
PMX
c
OP
V
PSP
BO
PAL
BSP
cav.
PRO
PT
bpt.p.
LSP
5 cm
B
LSP
N
F
PMX
P
PF
SQ
PO

Fig. 6. *Hypsilophodon foxii.* Skull R2477, × 1. A, palatal view, compare with Pl. 1, fig. 2; B, ventral view of the skull roof. Abbreviations: c, foramen for internal carotid artery; cav., cavity in the premaxillae; bpt. p., basipterygoid process. For other abbreviations see page 21.

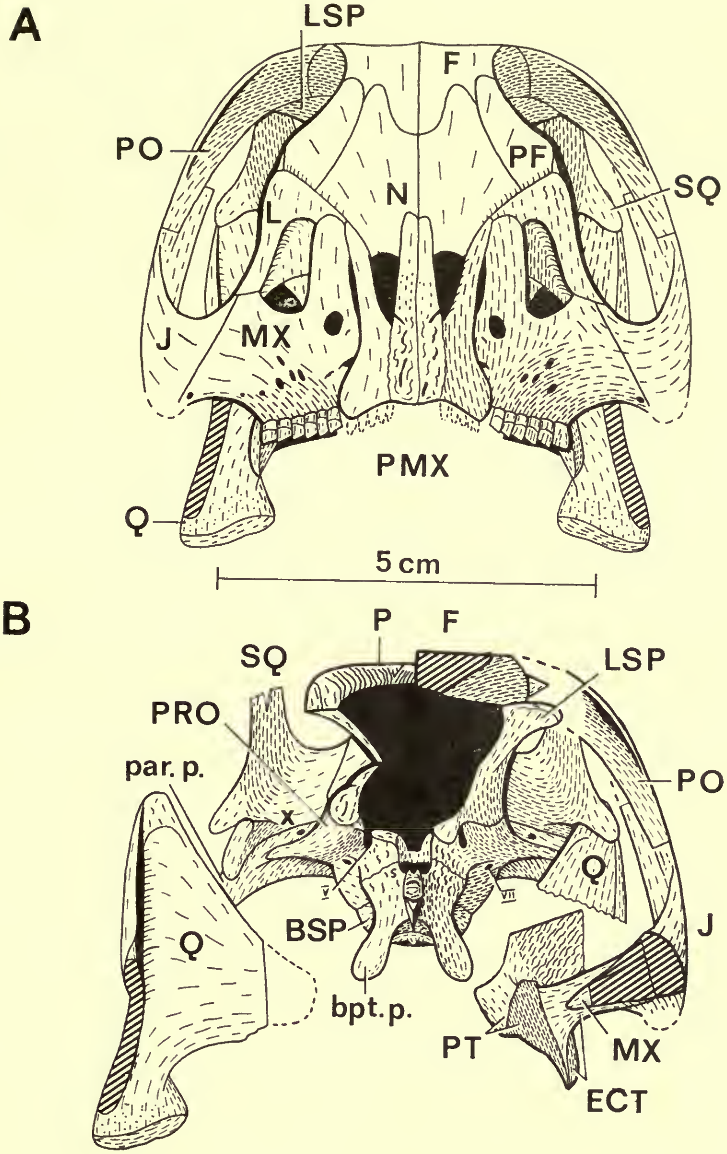
A
LSP
F
PO
PF
SQ
N
L
J
MX
PMX
Q
5 cm
B
P
F
SQ
LSP
PRO
par. p.
PO
x
Q
s
V
VII
J
BSP
Q
bpt. p.
PT
MX
ECT

FIG. 7. *Hypsilophodon foxii*. Skull R2477, × 1. A, anterior view; B, anterior view with skull sectioned through the middle of the orbits with the frontal, orbital and palatal bones of the right side removed and the quadrate displaced. Paroccipital process restored from R194. Abbreviations: bpt. p., basipterygoid process; par. p., paroccipital process; s, sella turcica; x, remnant of post-temporal fenestra; V, trigeminal foramen; VII, facial foramen. For other abbreviations see page 21.

The ventral surface (Text-fig. 6A) is transversely concave with five marginal thecodont teeth, each with a foramen medial to it. In R5830 and R8367 the median surface of the tapering ventral sheet and of the anterior process form one continuous flat sutural surface for the other premaxilla. In R197 and R2477 (Text-fig. 4B) these two surfaces are separated by a large depression which communicates with the exterior ventrally (Text-fig. 6A). Above the tapering ventral sheet there is a large channel which tapers in the opposite direction (Text-fig. 5A) with longitudinal ridges. This channel receives the anterior process of the maxilla and also the median vomer more postero-ventrally (Text-figs. 4B, 5C). Above this channel the surface is slightly concave. In R2477 the dorsal part of the posterior process sutures medially with a flange on the nasal (Text-figs. 4A, B). The sutural union is delimited by a slight edge which then curves antero-ventrally. In R197 the posterior process contacts the maxilla all along its posterior border (Text-fig. 2A).

Maxilla (MX). The maxilla consists of a thick rod with ten or eleven tooth-sockets (Swinton 1936, fig. 1). On the medial surface (Text-fig. 5A) there is a longitudinal ridge, convex transversely, which is continued anteriorly as a process. This process, triangular in cross-section, is slightly off-set from the rest of the ridge (Text-fig. 5C) and it bears strong sutural ridges. The two maxillary processes and that of the vomer fit tightly into a cavity enclosed by the premaxillae (Text-figs. 4B, 5A, C). The limit of overlap on the lateral surface is indicated by an edge that is a continuation of the sharp edge at the anterior end of the tooth row.

Above the main tooth-bearing region the maxilla consists of two thin fenestrated sheets which enclose the antorbital fossa (Text-figs. 4, 5, 60B, C). The lateral sheet arises from the side of the main body that it overhangs (Text-fig. 6A). This sheet has several foramina of varying size (Text-fig. 4A) while, more dorsally, it forms the anterior and ventral margins of the antorbital fenestra. The medial sheet forms a thin dorsal edge to the main body immediately above the roots of the teeth. This sheet has a much shallower vertical curve than the lateral sheet that it joins in the middle of the antero-dorsal part (in front of the antorbital fenestra, Text-fig. 5A). The more dorsal part of the medial sheet is overlapped by the thin sheet of the lachrymal (Text-fig. 5A) with which it forms the medial wall of the antorbital fenestra (Text-fig. 4A) and fossa. There is a large fenestra anteriorly in the medial sheet of the maxilla, while posteriorly, where it tapers to nothing, it borders another large fenestra with the lachrymal (Text-fig. 5A). The posterior margin of the latter is formed partly by the palatine bar and possibly also by the maxilla below. Posterior to this bar the antorbital fossa opens dorsally and posteriorly (Text-fig. 5) with the sides, especially medially, becoming progressively shallower (Text-fig. 5A). The medial wall of this part is formed by the main body of the maxilla with the thin lateral sheet curving dorso-laterally. The jugal forms an inwardly projecting ledge which roofs the more lateral parts of the fossa (Text-figs. 5B, C). The posterior end of the maxilla is sharp-edged and straight, making an angle of about 45 degrees with the vertical.

In R2477 the lateral sheet contacts the premaxilla only dorsally (Text-fig. 4A) and there is a narrow vacuity. The lateral sheet is extremely thin yet it has a perfect edge and it is the same on both sides. Consequently the thin anterior edge was not completely ossified in R2477 ; this, however, must be an individual variation because in R197 the lateral sheet is proportionately larger with an extra foramen and is completely overlapped by the premaxilla (Text-fig. 2). The lachrymal overlaps the medial surface of the medial sheet while posteriorly it contacts the thin edge of the lateral sheet in R2477 (Text-fig. 4A), though not in R197 (Text-fig. 2A). Ventral to the bridging bar of the palatine there is part of the medial sheet of the maxilla which probably also touched the lachrymal. The main body of the palatine is sutured diagonally on to the medial surface of the maxilla (Text-figs. 4B, 5A, C) with fine parallel suture ridges postero-ventrally but the surface is more irregular antero-posteriorly near the bar. The lateral sheet of the maxilla forms an overlapping suture with the jugal in R2477 (Text-fig. 4A) but in R197 (Text-fig. 2A) only the edge fits against the jugal more anteriorly. The jugal also sutures to the lateral part of the wedge-shaped posterior end of the maxilla which, with the medially directed process it bears (Text-fig. 5B), fits into a groove in the ectopterygoid.

Nasal (N). The nasals are rather thin and one slightly overlaps the other. The lateral margin of the nasal is turned downwards anteriorly to form a vertical sheet, the lower part of which is overlapped by the posterior process of the premaxilla. The tapering posterior part of the nasal overlaps the frontal while more laterally it is overlapped to a progressively greater extent by the prefrontal (Text-figs. 5B, 6B). This is greatest near the lateral edge where the prefrontal fits into a groove in the side of the nasal. This groove continues on to the latero-ventral edge of the nasal where it receives the lachrymal.

Parietal (P). In dorsal view (Text-fig. 5B) the anterior part of the single parietal is flat but the sides are obliquely concave and transversely constricted with a thin median edge. In anterior or posterior view (Text-fig. 8) there are two postero-lateral wings which are twisted along their long axis ; the axis is somewhat obliquely inclined. In ventral view the parietal is laterally convex and transversely concave, with the sides becoming progressively steeper more posteriorly (Text-fig. 6B).

The parietal overlaps the frontals anteriorly ; the slightly concave suture surface bears strong ridges which become weaker laterally (Text-fig. 7B). The median process of the parietal fits between the frontals and is itself overlapped slightly (Text-figs. 5A, 6B). The antero-lateral corner forms a vertical facet with strong sutural ridges for the postorbital (Text-fig. 4B). The anterior part of the ventral edge is flat, then grooved (the laterosphenoid fitted against this region) while more posteriorly this edge is sharp (Text-fig. 6B). The parietal enclosed the dorsal part of the supraoccipital (Text-fig. 5A).

Frontal (F). The frontals are elongate and form most of the dorsal margin of the orbits. In dorsal view (Text-fig. 5B) the central part of each bone is slightly concave transversely. The orbital rim, which bears well-developed insertion markings, is quite thin because the ventral surface above the orbits is obliquely concave (Text-fig. A4) ; the plane of the orbital circle makes an angle of about 45 degrees with the mid-line (Text-fig. 7B). This obliquely concave surface forms a very prominent and sharp-edged ridge ventrally (Text-fig. 6B) where it meets another concave surface,

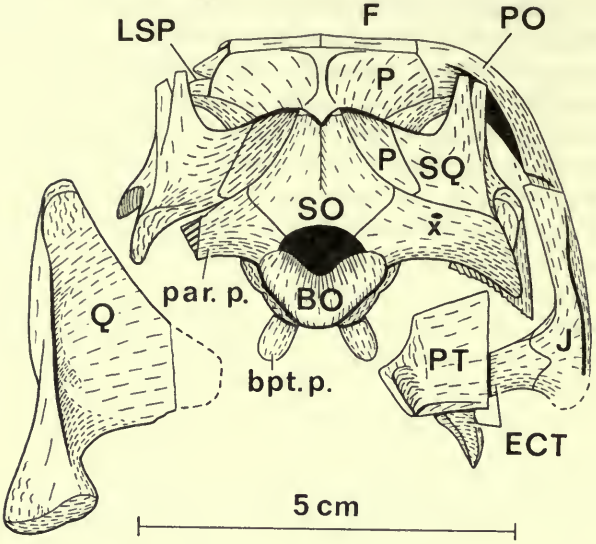

FIG. 8. *Hypsilophodon foxii.* Skull R2477, × 1. Abbreviations: bpt. p., basipterygoid process; par. p., paroccipital process; x, remnant of post-temporal fenestra. For other abbreviations see page 21.

the 'transverse' plane of which varies so that the curve is always perpendicular to that of the orbital surface. This medial curved surface is more strongly concave anteriorly.

The sutural markings on the thin anterior part of the edge between the frontals are very slight but on the thick central part they are well developed, consisting of a cone-within-cone pattern (Text-fig. 5A). On the thinner posterior part they are deeper, more vertical but less regular. The frontals are sutured to the parietal, the prefrontals and the squamosals. Postero-laterally on the ventral surface there is a slight depression which, together with the larger one on the postorbital, receives the head of the laterosphenoid (Text-fig. 6B). The postorbital itself sutures on to a well-developed spike (Text-fig. 7B) of the frontal.

Jugal (J). The outer orbital edge of the jugal is gently rounded and medial to this the jugal floors the ventral part of the orbit (Text-fig. 5B). Anteriorly this floor is obliquely inclined, facing medially and somewhat postero-dorsally but posteriorly the plane shifts until it faces anteriorly (Text-fig. 7A). The inner edge of this orbital floor is rounded anteriorly but becomes very thin and sharp-edged more postero-dorsally (Text-fig. 4B). The remainder of the jugal is an extremely thin sheet of bone. Anteriorly the jugal fits against the ventral edge of the thick part of the lachrymal. The sutural relationships with the maxilla and lachrymal vary in R197 (Text-fig. 2A) and R2477 (Text-fig. 4A). Posteriorly the jugal forms an 'M'-shaped suture with the pointed ends of the maxilla and ectopterygoid (Text-fig. 6A). The postero-dorsal part of the jugal has an overlapping suture with the tapering end of the postorbital (Text-fig. 4A). The thin part of the jugal overlaps the quadratojugal (Text-fig. 2A).

Quadratojugal (QJ). The sheet-like quadratojugal is perforated by a relatively large foramen (Text-fig. 2A). The edge of this foramen and the ventral edge of the bone are rounded while the dorsal and posterior edges are thinner and sharp. The anterior edge is hidden by the overlapping jugal. Postero-dorsally the quadratojugal is overlapped by the quadrate but more ventrally the position is reversed, with the quadratojugal extending nearly to the mandibular condyle (Text-figs. 3, 4A).

Quadrate (Q). From its rounded condylar region the main body of the quadrate rises, twisting through 45 degrees, to form a head (Text-fig. 4A). This head, triangular in cross-section, inserts in a socket in the squamosal ; its anterior (Text-fig. 7B) and inner (Text-fig. 5A) surfaces are covered with markings of ligamentous insertions. The main body of the quadrate and its pterygoid flange, set at about 70 degrees to one another, form the outer (Text-fig. 3) and the posterior (Text-fig. 7A) borders respectively of the lower temporal vacuity. The anterior and posterior edges of the main body of the quadrate are thin and sharp but its shaft is thicker and more rounded. For most of its height the pterygoid flange arises from the middle of the main body but dorsally its origin migrates backwards and takes part in the formation of the dorsal head of the quadrate (Text-figs. 5A, 8). A process of the squamosal fits between these two sheets of the quadrate in this region. The junction region between these two sheets is laterally concave along most of its length posteriorly (Text-fig. 8) and also anteriorly (Text-fig. 7B), but here the angle is more acute. The antero-medial face of the shaft is slightly concave dorso-ventrally (Text-fig. 7B) with well-developed pore markings.

There is very extensive overlap between the pterygoid flange and the alar process of the pterygoid. Neither of these two sheets is complete, but the shape of the missing parts of each is outlined on the more basal parts of the other. The quadratojugal has an overlapping suture with the lateral sheet of the quadrate and the limits of the suture are marked by an edge (Text-figs. 3, 4A).

Squamosal (SQ). This bone forms the postero-dorsal corner of the skull (Text-fig. 3), the lateral part of the occipital crest (Text-fig. 5B) and the posterior portion of the upper temporal bar. It is a roughly quadriradiate bone with rather unequally developed processes. The external surface (Text-fig. 4A) at the junction of the two larger processes, which are anteriorly and medially directed, is strongly convex while the inner surface (Text-fig. 7B) is concave forming the latero-posterior wall of the supratemporal fossa. Ventro-laterally there are two smaller processes which border the deep socket for the head of the quadrate. The posterior process forms a continuous sheet with the medial process and in posterior view (Text-fig. 8) the surface passing laterally is basically gently convex and then concave but dorsally above the socket there is a strongly convex part. In lateral view (Text-fig. 4A) there is an edge joining the lateral edge of the anterior process to the posterior edge of the posterior process (Text-fig. 5B). In ventral view (Text-fig. 6B), the large anterior concave area and the socket are separated by a wide bridge of bone, which shortly tapers as it passes antero-laterally and the surface of which is concave in this direction. The edges of the bone are thin and sharp. The medial process overlaps the

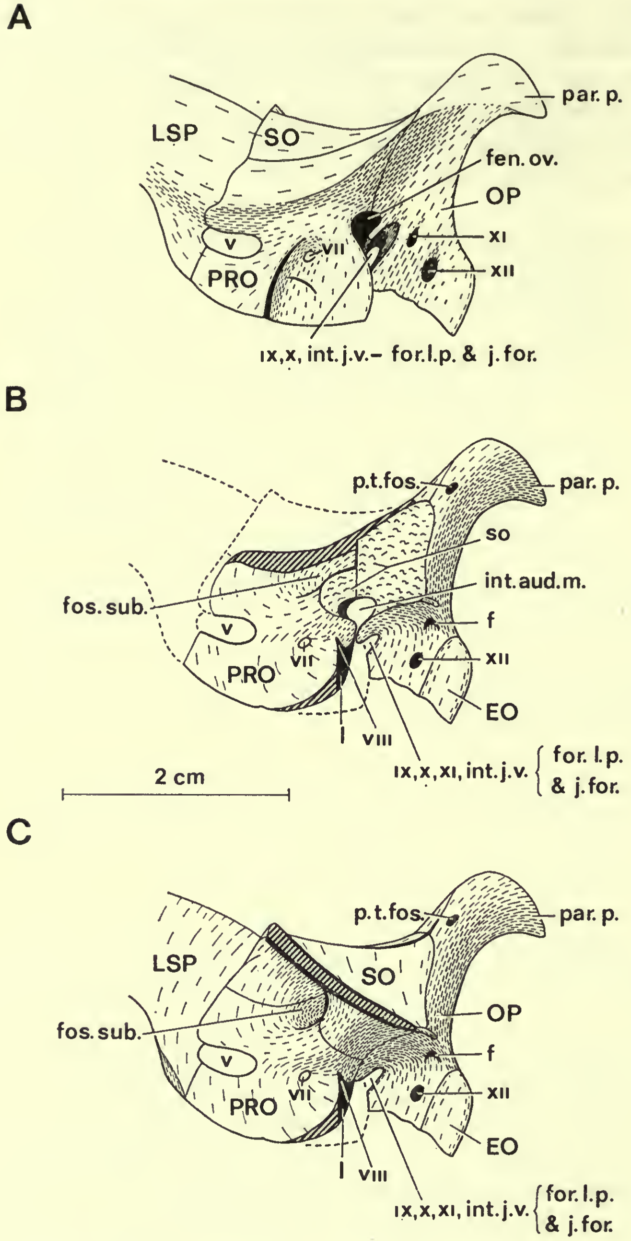
A
LSP
SO
par. p.
fen. ov.
OP
XI
XII
V
VII
PRO
IX,X, int.j.v.– for.l.p. & j.for.
B
p.t.fos.
par. p.
SO
int.aud.m.
fos. sub.
f
V
VII
XII
PRO
EO
l
VIII
IX,X,XI, int.j.v. { for. l.p. & j.for.
2 cm
C
p.t.fos.
par. p.
LSP
SO
OP
fos. sub.
f
V
VII
XII
PRO
EO
l
VIII
IX,X,XI, int.j.v. { for. l.p. & j.for.

Fig. 9. *Hypsilophodon foxii.* Side-wall of braincase, composite : EO, exoccipital R8367 ; LSP, laterosphenoid R2477 ; OP, opisthotic R194, R2477 ; SO, supraoccipital R8366. × 1·5 for R2477. A, ventro-lateral view ; B, dorso-medial view with supraoccipital removed. C, as B but with supraoccipital sectioned. Abbreviations : f., foramen ; fen. ov., fenestra ovalis ; for. l. p., foramen lacerum posterius ; fos. sub., fossa subarcuata ; int. aud. m., internal auditory meatus ; int. j. v., internal jugular vein ; j. for., jugular foramen ; l., lagenar recess ; par. p., paroccipital process ; p.t. f., remnant of post-temporal fenestra ; so., surface for supraoccipital ; foramina for cranial nerves in Roman numerals, other abbreviations see Fig. 60

parietal anteriorly. The ventral edge of this process is sutured to the opisthotic while the posterior process is overlapped by the paroccipital process (Text-figs. 7B, 8). The anterior process is overlapped laterally by the posterior process of the postorbital.

Lachrymal (L). The main part forms the dorsal border of the antorbital fenestra while the medial sheet forms an inner wall (Text-fig. 3). In lateral view (Text-fig. 3) the main part is gently convex transversely and longitudinally. Ventrally it is hollowed out to form a thin and sharp edge which overhaps the base of the medial sheet. The plane of this sheet is at an angle to that of the main part so that they are wider apart posteriorly. Here the lachrymal has a posterior surface (Text-fig. 5B) which forms part of the margin of the orbit. The lachrymal foramen is on this surface and its duct follows the curved dorsal margin of the lachrymal in the junction region (Text-figs. 60C, D). It opens at the pointed anterior end medial to the maxilla. The sutural relationship with the maxilla and jugal varies in R197 (Text-fig. 2A) and R2477 (Text-fig. 4A). The end of the palatine bar sutures to the medial edge of the lachrymal just anterior to the jugal (Text-fig. 5B). Dorsal to this there is a groove along the postero-medial edge of the lachrymal (Text-fig. 4B) in which there is still a small piece of bone. The original bone was a slender rod. The dorsal edge of the lachrymal is sutured to the prefrontal and nasal ; this edge has a groove to receive the prefrontal while more anteriorly its edge fits into a groove on the edge of the nasal.

Prefrontal (PF). This bone forms the edge of the orbit and consists of two tapering sheets ; the dorsal one (Text-fig. 5B) is gently convex antero-posteriorly while the lateral one is concave (Text-fig. 4A), obliquely inclined and slightly twisted along its longitudinal axis. The medial surface (Text-fig. 5A) is concave but more gently angled and the long edges are sharp. The prefrontal overlaps both the nasal and the frontal (Text-figs. 5B, 6B). The anterior edge fits into a groove on the dorsal edge of the lachrymal. The lateral corner of the bone is thick with well-developed suture pits and ridges for the supraorbital.

Supraorbital (SOB). The supraorbital is preserved in the right orbit of R197 (Text-fig. 2B) and there is one from R194 (see Text-fig. 3). The shaft of the bone is curved and tapers, with an oval cross-section and sharp edges, and is slightly twisted along its longitudinal axis. Anteriorly there is a dorso-medial flange that is also present in R197 but there is no sutural area corresponding to it on the prefrontal of R2477. There is a transversely concave area on the outside of the flange with a slight ridge on the shaft. The dorso-lateral surface and the posterior part of the inner surface are covered with fine surface markings. More proximally it is smooth but with several slight ridges running diagonally across the shaft.

Postorbital (PO). This is a triradiate, sharp-edged bone forming the posterior wall of the orbit and the anterior part of the upper temporal bar. The outer surface is flat antero-posteriorly and curved transversely (Text-fig. 7B). The slender and tapering posterior and ventral processes (Text-fig. 5B) are in the same plane. The posterior process is thinner than the ventral, which latter has a medial ridge and is triangular in cross-section (Text-fig. 6B). This ridge becomes thicker dorsally where it forms the ventral part of the medial process (Text-fig. 6B). The medial process is short but stout with a dorsal ridge (Text-fig. 5B) which links a similar ridge on the parietal to the dorsal edge of the posterior process. The surface behind this edge is slightly concave and is continuous with the ventral surface with which it forms a twisted plane (Text-figs. 5B, 6B).

There is a very strong union between the medial process of the postorbital and the adjacent bones. Ventrally the thick medial process has two large cavities, one lateral and ventral to the other, which are partly separated by a thin dividing wall. The dorso-medial cavity is for the large spike on the corner of the frontal (Text-fig. 7B). This spike is bounded on all sides, though to a lesser extent ventrally, by the postorbital which also overlaps the frontal with a small anterior flange (Text-figs. 5B, 6B). The roof of the ventro-lateral cavity forms an oval depression (Text-fig. 6B) with the adjacent surface of the frontal. This depression, the side-walls of which become deeper as they pass laterally, is for the large head of the laterosphenoid (Text-fig. 7A). Posteriorly there is a small sutural surface for the parietal. The tapering end of the posterior process overlaps the anterior process of the squamosal while the ventral process overlaps the jugal (Text-figs. 3, 4A).

Pterygoid (PT). The triradiate pterygoid has long and thin alar processes to the adjacent bones. Those for the palatine and ectopterygoid form a sheet (Text-fig. 6A) which is slightly concave antero-posteriorly. Approximately perpendicular to this sheet, to which it is linked by a thickened connecting region, is the very broad alar process for the quadrate (Text-figs. 4B, 6A). In medial view (Text-fig. 4B) the quadrate process is concave dorso-ventrally apart from the obliquely convex antero-dorsal corner. Ventrally there is a concave border delimited by an edge that runs parallel to the ventral margin. The anterior part is thicker, covered with insertion markings and has a centrally situated depression. This depression with the adjacent small process receives the basipterygoid process of the basisphenoid (Text-figs. 5C, 6A). The lateral surface of the quadrate process has a well-defined sutural area (Text-fig. 4A) for the quadrate.

In ventral view (Text-fig. 6A) there is a well-defined corner on the centre of the connecting region. The anterior edge of the connecting region is sharp but becomes rounded at the base of the quadrate process (Text-fig. 7B). The anterior part of the palatine process is missing but the part of the palatine that was overlapped is visible (Text-fig. 6A). The pterygoid overlaps the ectopterygoid ventrally with a broad process which tapers to a point.

Ectopterygoid (ECT). The main part consists of a bar, triangular in cross-section, which forms two equal halves at right angles to each other (Text-figs. 5C, 6A, 7B) plus a medial flange (Text-fig. 5C). The dorsal ridge on the anterior half of the ectopterygoid is gently rounded with a convex surface in front of it (Text-fig. 5C). More medially and posteriorly this edge becomes thinner and sharper, with irregular bumps, and the surface medial to it is concave. In the central region this surface is large because it continues on to the medial flange (Text-fig. 5C). The other edges of the bone are thin and sharp. The lateral end of the ectopterygoid is strongly

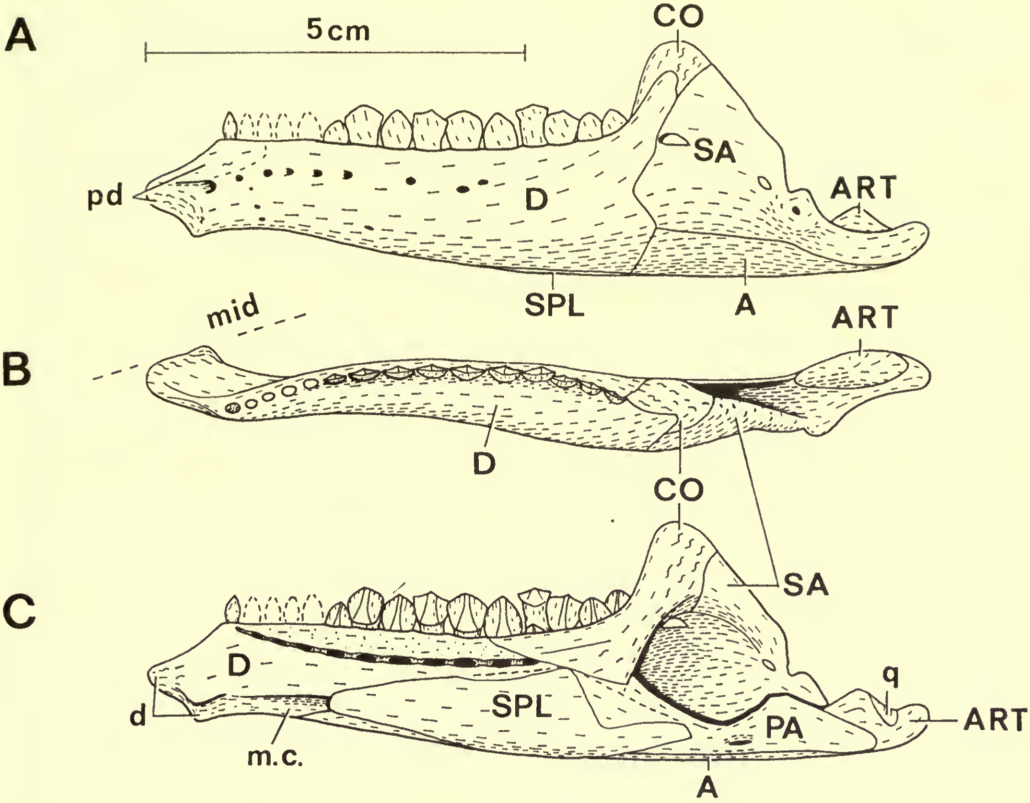

Fig. 10. *Hypsilophodon foxii*. Mandibular ramus, × 1 for R196 with details from R193, R197 and R2477. A, antero-lateral view; B, dorsal view; C, postero-medial view. Abbreviations: d., surface for dentary; m.c., Meckelian canal; mid, midline; pd, surface for predentary; q, surface for quadrate. For other abbreviations see page 21.

sutured to the jugal (Text-figs. 4B, 5, 6A, 8). The antero-ventral surface of the anterior half of the bone is excavated to form a deep groove for the sharp posterior edge of the maxilla (Text-figs. 5, 6A, 7B). The medial flange of the ectopterygoid is sunk into the dorsal surfaces of the pterygoid (Text-fig. 5C).

Palatine (PAL). The palatine consists of a broad base, sutured to the medial surface of the maxilla (Text-figs. 4B, 5A, C), and bears a thin alar process from approximately along the middle and perpendicular to the base (Text-figs. 5A, C). Dorsally and ventrally the surface of the palatine is continuous with the adjacent surface of the maxilla (Text-figs. 5C, 6A). Anteriorly the palatine is much thicker and set at about 70 degrees to the maxilla. The lateral end of this thick part of the palatine forms a bar, triangular in cross-section, which bridges the antorbital fossa to suture with the medial surface of the lachrymal (Text-figs. 5B, 5C). The dorsal surface (Text-fig. 5C) in slightly convex longitudinally and slightly concave transversely, with this

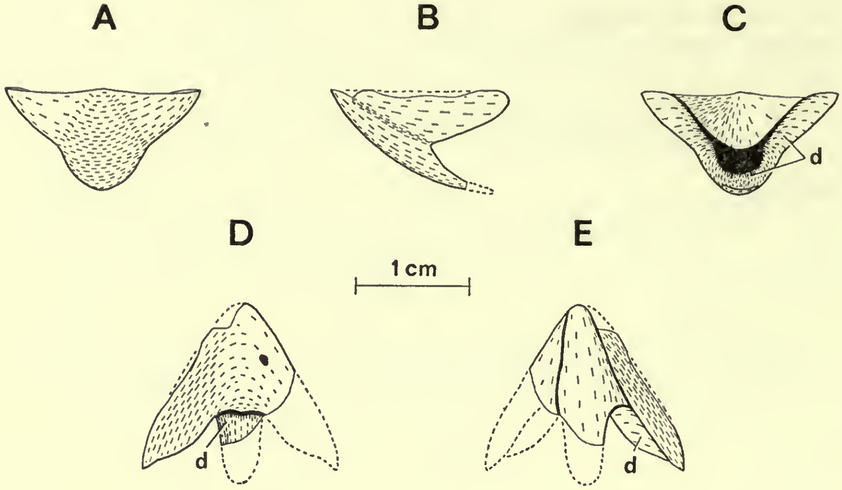

FIG. 11. *Hypsilophodon foxii.* Predentary R2470, × 1·5. A, anterior view; B, lateral view; C, posterior view; D, dorsal view; E, ventral view. Abbreviation: d, surface for dentary.

curve becoming stronger on the posterior part of the bone where the alar process is slightly convex (Text-fig. 4B). The thick anterior edge forms a surface, tapering medially, which is convex dorso-ventrally and straight transversely except for the medial part which is concave (Text-fig. 5C). In medial view (Text-fig. 4B) the bone is gently convex with a concave region where it joins the alar process. The curve continues on to the thicker anterior part of the process. Posteriorly the alar process overlapped the pterygoid. This sutural surface is bordered laterally by a thickened edge (Text-fig. 6A). The anterior end was probably sutured to the vomer. However, there is no definite sutural surface on the anterior part of the palatine which, like the posterior part of the vomer, is damaged and incomplete.

Vomer (V). The tapering head of this median bone is triangular in cross-section and fits between the maxillae (Text-fig. 6A). Ventrally the head sutured to the floor of the premaxillae and the posterior limit of this suture is marked by a step (Text-fig. 6A). Slightly behind the head there is a dorsal groove that was for the median cartilaginous septum. The groove becomes deeper as it passes posteriorly so that the rest of the vomer consists of two thin sheets separated dorsally and curving out laterally (Text-figs. 5C, 6A). Laterally there is a longitudinal ledge (Text-fig. 4B), the dorsal surface of which is convex dorso-ventrally while the ventral surface is concave. This ledge was probably for the anterior part of the palatine. Ventral to this ridge in R194 there is a foramen, the ventral margin of which has been lost in R2477 (Text-fig. 4B).

The lower jaw consists of seven bones and the two rami are linked anteriorly by the median predentary. Only one *predentary* (PD) is known (Text-fig. 11) and this was preserved next to the dentary (see Nopcsa 1905, fig. 3). The dorsal surface

(Text-fig. 11D) is gently concave transversely while postero-medially the surface is convex antero-posteriorly. The dorsal edge is sharp. The sides are gently convex with a groove running diagonally back from the anterior end (Text-fig. 11B). The paired lateral processes overlap the adjacent lateral surface of the dentaries (Text-figs. 3, 10A). Passing medially each process overlaps the dorsal edge of the dentary to a progressively greater extent so that the anterior tip fits into a groove on the posterior surface of the predentary (Text-fig. 11C). The symphysial region is also overlapped by the ventral process of the predentary ; the process is thin and transversely curved (Text-figs. 11D, E).

Dentary (D). In lateral view (Text-fig. 10A) the spout-like anterior end of the dentary is longitudinally convex but the rest of the bone is concave, the surface sweeping gently postero-laterally. The corresponding curves on the medial surface (Text-fig. 10C) are concave and then convex. The two rami diverge posteriorly, each becoming progressively deeper and thicker, the additional thickness being lateral to the tooth row (Text-fig. 10B). The transverse curve of the lateral surface becomes more convex posteriorly while, apart from the ventral Meckelian canal, all the medial surface (Text-fig. 10C) is gently convex. This canal ends just behind the symphysis and is deeper posteriorly, with the dorsal part enclosed by an edge from the dentary. The splenial covered most of this canal ; the canal carried the mandibular artery and vein plus the palatine ramus of the trigeminal nerve as in modern lizards (Romer 1956). About half-way along the dentary the canal opens into the adductor fossa, which greatly increases in depth (Text-fig. 12) and width posteriorly. Close to the symphysis the ventral edge is sharp ; the rest is rounded. There are several foramina along the lateral surface of the dentary which may have transmitted nerves and nutrient blood vessels to the lips. The most anterior and largest of these foramina probably represents the mental foramina through which a branch of the fifth nerve emerged (Gilmore 1909).

Anteriorly the two dentaries meet at a median and somewhat obliquely inclining contact surface (Text-figs. 10B, C). The splenial and coronoid overlap the dentary medially (Text-fig. 10C). The part of the dentary overlapping the angular and surangular (Text-fig. 10C) is thin but the part touching the coronoid is thick with strong sutural markings.

Splenial (SPL). This is thin and was applied to the inner surface of the mandibular ramus (Text-fig. 10C). It is gently convex longitudinally and more strongly so transversely, especially the ventral part that wraps round the ventral edge of the ramus and is visible in lateral view (Text-fig. 10A). This ventral edge is thick and rounded ; the other edges are thin and sharp.

Angular (A). This is thin and tapering (Text-fig. 10A) and the ventral part is transversely convex. Dorsally it overlaps the surangular (Text-fig. 10A) while ventromedially it overlaps the prearticular and part of the articular and is itself overlapped by the splenial (Text-fig. 10C).

Surangular (SA). This is thin and in lateral view (Text-fig. 10A) is transversely convex ; longitudinally the dorsal part is gently convex, the ventral part gently

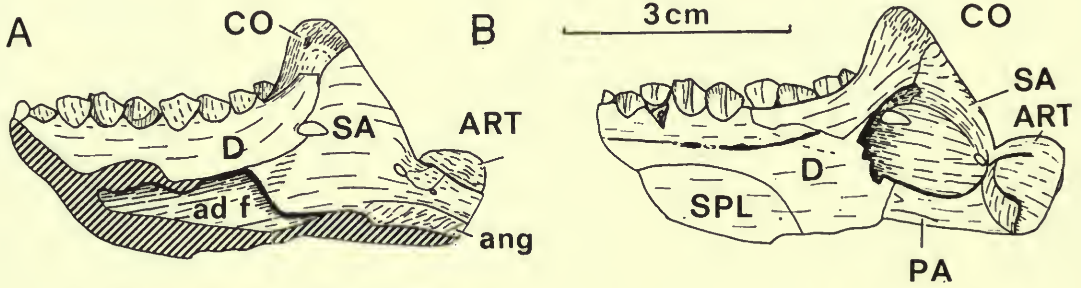
A
CO
SA
D
ART
ad f
ang
B
3cm
CO
SA
ART
D
SPL
PA

FIG. 12. *Hypsilophodon foxii.* Mandibular ramus R2477, × 1. A, lateral view; B, medial view. Abbreviations; ad. f., adductor or supramandibular fossa; ang., surface for angular. For other abbreviations see page 21.

concave. There are three foramina through the bone, two smaller ones posteriorly and one large one anteriorly, which were probably for the cutaneous branches of the inferior alveolar nerve as in modern lizards (Oelrich 1956). The most dorsal part of the anterior edge fits into a groove in the coronoid. The dorsal edge is thick, especially close to the coronoid. This edge also forms a well-developed boss just in front of the articular. The part overlapping the articular is thick and roughly oval in cross-section with a rounded dorsal edge.

Prearticular (PA). This is flat, tapers posteriorly and overlaps the dentary and is itself overlapped by the splenial and the coronoid (Text-fig. 10C). The ventral edge is overlapped by the angular. The prearticular then widens out again. The posterior part consists of two transversely convex curves separated by a thin slit (Text-fig. 10C) through which the chorda tympani branch of the seventh nerve probably passed as in other reptiles (Romer 1956). More posteriorly the bone becomes transversely convex and then flat and overlaps the articular.

Articular (ART). The articular is roughly triangular in lateral view with one apex dorsal in position (Text-fig. 10A). The rounded anterior edge is thin but the rest of the bone is much thicker. The ventral edge forms a flat surface while the posterior edge, which is concave in lateral view (Text-fig. 10A), is gently convex transversely and formed the articular surface for the quadrate. The articular is overlapped laterally by the surangular, ventrally by the angular and medially by the prearticular.

ii) TEETH AND TOOTH REPLACEMENT

Dental formula. There are five teeth on each premaxilla (Text-figs. 2, 4). The number of maxillary teeth is ten (Text-fig. 6A, left side) or eleven (R197, R2477, Text-fig. 6A and R5862, Swinton 1936, fig. 1). The predentary is toothless and the number of teeth borne by the dentary is not certain as the dentaries of R197 and R2477 are incomplete anteriorly. In R8366 the anterior part of the dentary is preserved and this bears four smaller alveoli at the front. In R2470 the roots of teeth are preserved in these four smaller alveoli. In R196 (Text-fig. 10) the complete dentary is preserved but it is slightly damaged and some of the teeth are missing ; the most anterior of the smaller teeth is preserved and, assuming that there were three more, the original count would have been 14. In the large individual R192, the anterior part of the jaw is missing but there are 13 teeth of which only the most anterior is small. A complete dentary is needed to show the number of teeth but there were certainly more than on the maxilla, not less as believed by Hulke (1882) and Parks (1926).

Premaxillary teeth. The five premaxillary teeth are preserved *in situ* on the left side of R197 (Text-fig. 2A). In the toothless premaxilla R8367 the sockets for the teeth are visible and these closely resemble those of the maxilla as figured by Swinton (1936, fig. 1). A loose tooth is figured by Hulke (1882, pl. 72, figs. 3–4) and one from R196 in Text-fig. 13. The root is separated from the head by a slight constriction and is circular in cross-section. The root is open with a large pulp cavity which extends into the crown (Hulke 1882). The crown is slightly compressed laterally

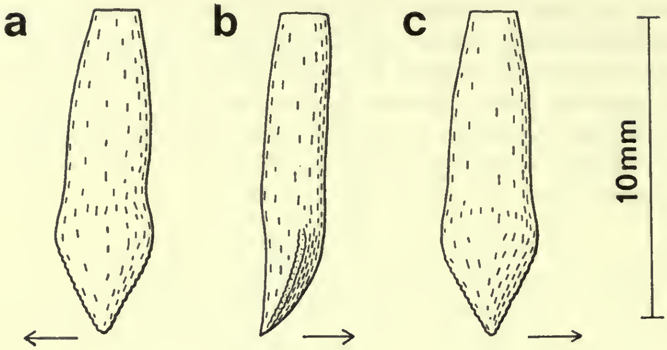

FIG. 13. *Hypsilophodon foxii.* Predentary tooth R196, × 4. a, lateral view; b, anterior view; c, medial view. Arrow in text-figs. 13 to 16 points anteriorly or laterally depending on the view.

with the outer surface of its cross-section less convex than the inner. The pointed crown has sharp edges anteriorly and posteriorly which bear a series of fine serrations. On the medial surface (Text-fig. 13c) there is a slight depression running diagonally towards the tip on each side. Both surfaces are smooth – that of the root is rather matt while that of the crown is very shiny and obviously thickly enamelled on both sides (visible in section of R2472). There are several minute striae on both sides of the crown.

Maxillary and dentary teeth. These are preserved in skulls (Text-figs. 2, 6A, 12) and loose teeth were figured by Hulke (1873, pl. 18, figs. 4–6; 1882, pl. 72, figs. 5–9), Swinton (1936, figs. 2–3) and in Text-figs. 14–16. The crowns of both types are laterally compressed and wider than the root, which is cylindrical and tapering. One side of the crown (the lateral side of the maxillary teeth and the medial side of the dentary teeth) is covered with a thick layer of enamel and bears several longitudinal ridges. On the upper teeth these ridges are all weak but on the lower teeth the central ridge is extremely well developed. The other side of the tooth is smooth and shiny. Ground sections show that there is a thin layer of enamel on unworn teeth (R8419), as Swinton (*in* Sternberg 1940) suggested, and in worn teeth (R2472) as well. In the section of the unworn dentary tooth R8419, in which the width of the crown is 5·5 mm, the medial enamel layer at 0·1 mm is about five times as thick as the lateral layer. The thickly enamelled edge of the tooth was more resistant to wear and formed a sharp edge to the worn surface of the tooth. The obliquely inclined occlusal surface of some teeth is gently concave transversely and flat longitudinally.

Maxillary teeth in longitudinal section curve slightly medially (Text-fig. 14a). The root is about twice as long as the unworn crown. A depression runs along the anterior edge of about half of the root and continues a little way on to the crown (Text-fig. 14A). The crown of each tooth slightly overlaps the tooth behind and fits against this anterior depression. The boundary between the root and the crown is formed by a slight cingulum. The crown is laterally compressed and, apart from the

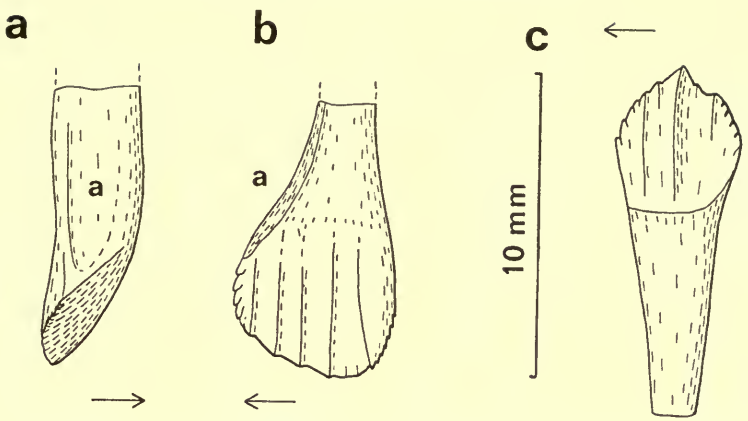

FIG. 14. *Hypsilophodon foxii.* Unworn maxillary tooth R8367, × 4. a, anterior view; b, lateral view; c, unworn dentary tooth right side R8367, × 4, lateral view. Abbreviation: a, depression for the more anterior tooth.

slight longitudinal ridges, the outer thickly enamelled surface is flat; the inner surface is very slightly concave longitudinally, gently convex transversely. In an unworn tooth the rounded apex is somewhat posterior to the centre of the crown. The number and degree of development of the longitudinal ridges on the enamelled lateral surface of the crown varies. There are usually three ridges which reach the cingulum: an obliquely inclined ridge on the antero-dorsal edge of the crown, another from the apex and a third close to the posterior edge of the crown. Extra ridges may be developed on the wider anterior part between the oblique ridge and the apex ridge. Up to three ridges may be present and may or may not reach the cingulum. The anterior edge bears several small crenellations and there are a few others between the apex and the posterior ridge. There are numerous faint longitudinal ridges on the thinly enamelled medial side.

Dentary teeth (Text-figs. 15, 16) are orientated in the reverse way to those of the maxilla. The ridged and thickly enamelled surface is medial, instead of lateral; the tooth curves laterally, instead of medially; more of the crown is posterior, instead of anterior to the apex and the oblique ridge is posterior instead of anterior. The cingula of dentary teeth are more strongly developed, the apices are more pointed and more central on the crowns. However, the striking difference is the prominent development of the apical ridges of the dentary teeth. The other longitudinal ridges are faint, resembling those of the maxillary teeth, but the apex ridge is very large and forms a well-developed 'spike' as the crown is worn. In large teeth there may be several fine longitudinal ridges on the lower half of the apex ridge. The degree of development of the anterior ridge varies and it may be practically absent. The number and lengths of the ridges developed between the apex and the posterior oblique ridge vary: there may be an anterior long one plus a short one, or just an anterior short one. The anterior and posterior edges both have numerous fine crenellations.

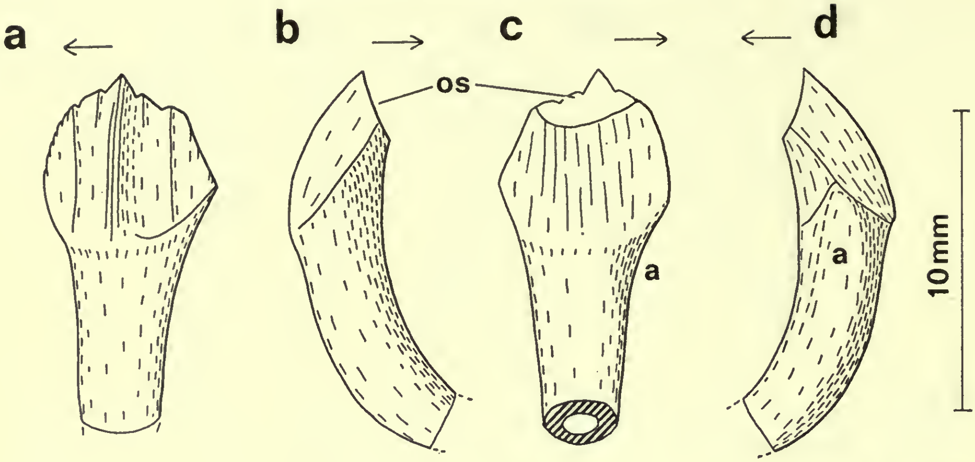

FIG. 15. *Hypsilophodon foxii.* Worn dentary tooth, right side, R8367, × 4. a, medial view ; b, posterior view ; c, lateral view ; d, anterior view. Abbreviations : a, depression for the more anterior tooth ; os, occlusal surface.

Special foramina and replacement teeth. On the medial surface of the maxilla above the tooth row there is a series of foramina connected by a shallow groove (Text-fig. 5A). Each foramen corresponds to a tooth position and is situated directly above it. The edges of the foramina are straight ventrally and gently concave dorsally. The bone surface between the foramina and the tooth row is pitted. The foramina open into the alveoli of the functional teeth. A comparable series is present on the dentary (Text-fig. 10C). In certain cases (maxilla of R5862 and R6372, dentary of R2477 and R8366) a replacement tooth is visible through a foramen.

Edmund (1957) discussed the function of the special foramina in ceratopsians and hadrosaurs. He concluded that these foramina were for the admission of parts of the dental lamina or for the admission of young replacement teeth produced by the lamina. Edmund (1957 : 13) noted that the foramina 'are not seen in primitive forms, are seen in some of the more advanced forms, and are best developed in forms with very high alveolar walls. This definitely points to their function as orifices for the admission of dental germinal material.' While not disputing Edmund's conclusion concerning the function of these foramina, it should be noted that they are well developed in *Hypsilophodon* (Text-figs. 5A, 10C), *Dysalotosaurus*, *Camptosaurus* and *Iguanodon* (see Galton in press). Their absence in other lower ornithopods is probably more apparent than real and reflects the state of preservation of the material. These foramina represent a *preadaptation* for the development of a dental battery consisting of vertical tooth series, because high alveolar walls can be developed (Galton in press). This potential was realized independently in two lines of ornithischians, the hadrosaurs and the ceratopsians.

In *Hypsilophodon* a small replacement tooth is preserved in the alveolus where it is closely applied to the medial surface of the functional tooth. At a later stage in

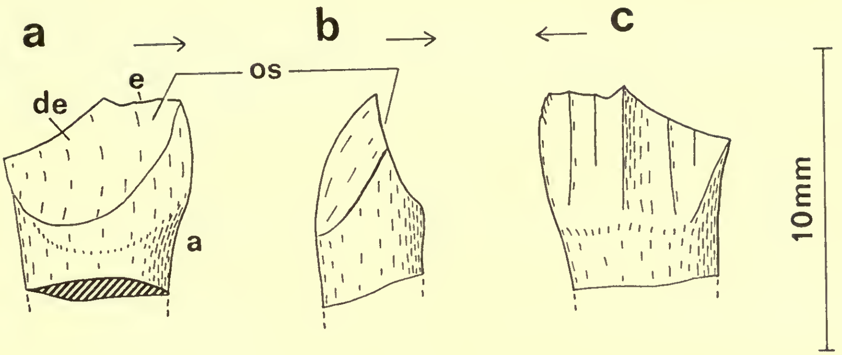

FIG. 16. *Hypsilophodon foxii.* Well-worn dentary tooth, right side, R8367, ×4. a, lateral view; b, posterior view; c, medial view. Abbreviations: a, depression for the more anterior tooth; de, dentine; e, enamel; os, occlusal surface.

its development the replacement tooth is more lateral in position because it is underneath the functional tooth. When this situation is visible, as in the dentary of specimens R192, R196 (Text-fig. 10C) and R2477 (Text-fig. 12B), the root of the functional tooth is much shorter than the original length of the crown. Resorption of the root must therefore have occurred because in an unworn tooth the root is about twice as long as the crown. A functional tooth in this condition was readily shed so that the replacement tooth could continue growing upwards into its position.

In the case of the premaxilla the bone medial to the tooth row is obliquely inclined (Text-fig. 5B) rather than vertical as in the maxilla and dentary. However, the situation is similar because the replacement tooth is close to the medial surface of the functional tooth and lateral, but also ventral, to the foramina. There are five premaxillae with teeth – 24 preserved in all – but only one case (R5830) preserves a non-functional replacement tooth in the alveolus.

Sequence of tooth replacement. In a study of tooth replacement in reptiles Edmund (1960) found that all the teeth with 'odd' numbers in a numbered tooth series are replaced in sequence, followed by all the 'evens'. The pattern of waves of tooth replacement in most cases pass anteriorly so that the teeth of each 'odd' or 'even' series erupt progressively from back to front. In *Hypsilophodon* this general pattern is discernible in the tooth rows of the premaxilla, maxilla and dentary. It is especially clear in the right maxilla of R2477 in which ten teeth (Text-fig. 6A) are well preserved. If the youngest tooth and the most worn tooth are designated as stages 1 and 6 respectively, then the stage of eruption of the remaining teeth can be assessed on this scale (Table IV). Apart from the first tooth, the teeth in the right maxilla clearly show that replacement is alternate, with replacement waves passing anteriorly. Both 'odd' and 'even' tooth series show two replacement waves – the junction of those of the 'odd' series is between tooth 3 and 5 and that of the 'even' teeth between 8 and 10. The first tooth is out of sequence as is also the case on the left maxilla (likewise the last tooth of the dentary); these teeth, however, are small and have no wear surfaces. The replacement sequence of the premaxillary teeth of R2477 is not apparent. In specimen R8367, however, where the functional teeth have been lost, there are replacement teeth in the medial part of sockets 1, 3 and 5 but not in 2 and 4, so here too the replacement appears to have been alternate.

TABLE IV

Stages of eruption of teeth at various positions along the jaw in R2477

Tooth position	1	2	3	4	5	6	7	8	9	10	11	12	13
a) Left maxilla	6	x	x	6	5	2	5·5	5	2	5·5	4·5	–	–
b) Right maxilla	1	3·5	5	4	2	5	3	6	5	2·5	–	–	–
c) Right dentary	x	x	x	x	5·5	2·5	6	3	2	5	2	6	1

iii) ACCESSORY ELEMENTS

Hyoid apparatus. In specimens R192 and R196 there are remains of a slender element preserved medial to the mandibular ramus. In R196 this element is gently curved along its length and transversely flattened – it is about 2·5–3·0 mm wide and more than 40 mm long, being broken at both ends. In R197 (Text-fig. 2C) the edges are more rounded while in R192 the small pieces that are preserved on both sides are definitely rod-like. These are regarded as the first ceratobranchial because this is the dominant and most highly ossified element of the hyoid apparatus in modern reptiles (see Ostrom 1961).

Sclerotic ring. Hulke (1873 : 523), when referring to an individual *in situ* in marl (remains as specimens R2466–76), noted that in the orbit there were 'several small osseous scales which [he] judged to be vestiges of a sclerotic ring'. Subsequently (1874, 1882) he figured the 'thin bony scales' of another specimen, R2477. Nopcsa (1905) reinterpreted this specimen correctly and showed that the sclerotic plates were the wear surfaces of the dentary teeth. He therefore concluded that there was no sclerotic ring in *Hypsilophodon.* Hulke's original observation (1873) on R2466–76, however, has been confirmed by the further preparation of the skull material. Further, a nearly complete sclerotic ring is preserved in one orbit of R2477 (Plate 1, fig. 3) with several plates in the other orbit. Plates are also preserved in R192 and R197 (Text-fig. 2B).

The presence of a sclerotic ring in *Hypsilophodon* is not surprising because it has been found in several dinosaurs (Edinger 1929, Ostrom 1961) and in *Parksosaurus* (Galton, in press, fig. 1). Where it can be determined, the sclerotic pattern of dinosaurs conforms to pattern A of Lemmrich (1931), with two positive plates and two negative plates. The ring is divided into four quadrants which are not necessarily equal in size. The positive plates are dorsal and ventral in position and overlap another plate at both ends. The negative plates are anterior and posterior in position and are overlapped by another plate at both ends. The sclerotic ring of *Corythosaurus* (see Ostrom 1961) and *Lambeosaurus* (see Russell 1940) consists of 14 plates while in *Anatosaurus* there are 13 plates (see Edinger 1929).

The sclerotic ring of *Hypsilophodon* consists of 15 plates (Text-fig. 17). The anterodorsal quadrant has been eliminated because the dorsal positive plate overlaps the

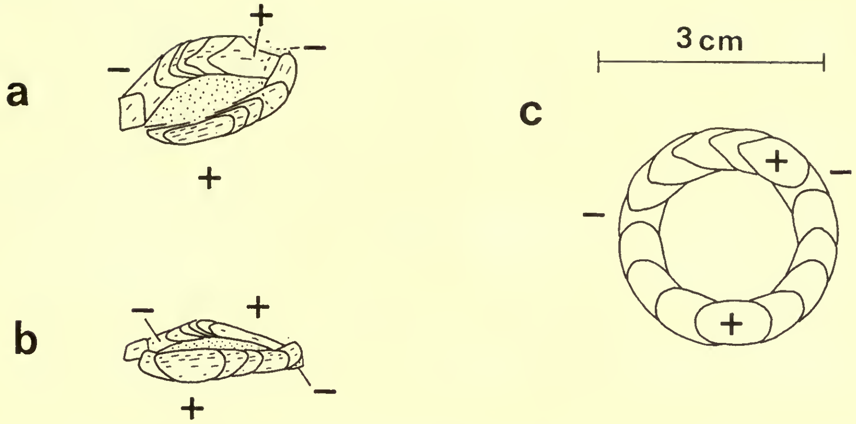

FIG. 17. *Hypsilophodon foxii.* Sclerotic ring R2477, × 1. a, lateral view ; b, ventral view ; c, reconstruction.

anterior negative plate with no intervening plates. Although not previously reported in dinosaurs this condition is known in several birds including all the members of the family Phasionidae (partridges and pheasants ; Lemmrich 1931). The antero-ventral quadrant has four intervening plates ; the postero-ventral quadrant has three and the postero-dorsal quadrate has four.

The individual plates of the ring are gently convex longitudinally. In cross-section the outer part is gently convex and the middle and inner parts are gently concave. In R197 (Text-fig. 2B) there is an isolated plate which is sub-rectangular in outline with rounded edges ; this appears to be a positive or a negative plate. The long edges of the individual plates in R2477 are damaged but the overlapping part of each plate in the postero-dorsal quadrant clearly tapers to a point. This is not shown by the other plates but a comparable difference is shown in the ring of *Sphenodon* (Edinger 1929, fig. 23).

The length of the longest plate as preserved in R2477 has been used as the length of the individual plates in the reconstruction. An overlap of about a half has been assumed because this appears to be the amount of overlap between adjacent plates in birds and reptiles (see Edinger 1929, Lemmrich 1931). The sclerotic ring is shown overlapped by the supraorbital, but this may not be correct. As reconstructed the diameter of the ring may be too large if some of the plates were smaller than the one measured. In addition the degree of overlap may have been greater than half ; it certainly is as preserved but this may be a post-mortem effect. The overlap would also be reduced if, as was probably the case, the sclerotic ring were placed more ventrally in the orbit than in the reconstruction.

Stapes. Unfortunately no trace of a stapes was found in the prepared skulls. However, it is reasonable to assume that it was a rod-shaped element which, as in hadrosaurs (Ostrom 1961), ran from the fenestra ovalis to a tympanum supported between the quadrate and the paroccipital process.

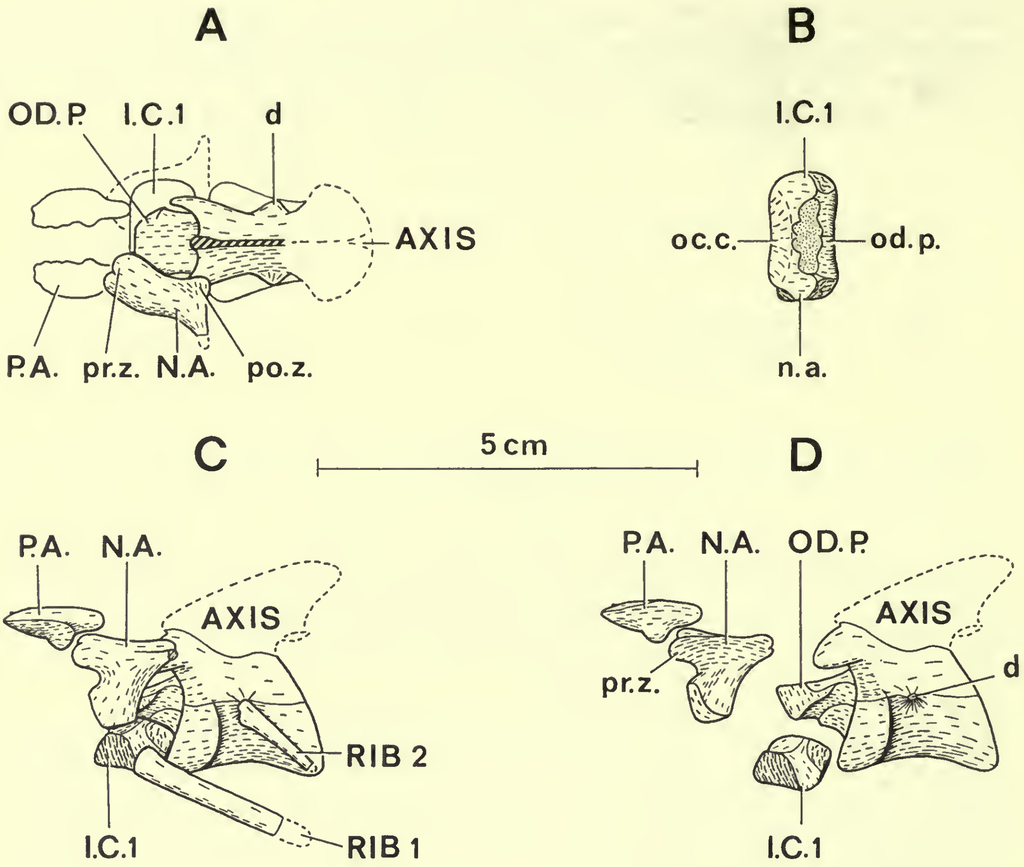

b) *The vertebral column and ribs*

The vertebral column can be assembled from specimens R196 and R196a. The complete presacral series consists of 24 vertebrae – 9 cervicals and 15 dorsals. There are 6 sacral and about 45 to 50 caudal vertebrae.

i) PROATLAS, ATLAS AND AXIS

Proatlas. That of R2477 is presumed to be the left but this, together with the orientation shown in Text-fig. 18G, is only tentative. The proatlas of R196 is only two-thirds the size of that of R2477 although the atlas and axis are slightly larger.

Atlas. This consists of an intercentrum, an odontoid process and two neural arches. The intercentrum (Text-fig. 18) is a subcrescentic bone which anteriorly has a large shallow depression for the occipital condyle (oc.c. Text-figs. 18B, H). This depression is obliquely inclined with a sharp edge ventrally. More laterally

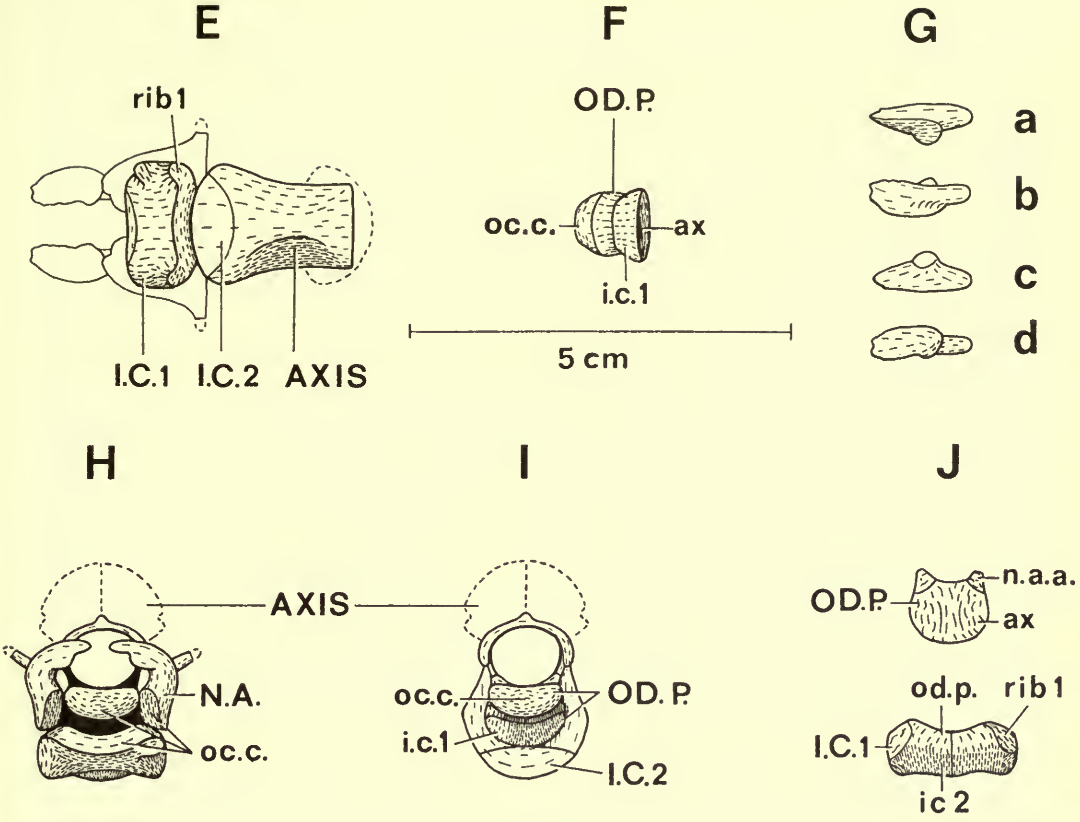

FIG. 18. *Hypsilophodon foxii*. Proatlas, atlas and axis R2477, ×1. A, dorsal view, right neural arch removed; B, atlas intercentrum, dorsal view; C, lateral view with ribs (rib 2 from R196); D, proatlas with atlas in medial view, axis in lateral view; E, ventral view; F, odontoid process of axis in ventral view; G. proatlas, view a = C, b = A, c = D, d = E; H, anterior view; I, axis in anterior view; J, odontoid process and intercentrum of axis in posterior view. Abbreviations: IC. 1, intercentrum of atlas; IC. 2, intercentrum of axis; OD.P., odontoid process of axis; P.A., proatlas; N.A., neural arch of atlas; RIB 1 and 2, ribs of atlas and axis; ax., surface for axis; d, diapophysis; i.c., surface for intercentrum; n.a., surface for neural arch of atlas; n.a.a., surface for neural arch of axis; oc.c., surface for occipital condyle; od.p., surface for odontoid process; po.z., postzygapophysis; pr.z., prezygapophysis; rib 1., surface for rib of atlas.

there are two surfaces, facing antero-dorsally and laterally, for the neural arches (n.a. Text-figs. 18B, C, D). The central part of the dorsal surface is sunken with an irregular though symmetrical outline (Text-fig. 18B). Ventrally (Text-fig. 18E) the surface is concave antero-posteriorly, forming a distinct edge with the anterior and posterior articular surfaces. Posteriorly, this surface medial to the rib facet is concave transversely but the remainder of the surface is convex. This ventral surface is covered with well-developed insertion markings. On the left side the anterior corner has a very irregular appearance (see Text-fig. 18E) which is not due to breakage and must be an individual variation.

The dorsal surface of the odontoid process is transversely concave next to the axis but becomes planar anteriorly (Text-fig. 18J). The ventral surface of the wedge-shaped odontoid is transversely convex. The anterior crescentic area is flat apart from a slight median depression (oc.c. Text-fig. 18H) with which the occipital condyle articulated. The base is gently concave and the intercentrum articulated with this surface (i.c. 1 Text-fig. 18I). Between these two surfaces and forming an obtuse edge with each there is a concave area which, after a slight constriction, passes on to the lateral surface to form a shallow depression (Text-fig. 18D). There is a sharp edge antero-dorsally but more posteriorly the surface is indented slightly with a gentle convex curve (Text-figs. 18A, D).

The neural arches (or neurocentra) are rather irregularly shaped bones which did not meet each other dorsally. Ventrally there are two articular surfaces (Text-fig. 18D); the larger posterior surface across the thicker part of the bone is for the intercentrum, the other faces slightly medially and contributes to the articulation for the occipital condyle (oc.c. Text-fig. 18H). Above these facets the outer surface is convex (Text-fig. 18C) and the inner slightly concave (Text-fig. 18D). On the outer surface where the shaft is constricted there is a well-defined bump. Anteriorly the region of the prezygapophysis forms a thin, curved sheet with two lobes (Text-fig. 18A). The postzygapophyseal process is slender and directed postero-dorsally and laterally (Text-figs. 18A, H). Medial to this the dorsal surface is concave. The ventro-medial surface is concave apart from the flat postzygapophysis, facing ventro-medially.

The atlantal rib (Text-fig. 18A) is long, laterally flattened and oval in cross-section. The head, which articulated with the intercentrum, is slightly expanded with an obliquely inclined concave surface. In R196 there is another single-headed rib next to the axis but it is slenderer than the atlantal rib of R2477 which is a smaller animal. It has also, close to its head, a small ventral plate which is presumably the remains of the capitulum (Text-fig. 18C); it is probably the axial rib because the rib of the third cervical vertebra was in position (Text-fig. 19).

Axis. The centrum is plano-concave with a shallow posterior depression. Anteriorly there is an oval intercentrum (Text-fig. 18E), triangular in sagittal section, with a sharp anterior edge. The neural arch has a well-developed and laterally compressed neural spine (Text-fig. 18A) which posteriorly is laterally expanded to form a frill-like plate (Text-figs. 18H, 20B). The ventral part of this plate is thicker and bears postzygapophyses which face ventro-laterally and slightly posteriorly. Anteriorly the neural spine is slightly thickened to form a projecting knob (Text-fig. 20B). The prezygapophyses are transversely convex and the postzygapophyses of the atlas articulated round their lateral surface. The ventral edge of the prezygapophysis continues on to the neural arch as a ridge below which the surface of the neural arch is concave (Text-fig. 18D). This concave area is continuous with the depression on the side of the odontoid process. The diapophysis (d. Text-fig. 18D) is small and is traversed by the rather indistinct suture between the neural arch and centrum. There does not appear to be a corresponding parapophysis on the centrum but this region is slightly damaged. However, it was probably absent because the rib of the axis appears to have been single-headed.

ii) CERVICAL VERTEBRAE 3 TO 9

The centra of cervical vertebrae 3 to 7 are opisthocoelous while those of 8 and 9 are amphicoelous. The centrum of the third cervical vertebra is laterally compressed; anteriorly there is a sharp ventral edge which widens out posteriorly where it is covered with well-developed surface markings. The remainder of the centra are also laterally compressed but ventrally the lateral surface curves outwards again to form a thickened keel (Text-figs. 19, 20A). The rounded ventral surface of this keel is covered with strongly developed and irregular surface markings.

The neuro-central suture bisects the parapophysis and is clearly visible in all cervicals (Text-fig. 19). The parapophyses of cervical vertebrae 8 and 9 are the largest. The diapophysis shows a progressive increase in robustness and length. In the fifth cervical it runs into the base of the prezygapophysis, in cervical vertebrae 6 to 9 the diapophysis is progressively more antero-dorsal in position on the side of the prezygapophysis. The angle which the diapophysis makes with the vertical in the transverse plane varies from 140 degrees in the third vertebra to 155 degrees in the fifth and then to 80 degrees in the ninth. The postzygapophysis of the third vertebra is quite slender with a well-developed dorsal ridge but distally it is flatter and broader. The remaining postzygapophyses are wider and thicker so that the dorsal ridge becomes progressively less conspicuous. Distally the postzygapophyses are broader and flatter but the separation of this region is less well marked. On this distal part in cervical vertebrae 6 and 7 there are well developed and irregular surface markings.

In cervical vertebrae 3 and 4 the neural spine was probably only a slight ridge; in 5 and 7 it is small and thick with a triangular lateral outline while in 8 and 9 it is much larger, forming a thin triangular sheet. In cervical vertebrae 3 and 4 the pre- and postzygapophyses form a continuous curve with the neural arch (Text-fig. 20B). In the fifth there is a distinct excavation of the wall of the neural arch and the line of the postzygapophysis continues antero-medially to the end of the neural spine. In cervical vertebrae 6, 7 and 9 this lateral space between the pre- and postzygapophyses becomes slightly deeper anteriorly and slightly wider. However, in cervical 8 this space forms a narrow cleft as the body of the neural arch is considerably enlarged. On the flat area so formed are well-developed insertion markings which are adjacent to those on the postzygapophyses of the preceding vertebra.

The third rib, like those of the remaining cervicals, is double-headed. The tuberculum is longer and wider than the capitulum. This rib lacks the anteriorly directed spine present on the fourth rib (Text-fig. 19). The ribs of cervicals 4 to 9 show a number of progressive trends as illustrated (Text-figs. 19, 20). The capitulum becomes longer, the anteriorly directed spine is reduced and the ribs become longer and wider so that they are more sheet-like. In the seventh to ninth ribs the lateral surface is convex, the medial surface concave, the anterior edge thick and rounded and the posterior part thin and sharp-edged. In the eighth and ninth ribs there is a non-articular extension of the capitulum on its medial side.

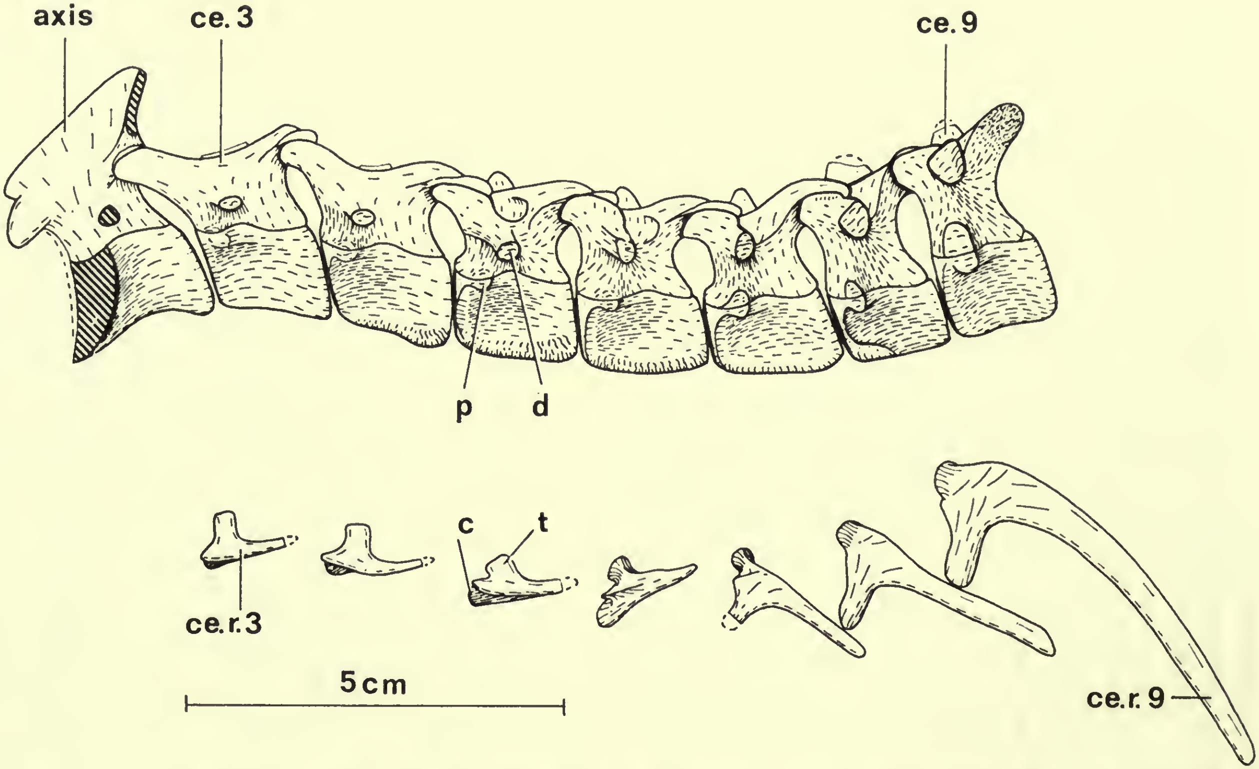
axis
ce. 3
ce. 9
p
d
c
t
ce.r.3
5 cm
ce.r. 9

Fig. 19. *Hypsilophodon foxii.* Cervical vertebrae 2 to 9 of R196, × 1. Lateral view with ribs displaced. Abbreviations: c, capitulum; ce., cervical vertebra; ce.r., cervical rib; d, diapophysis; p, parapophysis.

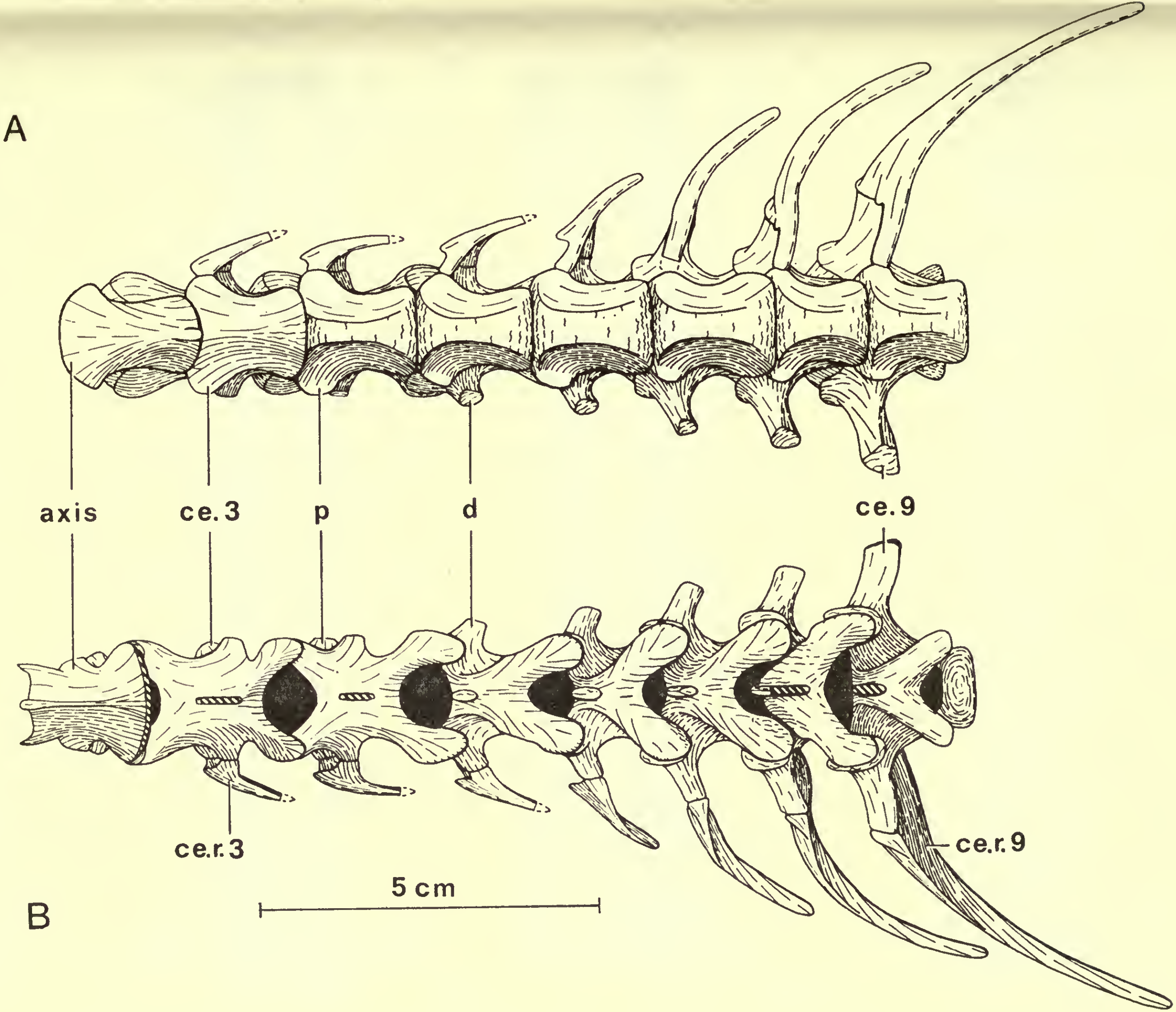
A
axis
ce. 3
p
d
ce. 9
B
ce.r. 3
5 cm
ce.r. 9

FIG. 20. *Hypsilophodon foxii.* Cervical vertebrae 2 to 9 of R196 with ribs in position, × 1. A, ventral view; B, dorsal view. Abbreviations as in Text-fig. 19.

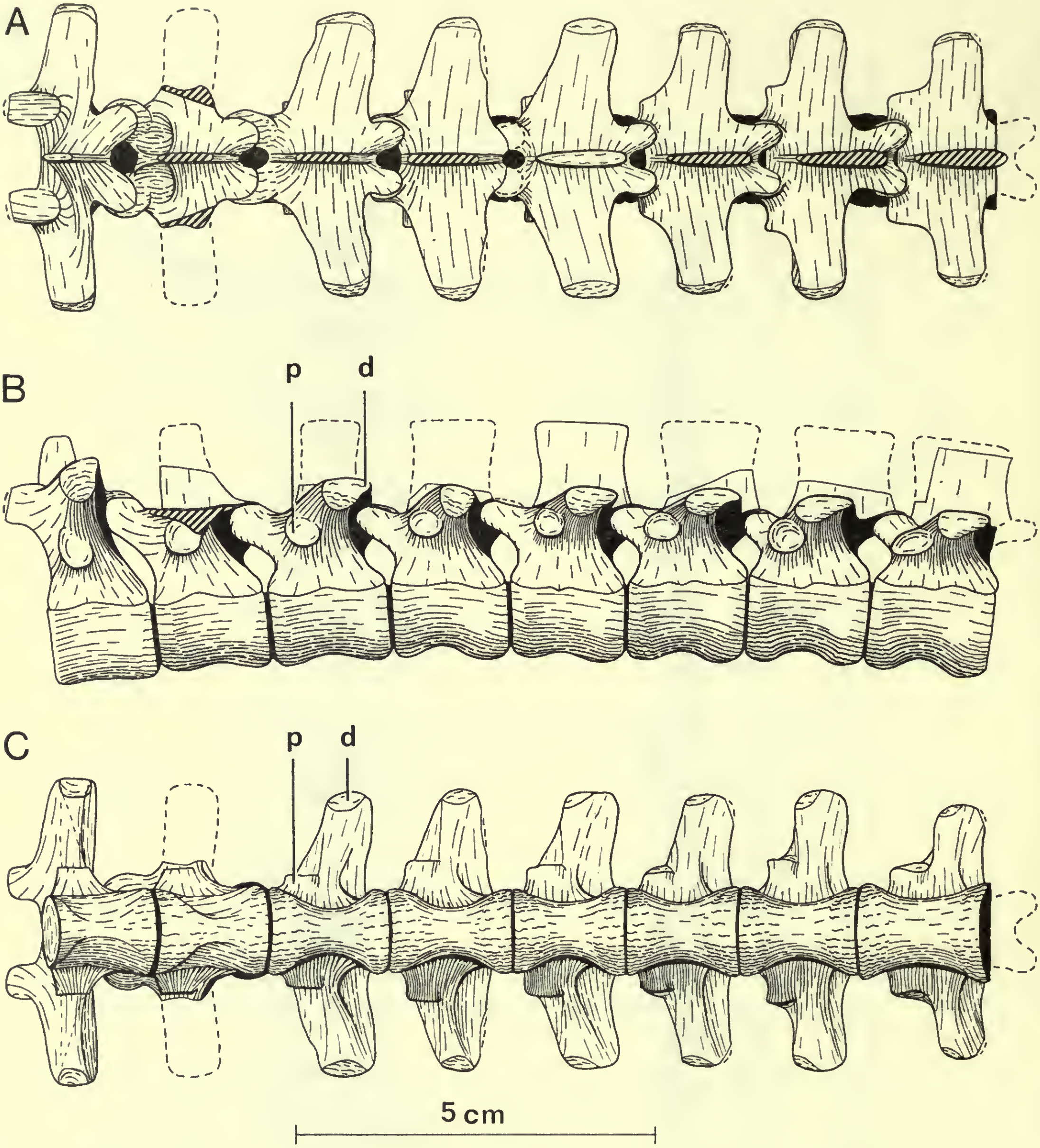

FIG. 21. *Hypsilophodon foxii*. Dorsal vertebrae 1 to 8 of R196, × 1. A, dorsal view; B, lateral view; C, ventral view. Abbreviations: d, diapophysis; p, parapophysis.

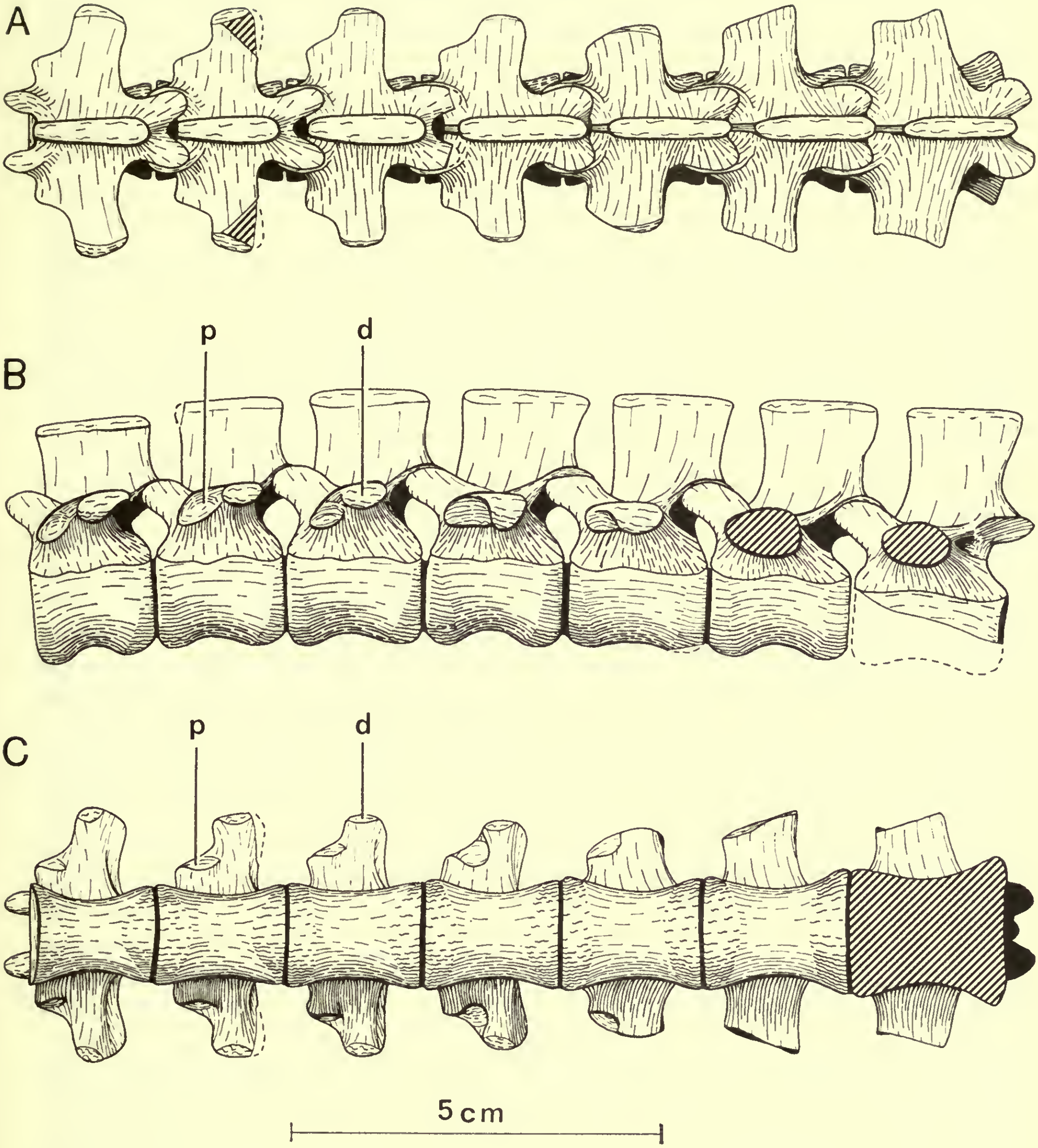

FIG. 22. *Hypsilophodon foxii*. Dorsal vertebrae 9 to 15 of R196 (supplementary details from R2477a), × 1. Views and abbreviations as in Text-fig. 21.

iii) DORSAL VERTEBRAE (Text-figs. 21, 22)

All the centra are amphicoelous. The posterior face of the last dorsal vertebra has two lateral concave areas separated by a dorso-medial ridge. The length of the centrum increases slightly with each successive vertebra. In the first dorsal the middle part of the centrum is laterally compressed so that a thin ventral edge is formed (Text-fig. 21C). The degree of compression decreases posteriorly, so that this ventral part becomes thicker and more rounded. The thicker anterior and posterior regions of the centra are covered with muscle insertion markings which are especially strong ventrally.

The diapophysis remains at about the same height on the neural arch throughout the series (Text-figs. 20B, 21B). The level of the parapophysis drops quite sharply from dorsals 1 to 4 but behind this there is only a very slight drop. The diapophysis and parapophysis become progressively closer together and are united in the last two dorsal vertebrae. In the first dorsal the prezygapophyses are large and wide apart but in the next five vertebrae they become progressively smaller and closer together (Text-fig. 20A). Posteriorly the prezygapophyses become slightly longer and the level varies as shown in Text-fig. 21B. The articular surfaces of all the prezygapophyses make an angle of about 45 degrees with the horizontal.

The angle between the transverse process and the vertical varies from 60 degrees in the first dorsal to 70 degrees in dorsal 4 and 85 degrees in dorsal 8, the processes being more or less horizontal in the remainder. The bases of the transverse processes of the first five dorsal vertebrae become more ventral (Text-fig. 20B) and posterior (Text-fig. 20C) in position. The thin overhanging part at the base of the transverse process is reduced, passing posteriorly, so that more of the diapophysis becomes visible in dorsal view (Text-fig. 20A). In the sixth dorsal the dorsal edges of the diapophysis and the transverse process form a continuous curve. Posteriorly at its base the transverse process forms a flattened sheet which continues as the postzygapophysis. This sheet is small in the first dorsal but considerably larger in the second ; it is then progressively reduced and is absent in the fourteenth and fifteenth dorsals. The first neural spine is thin, the fifth is thicker and larger (Text-fig. 20A, B) while the last seven dorsals have a well-developed thickening dorsally so that a thick edge is formed (Text-fig. 21B).

All except the last one or two dorsal ribs are double-headed. Anteriorly the thoracic ribs are curved, especially near their upper ends, with a superficially flattened and broad distal part. Posterior to the seventh dorsal vertebra the ribs become progressively shorter, straighter and the lateral expansion is lost. The capitulum is borne on the proximal end of the rib while the tuberculum is on a more dorsolaterally placed step and faces dorso-medially. On the anterior ribs the tuberculum is widely separated from the capitulum but more posteriorly the two heads are progressively closer together ; thus they are scarcely distinguishable on dorsal rib 14 while rib 15 is single-headed. These last two ribs are fused with the end of the transverse process.

The sternal segments of the dorsal ribs are always present but are not always ossified. In R196 the sternal segments of the first three dorsal ribs and part of the fourth (Text-fig. 37E) are preserved on the left side together with parts of the first three of the right side (Text-fig. 37B). The first three segments contact the thick and roughened dorso-lateral edge of the sternum while the fourth contacts the distal part of the third (Text-fig. 37E). Distally the first three segments become dorso-ventrally flattened and thicker. In *Parksosaurus* the first six dorsal ribs have sternal segments (Parks 1926) and this may have been the case in *Hypsilophodon.*

iv) SACRAL VERTEBRAE

There are two distinct types of sacrum found in *Hypsilophodon* ; the significance of this dimorphism will be discussed below (p. 122).

The sacrum of R196 (Text-fig. 23) consists of six coossified centra. But the ribs of the first vertebra are borne on the transverse processes and do not contact the ilium (Text-figs. 23, 25C) ; there are only five pairs of sacral ribs, which belong to vertebrae 2–6. This is the *pentapleural* condition. Therefore, strictly speaking, the 'first sacral' vertebra is a dorsal ; R196 has 16 dorsal vertebrae and 5 true sacrals. Functionally, however, this last dorsal vertebra is an integral part of the sacrum because the expanded posterior part of its massive centrum has an extensive sutural contact with the first true sacral ribs (i.e. the ribs of the second vertebra, Text-figs. 23, 25E).

The sacra of *Parksosaurus, Thescelosaurus* and *Dysalotosaurus* are very similar to this. In his description Parks (1926) – followed by Sternberg (1940) and Janensch (1955) – numbered the massive dorso-sacral vertebra as S1 and the other five vertebrae as S2–S6 ; yet, oddly enough, the five pairs of sacral ribs borne by those five vertebrae were numbered 1–5. Thus the second vertebra bears the first rib, the third vertebra the second rib and so on down the series. Confusing though this may seem, for the sake of consistency the same system of numbering will be applied to the pentapleural sacrum of *Hypsilophodon.*

By contrast, in R193 and R195 the first vertebra (Text-figs. 24, 25B, 27) *is* a true sacral because its ribs suture with the centrum and neural arch and contact the pubic peduncles of the ilia ; thus the sacrum in these individuals has 6 pairs of sacral ribs. This is the *hexapleural* condition, with only 15 dorsal vertebrae but with 6 sacrals. Because the ribs of sacral vertebrae 2–6 (numbered 1–5) are obviously homologous to the 5 true sacral ribs of R196 and to those of other lower ornithopods, Parks' system of numbering will be applied also to the hexapleural sacrum of *Hypsilophodon,* with the second vertebra bearing the *first* rib and so on. The problem then arises : how should the rib borne by the first sacral vertebra be numbered in hexapleural individuals? The solution adopted, is to call it the 'new sacral rib' (Text-figs. 24, 25B, 27 ; see Section vi). Though this too may be confusing, it seems likely that worse confusion would result from a complete renumbering.

In R196 the anterior end of the first centrum is transversely expanded (Text-fig. 23C) and its face is markedly concave (Text-fig. 25C). The slightly expanded posterior surface of centrum 6 is very gently concave (Text-fig. 26D). Each zygapophysis makes about a right angle with the other but they are closer together posteriorly. The postzygapophyses of sacrals 1 to 5 fit into a square space formed by the anterior edge of the neural arch and the prezygapophyses of the next vertebra. In sacral 1 the

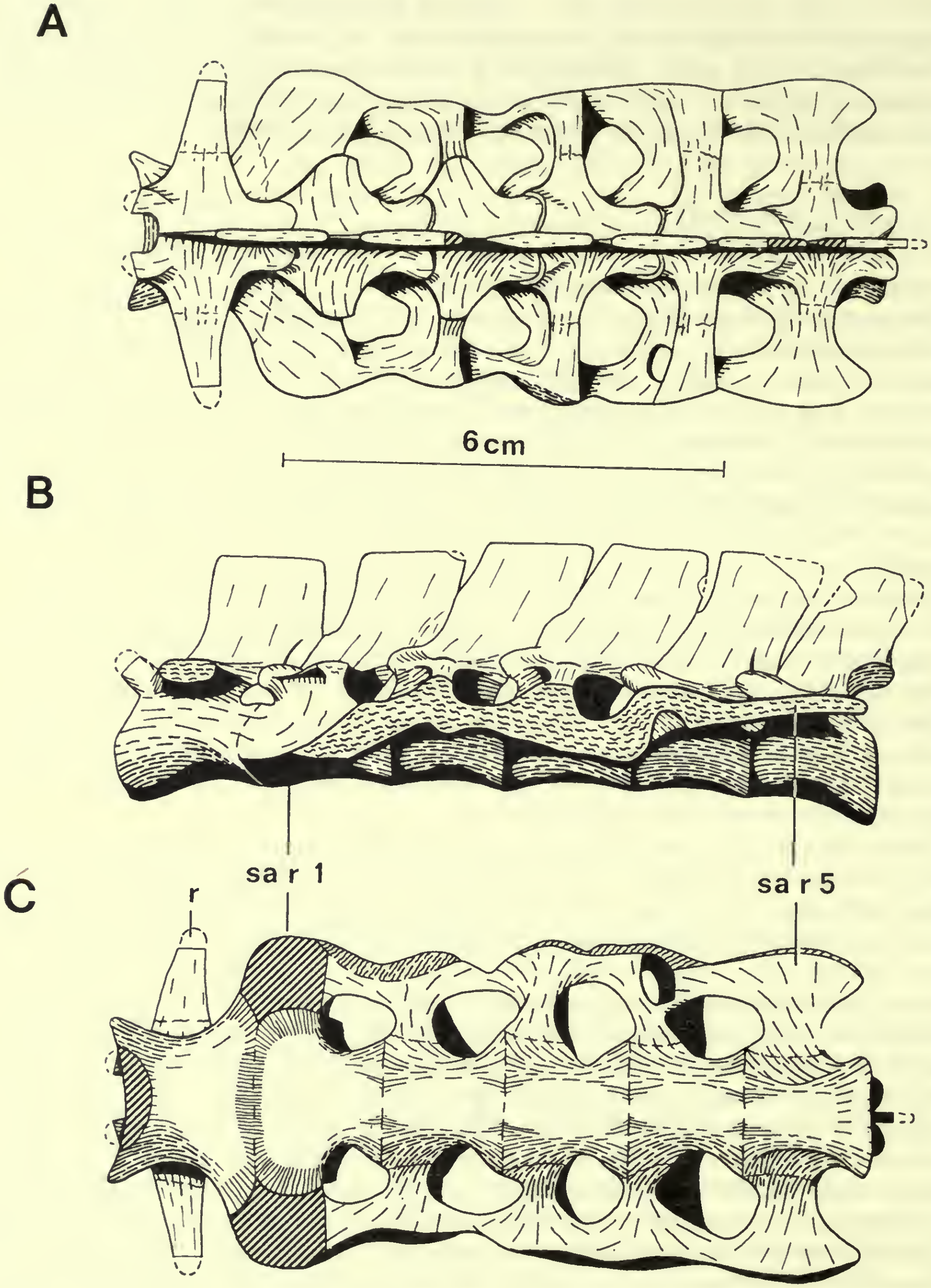

FIG. 23. *Hypsilophodon foxii*. Sacrum of R196 – pentapleural type, × 1. A, dorsal view; B, lateral view; C, ventral view. Abbreviations: r, rib of first sacral vertebra (dorsosacral); sa, sacral vertebra; sa r, sacral rib.

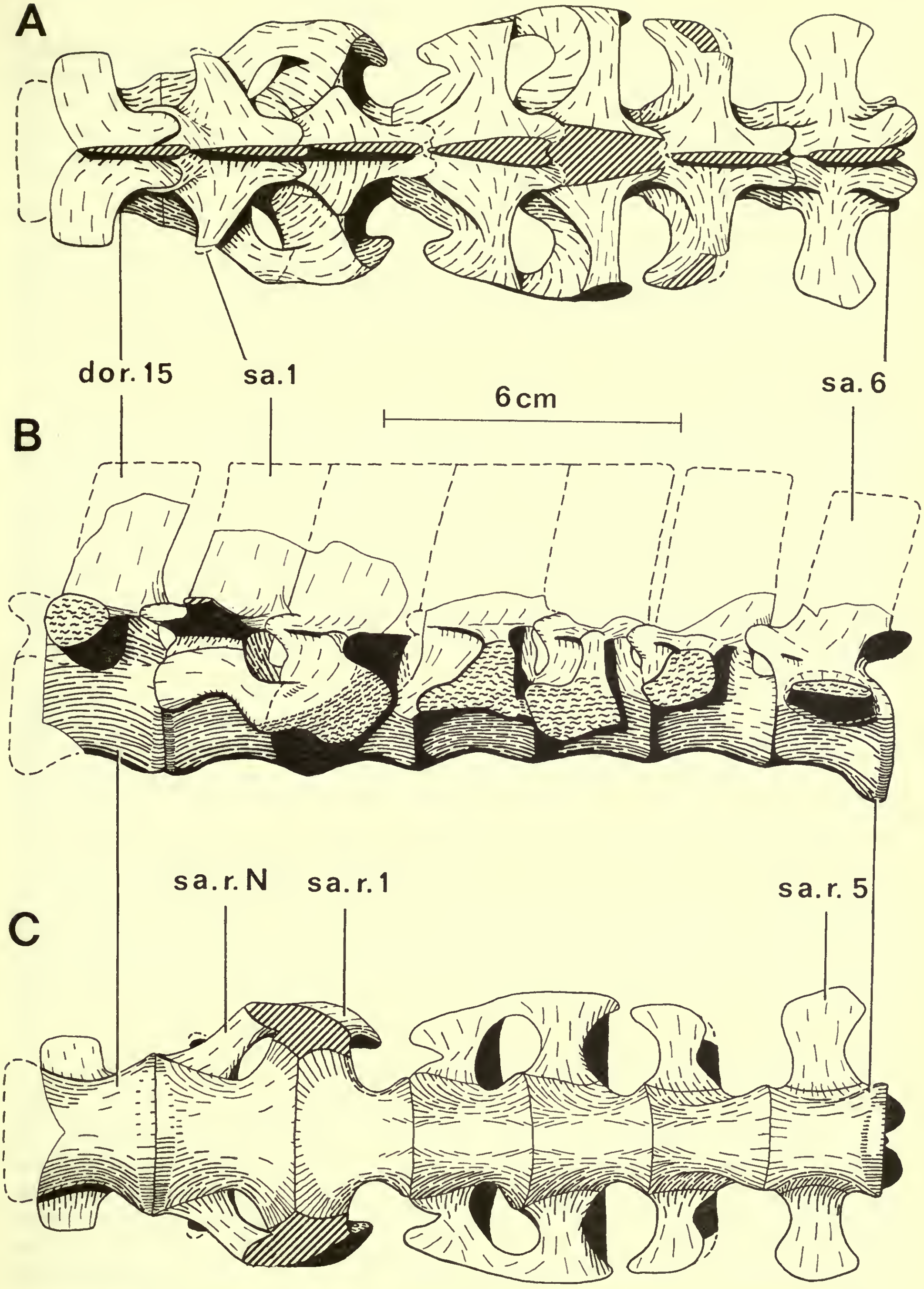
A
dor. 15
sa. 1
sa. 6
6 cm
B
sa. r. N
sa. r. 1
sa. r. 5
C

FIG. 24. *Hypsilophodon foxii.* Last dorsal vertebra and sacrum of R193 – hexapleural type, × ¾. A, dorsal view, B, lateral view; C, ventral view. Abbreviations: dor, dorsal vertebra; sa, sacral vertebra; sa r, sacral rib; sa r N, new sacral rib.

transverse process is large and bears a free rib on its distal end. In the remaining sacral vertebrae the transverse process is sutured ventrally and also (except in sacral 2) laterally to a sacral rib. The angle between the distal part of the transverse process and the vertical varies, being 70 degrees in sacral 1, 90 degrees in sacral 4 and 100 degrees in sacral 6. In sacral vertebrae 1 and 6 the sides of the neural arch are excavated so that the anterior end of the base of the neural spine is thin. Posteriorly there is a slight increase in thickness from sacral 1 to 3, then a decrease to sacral 6. The lower half of each neural spine is thin anteriorly and posteriorly so that the edges of adjacent spines touch. The anterior thin sheet is especially large in sacrals 5 and 6 while the posterior thin sheet, which is developed between and above the postzygapophyses, is largest in sacral 5 but absent in sacral 6.

v) SACRAL RIBS

The central sutures are not clearly visible in R196 (Text-fig. 23) but can be seen in the four sacral vertebrae of R195, in which the different parts have been dissociated (Text-figs. 25B, E, F, 26A, 27; for sac. r. N see Section vi), and in R193 (Text-figs. 24, 26B, C). Each sacral rib projects not from the middle of the centrum, but more anteriorly, so that its anterior edge is borne by the centrum of the preceding vertebra. The base of each rib contacts the lower surface of the transverse process and it is sunk into the side of the neural arch. The flat ventral surface of the first sacral rib is level with the ventral surface of the centrum (Text-fig. 23B). Proximally the bases of the remaining sacral ribs are high on the centrum, with the second slightly higher than the others.

In R196 the dorsal parts of the sacral ribs vary (Text-figs. 23A, B). In the first sacral rib the dorsal part is thin with a sharp dorsal edge. In the second and third sacral ribs it is still thin, but its dorsal edge is thicker and is attached to the end of the transverse process. In the fourth sacral rib all the dorsal part is thicker and postero-dorsally inclined. There is a progressive dorso-ventral flattening of the more distal part of sacral ribs 3, 4 and 5 (Text-fig. 23B) so that the fifth rib (Text-fig. 26D) is practically horizontal and the thickened dorsal edge has merged with the rest of the rib. On the dorsal surface of the ribs and transverse processes there are well-developed markings across the line of suture. These are absent on the second sacral vertebra, the transverse process of which does not contact a sacral rib at its lateral end; consequently the muscles concerned presumably attached to the end of this process.

vi) THE HEXAPLEURAL TYPE OF SACRUM

In specimens of this type (R193, R195, R2477a, R5829, R5830) the rib of the first sacral vertebra is no longer a free dorsal rib, but has become a sacral rib; this vertebra is therefore a true sacral rather than a dorso-sacral vertebra. The rib is no longer attached to the transverse process, but is borne ventrally and sunk into the side of the centrum and neural arch (Text-figs. 24, 25B, D, 27). The rib base is enlarged antero-posteriorly and is partially borne by the centrum of the preceding vertebra (Text-figs. 24B, 25B, D, 27B). Thus, in comparison with the pentapleural type with five sacral ribs (Text-fig. 23; R2477b, R8422), there is an additional sacral rib which is termed the 'new sacral rib' (see above). This rib has a constricted shaft beyond which it is slightly expanded and meets an anterior projection from the proximal end of the first sacral rib. The distal face of this new rib forms a smooth and slightly concave surface (shown in R195, right rib).

The new position of the rib of the first sacral vertebra has resulted in a few differences in the form of the vertebra when compared with that of the first sacral (dorso-sacral) of the pentapleural type described above. The transverse process, because it no longer bears the rib, is very thin dorso-ventrally. In anterior view (Text-figs. 25B, D) it tapers to a point and there is no distal facet. There are no well-developed muscle scars on the distal part of the dorsal surface as the muscles concerned inserted on the lateral end of the process. Anteriorly the sides of the neural arch and the centrum are recessed for the new sacral rib.

The sacrum of R5829 differs somewhat from the other hexapleural sacra. The new sacral rib is rather damaged but it was certainly sutured to the side of the first sacral centrum and neural arch. Dorsally the right transverse process of the first sacral vertebra bears well-developed muscle scars. These insertion markings are found only when a rib is present and they run across the line of suture between the rib and the transverse process. Because these markings are complete the proximal part of the new sacral rib is still attached to the end of the transverse process (the rest of the rib is lost). Consequently the new sacral rib in R5829 has the same connections with its vertebra as do the other sacral ribs. The first sacral rib (i.e. the rib of the second sacral vertebra) bears an anteriorly directed process that would have met the new sacral rib. However, the dorsal edge of the first sacral rib is thickened; it is sutured to the end of the transverse process and there are muscle striations running across the line of suture. This is in contrast to all other sacra, pentapleural or hexapleural, in which this rib has a sharp dorsal edge and there is no contact with the distal end of the transverse process.

vii) OTHER VARIATIONS IN THE SACRUM

The degree of contact between the neural spines of the sacral vertebrae varies (Text-figs. 23B, 24B, 27B). In R193 and R196 the part of the spine adjacent to the contact edge consists of a thin sheet. In R195 and R2477a the whole of the neural spine is thick with well-developed sutural ridges along the contact edge (Text-fig. 25E). In addition there is a small sutural contact between the neural spine bases of the fifteenth dorsal vertebra and the first sacral vertebra (Text-fig. 25B). This contact is also present in R5829 but there are no comparable sheets between the zygapophyses of the other specimens. The degree of fusion of the neural spines is an individual variation because it is not related to the size of the specimens (see list below). The ankylosis of the neural arch and the centrum of the sacral vertebrae appears to be an age variation. The length of the first three centra of the sacrum is the best index of size available. The neural arch and centrum are separate (as are the individual centra) in R5830 (38 mm), and R195 (51 mm) but they are all ankylosed in R2477a (± 50 mm), R2477b (54 mm), R196 (55 mm), R5829 (± 67 mm),

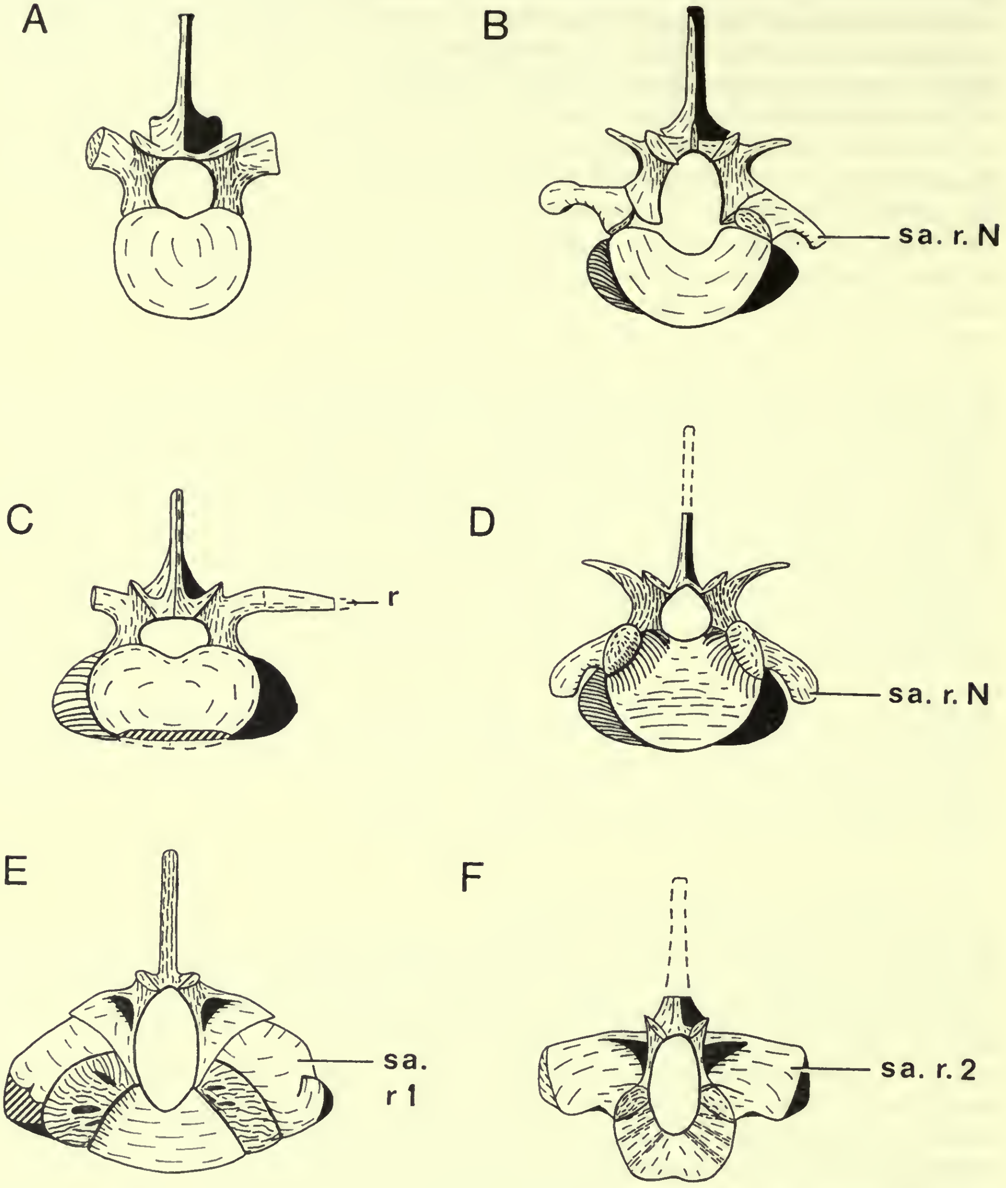

Fig. 25. *Hypsilophodon foxii.* Anterior view of vertebrae. Dorsal vertebra: A, fifteenth of R195, × 1. Sacral vertebrae: B, first of R195, × 1; C, first of R196 (dorso-sacral), × 1; D, first of R193, $\times\frac{2}{3}$; E, second of R195, × 1; F, third of R193, $\times\frac{2}{3}$. Abbreviations: r, rib of first sacral vertebra; sa r, sacral rib; sa r N, new sacral rib.

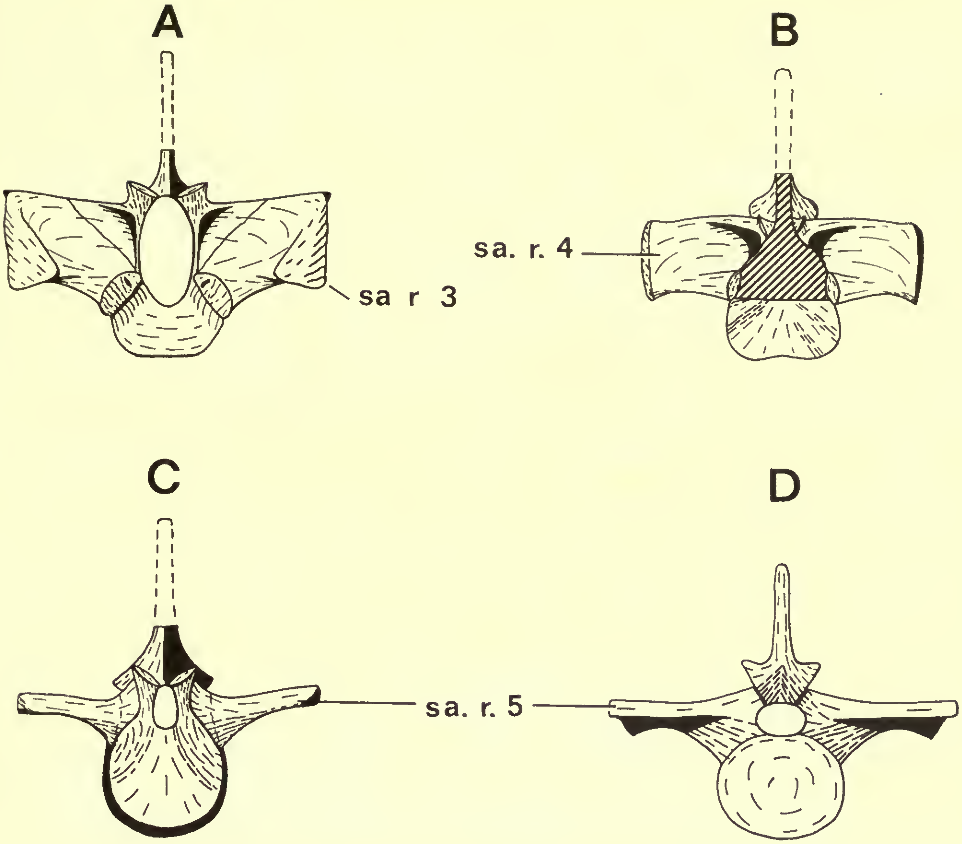

FIG. 26. *Hypsilophodon foxii.* Anterior view of sacral vertebrae. A, fourth of R193, × $\frac{2}{3}$; B, fifth of R193, × $\frac{2}{3}$; C, sixth of R193, × $\frac{2}{3}$; D, posterior view of sixth of R196, × 1. Abbreviations: sa r, sacral rib.

R8422 (71 mm) and R193 (75 mm). The anterior face of the centrum of the first sacral varies; it is transversely concave in R196 (Text-figs. 23C, 25C), almost flat in R195 (Text-figs. 25B, 27C) while in R193 (Text-figs. 24C, 25D) the medial part is flat with deep dorso-lateral depressions in the region of the new sacral rib. The ventral surface of the first two centra varies: the medial part of the first of R196 (Text-fig. 23C) is rather flat while in R193 (Text-fig. 24C) and R195 (Text-fig. 27C) it is transversely convex and longitudinally concave; that of the second is transversely concave in R195 and R196 but convex in R193.

viii) CAUDAL VERTEBRAE AND CHEVRONS

In the small individual R196 the first 19 caudals are present while in the larger individual R196a there are 29 from the posterior part of the tail. The first vertebra without a transverse process is the eighteenth caudal of R196 and the ninth preserved

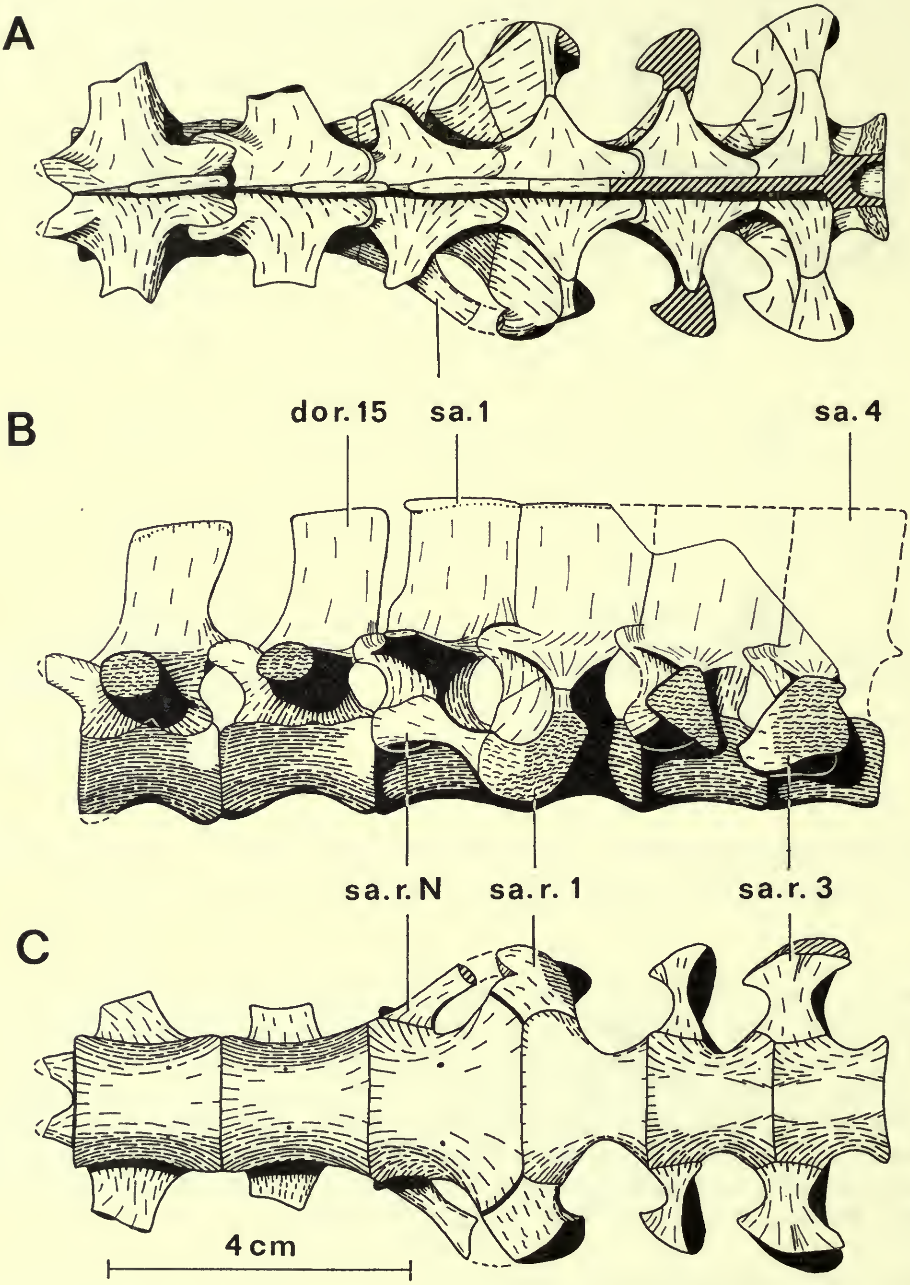
A
B
dor. 15
sa. 1
sa. 4
sa. r. N
sa. r. 1
sa. r. 3
C
4 cm

FIG. 27. *Hypsilophodon foxii.* Dorsal vertebrae 14, 15 and sacral vertebrae 1 to 4 of R195, × 1. A, dorsal view; B, lateral view; C, ventral view. Abbreviations: dor, dorsal vertebra; sa, sacral vertebra; sa r, sacral rib; sa r N, new sacral rib.

vertebra of R196a. This suggests that the first 9 tail vertebrae are missing in the latter series, those present being caudals 10 to 38. The most posterior caudals present are not greatly shortened. A comparison with the tail in *Thescelosaurus* (see Gilmore 1915) indicates that 10 or so vertebrae are probably missing from the distal end of the tail of the larger specimen.

The first caudal centrum is opisthocoelous but the remaining centra are amphicoelous. Throughout the series the centra become progressively lower and thinner. Posterior to the eighteenth caudal the lateral and ventral surfaces become flatter so that the ventral edge is square in section. In addition there is a square dorsal outline above. All the transverse processes point slightly upwards at an angle of about 10 degrees to 15 degrees to the horizontal. The distal part is postero-ventrally directed only in the first caudal (Text-figs. 28A, C, 30A, C). Some of the variation in the horizontal plane (Text-figs. 29, 31) is due to distortion. The transverse process of the seventeenth caudal is represented by a very slight bump with no trace at all on the eighteenth.

In the first 12 caudal vertebrae the articular surfaces of the zygapophyses become progressively smaller, more vertical and closer together but then remain constant in the remaining caudals preserved. In lateral view (Text-fig. 28A) the prezygapophyses become thinner but the length remains about the same. However, internally the space at the base of the prezygapophyses is filled in with bone. By caudal 12 the postzygapophyses have become round vertical plates close together on the edge of the neural spine. They are embraced by the correspondingly small prezygapophyses.

The main body of the neural arch becomes progressively lower and thinner along the series. The neural spine of the first caudal is slightly taller and narrower than in the last sacral vertebra. The thin anterior part is less extensive but the part of the spine dorsal to the postzygapophyses is thicker. The anterior thin part is progressively reduced in the first six caudals so that the neural spine is slightly shorter ventrally (Text-fig. 28A). Posterior to the ninth caudal the neural spines become progressively lower but the ventral part becomes wider. The neural spines seem to disappear at about the thirty-sixth caudal in R196a.

The first chevron is borne between the centra of the first two caudals and was found in place in R196 (Text-fig. 28A). In R193 this region had already been prepared but a chevron was originally present because these two centra have the same facets (Text-fig. 30A). Hulke (1882 : 1046) stated that the second caudal has 'a single facet, the first chevron being articulated with the second and third caudal vertebrae'. However, the condition of the second centrum cannot be determined from his figure (Hulke 1882, pl. 74, fig. 9) and this specimen cannot be found. The first chevron is a small nubbin of bone that is slightly flattened dorso-ventrally (Text-fig. 28A). The ventral part is damaged and there may have been bone enclosing the haemal artery. The second chevron appears to be flattened antero-posteriorly while the third is circular in cross-section and tapers distally (Text-figs. 28A, B). In the fourth and successive chevrons the distal part becomes longitudinally expanded and flat while the proximal part becomes narrower with the formation of a short shaft region. In all the chevrons the articular surface for the preceding centrum is slightly smaller than that for the posterior one.

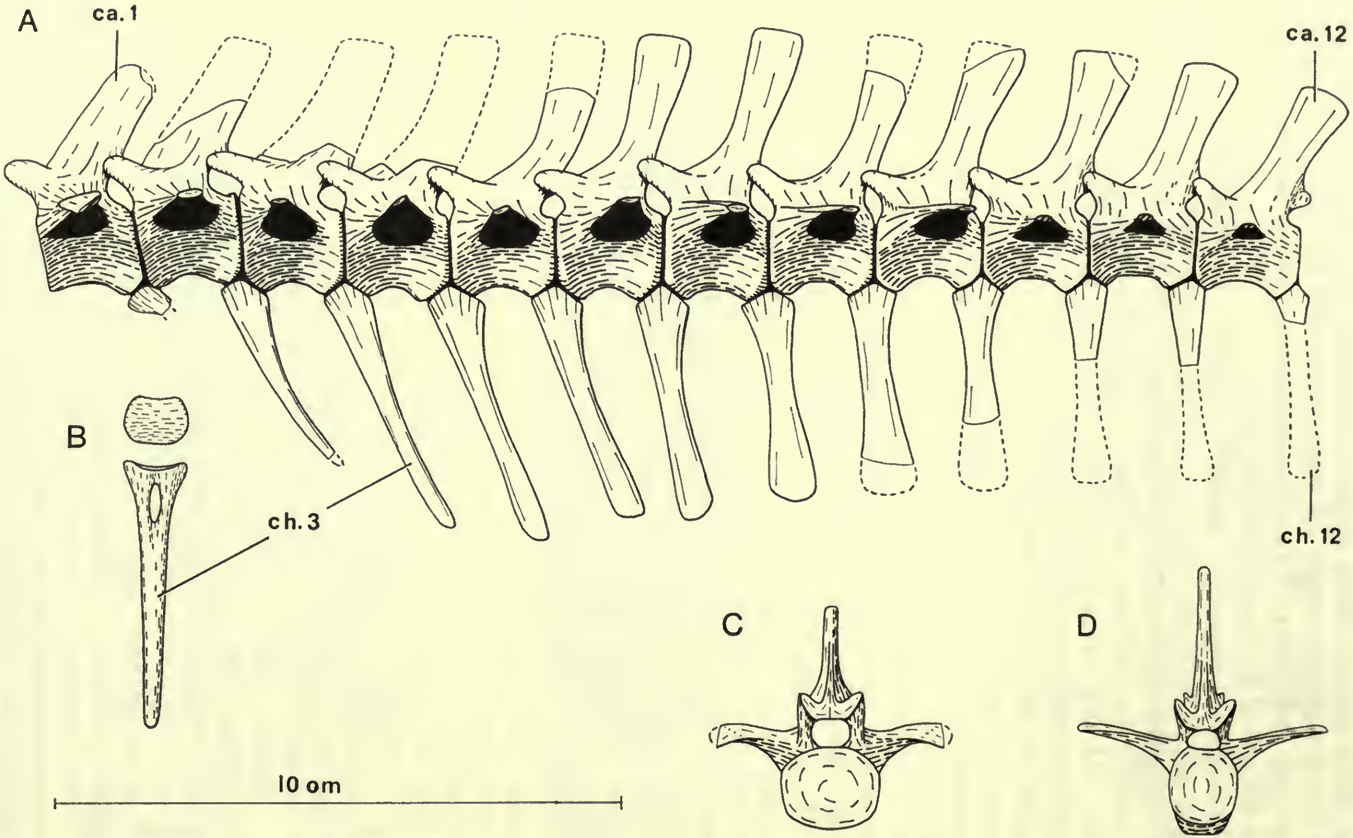

FIG. 28. *Hypsilophodon foxii.* Caudal vertebrae R196, × ¾. A, lateral view caudals 1–12 with chevrons; B, dorsal and anterior views of chevron 3; C, anterior view of caudal vertebra 1; D, anterior view of caudal vertebra 6. Abbreviations: ca, caudal vertebra; ch, chevron.

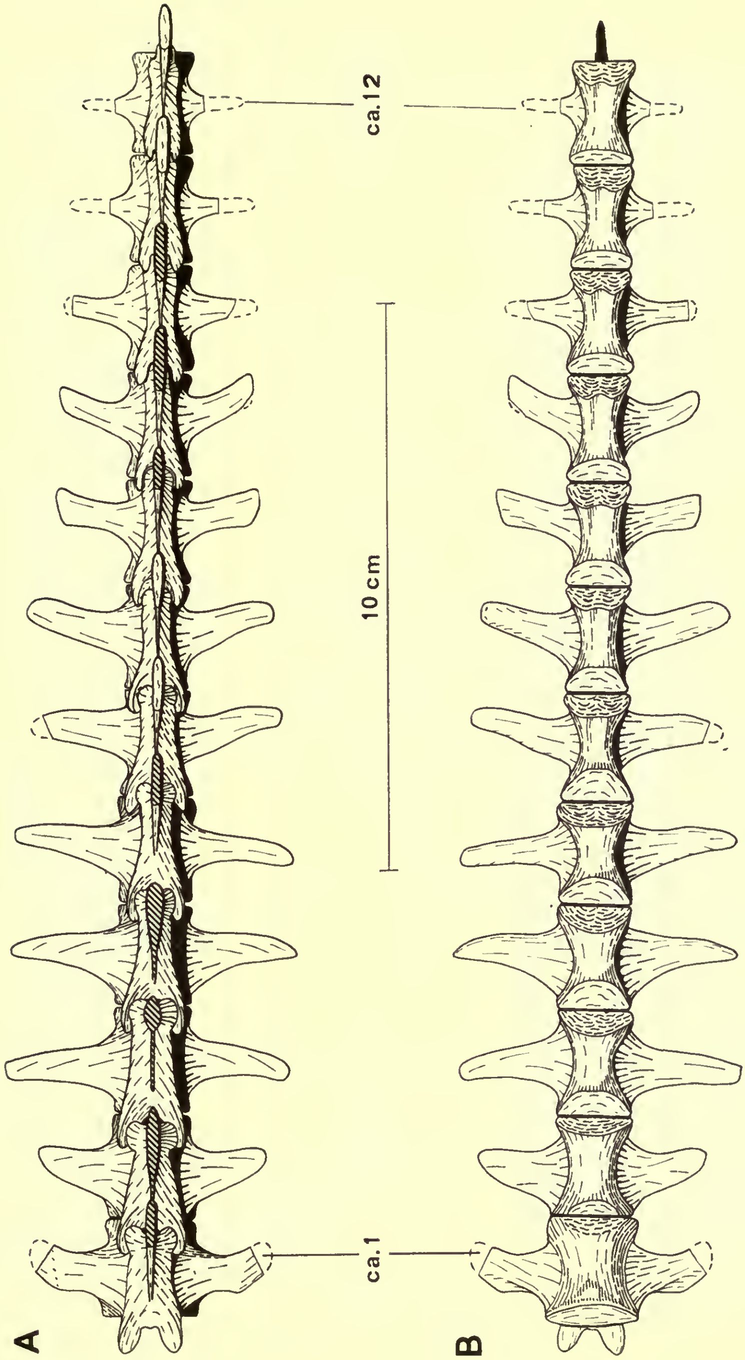

FIG. 29. *Hypsilophodon foxii.* Caudal vertebra 1–12 of R196, × ¾. A, dorsal view; B, ventral view. Abbreviation: ca, caudal vertebra.

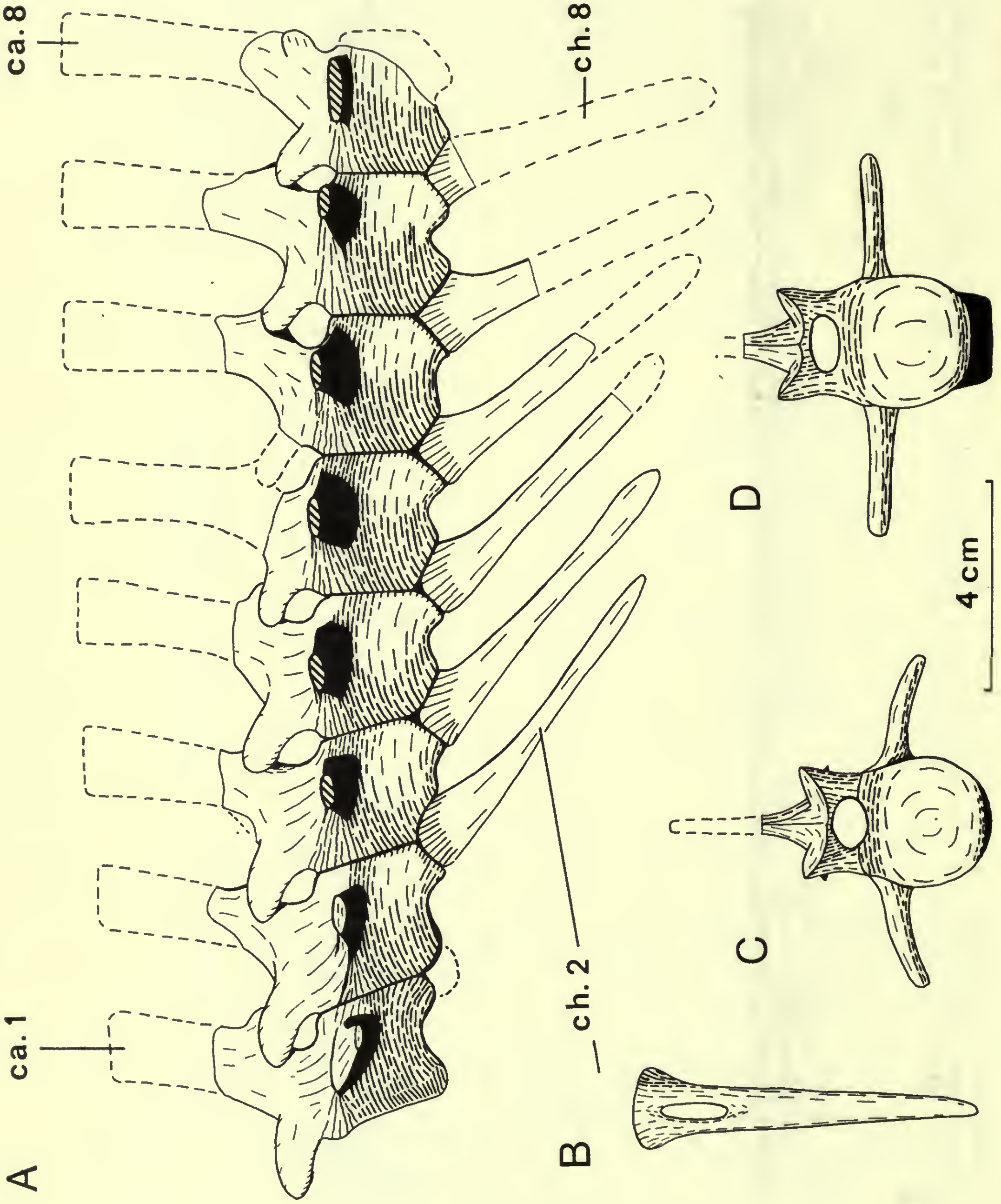

FIG. 30. *Hypsilophodon foxii.* Caudal vertebrae R193, × ¾. A, lateral view of caudals 1–8 with chevrons; B, anterior view of chevron 2; C, anterior view of caudal vertebra 1; D, anterior view of caudal vertebra 2. Abbreviations: ca, caudal vertebra; ch., chevron.

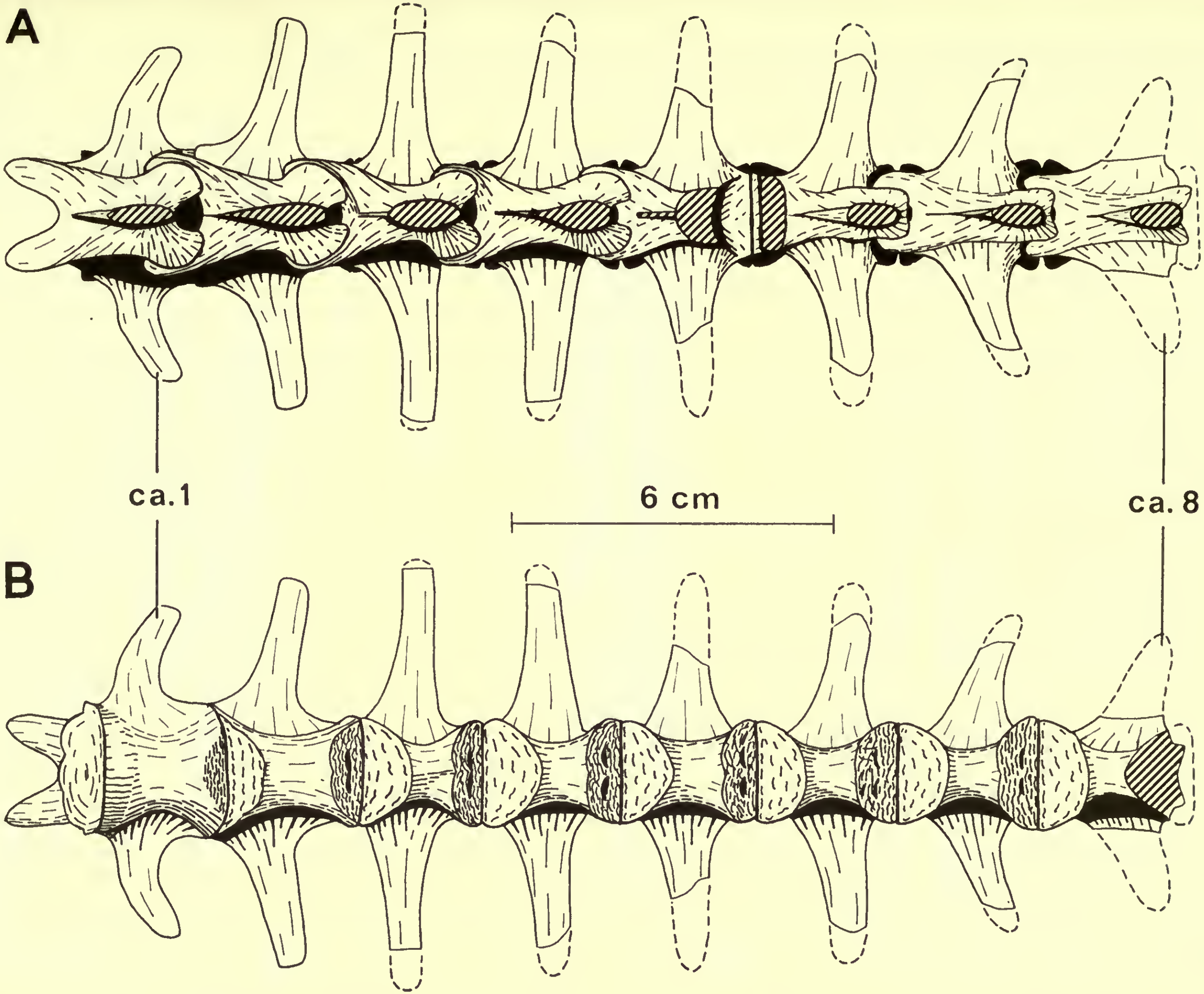

Fig. 31. *Hypsilophodon foxii.* Caudal vertebrae 1–8 of R193, × ¾. A, dorsal view ; B, ventral view. Abbreviation : ca., caudal vertebra.

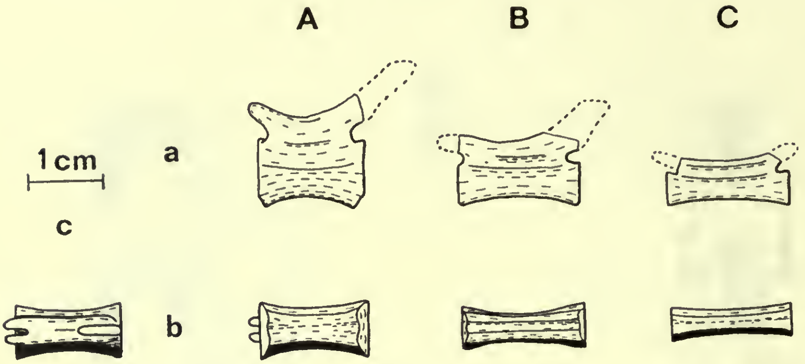

FIG. 32. *Hypsilophodon foxii.* Caudal vertebrae of R5830, × 1. A, about the twenty-fourth; B, about the twenty-eighth; C, about the thirty-seventh; a, lateral view, b, ventral view; c, dorsal view.

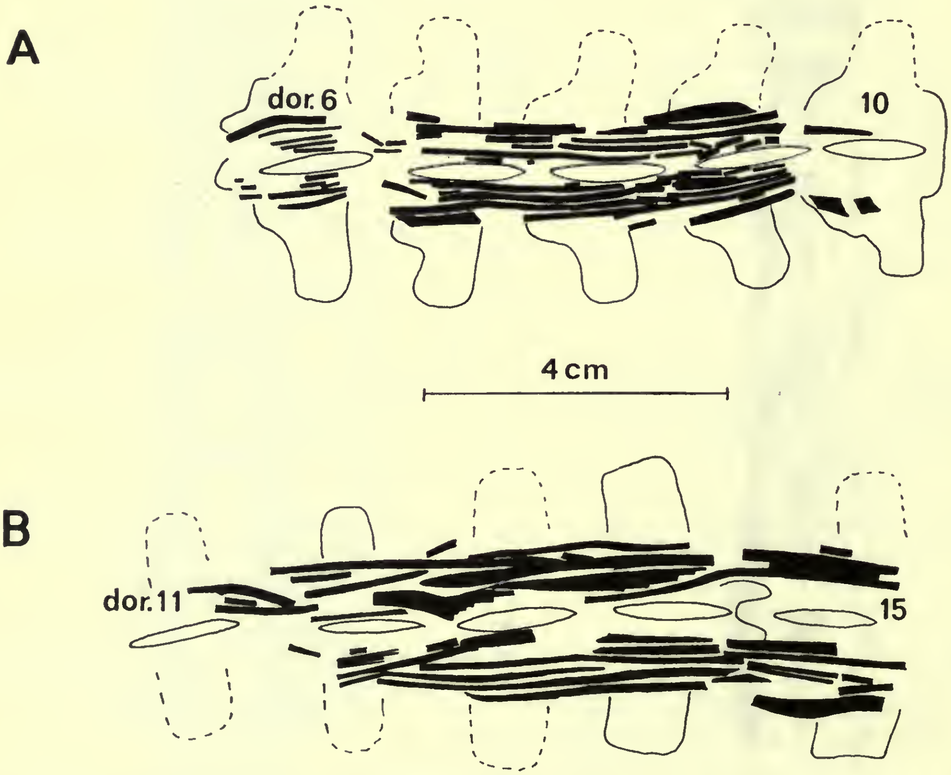

FIG. 33. *Hypsilophodon foxii.* Ossified tendons of R196, × 1. A, dorsal vertebrae 6–10 in dorsal view; B, dorsal vertebrae 11–15 in dorsal view; C, sacrum in dorsal view; D, caudal vertebrae 13–18 in lateral view. Abbreviations: ch., chevron; dor., dorsal vertebra; sa., sacral vertebra: t.p., transverse process.

c) *Ossified tendons*

Anteriorly, fragments of ossified tendons remain on the fifth dorsal of R196 but no tendons were found when the third dorsal was prepared. These vertebrae were in natural articulation and the fourth dorsal vertebra probably marks the anterior limit of the ossified tendons. Most of the tendons of the dorsal and sacral series of R196 lie immediately above the neural arches. However, this may not be natural because in R195 and R2477 the tendons occurred along the sides of the neural spines. In R195 the individual tendons span at least five vertebrae, running horizontally and close to one another; they do not show the rhomboidal arrangement present in *Iguanodon* (see Dollo 1887) and the hadrosaurs (Lull & Wright 1942, Colbert 1962). The number of tendons on one side of a vertebra varies from six to nine but originally there were probably many more.

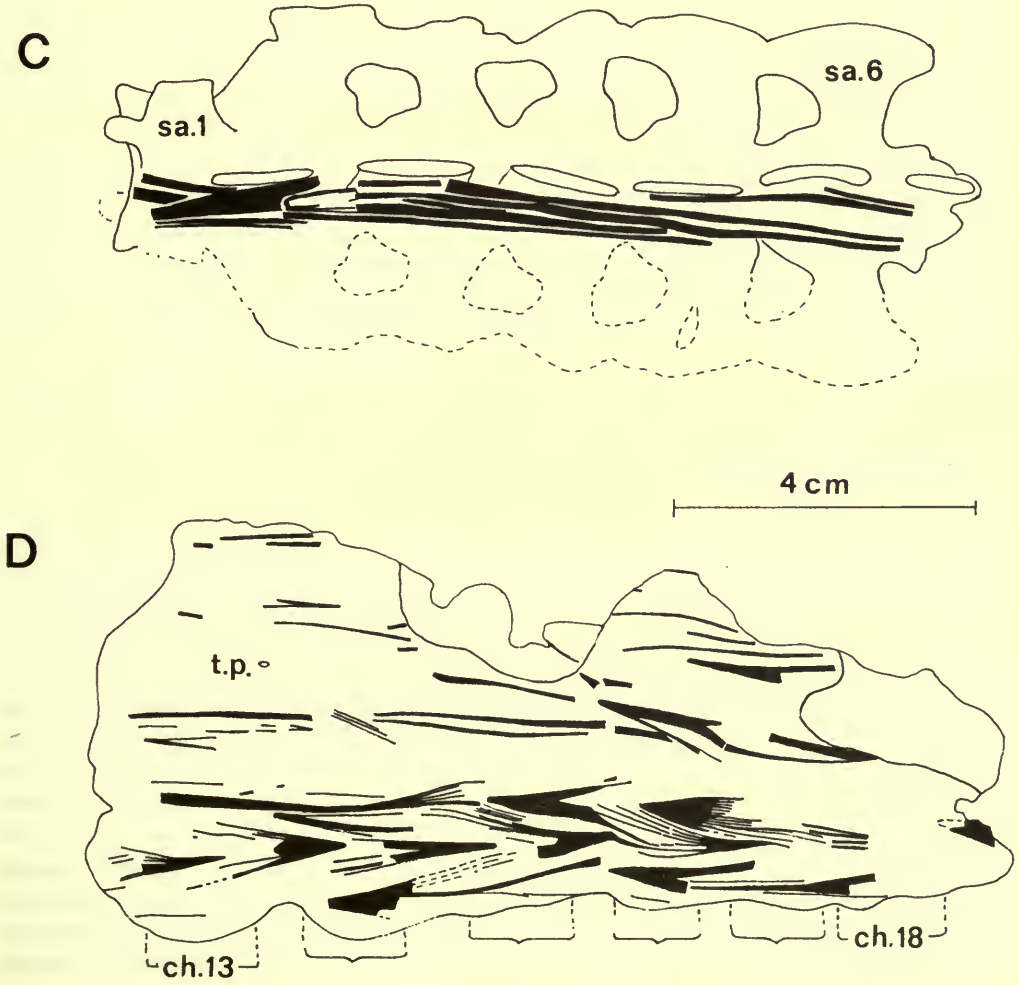

Only a few tendons were found when the proximal part of the tail of R196 was prepared and this probably reflects the original situation. The tendons on the chevrons of caudal vertebrae 14 to 17 are well preserved (Text-fig. 33D) and each consists of a flat sheet of bone, with fine longitudinal striations, one end of which tapers to a point while the other splays out into a series of fine rays. The complete series of rays is not preserved for any single tendon but there were at least ten per tendon. Each tendon is intervertebral in position and is about the same length as one of the adjacent centra. The tendons are arranged in rows, the individual tendons of which point in the same direction (Text-fig. 33D) while adjacent rows point in the opposite direction.

The posterior third, at least, of the tail was ensheathed by a large number of ossified tendons (Text-fig. 62). On one side of the twenty-seventh caudal of R196a there are 28 tendons in a width of 23 mm. However, there are many more than this because there are others below and, in addition, quite a few appear to have been removed during preparation. The individual tendons can be followed for a length of only two centra at the most but, because they are rather damaged, they may originally have been considerably longer. The splaying of the end of the tendon into many rays is visible in several places with both anteriorly and posteriorly pointing tendons represented.

In the dorsal and sacral series of R196 (Text-figs. 33A–C) the splaying is visible in a few places. However, all of these point anteriorly with a posterior splaying. There are a few anterior ends that are different, being slightly flattened laterally with a few strongly developed ridges and an uneven surface. Individual tendons are much longer than those of the tail and for most of their length are circular in cross-section, but they have the same fine longitudinal striations as the tendons of the caudal series.

d) *Appendicular skeleton*

i) THE PECTORAL GIRDLE

Scapula. This is about the same length as the humerus, is twisted along its length and, in addition, bowed (Text-fig. 34B) so that it followed the outer contour of the rib cage. The anterior end of the base of the scapula bears a triangular facet (cl. Text-figs. 34A, 35A) with a rounded articular surface which was probably for the clavicle. In ornithischians the clavicle itself is preserved in *Protoceratops* (see Brown & Schlaikjer 1940) and psittacosaurs (Osborn 1924). The anterior edge of the scapular blade is thin and rounded as is the posterior edge, apart from the dorsal part which is sharp. The dorsal edge is thicker where it cuts across the body of the blade and it is rather bumpy. This dorsal end-surface probably carried a cartilaginous suprascapula as described in *Parksosaurus* by Parks (1926). The lateral surface of the scapula immediately behind the clavicular facet forms a well-developed depression (Text-figs. 34A, 35A). This is continued diagonally upwards as a concave surface running along the convex curve of the scapula to meet another diagonally inclined depression from the glenoid region. Ventrally the central part forms a

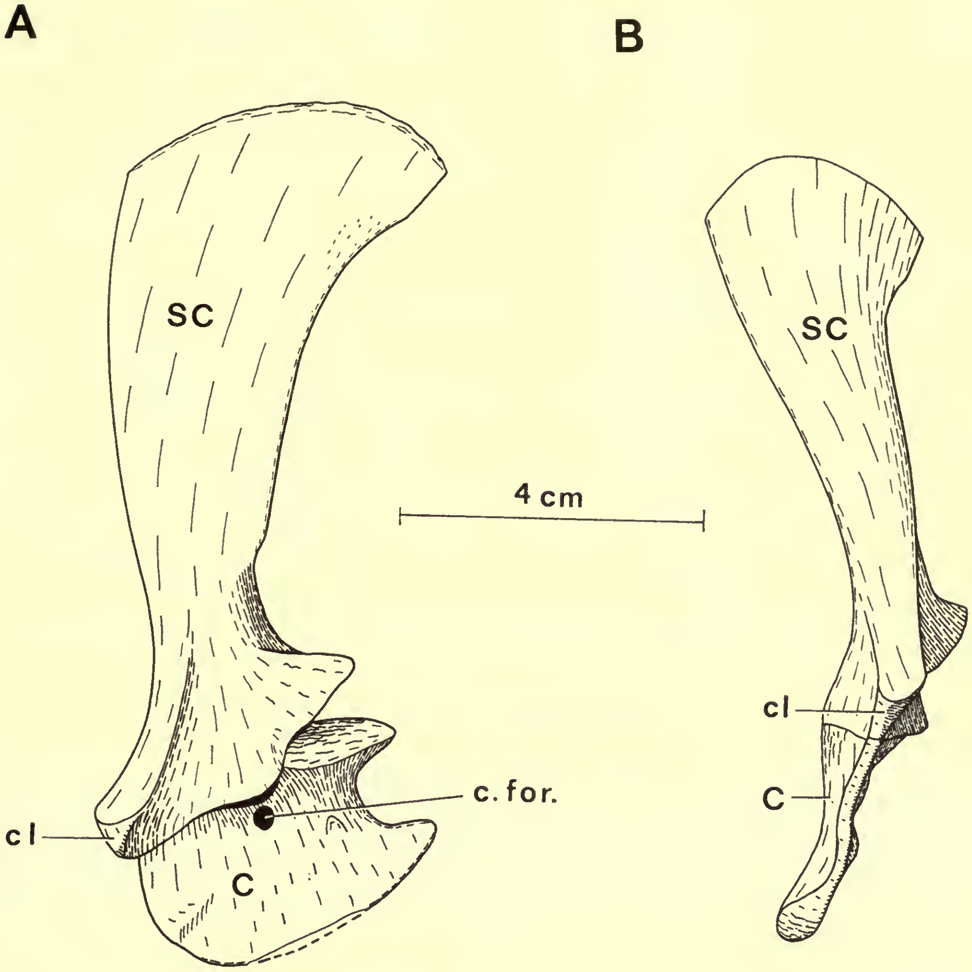

FIG. 34. *Hypsilophodon foxii*. Scapula and coracoid R196, × 1. A, lateral view; B, anterior view. Abbreviations: C, coracoid; SC., scapula; c. for., coracoid foramen; cl., facet for clavicle; gl. cav., glenoid cavity.

rounded surface that projects beyond the coracoid (Text-fig. 34). The medial surface (Text-figs. 34B, 35B) is slightly concave dorso-ventrally and convex antero-posteriorly. The ventral part forms a broad convexity which is crossed by a groove leading from the coracoid foramen (Text-fig. 35B).

The scapulae show a certain number of individual variations. Posteriorly the junction of the shaft and the blade forms a step in R196 (Text-fig. 34A) and R192 which is practically absent in R5829 and R5830 (Text-fig. 36A). The shaft is more strongly twisted in R196 (Text-fig. 34) than it is in R192, R5829 and R5830 (Text-fig. 36). The coracoid groove is deeper in R196 (Text-fig. 35B) than it is in R5829

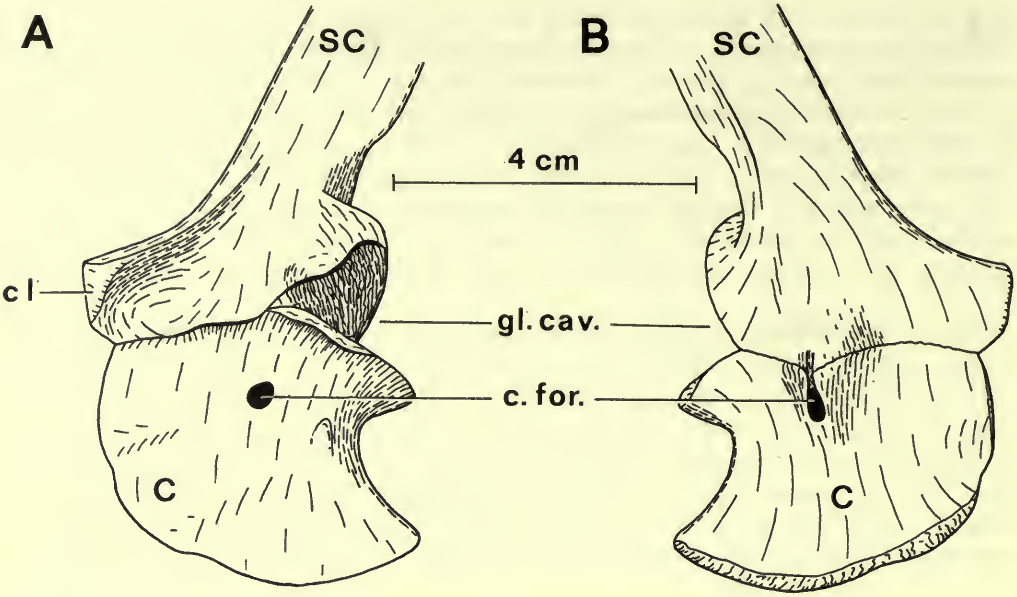

FIG. 35. *Hypsilophodon foxii.* Scapula and coracoid R196, × 1. A, ventro-lateral view ; B, dorso-medial view. For abbreviations see Text-fig. 34.

or R5830. All these are random variations independent of size. The lateral edge running from the facet for the clavicle is strongly developed in R192, R196 (Text-fig. 34A) and R5829 but weakly so in R5830 (Text-fig. 36A). The sutural surface with the coracoid has well-developed ridges in R196 which are absent in R5830. The general curves of the scapula (and coracoid) of R196 (Text-figs. 34, 35) and R5829 are more strongly developed than in R5830 (Text-fig. 36) ; all these differences are probably due to the smaller size of R5830.

Coracoid. The coracoid is thin except for the dorsal part. The inner surface (Text-figs. 34B, 35B) is concave dorso-ventrally and convex antero-posteriorly, with a strongly developed depression on the antero-ventral part where the edge is very thin (Text-fig. 35B). Dorsally, the inner surface has a large raised area in the middle. The coracoid foramen (Text-fig. 35B), which extends diagonally forwards and downwards through the bone (visible in R5830), is located in the posterior part of this area. A well-marked groove (Text-fig. 35B) extends dorsally from the coracoid foramen and continues on to the scapula.

Sternum. The right sternal bone is longer than the left (Text-fig. 37), but this is presumably an individual variation. The antero-medial part is thick with an irregular sutural surface (Text-fig. 37D). Anteriorly the ventral and medial surfaces are covered with large bumps (Text-fig. 37B). The anterior edge is rounded medially but becomes sharp-crested laterally. The bone behind this edge is moderately thick

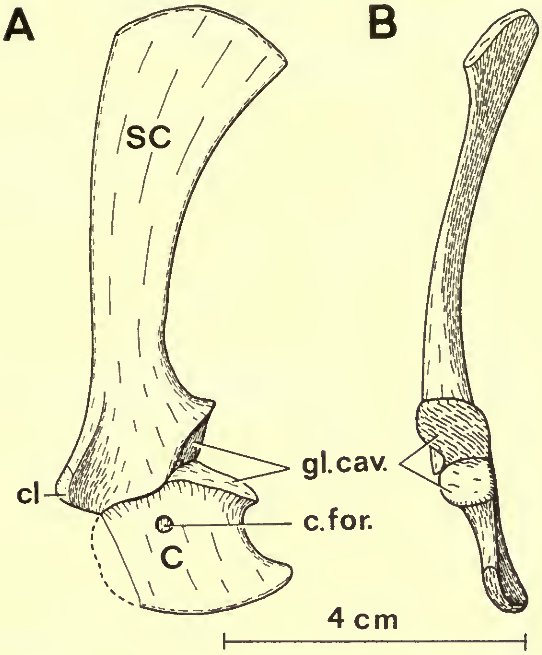

Fig. 36. *Hypsilophodon foxii.* Scapula and coracoid R5830, × 1. A, lateral view; B, posterior view. For abbreviations see Text-fig. 34.

as is the postero-lateral edge. The latter edge has an irregularly pitted surface that contacted the ends of the sternal sections of the first three dorsal ribs (Text-figs. 37B, E). The postero-medial part of the sternum is very thin.

ii) THE FORELIMB

Humerus. As a result of the twisting of the shaft (Text-fig. 38) the moderately expanded distal end of the humerus is set at an angle to the broader proximal end that carries the anteriorly directed delto-pectoral crest (Text-fig. 38E). This crest becomes progressively thicker distally towards the apex and the edge is rounded. In the region of the apex the crest has a flat surface, facing antero-laterally (Text-fig. 38D), which becomes rounded more distally to merge with the shaft. The broad proximal end with the delto-pectoral crest forms a longitudinally concave and transversely twisted anterior surface (Text-fig. 38C). Proximally the posterior edge is thin but it becomes thicker and rounded, forming a slight ridge where it meets the concave surface at the base of the delto-pectoral crest (Text-fig. 38C). This ridge continues on to the shaft, which is slightly oval in cross-section, and runs to the ventral ulnar condyle. The anterior intercondylar groove is wider, deeper and continues further along the shaft (Text-figs. 38D, F) than the posterior intercondylar groove (Text-figs. 38B, F).

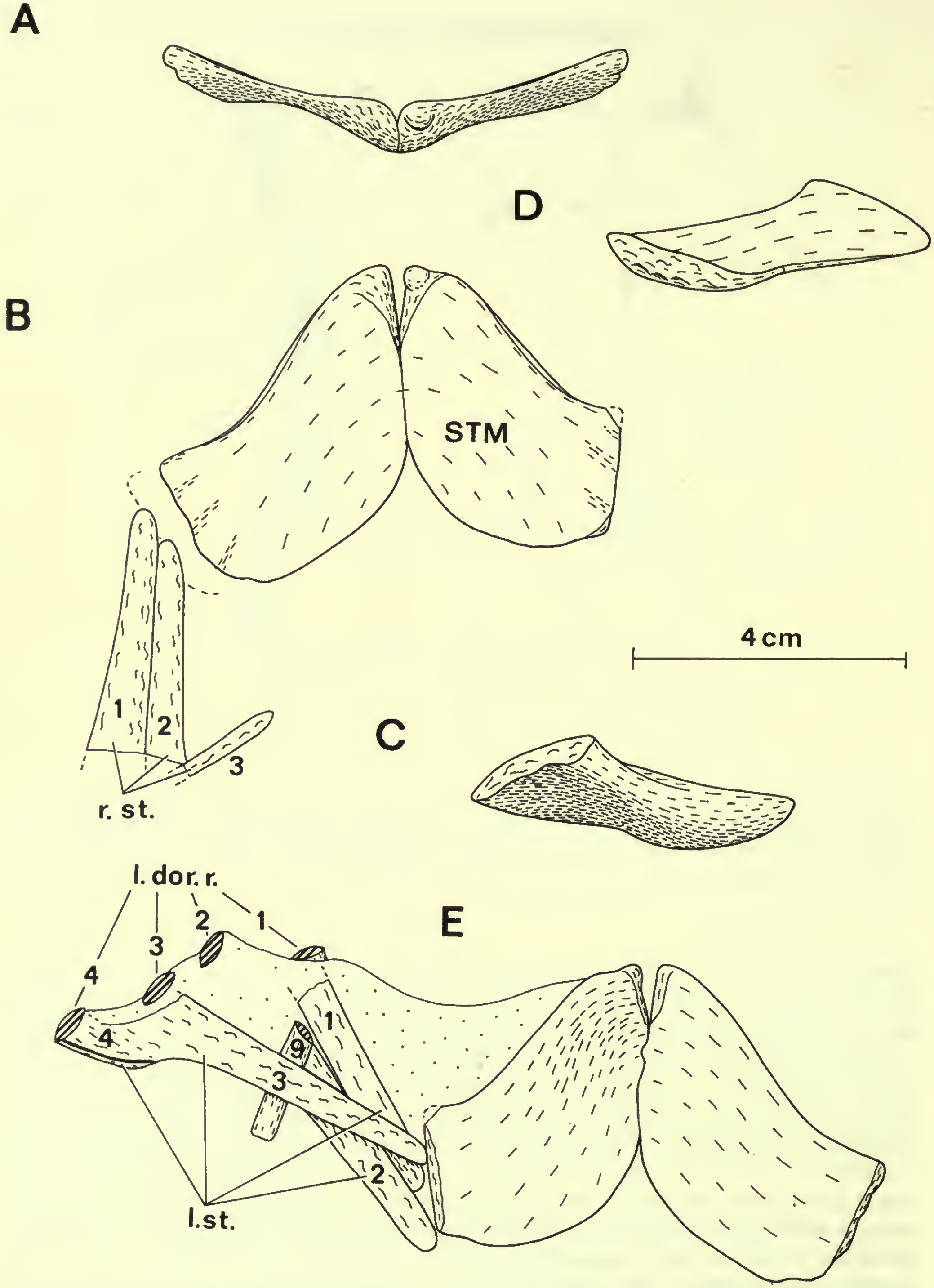

FIG. 37. *Hypsilophodon foxii.* Sternum R196, × 1. A, anterior view; B, ventral view with sternal section of dorsal ribs 1–3 displaced slightly; C, lateral view right sternal bone; D, medial view of right sternal bone; E, dorsal view with dorsal ribs 1–4. Abbreviations: STM, sternum; l dor r, dorsal ribs of left side; l st, sternal segments of left dorsal ribs; r st, sternal segments of right dorsal ribs.

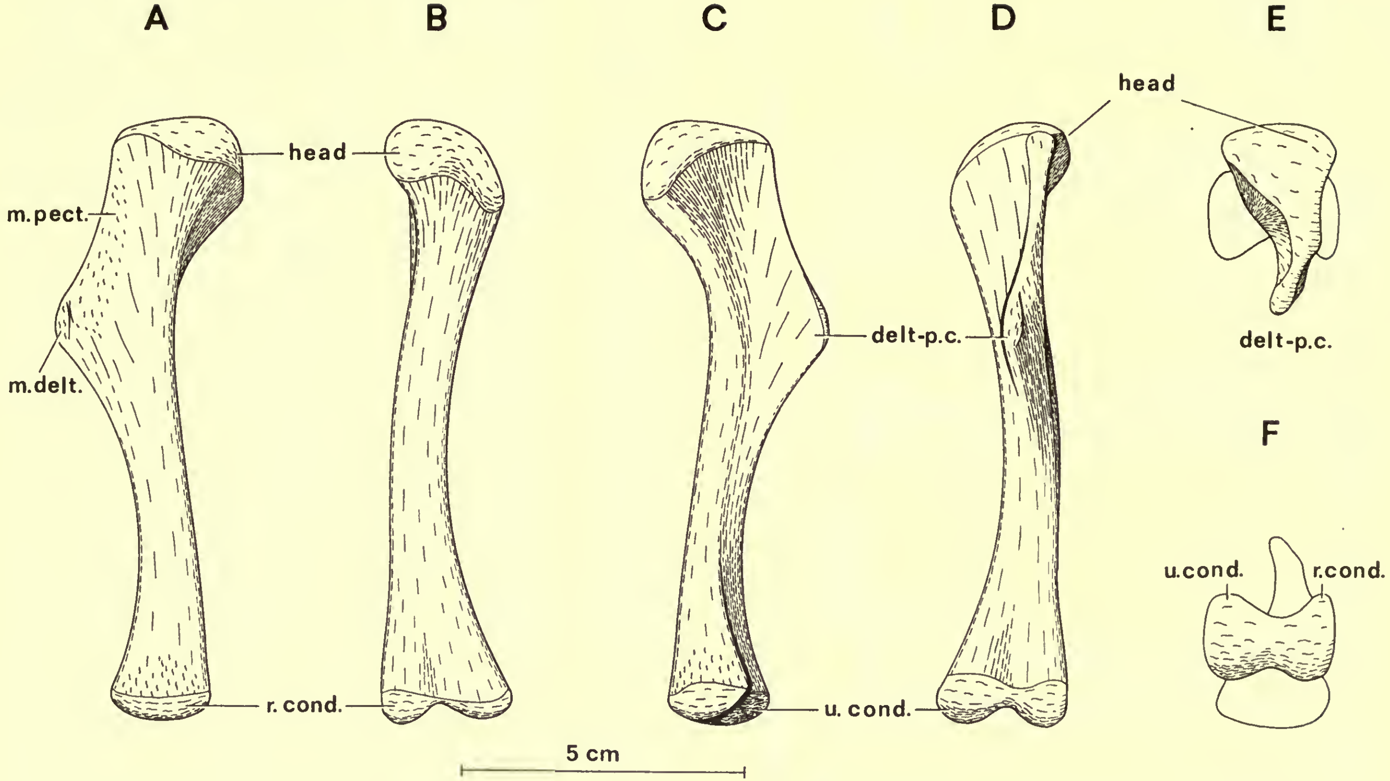
A
B
C
D
E
head
m.pect.
m.delt.
head
r. cond.
delt-p.c.
u. cond.
head
delt-p.c.
F
u.cond.
r.cond.
5 cm

Fig. 38. *Hypsilophodon foxii.* Humerus R196, × ¾. A, lateral view ; B, posterior view ; C, medial view ; D, anterior view ; E, proximal view ; F, distal view. Abbreviations : delt-p.c, deltopectoral crest ; m delt., M. deltoideus ; m pect., M. pectoralis ; rc or r cond., radial condyle ; uc or u cond., ulnar condyle.

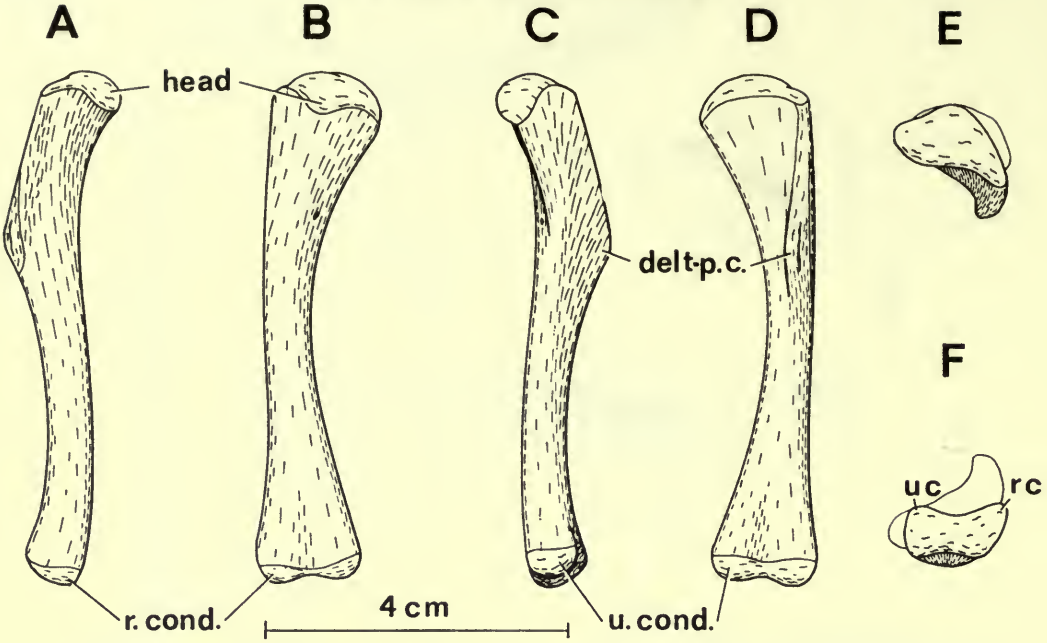

FIG. 39. *Hypsilophodon foxii.* Humerus R5830, × 1. Views and abbreviations as in Text-fig. 38.

The shaft is more twisted in R196 (Text-fig. 38) and R5829 than it is in the smaller R5830 (Text-fig. 39). A comparable difference occurs between small, medium-sized and larger humeri in *Protoceratops* (Brown & Schlaikjer 1940, fig. 27), so this is probably an age variation.

Ulna. The olecranon process is moderately well developed. The edges of the proximal end (Text-fig. 40E) continue along the tapering shaft to the slightly expanded and somewhat compressed distal end. The shaft is roughly triangular in cross-section with a slightly concave medial surface which becomes more strongly so distally (Text-figs. 40C, E). The dorsal ridge (Text-figs. 40D, E) continues to the thick and rounded antero-lateral (radial) edge of the distal end. The rounded medial edge (Text-figs 40C, E) continues to the sharp postero-medial edge of the distal end. The larger lateral edge continues as a well-defined edge on the outside of the shaft but merges with the convex lateral face of the distal end. The middle part of the shaft anterior to this ridge is slightly concave. Proximally there is a well-defined rugose bump (u, Text-fig. 40) while distally there are two rugose areas (v, w, Text-fig. 40).

Swinton (1936, fig. 6) figured the ulna and radius of R5830; he stated (: 564) that 'the right ulna . . . is preserved in perfect condition' and gave the length of the radius (: 566) and ulna (: 565). However, the forearm on both sides is represented only by proximal ends with that of the right radius mounted as a distal end. There are several odd distal ends in the Hooley Collection that have been referred to R5830, but none of these definitely fits on to the bones from the mounted skeleton.

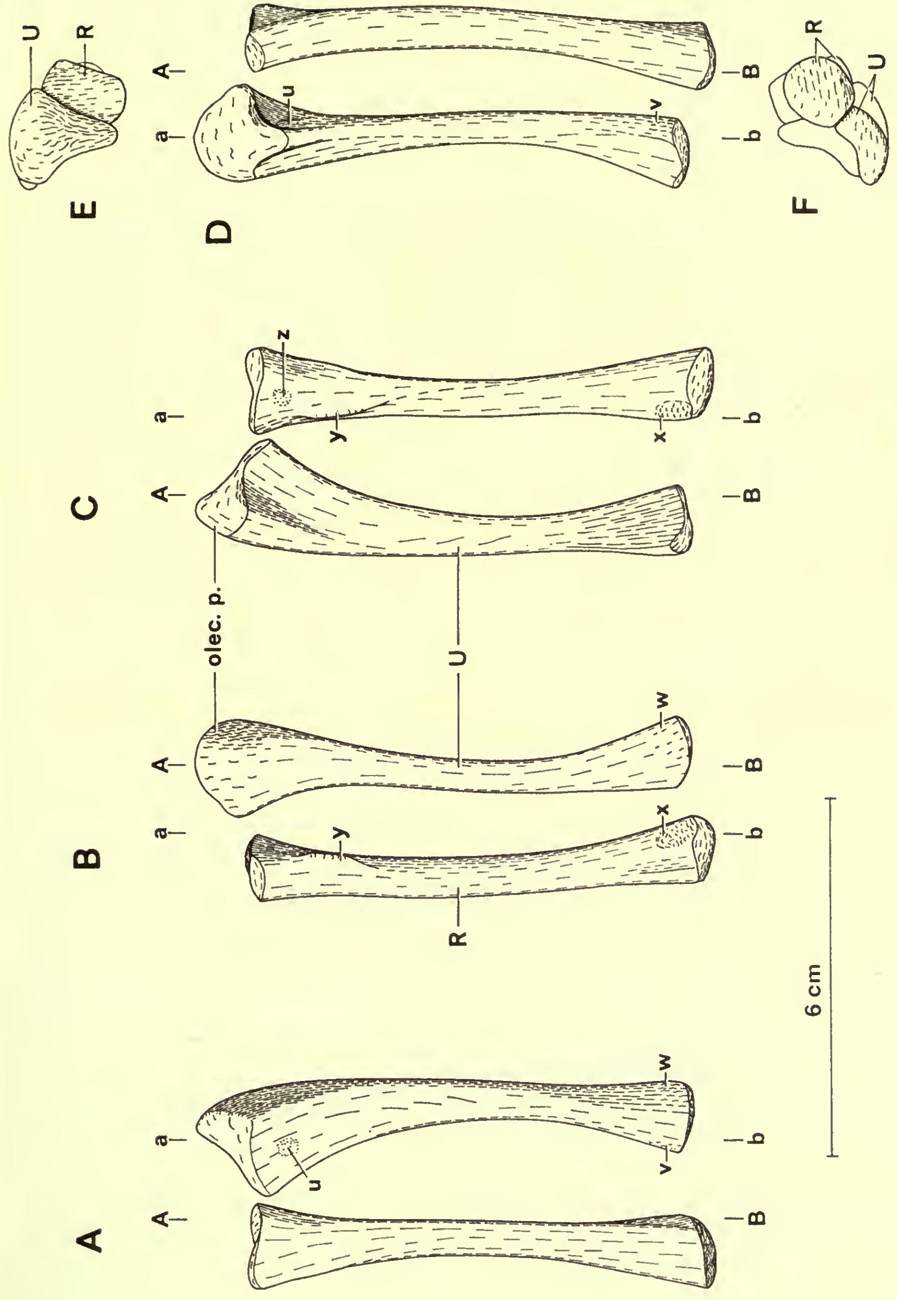
A
a
A
B
b
u
v
w
B
a
A
R
y
x
b
B
olec. p.
U
w
C
A
a
z
y
x
B
b
D
a
A
u
v
b
B
E
U
R
F
R
U
6 cm

Fig. 40. *Hypsilophodon foxii.* Radius and ulna R196, × ¾. In views A–D the radius and ulna have been separated – for natural articulation superimpose line AB on ab in each case. A, lateral view; B, ventral or posterior view; C, medial view; D, dorsal or anterior view; E, proximal view; F, distal view. Abbreviations: olec. p., olecranon process; R, radios; U, ulna; u, v, w, x, y, z, areas with rugose surface markings.

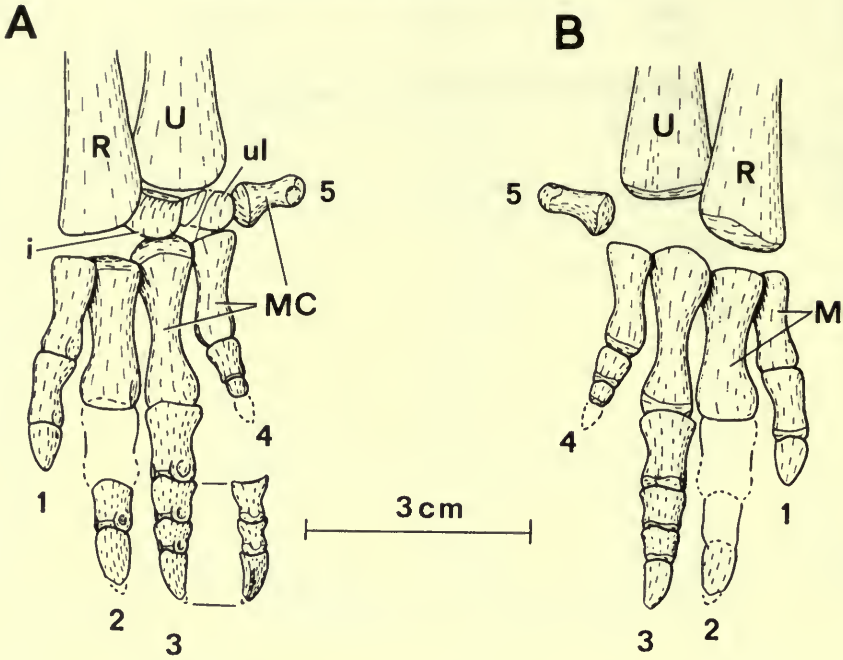

FIG. 41. *Hypsilophodon foxii.* Manus R196, × 1. A, dorsal view; B, ventral view. Abbreviations: MC, metacarpal; R, radius; U, ulna; 1–5, digits; i, intermedium; ul, ulnare.

Radius. The articular surface on the proximal end is concave along one diagonal and convex across the other (Text-fig. 40E). The shaft is subtriangular in section. The medial edge in the middle of the shaft is sharp but it is more rounded proximally and distally. The lateral edge is very slight and gently rounded distally. Proximally there is a well-defined ridge with insertion markings (y, Text-figs. 40B, C) while distally there is a rugose area (x, Text-figs. 40B, C).

Carpals. As noted by Hulke (1882), the wrist of the only complete manus (Text-fig. 41) is traversed by a seam of carbonaceous material that has obliterated the radiale and distal carpals and bisected the ulnare. The dorsal surfaces of the *ulnare* and of the adjacent *intermedium* of R196 are transversely concave (Text-fig. 41A). As preserved, it is impossible to determine the shape of the ulnare. The distal surface of the intermedium is rounded transversely and probably articulated against the distal carpals. The only trace of a *distal carpal* in R196 is a small corner which is wedged medially between the ulnare and metacarpal IV (Text-fig. 41A). The space between the radius and metacarpals I and II may indicate the outline of the *radiale.*

Three rather distorted carpal bones were obtained from the disarticulated partial manus of R2473 (Hulke 1873, pl. 18, fig. 3). These were matched with elements in the Hooley Collection that have now been referred to R5830. The *intermedium* corresponds closely with that of R196. The dorsal (Text-fig. 42a) and ventral

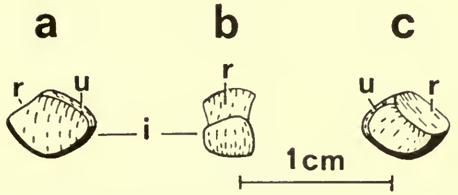

FIG. 42. *Hypsilophodon foxii.* Intermedium R5830, × 2. a, dorsal view; b, lateral view; c, ventral view. Abbreviations: i, intermedium; r, surface for radius; u, surface for ulna.

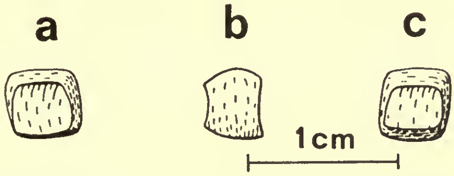

FIG. 43. *Hypsilophodon foxii.* Bone 1, R5830, × 2. Views as in Text-fig. 42.

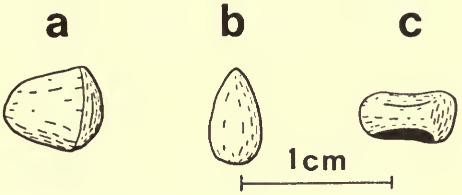

FIG. 44. *Hypsilophodon foxii.* Bone 2, R5830, × 2. Views as in Text-fig. 42.

(Text-fig. 42c) surfaces are transversely concave with a polished surface. The surface for the radius (r, Text-fig. 42) is concave but the remaining surfaces are convex laterally and transversely. These slope slightly inwards as the ventral surface is slightly smaller than the dorsal. The other two bones have been tentatively orientated as shown in Text-figs. 43 and 44. The second bone is a cube with a transversely concave dorsal surface and a similar but slightly smaller ventral surface (Text-figs. 43a, c). The four articular sides are gently convex laterally and transversely. This bone is either the radiale or the ulnare. The third bone has an irregular shape (Text-fig. 44) without the polished surfaces of the intermedium and the second bone; in this it resembles the distal tarsals.

Hulke (1882, pl. 79) showed the space in the wrist of R196 bounded proximally by the radius, intermedium and ulnare and distally by metacarpals I, II and III. Abel (1911, fig. 12) in his reconstruction closed this space so that there is practically no room for the radiale and none for any distal carpals. In contrast Steiner (1922, fig. 17) put the radiale and two distal carpals in this space, with a small first distal carpal and a second which is larger than the ulnare. Though Steiner's figure is

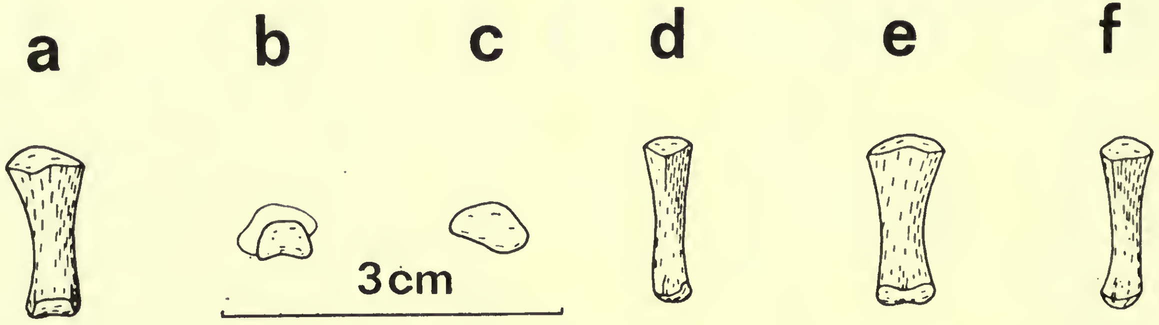

FIG. 45. *Hypsilophodon foxii.* Third metacarpal R5830, × 1·5. a, dorsal view ; b, distal view ; c, proximal view ; d, lateral view ; e, ventral view ; f, medial view.

'after Hulke', Hulke did not in fact indicate these details. Heilmann (1926, fig. 116) showed a radiale and the dotted outline of four distal carpals. In *Thescelosaurus,* the two distal carpals are equal in size and much smaller than the ulnare (Gilmore 1915, fig. 11). However, if the second bone (Text-fig. 44) is a distal carpal then Steiner's reconstruction (1922) may be correct.

Metacarpals. The third metacarpal (Text-fig. 45) has a well-rounded proximal end with well-defined lateral and medial edges. The shaft in cross-section is a circle slightly flattened dorso-ventrally. The muscle grooves on the distal condyles are not strongly developed. There is no dorsal intercondylar groove and the ventral one is shallow. The size and shape of the metacarpals are shown in Text-fig. 41. As preserved the distal ends of metacarpals I, II, and III are inclined at an angle of about 45 degrees to a line through the carpus. The proximal ends are inclined at a slightly steeper angle and, though the area of contact is small, they are packed together. The proximal end surface of metacarpals II and III are rounded and slope. Metacarpal III is more slender and longer than metacarpal II. The proximal end of metacarpal IV is triangular and the condylar region is in the same plane as the carpus. Metacarpal V as preserved is set at quite an obtuse angle to the others but in life this was probably less marked.

Phalanges. The phalangeal counts of the first three digits are definitely 2, 3 and 4 respectively. The fourth metacarpal bears two phalanges and Hulke (1882) noted that the distal half of the second of these was missing, as was the continuation of the digit. Further development has exposed the ventral surface and the distal articular surface is practically complete so that only a small part of this phalanx is missing. Metacarpal V has a distal condyle but there is no evidence concerning the number of phalanges. Gilmore (1915 : 600) tabulated the phalangeal formula of *Hypsilophodon* as 2, 3, 4, 3, 2. This may be correct but the evidence from specimen R196 suggests the formula 2, 3, 4, 3 (? +), 1 (? +).

iii) THE PELVIC GIRDLE

Ilium. In external view (Text-figs. 46A, 48, 49) the dorsal part of the ilium of *Hypsilophodon* forms a thin and almost flat sheet of bone ; ventrally the bone is much thicker and the surface curves outwards to the acetabulum. The dorsal edge is sharp with a bevel running along most of its length. The posterior edge is rather square in section with a rugose surface while the postero-ventral edge is sharp. The anterior process of the ilium curves outwards with the lateral surface facing slightly dorsally (Text-figs. 50A, 51A). This curvature enabled the process to clear the adjacent ribs, provided a larger insertion area for part of the M. dorsalis trunci and permitted a more fore-and-aft action of the M. ilio-tibialis 1 (Text-fig. 49, see Galton 1969). In addition the amount of antero-ventral curvature varies a great deal between individuals ; the ilia can be arranged in a series that shows a progressive increase in the degree of curvature (Text-figs. 49A, 46A, 48A and 48B). This variation is independent of the sacral type because only R196 has a pentapleural sacrum. The outer edge of the ventral margin of the anterior process is rounded in all specimens, but the inner edge is more variable. In R196 (Text-figs. 51B, C) it is rounded

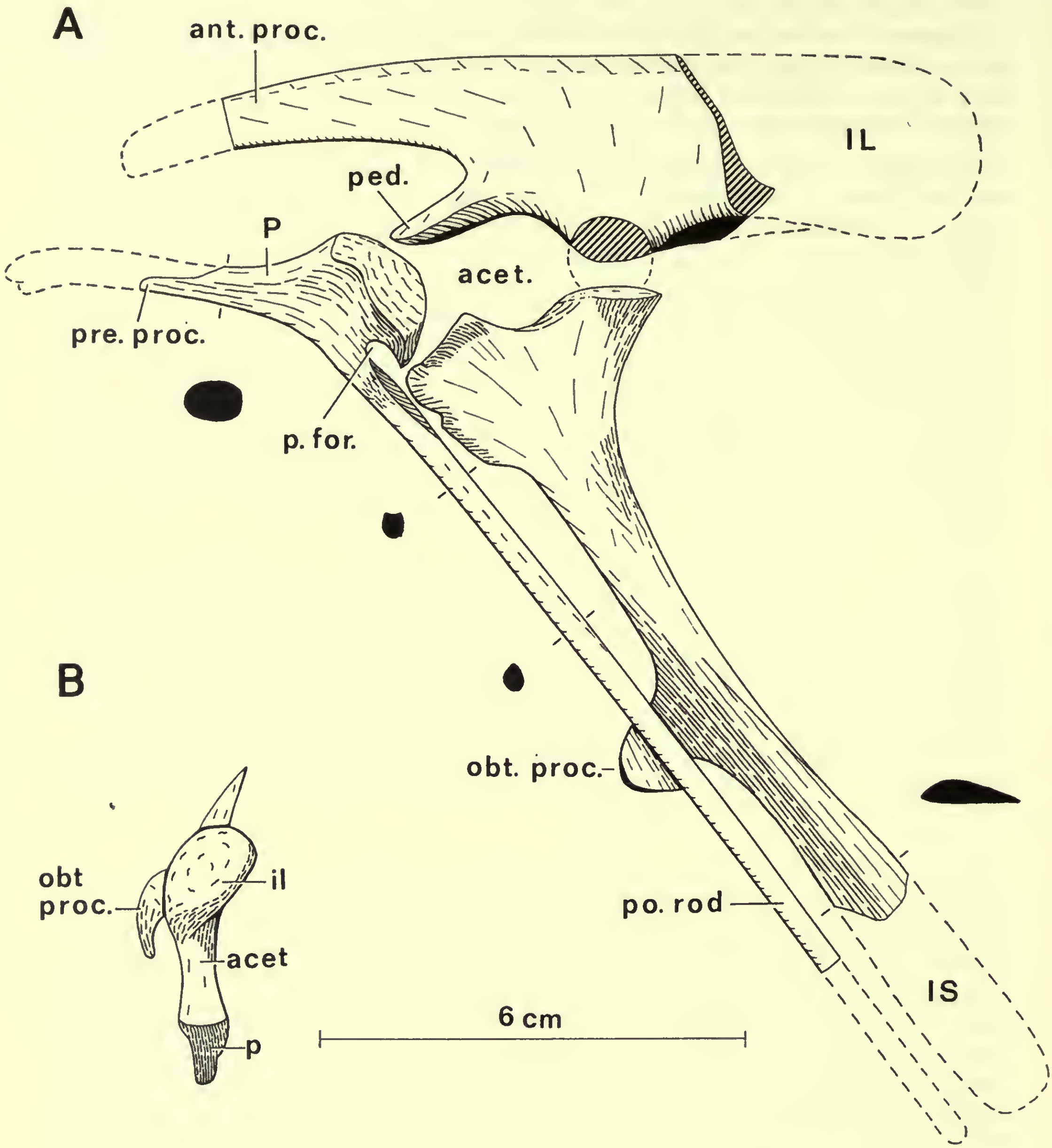
A
ant. proc.
IL
ped.
P
acet.
pre. proc.
p. for.
B
obt. proc.
obt
proc.
il
acet
p
po. rod
IS
6 cm

FIG. 46. *Hypsilophodon foxii.* Pelvic girdle R195, × 1. A, lateral view; B, acetabular view of ischium. Abbreviations for Text-figs. 46–53. IL, ilium; IS, ischium; P, pubis; acet., acetabulum; ant. proc. or a. p., anterior process; brev. sh., brevis shelf; il., surface for ilium; is., surface for ischium; obt. p., obturator process; p., surface for pubis; ped., peduncle; p. for., pubic foramen; po. rod., post-pubic rod; pre. proc., prepubic process.

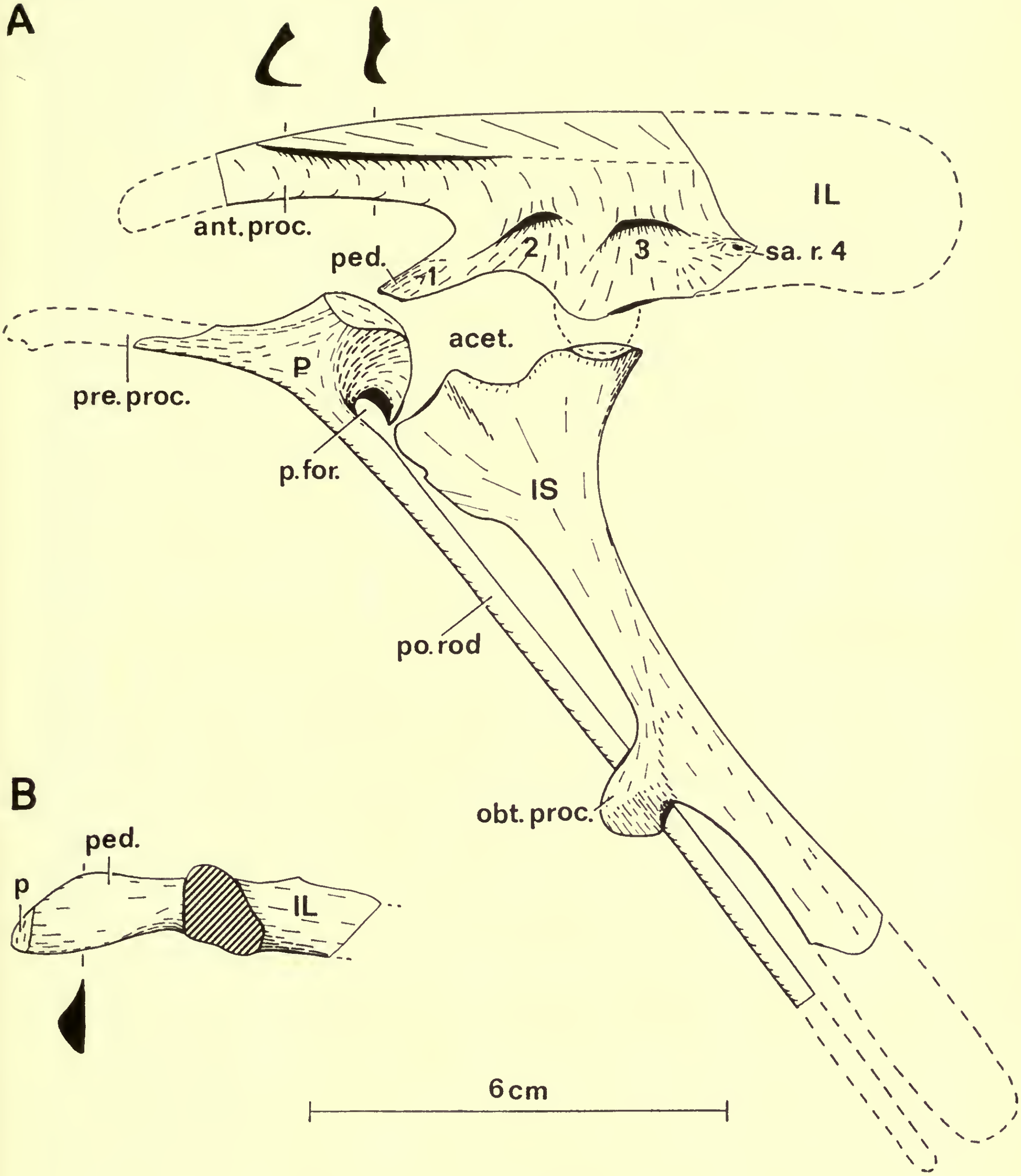
A
IL
ant. proc.
ped.
1
2
3
sa. r. 4
acet.
P
pre. proc.
p. for.
IS
po. rod
obt. proc.
B
ped.
p
IL
6 cm

FIG. 47. *Hypsilophodon foxii.* Pelvic girdle R195, × 1. A, medial view; B, acetabular part of the ilium. For abbreviations see page 84.

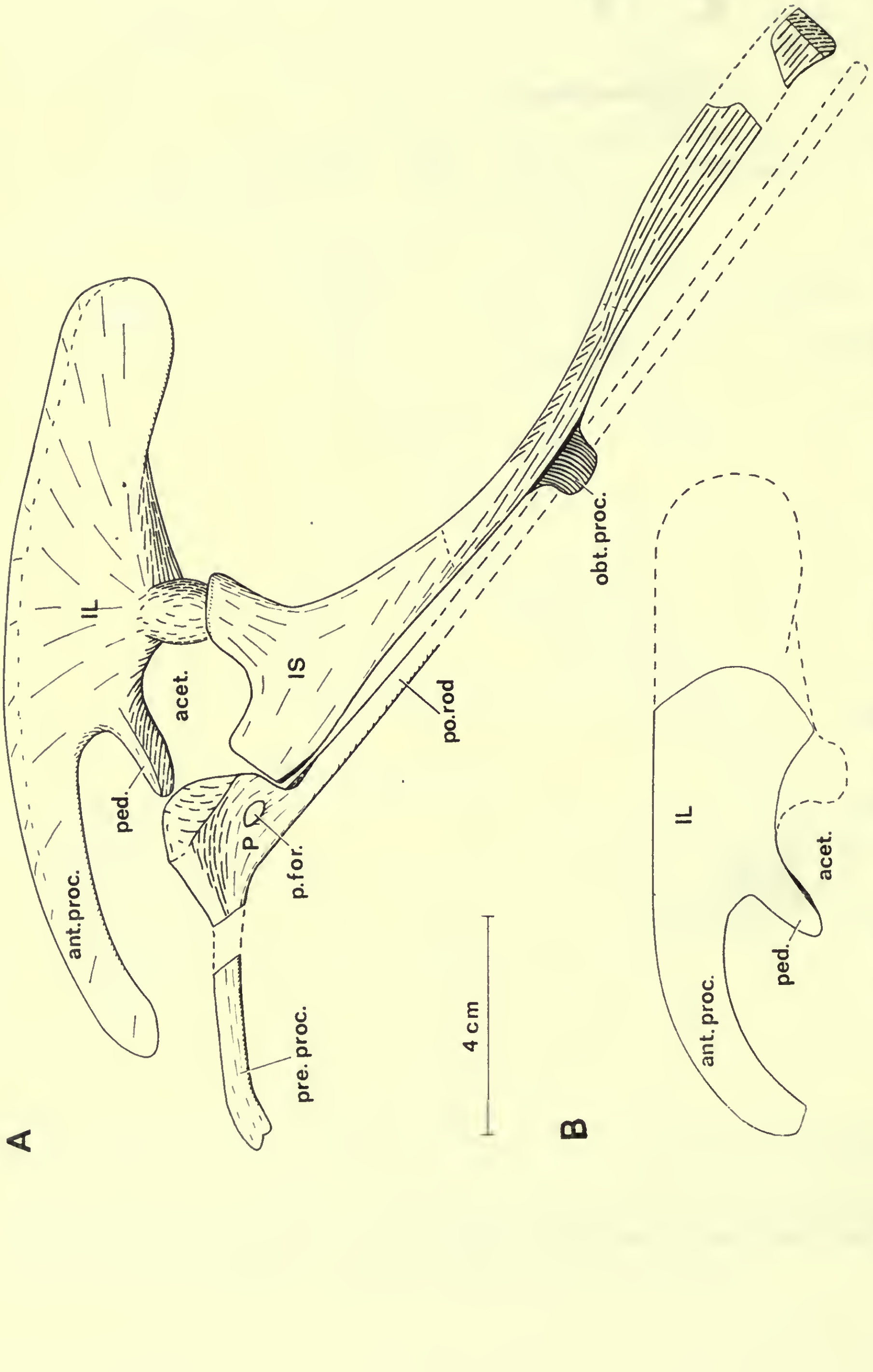
A
IL
acet.
IS
po.rod
obt.proc.
ped.
ant.proc.
P
p.for.
pre.proc.
4 cm
B
IL
acet.
ped.
ant.proc.

FIG. 48. *Hypsilophodon foxii.* A, pelvic girdle R196, × ¾, lateral view; B, ilium R2477a, × ¾, lateral view. For abbreviations see page 84.

and somewhat thicker than the rest of the process. In R2477a the inner part forms a small ledge, which in R193 (Text-figs. 50B, C), R2477b and R195 (Text-fig. 47A) shows a progressive increase in size. This ledge is mainly sharp-edged, though it becomes reduced and rounded both anteriorly and posteriorly. This variation too is independent of the sacral type. The slender anterior peduncle is triangular in section with a sharp outer edge (Text-fig. 47B) which disappears posteriorly. Its ventral surface is broad and flat. It is broader in forms with the hexapleural sacrum (Text-figs. 47B, 50C) than in those with the pentapleural type (Text-figs. 51C, R2477b).

A prominent ridge runs along the medial surface (Text-figs. 47A, 50B, 51B) of the anterior process. Ventral to this there is a longitudinal depression which is bordered by the internal ledge mentioned above. Anteriorly another, much smaller, ridge runs diagonally across the process. The thicker ventral region of the ilium bears the rugose facets for the sacral ribs. The ledge below these sacral facets is sharp-edged except for the section that lies internal to the ischiadic head of the ilium.

In all the ilia the first sacral rib fits on to the dorso-medially facing inner surface of the peduncle. The facets for the remaining sacral ribs are more anteriorly placed in R196 (Text-fig. 51B) than they are in R193 (Text-fig. 50B) and R195 (Text-fig. 47A), both of which have a hexapleural sacrum. In both types there is a projecting edge above facets 2 and 3. There is a similar edge above facet 4 in R196 but this facet is only partly on the brevis shelf (Text-fig. 51). In R195 the whole facet is on the brevis shelf and, anteriorly at least, there is a dorsal edge (Text-fig. 47A). In R193 there is no dorsal edge and the facet is obliquely inclined (Text-fig. 50), in contrast to its much more vertical position in the others.

Pubis. The anterior end of the pubis is slightly flattened (Text-fig. 48A). The outer surface of the prepubic process is flat with well-developed striations (Text-fig. 49) and the ventral edge is grooved. The function of the prepubic process has been discussed elsewhere (Galton 1969, 1970a) and it was suggested that the striations were for a limb muscle (M. ilio-femoralis internus, M. pubo-tibialis or M. ambiens). The ventral part of the stout acetabular region is laterally constricted and has a rounded ventral edge (Text-fig. 52B). The outer surface (Text-figs. 46A, 48A, 49A) is hollowed anteriorly into a shallow and approximately circular depression, but above the obturator foramen this surface is convex. The inner surface (Text-fig. 47A) is slightly concave anteriorly, but it is convex at the root of the post-pubic rod. Posteriorly the inner surface is strongly concave and funnels into the obturator foramen (Text-fig. 47A). The postero-dorsal articular region is rough-textured and, except anteriorly, is sharp-edged.

The obturator region is variable. Among the smaller individuals there is a notch in R195 (Text-fig. 47A) but a foramen in R196 (Text-fig. 48A) ; among the larger individuals there is a notch in R5829 but a foramen in R193 (Text-fig. 49A). It is apparent that this is an individual variation. In those specimens where closure of the notch has occurred, R196 shows no trace of a suture, while in R193 a suture is visible on the lateral surface only ; in the latter specimen there is no evidence as to when closure occurred (growth stages of the same individual would be needed for this). Anteriorly the post-pubic rod has a dorsal sheet which may be variously

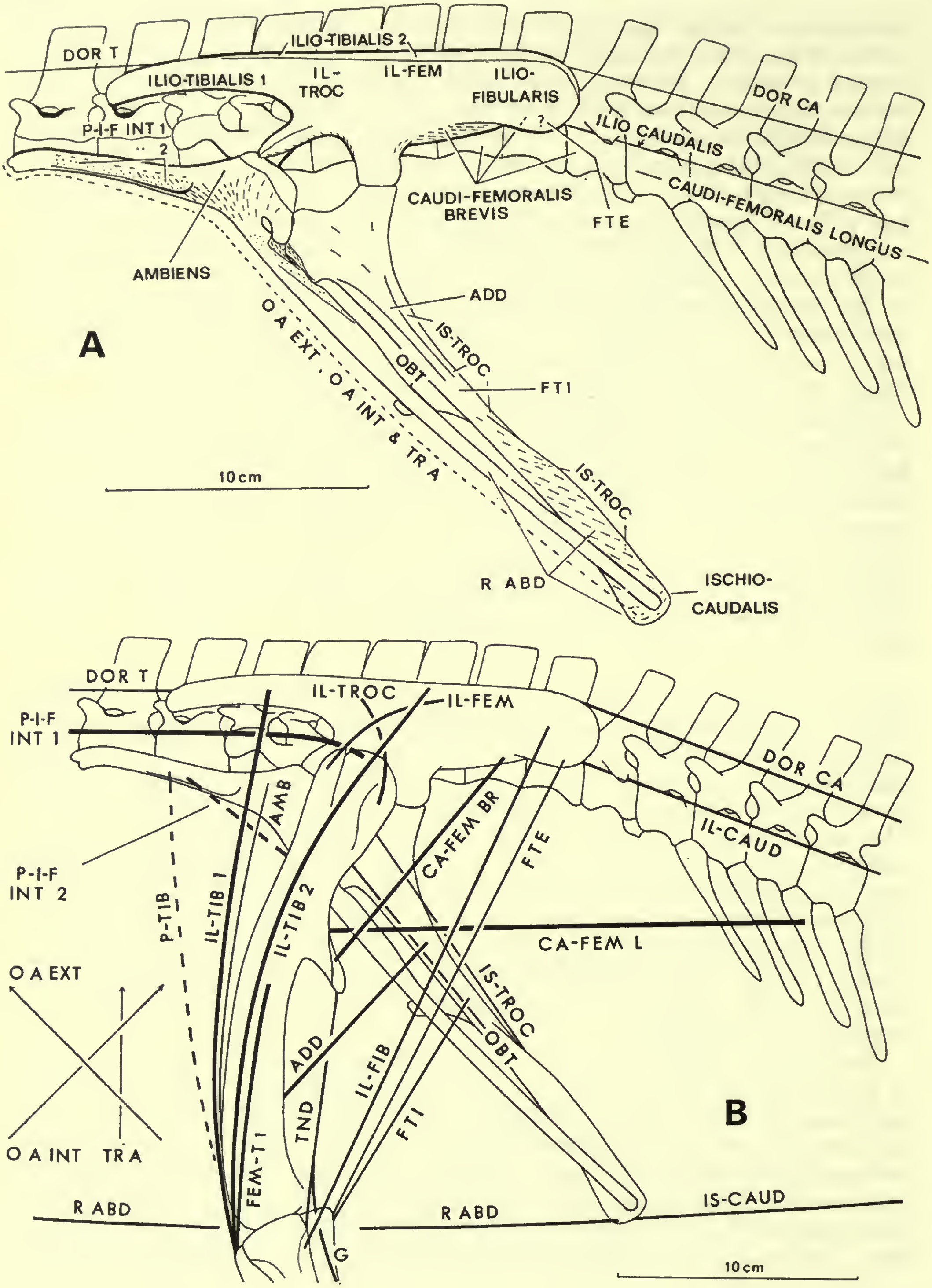
A
DOR T
ILIO-TIBIALIS 2
ILIO-TIBIALIS 1
IL-TROC
IL-FEM
ILIO-FIBULARIS
?
DOR CA
ILIO CAUDALIS
P-I-F INT 1
2
CAUDI-FEMORALIS BREVIS
FTE
CAUDI-FEMORALIS LONGUS
AMBIENS
ADD
IS-TROC
OBT
O A EXT, O A INT & TR A
FTI
10 cm
IS-TROC
R ABD
ISCHIO-CAUDALIS
B
DOR T
IL-TROC
IL-FEM
P-I-F INT 1
AMB
CA-FEM BR
FTE
DOR CA
IL-CAUD
P-I-F INT 2
P-TIB
IL-TIB 1
IL-TIB 2
CA-FEM L
O A EXT
IS-TROC
ADD
OBT
IL-FIB
TND
FTI
O A INT
TR A
FEM-T1
R ABD
R ABD
IS-CAUD
G
10 cm

developed. In R196 it is absent (Text-fig. 48A); in R195 it is small and faces dorso-medially (Text-figs. 47A, 48A); in R5829 it is larger; and in R193 it is very well developed (Text-fig. 49A). The edge is thickened in R193, forming with the most anterior part a triangular area with an irregular surface.

Ischium. The ischium consists of a proximal head-region which is separated from the large flat blade region by a constricted shaft (Text-figs. 46A, 48A, 49A, 53). Ventrally the head and shaft merge in R196 (Text-fig. 48A) and R5830 (Text-fig. 53E) but this junction becomes progressively more marked in the series R5829, R195 (Text-fig. 46A) and R193 (Text-fig. 49A). This is probably an individual variation. The shaft is twisted so that the blade is at an angle of about 45 degrees to the head. The inner surface of the blade therefore faces dorso-medially. This surface and the internal surface of the head meet along a diagonal line which continues distally on to the base of the obturator process (Text-fig. 47A). In relation to the rest of the ischium the acetabular region is longer in R196 (Text-fig. 48A) than it is in R193 (Text-fig. 49A) or R195 (Text-fig. 46A) and the ventral part is lengthened to a corresponding degree. At the anterior end of the acetabular region there is an internal expansion which is more strongly developed in R196 (Text-fig. 53D) than in R195 (Text-fig. 46B). The internal surface below this process forms a shallow depression.

The dorsal edge of the shaft is rounded. Ventrally, the shaft is sharp-edged and distally this edge curves abruptly downwards and inwards to form the obturator process (Text-fig. 47A). Posteriorly, the shaft gradually thins out as it merges into the blade region. This continuation of the shaft tends to cross from the outer to the inner edge because of the outward curve of the blade relative to the shaft. The distal part of the ischium is straight, flat and blade-like. Anteriorly, on the dorsal

FIG. 49. *Hypsilophodon foxii.* A, pelvic girdle R193 in lateral view to show areas of attachment of the individual muscles. Data also from R196 and 28707. Figure from Galton (1969, fig. 6; see fig. 7 for stereo-photograph of pubis and ischium R193) in which the areas are described. B, reconstruction of the pelvic region showing the lines of action of the individual muscles. Data from R193, R196, R5830 and 28707. Figure from Galton (1969, fig. 4). Compare with Text-fig. 55.

The muscles have been abbreviated as follows:

ADD	M. adductor femoralis	IS-CAUD	M. ischio-caudalis
AMB	M. ambiens	IS-TROC	M. ischio-trochantericus
CA-FEM BR	M. caudi-femoralis brevis	LIG	ligaments for holding head in acetabulum
CA-FEM L	M. caudi-femoralis longus		
DOR CA	M. dorsalis caudae	O A EXT	M. obliquus abdominis externus
DOR T	M. dorsalis trunci	O A INT	M. obliquus abdominis internus
FEM-T 1, 2 & 3	M. femoro-tibialis 1, 2 and 3	OBT	M. obturator internus
F T E	M. flexor tibialis externus	P-I-F INT 1	dorsal part of M. pubo-ischio-femoralis internus
F T I	M. flexor tibialis internus		
G	M. gastrocnemius	P-I-F INT 2	ventral part of M. pubo-ischio-femoralis internus
IL-CAUD	M. ilio-caudalis		
IL-FEM	M. ilio-femoralis	P-TIB	M. pubo-tibialis
IL-FIB	M. ilio-fibularis	R ABD	M. rectus abdominis
IL-TIB 1 & 2	M. ilio-tibialis 1 (sartorius) and 2	TND	tendon inserting on fibula
IL-TROC	M. ilio-trochantericus	TR A	M. transversus abdominis

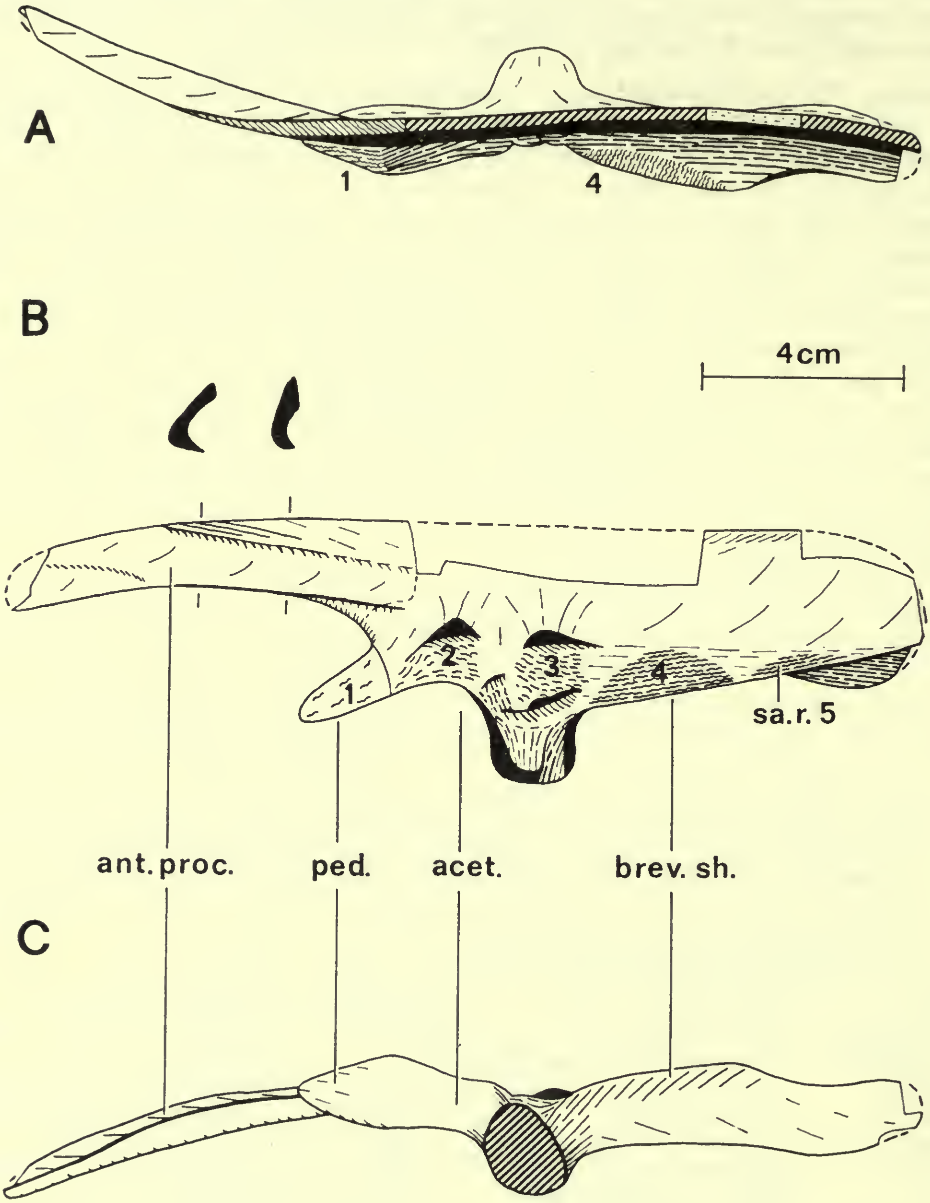
A
1
4
B
4cm
2
3
1
4
sa.r. 5
ant. proc.
ped.
acet.
brev. sh.
C

FIG. 50. *Hypsilophodon foxii*. Ilium R193, × ⅔. A, dorsal view; B, medial view; C, ventral view. For abbreviations see page 84.

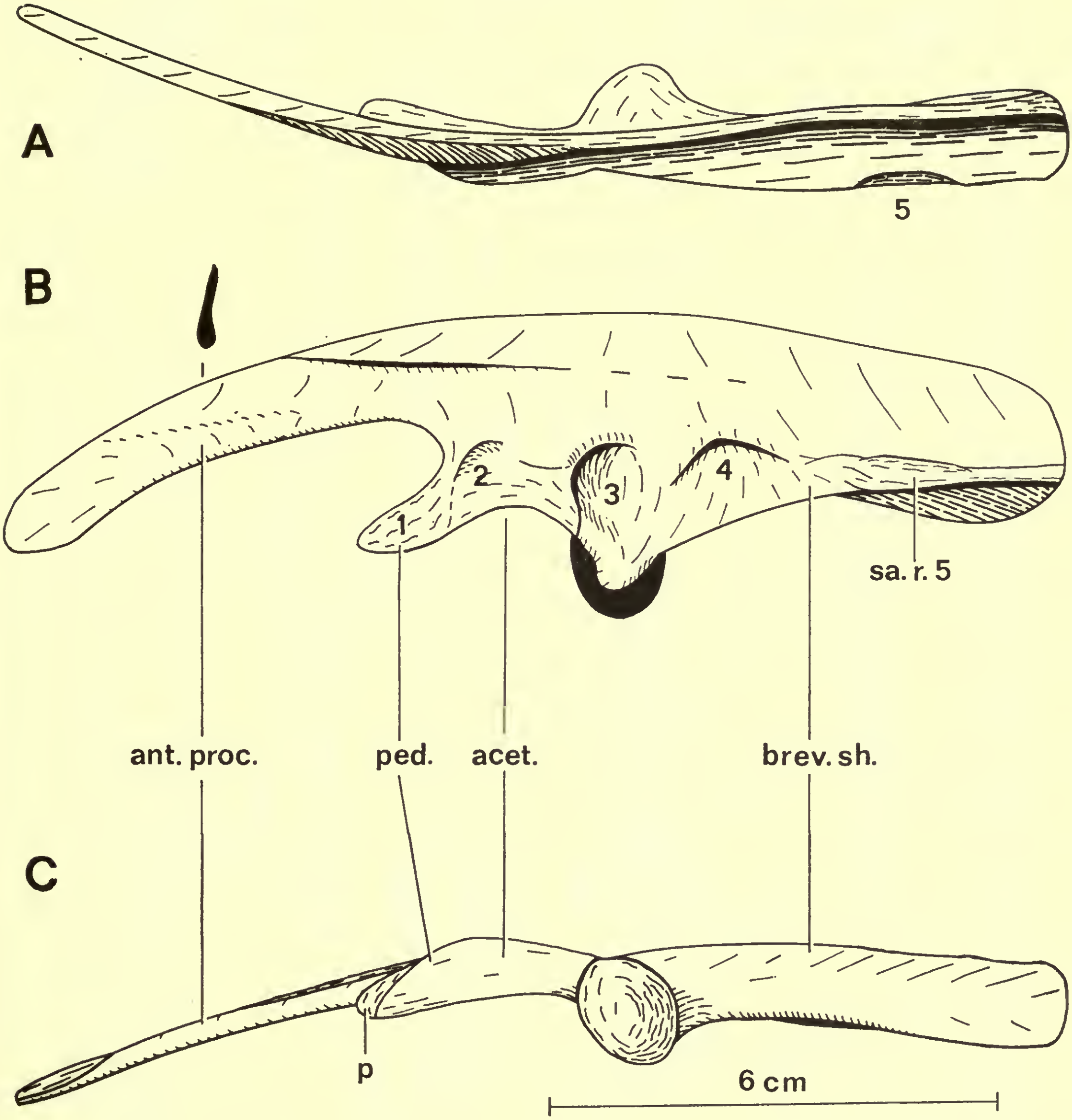
A
5
B
1
2
3
4
sa. r. 5
ant. proc.
ped.
acet.
brev. sh.
C
p
6 cm

FIG. 51. *Hypsilophodon foxii*. Ilium R196, × 1. A, dorsal view; B, medial view; C, ventral view. For abbreviations see page 84.

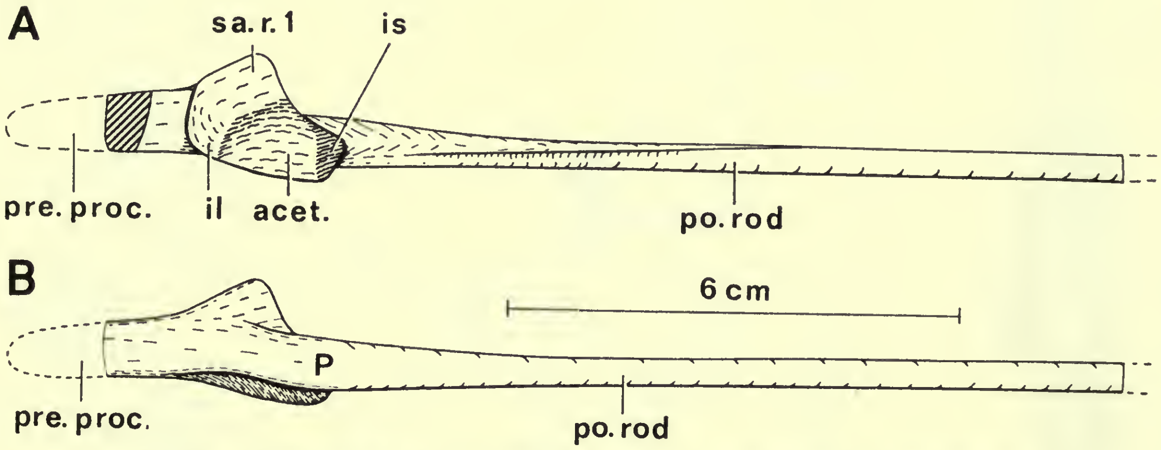
A
sa. r. 1
is
pre. proc.
il
acet.
po. rod
B
6 cm
P
pre. proc.
po. rod

FIG. 52. *Hypsilophodon foxii.* Pubis R195, × 1. A, dorsal view ; B, ventral view. For abbreviations see page 84.

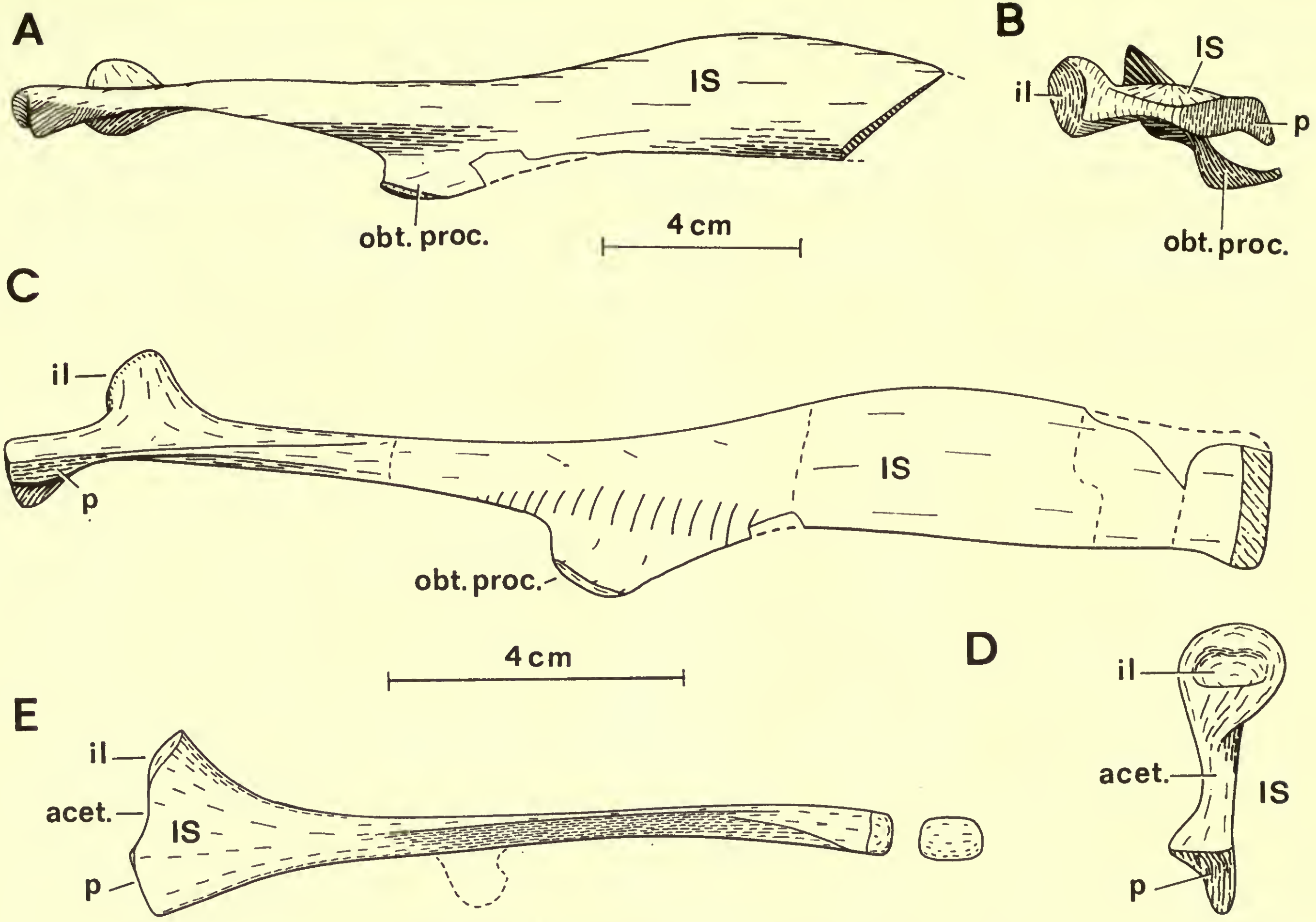
A
IS
obt. proc.
4 cm
B
IS
il
p
obt. proc.
C
il
p
IS
obt. proc.
4 cm
D
il
acet.
IS
p
E
il
acet.
IS
p

FIG. 53. *Hypsilophodon foxii.* Ischium R193, × ⅔. A, ventral view; B, proximal view. Ischium R196, × 1. C, ventral view; D, proximal view. Ischium R5830, × 1. E, lateral view. For abbreviations see page 84.

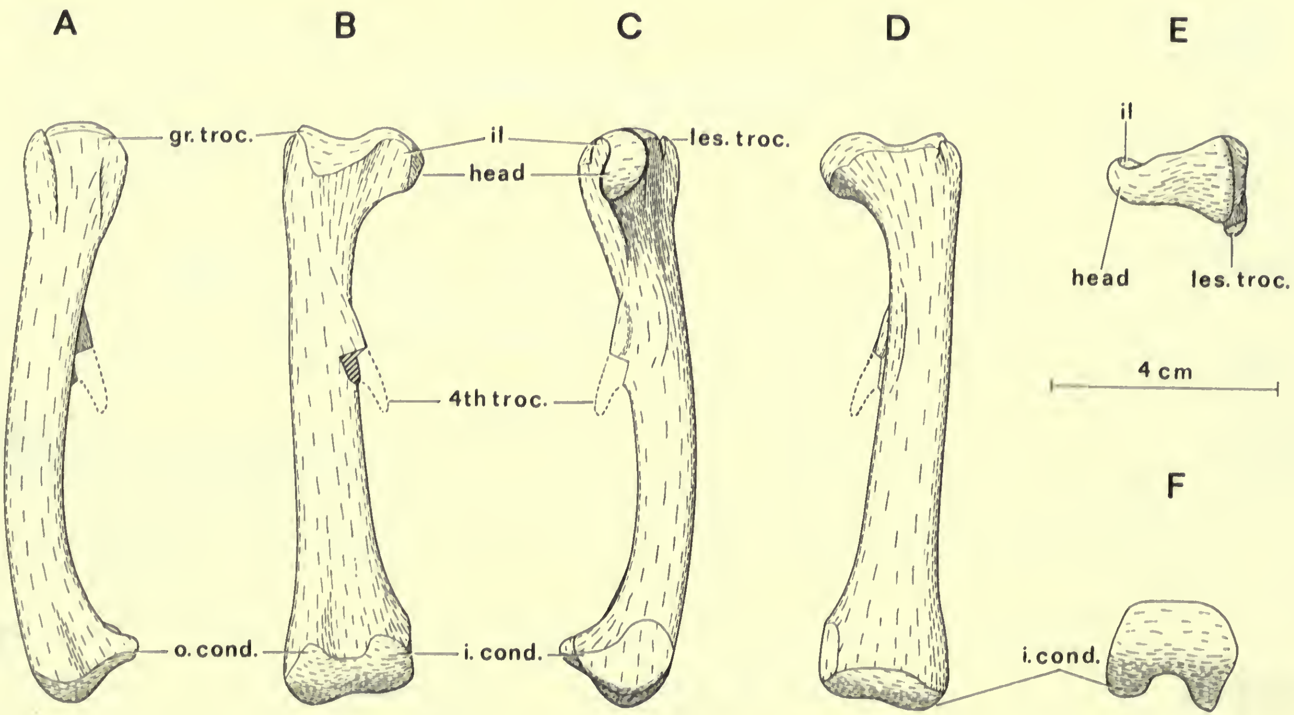
A
B
C
D
E
gr. troc.
il
head
les. troc.
4th troc.
o. cond.
i. cond.
il
head
les. troc.
4 cm
F
i. cond.

FIG. 54. *Hypsilophodon foxii.* Femur R5830, × ¾. A, lateral view ; B, posterior view ; C, medial view ; D, anterior view ; E, proximal view ; F. distal view. Abbreviations : gr. troc., greater trochanter ; i. cond., inner condyle ; il., depression for ischiadic head of ilium ; les troc, lesser trochanter ; o. cond, outer condyle ; 4th troc, fourth trochanter.

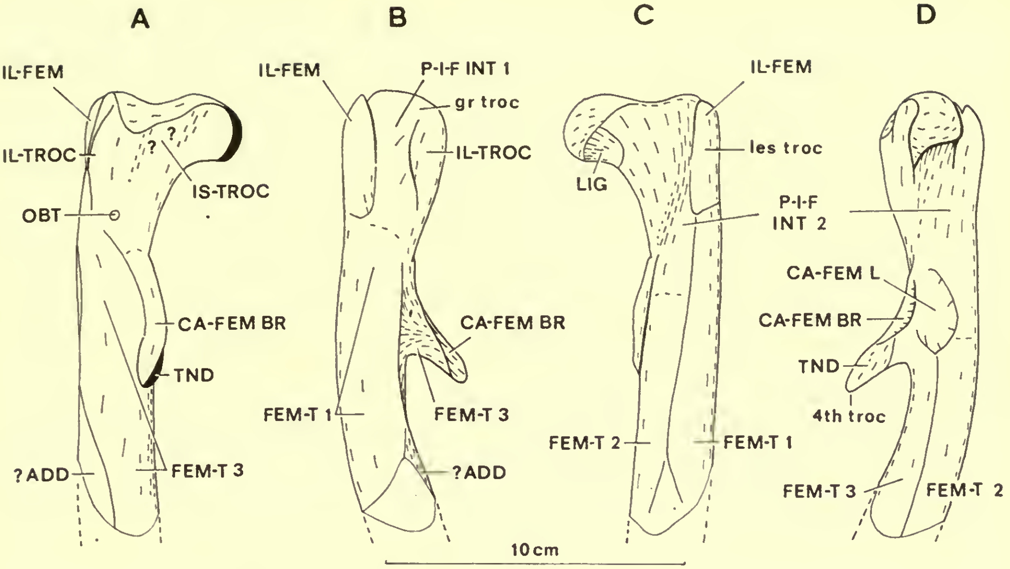

FIG. 55. *Hypsilophodon foxii*. Femur showing the areas of attachment of the limb muscles, mainly R193 with data from R196 and R5830. From Galton (1969, fig. 10; see fig. 8 for stereo-photograph of femur of R193) in which the areas are described. A, posterior view; B, lateral view; C, anterior view; D, medial view. Abbreviations: gr. troc., greater trochanter; les. troc., lesser trochanter; 4th troc, fourth trochanter. For abbreviations of muscles see Text-fig. 49.

surface of the blade, there is a definite depression above the obturator process (Text-fig. 47A). In R196 alone, a groove is present along the upper region of the outer surface of the blade. The dorsal edge of the blade is sharp. Ventrally, it is also sharp-edged, but it thickens distally to form an almost square edge. The distal end of the blade is swollen, with a rugose surface (Text-fig. 53E).

iv) THE HINDLIMB

Femur. The shaft of the femur is twisted so that the outer surface at the proximal end becomes the anterior surface more distally (Text-fig. 54D). The lesser trochanter is somewhat triangular in section (Text-fig. 54E) and is separated from the greater trochanter by a short cleft (Text-fig. 54D). The lesser trochanter is set slightly away from the external surface of the greater trochanter but gradually merges with the shaft more distally (Text-fig. 54A). Proximally the outer surface of the greater trochanter is flat but near the posterior edge there is an 'S'-shaped ridge that separated the insertion area of the M. pubo-ischiofemoralis internus 1 from the more posterior M. ilio-trochantericus (Text-fig. 55B; see Galton, 1969 in which the areas of muscle attachment on the femur of R193 are discussed). Running diagonally across the posterior face of the head is a strongly concave depression (Text-figs. 54B, E) which is bounded internally by a stout ridge.

Behind the head the neck and shaft form an acute though rounded edge which is continuous with the sharper outer edge of the pendant fourth trochanter pointing posteriorly. The large fourth trochanter probably improved the leverage of the M. caudi-femoralis brevis (from brevis shelf of ilium; Text-fig. 49) during the first half of femoral protraction (see Galton 1969). The outer surface (Text-fig. 55A) of the fourth trochanter is gently concave, the curve continuing that of the adjacent shaft. In internal view (Text-fig. 54C) most of the shaft is convex, but at the base of the fourth trochanter there is a depression, quite deep (R193, Text-fig. 55D; R195, R2477b) or very shallow (R196, R5829, R5830, Text-fig. 54C), which probably served for the insertion of the caudi-femoralis longus muscle (Text-fig. 55D; see Galton 1969). The shaft is narrowest just above the fourth trochanter where its cross-section is roughly quadrilateral with rounded edges. Below this it is roughly circular with a slight antero-posterior flattening. The anterior face (Text-fig. 54D) forms a progressively flatter convex curve and there is practically no anterior intercondylar groove (Text-fig. 54F). Posteriorly the outer condyle is almost as large as the inner and the surface becomes concave towards the base of the condyles with a deep but quite wide intercondylar groove (Text-figs. 54B, F).

Tibia. The proximal end is only moderately expanded (Text-fig. 56E) with a flat and slightly inclined surface (Text-fig. 56B). The proximal condyles (Text-fig. 56B) are rounded and approximately equal in size and they shortly merge with the convex shaft. The outer condyle bears a much smaller condyle on its antero-lateral face (Text-fig. 56A) against which the fibula fitted. The cnemial crest of the tibia is small and forms a rounded edge (Text-fig. 56D) which is continued somewhat diagonally down the shaft, passing internally to merge with the base of the inner malleolus (Text-fig. 56D). The depression between the distal malleoli continues along about a quarter of the shaft (Text-fig. 56D). In anterior view (Text-fig. 56D) the medial part of the inner malleolus is convex while the lateral part below the intercondylar groove is transversely concave and more obliquely inclined. In posterior view (Text-fig. 56B) there is a distal sharp edge backing the malleoli. The surface above the outer malleolus is convex but that above the inner malleolus is concave.

The shaft of the tibia is basically triangular in section but the sharpness of the edges varies. In R196, R752 and R5830 (Text-fig. 56) these edges are rounded apart from that above the outer malleolus. In R199 (Hulke 1882, pls. 80 and 81) the edges are more marked and the edge above the outer malleolus is much sharper and forms a step. The edge visible in anterior view above the inner malleolus also varies. In R193, R199 and R5830 (Text-fig. 56D) it is smooth, forming a gentle and continuous curve on the shaft. In R196 and R5829 this edge, about a third up, is considerably enlarged and swollen, the area being covered with well-developed surface markings. All of these seem to be individual variations.

Fibula. Only in R5830 are both ends well preserved. Swinton (1936 : 568) noted that the right fibula of this specimen was complete and figured it as such (Swinton 1936, fig. 7) but the middle two-thirds is restored in plaster. The proximal surface is transversely rounded and articulated during adduction with the groove on the outer condyle of the femur. The concave curve of the medial surface (Text-fig. 56E) continues on to the proximal third of the shaft but below this the shaft is oval in cross-section. In S.M. 4127 the upper half of the fibula is slightly curved, with a concave anterior outline, and it is set at a slight angle to the distal half. Distally the fibula is backed to a progressively greater extent by the outer malleolus of the tibia. This part of the fibular shaft in R193 is laterally expanded with a sharp inner edge ; the anterior surface is slightly concave longitudinally while the posterior surface against the tibia is flat. The outer edge is gently convex and this, together with the anterior surface, sweeps out to the distal head ; the latter is rounded in outline apart from the flat area against the tibia. The edges of the distal end are rounded but the end surface is flat and fitted against the calcaneum.

Astragalus. This consists of two sheets of bone, one capping the distal end of the tibia (Text-fig. 57E), the other an ascending process that wraps round part of the anterior surface of the tibia (Text-figs. 56D, G). The ascending process ends in a tooth-like structure set out in slight relief from the adjacent bone (Text-figs. 56D, 57A, B). Below this ' tooth ' the ascending process is very thick and continues posteriorly as a broad ridge across the concave proximal surface (Text-fig. 57A) while medial to this ridge there is a large depression. This proximal surface was closely applied to the distal end of the tibia (compare Text-figs. 57A, 56F). The astragalus thins posteriorly and ends in a sharp edge (not visible in Text-fig. 56B) closely applied to the adjacent surface of the tibia. Though there is a gap below the inner corner of the fibula in R5830 (Text-fig. 56D) this area in R196 is filled by bone that appears to belong to the astragalus. This is confirmed by the presence of a broken surface on the external proximal corner of the astragalus of R5830 (Text-fig. 57D). The shape of this part of the bone is indicated by the adjacent surfaces of the fibula and calcaneum.

Calcaneum. The outer surface (Text-fig. 56A) is gently concave and forms a definite edge, indented in several places (Text-fig. 56E), with the curved antero-distal surface for distal tarsal 1. The proximal surface against which the fibula fitted is concave (Text-fig. 57A), the depression continuing medially on to the inner surface (Text-fig. 57C). The posterior surface for the outer malleolus of the tibia is a large depression (o, Text-figs 57C, D) which forms a thin and sharp edge with the outer edge (Text-fig. 57D). This obliquely inclined depression forms sharp diagonal edges with the proximal (Text-fig. 57A) and distal (Text-fig. 57E) surfaces. The medial view (Text-. fig. 57C) shows five surfaces, three of which I have designated (f, d.2 and o). The surface (a) for the main part of the astragalus is flat and above this there is a concave surface (e) for the dorso-laterally directed process of the astragalus. A medially directed corner (see Text-fig. 57A) is formed by the contact edges of surfaces e, f and o. However, the antero-distal part of the depression (e) is also continuous with those surfaces for the fibula (f) and tibia (o).

Distal tarsal 1. This is an irregularly flattened plate of bone with rounded edges which are indented in several places. Most of the proximal surface (Text-fig. 57F) with which the astragalus articulated is slightly convex, apart from a central concave

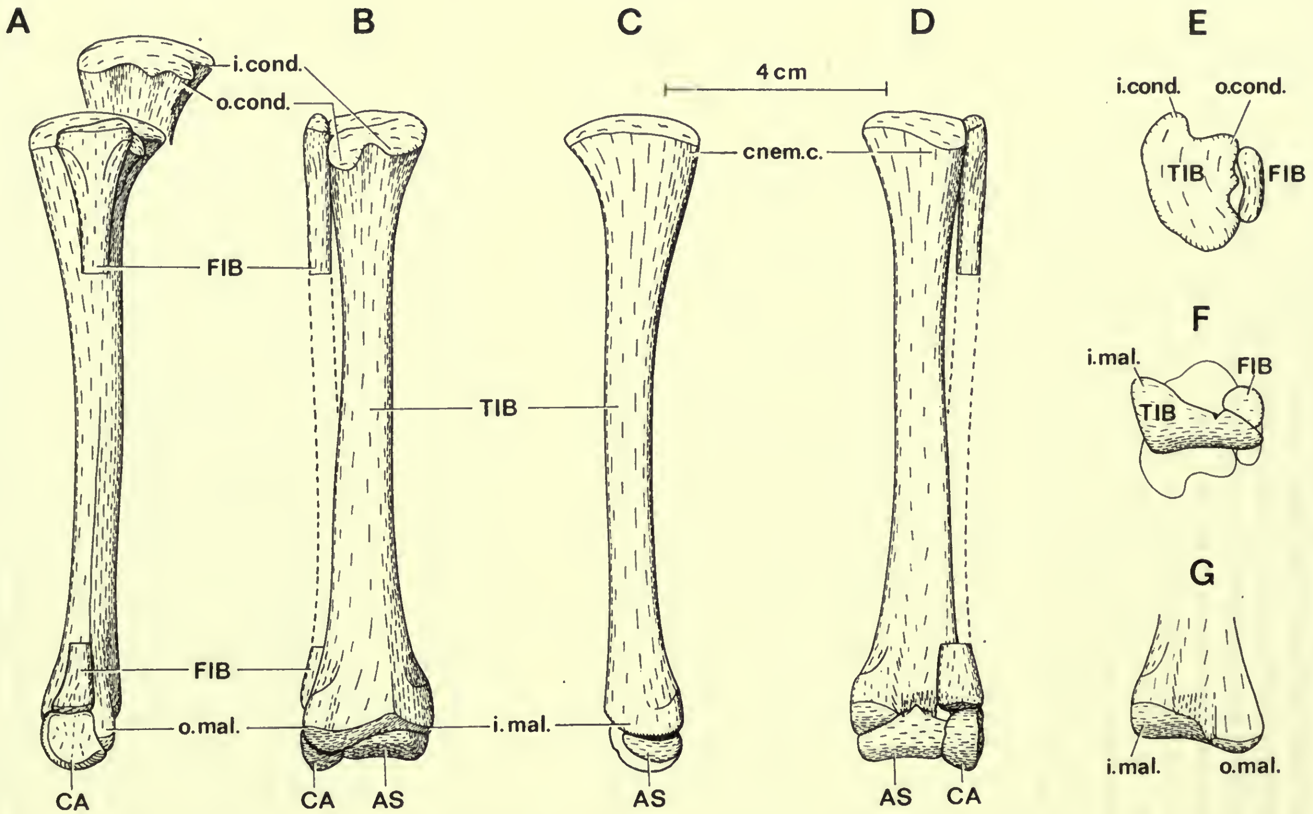
A
B
C
D
E
F
G
i.cond.
o.cond.
FIB
TIB
FIB
o.mal.
i.mal.
CA
CA
AS
AS
AS
CA
4 cm
cnem.c.
i.cond.
o.cond.
TIB
FIB
i.mal.
FIB
TIB
i.mal.
o.mal.

Fig. 56. *Hypsilophodon foxii*. Tibia, fibula, astragalus and calcaneum R5830, × $\frac{3}{4}$. A, lateral view; B, posterior view; C, medial view; D, anterior view; E, proximal view; F, distal view of tibia and fibula; G. anterior view of distal part of tibia. Abbreviations: AS, astragalus; CA, calcaneum; FIB, fibula; TIB, tibia; cnem. c., cnemial crest; i. cond., inner condyle; i. mal., inner malleolus; o. cond., outer condyle; o. mal., outer malleolus.

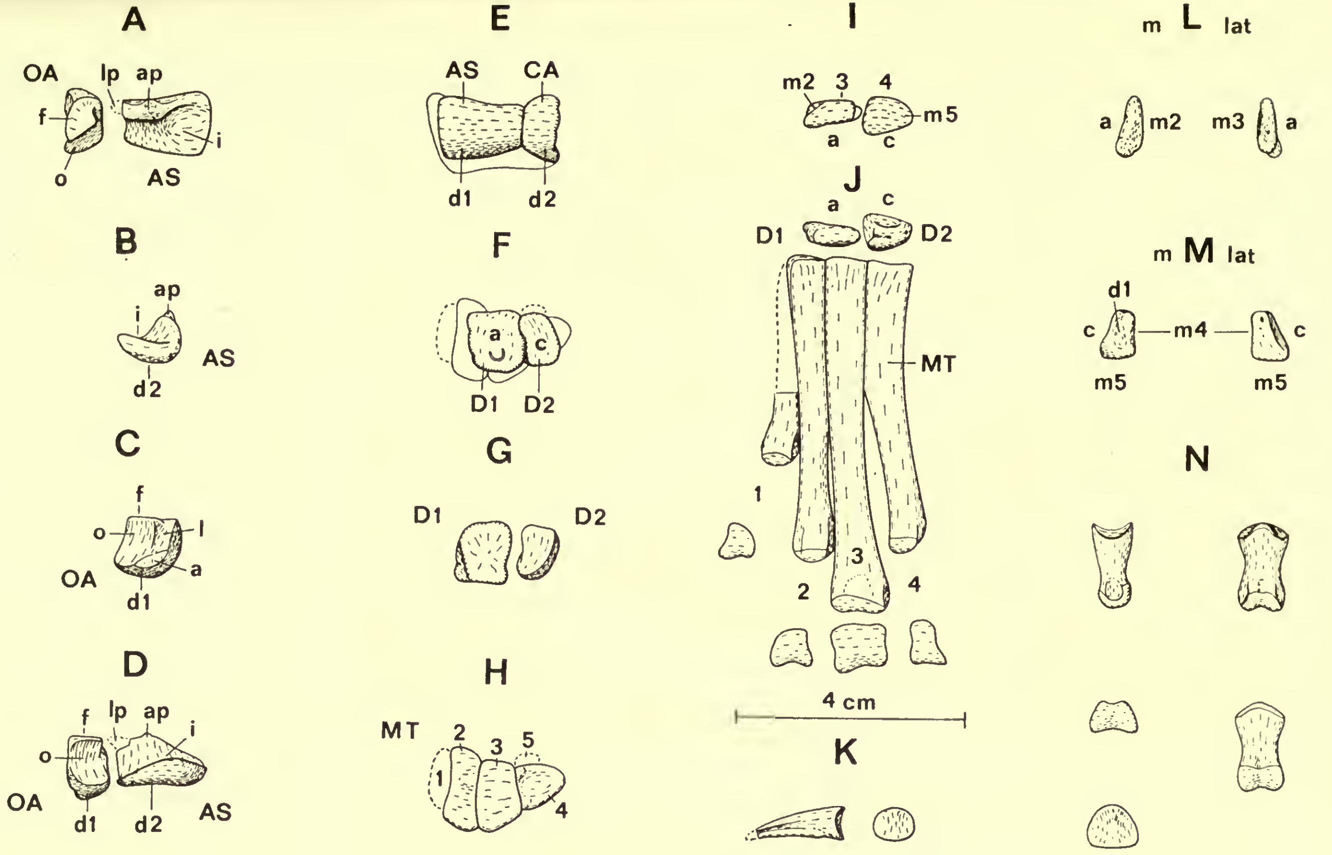
A
OA
lp
ap
f
o
AS
i
B
ap
i
AS
d2
C
f
o
l
OA
a
d1
D
f
lp
ap
i
o
OA
d1
d2
AS
E
AS
CA
d1
d2
F
a
c
D1
D2
G
D1
D2
H
MT
2
3
5
1
4
I
m2
3
4
m5
a
c
J
a
c
D1
D2
MT
1
3
2
4
4 cm
K
m
L
lat
a
m2
m3
a
m
M
lat
d1
c
m4
c
m5
m5
N

FIG. 57. *Hypsilophodon foxii.* R5830, × $\frac{3}{4}$. A, astragalus and calcaneum, proximal view ; B, astragalus, lateral view ; C, calcaneum, medial view ; D, astragalus and calcaneum, posterior view ; E, astragalus and calcaneum, distal view ; F, distal tarsals, proximal view of metatarsus ; G, distal tarsals, distal view ; H, metatarsus, proximal view ; I, distal tarsals, ventral view ; J, distal tarsals and metatarsus, dorsal view with distal view of metatarsals I to IV ; K, ungual phalanx, lateral and proximal views ; L, distal tarsal 1, medial and lateral views ; M, distal tarsal 2, medial and lateral views ; N, phalanx, lateral, dorsal, distal, ventral and proximal views. Abbreviations : AS, astragalus ; CA, calcaneum ; D, distal tarsal ; MT, metatarsal ; a, surface for astragalus ; ap., anterior ascending process ; c, surface for calcaneum ; d, surface for distal tarsal ; f, surface for fibula ; i or im, surface for inner malleolus ; l, surface for lateral process ; lp., lateral process ; m, surface for metatarsal ; o, surface for outer malleolus.

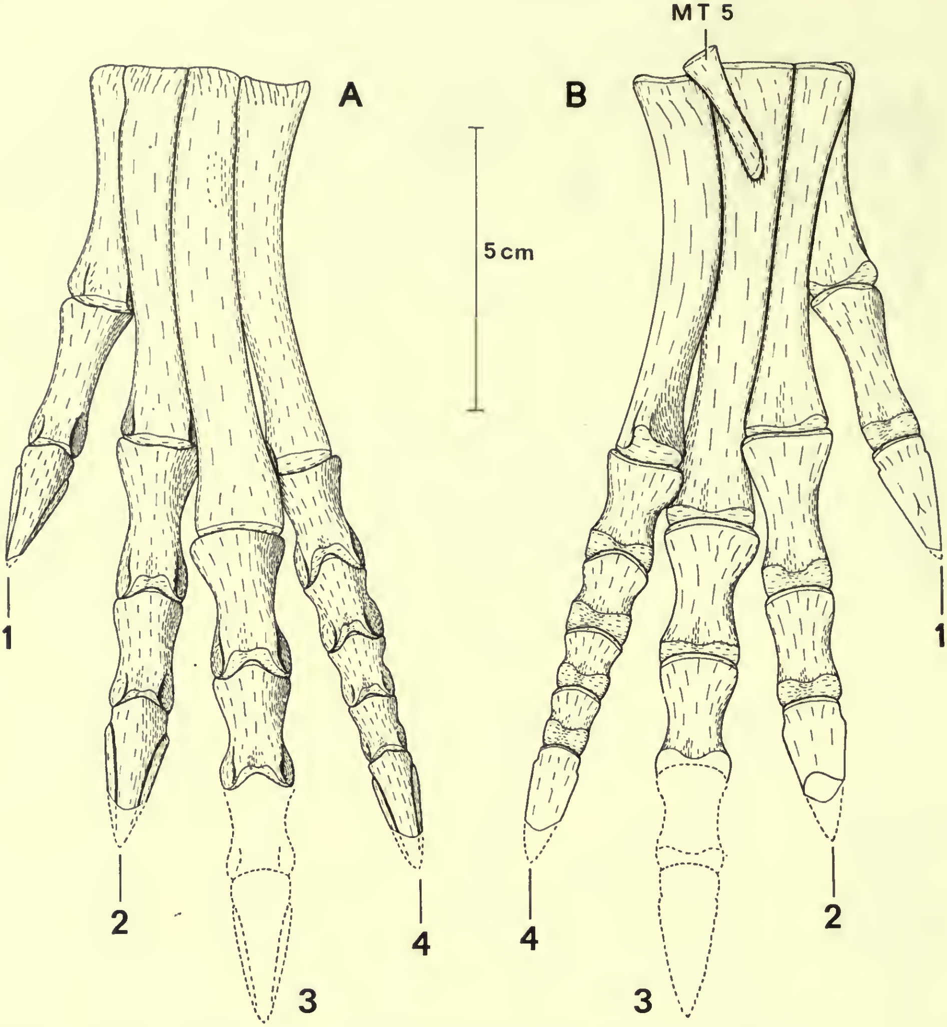

FIG. 58. *Hypsilophodon foxii*. Pes R196, ×$\frac{3}{4}$. A, dorsal view; B, ventral view with details of metatarsal V from SM 4127. Abbreviations: MT, metatarsal; 1–5, digits.

region in the ventral half. Most of the distal surface (Text-fig. 57G) is flat with radiating surface markings; the proximal end of metatarsal III articulated with the lateral two-thirds of this surface. The ventro-medial corner is bevelled to form a distinct depression (Text-fig. 57G). A well-developed boss on metatarsal II (Text-fig. 57H) fitted into this depression while the remainder of the lateral part articulated with the flat surface of this distal tarsal (cf. Text-figs. 57G, H).

Distal tarsal 2. This is a rather irregular wedge-shaped bone. The proximal (Text-fig. 57F) and distal surfaces (Text-fig. 57G) are concave. The inner surface (d.1 Text-fig. 57M) is markedly concave and fitted against the lateral surface of distal tarsal 1. This depression continues a short distance on to the dorsal surface (Text-fig. 57J). The outer and ventral surface (Text-fig. 57J) form a continuous and obliquely inclined curve progressively increasing with width (Text-fig. 57M). The reduced fifth metatarsal articulated with the wide ventral part of this surface.

Metatarsals. The relative length of the metatarsals varies, but metatarsal III is always the longest and stoutest with metatarsal I about half as long. In R5830 metatarsals II and IV are approximately equal but in all other specimens metatarsal II is slightly shorter than metatarsal IV. The anterior (dorsal) surface of the metatarsus is transversely convex (Text-figs. 57H, 58A) with well-marked corners which become more rounded distally. Proximally the metatarsals are expanded antero-posteriorly with the anterior face sweeping upwards so that a deep articular surface is formed, especially large in metatarsals II and III (Text-fig. 57H). The posterior surface of the metatarsus is concave (Text-figs. 57H, 58B), although the individual metatarsals are gently convex and becoming more strongly curved distally.

The distal articular condyle of metatarsal I is not reduced (Text-figs. 57J, 58) and the adjacent part of the shaft is subtriangular in cross-section. The shaft becomes more compressed so that the proximal part is thin and flat with almost no proximal articular surface. The amount of the first metatarsal visible in ventral view (Text-fig. 58B) progressively decreases because the flattened proximal part wraps round on to the dorso-lateral surface of the second metatarsal (Text-fig. 58A). The proximal end of metatarsal II is bioconcave with a well-developed bump towards its rear surface (Text-fig. 57H) which fitted against the step on distal tarsal 1. The medial surface is rounded beyond the end of metatarsal I, while the flat lateral surface against metatarsal III is reduced distally so that the shaft becomes almost circular in section. The proximal end of metatarsal III has an irregular surface which fitted against distal tarsal 2. The cross-section of the shaft near the distal end is a dorso-ventrally flattened circle. The proximal end of metatarsal IV is concave, with a well-developed bump on each of the inner corners (Text-fig. 57H), and it contacted distal tarsal 2. Most of the shaft is somewhat triangular in outline with a sharp lateral edge formed by the junction of the gently convex anterior and posterior surfaces. The distal half diverges laterally and also slightly posteriorly from metatarsal III. In ventral view (Text-fig. 58B) there is an edge on the medial margin which gradually passes laterally until it merges with the roots of the outer condyle. The shaft internal to this ridge is convex but external to it is gently concave. This ridge is also well developed in R200 and S.M. 4127 but it is absent in R5830; its development is probably related to size. Metatarsal V is reduced to a splint which is well preserved in S.M. 4127 (basis for Text-fig. 58B). The proximal end is transversely expanded to form a head, oval in section and with a rounded end which articulated with the posterior surface of distal tarsal 2. The distal end has an obliquely inclined articular surface but no phalange was found.

Phalanges. The proximal ends of the first and last phalanges of each digit do not bear a well-developed dorsal process as do the other phalanges (Text-fig. 58A). These processes appear to be less strongly developed in R5830 than they are in R196; this is probably due to the difference in size. The proximal ends (Text-fig. 57N) are concave with a median ridge so that two depressions are formed. These are shallow in the first and ungual phalanges (Text-fig. 57K) but are well developed in the others. The lateral muscle grooves are well developed on the distal condylar head (Text-fig. 57N). The central depression is continued dorsally on to the non-articular part and the resulting cavity received the dorsal process of the next phalanx. The ungual phalanges are slender (Text-figs. 57K, 58) and the grooves for the claw are well developed.

e) *Dermal armour*

A few thin sheets of bone are present close to the skull of specimen R2477. Hulke (1874, pl. 3, fig. 1) figured these and regarded them as thin scutes, noting that they were 'irregularly polygonal' in outline with one surface granular, the other smooth and furrowed by a vascular net. In a later paper (1882) they were figured but neither labelled nor mentioned. Nopcsa (1905, fig. 4) figured them and noted (: 205) that *Hypsilophodon* was 'clad with a thin but well developed dermal armour consisting of comparatively large yet thin and flat, feebly punctured plates'. He also noted that they showed the same feebly grooved sculpture and could not be referred to any part of the endoskeleton. Romer (1956 : 428) noted that '*Hypsilophodon* had a paired row of thin dorsal plates presumably retained from the thecodont ancestors'.

The thin overlapping plates of bone were shown by Nopcsa (1905, fig. 4) but it is impossible to determine their original shape as all the edges are broken. The plates lie lateral to the distal parts of the dorsal ribs of individual 'a' and very close to a skull that probably belongs to another individual (Hulke 1874, pl. 3, fig. 1, 2 ; Galton 1967, photograph fig. 23). However, it is not certain to which individual the plates belong. Consequently there is no evidence to show that the plates were paired or dorsal in position. Both surfaces are rough, lacking the smooth finish of other bones, with various small and irregularly shaped depressions.

It is possible that these plates formed part of a dermal armour. However, if such were the case it is surprising that they have not been preserved in any of the other specimens. In R194 there is a similar plate, about a square inch in size, but it is so eroded that it could be anything. It is particularly surprising that these elements were not preserved in R196 because this skeleton is so complete in all other respects. Nopcsa (1905) could not identify these plates as any part of the endoskeleton but they could be the remains of a damaged sternum. Consequently, although they may well represent dermal armour, further material is needed to confirm this identification. Dermal armour is present in most thecondontians but *Hypsilophodon* is the only ornithopod in which dermal armour has been reported. In stegosaurs and ankylosaurs dermal plates formed a strong armour.

V. *CAMPTOSAURUS VALDENSIS*–A LARGE *HYPSILOPHODON FOXII*

Lydekker (1888) noted that the damaged left femur R167 (Pl. 2, fig. 4) might, because of its greater size, represent a species distinct from *Hypsilophodon foxii*. He also catalogued a small mandibular ramus R180 as that of a young *Iguanodon* (Owen 1864, pl. X figured it as this). In the same year he stated (1888*a*) that this ramus might belong to a smaller adult form, allied to *Laosaurus* or *Dryosaurus*, in which case the femur R167 might belong to the same form. Subsequently (1889) he noted that the femur was very similar to that of *Camptosaurus leedsi* from the Oxford Clay, which is itself very similar to the femur of the North American *Camptosaurus*. Because there was no other evidence of a *Hypsilophodon* of these dimensions he made the femur R167 the type of a new species, *Camptosaurus valdensis*, to which he provisionally referred the mandibular ramus. He listed the femur and jaw as *Camptosaurus valdensis* in the supplement to his catalogue (1890).

Gilmore (1909) noted that the fourth trochanter of R167 was on the proximal half of the shaft and he opined that, because in the American *Camptosaurus* it is on the distal half, this femur must be distinct from *Camptosaurus*. There are other differences between the two. The lesser trochanter of R167 is not expanded anteroposteriorly and the cleft separating it from the greater trochanter is shallow and ends level with the middle of the head. In the American *Camptosaurus* (Gilmore 1909, fig. 42–1) and *C. leedsi* (Lydekker 1889, fig. 3) the trochanter is expanded and the cleft is deep and ends level with the bottom of the head. In addition, *Camptosaurus* has a well-developed anterior intercondylar groove which is absent in R167.

In the characters cited (the position of the fourth trochanter, the shape of the lesser trochanter, the depth of the cleft between the lesser and greater trochanters and the absence of a marked anterior intercondylar groove) the femur R167 agrees with those of *Hypsilophodon* (Text-figs. 54, 55). Consequently this femur is regarded as belonging to the genus *Hypsilophodon*.

Lydekker (1888, 1889) emphasized the large size of the femur R167 in comparison with those of *Hypsilophodon foxii*; Swinton (1936*b*) stated that it is half as large again as any femur known in that genus. The total length of R167 is unknown but the minimum distance between the proximal end and the distal surface of the fourth trochanter is 108 mm (see Text-fig. 1f). The distance in R5829 (the largest femur generally regarded as *Hypsilophodon foxii*) is 87 mm, so R167 is not quite 25 per cent as large again. The femur of R167 is therefore regarded, not as representing a new species but, on the contrary, as a femur of *Hypsilophodon foxii* from the largest individual hitherto found, which would have been about 7·5 ft or 2·28 m long.

The teeth of the mandibular ramus (R180) mentioned above resemble the corresponding teeth of *Iguanodon atherfieldensis* (see Hooley 1925). Therefore this ramus is referred to a young *Iguanodon*, following Owen (1864) and Lydekker (1888). This was the only other specimen referred to *Camptosaurus valdensis*; consequently the genus *Camptosaurus* is not so far represented in the Wealden of the Isle of Wight.

VI. ASPECTS OF CRANIAL ANATOMY

a) *The foramina of the braincase*

The foramina for the *olfactory*, *optic* and *trochlear nerves* (I, II and IV) are not preserved because the more anterior part of the braincase was cartilaginous. The same is true of the dorsal boundary of the large foramen for the oculomotor nerve III. The dorsal edge of the parasphenoid is concave and probably formed the ventral border to this foramen (III, Text-fig. 60A). The resulting foramen bears exactly the same relationship to the surrounding structures as does the foramen for the oculomotor in hadrosaurs (see Ostrom 1961, fig. 12).

Trigeminal foramen (V, Text-figs. 4B, 9, 60A). This large foramen is enclosed mainly by the prootic but anteriorly it is bordered by the laterosphenoid. On the lateral surface of the laterosphenoid there is a short groove which passes anterodorsally from the trigeminal foramen (Text-figs. 9A, 60A). The deep ophthalmic ramus (V_1), a sensory tract from the snout that branches off close to the braincase, probably ran in this groove. In hadrosaurs there is another groove running ventrally for the maxillary and mandibular rami (V_2 and V_3) ; in *Hypsilophodon* there is no well-developed groove but the common course of these two rami is faintly discernible, probably passing postero-ventrally to the edge of the step running from the base of the basipterygoid process (Text-figs. 4B, 60A). There is a slight depression on the posterior face of this edge which was probably for those two rami. The maxillary ramus (V_2) presumably passed forwards above the base of the pterygoid process while the mandibular ramus (V_3) continued ventrally ; these routes are visible in hadrosaurs (Ostrom 1961) but not in *Hypsilophodon*.

Abducent nerve (VI). The abducent of hadrosaurs arises from the floor of the metencephalon and passes through bone in a long canal, part of which is lateral to the sella turcica, to emerge through the oculomotor foramen (Ostrom 1961). The position appears to be the same in *Hypsilophodon* but the part in the lateral wall of the sella turcica is not enclosed by bone. The exit of a canal into this part of the sella turcica is visible on both sides in R2477 but its entrance into the inner wall of the braincase cannot be located.

Facial nerve (VII) passes through a small foramen in the prootic (Text-figs. 9, 60A). Leading ventrally from this there is a groove which continues ventrally medial to the groove already mentioned for V_2 and V_3. The anterior branch (palatine ramus) of the facial nerve presumably ran in this groove and then passed ventral to the basipterygoid process.

In medial view (Text-figs. 9B, C) the posterior part of the prootic of *Hypsilophodon* shows a process which meets a corresponding process of the opisthotic. The anterior opening bounded by the prootic was probably for the *auditory nerve* (VIII). The posterior opening bounded by the opisthotic is interpreted as a combined *foramen lacerum posterius* (for cranial nerves IX, X and XI) and *jugular foramen* (for the internal jugular vein). This common opening is separated from the *internal auditory meatus*, the *inner ear cavity* and the *fenestra ovalis* by a thin bony partition (Text-fig. 9A). A similar partition is mentioned by Gilmore (1914) in *Stegosaurus*. Medially (Text-fig. 9C) the three cranial nerves share a single opening but more laterally there is a small tunnel in the posterior wall which forms a separate exit visible in lateral view (Text-fig. 9A). This posterior opening was probably for the *accessory nerve* (XI) while the *glossopharyngeal* (IX) and *vagus* (X) nerves remained in the main foramen. In hadrosaurs the foramen for the accessory nerve is completely separate from the other two (Ostrom 1961). The foramen for the *hypoglossal* nerve (XII) is completely enclosed by the opisthotic (Text-figs. 9A, C).

In medial view (Text-figs. 9B, C) there are three features of the braincase which are not associated with cranial nerves : the fossa subarcuata, the lagenar recess and the opening for the vena cerebralis posterior. The sutural region between the supraoccipital and the prootic is excavated to form a large and tapering tunnel. A similar structure is present in *Plateosaurus*, interpreted by Janensch (1936, fig. 3) as the *fossa subarcuata*. The structure of the middle ear of *Hypsilophodon* cannot be determined but was probably similar to that of hadrosaurs as described by Ostrom (1961). In *Hypsilophodon* only part of the *lagenar recess* is visible ; this forms a concave depression on the postero-ventral part of the prootic ventral to the fenestra ovalis. On the opisthotic immediately above the medial opening of the hypoglossal nerve there is an opening (f, Text-figs. 9B, C) which leads into a small tunnel. Janensch (1955) labelled a similar opening in *Dysalotosaurus* as the vena cerebralis posterior ; he had discussed this identification in an earlier paper (1936).

b) *The paroccipital process and the post-temporal fenestra*

What appears to be part of the suture between the exoccipital and the opisthotic is visible on the medial surface of R8418 (Text-fig. 9B). The suture forms a clearly defined edge which, because the bone surface is well formed with faint markings, is not the result of displacement along a crack. Consequently it appears that in *Hypsilophodon* the exoccipital portion is restricted to the lateral part of the occipital condyles. The part through which the foramina pass is part of the opisthotic as is the paroccipital process.

Langston (1960) described a fragmentary skull of a hadrosaur in which the main occipital part of the paroccipital process appeared to be formed by the exoccipital. Overlapping this anteriorly but not extending to its distal end was a smaller process formed by the opisthotic. The tapering part of the prootic overlapped the base of the opisthotic anteriorly. However, the form of the paroccipital process was quite normal and it should be noted that several of the suture lines are shown dotted. Langston stated that in camptosaurs the opisthotic does not form part of the paroccipital process. Regarding the position in *Camptosaurus* Gilmore (1909 : 207) stated that 'the exoccipital and opisthotic are firmly coalesced, and there is no indication of the position of the suture that evidently was early obliterated'. He regarded the portion forming the occipital condyle as exoccipital and the rest, including the paroccipital process, as opisthotic. Janensch (1955) considered that in the hypsilophodont *Dysalotosaurus* all the bone behind the prootic was exoccipital with no mention of the opisthotic. Information from other specimens is needed to ascertain whether the paroccipital process of ornithischians is usually formed by the opisthotic or by the exoccipital.

In hadrosaurs the very small post-temporal fossa is bordered ventrally by the paroccipital process (see Langston 1960) while in *Hypsilophodon* it is totally enclosed by the paroccipital process (Text-figs. 7B, 8, 9B). Leading antero-medially and dorsally from the resulting foramen is a slight depression which soon disappears. However, more anteriorly on the side of the supraoccipital there is a well-defined groove which passes medial to the parietal to enter the braincase (Text-fig. 60A).

The anterior groove and the posterior depression are in line, bearing the same relationship to the edge of the supraoccipital, so it is reasonable to conclude that the same structure occupied both. The resulting course rules out a nerve so this structure must have been a blood vessel, presumably the vena capitis dorsalis. Cox (1959) pointed out that in *Sphenodon* (O'Donoghue 1929) and *Lacerta* (Bruner 1907) the vena capitis dorsalis, which drains the muscles of the spino-occipital region, runs anteriorly through the post-temporal opening. Just before it enters the braincase it receives an anterior factor, the sinus-like vena parietalis, from above the parietal bone. In *Lacerta* the vena capitis dorsalis passes through the posterior end of the great parietal fissure (between the parietal and the prootic) to join the vena cerebralis media (Bruner 1907). In *Hypsilophodon* the route is similar though it is between the parietal and the supraoccipital. On the parietal there is a slight depression, running antero-dorsally from the projection on the ventral edge (Text-fig. 60A), which was probably for the vena parietalis. Consequently a vena capitis dorsalis ran along the lateral surface of the supraoccipital and the paroccipital process of *Hypsilophodon*. The presence of this vessel confirms the identification of the foramen in the paroccipital process as the remnant of the post-temporal fossa.

c) *The eye*

The orbit of *Hypsilophodon* (Text-fig. 3) is large and the interorbital septum, which was presumably present, was very high. As reconstructed the sclerotic ring is also large though, as noted above, it may have been slightly smaller than shown. The orbital surfaces of the prefrontal, frontal, postorbital and jugal are all inclined rather obliquely (Text-figs. 4A, 5A, 6B). In addition the dorsal edge formed by the prefrontal, frontal and postorbital is cut back, forming a sharp and well-defined edge to the orbit. All these features indicate that the eye of *Hypsilophodon* was large and filled the orbit as in birds.

In dorsal view (Text-fig. 5B) the striking features about the skull are the largeness of the orbits and the narrowness of the frontals. The eye of *Hypsilophodon* would have projected slightly and this is confirmed by the shape of the supraorbital that curves out laterally. The rather oblique configuration of the orbit in dorsal view (Text-fig. 5B) suggests that the fields of view overlapped slightly when the eyes looked more anteriorly. Certainly in anterior view (Text-fig. 7A) much of the posterior part of the orbit is visible.

In *Hypsilophodon* the sclerotic ring is only slightly convex in transverse section. Underwood (1970) notes that this form indicates that there was a sharp change of curvature between the posterior and anterior segments of the eye, with a well-developed sulcus, indicating good powers of accommodation and diurnal habits. Underwood also states that the diameter of the inner and outer edge of the ring gives an indication of the relative size of the cornea. An inner diameter of about a third or less of the outer is a fair indication of diurnal habits. This cannot be accurately applied to the ring of *Hypsilophodon* because the reconstruction is rather tentative with regards to these measurements. However, it seems likely that *Hypsilophodon* had quite good powers of accommodation and was diurnal in its habits.

The form of the orbit might suggest that *Hypsilophodon* was arboreal but, as discussed below, *Hypsilophodon* was not specifically adapted for tree-climbing and was probably cursorial. *Heterodontosaurus* (Crompton & Charig 1962), *Parksosaurus* (Parks 1926, Galton in press) and *Dysalotosaurus* (Janensch 1955) are other ornithopods with large orbits and these, as shown by the proportions of their hindlimbs, were probably also fast runners. Outside the Ornithischia the closest approach to the relative largeness of the orbits is in *Ornithomimus* (see Romer 1956, fig. 81A), a definitely cursorial animal.

The function of the sclerotic ring must be considered. Edinger (1929) showed by experiments on the lizard *Ophisaurus* that the plates do not change their relative position and, consequently, do not aid in the dilation of the pupil as has been suggested. However, they must aid in supporting and maintaining the shape of the eyeball. Ostrom (1961) considered it unlikely that this was their function because forms with sclerotic rings occupy an extremely wide range of habitats and, in addition, related forms without rings may occupy the same habitat as forms with them. He therefore concluded that the function of these structures has not yet been determined. Colbert (1962) noted that the function of the sclerotic ring was debatable. However, Walls (1942) discussed the function of the sclerotic ring as follows. The typical sauropsid sclera consists mainly of a cartilaginous cup of which the open rim extends quite close to the edge of the cornea. The remaining zone of the sclera is occupied by the sclerotic plates which are lacking only in crocodilians and snakes. Because the plates are flat or concave they do not continue the rotundity of the equatorial sclera smoothly into the sharper curve of the cornea. On the contrary the sclero-corneal junction is depressed or concave to form a broad annular sulcus. Walls (1942 : 275) stated that 'the production of a sulcus is the whole meaning, physiologically, of the sauropsidan ossicular ring. It stiffens the concavity against the force of the intraocular pressure which, if unresisted, would evaginate it. This pressure rises slightly during accommodation, which it does not do in fishes, amphibians or mammals.' He noted that the presence of a sclero-corneal sulcus resulted in the ciliary body touching the lens. The striated ciliary muscles are arranged in such a way that they cause the ciliary process to squeeze the lens so that its anterior surface becomes more rounded (for figures showing the mechanism of accommodation in the eyes of reptiles and birds see also Young 1962, figs. 218, 293).

The sclerotic ring is absent in crocodiles, snakes and mammals. Walls (1942) suggested that the loss of the sclerotic ring in modern crocodiles can be attributed to the adoption of nocturnal habits in which the images are crude and accommodation useless. The eye of snakes, when compared with that of lizards (see Young 1962, fig. 238), shows that many structures have been lost and that there are various improvisations to give the same results. Walls (1942) suggested that a burrowing mode of life in the ancestral snake led to the loss of many structures in the eye so that when snakes subsequently came above ground they had to adapt what was left. This theory has been disputed but a phase of nocturnal existence would be adequate to explain the loss of the sclerotic ring. In mammals accommodation relies on the elasticity of the lens capsule to supply the actual force of accommodation. Walls

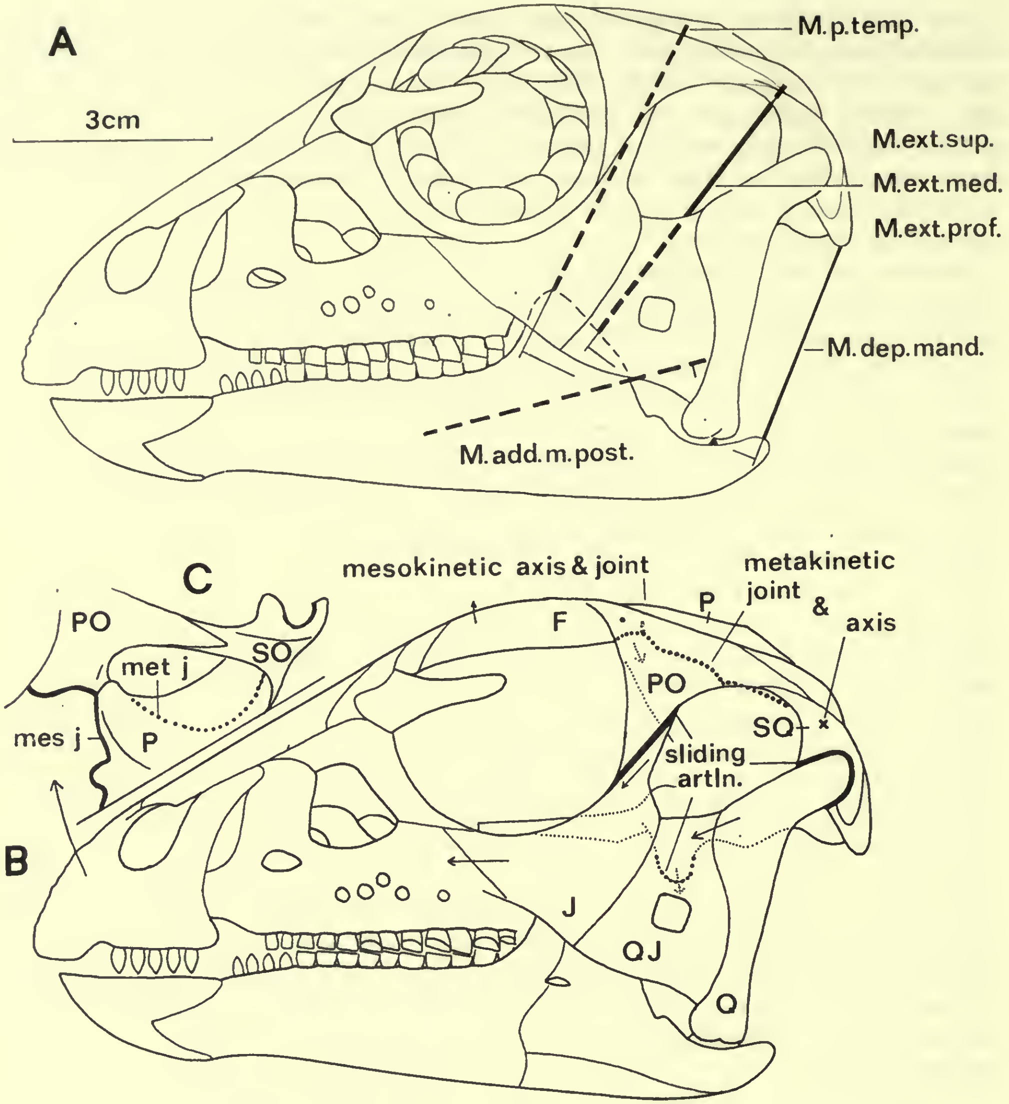
A
3cm
M.p.temp.
M.ext.sup.
M.ext.med.
M.ext.prof.
M.dep.mand.
M.add.m.post.
C
PO
SO
met j
mes j
P
mesokinetic axis & joint
metakinetic joint & axis
B
F
P
PO
SQ
sliding artln.
J
QJ
Q

FIG. 59. *Hypsilophodon foxii.* Skull R2477, × 1. A, the lines of action and moment arms of the jaw muscles. Abbreviations for the muscles in Text-figs. 59A and 60 :

M. add. m. post.	M. adductor mandibulae posterior
M. dep. mand.	M. depressor mandibulae
M. ext. med.	M. adductor externus medialis
M. ext. prof.	M. adductor externus profundus
M ext. sup.	M. adductor externus superficialis
M. prot. pt.	M. protractor pterygoidei
M. pt. dor.	M. pterygoideius dorsalis
M. p. temp.	M. pseudotemporalis
M. pt. vent.	M. pterygoideus ventralis
Pt. D.	M. pterygoideus D (anterior division of M. pt. dor.)
Pt. V.	M. pterygoideus V (anterior division of M. pt. vent.)

B, the regions of movement in the skull, lateral view ; for discussion see page 110 ; C, the regions of movement in the skull roof. Abbreviations : mes j, mesokinetic joint ; met j, metakinetic joint ; sliding artln., sliding articulations. For abbreviation of skull bones see page 109.

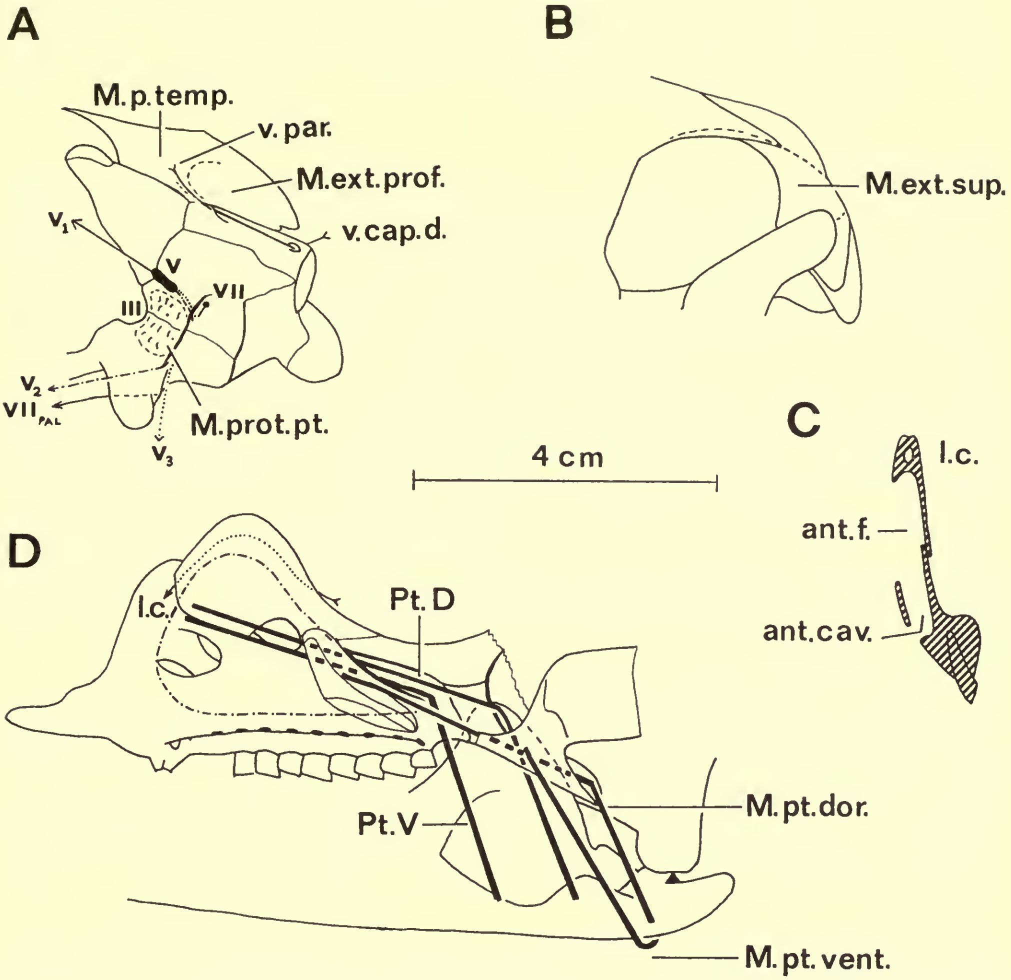
A
M.p.temp.
v. par.
M.ext.prof.
V₁
v.cap.d.
V
VII
III
V₂
VII PAL
V₃
M.prot.pt.
B
M.ext.sup.
4 cm
C
l.c.
ant.f.
ant.cav.
D
l.c.
Pt.D
Pt.V
M.pt.dor.
M.pt.vent.

FIG. 60. *Hypsilophodon foxii.* Details of the skull R2477, × 1. A, braincase in lateral view to show areas of muscle attachment and routes of nerves and blood vessels, compare with Text-fig. 4B ; B, area of origin of M. adductor externus superficialis, compare with Text-figs. 3, 4A ; C, vertical section through the lachrymal and maxilla taken along line below middle of lachrymal ; D, medial view to show lines of action of pterygoideus musculature, compare with Text-figs. 5A, 10B and Pl. 2, fig. 2. Abbreviations : ant. cav., antorbital cavity or fossa ; ant. f., antorbital fenestra ; l.c., lachrymal canal ; v, cap. d., vena capitis dorsalis ; v. par., vena parietalis ; III, oculomotor foramen ; V, trigeminal nerve ; V_1, ramus ophthalmicus ; V_2, ramus maxillaris ; V_3, ramus mandibularis ; VII, facialis nerve ; VII_{pal} ramus palatinus. For abbreviations of muscles see page 108.

(1942) noted that mammals originated from forms with small bodies which were almost certainly nocturnal.

It is apparent that the sclerotic ring of dinosaurs, as in other sauropsids, was essential for accommodation because it maintained the shape of the sulcus. The absence of the ring in animals occupying the same terrestrial habit as others with it can be explained by a nocturnal phase in the ancestry of the former.

d) *Jaw musculature*

Apart from the cranial crests and specializations associated with the large dental batteries the hadrosaur skull is basically similar to that of *Hypsilophodon*. Ostrom (1961), who used about 80 skulls, gave a detailed account of their cranial musculature. By using this account in conjunction with the skull of R2477 a good idea of the jaw musculature of *Hypsilophodon* can be obtained. The inferred lines of action of the muscles are shown in Text-figs. 59, 60D. Ostrom (1961) followed the tripartite division of the mandibular musculature established by Luther (1914) and Lakjer (1926). These divisions are separated on their function and innervation rather than on their position. The adductor mandibulae group, which includes the superficial muscles of the temporal region, functions to close the jaws. Medial to this in forms with a kinetic skull is the constrictor dorsalis group which elevates the maxillary segment. The last group, the intermandibular muscles, aids in swallowing and respiration. The remaining muscle concerned with jaw movement is the M. depressor mandibulae – a branchial muscle which acts to open the lower jaw.

i) ADDUCTOR MANDIBULAE GROUP

The adductors are separated into external, internal and posterior masses according to their relationship with the branches of the trigeminal nerve (Luther 1914, Lakjer 1926 ; see Ostrom 1961 for details).

M. adductor mandibulae externus. This is the most variable of the adductor muscles in fishes, amphibians and reptiles and is typically divided into three parts : partes superficialis, medialis and profundus.

Pars superficialis. Origin : on the lateral surface of the squamosal of *Hypsilophodon,* anterior and dorsal to the head of the quadrate, there is a well-defined depression (Text-fig. 4A). This depression forms a sharp edge, slightly undercutting the flat dorsal surface (Text-fig. 5B) ; it is continued anteriorly on to the ventral edge of the postorbital as a bevel (Text-figs. 4A, 60B). However, Ostrom (1961, fig. 34) concluded that the very similar depression in hadrosaurs was for the pars superficialis, although the reptilian pars superficialis typically originates on the medial surface of the upper temporal arch and rarely develops a prominent scar. As Ostrom noted, the position and shape of the depression in hadrosaurs suggest that it is an extension of the lower temporal fenestra and is consequently a reflection of the superficial temporal muscle. Only a small area is involved and this would concentrate the stresses, resulting in the prominent scar (Ostrom 1961). Insertion : there are no well-defined insertion markings to indicate the area of insertion in

Hypsilophodon or hadrosaurs. However, it probably inserted on to the postero-dorsal edge of the surangular and to its medial surface. The more dorsal part of this edge near the coronoid is much thicker (Text-fig. 10B), the reverse of the position in hadrosaurs, but it lacks the well-defined and slightly concave dorsal surface present in hadrosaurs. The partes medialis and profundus probably inserted in the same region.

A more lateral subdivision of the superficialis, the *M. levator, anguli oris,* was possibly present on the ventral border of the jugal. Ostrom (1961) noted that this border in hadrosaurs and *Iguanodon* shows a pronounced ventral lobe which was possibly for this muscle. A similar lobe is well developed in *Protoceratops* and was probably for the same muscle (Haas 1955) as was the large lobe in *Heterondontosaurus* (see Crompton & Charig 1962, fig. 1B 'J.F.'). The anguli oris probably inserted in front of the coronoid and on the quadratomaxillary ligament (Ostrom 1961) or possibly on to the outer surface of the coronoid region.

Pars medialis. Origin : in modern reptiles this muscle is medial to the pars superficialis but occupies a similar position. In hadrosaurs there is a well-defined area for the pars medialis on the medial surface of the postorbital and the lateral process of the squamosal ; it is bounded posteriorly by a well-defined ridge on the squamosal (Ostrom 1961, fig. 36). This ridge is absent in *Hypsilophodon* but the area occupied by the medialis was probably the same.

Pars profundus. Origin : in modern Sauropsida this muscle fills most of the upper temporal fenestra. In hadrosaurs Ostrom (1961, fig. 38) located this origin chiefly on the parietal and squamosal next to the medialis. The anterior limit is defined by a gentle ridge running postero-dorsally across the side of the parietal. In *Hypsilophodon* the anterior limit is marked by the edge of a slight depression on the ventro-medial half of the parietal (Text-fig. 60A). Consequently the pars profundus probably originated from the ventro-medial part and the lateral wing of the parietal and, in addition, from the anterior surface of the medial process of the squamosal.

M. adductor mandibulae internus

M. pseudotemporalis. Origin : in modern reptiles the M. pseudotemporalis originates from the deep position in the anterior part of the upper temporal fenestra, passing anterior to the trigeminal foramen. The posterior limit of this muscle is formed by the area of the previous muscle. In *Hypsilophodon* the M. pseudotemporalis overlapped the M. externus profundus dorsally to originate from the median crest (Text-fig. 60A). More anteriorly a ridge sweeps laterally across the parietal on to the postorbital ; it is continued by the dorsal edge of the postorbital. The region delimited by this ridge (Text-fig. 5B) indicates the anterior limit of the M. pseudotemporalis. Insertion : Ostrom (1961) deduced that this muscle must have inserted on to the coronoid in hadrosaurs although there is no distinct scar on that element. In *Hypsilophodon* there are, in contrast, well-developed insertion markings for the M. pseudotemporalis on the lateral, dorsal and medial surfaces of the coronoid bone (Text-figs. 10, 12).

M. pterygoideus. This muscle, which is not homologous with the mammalian muscle of that name, is divided into two parts in modern reptiles and birds. In hadrosaurs Ostrom (1961, figs. 42, 43) placed the origin of the pars dorsalis on the well-developed maxillary shelf formed by the postero-medial part of the maxilla and by the ectopterygoid. In *Hypsilophodon* there is no equivalent shelf region on the maxilla but the dorso-medial surface of the ectopterygoid is similar to that of hadrosaurs. The *pars dorsalis* probably originated from the concave surface of the ectopterygoid. Posteriorly this surface is medially directed (Text-figs. 4B, 5C) but more anteriorly it is dorsally directed (Text-fig. 5C) because the surface is twisted along its length. There is no trace of the area of insertion but it was probably on the medial surface of the articular postero-ventral to the quadrate as in hadrosaurs (Ostrom 1961, fig. 41).

In hadrosaurs the *pars ventralis* probably originated from two depressions on the ventro-medial surface of the pterygoid (Ostrom 1961, fig. 42). In *Hypsilophodon* it probably originated from a corresponding flat surface formed by the pterygoid and ectopterygoid (Text-figs. 4B, 6A, 60D). This muscle wraps round the ventral border of the retroarticular process to insert on the lateral surface. In *Hypsilophodon* there is a slight depression on the region below the mandibular condyle in R192 which was probably for this muscle. In hadrosaurs there is a well-defined depression which corresponds in position to that of the pars dorsalis on the opposite side (Ostrom 1961, fig. 41). The areas of origin of the pars dorsalis and ventralis are discussed below in more detail in Section (g.)

M. adductor mandibulae posterior. In sauropsids this muscle originates in the postero-ventral corner of the temporal region and links the quadrate with the posterior part of the inframandibular fossa. In hadrosaurs the anterior surface of the quadrate shows a well-developed depression, extending on to the lower third of the pterygoid flange, which was the area of origin of the M. adductor posterior (Ostrom 1961, fig. 46). The area was presumably the same in *Hypsilophodon* though the depression is not visible on the pterygoid flange (Text-fig. 7B). The insertion in *Hypsilophodon* was clearly into the deep inframandibular fossa. This tapers anteriorly (Text-fig. 12A) and ends (apart from the Meckelian canal running forwards) level with tooth 7. The wall formed by the dentary bears well-developed insertion markings and this was evidently a powerful muscle.

ii) CONSTRICTOR DORSALIS GROUP

Three divisions of the constrictor dorsalis group are recognized by Lakjer (1926). Two of these, the M. protractor pterygoidei and M. levator pterygoidei, are concerned with movement of the dermal skull roof and palatoquadrate (maxillary segment) relative to the braincase (occipital segment). The third division, the M. levator bulbi, is concerned with movements of the eyelid. The first two muscles are absent in modern akinetic skulls such as those of Crocodilia, Chelonia and Mammalia.

Ostrom (1961) failed to find any evidence of insertion areas for the levator and protractor pterygoidei muscles in hadrosaurs but suggested that the M. levator bulbi was present. He noted (: 108) that 'anterior and ventral to the trigeminal foramen, located on the laterosphenoid between the bony grooves for the profundus and maxillary branches of the trigeminal nerve, is situated a moderately concave, antero-laterally facing, triangular surface which may have served as the origin site of the M. levator bulbi'. He stated that the position of this surface on the lateral wall of the braincase and the direction it faces, directly towards the orbit, supported this interpretation. Ostrom stated that the akinetic nature of the skull ruled out the possibility that this area was for either a levator or a protractor pterygoidei and that, in addition, no other site for the M. levator bulbi was found on any of the numerous skulls examined.

In *Hypsilophodon* there is an equivalent slightly concave surface, with insertion markings, which bears the same relationships to the profundus (V_1) and maxillary branches (V_2) of the trigeminal nerve (Text-figs. 4B, 60A) but, in contrast, it is on the prootic and basisphenoid. In hadrosaurs there are no sutures in this region so this surface could also be on the prootic and basisphenoid. It is considered likely that the concave surface in hadrosaurs is the same as that in *Hypsilophodon.*

Oelrich (1956) gave a detailed account of the anatomy of the skull of the lizard *Ctenosaura.* He showed a concave surface on the prootic and basisphenoid, immediately below the trigeminal foramen. This surface bears exactly the same relationship to the surrounding bones and nerves as that on the same bones in *Hypsilophodon* (compare Text-fig. 4B with Oelrich 1956, fig. 8). In fig. 53 Oelrich shows a muscle which clearly originates from this surface but it is not labelled. However, a comparison with fig. 35 shows that this is the M. protractor pterygoidei. Oelrich (1956 : 45) stated that the M. protractor pterygoidei 'forms the lateral wall of the tympanic cavity. It is a large fan-shaped muscle arising from the lateral surface of the anterior inferior process of the prootic, the lateral surface of the alar process of the basisphenoid, and the posterior border of a tendon which extends from the proximal end of the pila antotica to the cartilage covering the anterior tip of the basipterygoid process just above the condyle'. This suggests that the surface on the prootic and basisphenoid of *Hypsilophodon* could have been for the M. protractor pterygoidei. However, the relationship of this surface to the branches of the trigeminal nerve clearly shows that it is the same as that in hadrosaurs which, as Ostrom (1961) suggests, may have been for the M. levator bulbi. This possible difference may be related to differences of kinetism. The skull of *Ctenosaura* is kinetic with the M. protractor pterygoidei moving the ventral part of the braincase away from the parietal. Presumably this was the position in the kinetic ancestor of hadrosaurs. When the skull became akinetic the M. protractor pterygoidei was lost. In *Ctenosaura* (Oelrich 1956, figs. 7, 8, 35) the M. levator bulbi originates from the pila antotica which passes anteriorly from the area of origin of the M. protractor pterygoidei. If the situation was similar in the ancestor of hadrosaurs the M. levator bulbi had only to shift slightly posteriorly to occupy the surface originally occupied by the M. protractor pterygoidei. In *Ctenosaura* this surface faces antero-laterally directly towards the orbit and would provide an excellent surface for the M. levator bulbi. However, the surface in hadrosaurs may have been occupied by a M. protractor pterygoidei which formed the lateral wall of the tympanic cavity.

It is rather difficult to determine the composition of the constrictor dorsalis group in *Hypsilophodon.* If the skull was metakinetic then the group must have been as in *Ctenosaura* with the M. protractor pterygoidei on the prootic and basisphenoid and the M. levator bulbi on the more anterior pila antotica. In this case the M. levator pterygoidei would have originated from the parietal but there is no trace of such an origin in *Hypsilophodon.* However, this is hardly surprising because this muscle would have been only a slip and unlikely to leave any trace. If the skull of *Hypsilophodon* was akinetic then the position could still have been as in *Ctenosaura* with the lateral wall of the tympanic cavity formed by the M. protractor pterygoidei. The M. levator bulbi may have originated from the area on the prootic and basisphenoid previously occupied by the M. protractor pterygoidei but, as discussed in the next section, there are certain features which indicate that the skull might have been kinetic.

iii) CONSTRICTOR VENTRALIS GROUP

These muscles are thin sheets which link the two mandibular rami. Ostrom (1961) figured one specimen which shows a possible area of origin of the M. mylohyoideus but concluded that the position was indeterminable ; the same is true for *Hypsilophodon.*

iv) M. DEPRESSOR MANDIBULAE

As in all reptiles this branchial muscle linked the retroarticular process of the mandible to the dorsal occipital surface of the skull. In hadrosaurs there is an insertion area on the medial surface of the retroarticular process (Ostrom 1961) but its position cannot be determined in *Hypsilophodon.* Ostrom concluded that in hadrosaurs the depressor fibres originated from the tip of the paroccipital process, the form of which was probably determined by the stresses imposed by this muscle. This was presumably the case in *Hypsilophodon* also (Text-fig. 59A).

e) *Kinetism*

Versluys (1910) introduced the concept of kinetism with respect to the reptilian skull. A kinetic skull is one in which there is a movable joint between two segments of the braincase (neurocranium and/or dermal roofing bones). Frazetta (1962) recognized three types which are distinguished by the position of the hinge region. In prokinesis the hinge is between the nasal and frontal bones, in mesokinesis it is between the frontals and parietal, while in metakinesis it is between the parietal and supraoccipital (or other bones of the occipital series). A kinetic skull may have one joint (monokinetic) or two (amphikinetic). In addition there may be movement between individual parts of the maxillary segments (dermal skull roof and palatoquadrate).

In *Hypsilophodon* the nasals are overlapped by the frontals while the lateral part of this sutural region is overlapped by the dorsal sheet of the prefrontal (Text-figs. 5B, 6B) so it is unlikely that there was any movement in this region. The suture between the frontals and the parietal consists of a well-developed set of interdigitating ridges and grooves (Text-fig. 7B). At first sight it would appear that this suture was immobile but it is comparable to the frontoparietal suture of a large skull of *Varanus* at which movement occurred (Frazetta 1962). The presence of a good sutural system and a slight hinging action are not necessarily incompatible because the former compensates for any weakness resulting from the latter. The frontal of *Hypsilophodon* has a laterally directed spike which is enclosed by the postorbital (Text-figs. 4B, 7B, 8). The postorbital probably remained fixed in position with respect to the parietal because there is a suture between them and because it received the head of the laterosphenoid ventrally (Text-fig. 6B). In addition the postorbital overlaps the squamosal with which it forms the temporal bar. As the pars superficialis, the pars medius and part of the pars profundus of the M. adductor mandibulae externus originated on this bar it is unlikely that there was any movement between its two parts. A slight hinging may have occurred at the fronto-parietal suture (mesokinetic joint) with the mesokinetic axis on the line across the frontals joining the two laterally directed spikes. These spikes would have allowed rotation yet kept the frontals fixed relative to the postorbital and close to the parietal. In *Varanus* the lateral part of the frontal and parietal fits into a concavity of the postorbital (Frazetta 1962, fig. 1a). The presence of a process anterior and posterior to the fronto-parietal suture also ensures that the frontal and parietal remain close together even though a hinging action is possible.

If the skull of *Hypsilophodon* was mesokinetic then there would have been some other cranial movements (Text-fig. 59B). The postorbital has a long overlapping and smooth contact surface with the jugal so it is likely that a sliding action was possible at this suture. In the palate the pterygoid contacts the articular surface of the basipterygoid process (Text-fig. 5C) at which movement would obviously be possible. The nature of the sutures in the palatal region shows that there was no other plane of movement there. The palatine is firmly sutured to the maxilla as is the ectopterygoid. The ectopterygoid bears a triangular flange of which the apex is medially directed. This flange is recessed into the dorsal surface of the pterygoid (Text-fig. 5C) which borders it anteriorly and posteriorly. Consequently movement of the pterygoid on the ectopterygoid was impossible, which meant that a sliding articulation with the palatine was out of the question.

The relationship between the parietal and bones of the occipital series remains to be considered. Posteriorly the parietal is overlapped by the squamosal, the posterior process of which overlaps the distal part of the paroccipital process (Text-figs. 7B, 8). The occiput in posterior view (Text-fig. 8) appears rather solid but the medial part of the parietal is not sutured to the underlying supraoccipital (Text-fig. 5A). The postero-ventral edge of the parietal and squamosal together form a convex curve (Text-fig. 5B) so the transversely orientated metakinetic axis would have been restricted to a small part of this edge. A hinging action would have involved only a slight movement of the squamosal away from the paroccipital process and this may have been possible (Text-fig. 59B).

No sliding could occur at the joint between the supraoccipital/prootic and the laterosphenoid because of the curved shape of the laterosphenoid and the nature of its suture with the prootic (Text-figs. 4B, 5C, 7B, 9). If the skull was metakinetic then the maximum movement would have been at the anterior end of the laterosphenoid. This is expanded laterally to form a well-developed head (Text-figs. 4B, 6B, 7B) which fits into a depression in the postorbital and frontal, opening ventrally with vertical sides. The depression becomes progressively deeper passing laterally (Text-fig. 7B) so that contact would have been maintained if the head of the laterosphenoid had moved ventrally. The head tapers laterally (Text-figs. 6B, 7B) and the dorsal part of the lateral half is rounded antero-posteriorly (Text-figs. 4B, 7B). The surface of the rounded part of the head and of the lateral part resembles that of the basipterygoid and was possibly an articular surface. In lizards (Frazetta 1962), and presumably in some individuals of *Sphenodon* (Ostrom 1962), the ventral part of the braincase moves slightly antero-posteriorly relative to the parietal. In *Hypsilophodon* the posterior wall of the depression in the frontal and postorbital is quite shallow so, with a slight ventral displacement, such an antero-posterior movement might have been possible. As discussed above (Section d ii) there is a surface on the prootic and basisphenoid which was possibly the area of origin of the M. protractor pterygoidei, one of the muscles necessary to effect the kinetic movements.

Cox (1959) noted that the vena capitis dorsalis passes through the post-temporal fenestra in living reptiles. It is significant that the remnant of the post-temporal fossa is totally enclosing by the paroccipital process in *Hypsilophodon.* In hadrosaurs in which the skull was akinetic Langston (1960) showed that the paroccipital process forms the ventral border to the remnant of the post-temporal fossa. In a metakinetic skull with a close but movable contact between the opisthotic and the squamosal, the vena capitis dorsalis, if it passed between those two bones, would have been subjected to pressure changes. The course of this vessel through the paroccipital process suggests that such a movement occurred because, had it not done so, such enclosure would have been unnecessary. From the nature of the material it is impossible to prove one way or the other but I consider that the skull of *Hypsilophodon* may have been mesokinetic and metakinetic (Text-fig. 59B). However, I do not know what function these movements would have served in a herbivore. It would be helpful to know something of the selective advantages conferred by the quite complex kinetic movements which, according to Frazetta (1962), are retained in the herbivorous lizards *Ctenosaura* and *Uromastix.*

f) *Streptostyly*

A streptostylic skull is one in which the quadrate moves relative to the other bones of the skull. This term is not interchangeable with kinetic because the two types of movement involved can occur independently or together. The head of the quadrate of *Hypsilophodon* is triangular in outline with a rounded articular surface (Text-fig. 4A) which fitted quite closely into a socket in the squamosal (Text-fig. 6B). The quadrate may have been loosely connected to the quadrotojugal but the likelihood of movement was minimal because, although the quadratojugal overlapped the quadrate ventrally, dorsally the situation was reversed. The lateral surface of the quadrate forms an angle of about 50 degrees with the pterygoid flange. Movement of the quadrate relative to the pterygoid must have been in the plane of this flange so the dorsal part of the quadratojugal would have restricted movement anteromedially ; the ventral part would have restricted it postero-laterally. The quadratojugal is overlapped by the jugal and, although a slight amount of sliding is conceivable, the parting of this contact necessary for the independent movement of the quadrate is considered unlikely. In addition the presence of the jugal on the lateral surface would have limited the amount of posterior movement.

In medial view the quadrates of R2477 (Text-fig. 4B, Pl. 1, fig. 3) and R192 clearly show the postero-lateral limits of the contact area with the alar process of the pterygoid. This is indicated by a distinct step in the level of the surface. The region of the quadrate on which this outline is preserved is curved in cross-section so that it is concave in medial view. This curved part is on the shaft, the posterior edge of which is sharp and makes an angle of about 110 degrees with the plane of the pterygoid flange. The postero-lateral part of the alar process of the pterygoid would have been curved in cross-section with a convex lateral surface. It is apparent that any movement between the quadrate and the pterygoid must have been one of sliding. The curved distal part of the alar process would have fitted against the concave part of the quadrate shaft and would have limited the anterior movement of the quadrate. In addition the curved nature of this distal part would have reduced the likelihood of any movement of the quadrate away from the pterygoid.

I consider that the contacts with surrounding bones would have prevented any independent movement of the quadrate. However, a slight movement of the quadrate with the quadratojugal and jugal relative to the postorbital, squamosal and braincase may have occurred if, as was possibly the case, the skull was mesokinetic (Text-fig. 59B).

g) *The antorbital fenestra*

In thecodontians such as *Euparkeria* (Ewer 1965) and *Stagonolepis* (Walker 1961) the large antorbital fenestra is bounded dorsally by the lachrymal and ventrally by the maxilla. In *Hypsilophodon* the antorbital fenestra is actually represented by the two internal antorbital fenestrae in the medial wall of the maxilla, visible in lateral view (Text-figs. 4A, B). The lateral opening will be called the external antorbital fenestra while the space totally enclosed by the maxilla is the antorbital fossa (Text-figs. 60C, D). The medial sheet of the maxilla and lachrymal is present in *Heterodontosaurus* and *Fabrosaurus* (Crompton, personal communication), both of which are from the Upper Triassic, but the external antorbital fenestra is large (for *Heterodontosaurus* see Crompton & Charig 1962). In *Parksosaurus* (see Parks 1926, Galton in press) the lateral sheet of the maxilla is large and the external antorbital fenestra is small. In *Dysalotosaurus* (see Janensch 1955) both the external antorbital fenestra and the lateral sheet of the maxilla are small but a large sheet from the premaxilla encloses part of the antorbital fossa. *Camptosaurus* in lateral view is similar and Gilmore (1909 : 214–215) mentioned that the lateral foramina in the maxilla 'are received by a large, elongate cavity situated at the base of the dorsal process between the thin inner and outer walls, and which opens posteriorly'.

The important point is that in these lower ornithopods there is a large fossa which opens posteriorly into the ventral part of the orbit below the eye. This cavity represents the antorbital fenestra, which in thecodontians also opens posteriorly

(Walker 1961, Ewer 1965). Consequently the obliteration of the antorbital fenestra, at least in these lower Ornithischia, was more apparent than real because it was merely enclosed medially and laterally to a varying extent by thin sheets of bone.

The function of the antorbital fenestra of thecodontians has been discussed by Walker (1961) and Ewer (1965). Both agree that in the more advanced forms the fenestra was for the origin of an anterior portion of the pterygoideus muscle. Walker (1961) kept the insertion of this portion on the lower jaw close to the articulation so that it effected a rapid movement of the jaw at the beginning of the bite. Ewer (1965) placed the insertion more anteriorly on the jaw so that this portion provided power for the initial phase of the bite.

In *Hypsilophodon* the only possible exit for a muscle from the antorbital fossa is posteriorly across the floor of the orbit. This opening in R2477 is about 4 mm wide and it is restricted dorso-laterally by the projecting edge of the jugal (Text-figs. 5B, C). As noted above, the M. pterygoideus dorsalis probably originated from the dorsal surface of the ectopterygoid. An anterior portion of this muscle may have extended anteriorly into the antorbital fossa. This portion would have passed across the floor of the orbit, over the edge of the ectopterygoid (Text-fig. 5C) and medial to the coronoid to insert on the lower jaw. Only a small slip or a tendon could have followed this route and the main part of the muscle must have been in the antorbital fossa. However, the morphology of the dorsal surface of the ectopterygoid indicates that, if the M. pterygoideus dorsalis extended anywhere, it would have passed on to the adjacent surface of the palatine. On the anterior part of the palatine there is a slight transverse step which may indicate the limit of such an extension (Text-figs. 5C, 60D).

When discussing the function of the antorbital fenestra it is assumed that the muscle concerned is derived from the M. pterygoideus dorsalis, as is the pterygoideus D of crocodiles (Lakjer 1926), but this anterior extension could have been part of the M. pterygoideus ventralis. In *Hypsilophodon* this latter probably originated from the ventral surface of the pterygoid and ectopterygoid (Text-figs. 4B, 60D). It is possible that a portion of this muscle passed through the vacuity between the ectopterygoid, palatine and maxilla (Text-figs. 5A, 6A) from an origin in the antorbital fossa (Text-fig. 60D). In specimen R2477 this vacuity is a rather square oval, 6 mm × 4 mm. The lateral wall of the maxilla becomes progressively shallower posteriorly and its edge more rounded. The topography of this part of the maxilla suggests that whatever originated from the antorbital fossa may have passed postero-ventrally through this palatal vacuity (Text-figs. 5A, C, Pl. 1, fig. 1, Pl. 2, fig. 2). If a cord be passed from the top of the antorbital fossa to its posterior opening, across the maxilla and through this vacuity, it forms a gentle curve. From the figures of the skull it would appear that a similar course would have been possible in the thecondontians *Euparkeria* (Ewer 1965), *Stagonolepis* (Walker 1961) and *Ornithosuchus* (Walker 1961).

The function of this postulated anterior portion of the pterygoideus in *Hypsilophodon* is not certain. If the insertion of this portion was close to the articulation it would have aided the rest of the pterygoideus in rapidly closing the jaw to effect a cropping action of the anterior horny beaks (function the same if portion was from the pars dorsalis). Such a course would give a very long muscle with a moderately straight course. However, the much more powerful M. adductor posterior, the moment arm of which is quite short, would have been much more effective. If the insertion was more anterior the pull of this muscle would tend to be in the plane of the occlusal surface of the teeth. As a result this would add to the shearing force at these surfaces (see Section h). To be effective this insertion should have been some way forward in the region below the coronoid but there is no evidence to show whether or not this was the case.

The enclosure of the antorbital fenestra in lower ornithischians without its obliteration is rather interesting. These forms could be regarded as demonstrating stages in its closure, the space enclosed having no function, but this is not very satisfactory. In the line leading to *Parksosaurus* this fossa was retained from the Upper Triassic right through to the Upper Cretaceous (Edmonton Formation) and it still retained a posterior exit. If this fossa was functionless it is surprising that it remained for such a long time in a region which was important in supporting the tooth row. A slip of the pterygoideus muscle (pars ventralis and/or dorsalis) probably originated from this space and this slip must have remained functional in these lower ornithopods.

h) *Jaw action*

Information concerning the mode of action of the jaws can be deduced from the arrangement and wear of the teeth, the nature of the jaw articulation and the lines of action of the musculature as reconstructed from the form of the skull. In *Hypsilophodon* there are several features indicating that an antero-posterior movement of the lower jaw was not possible. The inclination of the glenoid surface of the articular at about 30 degrees to the tooth row (Text-fig. 10A) would have prevented any significant retraction of the mandibles. The anterior convergence of the tooth rows (Text-figs. 6A, 10B) would have prevented any mandibular protraction. In addition the tooth rows are slightly curved with the individual teeth forming a rather jagged edge. It is therefore concluded that mandibular movement consisted only of a hinge movement about the condyle of the quadrate. The occlusal surfaces in *Hypsilophodon* are at an angle of about 10 degrees to the vertical for anterior teeth or about 25 degrees for more posterior teeth. These angles are rather approximate because the precise orientation of the maxillae is not absolutely certain. The occlusal surfaces were certainly not vertical because in that case the lower jaw would not fit between the maxillae.

In *Hypsilophodon* the maxillary and dentary teeth are thickly enamelled on one side and are transversely curved in opposite directions (Text-fig. 61). The convex surface bears thick enamel in both cases and, as the enamel was more resistant it formed a sharp edge while the rest of the tooth formed an obliquely inclined occlusal surface (Text-figs. 15, 60, 61). The sharpness of the enamelled edge is enhanced by the presence of serrations formed by the wear of the longitudinal ridges on the enamelled surface of the crown. In particular the apex ridge of each dentary tooth is very large and formed a prominent spike on the cutting edge (Text-figs. 15c, 16c).

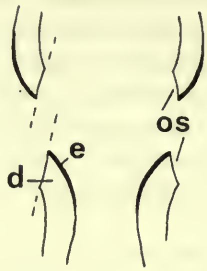

Fig. 61. *Hypsilophodon foxii.* Diagrammatic cross-section through dentition assuming that occlusal surface of maxillary and dentary teeth equally spaced apart. Abbreviations : de, dentine ; e, thickly enamelled surface ; os, occlusal surface.

When a force is applied across two obliquely inclined but parallel surfaces it can be resolved into two components using a parallelogram of forces. One component, that responsible for a crushing action, acts perpendicular to the occlusal surfaces. The other component, that responsible for a shearing action, acts parallel to the occlusal surface. With the angle of the occlusal surfaces at about 10–25 degrees to the vertical it is apparent that the shear component represented the greater proportion of the total force exerted across the obliquely inclined occlusal surfaces of *Hypsilophodon*. In addition, the sharp enamelled edges of both teeth would have had a cutting action.

The lateral relationship of the occlusal surfaces of the maxillary and dentary teeth cannot be determined from the skull material. The above analysis is based on the assumption that the lower teeth were the same distance apart transversely as the corresponding uppers (Text-fig. 61). However, the dentary teeth were probably closer together so that an oblique movement was possible with the teeth of only one side in opposition at a time. The amount of shift needed is quite small and, because the articulation surface of the quadrate (Text-fig. 6A) is much wider than that of the articular (Text-fig. 10B), such a movement may have been possible. This oblique movement would have resulted from the asymmetrical contraction of the jaw adductor muscles. With such a movement the sharp enamelled edges would have cut past each other and the action at the occlusal surface would have been almost exclusively one of shear.

The jaw adductor muscles insert on to the coronoid and the adjacent bones (Text-figs. 59, 60D) and their force is applied between the fulcrum (the glenoid cavity) and the resistance (food between the teeth). As a result, the lower jaw forms a third class lever with the adductor muscles acting somewhat obliquely. When an obliquely inclined muscle inserts on to a straight lever the effective force (i.e. the moment arm) can be increased by elevating the point of application above the axis or, alternatively, the fulcrum can be depressed below the line of the tooth row. In both cases the force exerted by the muscle is increased without decreasing the gape possible ; this would be decreased if the point of insertion were moved along the axis further away from the fulcrum. In *Hypsilophodon* the coronoid process is large so that the moment arms of the M. pseudotemporalis and the M. adductors externus, medius and profundus were lengthened (Text-fig. 59A). The glenoid cavity is set below the level of the tooth row so that the moment arm of all the main adductor muscles was increased.

The average line of action, together with the moment arm, is indicated for each muscle in the reconstruction of the skull (Text-fig. 59A). Although not absolutely accurate this reconstruction is adequate for general conclusions regarding the relative size of each muscle and its moment arm. The M. pseudotemporalis and the three divisions of the M. adductor externus were the main adductors. The M. pseudotemporalis has the longest moment arm but it was probably not so important as the other three muscles combined (they have a common line of action). The M. adductor mandibulae posterior was a large muscle but it had a small moment arm. Consequently it was important for the initial closing movements but then probably functioned mainly to prevent disarticulation of the jaw. The M. pterygoideus dorsalis and ventralis were probably not very large. Their extremely small moment arm means that they probably functioned chiefly to aid the M. adductor posterior in preventing disarticulation of the lower jaw. As discussed in Section (g) it is possible that an anterior portion from the antorbital fenestra inserted more anteriorly on the jaw (Text-fig. 60D). The only muscle acting to open the jaw, the M. depressor mandibulae, had a small moment arm. This means that the muscle had a fast action but exerted little force. However, there was little resistance to overcome and the weight of the lower jaw itself would have aided its own depression. It is apparent that the main adductors had a good mechanical position and the slight forward inclination of the quadrate helped it to resist the forces developed. The teeth formed an efficient apparatus for dealing with plant food as they combined cutting, shearing and crushing.

The food was obtained initially by the cropping action of the anterior horny beaks. As Nopcsa (1905) noted, the premaxillae are rugose anteriorly, indicating the presence of a horny beak. The pointed predentary has a fairly smooth outer surface but the only specimen available (Text-fig. 11) is from a small individual. The predentary was probably also covered by a horny beak because this is the case in other ornithischians (e.g. hadrosaurs, Ostrom 1961). More posteriorly the premaxillary teeth presumably bit outside the predentary. In ventral view (Text-fig. 6A) there is a step between the line of the tooth row of the premaxilla and maxilla. In addition, much of the maxilla is visible lateral to the tooth row which, as a result, is overhung (Text-fig. 3). The dorsal view of the lower jaw (Text-fig. 10B) shows a similar situation with much of the dentary lying lateral to the tooth row. I believe that the corner of the mouth probably did not extend much further back than the anterior end of the maxillary tooth row. Consequently the mouth was small and there was quite a large space lateral to the tooth rows of the maxillary and dentary which was necessary if the animal was to chew its food (see below: 150) The tongue would have moved the food around so that it was chewed several times while the space lateral to the tooth rows would have received the food prior to its next passage between the occlusal surfaces.

VII. ASPECTS OF POST-CRANIAL ANATOMY

a) *Individual variation*

There is a surprising amount of variation between the few specimens of *Hypsilophodon foxii* represented by articulated material. Certain of these variations are found also in *Thescelosaurus neglectus* (see Galton in press *a*). Details of variations with age and sex are available for *Protoceratops andrewsi* (Brown & Schlaikjer 1940) but, apart from this, there is very little information in the literature concerning variation in other species of dinosaur.

The most notable variation is the presence of the additional sacral rib in the hexapleural sacrum in contrast to the pentapleural type (see page 57). In Ornithischia the number of sacral vertebrae may vary between different species of the same genus, e.g. *Camptosaurus dispar* with 5 and *C. browni* and *C. depressus* with 6 (Gilmore 1909); *Iguanodon mantelli* with 5 and *I. bernissartensis* with 6 (Boulenger 1881, Dollo 1883). These are generally considered to be valid species. However, in the case of *Iguanodon*, van Beneden (1881) regarded the variation in the sacral count as an individual or sexual variation; Hooley (1912) also regarded it as a sexual variation (with *I. mantelli* as the female), although later (1925) he treated the two forms as separate species. Nopcsa (1918, 1929) considered that male ornithischians were characterized by the presence of extra sacral vertebra(e). In *Camptosaurus* the sacral difference is associated with several other differences (see Gilmore 1909, Nopcsa 1918, 1929) while in *Iguanodon* there are even more (see Nopcsa 1918, 1929, Dollo 1883, Abel 1927). However, in *Hypsilophodon* there are only a few other significant differences associated with that of the sacrum. In the pentapleural specimen R196, when compared with the hexapleural specimens, the peduncle of the ilium is narrower, the facets on the ilium for sacral ribs 2 to 5 are more anteriorly placed and the sub-acetabular part of the ischium is longer. A size difference is often used as a basis for specific separation with fossil material but there is no justification for this because the largest sacra of each type are about the same size (length of first three centra 75 mm in R193, 71 mm in R8422). The close similarity of the teeth and post-cranial skeletons of individuals with the two sacral types clearly shows that they are the same genus *Hypsilophodon*. The specific identity or separateness of the two sacral types depends on the taxonomic significance attached to the presence of the additional sacral rib.

In living birds the number of sacral vertebrae does not vary within a species (Nopcsa 1929) and this is apparently also the case in reptiles (Werner 1895). However, the sacral count can vary in man: there are usually five lumbar and five sacral vertebrae but this count can be four and six or six and four (Brash & Jamieson 1943). Consequently the number of sacral vertebrae (and hence ribs) can vary within a species. In view of the position in man and the individual variation shown by R5829 I consider that the two sacral types are best regarded as individual variations of *Hypsilophodon foxii*. However, even if the two types were to be regarded as separate species it would be inadvisable to give them taxonomic status because the sacral type of the holotype of *Hypsilophodon foxii* is not known.

The presence of an extra sacral rib (or vertebra) cannot be regarded as an age variation because the smallest specimen available (R5830) already has the extra sacral rib. The sacral difference in *Hypsilophodon* probably represents a sexual dimorphism, with the hexapleural type as the male. The sacral type can be determined in only eight individuals, there are five hexapleural forms and three pentapleural forms. It is interesting that Nopcsa (1929) used the high ratio of *Iguanodon bernissartensis* (regarded as the female) to *I. mantelli* (23 : 1) at Bernissart as evidence for herding in this species (*I. mantelli*).

The specimens of *Hypsilophodon* show quite a few other variations which were mentioned in the descriptions of the individual elements. The differences that appear to be correlated with the sacral difference have already been noted. Individual variations relate to the presence of the cavity in the premaxillae ; the contacts of the lateral sheet of the maxilla with the premaxilla and with the lachrymal and jugal ; various features of the sacrum ; the degree of ventral curvature of the anterior process of the ilium and the size of the medial ledge along its ventral edge ; the opening or closure of pubic foramen in small or large individuals ; the cross-section of the post-pubic rod ; the outline of the ventral junction between the head and shaft of the ischium ; the degree of development of the depression at the base of the fourth trochanter of the femur ; the form of the edges of the tibia ; and the outline of the posterior junction between the shaft and the blade of the scapula. Variations related to increased size probably include the ankylosis of the neural arches, ribs and centra of the sacral vertebrae ; the presence of strong sutural ridges between the scapula and coracoid ; the greater angularity of the edges of the scapula and coracoid and the greater degree of twisting of the shaft of the scapula and humerus.

b) *The first sacral rib*

In the reconstructions of *Hypsilophodon* by Hulke (1882), Marsh (1895, 1896*a*, *b*), Swinton (1934, 1936*a*) and von Huene (1956) the iliac peduncle is shown square-ended with the first sacral rib fitting on to the base of the anterior process. However, the first sacral rib actually fits against the iliac peduncle (Text-figs. 47A, 50B, 51B). This is the same as in *Thescelosaurus* (see Gilmore 1915, Galton in press *a*), *Camptosaurus* (see Gilmore 1909) and *Dysalotosaurus* (see Janensch 1955).

The peduncle region in *Hypsilophodon*, like that in most other Ornithischia, is quite slender and roughly triangular in cross-section (Text-fig. 47B) with the facet for the first sacral rib facing dorso-medially. As a result of the wedge-shaped cross-section the acetabular margin of the peduncle is horizontal yet there is a broad sutural surface with the first sacral rib. The slender peduncle region is therefore backed by the first sacral rib through which the thrust from the femur is transmitted to the vertebral column. This becomes progressively more important as the vertebral column is held more vertically. The first sacral rib is extremely thick and almost cubical (Text-fig. 27). The ends of sacral centra 1 and 2 form a large contact surface and then flare out to embrace the proximal part of the first sacral rib (Text-fig. 27B). This is also the case in *Thescelosaurus*, *Camptosaurus*, the English '*Camptosaurus*' *prestwichi* (see Gilmore 1909) and *Dysalotosaurus*. In these dinosaurs, as was probably the case in all lower Ornithopoda, the first sacral rib performed a key rôle in strengthening the iliac peduncle.

In *Hypsilophodon* the additional sacral rib in the hexapleural type of sacrum must have acted as an anterior brace for the first sacral rib and, in addition, helped to spread the thrust anteriorly. In R5829 this action was enhanced by the sutural union of the new sacral rib with the transverse process of the first sacral vertebra. It is perhaps relevant that the peduncle is more expanded transversely in forms with a hexapleural sacrum than in the other type but more specimens are needed to confirm this difference and, in addition, to provide more information about the union between the neural spines. In R195, which has a hexapleural sacrum, the edges of the neural spines of sacral vertebrae 1 and 2 are thick and closely united by a suture (Text-figs. 25E, F, 27B). Such a suture would further strengthen the union between the two vertebrae supporting the first sacral rib. However, the union between the neural spines is variable even in the few sacra available.

The iliac peduncle is slender and only the tip could have contacted the pubis. Here there is a small rugose area running diagonally across the end of the peduncle (Text-figs. 47B, 51C). This sutural surface is surprisingly small in comparison with the corresponding surface on the pubis (Text-fig. 52A). Anterior to the concave acetabular region, which in life was probably covered by cartilage, there are two distinct areas which are separated by a slight edge (Text-figs. 46A, 52A). Anteromedially there is a slightly convex area (sa. r. 1) of which the plane is inclined slightly more medially than that of the similar but smaller outer area (il.). It would appear that the ilium sutured with the outer area while the inner one was for the first sacral rib. The ventral surface of this rib in R195 (well preserved on left side, Text-fig. 27C) forms a large flat surface against which the pubis fitted. Consequently the pubis contacted the first sacral rib in addition to the ilium. A similar contact between the pubis and the first sacral rib is present in *Thescelosaurus* (see Galton, in press *a*) but, because the relevant areas of the ilium, pubis and sacrum are not known, it is impossible to determine the position in *Parksosaurus*. It is probable that the pubis articulated with the first sacral rib in *Dysalotosaurus*, to judge from the figures by Janensch (1955), but this possibility is not mentioned. The acetabular aspect of the pubis is very similar to that of *Hypsilophodon* but the broad anterior articular surfaces form one rounded curve. The peduncle of the ilium is almost identical in internal and external views but the acetabular view is not given. The first sacral rib has the same square shape but only the lateral view is given. The pubis of the mounted skeleton of *Iguanodon atherfieldensis* in the British Museum (R5764) has a broad dorsal surface which contacts a corresponding surface on the first sacral rib when the ilium is in articulation with both bones ; Hooley (1925) does not mention this.

c) *Limb articulation and posture*

i) FORELIMB

Both scapulae were displaced in specimen R196 so the original position cannot be determined. However, in several specimens of *Iguanodon* and hadrosaurs the scapula is preserved lying parallel to the vertebral column which, as Lull & Wright (1942) noted, was probably its position in life. It is reasonable to assume that this was also the case in *Hypsilophodon* (Text-fig. 62). The ventral edge of the coracoid is rough and bore a cartilaginous extension so there is no direct evidence concerning the angle at which the coracoid was held. When the transverse curve of the scapula and coracoid (Text-fig. 34B) is compared with that of the anterior dorsal ribs it appears that the coracoid probably made an angle of about 35 degrees (± 5 degrees) above the horizontal.

In reconstructions of bipedal dinosaurs the humerus is usually shown held vertically below the glenoid. Gregory (*in* Osborn 1917) and Sternberg (1940, 1965) pointed out that in this position the head of the humerus is out of the glenoid cavity. They concluded that the humerus was held more laterally while Sternberg (1965) thought that the ornithopod humerus was actually held horizontal. If maintaining contact between the limits of the articular surfaces of the humerus and the glenoid cavity was the factor limiting the range of movement, then this range was very restricted in the transverse plane. In *Hypsilophodon* this range would have been about 30 degrees: from 35 to 65 degrees to the vertical (or 90 to 120 degrees to the lateral surface of the coracoid). However, in the crocodile the range of movement is at least 90 degrees: from horizontal and lateral to vertically below the body in the high walk and the gallop (Cott 1961). It would be surprising if the range of movement was less than this in *Hypsilophodon*. It should be noted that the articular surface of the humerus is formed by all of the proximal end, not just the convex surface of the dorso-laterally directed 'head' (see Text-fig. 38). Consequently this 'head' can be completely out of the glenoid (i.e. visible in lateral view) but the more medial part of the articular surface is still in the glenoid. Although the humerus could have been held much more laterally than shown in most reconstructions the vertical pose was probably quite normal. The anterior limit of movement of the humerus can be determined because the anterior edge of the head comes up against the scapula. The edge of the glenoid in this region is reduced, forming a depression (Text-fig. 35A) into which fitted the humerus. The anterior limit is such that the delto-pectoral crest is approximately perpendicular to the adjacent lateral surface of the scapula.

The elbow joint, radius and ulna are similar to those of other dinosaurs. The articulations at the wrist cannot be determined because this region is badly preserved. The manus was undoubtedly capable of grasping. The phalanges of the first three digits are well formed (Text-fig. 41) and the third digit, with four phalanges, must have been capable of a large amount of flexion. Distally the fifth metacarpal has a definite condylar end with a well-defined articular surface which undoubtedly carried at least one phalanx. This metacarpal is certainly small but this does not necessarily mean that digit V was reduced. Metacarpal V of *Iguanodon*, relative to the other metacarpals, is proportionally only slightly larger than that of *Hypsilophodon* yet it bears four well-developed phalanges – the longest set in the hand (see Hooley 1925). In hadrosaurs the fifth metacarpal is about a third of the length of metacarpal III but it still bears three small phalanges (see Parks 1920 for *Kritosaurus*, Lull & Wright 1942 for *Anatosaurus*).

Proximally the lateral corner of metacarpal IV (Text-fig. 41B) closely resembles the medial corner of metacarpal I and, in the absence of metacarpal V, it would be assumed that digit V was completely reduced. This indicates that metacarpal V was not held alongside metacarpal IV but set at an angle, though this has probably been somewhat exaggerated as preserved in this specimen. The proximal end of metacarpal V, which articulated with the ulna, is slightly concave with a relatively extensive articular surface dorsally and ventrally. This indicates that quite a wide range of movements were possible, including a certain degree of ventral rotation. With metacarpal V in the same plane as the other metacarpals (Text-fig. 41) its phalanges would face ventro-medially because, as a result of the twisted shaft, the distal articular surface is set at an angle of about 135 degrees to the horizontal (a line through the transverse plane of the carpus). In this feature it is comparable to the human first metacarpal, the distal end of which makes a similar angle (45 degrees in this case). The condylar regions of metacarpals II to V are horizontal in man. However, as preserved it appears that in *Hypsilophodon* those of metacarpals II and III are set at an angle of 45 degrees to the horizontal so that these digits face ventro-laterally (Text-fig. 41B). With the fifth digit facing ventro-medially its joint surfaces are perpendicular to those of the second and third digits. This reduced the amount of ventral rotation necessary before the fifth digit was truly opposable. However, more material is needed to confirm the nature of the distal articular surfaces of metacarpals II, III and V.

ii) HINDLIMB

The femur was certainly held beneath the body. With its head set on a well-developed neck perpendicular to the shaft, no other pose was possible. The distal surface is somewhat obliquely inclined in posterior view (Text-fig. 54D). However, the corresponding surface of the tibia slopes the other way (Text-fig. 56B) so that the tibia moved more or less antero-posteriorly on the femur. The range of movement of the tibia cannot be determined because this depended on the restraining action of the knee capsule ligaments. The head of the fibula articulated with the groove on the lateral surface of the outer condyle of the femur when the knee was fully flexed.

In dinosaurs the joint between the tibia/fibula and the proximal tarsals was rendered immobile in various ways to form a mesotarsal joint. In ornithischians the joint is between the proximal and the distal tarsals, with both the astragalus and the calcaneum firmly attached to the tibia/fibula. In *Hypsilophodon* the distal end of the tibia is broad and backs the calcaneum as well as the fibula. The astragalus wraps round the inner malleolus with an anterior ascending process which was attached by ligaments to the adjacent part of the tibia (strong insertion markings here, see Text-fig. 56G). With a digitigrade pose the metatarsals, because they meet the tibia at an obtuse angle, would tend to rotate the astragalus anteriorly but the anterior process of the astragalus prevented this. The proximal tarsals, although firmly attached to the tibia and fibula, were not fused to them because they have shifted in most specimens. However, apart from small specimens (e.g. R5830) it appears that the astragalus and calcaneum were ankylosed together because no division is visible between them in larger specimens.

The functional ankle joint was between the proximal and distal tarsals, which were firmly attached to the tibia/fibula and to the metatarsus respectively. The range of possible movement at this joint is easily determined because the markedly convex articular surface of the calcaneum must have retained contact with the second distal tarsal. This gives a minimum angle of 60 degrees between the tibia and the metatarsus and a maximum of 180 degrees.

There was probably no movement between the distal tarsals and the metatarsals. Distal tarsal I fits across the joint between metatarsals II and III, engaging a small boss on metatarsal II, and there are well-developed radial striations indicating a strong ligamentous connection. The corresponding surfaces of distal tarsals I and II are of similar form so that they made a good fit. There were probably cartilaginous elements for the rest of metatarsals I and II which, together with the proximal and distal tarsals, were surrounded by a strong joint capsule. Metatarsals I to IV were closely applied to each other with broad contact surfaces so it is very unlikely that there was any movement between them and the metatarsus was therefore rigid.

In the reconstructions of the foot by Hulke (1882, pl. 82) and Abel (1912, fig. 293) the fifth metatarsal, relative to the other metatarsals, is shown much too long; but in Marsh (1895, fig. 9), Heilmann (1926, fig. 115) and Romer (1966, fig. 241) it is correctly drawn. In all these reconstructions the fifth metatarsal is shown lateral to metatarsal IV and also, except in those by Hulke and Romer, closely applied to the lateral edge of metatarsal IV. Proximally this edge is moderately rounded (Text-fig. 57H) but it soon becomes extremely sharp-edged so it is unlikely that metatarsal V occupied this position. The second distal tarsal is wedge-shaped in lateral view (Text-fig. 57M) with a broad and rounded ventral articular surface (Text-fig. 57J) for metatarsal V. In S.M. 4129 metatarsal V is preserved across the ventral surfaces of metatarsals IV and III with its proximal end in contact with distal tarsal 2. Metatarsal V is on the ventral surface of the metatarsus in all the other specimens where it is preserved (R193, R196, R200) and this was probably its natural position. In *Thescelosaurus* metatarsal V is ventral to metatarsal IV (Gilmore 1915, fig. 16) while Parks (1926 : 37) noted that in *Parksosaurus* metatarsal V is 'known only by a small bone under the palmar surface of the left foot'.

iii) QUADRUPEDAL OR BIPEDAL POSE AND THE POSTURE OF THE VERTEBRAL COLUMN

In the reconstructions by Hulke (1882) and Heilmann (1916) *Hypsilophodon* is shown in a quadrupedal pose while Marsh (1895), Abel (1922, 1925), von Huene (1956), Swinton (1962) and Colbert (1965) show it as a biped. In the reconstructions by Smit (*in* Hutchinson 1894) and Swinton (1934, 1936*a*, 1954) both poses are given. Heilmann (1916, 1926) noted that *Hypsilophodon* was not normally bipedal because the structure of its pelvic girdle was similar to that of the completely quadrupedal *Stegosaurus*. Consequently the form and proportions of the limbs must be considered to see whether or not *Hypsilophodon* could have run quadrupedally.

The manus is very small, when compared with the pes from the same individual (Text-figs. 41, 58), and it is adapted for grasping rather than for locomotion. The long bones of the forelimb are smaller and much more slender than those of the hindlimb. Consequently it is unlikely that the forelimb supported the body while the animal was running. *Hypsilophodon* has a forelimb 58·6 per cent of the length of the hindlimb ; if the metacarpals and metatarsals are included, the ratio is 52·5 per cent. The hindlimb would have greatly outstepped the forelimb and this would have been especially significant if the animal remained on all fours while trying to run. In order for the hindlimbs to make their full stride while the animal is quadrupedal the acetabulum must have been much higher than the glenoid cavity. As a result the dorsal vertebral series would have to be obliquely inclined and rise upwards to the pelvis. The presence in R196 of an uninterrupted series of ossified tendons from the fifth dorsal vertebra to the end of the sacrum indicates that this part of the column was relatively rigid with only a limited amount of bending in the sagittal plane. The sacral series would also be obliquely inclined and the column would curve downwards again only at the anterior part of the tail. These points are shown in Heilmann's reconstructions (1916, fig. 76) and the dorsal and sacral series are at an angle of 25 degrees to a line passing through the manus and pes. The knee is still quite strongly flexed and for a full stride this angle would be even larger. The overstepping effect and the resulting pose make it impossible for *Hypsilophodon* to have run quadrupedally.

To run efficiently it is important that the limb be positioned under the body because this lengthens the stride, improves the leverage exerted by each segment of the limb during propulsion and reduces the amount of lateral swinging of the limb during recovery. The lengthening of the distal parts of the hindlimb is an adaptation for fast running with a fore and aft movement of the limb but the distal parts of the forelimb are not elongated (Table V). In fast running quadrupedal ungulates and carnivores the fore and hindlimbs are modified to a comparable degree (see ratios in Gregory 1912). The restriction of cursorial adaptations to the hindlimbs in *Hypsilophodon* clearly shows that the animal was bipedal.

To move bipedally, the hindlimb should be long relative to the trunk (Ewer 1965). The trunk length can be taken as the distance between the glenoid cavity and the acetabulum. If the leg length be taken as femur and tibia, then the ratio leg length : trunk length is 1·26 which is higher than in modern lizards which are facultatively bipedal (see Ewer 1965, fig. 16 – *Basiliscus* – 1·05). However, because *Hypsilophodon* was digitigrade, the third metatarsal should also be included in the leg length, increasing the ratio to 1·59. The trunk is clearly short enough, relative to the hindlimb, for bipedal locomotion. The tail, which is an important balancing organ for facultatively bipedal lizards (Snyder 1962), is sufficiently long in *Hypsilophodon* for this purpose. In addition the rigidity of the posterior two-thirds of the tail, which is ensheathed in ossified tendons, would increase its efficiency as a balancing organ. The small size of the head and forelimbs made balancing easier because it reduced the weight anteriorly. It is therefore apparent that *Hypsilophodon* ran bipedally and could not have done so quadrupedally.

As discussed elsewhere in detail (Galton 1970) I consider that the sacrum of hadrosaurs and iguanodontids was held horizontally while running. This is the pose in living bipeds apart from primates and facultatively bipedal lizards. It was

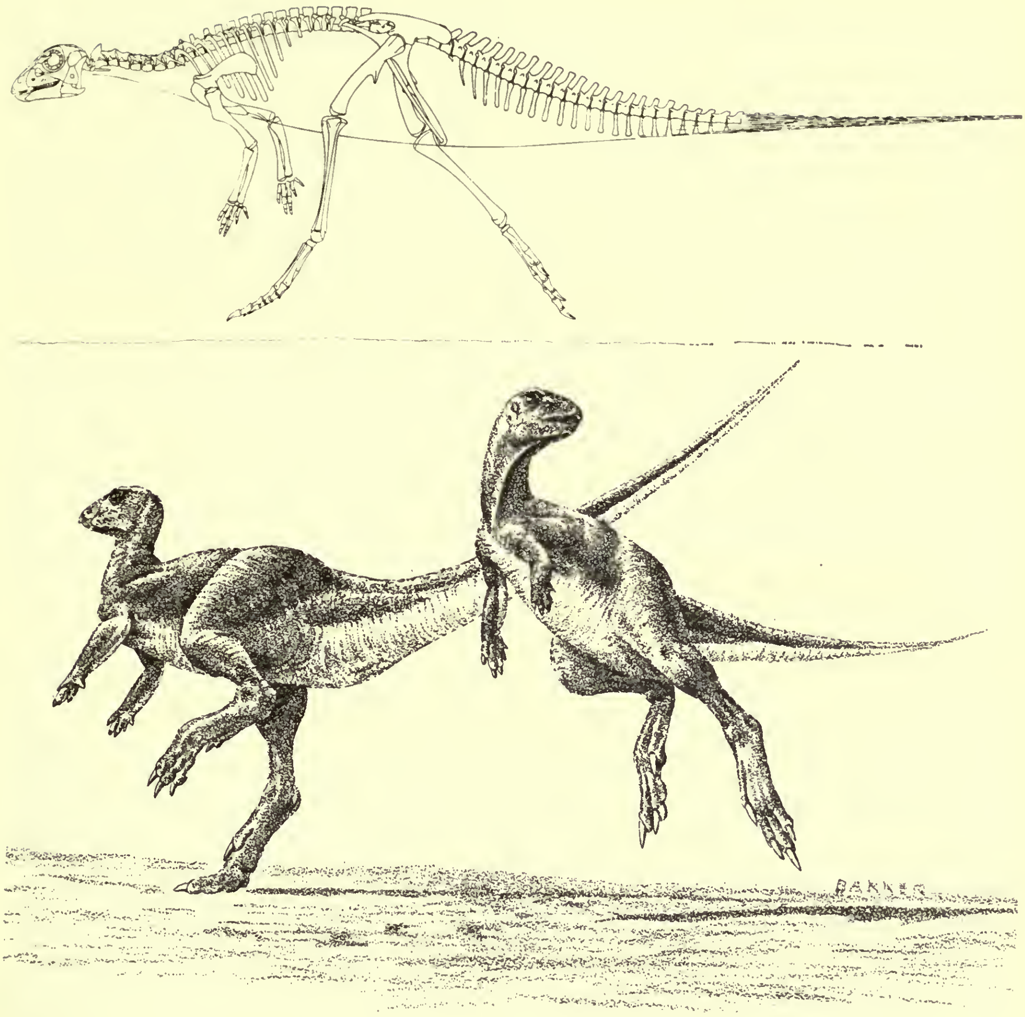

Fig. 62. *Hypsilophodon foxii*. Skeletal and flesh reconstruction showing bodily proportions of an animal about 1·36 m., or 4.5 ft. long (based mainly on R 196, see p. 19). Flesh reconstruction kindly provided by Mr R. T. Bakker of Harvard University.

probably the case in *Hypsilophodon* but the anatomical evidence is not nearly so conclusive as it is for hadrosaurs. Ossified tendons are well developed in *Hypsilophodon* but there is no rhomboidal pattern comparable to that in hadrosaurs. However, this would not seem necessary because *Hypsilophodon* is quite small (specimens known up to 2·28 m). Indeed, the presence of any ossified tendons in an animal of this size is surprising. The tendons of the dorsal series, arranged in parallel rows, would have been quite adequate to prevent a ventral sagging of the column in a horizontal pose and this was probably their function.

The pubic peduncle of the ilium (Text-figs. 46A, 48, 49) is slender but this region was not weak because it is backed by the massive first sacral rib (see Section b), through which the thrust of the femur would have been transmitted to the vertebral column. The vertebral column could have been swung to 40 degrees above the horizontal, the standard 'upright pose', without any danger. However, with a horizontal vertebral column the femur would still bear against the strongest part of the ilium. The central part of the acetabular margin is the thickest and it has the maximum height of ilium above it. In addition the thrust from the femur would be distributed much more evenly through the sacral ribs and would be perpendicular to the vertebral column.

Hypsilophodon was undoubtedly bipedal except when resting on the ground. In slow walking the vertebral column was probably held at about 30 degrees to the horizontal. In this 'upright' pose the animal was in the most advantageous position for catching sight of predators and it could reach foliage at a higher level than if it was quadrupedal or horizontal. However, when running it would seem likely that the vertebral column was held more or less horizontally (Text-fig. 62). This pose, which is the most effective for fast running, is only possible if the animal is completely adapted for bipedal locomotion and has a tail that can provide the necessary counterbalance.

VIII. WAS *HYPSILOPHODON* ARBOREAL?

a) *Historical survey*

Since Hulke (1882 : 1055) concluded that '*Hypsilophodon* was adapted to climbing upon rocks and trees' there has been a considerable amount of discussion on this matter. Abel (1912) argued from the structure of the hind-foot that *Hypsilophodon* was arboreal and that in this it retained the original habitat of the ancestor of all the dinosaurs. In his reconstruction the first toe is shown as being opposable to the remaining three toes, which are shown curving strongly backwards (Text-fig. 63). Abel said that this curvature was natural, rather than due to a post-mortem contraction of the tendons, because the position and attitudes of the articular surfaces would permit no other reconstruction. He considered that this was not a raptorial foot because the structure of the teeth clearly showed that *Hypsilophodon* was herbivorous. Abel concluded that the opposability of the hallux in combination with the strong flexural capabilities of the remaining toes clearly proved that *Hypsilophodon* was arboreal. He suggested that the foot was used to grip round branches as in an arboreal bird.

Heilmann (1916) agreed that *Hypsilophodon* lived in trees but regarded this as a secondary adaptation from a ground-living ancestor. He believed that, because the first metatarsal of *Hypsilophodon* was shortened exactly as in the ground-living dinosaurs, the ancestor of *Hypsilophodon* must also have been terrestrial. A result of this shortening of the first metatarsal is that the first toe arises at a higher level on the foot than the other three toes. Heilmann thought that this would have prevented *Hypsilophodon* from gripping like an arboreal bird in which all the toes arise

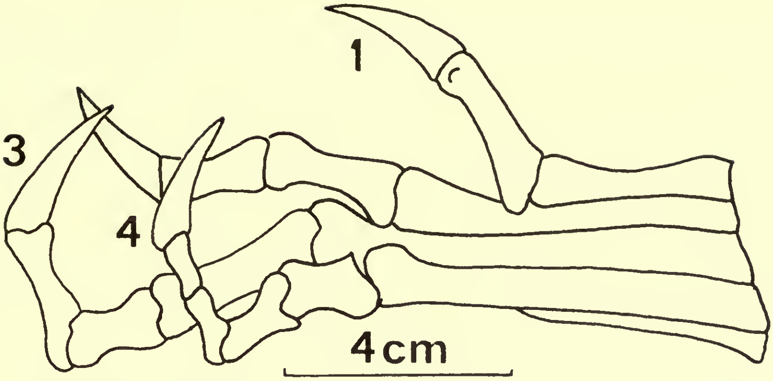

FIG. 63. *Hypsilophodon foxii.* Pes as figured by Abel, based on R196 and figures in Hulke (1873, 1882). After Abel (1912, fig. 283).

at the same level. He felt that the foot was more reminiscent of that of a monkey and, as a result, this secondary adaptation to an arboreal mode of life was analogous to that of the tree kangaroo *Dendrolagus*.

Abel (1925) admitted the correctness of Heilmann's conclusion that *Hypsilophodon* was secondarily arboreal. He opined that the first metatarsal was not further reduced because it was probably used in climbing and extended the analogy with *Dendrolagus* as a basis for reconstructing the pose of *Hypsilophodon.* He thought that the sharp and strongly arched claws of the hind-foot of *Hypsilophodon* would have rendered movement on the ground difficult. He referred to his own reconstruction of the fore-arm (1911) and pointed out that in *Hypsilophodon,* in contrast to the other dinosaurs, the radius was distinctly bowed. He cited Carlsson (1914), who had shown that *Dendrolagus* differed in the same manner from the large ground kangaroo *Macropus.* Carlsson regarded this enlargement of the space between the fore-arms in *Dendrolagus* as an adaptation to an arboreal mode of life.

Heilmann (1926) disagreed with Abel's conclusion that *Hypsilophodon* was arboreal (and, presumably, with his own similar conclusion of 1916). He pointed out that the cursorial *Procompsognathus triassicus* has ungual phalanges which are even more markedly bent than those of *Hypsilophodon.* Although Abel's reconstruction of the foot was based mainly on the figures of Hulke, Heilmann noted that it did not look like these ; furthermore, the individual elements did not agree with the measurements given by Hulke. In addition Heilmann thought that in Abel's reconstruction the first toe would collide with the second metatarsal. He again pointed out that the proximal position of the hallux made it impossible for *Hypsilophodon* to grasp in a fashion similar to that of an arboreal bird. In order to grip a branch the first metatarsal of *Hypsilophodon* must have been movable, as is the first metacarpal in the human hand. Heilmann showed that this was not the case by quoting Hulke (1882 : 1053), who wrote that the proximal ends of the metatarsals 'are in closest mutual apposition'. Heilmann considered that the foot was not specialized for climbing. He reconstructed the foot using Hulke's figures, and the toes are shown straight with no opposability of the hallux. He also thought that the hand was not specialized for climbing. Heilmann reiterated his belief that *Hypsilophodon* was quadrupedal (see above, page 127) but did not explain why this would have prevented *Hypsilophodon* from being arboreal, especially as his reconstruction (1916) showed *Hypsilophodon* climbing with a quadrupedal pose. Lastly, he pointed out that the presence of dermal armour was unexpected if *Hypsilophodon* was a tree climber, because arboreal animals are not usually so equipped.

Abel (1927) noted Heilmann's conclusion that *Hypsilophodon* was not arboreal but did not answer any of the points raised. He admitted that the tail of *Hypsilophodon* could not have been prehensile because of the ossified tendons (an objection that was not raised by Heilmann) but noted that a non-prehensile tail occurs in some tree-geckos. Abel also took further examples from Carlsson (1914) to show that the enlargement of the space between the fore-arms is an arboreal adaptation.

Swinton (1936) suggested that the arm in *Hypsilophodon* had a greater range of brachial movement than in *Thescelosaurus*, *Camptosaurus* or *Iguanodon*. The reasons given were the more medial position of the articular head of the humerus, the more proximal position of the delto-pectoral* crest and the fact that the humerus is longer than the scapula. Swinton admitted that the hand was not specialized for climbing. However, he pointed out that the three relatively elongated middle digits and the long, thin, pointed and curved unguals show that the hand was suitable for grasping, provided that no great weight was to be supported. Concerning the foot he noted that, even in Heilmann's reconstruction (1926), the first metatarsal is shown diverging distally from the rest. He considered that the first digit was opposable even though it was more proximally placed on the metatarsus. He pointed out that in the human hand some opposable action of the thumb is still possible even when the first metacarpal is forcibly kept against the second. However, Swinton (1936) admitted that the amount of opposability was probably exaggerated by Abel who argued on the basis of an unnaturally retracted foot.

Though some elongation of the hindlimb has taken place, the tibia being longer than the femur, Swinton (1936) pointed out that truly cursorial animals have an elongate metatarsus – a modification lacking in *Hypsilophodon*. Swinton also noted (1936 : 576) that in '*Hypsilophodon* (and even more so in *Thescelosaurus*) the fourth trochanter extends at least to the distal half of the bone, and this suggests that though the muscles may have been powerful their mere presence in this position hampered femoral movement to some extent'. From the structure of the hindlimb he concluded that, although bipedal, *Hypsilophodon* could not run fast but that the musculature was sufficient for climbing and balancing. In addition he noted that the tail must have been a rigid structure because of the presence of ossified tendons and that it must have helped in balancing. Swinton (1934) noted that dermal armour was shown in Heilmann's reconstruction (1916) but that, as it was only light, this was not a serious objection to *Hypsilophodon*'s being arboreal. Later (1936*a*) he pointed out that this armour was insufficient to protect *Hypsilophodon* from contemporary carnivores and that it was probably not fleet enough to escape by running. He suggested that, in times of danger, *Hypsilophodon* climbed up into the trees where, in addition, it obtained its food.

---

* Swinton (1936 : 575) actually cited 'the more proximally placed radial crest' but no such structure was mentioned in his description (: 563–564) and, from the context, it is apparent that he meant the delto-pectoral crest. He mentioned (: 564) that the deltoid crest was more proximally placed than in the other genera, 'a point which will be considered further later'.

More recently, Swinton (1962 : 24) wrote that 'it has been thought that the lengths of the fingers and toes of *Hypsilophodon* indicate that it could climb trees ; but this is probably a wrong assumption, though the animal could no doubt run up sloping trunks'. However, the accompanying reconstruction (pl. 9) showed *Hypsilophodon* well up a tree. Romer (1956 : 414) noted that in '*Hypsilophodon*, digit I diverges from its neighbours, as in *Thescelosaurus*, but is relatively long, with digital articulations suggesting a clutching power and hence habits possibly somewhat arboreal in nature for ancestral ornithischians'. More recently (1966 : 158) he noted that 'some structural features of *Hypsilophodon* suggest arboreal habits comparable to those of the tree-kangaroo of Australia'. These features, which have been mentioned above, can be summarized according to the region concerned as follows :

b) *Summary of the purported anatomical evidence that* Hypsilophodon *was arboreal*

i) Grasping capabilities of the pes :
  A) Strong flexural ability of the long toes and the long, thin, pointed and curved unguals.
  B) Opposability of the hallux.
ii) Grasping capabilities of the manus :
  A) Length of the middle three digits.
  B) Long, thin, pointed and curved unguals.
iii) Wider range of brachial movements possible :
  A) Humerus longer than scapula.
  B) More proximal position of the deltopectoral crest of the humerus.
  C) Medial position of the articular head of the humerus.
iv) Nature of fore-arm with a marked bowing of the radius which, by analogy with *Dendrolagus*, is an arboreal adaptation, and which is not found in other dinosaurs.
v) Rigid tail an aid to balancing.
vi) Dermal armour only light and therefore inadequate as a protection from ground-living predators.
vii) Limited running capabilities on the ground resulting from the structure of the hindlimb :
  A) Sharp and strongly arched claws hampered movements.
  B) Metatarsus not elongated as in truly cursorial forms.
  C) The low position of the insertion of leg muscles on the fourth trochanter of the femur.

c) *Discussion of this evidence*

i) GRASPING CAPABILITIES OF THE PES

Abel (1912), when discussing his reconstruction of the foot (see Text-fig. 63), considered that the pose shown was natural because the nature of the articular surfaces permitted no other reconstruction. If this is correct then *Hypsilophodon* must have found it rather difficult to change its grip! However, the nature of the flexural abilities of the toes as determined by the articular surfaces, together with the lengths of the phalanges and the nature of the unguals, is no different in *Hypsilophodon* from what it is in the hypsilophodontids *Thescelosaurus* (see Gilmore 1915), *Parksosaurus* (see Parks 1926), *Dysalotosaurus* (see Janensch 1955, 1961) and the psittacosaurid *Psittacosaurus* (Colbert 1962, fig. 29). Outside the Ornithischia the digits of the feet are also very similar in most pseudosuchians (*Hesperosuchus*, see Colbert 1952), coelurosaurs (*Coelophysis*, Colbert 1962, fig. 8) and prosauropods (see comparison of feet of *Hypsilophodon* and *Anchisaurus* in Galton, 1970*a*, *Plateosaurus* in von Huene 1926). Even in the relatively short phalanges of larger dinosaurs the articular surfaces are still very similar; the unguals of *Camptosaurus* (see Gilmore 1909) and *Iguanodon* (see Hooley 1925) are moderately curved. However, the unguals of ornithomimids, which are regarded as cursorial dinosaurs *par excellence* (Osborn 1917, Colbert 1962, Romer 1956, 1966) are even more pointed, longer and thinner than those of *Hypsilophodon*. It is apparent that digits II to IV of the foot of *Hypsilophodon* closely resemble those of many other dinosaurs.

Only in specimen R196 are the feet well preserved with articulated phalanges and Abel (1912) clearly based his reconstruction on this specimen. As drawn (Text-fig. 63) metatarsal V is too long and the length and proportions of most of the phalanges are incorrect. However, the first metatarsal is shown closely applied to the side of metatarsal II and its first phalanx is quite accurately drawn from the right foot. An examination of the complete first digit of the left foot (Pl. 2, fig. 3) shows that the curved ungual should point ventrally. The correctness of this articulation is confirmed by comparing the distal articular end of the first phalanx with the corresponding region on digits II to IV (see Text-fig. 58). Consequently Abel (1912) in his reconstruction rotated the first ungual through 180 degrees so that it pointed dorsally instead of ventrally.

In R196 the first metatarsal is closely applied along its whole length to metatarsal II as drawn by Abel (1912) and Heilmann (1926). Swinton (1936) stated that Heilmann (1926 : 162) showed the end of metatarsal I diverging distally. However, it would appear that Swinton had looked at figure 115 (4), that of *Anomoepus* (foot reconstructed from footprints from the Upper Triassic of the Connecticut Valley, in which metatarsal I indeed diverges), rather than figure 115 (3) of *Hypsilophodon*, in which metatarsal I is shown closely applied to metatarsal II. Swinton noted that in the human hand some opposable action of the thumb is still possible even when the first metacarpal is kept closely approximated to the second. However, metacarpal I cannot be closely approximated to metacarpal II because there are muscles that get in the way. In addition, this opposability of the thumb is rather ineffective and is merely a result of the angle of the distal articular condyle of metacarpal I. With the wrist held horizontally this angle is about 45 degrees to the horizontal so that the phalanges of digit I can be moved towards those of the adjacent digit (i.e. ventrolaterally). In *Hypsilophodon* the plane of the condyle of metatarsal I is approximately horizontal so that the phalanges of digit I can move only ventrally or even slightly ventro-medially. The fifth digit of the human hand would provide a better analogy. In both cases no amount of distal divergence will make the digit opposable, only a considerable amount of ventral rotation of metacarpal V (or metatarsal I).

The first metatarsal of *Hypsilophodon* has a greatly compressed proximal portion which wraps round on to the dorso-lateral surface of the second metatarsal (see description and Text-fig. 58). In addition, there is practically no proximal articular surface. There is no isolated first metatarsal but it would closely resemble that of *Parksosaurus* (Parks 1926, figs. 15, 16). In both *Hypsilophodon* and *Parksosaurus* the form of the first metatarsal shows that any lateral movement away from the second metatarsal was impossible and, as a result, ventral rotation was out of the question. Consequently the most important argument for regarding *Hypsilophodon* as a tree-climber, the opposability of the hallux, is based on misinterpretations of the material.

ii) GRASPING CAPABILITIES OF THE MANUS

The ungual phalanges of the manus resemble those of the pes but Swinton (1936 : 676) exaggerated slightly in describing them as long and thin. He also mentioned the 'comparatively elongated three middle digits' while, as can be seen in Text-fig. 41, the fourth digit is in fact quite short. Although Abel, Heilmann and Swinton argued that the hallux of *Hypsilophodon* was opposable, they did not discuss the possibility that the fifth digit of the hand was opposable as may have been the case (see page 126).

The hand of *Hypsilophodon* could probably grasp objects very well, provided that they were small. The manus is much smaller than the pes (Text-figs. 41, 58, both from specimen R196) with metacarpal III, the longest in the hand, being shorter than the rudimentary metatarsal V. The small size of the manus would have restricted its usefulness as an aid in climbing, but a grasping hand is not confined to arboreal forms. The fifth digit of *Iguanodon* bears phalanges (more than any other digit) and metacarpal V, which has a concave proximal surface, is set at quite an angle to metacarpal IV (Hooley 1925). The fifth digit of hadrosaurs is similar (Parks 1920, Lull & Wright 1942). Consequently the fifth digit, which was certainly adapted for grasping, may have been opposable, even though these ornithopods (length 6–9 m) were much too large to climb trees. The coelurosaurs *Ornitholestes* and *Struthiomimus* are supposed to have had an opposable first digit (Osborn 1917) ; and the hand of the coelurosaur *Coelophysis*, with its long second and third digits, was probably also a good grasping organ (Colbert 1962). The coelurosaurs are generally regarded as cursorial forms (Colbert 1962, Romer 1966).

iii) WIDER RANGE OF BRACHIAL MOVEMENTS POSSIBLE

Swinton (1936) believed that the humerus of *Hypsilophodon* was longer than the scapula. However, he based this view on specimen R5829, in which both scapulae are unnaturally shortened because of the loss of their dorsal ends. In R5830, R196 and R192 the humerus is about the same length as the scapula (see Table II). Swinton also pointed out that the delto-pectoral crest was rather proximal in position in *Hypsilophodon*. However, its position in *Dysalotosaurus* (see Janensch 1955) and

Iguanodon atherfieldensis (see Hooley 1925) is almost identical. Lastly, Swinton thought that the head of the humerus was rather medial in position. However, differences in the position of the head in *Hypsilophodon*, *Thescelosaurus* (Sternberg 1940, fig. 14b, Galton, in press *a*), *Camptosaurus* (Gilmore 1909, fig. 26) and *Iguanodon* (Hooley 1925, fig. 7 – IV) are minimal and lack any real significance. It is therefore concluded that the range of brachial movements was not greater developed in *Hypsilophodon*.

iv) LARGE FORE-ARM SPACE

The radius and ulna of *Hypsilophodon* are slender but the degree of development of the fore-arm space is comparable to that of *Thescelosaurus*, *Dysalotosaurus* and *Camptosaurus nanus* ; the radius and ulna are very similar in form in the first two genera. The fore-arm space of *Iguanodon atherfieldensis* is also quite well developed. This space is therefore not uniquely large in *Hypsilophodon*, and it is not true that *Hypsilophodon* differs from all other dinosaurs in the same way that the arboreal *Dendrolagus* differs from ground-living kangaroos.

v) RIGID TAIL AS A BALANCING ORGAN

The ensheathing tendons must have made the posterior two-thirds of the tail rather rigid. They would have enhanced the effect of the vertical articular surfaces of the pre- and post-zygapophyses of the caudal vertebrae from about the tenth vertebra onwards. The attitude of these facets must have restricted movement laterally while the ossified tendons would have also restricted it dorso-ventrally. The base of the tail was much more flexible because the absence of tendons in this region is probably natural and the articular planes of the zygapophyses are at about 45 degrees to the vertical. However, the distal part of the tail is also ensheathed in ossified tendons in the other hypsilophodontids in which this region is well preserved, namely *Parksosaurus* and *Thescelosaurus*. The tail is ensheathed in several dinosaurs, including two from the Lower Cretaceous of Montana – an ornithopod (Ostrom, personal communication) and a theropod (*Deinonychus*, Ostrom 1969). *Hypsilophodon* is thus not unique in having a rigid tail, which would have been useful while running on the ground. The rigidity would have increased the efficiency of the tail as a dynamic stabilizer when the animal rapidly changed its direction (see discussion for *Deinonychus* in Ostrom 1969 : 68).

vi) DERMAL ARMOUR

Hypsilophodon is the only ornithopod in which any trace of armour has been found ; other ornithopods were even less well protected against predators.

vii) LIMITED RUNNING CAPABILITIES

The ungual phalanges of *Hypsilophodon* do not differ from those of most other dinosaurs. In order to discuss the proportions of the hindlimb of *Hypsilophodon* the ratios for other Ornithopoda are given in Table V. Those for certain Saurischia are also given, together with those for perissodactyls and artiodactyls considered by Gregory (1912) as cursorial.

The ratio of tibia : femur in *Hypsilophodon* is, together with that of its closest relative *Parksosaurus*, higher than in any other post-Triassic ornithopod. Indeed the tibia is longer than the femur in only a few ornithischians. This ratio is higher only in the saurischian *Struthiomimus* and in a few of the cursorial perissodactyls and artiodactyls. The ratio of the third metatarsal : femur is larger in *Hypsilophodon* than it is in any other ornithischian. However, it is low in comparison with *Struthiomimus* and *Coelophysis* and, amongst the cursorial ungulates, the ratio is lower only in *Eohippus*. The ratio of the combined length of the tibia and third metatarsal : femur indicates the degree of elongation of the lower segment of the leg. This ratio in *Hypsilophodon* (at 1·78 or 1·73) is higher than in any other post-Triassic ornithischian while in the saurischians it is higher only in *Coelophysis* (1·67 or 1·86) and *Struthiomimus* (1·90 or 1·99). However, coelurosaurs and more especially the ornithomimids are generally regarded as the dinosaurs most highly adapted for fast running (Osborn 1917, Colbert 1962, Romer 1956, 1966). This last ratio shows that amongst the Ornithischia *Hypsilophodon* was the best adapted for fast running. It falls in the middle range of the cursorial species listed by Gregory (1912) and is better adapted than *Eohippus*, *Mesohippus*, the race-horse and *Tragulus napu*.

The ratio of X : femur, where X is the minimum length between the neck of the femur and the distal surface of the fourth trochanter (Text-fig. 1f), is certainly lower in most Theropoda than it is in *Hypsilophodon* ; the fourth trochanter is closer to the head even in *Gorgosaurus*. With a low value for this ratio the caudifemoralis longus muscle has a smaller moment arm and a faster action. This is an adaptation that is important in cursorial animals (Gregory 1912) and, although the fourth trochanter is relatively low in *Hypsilophodon*, it is even lower in other ornithischians that were less well adapted for fast running.

It is concluded that *Hypsilophodon* was not specifically specialized for an arboreal mode of life but, on the contrary, was cursorial. Individuals may occasionally have gone up into the trees but this would have occurred no more frequently than in any other small (up to 2·28 m long) and active dinosaur (see below : 149).

IX. GENERALIZED FEATURES OF *HYPSILOPHODON*

Hypsilophodon has been correctly regarded as a very primitive ornithopod and the more noteworthy features will be considered briefly with comments on the position in other ornithopods. Unfortunately the number of genera with which comparisons can be made is necessarily limited by inadequacies in the fossil record or in the published accounts. The relationships of *Hypsilophodon* are summarized below (: 150).

The snout is short, the skull deep with a large orbit and there is a supraorbital (Text-fig. 3) as in *Heterodontosaurus* (see Crompton & Charig 1962, Galton 1970*a*), *Parksosaurus* (Parks 1926, Galton in press), *Dysalotosaurus* (Janensch 1955) and in

TABLE V

Hindlimb measurements and ratios of dinosaurs and cursorial ungulates
(Measurements in mm)

		F	T	MT	$\frac{X}{F}$	$\frac{T}{F}$	$\frac{T + MT}{F}$	$\frac{MT}{F}$	$\frac{MT}{T}$
ORNITHISCHIA									
Hypsilophodon foxii	R5830	101	118	63	0·42	1·17	1·79	0·62	0·53
	R196	151	(178)	84	0·43	1·18	1·73	0·56	–
	R5829	200	238	–	0·43	1·19	–	–	–
Forelimb	R196	(105)^{H}	(88)^{U}	(24)^{MC}	–	(0·84)	(1·07)	(0·23)	(0·26)
Parksosaurus warreni[1]		270	320	151	0·49	1·18	1·74	0·56	0·47
Dryosaurus altus[2]		353	394	185	0·47	1·10	1·64	0·52	0·47
Dysalotosaurus[3]		–	–	–	0·45 0·47	1·10	1·69	0·59	0·54
Psittacosaurus[4]		162	179	93	0·50	1·10	1·68	0·57	0·52
Protiguanodon[4]		158	167	89	0·50	1·06	1·59	0·56	0·53
Stegoceras (Tröodon) validus[5]		222	220	85	–	0·99	1·33	0·38	0·38
Camptosaurus nanus[6]		242	231	97·5	0·54	0·95	1·31	0·40	0·42
Thescelosaurus edmontonensis[7]		320	290	–	–	0·90	–	–	–
Kritosaurus incurvimanus[8]		1045	943	363	0·54	0·90	1·24	0·35	0·38
Iguanodon atherfieldensis[9]		678	595	240	0·48	0·88	1·23	0·35	0·40
Thescelosaurus neglectus[10]		355	300	127	0·44	0·84	1·20	0·36	0·42

TABLE V (*cont.*)

	F	T	MT	$\frac{X}{F}$	$\frac{T}{F}$	$\frac{T + MT}{F}$	$\frac{MT}{F}$	$\frac{MT}{T}$
SAURISCHIA								
Ornithomimus brevitortius[11]	390	483	293	–	1·24	1·99	0·75	0·60
Struthiomimus altus[12]	480	540	370	0·33	1·12	1·90	0·77	0·68
Coelophysis bauri[13]	118	135	84	–	1·14	1·86	0·71	0·62 }
	209	224	126	–	1·07	1·67	0·60	0·56 }
Gorgosaurus[14]	1040	1000	594	0·39	0·96	1·53	0·57	0·59
Ornitholestes hermanni[12]	207	159	117	–	0·77	1·33	0·57	0·73
Anchisaurus[15]	210	147	98	0·41	0·70	1·17	0·47	0·66
Plateosaurus[16]	680	500	240	0·52	0·74	1·09	0·35	0·48
MAMMALIA								
Perissodactyla[17]								
Eohippus sp.	162	162	82	–	1·00	1·51	0·50	0·50
Mesohippus sp.	178	193	121	–	1·08	1·76	0·68	0·63
Neohipparion whitneyi	249	293	252	–	1·17	2·19	1·01	0·79
Equus caballus (race horse)	392	363	288	–	0·92	1·66	0·73	0·79
Artiodactyla[17]								
Tragulus napu	94	103	62	–	1·09	1·75	0·66	0·60
Odocoileus hemionus	253	295	255	–	1·16	2·13	1·00	0·86
Gazella dorcas juv.	140	176	132	–	1·25	2·20	0·81	0·75
Antilope cervicapra	183	223	183	–	1·21	2·34	1·00	0·82
Antilocapra americana	210	260	218	–	1·23	2·28	1·03	0·84

Abbreviations: F, femur; H, humerus; MC, third metacarpal; MT, third metatarsal; T, tibia; U, ulna ; X, fourth trochanter index, see Text-fig. 1f. Sources of measurements: 1, Parks 1926 and Edmund, personal communication; 2, Yale Peabody Museum No. 1876, 1884 for MT from a slightly smaller individual; 3, Janensch 1955; 4, Osborn 1924; 5, Gilmore 1924; 6, United States National Museum No. 2210; 7, Sternberg 1940; 8, Parks 1920; Hooley 1925; 10, Gilmore 1915; 11, Sternberg 1933; 12, Osborn 1917; 13, Colbert 1964; 14, Lambe 1917; 15, Lull 1953; 16, von Huene 1926; 17, Gregory 1912, all genera listed as cursorial.

the skulls referred to *Laosaurus* and *Dryosaurus* by Gilmore (1925). The snout is longer with a more elongated tooth row and a proportionally smaller orbit in *Camptosaurus* (Gilmore 1909), *Iguanodon* (Hooley 1925) and hadrosaurs (see Lull & Wright 1942. (Hadrosaurs will be mentioned only when there is a difference from *Iguanodon*.)

The posterior process of the premaxilla is short and slender as in thecodontians and, since it does not contact the prefrontal or the lachrymal, the nasal is not completely separated from the maxilla. This is also the case in *Parksosaurus* where this process, though short, is broad and has a good suture with the maxilla. The posterior process is long and contacts the prefrontal and lachrymal in *Heterodontosaurus*, *Dysalotosaurus*, *Camptosaurus* and *Iguanodon*.

In thecodontians the antorbital fenestra is large (Romer 1956) as was also the case in *Heterodontosaurus*. It is quite large in *Hypsilophodon* but is much smaller in *Laosaurus* and *Dryosaurus* and practically non-existent in *Parksosaurus*, *Dysalotosaurus*, *Camptosaurus* and *Iguanodon*. The quadratojugal was not excluded from the margin of the lower temporal fenestra by the jugal which, as a result, did not contact the quadrate. The jugal makes this contact and the quadratojugal is small in *Parksosaurus*, *Dysalotosaurus*, *Camptosaurus* and *Iguanodon*. The large size of the quadratojugal of *Hypsilophodon* (and the consequent reduction of the lower temporal fenestra) is a specialized feature.

Thecodontians had premaxillary teeth but these were lost in most ornithischians. They were retained in *Hypsilophodon*, *Heterodontosaurus*, *Thescelosaurus* (see Sternberg 1940, Galton in press *a*), *Stegoceras* (see Gilmore 1924), the ceratopsians *Protoceratops* and *Leptoceratops* (see Brown & Schlaikjer 1940) and the nodosaur *Silvisaurus* (Eaton 1960). The general form of the thickly enamelled side of the maxillary and dentary teeth resembles that of *Dysalotosaurus*, *Laosaurus* (see Marsh 1896), *Camptosaurus* and *Iguanodon*. There is a well-defined central ridge on each dentary tooth of *Hypsilophodon* as in *Laosaurus*. There is a strong central ridge on each maxillary tooth as well in *Dysalotosaurus* while in *Camptosaurus* the strong central ridge is restricted to the maxillary teeth. The thickly enamelled surface does not resemble that of *Heterodontosaurus*, *Fabrosaurus* (Ginsburg 1964), *Parksosaurus* or *Thescelosaurus*.

The lack of comparative data for the palate of thecodontians and of other lower ornithopods makes it difficult to recognize which characters of the palate of *Hypsilophodon* are generalized; it would appear that the palatines and pterygoids of opposite sides did not meet at the midline.

In the vertebral column the neural spines are low as in *Dysalotosaurus* (see Janensch 1961) and they are progressively taller in the series *Parksosaurus*, *Thescelosaurus*, *Camptosaurus* (see Gilmore 1912) and *Iguanodon* (see Casier 1960). The first chevron is reduced to a nubbin while in *Dysalotosaurus* it is much longer but it is absent in *Thescelosaurus* and *Camptosaurus*.

Dermal armour is present in most thecodontians and, if the plates described by Nopcsa (1905) were correctly described (see page 102), then *Hypsilophodon* is the only ornithopod in which dermal armour has been reported. In stegosaurs and ankylosaurs dermal plates formed a strong armour.

In the pelvis the ilium is low as in *Parksosaurus*. The ilium is progressively deeper in the series *Thescelosaurus, Dysalotosaurus, Camptosaurus* and *Iguanodon*. The prepubic process of *Hypsilophodon* is not short as in the Triassic ornithischians *Fabrosaurus* and *Heterodontosaurus* (Crompton & Charig, personal communication) which probably represent the primitive ornithischian condition (see Galton 1970*a*). The rod-like prepubic process of *Hypsilophodon* resembles that of *Dysalotosaurus* and the anterior end is not expanded slightly as it is in *Thescelosaurus* (Galton in press *a*) and *Dryosaurus*. In *Camptosaurus* the prepubic process is deep and transversely flattened and this is even more marked in *Iguanodon*. The postpubic rod extends to the end of the ischium as in *Thescelosaurus, Dysalotosaurus* and *Camptosaurus* but it is much shorter in iguanodontids, hadrosaurs, psittacosaurids and ceratopsians. The obturator process of the ischium is on about the same position on the shaft as it is in *Thescelosaurus*. The obturator process is progressively more proximal in the series *Parksosaurus, Hypsilophodon, Dysalotosaurus, Camptosaurus* and *Iguanodon*. The distal part of the ischium is straight, flat and blade-like as it is in *Thescelosaurus* and *Parksosaurus*. In *Dysalotosaurus, Camptosaurus* and *Iguanodon* the ischium curves ventrally and the distal part is much more massive.

The manus has five digits with four phalanges on the third digit. The latter large number has been reported only in *Thescelosaurus, Psittacosaurus* (see Osborn 1924) and in *Protoceratops, Leptoceratops* and *Monoclonius* (Brown & Schalikjer 1940). The distal end of the femur has practically no anterior condylar groove. This groove is shallow in *Thescelosaurus* and *Parksosaurus* and becomes progressively deeper in the series *Dysalotosaurus, Dryosaurus, Camptosaurus* and *Iguanodon* while in hadrosaurs the edges meet above the deep cleft. Posteriorly the outer condyle is almost as large as the inner while in the above-mentioned genera the outer condyle is sheet-like and much smaller than the inner condyle. The cnemial crest of the tibia is small as in *Pisanosaurus* (see Casamiquela 1967) and *Dysalotosaurus*; it is much larger in *Parksosaurus, Thescelosaurus, Camptosaurus* and *Iguanodon*. In the pes a rudimentary fifth metatarsal is present as is the case in many other ornithischians.

At first sight it would appear that the cursorial adaptations of *Hypsilophodon* would be specialized rather than generalized features for ornithischians. However, the hindlimb of *Pisanosaurus* (Casamiquela 1967) from the Triassic Ischigualasto Formation of Argentina was probably more highly adapted for fast running than was that of *Hypsilophodon*. The tibia and third metatarsal of *Pisanosaurus* are both slender with a metatarsal to tibia ratio of 0·59 as against 0·53 for *Hypsilophodon*. The metatarsus of Triassic ornithischians from the Connecticut Valley (*Anomoepus, Sauropus*, see Lull 1953) was also very slender and elongated. Skeletons of *Fabrosaurus* and *Heterodontosaurus* collected from the Upper Triassic of southern Africa show that both were bipedal and were adapted for fast running (Crompton, personal communication; see below: 149). The proximal position of the fourth trochanter of the femur and the elongate tibia and third metatarsal of the hindlimb of *Hypsilophodon* appears to have been more generalized than any other post-Triassic ornithischian. Increased size in ornithopods appears to have been correlated with a more distal position for the fourth trochanter of the femur and a relatively shorter tibia and third metatarsal (Table V). This probably occurred several different times during the history of the group : in *Camptosaurus*, in the line to *Iguanodon* and the hadrosaurs (Rozhdestvenskii (1966), in the pachycephalosaurids and in *Thescelosaurus* (see Galton in press *a*). A reversion to quadrupedality and increased size occurred in the line close to *Psittacosaurus* that led to ceratopsians and in the lines to ankylosaurs and stegosaurs (Text-fig. 64).

From the above survey it is apparent that *Hypsilophodon* retained many features of a generalized nature for ornithopods and, as a result, probably for ornithischians as a whole. *Hypsilophodon* occurred too late in time to have been directly ancestral to ankylosaurs, stegosaurs and most of the ornithopods. Rozhdestvenskii (1966) has shown that hadrosaurs were probably derived from *Iguanodon* that, like the most primitive pachycephalosaurid (see Galton, 1971), was a sympatric contemporary of *Hypsilophodon*. The large size of the maxilla and quadratojugal would debar *Hypsilophodon* from the direct ancestry of *Parksosaurus*. Its skull is inadequately known but it is possible that *Thescelosaurus* may have been derived from *Hypsilophodon* by a broadening of the frontals, a decrease in the size of the orbit, the specialization of the teeth and by graviportal modifications of the postcranial skeleton (see Galton in press *a*). The psittacosaurids and ceratopsians could have evolved from a form that was similar to *Hypsilophodon* but in which the prepubic process was much smaller.

The restricted geographical and stratigraphical occurrence of *Hypsilophodon* is obviously the result of accidents of the fossil record as known to date. The discovery of representatives of this genus in Jurassic or even in Triassic rocks is a distinct possibility. If the Triassic ancestor had a larger antorbital fenestra, a smaller quadratojugal, a small prepubic process and a more massive postpubic rod then it would make a good structural ancestor for all Jurassic and Cretaceous ornithischians (see below : 149).

X. SUMMARY

Several articulated specimens of *Hypsilophodon* were prepared mechanically and with acetic acid. Although no new material was included this enabled a more thoroughly detailed description of the osteology to be made. Only a few features are still uncertain : the contacts between the palatine, parasphenoid and vomer ; the transverse relationships between the tooth rows of the maxillae and lower jaw ; the form of the complete fibula ; the number and shape of some of the carpal bones and of the phalanges of the fifth digit of the manus.

The femur of *Camptosaurus valdensis* Lydekker (1889) is referred to *Hypsilophodon foxii*. It represents the largest individual recognized to date and was from an animal of about 2·28 m.

The paroccipital process of *Hypsilophodon* appears to be formed completely by the opisthotic, with the exoccipital restricted to the lateral part of the occipital condyle. This is in contrast to the position in the hadrosaur described by Langston (1960) in which the exoccipital appears to form most of the paroccipital process. Contrary to previous reports the skull has a supraorbital and also a sclerotic ring which was presumably essential for accommodation as is the case in living sauropsids.

The areas of attachment of the jaw muscles were, apart from those of the M. pterygoideus dorsalis and ventralis, similar to those described by Ostrom (1961) for the hadrosaur *Corythosaurus*. In *Hypsilophodon* the dorsal part of the coronoid is covered with very well-developed insertion markings which support Ostrom's contention that the M. pseudotemporalis inserted there. The area on the braincase of *Corythosaurus* where the M. levator bulbi may have originated could be prootic and basisphenoid rather than laterosphenoid. Originally this surface was for the M. protractor pterygoidei but, when the skull became akinetic, this surface may have become free and was then occupied by the M. levator bulbi. The M. protractor pterygoidei probably originated on the equivalent area in *Hypsilophodon*, the skull of which was possibly mesokinetic, metakinetic and amphistylic. The large antorbital fossa opened posteriorly across the floor of the orbit and was presumably for the anterior part of the M. pterygoideus dorsalis, the pterygoideus D, or possibly for a postulated equivalent of the M. pterygoideus ventralis. The moment arm of the jaw adductor muscles was lengthened by the presence of a large coronoid process and an off-set articulation with the quadrate. The anterior part of the premaxillae and the predentary were enclosed by a horny beak which was used to crop plants. The mouth was probably small with a large cheek pouch lateral to the tooth rows. The maxillary teeth are thickly enamelled on the lateral surface and they curve medially while with the dentary teeth the reverse is the case. The thickly enamelled edge was much more resistant than the rest of the crown and formed a sharp leading edge to an obliquely inclined occlusal surface between which and its fellow there was a high shear component. The cutting effect of this edge was enhanced by the presence of serrations produced by vertical and parallel ridges on the thickly enamelled surface. The foramina on the medial surface of the tooth-bearing bones, one per tooth, represent a preadaptation for the development of high alveolar walls.

There is a surprising amount of variation, the most interesting of which is the presence of an additional sacral rib in some individuals; this supports the contention of von Beneden (1881) and Nopcsa (1918, 1929) that the sacral count can vary within an ornithopod species. The massive first sacral rib backed the slender pubic peduncle of the ilium and keyed that bone to the pubis. The humerus could have been held vertically and the fifth digit of the manus may have been well formed and opposable.

Hypsilophodon was clearly bipedal as shown by the fore- to hindlimb ratio, the hindlimb to trunk ratio and the restriction of cursorial adaptations to the hindlimb. The arguments advanced to put *Hypsilophodon* up in the trees, the position it occupies in every textbook, are reviewed historically and discussed under the separate regions of the body concerned. The first metatarsal was closely applied along all its length to the adjacent part of metatarsal II. The first digit of the pes was not opposable and all the phalanges closely resemble those of other dinosaurs. The relatively small size of the grasping manus would have restricted its usefulness in climbing and the fore-arm space was not uniquely enlarged by a bowed radius. The rigid tail with its sheath of ossified tendons would have been useful as an aid to balancing and steering while running on the ground. If dermal armour was present then this was more protection than possessed by any other ornithopod. Far from having limited running capabilities *Hypsilophodon* was the ornithopod most highly adapted for fast running if the ratios of the length of the femur : tibia, femur : third metatarsal and the position of the fourth trochanter mean anything. The values for the first two ratios fall in the middle range of those for the living ungulates that Gregory (1912) considered cursorial.

Although *Hypsilophodon* is from the Lower Cretaceous it has retained several features that may be generalized for ornithischians. The skull has a short snout with the retention of premaxillary teeth, the orbit is large and there is a supraorbital. The premaxilla has a short and slender posterior process that does not meet the prefrontal or lacrymal and, as a result, the maxilla meets the nasal. The quadratojugal is not excluded from the margin of the lower temporal fenestra by the jugal which, as a result, does not contact the quadrate. The neural spines are low, a first chevrons (rudimentary) is present and there may have been dermal armour. The manus has five digits with four phalanges on the third digit. The ilium is low, the postpubic rod is long and the distal half of the ischium is straight and blade-like. The fourth trochanter is placed proximally on the femur ; the distal end of the femur has practically no anterior intercondylar groove while posteriorly the outer condyle is almost as large as the inner condyle. The long tibia has a small cnemial crest. The fifth metatarsal is vestigial but the first to fourth are relatively elongate and the hindlimb is adapted for fast running. Structurally *Hypsilophodon* is quite similar to the hypothetical ancestor of the other ornithischians of the Jurassic and Cretaceous.

XI. ACKNOWLEDGEMENTS

This paper is based on work done in the Zoology Department, King's College, University of London, which was made possible by a three-year Research Studentship from the Department of Scientific and Industrial Research (subsequently the Natural Environment Research Council). I am grateful to the following people who lent me material : Dr A. J. Charig of the British Museum (Natural History) (material of *Hypsilophodon* with permission to prepare it in acid, the holotype was kindly prepared by Mr R. Croucher) ; Mr Grapes of the Sandown Museum, Isle of Wight (foot) and Dr P. L. Robinson of University College London (three partial skeletons). I thank Drs A. J. Charig of the British Museum (Natural History), J. H. Ostrom of Yale University, New Haven, P. L. Robinson of University College London, D. A. Russell of the National Museum of Canada and A. D. Walker of the University of Newcastle upon Tyne for reading the manuscript at various stages and for all their comments. Dr A. W. Crompton of Harvard University kindly provided information about the Triassic ornithischian material collected from southern Africa. Finally my best thanks must go to Dr C. Barry Cox of King's College London for his constant help and encouragement during the course of this work.

XII. REFERENCES

Abel, O. 1911. Die Bedeutung der fossilen Wirbeltiere für die Abstammungslehre. 198 + 250 pp., 33 figs. In *Die Abstammungslehre*. Eds. A. Abel, E. Brauer *et al.* Jena.

—— 1912. *Grundzüge der Palaeobiologie der Wirbeltiere.* xvi + 708 pp., 470 figs. Stuttgart.

—— 1922. *Lebensbilder aus der Tierwelt der Vorzeit.* viii + 643 pp., 505 figs. Jena.

ABEL, O. 1925. *Geschichte und Methode der Rekonstruktion vorzeitlicher Wirbeltiere.* viii + 327 pp., 225 figs. Jena.

—— 1927. *Lebensbilder aus der Tierwelt der Vorzeit.* 2nd ed. viii + 714 pp., 551 figs. Jena.

ALLEN, P. 1955. Age of the Wealden in North-western Europe. *Geol. Mag.*, London, **92** : 265–281, 2 figs.

B.M. (N.H.) Handbook. 1962. *British Mesozoic fossils.* v + 205 pp., 72 pls. London.

BOULENGER, G. A. 1881. Sur l'arc pelvien chez les dinosauriens de Bernissart. *Bull. Acad. r. Belg. Cl. Sci.*, Bruxelles, (3) **1** : 600–608.

BRASH, J. C. & JAMIESON, E. B. 1943. *Cunningham's text-book of anatomy.* 8th ed. London.

BROWN, B. & SCHLAIKJER, E. M. 1940. The structure and relationships of *Protoceratops*. *Ann. N.Y. Acad. Sci.*, **40** : 133–266, 33 figs., 13 pls.

BRUNER, H. L. 1907. On the cephalic veins and sinuses of reptiles, with description of a mechanism for raising the venous blood pressure in head. *Am. J. Anat.*, Baltimore, **7** : 1–117, 17 figs., 3 pls.

CARLSSON, A. 1914. Über *Dendrolagus dorianus*. *Zool. Jb.* (*System*), Jena, **36** : 547–617.

CASAMIQUELA, R. M. 1967. Un nuevo dinosaurio ornithisquio Triásico (*Pisanosaurus mertii* ; Ornithopoda) de la formación Ischigualasto, Argentina. *Ameghiniana*, Buenos Aires, **4** : 47–64, 4 pls.

CASEY, R. 1963. The dawn of the Cretaceous period in Britain. *Bull. S.-East. Un. scient. Socs.*, Tunbridge Wells, England, **117** : 1–15, 3 figs.

CASIER, E. 1960. *Les Iguanodons de Bernissart.* 134 pp., 49 figs., 28 pls. Brussels.

CHATWIN, C. P. 1960. *The Hampshire basin and adjoining areas.* 3rd ed. 99 pp., 42 figs., 8 pls. London.

COLBERT, E. H. 1952. A pseudosuchian reptile from Arizona. *Bull. Am. Mus. nat. Hist.*, New York, **99** : 565–592, 35 figs., 2 pls.

—— 1962. *Dinosaurs. Their discovery and their world.* 288 pp., 47 figs., 100 pls. London.

—— 1964. Relationships of the saurischian dinosaurs. *Am. Mus. Novit.*, New York, **2181** : 1–24, 6 figs.

—— 1965. *The age of reptiles.* xiv + 228 pp., 66 figs., 20 pls. London.

COTT, H. B. 1961. Scientific results of an inquiry into the ecology and economic status of the Nile crocodile (*Crocodilus niloticus*) in Uganda and Northern Rhodesia. *Trans. zool. Soc. Lond.*, **29** : 211–356, 45 figs., 9 pls.

COX, C. B. 1959. On the anatomy of a new dicynodont genus with evidence of the position of the tympanum. *Proc. zool. Soc. Lond.*, **132** : 321–367, 17 figs.

CROMPTON, A. W. & CHARIG, A. J. 1962. A new ornithischian from the upper Triassic of South Africa. *Nature, Lond.*, **196** : 1074–1077, 1 fig.

DOLLO, L. 1882. Première note sur les dinosauriens de Bernissart. *Bull. Mus. r. Hist. nat. Belg.*, Bruxelles, **1** : 161–180, pl. 9.

—— 1883. Troisième note sur les dinosauriens de Bernissart. *Bull. Mus. r. Hist. nat. Belg.*, Bruxelles, **2** : 85–126, pls. 3–5.

—— 1887. Note sur les ligaments ossifiés des dinosauriens de Bernissart. *Archs Biol.*, Paris, **7** : 249–264, pls. 8–9.

EATON, T. H. Jr. 1960. A new armoured dinosaur from the Cretaceous of Kansas. *Paleont. Contr. Univ. Kansas*, Topeka, Ka., **25**, (8) : 1–24, 21 figs.

EDINGER, T. 1929. Über knocherne Schleralringe. *Zool. Jb.* (*Anat.*), Jena, **51** : 163–226, 61 figs.

EDMUND, A. G. 1957. On the special foramina in the jaws of many ornithischian dinosaurs. *Contr. Div. Zool. Palaeont. R. Ont. Mus.*, Toronto, **48** : 1–14, 6 figs.

—— 1960. Tooth replacement phenomena in the lower vertebrates. *Contr. Life Sci. Div. R. Ont. Mus.*, Toronto, **52** : 1–190, 58 figs.

EWER, R. F. 1965. The anatomy of the thecodont reptile *Euparkia capensis* Broom. *Phil. Trans. R. Soc.* (*B*), London, **248** : 379–435, 19 figs., pls. 32–34.

FOX, W. 1869. On the skull and bones of an *Iguanodon*. *Rep. Br. Ass. Advmt Sci.*, Norwich, **1868** : 65.

Fox, W. MS. List of fossils in the collection of Revd. W. Fox, at British Museum (Natural History).

Galton, P. M. 1967. On the anatomy of the ornithischian dinosaur *Hypsilophodon foxii* from the Wealden (Lower Cretaceous) of the Isle of Wight, England. Ph.D. thesis University of London, 513 pp., 70 figs. (Copy deposited in Palaeontology Library of the British Museum, Natural History.)

—— 1969. The pelvic musculature of the dinosaur *Hypsilophodon* (Reptilia : Ornithischia). *Postilla*, New Haven, Conn., **131** : 1–64, 17 figs.

—— 1970. Posture of hadrosaurian dinosaurs. *J. Paleont.*, Tulsa, Okla., **44** : 464–473, 5 figs.

—— 1970*a*. Ornithischian dinosaurs and the origin of birds. *Evolution*, Lancaster, Pa., **24** : 448–462, 6 figs.

—— 1971 A dome-headed dinosaur (Reptilia : Pachycephalosauridae) from the Wealden (Lower Cretaceous) of the Isle of Wight, England and the function of the dome of pachycephalosaurids. *J. Paleont.*, Tulsa, Okla., **45** : 40–47, 7 figs.

—— In press. Redescription of the skull and mandible of *Parksosaurus* (Ornithischia : Ornithopoda) from the Late Cretaceous with comments on the family Hypsilophodontidae (Ornithischia). *Contr. Life Sci. Div. R. Ont. Mus.*, Toronto, **89**, 1973 : 1–21, 9 figs.

—— In press *a*. Comments on the dinosaur *Thescelosaurus* (Reptilia : Iguanodontidae) from the Upper Cretaceous of North America. *J. Paleont.*, Tulsa, Okla.

Gilmore, C. W. 1909. Osteology of the Jurassic reptile *Camptosaurus* with a revision of the species of the genus, and descriptions of two new species. *Proc. U.S. natn. Mus.*, Washington, **36** : 197–332, 48 figs., pls. 6–20.

—— 1912. The mounted skeletons of *Camptosaurus* in the United States National Museum. *Proc. U.S. natn. Mus.*, Washington, **41** : 687–694, 4 figs., pls. 55–61.

—— 1914. Osteology of the armoured Dinosauria in the United States National Museum, with special reference to the genus *Stegosaurus*. *Bull. U.S. natn. Mus.*, Washington, **89** : 1–143, 73 figs., 37 pls.

—— 1915. Osteology of *Thescelosaurus*, an ornithopodous dinosaur from the Lance Formation of Wyoming. *Proc. U.S. natn. Mus.*, Washington, **49** : 591–616, 20 figs., pls. 79–82.

—— 1924. On *Trŏodon validus*, an ornithopodous dinosaur from the Belly River Cretaceous of Alberta, Canada. *Bull. Dep. Geol. Univ. Alberta*, Edmonton, **1** : 1–43, 3 figs., 15 pls.

—— 1925. Osteology of ornithopodous dinosaurs from the Dinosaur National Monument, Utah. *Mem. Carneg. Mus.*, Pittsburg, **10** : 385–409, 8 figs., pl. 18.

Ginsberg, L. 1964. Découverte d'un scélidosaurien (dinosaure ornithischien) dans le Trias supérieur du Basutoland. *C. R. Acad. Sci.*, Paris, **258** : 2366–2368, 1 fig.

Gregory, W. K. 1912. Notes on the principles of quadrupedal locomotion and on the mechanism of the limb in hoofed animals. *Ann. N.Y. Acad. Sci.*, **22** : 267–294, 7 figs.

Haas, G. 1955. The jaw musculature of *Protoceratops* and in other ceratopsians. *Am. Mus. Novit.*, New York, **1729** : 1–24, 11 figs.

Heilmann, G. 1916. *Fuglenes afstamning*. liii + 398 pp., 215 figs. Copenhagen (separates from *Dansk Ornithol. Foren. Tidsskr.*).

—— 1926. *The origin of birds*. iii + 208 pp., 142 figs., 2 pls. London.

Hooley, R. W. 1912. On the discovery of remains of *Iguanodon mantelli* in the Wealden beds of Brightstone Bay, Isle of Wight. *Geol. Mag.*, London, n.s. (5) **9** : 444–449.

—— 1925. On the skeleton of *Iguanodon atherfieldensis* sp. nov., from the Wealden shales of Atherfield (Isle of Wight). *Q. Jl geol. Soc.*, Lond., **81** : 1–60, 10 figs., pls. 1–2.

Huene, F. Von 1907. Die Dinosaurier der europäischen Triasformation. *Geol. paläont. Abh.*, Jena, N.F. **Suppl. 1** : 1–419, 351 figs., 111 pls.

—— 1926. Vollständige Osteologie eines Plateosauriden aus dem schwäbischen Keuper. *Geol. paläont. Abh.*, Jena, N.F. **15** : 139–180, 26 pls.

—— 1956. *Paläontologie und Phylogenie der niederen Tetrapoden*. vii + 716 pp., 690 figs. Jena.

Hughes, N. F. 1958. Palaeontological evidence for the age of the English Wealden. *Geol. Mag.*, London, **95** : 41–49.

Hulke, J. W. 1873. Contribution to the anatomy of *Hypsilophodon foxii*. An account of some recently acquired remains. *Q. Jl geol. Soc.*, Lond. **29** : 522–532, pl. 18.

—— 1873*a*. Contribution to the anatomy of *Hypsilophodon foxii*. *Abstr. Proc. geol. Soc., Lond.* **271** : 4–5.

—— 1873*b*. Supplemental note on the anatomy of *Hypsilophodon foxii*. *Abstr. Proc. geol. Soc., Lond.*, **273** : 1–2.

—— 1874. Supplemental note on the anatomy of *Hypsilophodon foxii*. *Q. Jl geol. Soc.*, Lond., **30** : 18–23, pl. 3.

—— 1882. An attempt at a complete osteology of *Hypsilophodon foxii*, a British Wealden dinosaur. *Phil. Trans. R. Soc.*, London, **172** : 1035–1062, pls. 51–82.

—— 1882*a*. An attempt at a complete osteology of *Hypsilophodon foxii*, a British Wealden dinosaur. *Proc. R. Soc.*, London, **33** : 276.

—— 1882*b*. [*Hypsilophodon*]. *Nature, Lond.*, **25** : 426.

—— MS. Manuscript catalogue of the collection of J. W. Hulke, at British Museum (Natural History).

Hutchinson, H. N. 1894. *Extinct monsters*. xxii + 270 pp., 58 figs., 26 pls. London.

Huxley, T. H. 1869. On *Hypsilophodon*, a new genus of Dinosauria. *Abstr. Proc. geol. Soc.*, Lond., **204** : 3–4.

—— 1870. On *Hypsilophodon foxii*, a new dinosaurian from the Wealden of the Isle of Wight. *Q. Jl geol. Soc.*, Lond., **26** : 3–12, pls. 1–2.

Janensch, W. 1936. Über Bahnen von Hirnvenen bei Saurischiern und Ornithischiern, sowie einigen anderen fossilen und rezenten Reptilien. *Pälaont. Z.*, Berlin, **18** : 181–198, 5 figs.

—— 1955. Der Ornithopode *Dysalotosaurus* der Tendaguru-Schichten. *Palaeontographica, Stuttgart*, **Suppl. 7**, Erste Reihe, III (3) : 105–176, 40 figs., pls. 9–14.

—— 1961. Skelettrekonstruktion von *Dysalotosaurus lettow-vorbecki*. *Palaeontographica*, Stuttgart, **Suppl. 7**, Erste Reihe, III (4) : 237–240, pl. 24.

Kirkaldy, J. F. 1939. The history of the Lower Cretaceous period in England. *Proc. Geol. Ass.*, London, **50** : 379–417, figs. 31–37, pls. 23–26.

—— 1963. The Wealden and marine Lower Cretaceous beds of England. *Proc. Geol. Ass.*, London, **74** : 127–146, 1 fig.

Lakjer, T. 1926. *Studien über die Trigeminus-versorgte Kaumuskulature der Sauropsiden*. 155 pp., 26 pls. Copenhagen.

Lambe, L. M. 1917. The Cretaceous theropodous dinosaur *Gorgosaurus*. *Mem. geol. Surv. Brch. Can.*, Ottawa, **100** : 1–84, 49 figs.

Langston, W. 1960. The vertebrate fauna of the Selma formation of Alabama. VI. The dinosaurs. *Fieldiana, Geol. Mem.*, Chicago, **3** (6) : 314–360, figs. 146–163, pl. 34.

Lemmrich, W. 1931. Der Skleralring der Vögel. *Jena. Z. Naturw.*, **65** : 513–586, 60 figs.

Lull, R. S. 1933. A revision of the Ceratopsia or horned dinosaurs. *Mem. Peabody Mus. Yale*, New Haven, Conn., **3** (3) : 1–135.

—— 1953. Triassic life of the Connecticut Valley. *Bull. Conn. St. geol. nat. Hist. Surv.*, Hartford, **81** : 1–331, 168 figs., 12 pls.

Lull, R. S. & Wright, N. W. 1942. Hadrosaurian dinosaurs of North America. *Spec. Pap. geol. Soc. Am.*, Washington, **40** : 1–242 pp., 90 figs., 31 pls.

Luther, A. 1914. Über die vom N. trigeminus versorgte Muskulature der Amphibien. *Acta Soc. Sci. fenn.*, Helsinforsiae, **44** (7) : 1–151, 92 figs., 1 pl.

Lydekker, R. 1888. *Catalogue of the fossil Reptilia and Amphibia in the British Museum* (*Natural History*). Part I. xxviii + 309 pp., 69 figs. London.

—— 1888*a*. British Museum Catalogue of fossil Reptilia, and papers on the enaliosaurians. *Geol. Mag.*, London, n.s. (3) **5** : 451–453.

—— 1889. On the remains and affinities of five genera of Mesozoic reptiles. *Q. Jl geol. Soc.*, Lond., **45** : 41–59, 9 figs.

—— 1890. *Catalogue of fossil Reptilia and Amphibia, in the British Museum* (*Natural History*). Part IV. xxiii + 295 pp., 66 figs. London.

LYDEKKER, R. 1891. On certain ornithosaurian and dinosaurian remains. *Q. Jl geol. Soc.*, Lond., **97** : 41–44, pl. 5.

MANTELL, G. A. 1849. Additional observations on the osteology of the *Iguanodon* and *Hylaeosaurus*. *Phil. Trans. R. Soc.*, London, **139**, 271–305, pls. 26–32.

MARSH, O. C. 1895. On the affinities and classification of the dinosaurian reptiles. *Am. J. Sci.*, New Haven, Conn., (3) **50** : 483–498, pl. 10.

—— 1896. The dinosaurs of North America. *Rep. U.S. geol. Surv.*, Washington, **16** (1) : 133–244, 66 figs., pls. 2–85.

—— 1896*a*. Restoration of some European dinosaurs, with suggestions as to their place among the Reptilia. *Geol. Mag.*, London, n.s. (4) **3** : 1–9.

—— 1896*b*. The classification of dinosaurs. *Geol. Mag.*, London, n.s. (4) **3** : 388–400.

NOPCSA, F. B. 1905. Notes on British dinosaurs I – *Hypsilophodon*. *Geol. Mag.*, London, n.s. (5) **2** : 203–208, 4 figs.

—— 1918. Über Dinosaurier. 4. Neues über Geschlechts-unterschiede bei Ornithopoden. *Zentbl. Miner. Geol. Paläont.*, Stuttgart, **1918** : 186–198, 12 figs.

—— 1929. Sexual differences in ornithopodous dinosaurs. *Palaeobiologica*, Wien, **2** : 187–200, 3 figs.

OAKLEY, K. P. & MUIR-WOOD, H. M. 1959. *The succession of life through geological time.* 3rd ed. vii + 94 pp. illust. London.

O'DONOGHUE, C. H. 1920. The blood vascular system of the tuatara, *Sphenodon punctatus*. *Phil. Trans. R. Soc.* (*B*), London, **210** : 175–252, 13 figs. pls. 6–8.

OELRICH, T. M. 1956. The anatomy of the head of *Ctenosaura pectinata* (Iguanidae). *Misc. Publs Mus. Zool. Univ. Mich.*, Ann Arbor, **94** : 1–122, 59 figs.

OSBORN, H. F. 1917. Skeletal adaptations of *Ornitholestes*, *Struthiomimus* and *Tyrannosaurus*. *Bull. Am Mus. nat. Hist.*, New York, **25** : 733–771, 23 figs., pls. 24–27.

—— 1924. *Psittacosaurus* and *Protiguanodon* : two Lower Cretaceous iguanodonts from Mongolia. *Am. Mus. Novit.*, New York, **127** : 1–16, 9 figs.

OSTROM, J. H. 1961. Cranial morphology of the hadrosaurian dinosaurs of North America. *Bull. Am. Mus. nat. Hist.*, New York, **122** : 35–186, 78 figs., 6 pls.

—— 1962. On the constrictor dorsalis muscles of *Sphenodon*. *Copeia*, New York, **1962** : 732–735, 1 fig.

—— 1964. *The strange world of dinosaurs.* 128 pp., illust. New York.

—— 1969. Osteology of *Deinonychus antirrhopus*, an unusual theropod from the Lower Cretaceous of Montana. *Bull. Peabody Mus. Yale*, New Haven, Conn., **30** : 1–165, 83 figs.

OWEN, R. 1855. Monograph on the fossil Reptilia of the Wealden and Purbeck formations. Part II. Dinosauria (*Iguanodon*) (Wealden). *Palaeontogr. Soc.* [*Monogr.*], London, **8** : 1–54, 19 pls.

—— 1864. Monograph on the fossil Reptilia of the Wealden and Purbeck formations. Supplement III. Dinosauria (*Iguanodon*) (Wealden). *Palaeontogr. Soc.* [*Monogr.*], London, **16** : 19–21, pl. 10.

—— 1874. Reptilia of the Wealden and Purbeck formation. Supplement V. Dinosauria (*Iguanodon*) (Wealden). *Palaeontogr. Soc.* [*Monogr.*], London, **27** : 1–18, 2 pls.

PARKS, W. A. 1920. The osteology of the trachodont dinosaur *Kritosaurus incurvimanus*. *Univ. Toronto Stud. geol. Ser.*, Toronto, **11** : 1–76, 22 figs., 7 pls.

—— 1926. *Thescelosaurus warreni*, a new species of ornithopodous dinosaur from the Edmonton formation of Alberta. *Univ. Toronto Stud. geol. Ser.*, Toronto, **21** : 1–42, 18 figs., 2 pls.

RIXON, A. E. 1949. The use of acetic and formic acids in the preparation of fossil vertebrates. *Mus. J.*, Lond., **49** : 116–117.

ROMER, A. S. 1956. *Osteology of the reptiles.* xxi + 772 pp., 248 figs. Chicago.

—— 1966. *Vertebrate paleontology.* 3rd ed. viii + 468 pp., 443 figs. Chicago.

ROZHDESTVENSKII, A. K. 1966. [New iguanodonts from Central Asia. Phylogenetic and taxonomic relationships between late Iguanodontidae and early Hadrosauridae.] *Paleont. Zh.*, Moskva, **1966** : 103–116, 4 figs. (in Russian).

RUSSELL, L. S. 1940. The sclerotic ring in the Hadrosauridae. *Contr. R. Ont. Mus. Palaeont.*, Toronto, **3** : 1–7, 2 figs., 2 pls.

SNYDER, R. C. 1962. Adaptations for bipedal locomotion of lizards. *Am. Zool.*, Utica, N.Y., **2** : 191–203, 8 figs.

STEINER, H. 1922. Die ontogenetische und phylogenetische Entwicklung des Vogel-flugelskelettes. *Acta. zool., Stockh.*, **3** : 307–360, 19 figs.

STERNBERG, C. H. 1933. A new *Ornithomimus* with complete abdominal cuirass. *Can. Fld. Nat.*, Ottawa, **47** : 79–83, 3 pls.

—— 1940. *Thescelosaurus edmontonensis*, n. sp. and classification of the Hypsilophodontidae. *J. Paleont.*, Tulsa, Okla., **14** : 481–494, 18 figs.

—— 1965. New restoration of hadrosaurian dinosaur. *Nat. Hist. Pap. natn. Mus. Can.*, Ottawa, **30** : 1–5, 2 figs.

STRAHAN, A. & REID, C. 1889. *The geology of the Isle of Wight.* 2nd ed. 349 pp., 84 figs., 5 pls. London.

SWINTON, W. E. 1934. *The dinosaurs.* xii + 233 pp., 20 figs., 25 pls. London.

—— 1936. Notes on the osteology of *Hypsilophodon* and on the family Hypsilophodontidae. *Proc. zool. Soc.*, Lond., **1936** : 555–578, 7 figs.

—— 1936*a*. A new exhibit of *Hypsilophodon. Nat. Hist. Mag.*, London, **5** : 331–336, illust.

—— 1936*b*. The dinosaurs of the Isle of Wight. *Proc. Geol. Ass.*, London, **47** : 204–220.

—— 1954. *Fossil amphibians and reptiles.* xiii + 114 pp., 67 figs., 17 pls. London.

—— 1962. *Dinosaurs.* 44 pp., 6 figs., 11 pls. London.

TOOMBS, H. A. 1948. The use of acetic acid in the development of vertebrate fossils. *Museums J.*, London, **48** : 54–55, 1 pl.

UNDERWOOD, G. 1970 The eye. In *Biology of the Reptilia.* **2**, *Morphology B.* : 1–97, 29 figs., Eds. C. Gans and T. S. Parsons. London.

VAN BENEDEN, P. J. 1881. Sur l'arc pelvien chez les Dinosauriens de Bernissart. *Bull. Acad. r. Belg. Cl. Sci.*, Bruxelles, (3) **1** : 600–608.

VERSLUYS, J. 1910. Streptostylie bei Dinosaurien, nebst Bemerkungen über die Verwandtschaft der Vögel und Dinosaurier. *Zool. Jb.* (*Anat.*), Jena, **30** : 175–260, 26 figs.

WALKER, A. D. 1961. Triassic reptiles of the Elgin area – *Stagonolepis, Dasygnathus* and their allies. *Phil. Trans. R. Soc.*, (*B*), London, **244** : 103–204, 25 figs., pls. 9–13.

WALLS, G. L. 1942. The vertebrate eye and its adaptive radiation. *Bull. Cranbrook Inst. Sci.*, Bloomfield, Mich., **19** : 1–785.

WERNER, F. 1895. Ueber sekundäre Geschlechtsunterschiede bei Reptilien. *Biol. Zbl.*, Leipzig, **15** : 125–140.

WHITE, H. J. O. 1921. *A short account of the geology of the Isle of Wight.* 219 pp., 1 pl., illust. London.

YOUNG, J. Z. 1962. *The life of the vertebrates.* 2nd ed. xvi + 820 pp., 514 figs. Oxford.

NOTE

Several papers of related interest have appeared in the three years since the manuscript of this article was last revised. I have given a full discussion of the mode of life of *Hypsilophodon* (Galton 1971b) with figures illustrating the comparisons made above (: 133–137) and with stereo-photographs of the manus and pes of R196 in dorsal view ; an abstract of this paper appeared a little earlier (1971*a*). Two other papers (Galton 1973, Galton in press) include reconstructions of the skull of *Hypsilophodon* in ventral and dorsal view respectively and figures of the skull.

Thulborn (1970, 1971, 1972) gives a detailed description of the anatomy of the Upper Triassic ornithischian *Fabrosaurus australis* and, on the basis of my figures of

Hypsilophodon (Galton 1967), refers *Fabrosaurus* to the family Hypsilophodontidae. However, my concept of this family (Galton 1971*a*, *b*, 1972, 1973 in press, in press *a*) is not as all-embracing as Thulborn's (1970, 1970*a*, 1971, 1971*a*, 1972) who includes all cursorial ornithopods with premaxillary teeth plus *Thescelosaurus* (for genera see Thulborn 1972, fig. 14). I agree with Thulborn (1970, 1971, 1972) that the Upper Triassic *Fabrosaurus* is very similar to the archetypal ornithischian from which all other ornithischians were originally derived. Indeed, the skull of *Fabrosaurus* with its flat maxilla, slender dentary and marginally positioned maxillary and dentary teeth (see Thulborn 1970, Galton 1973) is so primitive that I place that genus (along with *Echinodon* Owen from the Lower Cretaceous of England) in a separate family, the Fabrosauridae (Galton 1972). This family resembled living reptiles in not having muscular cheeks. In all other ornithischians described to date there is a large space lateral to the tooth rows which is overhung by the maxilla and floored by the massive dentary ; it is presumed that this space was bordered by cheeks (as noted on page 121 for *Hypsilophodon*) which prevented the loss of food from the sides of the jaws, as would otherwise have occurred when resistant plant material was chewed repeatedly. I attribute the spectacular success of ornithischian dinosaurs, the dominant 'small to medium' (up to 10 m) sized terrestrial herbivores of the Jurassic and Cretaceous periods (about 125 million years), to their development of cheeks (Galton, 1972, 1973).

Thulborn (1970, 1970*a*, 1971, 1971*a*, 1972) refers *Heterodontosaurus* (as '*Lycorhinus*') to the family Hypsilophodontidae. *Heterodontosaurus* has cheek teeth with planar wear surfaces and there is a caniniform tooth on each premaxilla and dentary (see Crompton & Charig 1962, Thulborn 1970*a*). I consider (Galton 1972) that these dental specializations justify the retention of the family Heterondontosauridae, to which I also refer *Geranosaurus* and *Lycorhinus*. Thulborn (1970, 1970*a*, 1971, 1972) follows current practice in placing *Thescelosaurus* (graviportal, premaxillary teeth ; see Sternberg, 1940) in the family Hypsilophodontidae and referring *Dysalotosaurus* (cursorial, no premaxillary teeth ; see Janensch, 1955) to the family Iguanodontidae. These taxonomic assignments are based on the respective presence or absence of premaxillary teeth, but I consider that this criterion should not be used to determine which genera should be included in the family Hypsilophodontidae (see Galton 1972). The skull of *Dysalotosaurus* is very similar to that of *Dryosaurus* (cursorial, no premaxillary teeth) ; I therefore place both those genera in the Hypsilophodontidae and refer *Thescelosaurus* to the Iguanodontidae (Galton 1972, in press, in press *a*).

The cursorial ornithopods of conservative aspect should be referred to the family Hypsilophondontidae, diagnosed as follows :

Head small, snout short, orbits large ; no large rostral beak, no caniniform teeth, maxillary and dentary teeth inset (longitudinal recess to maxilla, massive dentary) and with randomly formed wear surfaces which are not all in the same plane ; distal part of hind limb elongate (Galton 1972, in press). The genera and specimens that I refer to this family are shown in the phyletic chart (Text-fig. 64) and the relationships shown are based largely on the form of the femur (for discussion of various aspects of this chart see Galton 1972, in press, in press *a*).

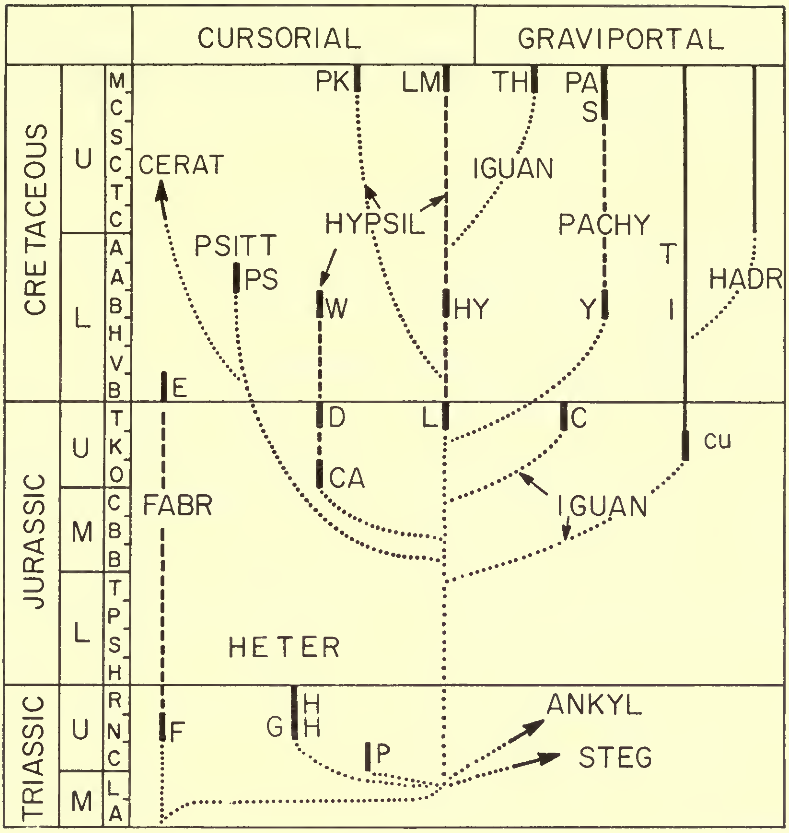
CURSORIAL
GRAVIPORTAL
CRETACEOUS
U
L
M C S C T C A A B H V B
JURASSIC
U
M
L
T K O C B B T P S H
TRIASSIC
U
M
R N C L A
PK
LM
TH
PA
S
CERAT
IGUAN
HYPSIL
PSITT
PS
PACHY
T
HADR
W
HY
Y
I
E
D
L
C
CU
CA
IGUAN
FABR
HETER
H
G
H
ANKYL
F
P
STEG

Fig. 64. Phylogeny of the Ornithopoda; modified from Galton (1972). Diagram to show phylogenetic relationships and the nature of the fossil record of lower ornithopods. The ages of the different genera are based on data in Charig (1967) and the stratigraphic distribution is by stages, the initials of which are given in the third column. Abbreviations: Classificationary units: ANKYL, Ankylosauria; CERAT, Ceratopsia; FABR, Fabrosauridae; HADR, Hadrosauridae; HETER, Heterodontosauridae; HYPSIL, Hypsilophodontidae; IGUAN, Iguanodontidae; PACHY, Pachycephalosauridae; PSITT, Psittacosauridae; STEG, Stegosauria. Genera: C, *Camptosaurus*; CA, '*Camptosaurus' leedsi*, R1993; CU, *Cumnoria* ('*Camptosaurus*') *prestwichi*, D, *Dryosaurus* and *Dysalotosaurus*: E, *Echinodon*; F, *Fabrosaurus*; G. *Geranosaurus* and *Lycorhinus*, H, *Heterodontosaurus*; HY, *Hypsilophodon*; I, *Iguanodon*; L, *Laosaurus*; LM, '*Laosaurus' minimus*; P, *Pisanosaurus*; PA, *Pachycephalosaurus*: PK, *Parksosaurus*; PS, *Psittacosaurus*; S, *Stegoceras*; T, *Tenontosaurus*; TH, *Thescelosaurus*; W, Wealden hypsilophodont (R184, R185, 36509, see above, p.7; to be described elsewhere); Y, *Yaverlandia* (Galton 1971). Actual fossil record of ornithopods indicated by ———; no fossil record indicated by - - - - - but genera in the same vertical line are closely related; postulated relationships indicated by ....

In this connection, however, it must be pointed out here that the Iguanodontidae as presently constituted are probably not a natural group, a monophyletic taxon. Text-fig. 64 shows that the 'family' comprises three lines of graviportal ornithopods arising independently from the Hypsilophodontidae: the Iguanodontidae *sensu stricto* (with *Cumnoria, Iguanodon* and *Tenontosaurus*), a line leading to *Camptosaurus*, and a line leading to *Thescelosaurus*.

OTHER REFERENCES

CHARIG, A. J. 1967. Subclass Archosauria. *In* Harland, W. B. *et al.* (Eds.) *The fossil record.* London (Geological Society of London) : 708–718, 725–731.

GALTON, P. M. 1971*a*. *Hypsilophodon*, the cursorial non-arboreal dinosaur. *Nature, Lond.*, **231** : 159–161, 2 figs.

—— 1971*b*. The mode of life of *Hypsilophodon*, the supposedly arboreal ornithopod dinosaur. *Lethaia*, Uppsala, **4** : 453–465, 5 figs.

—— 1972. Classification and evolution of ornithopod dinosaurs. *Nature, Lond.*, **239** : 464–466, 1 fig.

—— 1973. The cheeks of ornithischian dinosaurs. *Lethaia*, Uppsala, **6** : 67–89, 7 figs.

THULBORN, R. A. 1970. The skull of *Fabrosaurus australis*, a Triassic ornithischian dinosaur. *Palaeontology*, London, **13** : 414–432, 9 figs.

—— 1970*a*. The systematic position of the Triassic ornithischian dinosaur *Lycorhinus angustidens*. *Zool. J. Linn Soc.*, London, **49** : 235–245, 5 figs.

—— 1971. Tooth wear and jaw action in the Triassic ornithischian dinosaur *Fabrosaurus*. *J. Zool., Lond.*, **164** : 165–179, 9 figs.

—— 1971*a*. Origin and evolution of ornithischian dinosaurs. *Nature, Lond.*, **234** : 75–78, 4 figs.

—— 1972. The post-cranial skeleton of the Triassic ornithischian dinosaur *Fabrosaurus australis*. *Palaeontology*, London, **15** : 29–60, 14 figs.

INDEX

The page numbers of the principal references are printed in **bold** type; an asterisk (*) denotes a figure.

All anatomical terms refer to the species *Hypsilophodon foxii* Huxley.

abducent nerve, 104
accessory elements of skull, 46–7
adductor mandibulae muscles, 110–2
anatomical evidence that *Hypsilophodon* was arboreal, 133–7
anatomy, cranial, 103–22
  post-cranial, 122–30
Anatosaurus, 46, 125
Anchisaurus, 134, 139
angular, 39
Anomoepus, 134, 141
Antilocapra americana, 139
Antilope cervicapra, 139
antorbital fenestra, 117–9
  recess, 18
appendicular skeleton, 72–102
arboreal condition in *Hypsilophodon*, 130–7
armour, dermal, 102, 136, 140
articular, 41
articulation of limbs, 124–7
astragalus, 97, 98*, 99*
atlas, 48–50, 48*, 49*
axis, 48*, 49*, 50–1

balancing organ, rigid tail as, 136
Basiliscus, 128
basioccipital, 22
basisphenoid, 26–7
bipedal pose, 127–30
bones of skull and jaw, 21–41
brachial movements, wider range possible, 135–6
braincase, 34*
  foramina of, 103–5

Calamospondylus foxi, 7, 18
calcaneum, 97, 98*, 99*

Camptosaurus, 44*, 103, 105, 117, 122–3, 132, 134, 136, 140–2, 152
  browni, 122
  depressus, 122
  dispar, 122
  leedsi, 103
  nanus, 136, 138
  prestwichi, 123
  valdensis, 4, 7, **102–3**, 142 ; pl. 2, fig. 4
carpals, 80–3, 81*
caudal vertebrae, 63, 65
cervical vertebrae 3 to 9, 51, 52*, 53*
chevrons, 65
Coelophysis, 134–5, 137
  bauri, 139
condyles, 19
constrictor dorsalis muscles, 112–4
  ventralis muscles, 114
coracoid, 12*, 13, **73–4**, 73*, 74*, 75*
Corythosaurus, 46, 143
Cowleaze Chine, Isle of Wight, 5, 7, 9–10, **15–17**
cranial anatomy, 103–21
Ctenosaura, 113, 116
Cuckfield, Sussex specimen *not Hypsilophodon*, 7
Cumnoria, 152
Cyrena, 16

Deinonychus, 136
Dendrolagus, 131, 133, 136
dental formula, 41
dentary, 39
  teeth, 18, **42–3**, 44*
dentition, diagrammatic cross-section, 120*
depressor mandibulae, musculus, 114
dermal armour, 102, 136, 140
dorsal vertebrae, 54*, 55*, **56–7**, 59*
Dryosaurus, 103, 140–1, 150
  altus, 138
Dysalotosaurus, 44, 57, 105, 117, 123–4, 134–8, 140–1, 150

Echinodon, 150
ectopterygoid, 36–7
Eohippus, 137, 139
Equus caballus, 137, 139
Euparkeria, 117–8
eye, 106–10 ; see also sclerotic ring
exoccipital, 22

Fabrosaurus, 5, 117, 140–1, 150
  australis, 149
facial nerve, 104
fauna associated with *Hypsilophodon*, 17–18
features, generalized, of *Hypsilophodon*, 137–42
femur, 12*, 14, 19, 94*, 95*, **95–6** ; pl. 2, fig. 4
  fourth trochanter index, 13
fenestra, antorbital, 117–9
  post-temporal, 105–6
fibula, **96–7**, 98*
figured specimens of *Hypsilophodon*, BM(NH) numbers of, 10–2
foramina, of braincase, 103–5
  special, 44–5
forelimb, forearm, **75–83**, 124–6, 136
fossa, post-temporal, 105–6
Fox, W., collection, 7–8
frontal, 31–2

Gazella dorcas, 139
Geranosaurus, 150
girdle, pectoral, 72–5
  pelvic, 83–95
Goniopholis, 18
Gorgosaurus, 137, 139
grasping capabilities of *Hypsilophodon*, 133–5

hadrosaurs, 140–2
Hesperosuchus, 134
Heterodontosaurus, 107, 111, 117, 137, 140–1, 150
hexapleural type sacrum, 60–1
hindlimb, **95–102**, 126–7, 141
  measurements and ratios in dinosaurs and cursorial ungulates, 138–9
Hulke, J. W., collection, 9–10
humerus, 12*, 13, 18, **75**, 77*, **78**, 78*
hyoid apparatus, 46
Hypsilophodon from Wealden of Isle of Wight, 1–152, *passim*
  foxii, 5, **18–19**
    holotype, 19, 20*
    paratype, 19
    specimens used for osteology and reconstructions, 19
Hypsilophodon bed, 8, **15–18**
Hypsilophodontidae, 18–19, 150, 152
Hyracotherium, see *Eohippus*

Iguanodon, 5, 7, 18, 44, 71, 102, 111, 122, 124–5, 132, 134–6, 140–2, 152
  atherfieldensis, 18, 103, 124, 136, 138
  bernissartensis, 19, 122–3
  foxi, 5
  mantelli, 5, 18, 122–3
Iguanodontidae, 150, 152

ilium, 12*, 13, **83**, **87**, 90*, 91*
individual variation of *Hypsilophodon*, 122–3
intermedium, see carpals
ischium, 12*, 14, 19, **89**, 93*, **95**

jaw, lower, 37*, 38–9 ; see also mandibular ramus
  action, 119–21
  musculature, 110–4
    lines of action, 108*
jugal, 18, 32–3

kinetism, 114–6
Kritosaurus, 125
  incurvimanus, 138

Lacerta, 106
lachrymal, 35
Lambeosaurus, 46
Laosaurus, 103, 140
laterosphenoid, 27
Leptoceratops, 140–1
localities of *Hypsilophodon*, 17
lower jaw, 38–41
Lycorhinus, 150

Macropus, 131
mandibular muscles, see jaw musculature
  ramus, 37*, 40*
Mantell, G. A., collection, 7
manus, 14–15, 80*, 141
  grasping capabilities, 135
material of *Hypsilophodon*, 6–10
maxilla, 30–1
maxillary teeth, 18, **42–3**, 43*
measurements of *Hypsilophodon*, 12–15
Mesohippus, 137, 139
metacarpals, 82*, 83
metatarsals, 14–15, 99*, 101
methods, 6–15
Monoclonius, 141
musculature of jaw, 110–4
musculus adductor mandibulae externus, 110–1
  pars medialis, 111
  pars profundis, 111
  pars superficialis, 110–1
musculus adductor mandibulae internus, 111–2
musculus adductor mandibulae posterior, 112
musculus depressor mandibulae, 114
musculus pseudotemporalis, 111
musculus pterygoideus, 112

narial openings, 18
nasal, 31
Neohipparion whitneyi, 139
nerves of skull, 103–5
new sacral rib, 61

obturator process, 18
Odocoileus hemionus, 139
Ophisaurus, 107
opisthotic, 22, 26
orbit, see eye, sclerotic ring
orbitosphenoid, 27
Ornithosuchia, 18–19
Ornithosuchian dinosaur *Hypsilophodon*, 1–152
Ornitholestes, 135
  hermanni, 139
Ornithomimus, 107
  brevitortius, 139
Ornithopoda, 18–19
Ornithosuchus, 118
ossified tendons, 71–2
osteology, 18–102

pachycephalosaurids, 142
palatine, 37–8, 140
Paludina, 16
parasphenoid, 27
parietal, 31
Parksosaurus, 46, 57, 72, 107, 117, 119, 124, 134–7, 140–2
  warreni, 138
paroccipital process, 105–6
pectoral girdle, 72–5
pelvic girdle, 83–95, 84*, 85*, 86*, 88*, 141 ; see also ilium, ischium, etc.
pelvic region, reconstruction, 88*
pes, 14–15, 100*, 131* ; pl. 2, fig. 3
  grasping capabilities, 133–5
phalanges, 14–15, **83**, 99*, 101–2
Pisanosaurus, 141
Plateosaurus, 105, 134, 139
Polacanthus foxii, 18
Poole, H. F., collection, 10
pose of *Hypsilophodon*, quadrupedal or bipedal ?, 127–30
post-cranial anatomy, 122–30
postorbital, 35–6
post-temporal fenestra or fossa, 105–6
posture of limbs, 124–30
  of vertebral column, 127–30
prearticular, 41
predentary, 38*, 38–9
  tooth, 42*
prefrontal, 35
premaxilla, 18, 27, 30
premaxillary teeth, 18, **41–2**

preparation of material, 6, 142
proatlas, 48, 48*, 49*
Procompsognathus triassicus, 131
proötic, 26
Protiguanodon, 138
Protoceratops, 72, 78, 111, 140–1
  andrewsi, 122
psittacosaurids, 142
Psittacosaurus, 134, 138, 141–2
pterygoid, 36
pubis, 12*, 14, **87**, **89**, 92*

quadrate, 18, 33
quadrotojugal, 18, 33
quadrupedal pose of *Hypsilophodon*, 127–30

radius, 13, 79*, **80**, 136
reconstructions of *Hypsilophodon*, 129*
replacement teeth, 44–5
  sequence, 45–6
ribs, see vertebral column
  sacral, 60
    first, 123–4
running capabilities of *Hypsilophodon*, 136–7

sacral ribs, 18, 60
  first, 123–4
sacral vertebrae, 18, 57–60
sacrum, hexapleural type, 59*, 60–1
  pentapleural type, 58*
  other variations in, 61, 63
Sauropus, 141
scapula, 12*, 13, 18, **72–3**, 73*, 74*, 75*
sclerotic ring, 46–7, 47* ; see also eye
Silvisaurus, 140
skeleton, see osteology
skull, 20*, 21*, **21–38**, 23*, 24*, 25*, 28*, 29*, 32*, 108*, 109*, 137, 140 ; plate 1 ; pl. 2, figs. 1–2 ; see also braincase, cranial anatomy
snout, 137, 140
Sphenodon, 47, 106, 116
splenial, 39
squamosal, 33, 35
Stagonolepis, 117–8
stapes, 47
Stegoceras, 140
  (*Troodon*) *validus*, 138
Stegosaurus, 127
sternum, 74–5, 76*
stratigraphy of *Hypsilophodon* bed, 15–17
streptostyly, 116–7
Struthiomimus, 135, 137, 139
supraoccipital, 21–2
supraorbital, 35, 137
surangular, 39, 41

tail, rigid, as balancing organ, 136
tarsals, **97**, 99*, **100–1**
teeth, 18, **41–6**, 140
  sequence of replacement, 45–6
tendons, ossified, 70*, 71*, 71–2
Tenontosaurus, 152
Thescelosaurus, 57, 66, 83, 123–4, 127, 132–4, 136, 140–2, 150, 152
  edmontonensis, 138
  neglectus, 122, 138
tibia, 14, **96**, 98*
Tragulus napu, 137, 139
trigeminal foramen, 104
Trionyx, 18
trochanters, 19

ulna, 13, **78**, 79*, 136
Unio, 16
Uromastix, 116

Varanus, 115
variation, individual, in *Hypsilophodon*, 122–3
vertebrae, caudal, 63–71, 66*, 67*, 68*, 69*, 70*
  cervical, 51
  dorsal, 56–7, 62*, 64*
  sacral, 57–60, 62*, 63*, 64*
vertebral column, 48–70, 140
  posture, 127–30
vomer, 38

Wealden of Isle of Wight, *Hypsilophodon* from, 1–152

PETER M. GALTON, B.Sc., Ph.D.
Department of Zoology
KING'S COLLEGE LONDON UNIVERSITY
STRAND, LONDON, W.C. 2

Present address:
Department of Biology
UNIVERSITY OF BRIDGEPORT
BRIDGEPORT, CONN. 06602, U.S.A.

Peabody Museum of Natural History
YALE UNIVERSITY
NEW HAVEN, CONN., U.S.A.

PLATE 1

Hypsilophodon foxii

Fig. 1. Skull R2477, dorsal view. Compare with Text-fig. 5B.
Fig. 2. Skull R2477, palatal view. Compare with Text-fig. 6A.
Fig. 3. Skull R2477, left lateral view. Compare with Text-fig. 4A.
Fig. 4. Skull R2477, right lateral view. Compare with Text-fig. 4A.
Scale line represents 5cm.

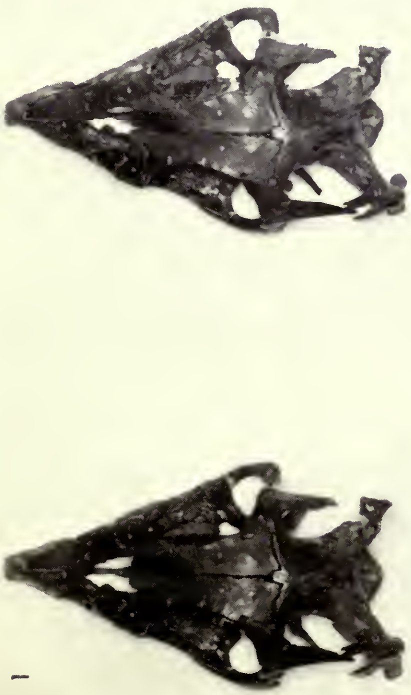

1

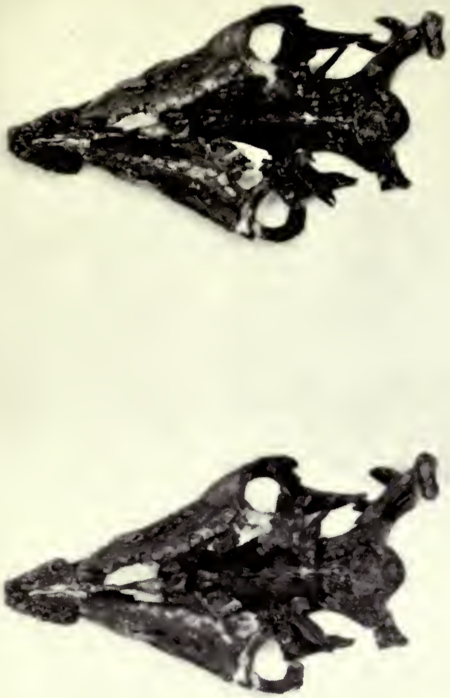

2

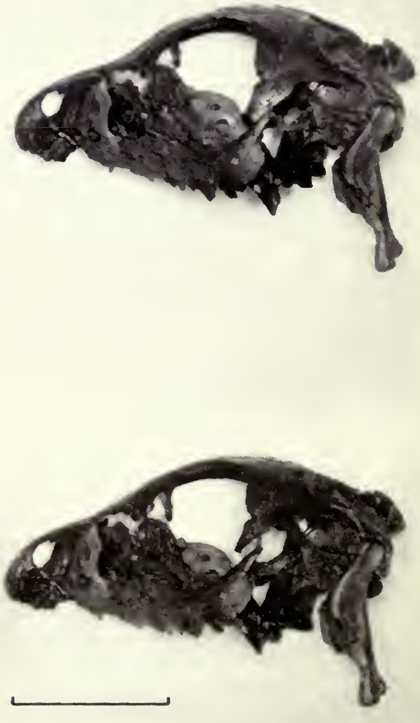

3

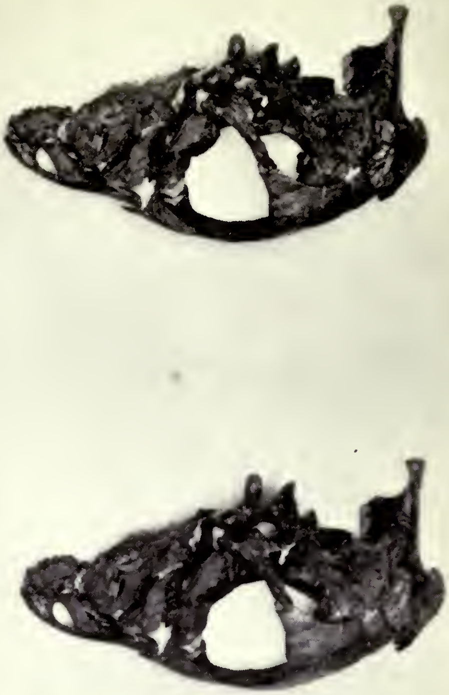

4

PLATE 2

Hypsilophodon foxii

FIG. 1. Skull R2477, dorsal view of palate and braincase. Compare with Text-fig. 5C.

FIG. 2. Skull R2477, medial view, compare with Text-figs. 4B, 60D.

FIG. 3. Pes R196, dorsal view of left pes.

FIG. 4. Femur R167, '*Camptosaurus valdensis*', from a large individual of *Hypsilophodon foxii*. a, anterior view ; b, posterior view.

Scale lines represent 5 cm.

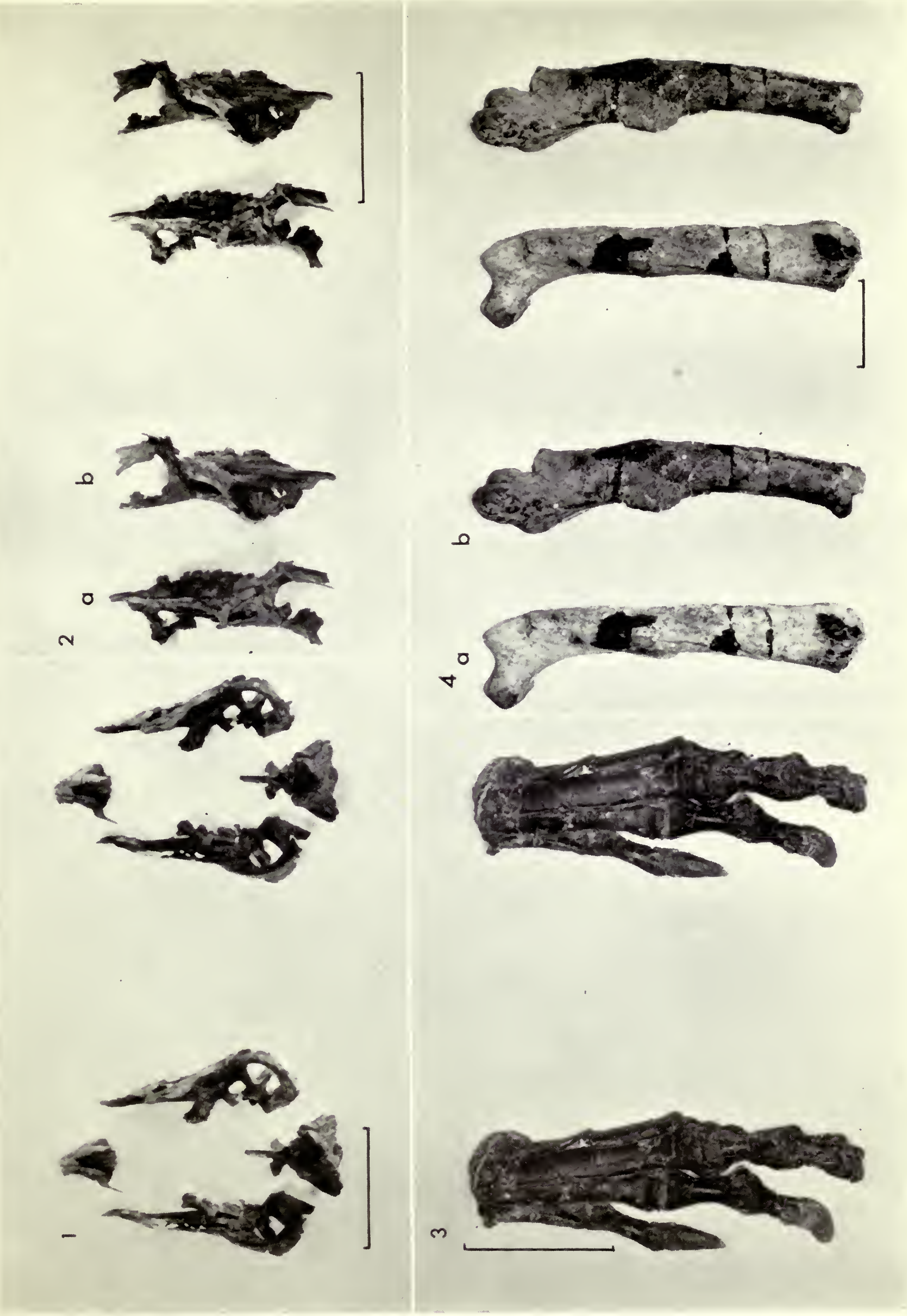
1
2
a
b
3
4
a
b

A LIST OF SUPPLEMENTS
TO THE GEOLOGICAL SERIES
OF THE BULLETIN OF
THE BRITISH MUSEUM (NATURAL HISTORY)

1. Cox, L. R. Jurassic Bivalvia and Gastropoda from Tanganyika and Kenya. Pp. 213; 30 Plates; 2 Text-figures. 1965. £6.
2. El-Naggar, Z. R. Stratigraphy and Planktonic Foraminifera of the Upper Cretaceous—Lower Tertiary Succession in the Esna-Idfu Region, Nile Valley, Egypt, U.A.R. Pp. 291; 23 Plates; 18 Text-figures. 1966. £10.
3. Davey, R. J., Downie, C., Sarjeant, W. A. S. & Williams, G. L. Studies on Mesozoic and Cainozoic Dinoflagellate Cysts. Pp. 248; 28 Plates; 64 Text-figures. 1966. £7.
   Appendix. Davey, R. J., Downie, C., Sarjeant, W. A. S. & Williams, G. L. Appendix to Studies on Mesozoic and Cainozoic Dinoflagellate Cysts. Pp. 24. 1969. 80p.
4. Elliott, G. F. Permian to Palaeocene Calcareous Algae (Dasycladaceae) of the Middle East. Pp. 111; 24 Plates; 17 Text-figures. 1968. £5.12½.
5. Rhodes, F. H. T., Austin, R. L. & Druce, E. C. British Avonian (Carboniferous) Conodont faunas, and their value in local and continental correlation. Pp. 315; 31 Plates; 92 Text-figures. 1969. £11.
6. Childs, A. Upper Jurassic Rhynchonellid Brachiopods from Northwestern Europe. Pp. 119; 12 Plates; 40 Text-figures. 1969. £4.75.
7. Goody, P. C. The relationships of certain Upper Cretaceous Teleosts with special reference to the Myctophoids. Pp. 255; 102 Text-figures. 1969. £6.50.
8. Owen, H. G. Middle Albian Stratigraphy in the Anglo-Paris Basin. Pp. 164; 3 Plates; 52 Text-figures. 1971. £6.
9. Siddiqui, Q. A. Early Tertiary Ostracoda of the family Trachyleberididae from West Pakistan. Pp. 98; 42 Plates; 7 Text-figures. 1971. £8.
10. Forey, P. L. A revision of the elopiform fishes, fossil and Recent. Pp. 222; 92 Text-figures. 1973. £9.45.

Printed in Great Britain by John Wright and Sons Ltd. at The Stonebridge Press, Bristol BS4 5NU

22 JUL 197

THE TAXONOMY AND MORPHOLOGY OF *PUPPIGERUS CAMPERI* (GRAY), AN EOCENE SEA-TURTLE FROM NORTHERN EUROPE

R. T. J. MOODY

BULLETIN OF
THE BRITISH MUSEUM (NATURAL HISTORY)
GEOLOGY Vol. 25 No. 2
LONDON: 1974

BRITISH MUS
22 JUL 19
NATURAL HIS

THE TAXONOMY AND MORPHOLOGY OF *PUPPIGERUS CAMPERI* (GRAY), AN EOCENE SEA-TURTLE FROM NORTHERN EUROPE

BY
RICHARD THOMAS JONES MOODY
Kingston Polytechnic

Pp. 153–186 ; 8 *Plates,* 15 *Text-figures*

BULLETIN OF
THE BRITISH MUSEUM (NATURAL HISTORY)
GEOLOGY Vol. 25 No. 2
LONDON: 1974

THE BULLETIN OF THE BRITISH MUSEUM (NATURAL HISTORY), *instituted in* 1949, *is issued in five series corresponding to the Departments of the Museum, and an Historical series.*

Parts will appear at irregular intervals as they become ready. Volumes will contain about three or four hundred pages, and will not necessarily be completed within one calendar year.

In 1965 *a separate supplementary series of longer papers was instituted, numbered serially for each Department.*

This paper is Vol. 25, *No.* 2, *of the Geological (Palaeontological) series. The abbreviated titles of periodicals cited follow those of the World List of Scientific Periodicals.*

World List abbreviation :
Bull. Br. Mus. nat. Hist. (Geol.)

© Trustees of the British Museum (Natural History), 1974

TRUSTEES OF
THE BRITISH MUSEUM (NATURAL HISTORY)

Issued 23 *May*, 1974 *Price* £2·85

THE TAXONOMY AND MORPHOLOGY OF *PUPPIGERUS CAMPERI* (GRAY), AN EOCENE SEA-TURTLE FROM NORTHERN EUROPE

By RICHARD THOMAS JONES MOODY

CONTENTS

	Page
INTRODUCTION	155
HISTORICAL REVIEW	156
SYSTEMATIC DESCRIPTION	161
SUMMARY AND CONCLUSIONS	182
ACKNOWLEDGMENTS	183
REFERENCES	184

SYNOPSIS

Comparative studies show that the chelonians *Eochelys longiceps* (Owen), *Lytoloma trigoniceps* (Owen) and *Lytoloma camperi* (Gray) are conspecific; the valid name is *Puppigerus camperi*, and a lectotype is designated. The species occurs in the Eocene of Belgium and England. All known skeletal elements are described, certain ontogenetic trends are described and discussed, and a few comments are made on the biology.

INTRODUCTION

IN THE collections of many Northern European museums are excellent examples of the cheloniids *Eochelys longiceps* (Owen), *Lytoloma trigoniceps* (Owen) and *Lytoloma camperi* (Gray). All three species are of Eocene age; *E. longiceps* occurs in the London Clay and Bracklesham Beds, *L. trigoniceps* in the Brackleshams only, and *L. camperi* in the Bruxellian of Belgium.

The history of *L. camperi* began in 1781, when Buc'hoz (dec. 6, pl. 3, cent. 2) figured an unnamed turtle carapace from the Sables de Bruxelles; this specimen was later to become one of the two syntypes of *Emys camperi* Gray (1831, p. 37). The species *Chelone longiceps* and *Chelone trigoniceps* were erected by Owen in 1841 and 1850 respectively. The arguments that raged during this period as to the marine or fresh-water affinities of Eocene turtles concerned (*inter alia*) *C. longiceps* and *C. trigoniceps* but not *E. camperi*, which everyone accepted as a marsh turtle.

Cope (1871) erected the new genus *Puppigerus*, with *C. longiceps* and *C. trigoniceps* among the included species, but he did not designate a type. Lydekker (1889*b*) designated *C. longiceps* as the type-species of *Puppigerus*, and, at the same time, transferred the species to the genus *Lytoloma*. *Lytoloma* had also been erected by Cope, in 1870, and is therefore a year older than *Puppigerus*. Lydekker's synonymy, however, is only subjective; and, in any case, the genus *Lytoloma* should have been ignored, being based on two indeterminate species (Zangerl 1953; Moody 1968).

The same author (Lydekker 1889*a*, *b*) discussed the morphology of the two British species and decided that both were cheloniid turtles. Dollo (1923) claimed the same for the species *camperi*, which too he referred to *Puppigerus*. The belief in the marine affinities of all these species has persisted. The species *Lytoloma longiceps* [*Chelone*] was made the type of the new genus *Eochelys* by Moody in 1968, who was then unaware that it was already the type of *Puppigerus* Cope. *Eochelys* thus became an objective junior synonym of *Puppigerus*.

In recent years Dr E. Casier, Dr R. Zangerl and I have worked separately on the morphology and taxonomy of the three species. Drs Zangerl and Casier have recently made their material available to me so that the possibly synonymous species could be compared on a wider basis. There is excellent associated material of *Puppigerus* in the Institut Royal des Sciences Naturelles de Belgique, Brussels. On the other hand, material from English localities in English museums consists mainly of well-preserved but isolated skeletal remains ; nevertheless a great deal of preparation and jig-saw type assembly carried out at the British Museum (Natural History) has made it possible to compare the prepared material with the associated remains in Brussels. The evidence undoubtedly indicates that the remains of the three species are identical.

HISTORICAL REVIEW

EMYS CAMPERI Gray

The history of the Eocene turtles under revision began with the illustration of a carapace by Buc'hoz in 1781. The specimen remained unnamed until 1784, when Burtin claimed – obviously incorrectly – that it should be referred to the species *Testudo corticata*, a name applied by Rondelet to the Recent Hawksbill Turtle (*Lepidochelys*). Faujas St Fond (1799) agreed with this but, according to Dollo (1923), stated that the specimen was similar to the Recent Green Turtle (*Chelonia mydas*). Cuvier (1812) also thought it was a sea-turtle but, on reflection, described and figured the carapace as one of the marsh turtles from the 'Environs de Bruxelles' (1824, pl. 15, fig. 16 and pl. 13, fig. 8). Gray (1831) regarded Cuvier's description of the turtles from Brussels as an indication of specific grouping and based a new species *Emys camperi* on the two specimens figured by Cuvier. It is fortunate that these syntypes have since proved conspecific, for Cuvier's illustrations are so inaccurate that they could never be regarded as representative of a single species.

The syntypes of *E. camperi* were separated after 1830 ; the original carapace illustrated by Buc'hoz remained in Brussels as I.R.S.N.B. 1687/R.4; the other and its counterpart were moved to Ghent to become G.M. 2250 and 2251 respectively. The latter were figured and described by Poelman (1868, figs. 1–2), the description confirming that the specimen had eight costal and nine neural plates. As it has not been confirmed whether the last two specimens are still in existence, the Brussels specimen is here designated as the lectotype of the species *E. camperi*. The belief that *E. camperi* was a marsh turtle persisted until 1923, when Dollo assigned the species to the marine genus *Puppigerus* Cope. Bergounioux (1933) disagreed with Dollo's assignment of *E. camperi* to the genus *Puppigerus* and claimed that the species would be more correctly referred to the American genus *Lytoloma*. He supported Dollo's view, however, that *E. camperi* was a marine turtle. His reconstruction of the animal bore little resemblance to the type material.

CHELONE LONGICEPS Owen

Ten years after Gray's erection of the species *E. camperi* upon the forms figured earlier by Cuvier, Owen (1841) described the species *Chelone longiceps* from the London Clay of the Isle of Sheppey; this form was destined to become the type species of both *Puppigerus* Cope 1871 (see Lydekker 1889*b*, p. 57) and *Eochelys* Moody 1968. *C. longiceps* was erected on skull and shell material correctly assigned to the one species. However, over the next fifty years there was much discussion of the possible synonymy of *C. longiceps* with *Emys parkinsonii*, a species erected by Gray (1831) on remains figured by Parkinson (1811) and Cuvier (1824) from the Isle of Sheppey.

Poelman (1868) decided that the two were synonymous and that *E. parkinsonii* was the senior name, a lead followed by Winkler (1869). This conspecific evaluation was in part correct, as one of the syntypes of *E. parkinsonii* (Parkinson 1811, fig. 2, pl. 18) was a juvenile of '*longiceps*' form, a fact noted by Owen (1842) in his description of *C. longiceps*. Since *C. longiceps* is here considered to be a subjective junior synonym of *E. camperi*, the question arises as to the possible synonymy of *E. camperi* and *E. parkinsonii*. Both are proposed on the same page of the same work (Gray 1831, p. 33), *E. parkinsonii* having line priority. The International Code of Zoological Nomenclature recommends (Recommendation 69B (12)) that the first-mentioned name should be used in such cases, all other things being equal. But all other things are *not* equal. *E. parkinsonii* was based on a series of individuals which do not all belong to the same species and from which no lectotype has been chosen, and to use that name in preference to *E. camperi* for all the material described in the present paper would only add to the confusion. It is therefore clear that the recommendation does not apply in this instance and that the name *E. camperi* should be retained.

The species *C. longiceps* and *C. trigoniceps* were regarded as valid by Lydekker, who assigned them in 1889 to the genus *Lytoloma*; this decision succeeded in stabilizing a synonymy confused by Dollo, who had noted the similarity of the two English species with Belgian forms referred variously to the genera *Pachyrhynchus* Dollo, *Erquelinnesia* Dollo and *Euclastes* Cope between 1886 and 1888. The synonymy of the various chelonians from the London Clay was discussed by Moody (1968), when an account of the taxonomic confusion regarding these specimens was given. As mentioned above, Moody erected the new genus *Eochelys* on the species *longiceps*, unaware that that species was already the valid type of *Puppigerus*.

CHELONE TRIGONICEPS Owen

The synonymy of the species *Chelone trigoniceps* followed similar lines to that of *C. longiceps*, the species being first described by Owen in 1849 and first figured, again by Owen, in Dixon's *Geology of Sussex* (1850, pl. XIII, fig. 4). Lydekker (1889*b*) assigned the species to the genus *Lytoloma* and this has generally been accepted until now.

Stratigraphical occurrence of *Lytoloma*

Sables de Wemmel	Wemmelian	U. Eocene
Barton Beds	Bartonian	U. Eocene
Sables de Bruxelles	Bruxellian	M. Eocene
Bracklesham Beds	Lutetian	M. Eocene
London Clay	Lower Ypresian	L. Eocene

The European material hitherto referred to *Lytoloma* includes the material housed in the I.R.S.N.B., Brussels, under the names *Lytoloma camperi*, '*L. bruxelliensis*' and '*L. wemelliensis*' and in the British Museum (Natural History) under the names *L. longiceps*, *L. trigoniceps* and *L. crassicostatum* (part). As indicated in the introduction to this paper the three Belgian species, *L. longiceps* and *L. trigoniceps* are doubtless all identical and the number of species in this genus is therefore only two.

The supposed differences between *L. longiceps* and *L. trigoniceps* were that *L. trigoniceps* attained greater size and that its interorbital bar was relatively much wider. The latter 'difference' is without doubt the result of distortion and crushing ; simple measurement (Table 1B) shows that the relative width of the interorbital bar is exactly the same in the two forms.

A summary of the measurements and indices recorded from the various species (Tables 1 and 2) confirms the comparative studies undertaken. The tables also show that *L. camperi* and *L. longiceps* are conspecific.

TABLE 1

Measurements and indices recorded from skulls now referred to the species *Puppigerus camperi* but formerly variously referred to the species *Lytoloma longiceps* and *L. trigoniceps* as well as to *L. camperi*

A. Distance of internal nares from snout/total length of palate

specimen	distance of internal nares from snout n mm	total length of palate p mm	$\frac{n}{p}$ (as %)
Lytoloma camperi			
I.R.S.N.B. R.19	23	52	44·2
I.R.S.N.B. R.18	28	56	50·0
I.R.S.N.B. R.17	45	87	51·7
I.R.S.N.B. R.16	47	92	51·1
Lytoloma longiceps			
H.M. 297	46	87	52·9
Spec. fig. Owen (1849)	46	86	53·6
B.M.(N.H.) R.2163	50	97*	51·5
Lytoloma trigoniceps	No measurements available		
Specimen referred by Lydekker (1889*b*) to *L. crassicostatum*			
B.M.(N.H.) 38954	34	72	47·2

* Estimated.

Table 1 (*cont.*)

B. Width of interorbital bar/length of orbit

specimen	width of interorbital bar i mm	length of orbit o mm	$\frac{i}{o}$ (as %)
Lytoloma camperi			
I.R.S.N.B. IG.8402	22	25	84·6
I.R.S.N.B. R.19	16	18	88·8
Lytoloma longiceps			
B.M.(N.H.) R.2613	25	27·5	90·9
B.M.(N.H.) 38954	24	26·5	90·6
Lytoloma trigoniceps			
B.M.(N.H.) 39771	29	32	90·6

Table 2

Measurements (in mm) and indices recorded from shells now referred to the species *Puppigerus camperi*

	Neural plate								
specimen	1st	2nd	3rd	4th	5th	6th	7th	8th	9th
L. camperi									
I.R.S.N.B. IG.9544	33	30	33	33	28	28	22·5	18	9
I.R.S.N.B. R.13	34	30	29	29	24	24	21	15	15
I.R.S.N.B. IG.8632	17	17	15	18	14	12	11	8	5
I.R.S.N.B. IG.8402/R.17	32	29	31	–	–	–	–	–	–
I.R.S.N.B. R.14	–	–	28	30	23	26	21	13	11
L. longiceps									
B.M.(N.H.) 38951	24	26	24	25	23	21·5	19·5	17	–
B.M.(N.H.) 38950	22	17·5	19	20	17	17	16	13	–

	Neural shield measurements					
	2nd		3rd		4th	
specimen	L	W	L	W	L	W
L. camperi						
I.R.S.N.B. IG.9544	69	72	65	71	75	65
I.R.S.N.B. R.13	62	68	58	62	61	61
I.R.S.N.B. IG.8632	34	49	34	51	34	45
I.R.S.N.B. IG.8402/R.17	66	72	–	–	–	–
L. longiceps						
B.M.(N.H.) 38951	52	62	50	63	58	56
B.M.(N.H.) 38950	44	56	41	51·5	45	48

Plastral index A

specimen	axillo-inguinal width a	½ width of plastron w	$\frac{a}{w}$ (as %)
L. camperi			
I.R.S.N.B. R.14	87	105	82·9
I.R.S.N.B. R.15	92	104	88·5
L. longiceps			
B.M.(N.H.) 45902	52	74	70 ±
B.M.(N.H.) 35721	64	80	80
B.M.(N.H.) 38951	70	95	73·6

TABLE 2 (*cont.*)

Plastral index B

specimen	axillo-inguinal width a	length from hyo-hyposuture to xiphi tip h	$\frac{a}{h}$ (as %)
L. camperi			
I.R.S.N.B. R.15	92	136	67·6
I.R.S.N.B. R.14	87	114	76·3
L. longiceps			
B.M.(N.H.) 38951	70	99	70·7
B.M.(N.H.) 25608	53	71	75·7
B.M.(N.H.) 38950	55	73*	75·3
B.M.(N.H.) R.1917	43	64	67·2
B.M.(N.H.) 35721	61	89	68·5

Xiphiplastral index

specimen	length of xiphiplastron x	length of plastron l	$\frac{x}{l}$ (as %)
L. camperi			
I.R.S.N.B. R.15	87	266	32·7
I.R.S.N.B. R.14	73	218	33·5
L. longiceps			
B.M.(N.H.) 38951	64	201	31·8
B.M.(N.H.) 25608	45	138	32·6
B.M.(N.H.) 35721	54	185	29·2
B.M.(N.H.) R.3964	48	156	30·7
L. camperi			
I R.S.N.B. IG.8632	40	127	31·5

*Estimated.

The obvious synonymy between *L. camperi* and *L. longiceps* is shown by a comparison of the skull I.R.S.N.B. IG.8402/R.17 (Figs. 2–5, Pl. 2) with either the type skull of *C. longiceps* figured by Owen (1849), which is missing presumed lost, or the skull H.M.297, also figured by Owen in 1849. Other comparisons can be made between shell and limb remains, and the similarity is confirmed by a comparison of the plastra of I.R.S.N.B. IG.8632 and B.M.(N.H.) 38951 (Pl. 8).

The belief that the three forms are conspecific renders it necessary to comment briefly on the synonymy. As mentioned above, the species *longiceps* was made the type of the new genus *Eochelys* by Moody (1968), who thought that the generic names *Lytoloma* and *Puppigerus* were both unsuitable. But the realization that *Puppigerus* is an objective senior synonym of *Eochelys*, and the placing of *camperi* and *longiceps* in subjective synonymy, together necessitate that all this material should now be called *Puppigerus camperi*.

This species is described in detail below.

A comparative table (p. 162) of the families Plesiochelyidae, Thalassemydidae, Toxochelyidae and Cheloniidae shows that *Puppigerus* is *not* a thalassemydid, as had been suggested by Cuvier (1824, writing about the material on which Gray later based *E. camperi*). Rather does it confirm Moody's belief (1968) that *Puppigerus* [*Eochelys*] is a cheloniid. In the same work Moody indicated that most British Eocene marine turtles were not toxochelyids.

SYSTEMATIC DESCRIPTION

Family **CHELONIIDAE**

Subfamily **EOCHELYINAE** Moody 1968

EMENDED DIAGNOSIS. Skull more or less triangular as seen from above ; dermal and epidermal elements few and regularly arranged (like Cheloniinae, unlike Carettinae). External naris faces forwards and/or upwards ; orbit faces slightly forwards and outwards, with frontal forming part of its rim. Secondary palate may be present, bounded by low, steep cutting edges ; position of internal naris extremely variable. Cervical vertebrae short and stout, articulating as in Recent members of the family. Limbs intermediate in structure between toxochelyids and Recent cheloniids, although humeral : femoral ratio is fully cheloniid. Carapace moderately arched, thickness of plates variable ; neurals eight or nine in number and generally unkeeled. Plastron cruciform, variously ossified, epiplastra wedge-shaped or slightly rounded. No sutural contact between carapace and plastron.

Subfamily includes genera *Puppigerus* Cope (objective junior synonym *Eochelys* Moody), *Argillochelys* Lydekker and *Eochelone* Dollo.

Genus ***PUPPIGERUS*** Cope 1871

TYPE-SPECIES. *Chelone longiceps* Owen 1841 by subsequent designation (Lydekker 1889*b*).

EMENDED DIAGNOSIS. Snout of moderate length in juveniles but very elongate, pinched and narrow in the adults of certain species. Occipital shield present in epidermal mosaic. Extensive secondary palate, with or without shallow median sulcus, large area occupied by palatine ; premaxilla and vomer narrow and elongate. Internal narial opening narrow or quite large ; area in front of opening flat, without swelling ridges. Ectopterygoid processes fairly small, anterior pterygoid area narrower than in *Argillochelys*. Basioccipital depression shallow and smooth. Mandible with elongate symphysis, more than one-third the length of the mandible itself ; dorsal surface of symphysial area very flat or gently concave. Vertebral column as in Recent cheloniids. Carapace more rounded than in *Argillochelys* ; eight or nine neural plates, each slightly longer than broad and with antero-lateral facets much shorter than postero-lateral facets ; vertebral scutes almost square ; fontanelles may be present between costal and peripheral plates in adult specimens. Plastron

COMPARATIVE TABLE

		Plesiochelys	*Thalassemys*	*Idiochelys*	*Toxochelys*	*Puppigerus* [*Lytoloma*]	*Argillochelys*	*Lepidochelys*	*Chelonia*
SKELETON	secondary palate	absent	absent	absent	absent	present	partially present	present	present
	double or plane joints between cervicals 6, 7 and 8	–	–	–	rare	present	present	present	present
	fore limb	as in freshwater turtle?	as in freshwater turtle?	as in freshwater turtle?	flipper-like	flipper-like	flipper-like	flipper-like	flipper-like
	hind limb	as in freshwater turtle	as in freshwater turtle	as in freshwater turtle	as in freshwater turtle	as in freshwater turtle	as in freshwater turtle	reduced cheloniid type	reduced cheloniid type
CARAPACE	general form	rounded or broadly cordiform	rounded or broadly cordiform	rounded or broadly cordiform	circular	broadly cordiform	broadly cordiform	broadly cordiform	broadly cordiform
	neural plates	9	9	partly suppressed	9	9	9	fragmented	8
	suprapygal plates	–	1	1	2	2	2	2	2
	peripheral plates	22	22	22	22	22	22	normally 24	22
	costo-peripheral fontanelles	absent	present	present	present	present in juvenile, often absent in adult	present in juvenile, often absent in adult	present	present
PLASTRON	sutural attachment to carapace	present	absent	absent	absent	absent	absent	absent	absent
	xiphiplastron	large and square	large and square	large and square	elongated, with notched insertion into hypoplastron	shorter, with notched insertion into hypoplastron	elongated, with notched insertion into hypoplastron	elongated, with notched insertion into hypoplastron	elongated, with notched insertion into hypoplastron
EPIDERMAL SHIELDS	width of vertebrals compared with pleurals	much wider	much wider	much wider	much narrower	much narrower	much narrower	much narrower	much narrower
	pleurals	4	4	4	4	4	4	normally 5	4
	marginals	24	24	24	24	24	24	normally 26	24

extensively ossified, with central fontanelle (if present) of variable size ; epiplastra wedge-shaped as in *Eretmochelys* and *Catapleura*, hyo-hypoplastral suture extensive, xiphiplastra short and broad. Texture of bone surface smooth and without pronounced pattern visible in *Argillochelys*.

Puppigerus camperi (Gray) [***Emys***]

1784 *Testudo corticata* (Rondelet) Burtin, p. 93, pl. 5.
1799 'Tortue Franche' (*Chelonia mydas*) Faujas St Fond, p. 60.
1824 Emydes de Bruxelles : Cuvier, p. 236, pl. 13, fig. 8.
1824 Emydes de Sheppey : Cuvier, p. 234, pl. 15, fig. 7.
1831 *Emys camperi* Gray, p. 33. Based upon Cuvier's figures of 1824.
1831 *Emys parkinsonii* Gray, p. 33.
1837 *Emys cuvieri* Galeotti, p. 45.
1841 *Chelone longiceps* Owen, p. 572.
1842 *Chelone longiceps* Owen : Owen, pp. 162, 172.
1849 *Chelone longiceps* Owen : Owen & Bell, p. 16, pls. 3–5.
1849 *Chelone trigoniceps* Owen & Bell, p. 31.
1849 *Chelone longiceps* Owen : Owen, p. 16, pls. 12–13.
1849 *Chelone trigoniceps* Owen : Owen, p. 31, pl. 25.
1849 *Chelone auticeps* Owen, pl. 25.
1850 *Chelone trigoniceps* Owen : Owen, p. 218, pl. 13.
1854 *Chelone longiceps* Owen : Owen, p. 72.
1868 *Emys camperi* Gray : Poelman, p. 105, pls. 1–2.
1868 *Emys parkinsonii* Gray : Poelman, p. 111, pl. 3.
1869 *Emys camperi* Gray : Winkler, p. 129, pls. 26–28.
1869 *Emys parkinsonii* Gray : Winkler, pls. 24, 25.
1870 *Puppigerus longiceps* (Owen) Cope, p. 235.
1886 *Pachyrhynchus longiceps* (Owen) Dollo, p. 138.
1886 *Pachyrhynchus trigoniceps* (Owen) Dollo, p. 138.
1889*b* *Lytoloma longiceps* (Owen) Lydekker, p. 57.
1889*b* *Lytoloma trigoniceps* (Owen) Lydekker, p. 53.
1889*b* *Lytoloma crassicostatum* (Owen) (part) Lydekker.
1909 *Emys camperi* Dollo, p. 111.
1923 *Puppigerus camperi* (Gray) Dollo, p. 416.
1933 *Lytoloma camperi* (Gray) Bergounioux, pp. 1–13, figs. 1–4.
1968 *Eochelys longiceps* (Owen) Moody, p. 131.

SYNTYPES. I.R.S.N.B. 1687 – Lectotype, designated herewith.
G.M. 2250, 2251 – Paralectotypes. (As yet no confirmation has been received that these specimens, figured by Poelman (1868), are still in Ghent.)

DESCRIPTION OF LECTOTYPE, I.R.S.N.B. 1687 (Fig. 1). Incomplete carapace, lacking most of the peripheral plates ; specimen very fragmentary on left-hand side ; nuchal incomplete ; nine neural and eight costal plates. On list of types housed in I.R.S.N.B. It is, without doubt, closer to the specimen figured by Cuvier (pl. 13, fig. 8) than the other syntype and is therefore designated herewith as the lectotype of *Puppigerus camperi*.

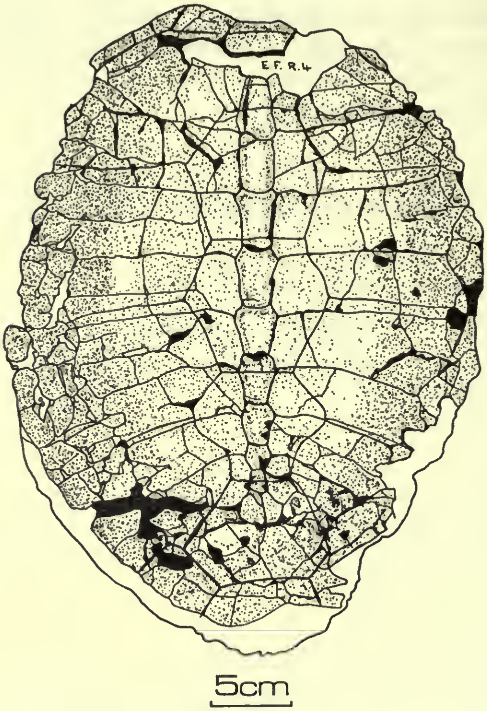

FIG. 1. *Puppigerus camperi* (Gray). Lectotype (I.R.S.N.B. 1687/R.4). From above, drawn from a photograph.

REFERRED SPECIMENS.

I.R.S.N.B. 1663, 1664, 1665, 1666, 1667, 1668, 1669, 1684, 1685, 1686, 1687/R.4, 1689, R.5, R.13, R.14, R.16, IG.8402/R.17, R.18, R.19
G.M. 2250, 2251, 2252
B.M.(N.H.) 25609, 28853, 30526, 35608, 35689, 37207, 37211, 38950, 38954, 38959, 39763, 39771, 44092, R.1025, R.1425, R.1475, R.1481, R.2163, R.8553
G.S.M. 57266, 57267, 92297, 92298
Hunterian Collection, R.C.S. H.M.297
Sedgwick Museum, Cambridge. C.20924, 20926, 20930, 20933
Maidstone Museum (M.M.) (G.S.M. TN). 9551, 9552, 9554, 9957

Also belonging to this species are two very poor fragmentary mandibles in the I.R.S.N.B. labelled, in Dollo's handwriting, '*Lytoloma bruxelliensis*' and '*Lytoloma wemelliensis*'. These are presumably the specimens upon which, in 1909, Dollo based those two names (they should in fact have been *L. bruxelliense* and *L. wemelliense*, the Greek noun λωμα being of the neuter gender). The names, however, were given without adequate indication and are certainly *nomina nuda*; since they cannot be formally connected with the specimens they are not included in the synonymy.

OCCURRENCE OF SPECIES.

Sables de Wemmel – Wemmelian – Upper Eocene. Belgium. (See Curry 1966.)
Sables de Bruxelles – Bruxellian – Middle Eocene. Belgium.
Bracklesham Beds – Lutetian to Auversian – Middle Eocene. England.
London Clay – Lower Ypresian – Lower Eocene. England.

The specimens referred to this species range widely in both size and state of preservation. The material studied includes numerous skulls, vertebrae, limb and girdle elements and shells, together with a few excellent associated skeletons (Pl. 1). The smallest known specimens are G.S.M. 57266 and B.M.(N.H.) 28853, of which the last has been prepared with the air-abrasive and has yielded a tremendous amount of skeletal material. The largest specimens are housed in the Belgian collections and reach a maximum length of 350 ± mm. From such a range of material the following specific diagnosis is drawn.

EMENDED DIAGNOSIS OF *P. camperi.* Snout region elongate in adult, tapering anteriorly to a point ; in side-view, premaxilla plus maxilla much longer than jugal plus quadrato-jugal. Extensive secondary palate, with narrow internal narial opening situated (in adult) in third quarter of ventral skull length ; very long vomer and premaxilla and short rounded palatine ; palatal surface pitted. Palatine extends backwards to form a shelf lying ventral to the pterygoid and small ectopterygoid process ; pterygoid bar narrow. Basioccipital depression fairly deep, without rugose surface. Braincase basically cheloniid, but with distinct specific characters (see description). Carapace of adult completely ossified, broadly cordiform and gently arched ; nine neurals and two pygals ; juvenile forms with costo-peripheral fontanelles. Plastron with small to medium-sized central fontanelle ; epiplastra wedge-shaped as in *Catapleura* ; entoplastron T-shaped ; xiphiplastron short and wide. Plastral index 70–85.

DESCRIPTION OF MATERIAL. There are many excellent skulls amongst the specimens listed above, and the following description is drawn from I.R.S.N.B. R.14, R.15, R.16, IG.8402/R.17, R.18 & R.19 ; B.M.(N.H.) 38954 & R.2613 ; and H.M.297. The previously noted similarity between the adult skulls formerly ascribed to the respective species *Emys camperi* (Pl. 2) and *Chelone longiceps* (H.M.297), is also apparent in the juvenile specimens I.R.S.N.B. R.19 (Pl. 3A) and B.M.(N.H.) R.1475, in which the snout region is much shorter. The progressive pinching in of the snout as seen in dorsal view is an outstanding ontogenetic trend. The snout of the juvenile is very similar in shape to that of *Chelone crassicostata* ; the snout of the adult, however, is pinched below the orbits and tapers anteriorly to a more pronounced and acutely pointed beak, as is shown particularly well in I.R.S.N.B. IG.8402/R.17 (Figs. 2–5). This pinching in of the snout is demonstrated by a growth series of *P. camperi* skulls (R.19, R.18, R.16 – see Plate 3) ; this same series also shows the progressive increase in the jugal index from 33·3 to 41·2 (Table 3). It is noticeable that despite this gradual increase in the jugal and quadratojugal indices within the *P. camperi* series, the premaxilla-maxillary length is still proportionally much greater than in the other eochelyines.

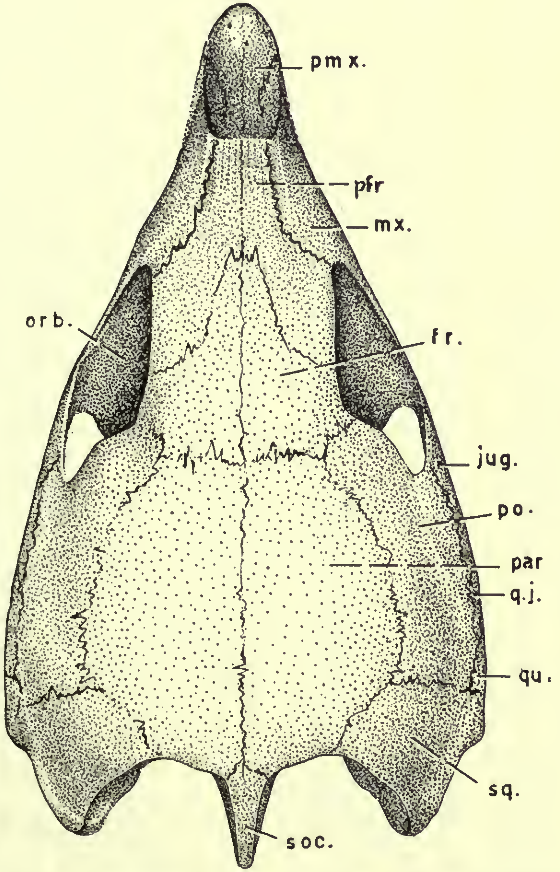
pmx.
pfr
mx.
orb.
fr.
jug.
po.
par
q.j.
qu.
sq.
soc.

FIG. 2. *Puppigerus camperi* (Gray). Reconstruction of skull × 1, based on I.R.S.N.B. IG.8402/R.17. From above. Abbreviations as on p. 184.

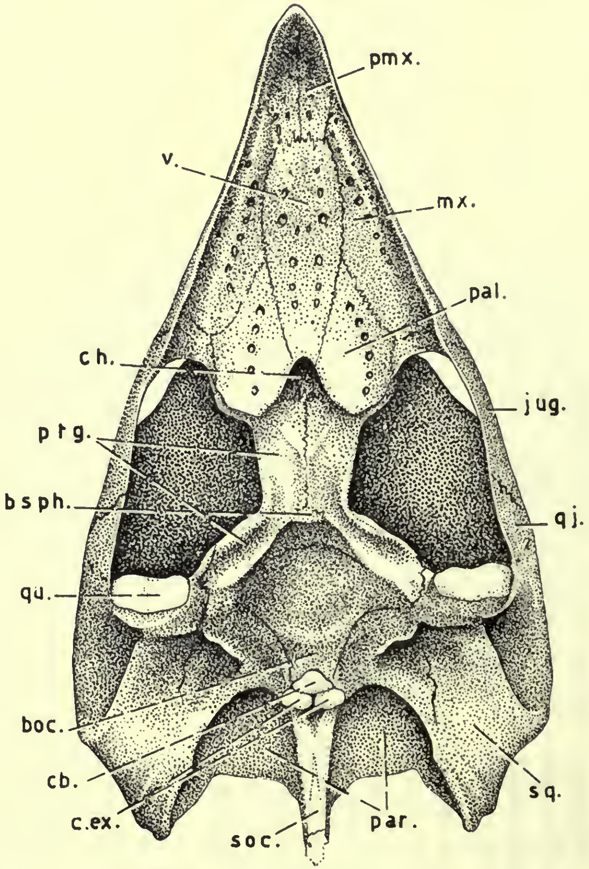
pmx.
v.
mx.
pal.
ch.
jug.
ptg.
bsph.
qj.
qu.
boc.
cb.
c.ex.
soc.
par.
sq.

FIG. 3. *Puppigerus camperi* (Gray). Reconstruction of skull × 1, based on I.R.S.N.B. IG.8402/R.17. From below. Abbreviations as on p. 184.

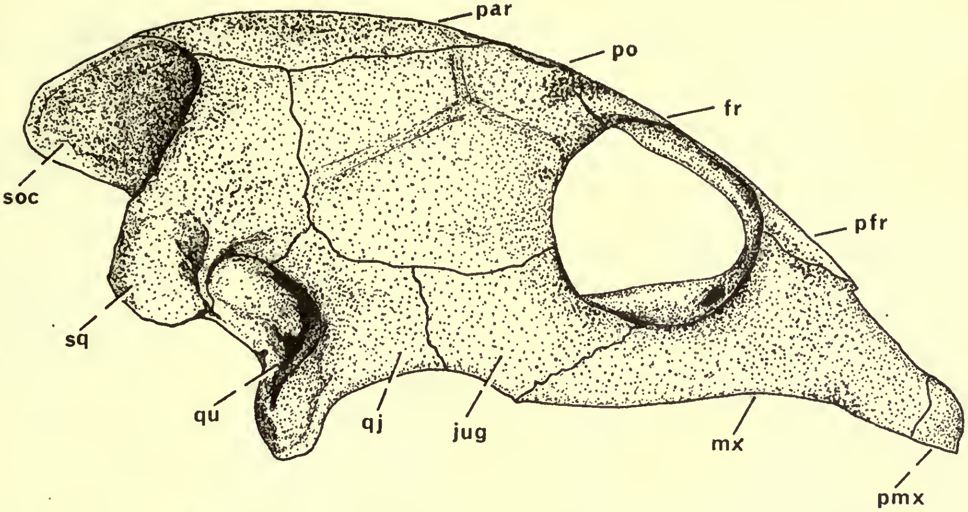
par
po
fr
soc
pfr
sq
qu
qj
jug
mx
pmx

FIG. 4. *Puppigerus camperi* (Gray). Reconstruction of skull × 1, based on I.R.S.N.B. IG.8402/R.17. From right side. Abbreviations as on p. 184.

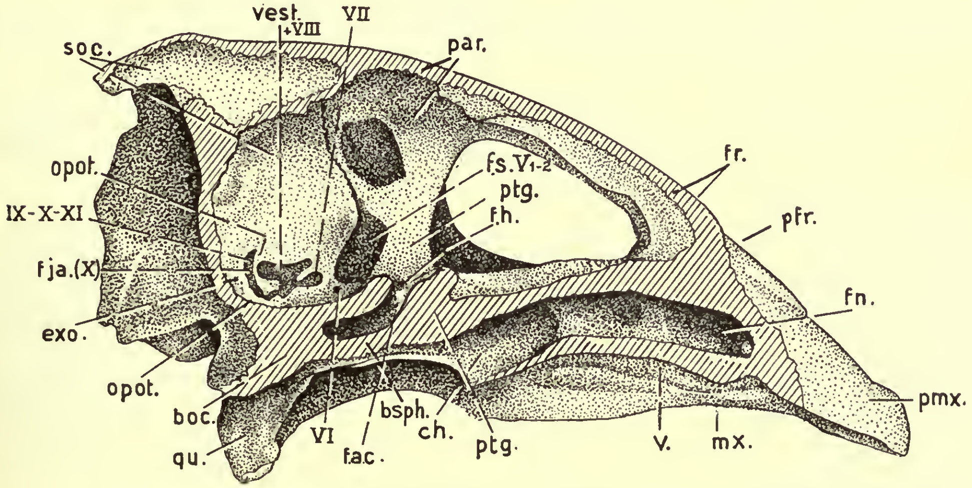
vest.
+VIII
VII
soc.
par.
opot.
IX-X-XI
f.s.V1-2
ptg.
f.h.
fr.
pfr.
fja.(X)
fn.
exo.
opot.
pmx.
boc.
bsph.
qu.
VI
ch.
f.ac.
ptg.
V.
mx.

FIG. 5. *Puppigerus camperi* (Gray). Reconstruction of skull × 1, based on I.R.S.N.B. IG.8402/R.17. Parasagittal section close to midline to show braincase. Abbreviations as on p. 184.

Table 4 shows that the internal narial opening is retreating backwards over the ventral surface of the skull as the animal grows. The premaxilla and vomer are elongate in this species, the vomer narrowing anteriorly but expanding slightly in the area of contact with the maxilla and palatine. The palatine is shorter and more rounded than in other species ; it often expands medially and posteriorly to reduce the front part of the internal narial opening to a narrow slit (shown well in I.R.S.N.B.

TABLE 3

Measurements (in mm) and indices recorded for the bones of the outside edge of the skulls of three eochelyine species

specimen	total length of premaxilla + maxilla m	length of jugal j	$\frac{j}{m}$ (as %)	length of quadrato-jugal q	$\frac{q}{m}$ (as %)
Puppigerus camperi					
I.R.S.N.B. R.19	27	9	33·3	7	25·9
I.R.S.N.B. R.18	33	11	33·3	5	15·1
I.R.S.N.B. R.17	46	20	43·5	8	17·3
I.R.S.N.B. R.16	51	22	43·1	13	25·5
Puppigerus crassicostatus					
B.M.(N.H.) 37213a	39	23	58·9	8	20·5
B.M.(N.H.) 25610	33	20	60·6	8	24·2
B.M.(N.H.) 35696	32	20	62·5	–	–
B.M.(N.H.) R.3964	–	19	–	7	–
Argillochelys cuneiceps					
B.M.(N.H.) 41636	41	33	80·5	16	39·0

TABLE 4

Measurements (in mm) to illustrate the variation in the position of the internal narial openings with size in *Puppigerus camperi*, and a comparison with other Eocene forms

specimen	length of skull below l	distance of narial opening from tip of snout d	$\frac{d}{l}$ (as %)	quarter in which choanae sited
Puppigerus camperi				
I.R.S.N.B. R.19	52	23	44·2	2
I.R.S.N.B. R.18	56	28	50·0	2–3
B.M.(N.H.) 38954	72	36	50·0	2–3
I.R.S.N.B. IG.8402/R.17	87	45	51·7	3
H.M. 297	87	46	52·9	3
I.R.S.N.B. R.16	92	47	51·1	3
Puppigerus crassicostatus				
B.M.(N.H.) 38955	56	22	39·3	2
B.M.(N.H.) 37213a	64	26	40·6	2
Argillochelys cuneiceps				
B.M.(N.H.) 41636	*c.* 91	26·5	29·1	1–2

R.16, Fig. 6) and to form a shelf ventral to the ectopterygoid process. The latter is not as pronounced as in either *C. crassicostata* or *Argillochelys*. The pterygoid bar is narrow in *P. camperi* and does not expand anteriorly to any great extent (Fig. 6). Posteriorly the pterygoid borders the fairly shallow, smooth, basisphenoid/basioccipital depression ; the quadrate ramus bears a deep groove running along its ventral surface, its antero-lateral margin curving downwards towards the basioccipital.

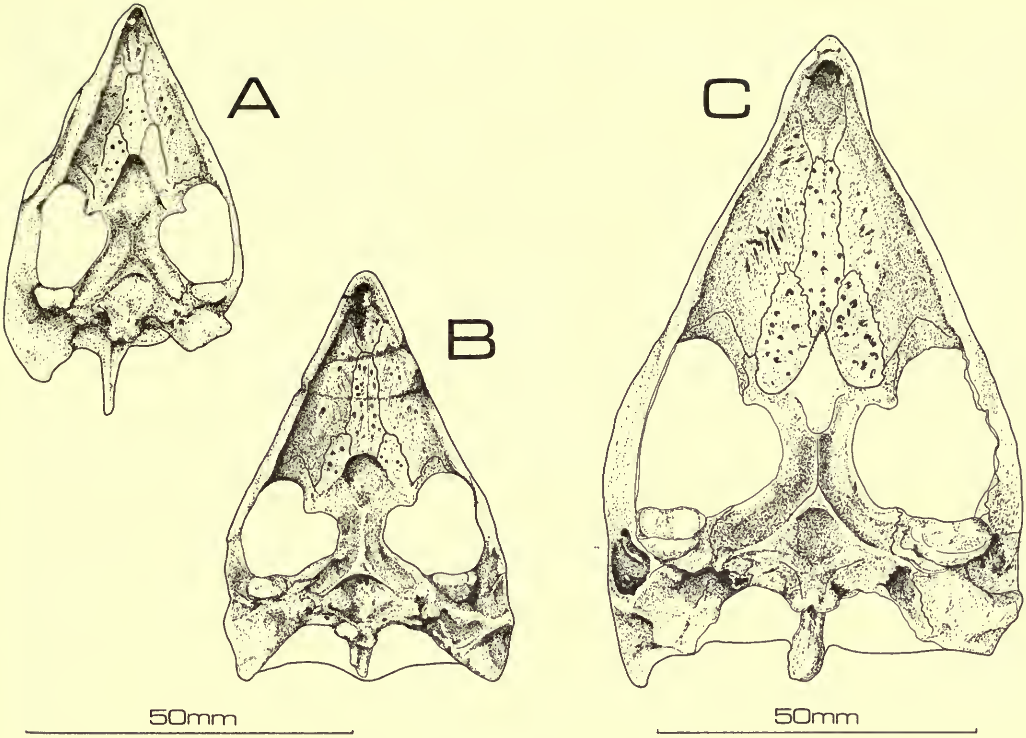

FIG. 6. *Puppigerus camperi* (Gray). Skulls, from below. A. I.R.S.N.B. R.19 B. I.R.S.N.B. R.18 C. I.R.S.N.B. R.16

Peculiar to the skull I.R.S.N.B. R.19 is the presence of a mid-line foramen, just behind the fronto-parietal suture (Pl. 3A, Fig. 7). This foramen is a definite opening and is not to be confused with the parasitic lesions that so often occur in London Clay specimens. The presence of this parietal foramen was first noted by Edinger (1933) and was later mentioned by Zangerl (1957) in a comparison with *Testudo denticulata*. The foramen is circular and has an anteroposterior diameter of 2·2 mm (Table 5).

TABLE 5

Comparative table

	length of skull mm	distance of parietal foramen from tip of snout mm	diameter of parietal foramen mm
Testudo denticulata R.Z. 612	42	*c.* 19·5	0·9
Puppigerus camperi I.R.S.N.B. R.19	65 (incomplete)	35	2·2

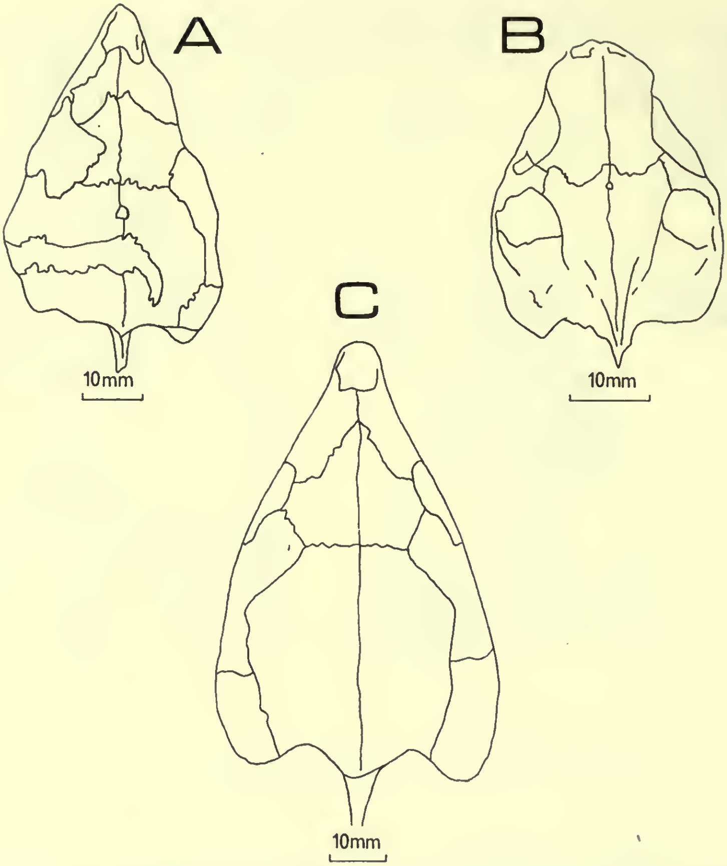

FIG. 7. Reconstructions of skulls of juvenile chelonians, from above, to show parietal foramen. A. *Puppigerus camperi* (based on I.R.S.N.B. R.19). B. *Testudo denticulata* (based on R.Z. 612). C. *Puppigerus camperi* (based on I.R.S.N.B. R.18).

Braincase

The braincase of *P. camperi* is known from the sectioned skull of the Belgian specimen I.R.S.N.B. IG.8402/R.17 (Fig. 5). The bones of the side-wall of the braincase are the pterygoid, parietal, prootic, supraoccipital, opisthotic and exoccipital. The bones of the floor are the basisphenoid, the anterior part of which, the rostrum basisphenoidale, is underlain by the pterygoid, and the basioccipital, which is encroached upon by the exoccipital just anterior to the foramen magnum.

The pterygoid extends upwards from beneath the basisphenoid to form the lower antero-lateral portion of the braincase, the crista pterygoidea. The sulcus cavernosus is well developed between the pterygoid and the rostrum basisphenoidale, much as in *Chelonia mydas*. Postero-laterally the pterygoid forms part of the border of the large foramen nervi trigemini. Laterally the pterygoid is narrower than in most other cheloniids, but not as narrow as in *Argillochelys*. The vertical pterygoid process fuses with the basisphenoid in the sella turcica region to form a wide shelf in front of and to the side of the dorsum sellae, thus providing a canal between the two bones for the internal carotid. The internal carotid canal therefore joins the sulcus cavernosus well forward of the foramen nervi trigemini ; in *Chelonia mydas* the canalis cavernosus is behind this foramen.

Part of the anterior border of the foramen nervi trigemini is formed by the ventral parietal element ; the suture between the parietal and the processus pterygoideus beneath it terminates posteriorly at that foramen. In I.R.S.N.B. IG.8402/R.17 the vertical parietal element is apparently pierced by a second large 'foramen' (Fig. 5). This 'foramen' is much reduced on the opposite side of the cavum cranii and, as the bone in that region is translucent in other sectioned skulls, it is probably due to damage and/or subsequent preparation. The vertical prootic component is reduced in lateral view because of the large foramen nervi trigemini anteriorly and the vestibulum posteriorly (Fig. 5) ; the internal surface area of the prootic is reduced in all eochelyines which have been sectioned, but it is possible that larger specimens were more heavily ossified.

Incomplete ossification may also be an important factor in reducing the internal dimensions of the opisthotic (Fig. 5), which is relatively smaller than in *Chelonia mydas* (Goodrich 1930, fig. 420) ; it forms an incomplete bar between the vestibulum and the foramen jugulare.

The exoccipital forms the posterior portion of the braincase wall and the posterior border of the foramen jugulare anterius ; it is pierced by the foramen for the twelfth nerve.

The dorsal portions of the basisphenoid and basioccipital form the floor of the braincase. The basisphenoid extends anteriorly over the suture of the pterygoid to the posterior area of the palatine ; its anterior portion forms the rostrum basisphenoidale, the complete structure of which is unknown because of damage by sectioning. The rostrum appears to have been elongate as in the Cheloniidae but the foramen arteriae cerebralis is much nearer to the dorsum sellae than in Recent forms and is connected ventrally with the pronounced sulcus cavernosus. The sella turcica is overhung by the dorsum sellae. The foramina of the nervus vidianus and nervus abducens are very small, but the processus clinoideus is quite large. Behind the dorsum sellae and the processus clinoideus the basisphenoid is a concave plate ; this plate is divided by a small ridge, the crista basisphenoidalis, which is less pronounced than in the toxochelyids or Recent cheloniids.

The basioccipital too is concave anteriorly, but is encroached upon posteriorly by the exoccipital ; only in the toxochelyids does the basioccipital extend backwards dorsally to the occipital condyle. The basis tuberculi basalis and crista basioccipitalis are reduced in *P. camperi*. The basioccipital is smooth on its dorsal surface, the numerous ridges typical of *Toxochelys* and *Chelonia* being absent.

The cavum labyrinthicum and cavum acustico-jugulare of the eochelyines are best known from species other than *P. camperi*. Both are very similar to those of Recent cheloniids and of the genus *Stegochelys* as described by Parsons & Williams (1961 p. 80). This is also true of the columella of *Puppigerus camperi* (known from the specimen B.M.(N.H.) 25599).

Endocranial cast

The endocranial cast (Fig. 8) of *P. camperi* taken from I.R.S.N.B. IG.8402/R.17 reflects very little of the actual brain morphology. The information provided by such casts is of general interest only and, in the main, simply illustrates the principal flexures of the brain (Fig. 8). This lack of detail has been noted previously by Zangerl (1960) and Gaffney (1968). Only in the massively constructed braincase of *Corsochelys haliniches* (Zangerl 1960) are the subdivisions of the brain partially reflected in the endocranial cast.

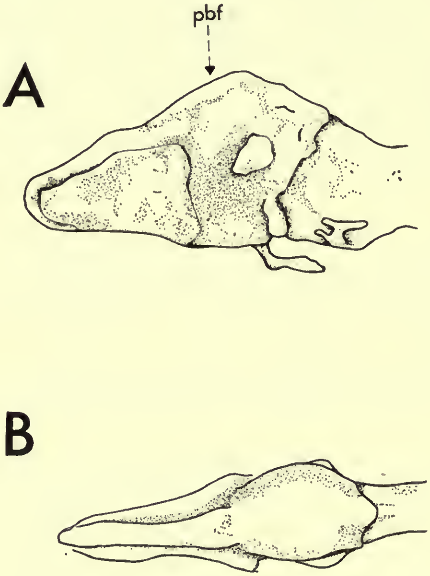

Fig. 8. *Puppigerus camperi* (Gray). Endocranial cast taken from sectioned skull, I.R.S.N.B. IG.8402 × ¾. A. From left side. B. From above. pbf – principal brain flexure.

Lower jaw

The lower jaw of *P. camperi* (Fig. 9; Pl. 2C) is well known from numerous Bruxellian and Bartonian specimens and from one excellent London Clay specimen, B.M.(N.H.) R.8553. The masticatory surface of the jaw is typically almost flat, but does show a very slight concavity in both the anteroposterior and transverse directions. The length of the symphysis is approximately one-half that of the mandibular ramus and the dorsal symphysial surface is always longer than the ventral. The ventral surface has a faint median ridge and a shallow depression posteriorly. The elongation of the symphysial region of the lower jaw is a close reflection of the elongate nature of the secondary palate.

Posterior to the mandibular symphyses of specimens I.R.S.N.B. R.15 and I.R.S.N.B. IG.8402/R.17 is evidence of the hyoid apparatus (Fig. 10; Pls. 1 & 2B); in the case of the latter specimen it is to be seen on the nodule bearing the carapace. In IG.8402/R.17 the copula is incompletely ossified and shaped like a tuning-fork;

in R.15 it is more heavily ossified, the body being complete and shield-like in appearance. The first cerato-branchial arches are also present; these are relatively common as skeletal fragments within fossils of this group.

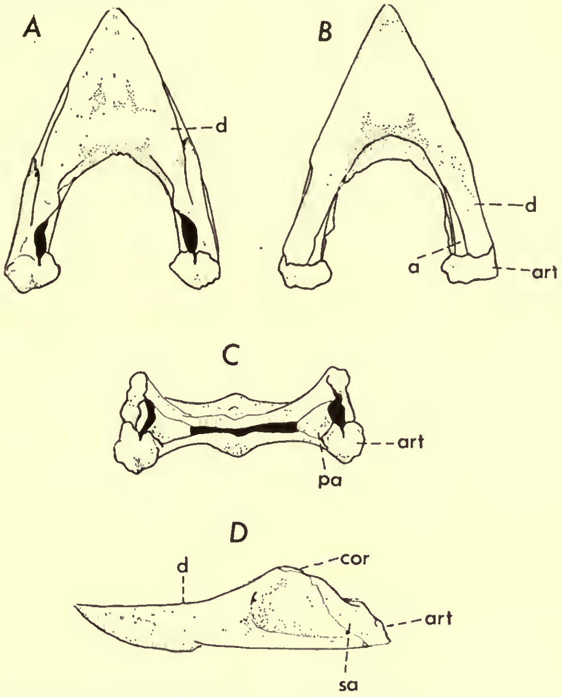

FIG. 9. *Puppigerus camperi* (Gray). Lower jaw × ½. A. From above. B. From below. C. From behind. D. From left side. Abbreviations as on p. 184.

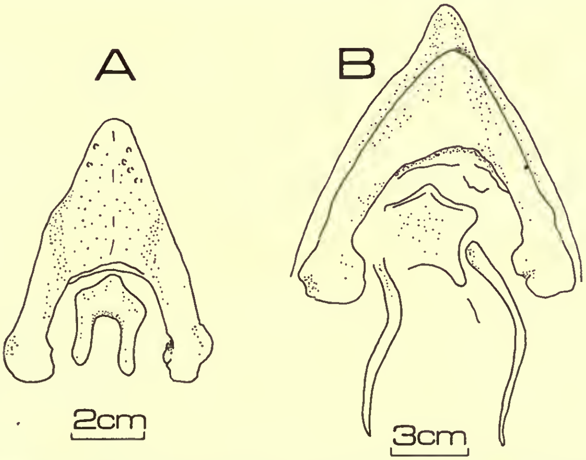

FIG. 10. *Puppigerus camperi* (Gray). Hyoid apparatus. A. Mandible and copula, from below (I.R.S.N.B. IG.8402). B. Mandible, copula and first ceratobranchial arch, from below (I.R.S.N.B. R.15).

Cervical vertebrae

The cervical vertebrae of *P. camperi* are known fully from the prepared specimen B.M.(N.H.) 28853 (Pls. 4–5) and, in lesser degrees, from the specimens I.R.S.N.B. R.14 and R.15 ; Plates 1 and 6 show the great similarity between the cervical vertebrae of *Puppigerus* and those of *Argillochelys*. As stated previously, they are also very similar to those of all other marine turtles. The immediate difference between the two vertebral series is in the articulation pattern for, whereas that of *P. camperi* B.M.(N.H.) 28853 is (2(3(4)5)6/7)8), that of *Argillochelys cuneiceps* S.M.C. 20937 is (2(3(4)5)6)7)8). The former pattern is characteristic of the advanced sea-turtles (Williams 1950). Other than this, the main differences between the two series are concerned with the depth of the hypapophysial keels and the position of certain zygapophysial surfaces.

In *P. camperi* the hypapophysial keels are exceptionally well-developed on the first five vertebrae and remain as significant features through to the last (eighth) cervical. In *Argillochelys* the keels are again present but, as in *Corsochelys haliniches* (Zangerl 1960) and *Dermochelys* (Völker 1913, pl. 31), are pronounced developments of only the second, third and fourth cervicals. In *Dermochelys* the keels acted as areas of attachment for sheaths of cartilage, and Zangerl postulated a similar rôle for those of *Corsochelys*. The actual function of the cartilaginous sheaths was unexplained, except that it was to be regarded as an advanced marine specialization ; my own investigation into this question has resulted in no firm conclusions.

Variation in the zygapophysial surfaces is evident in the second, third and fourth vertebrae of the two series (Pls. 4 & 6). In *Puppigerus camperi* (Pl. 4) the zygapophysial surfaces are more horizontal than those of *Argillochelys* (Pl. 6). This difference would suggest greater lateral movement within the forward neck region of *P. camperi*, which would certainly agree with the inshore mode of life postulated for this form (Moody 1970). The increased tilt of the surfaces in *Argillochelys* would restrict lateral movement but permit greater vertical movement. Once again comparison is made with the form *Corsochelys haliniches* (Zangerl 1960, pl. 32), in which the surfaces are also tilted vertically. Thus the variations in depth of the hypapophysial keel and in tilt of the zygapophysial surfaces may be specializations related to particular environments and modes of life. The cervicals of *P. camperi* show similarities with *Corsochelys* and *Caretta* (Zangerl 1960, pls. 31–33) ; the position of the neurocentral suture, however, is more like that of *Corsochelys*.

Dorsal vertebrae

The dorsal vertebrae of *P. camperi* have been prepared, together with the central part of the carapace, from the same specimen B.M.(N.H.) 28853 (Pl. 5). This specimen is a juvenile, so that the dorsal vertebrae are not completely fused together ; a ventral view shows large spaces between the first five centra. Spaces are also present between the rib heads and the synapophyses. All these spaces were filled with cartilage during the early stages of growth. Each dorsal vertebra (except the first) is fused to the corresponding neural plate ; the first, which lies beneath the nuchal plate, is somewhat similar to the eighth cervical in that it has a much reduced centrum and an elongate neural arch. The centrum of the first dorsal is procoelous to receive the condyle of the eighth cervical; and the whole vertebra is tilted forwards to an angle of some 45 degrees, the posterior portion of the neural arch touching the ventral surface of the nuchal plate. After the first, the centra of the dorsal vertebrae are much reduced, laterally compressed and constricted in the centre to give a waisted appearance. The ends of the centra of this immature specimen are flat. The dorsal blade formed by the fusion of the neural arches is very thin, although it does expand anteriorly with the rest of each arch to form the dorsal part of the synapophyses; the ventral portions of the latter are formed by the underlying centra. The neural arches are intercentral in position, each being extended forwards; the spinal nerve openings occur above the middle of each centrum. Hoffstetter & Gasc (1969) described the composition of the same region in *Pseudemys ornata*, which appears to be very similar.

The ribs arise intervertebrally, as in all turtles, and they arch upwards to fuse with the carapace. The tunnel formed between the vertebrae, ribs and costal plates is in life occupied by epaxial musculature (Vallois 1922, fig. 16); it is well developed as far back as the third rib, but is then reduced to a very small opening. The first rib is reduced and fused distally with the second (as is typical of sea-turtles). The notch between the articular facets of the two ribs is similar to that of the Cheloniidae.

Sacral and caudal vertebrae

The sacral vertebrae of *P. camperi* are known from the specimen H.M.297; another specimen, B.M.(N.H.) R.1480 (Fig. 11), has similar sacrals but is without a skull and cannot be determined with certainty. The sacrum of the latter specimen is made up of two sacral vertebrae and a modified first caudal, all ankylosed together. The centrum of the first sacral is strongly procoelous whilst the first caudal has a large

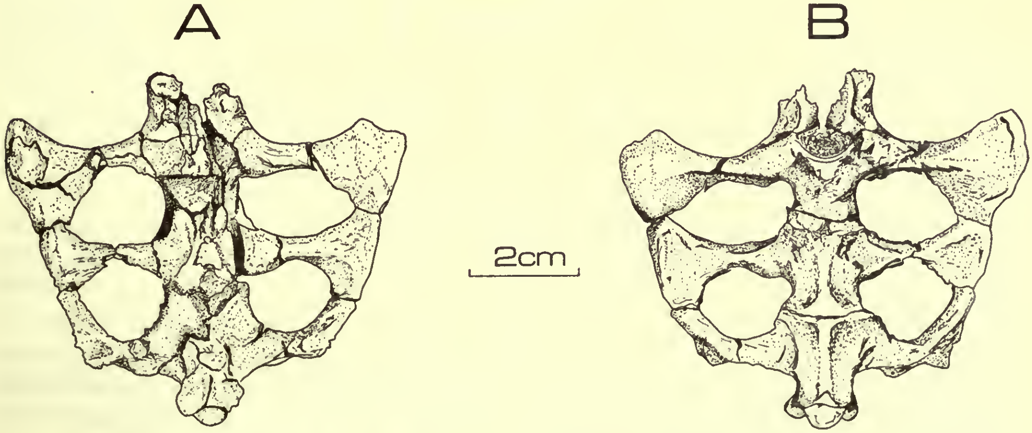

FIG. 11. *Puppigerus camperi* (Gray). Sacrum (B.M.(N.H.) R.1480). Specimen referred by Lydekker to *Lytoloma trigoniceps* (Owen). A. From above. B. From below.

condyle posteriorly; radiography, however, has failed to show whether all these vertebrae are procoelous. Sharp neural crests are visible and the first caudal bears large postzygapophyses. The first sacral rib is greatly expanded laterally and in side-view is thickened anteriorly. The second rib, although smaller, is also expanded. In H.297 the first sacral vertebra and rib are missing, but the other two vertebrae and ribs are very similar to those of B.M.(N.H.) R.1480. In both specimens the caudal rib is expanded anteriorly and curved distally.

Two caudal vertebrae remain attached to the sacrum of H.297, but the only other articulated caudal vertebrae attributable to this species are three vertebrae of specimen I.R.S.N.B. R.14 (Pl. 1A), the centra of which are similar to those of the dorsal vertebrae; they are 22 mm, 16 mm and 13 mm long respectively.

Girdles and limbs

The girdle and limb material prepared from the immature specimen B.M.(N.H.) 28853 (Pl. 5) shows clearly the peculiar mixture of cheloniid and toxochelyid characters noted for the Eochelyinae by Moody (1968). This is shown even better by disarticulated elements referred to mature specimens of the same species.

The pectoral girdle and fore limb definitely tend towards the cheloniid condition. The scapula (Pl. 5C) has a pronounced 'neck region' between the glenoidal and coracoidal facets and the base of the bifurcation, while the coracoid (Pl. 5E) is much longer than the dorsal process of the scapula. A table (Table 6) of the measurements and indices of the shoulder girdle in the Toxochelyidae, Eochelyinae and Recent Cheloniidae shows clearly the direct affinities between the latter two groups.

TABLE 6

Shoulder girdle measurement and indices of the Toxochelyidae, Eochelyinae and Recent Cheloniidae

specimen	Va	Vb	$\frac{Vb}{Va}$ (as %)	Vc	$\frac{Vc}{Va}$ (as %)	Vd	$\frac{Vd}{Va}$ (as %)
**Toxochelys latimeris*							
Y.P.M. 3602	26	13·5	51·9	34·5	132·7	–	–
C.N.H.M. PR.123	940	48·0	51·0	122·0	129·7	137	145·7
Puppigerus camperi							
B.M.(N.H.) 28853	26	15	57·7	29	111·5	41	157·7
**Lepidochelys kempi*							
C.N.H.M. 31334	76	25·5	46·7	90	118·4	118	142·5
B.M.(N.H.) 1940.3.13.1	40	18·5	46·2	47	117·5	57	162·5
**Chelonia mydas*							
C.N.H.M. 22066	153	89	58·1	183	119·6	304	198·7

Va = length of ventral prong of scapular fork from tip of process to edge across neck of scapula.
Vb = length of scapular neck from base of fork to ridge dividing glenoidal facet from carocoid suture face.
Vc = length of dorsal prong of scapular fork from tip of process to edge across neck of scapula.
Vd = maximum length of coracoid.

*After Zangerl (1953, tab. 5).

The humerus of *P. camperi* (Pl. 5D) has a straighter shaft than that of the toxochelyids and a more pronounced radial process, which latter is also situated further down the shaft. The humerus is similar to that of *Eochelone brabantica* and other cheloniids such as '*Chelone*' *vanbenedeni* Smets 1886, *Corsochelys haliniches* Zangerl 1960 and *Desmatochelys lowi* (Zangerl & Sloane 1960).

The radius and ulna are known only from a few specimens and are usually unassociated. The two bones lie close to each other in I.R.S.N.B. R.15 (Pl. 1B), and measure 41 mm and 32 mm respectively.

A comparison with the fore limb bones of the Recent Cheloniidae and the Toxochelyidae (Table 7) brings out two interesting points. First, as in the Recent cheloniids, the radius of *Puppigerus* is much larger than the ulna ; secondly, those two bones are proportionally shorter in relation to the humerus than those of either the Recent Cheloniidae or the Toxochelyidae.

TABLE 7

Measurements (in mm) and indices of the fore limb bones of the Eochelyinae, Recent Cheloniidae and Toxochelyidae

	length of humerus h	length of radius r	$\frac{r}{h}$ (as %)	length of ulna u	$\frac{u}{h}$ (as %)
EOCHELYINAE					
Puppigerus camperi					
I.R.S.N.B. R.15	74	41	55·4	32	43·2
RECENT CHELONIIDAE					
**Eretmochelys imbricata*					
C.N.H.M. 31009 (sub adult)	79	48	60·7	42	53·1
**Chelonia mydas*					
C.N.H.M. 22066 (adult)	213	140	65·7	110	51·6
TOXOCHELYIDAE					
**Toxochelys latimeris*					
Y.P.M. 3602	37	–	–	–	–
C.N.H.M. PR.123	130	–	–	65	50·0
**Toxochelys moorevillensis*					
C.N.H.M. PR.136	± 120	–	–	60	50·0

* After Zangerl (1953, tab. 8, p. 177).

Bones of the pelvic girdle and hind limb are much more commonly preserved than those of the pectoral girdle and fore limb. The bones prepared from B.M.(N.H.) 28853 (Pl. 5) allow a direct statistical comparison to be made with other turtles, and the index of 23·2 recorded for the area of the eochelyine ischium against the area of the pubis falls between the 14·9 and 46·3 recorded for *Eretmochelys* and *Toxochelys* respectively (Table 8). The development of a pronounced posterior spur on the ischium (Pl. 1A ; Fig. 12) distinguishes the girdle of this species from those of the Recent Cheloniidae. The general morphology of the pelvic girdle of *P. camperi* is, as in other eochelyines, intermediate between the toxochelyid and cheloniid conditions.

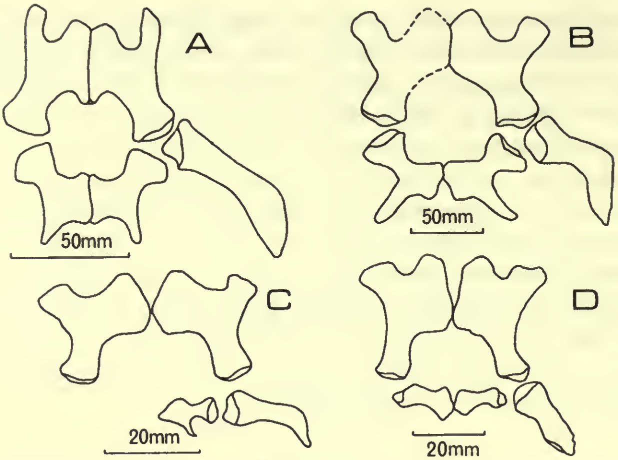

FIG. 12. Chelonian pelvic girdles. A. *Chelydra*. B. *Toxochelys*. C. *Puppigerus*. D. *Eretmochelys*. A, B and D from Zangerl, 1953, p. 163.

TABLE 8

Measurements (in mm²) and indices of surface areas of ischium and pubis in *Eretmochelys*, *Puppigerus* and *Toxochelys*

	area of pubis p	area of ischium i	$\frac{i}{p}$ (as %)
**Eretmochelys imbricata* C.N.H.M. 22352	2217	331	14·9
Puppigerus camperi B.M.(N.H.) 28853	2442	566	23·2
**Toxochelys moorevillensis* C.N.H.M. P.27391	2308	1069	46·3

* After Zangerl (1953, tab. 6, p. 164).

Several bones of the pelvic girdle and hind limb are present in the specimen I.R.S.N.B. R.15 (Pl. 1B), in which the femur and tibia may be measured and compared with the humerus, radius and ulna (Table 7). The femur is approximately 50 mm in length and, although morphologically identical to that of the Toxochelyidae, is shorter in relation to the humerus than that of even the Recent Cheloniidae. The index femur/humerus is 67·5, as against 70·9 for *Eretmochelys* and 75·1 for *Chelonia* (see Zangerl 1953, p. 177, tab. 8). The index tibia/humerus is 66·3 and is similar to those recorded for both Cheloniidae and Toxochelyidae. Partial pelves and hind limbs from other specimens (I.R.S.N.B. R.14 (Pl. 1A), IG.8632, B.M.(N.H.) 25608 and 38950) show the same characteristics as those described above. The femur/humerus ratio of I.R.S.N.B. IG.8632 is 65·6, as against the 67·5 recorded for the adult specimen I.R.S.N.B. R.15.

R.15 also includes two distal tarsals and all five metatarsals. The bones are very little disturbed and are of similar proportions to the same elements in the hind limb of modern sea-turtles. Distal tarsal III is rounded and similar to that of the species *Glarichelys knorri* Zangerl (1958). The lengths of metatarsals II–V are 19 mm, 20 mm, 20·5 mm and 15 mm respectively.

Carapace and plastron (Reconstruction Fig. 13)

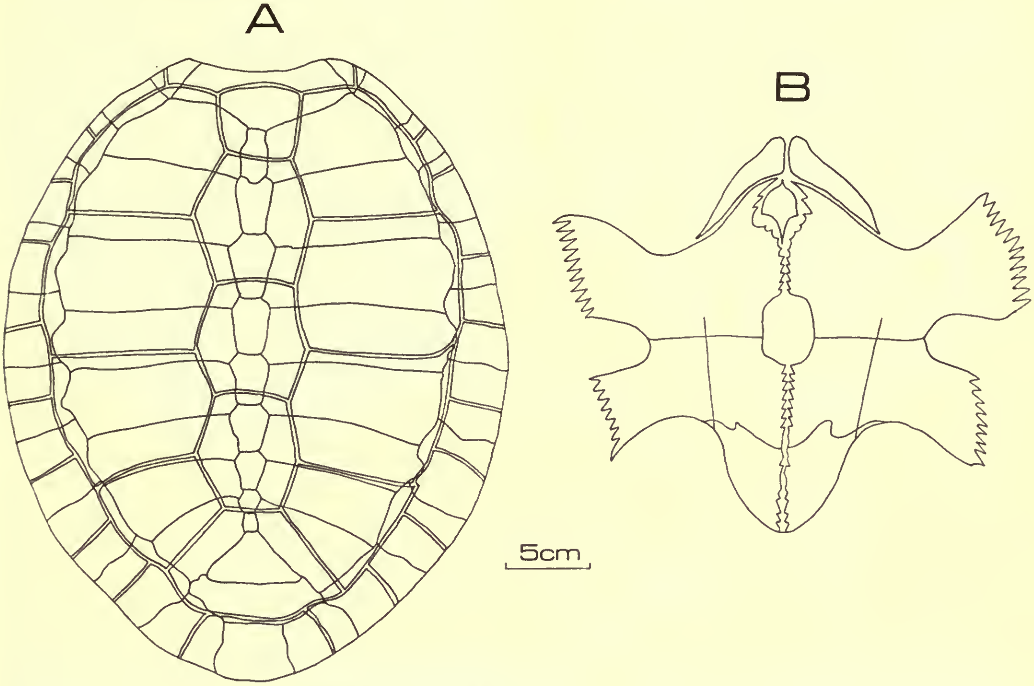

FIG. 13. *Puppigerus camperi* (Gray). Reconstructions of shell. A. Carapace. B. Plastron.

Several excellent shells of *P. camperi* are housed in the Brussels Institute; they are numbers I.R.S.N.B. R.13, R.14, R.15, IG.8402, IG. 8632, IG.9544, 1666 and the lectotype 1687/R.4. Most of them include remains of both carapace and plastron, so that the task of description is much simpler than it would be if one had to rely solely on British material. Comparative measurements of specimens from both countries are listed in Table 2 to support the subjective synonymy of the species *P. camperi* and *P. longiceps*. Variation in the neural and pygal plates of the several carapaces is only very slight and the pattern of the central dermal plates is characteristically constant; this contrasts with the condition in *Argillochelys antiqua*, where the relationship between the first and second neurals is inconstant and the sizes of the last three extremely variable. In *P. camperi* the first neural is usually biconvex and the last three neurals always become progressively shorter. A comparison with other eochelyines emphasizes the invariability of the central dermal plate pattern.

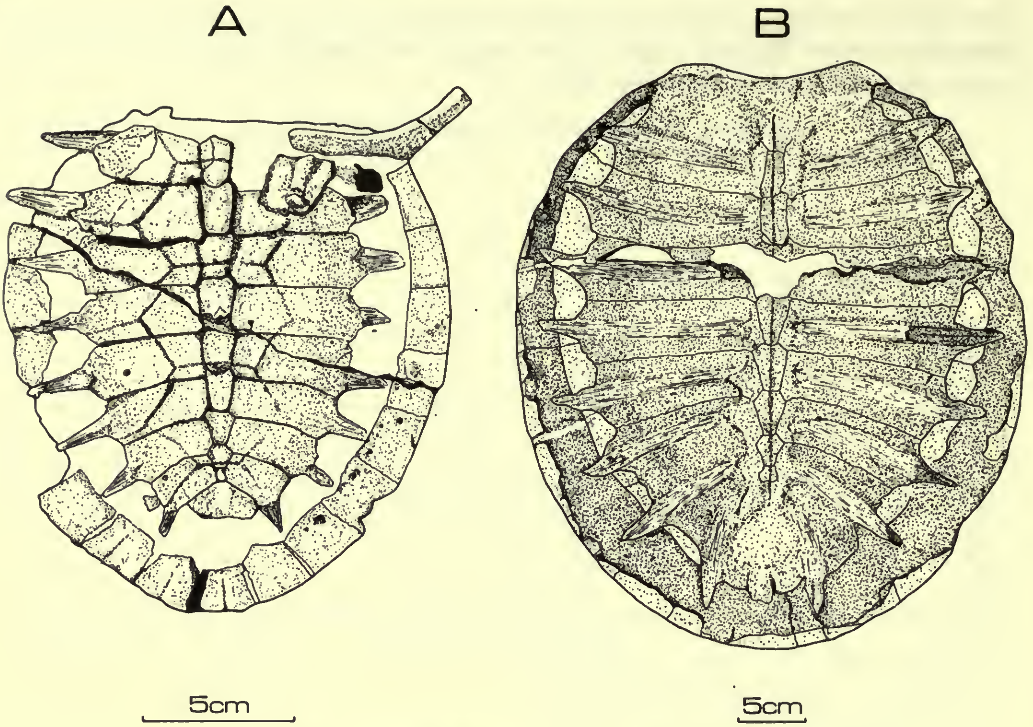

Fig. 14. *Puppigerus camperi* (Gray). Carapaces from above.
A. I.R.S.N.B. IG.8632. B. I.R.S.N.B. IG.1663.

In the juvenile specimens I.R.S.N.B. IG.8632 and G.S.M. 57266 the carapace is not completely ossified and large costo-peripheral fontanelles are present along its margin, from the nuchal to the pygal plates. In IG.8632 (Fig. 14A) the second suprapygal is missing, perhaps because of imperfect preservation. As the animal grows the costal and peripheral plates gradually occlude the lateral fontanelles (Fig. 15); the carapace of the adult is completely ossified, e.g. in I.R.S.N.B. IG.9544 (Pl. 7B). This closure of the lateral fontanelles occurs only in *Puppigerus* and, in consequence, the peripheral plates of that genus are larger than those of related forms. Another change in the development of the carapace is seen in the lengthening and rounding of the epidermal scutes in the adults, for those of the juveniles are relatively broader and much more angular (Fig. 15). In specimen IG.9554 the outlines of the vertebral scutes are double and indicate successive growth stages (Pl. 7B). The ontogenetic changes described above for the Belgian specimens are also visible in certain British carapaces, which range from the very well-preserved juvenile G.M. 57266 to the large adult B.M.(N.H.) 38951.

All the British specimens are incomplete; the main casualties are the peripheral plates, which are known from very few specimens indeed. But, in spite of these preservational defects, the carapaces of *P. camperi* can be easily recognized through the description given above and by the constancy of the plate pattern.

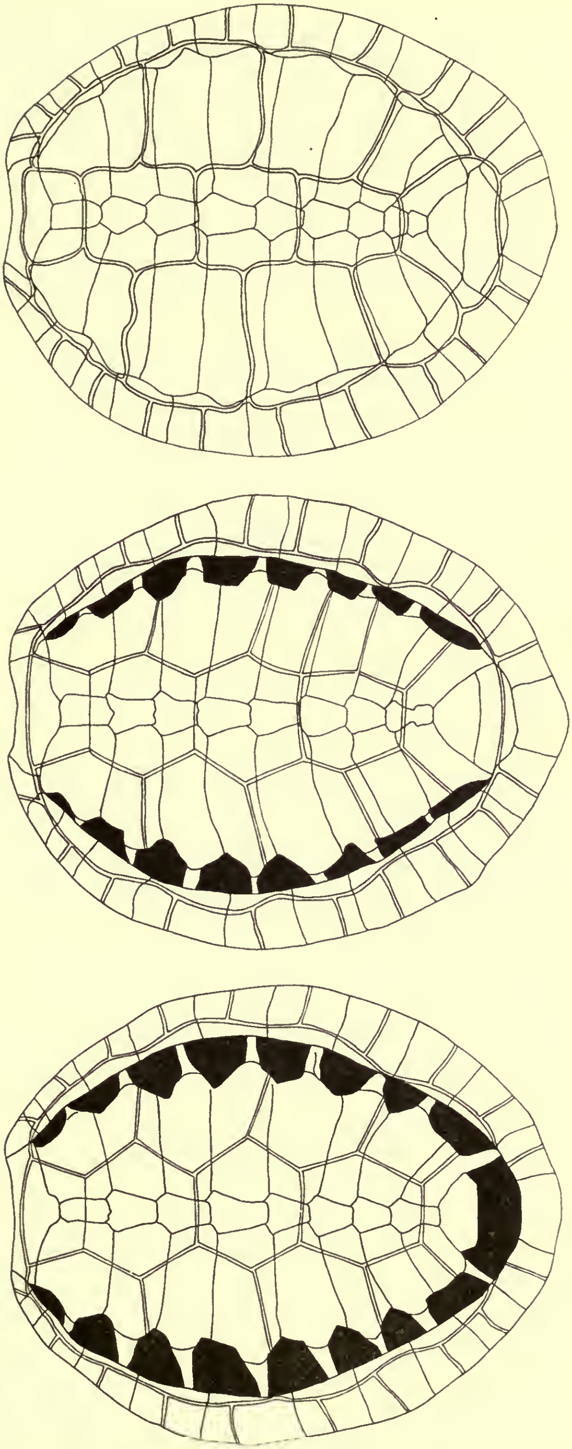

Fig. 15. *Puppigerus camperi* (Gray).
Growth series of carapaces (not to scale) to show increased ossification during ontogeny.

The plastra of the two Belgian specimens I.R.S.N.B. R.14 and R.15 (Pl. 1) are, without doubt, the best examples of the ventral shell of *P. camperi*. Both have all their plates and in R.15 each plate is in its correct position. The epiplastra are shown beautifully in the latter specimen and are typically wedge-shaped, like those of the genus *Catapleura* (Schmidt 1944). The xiphiplastra are shorter and broader than those of *Argillochelys*, sutural contact existing along their whole length, and their notched contact with the hypoplastra is less acute. The difference between the notched contacts of *P. camperi* and those of *Eochelone brabantica* is even more pronounced. The specimens I.R.S.N.B. IG.8632 (Pl. 8A), IG.8402 (individual plates), and B.M.(N.H.) 25608, 28853, 38950 and 38951 (Pl. 8B) also illustrate the form of the plastron in *P. camperi*.

The central fontanelle, which Cuvier (1824) used as one of the characters justifying his association of this form with the 'émydes', is a consistent feature throughout the ontogeny of *P. camperi* (Pl. 8). In forms such as *Lepidochelys olivacea olivacea*, however (see Zangerl 1958, Abb. 27), this fontanelle varies greatly in size.

The plastral indices recorded for *P. camperi* show a high intraspecific variability, with a range of 70–90 for plastral index A and of 65–75 for plastral index B (Table 2). It is therefore recommended that isolated plastral material should be identified not only on these indices but also on other proportional differences, including the slight variation in xiphiplastral lengths of the three genera *Argillochelys*, *Eochelone* and *Puppigerus*.

The terminology of the various shell elements is explained by Zangerl (1969).

SUMMARY AND CONCLUSIONS

The account given represents a taxonomic and morphological study of all available material hitherto referred to the species *Lytoloma camperi*, *L. longiceps* and *L. trigoniceps* of Belgium and England. All this material is recognized as conspecific, the rules of priority requiring that the species be called *Puppigerus camperi*.

The morphology of this species is mainly cheloniid but the pelvic girdle and hind limb retain several primitive characters. The functional purpose of a combination of cheloniid fore limb and toxochelyid hind limb was probably to enable alternate slow cruising and rapid paddling (Zangerl 1953). Although this type of movement is postulated for this species and many others of similar morphology, no light is thrown on to the habitat or feeding habits of the animal. The jaws of *P. camperi* are characteristic elements but they too give little information as to the likely feeding habits. Dollo (1909) stated that *Lytoloma bruxelliensis* fed on oysters but, although the feeding habits of turtles are in some species restricted to particular diets, they generally vary according to the availability of food.

In *Chelydra serpentina*, the Recent snapping turtle, the form of the jaw suggests a diet consisting exclusively of fish or other animals ; this, however, is not so, for the turtle is known to consume large quantities of vegetable material (Lagler 1943). Nor is a secondary palate an invariable indicator of a durophagous diet, for it occurs in plant-eaters such as *Chelonia mydas*.

The sediments in which *P. camperi* is found contain great quantities of vertebrate and invertebrate material and, in the case of the London Clay, an abundance of plant material too. The size of the secondary palate varies considerably in the Eochelyinae and this suggests a variation in diets, but as yet no one knows what *P. camperi* fed on.

The limb pattern and the suggested type of locomotion would tend to indicate a wider variety of ecological niches in the Eochelyinae than is found in freshwater forms. It is probable that the eochelyines dwelt mainly on the coast and in coastal inlets but could also travel into the open sea.

As in the toxochelyid turtles described by Zangerl (1953), parasitic lesions are very common. Some of the specimens are badly affected, with infestations occurring mainly on the shell plates but also on the skulls. The skull infestations sometimes penetrate the bone and may have been the cause of death. Thicker bone often surrounds the cavities caused by the parasites.

Most of the London Clay and Bartonian specimens are disarticulated and incomplete, but some specimens do retain attached skulls or limb fragments, indicating that scavenging and current action were not severe.

Specimens are more frequently damaged (crushed and distorted) by post-depositional compaction and are often destroyed by pyritization. The Belgian material occurs in a sandstone and is often complete in its preservation ; this suggests very peaceful burial conditions.

ACKNOWLEDGMENTS

I should like to thank Drs E. Casier, A. J. Charig and R. Zangerl for their valuable help and encouragement and Drs Charig and Zangerl for their reading of the manuscript. Thanks are also due to Messrs C. A. Walker and P. J. Whybrow of the British Museum (Natural History) for their assistance in the preparation of material. I acknowledge the kind help and attention of Dr G. E. Quinet and the staff at the Institut Royal des Sciences Naturelles, Brussels ; Miss J. Dobson of the Hunterian Museum, Royal College of Surgeons, London ; Dr D. Russell of Paris ; Mr R. V. Melville, Dr R. Casey, Mr E. P. Smith and Mr C. J. Wood of the Institute of Geological Sciences, London ; and Dr C. L. Forbes of the Sedgwick Museum, Cambridge. The photographs were taken by Dr E. Casier, Mr T. W. Parmenter, Dr R. Zangerl and myself, and the figures organized with the help of Mr R. Andrews of Kingston.

This programme of research has been made possible by grants from the Natural Environment Research Council and the Central Research Fund of London University.

ABBREVIATIONS

The names of Museum and other collections have been abbreviated as follows :

B.M.(N.H.)	British Museum (Natural History), London
C.N.H.M.	Field Museum of Natural History, Chicago
G.M.	Geological Museum, Institute of Geological Sciences, London
H.M.	Hunterian Museum, Royal College of Surgeons, London
I.R.S.N.B.	Institut Royal des Sciences Naturelles de Belgique, Brussels
M.M.	Maidstone Museum
R.Z.	Rainer Zangerl's private collection
S.M.C.	Sedgwick Museum, Cambridge
Y.P.M.	Peabody Museum of Natural History, Yale University, New Haven

Other abbreviations

a	os angulare
art	os articulare
boc	os basioccipitale
bsph	os basisphenoideum
cb	condylus basioccipitalis
cex	condylus exoccipitalis
ch	internal narial opening
cor	os coronoidum
d	os dentale
exo	os exoccipitale
fac	foramen arteriae cerebralis
fh	fossa hypophyeos
fja	foramen jugulare
fn	foramen nasale internum
fr	os frontale
fs	foramen nervi trigemini
i	ilium
is	ischium
jug	os jugale
mx	os maxillare
opot	os opisthoticum
orb	orbit
p	pubis
pa	os praearticulare
pal	os palatinum
par	os parietale
pbf	first principal brain flexure
pfr	os prefrontale
pmx	os preamaxillare
po	os postorbitale
ptg	os pterygoideum
qj	os quadrato-jugale
qu	os quadratum
sa	os surangulare
sq	squamosal
soc	os supraoccipitale
v	vomer
vest	vestibule

Cranial nerves

V	trigeminal
VII	facial
VIII	acoustic
IX	glossopharyngeal
X XI	vagus and accessory
XII	hypoglossal

REFERENCES

Bergounioux, F. M. 1933. Sur l'*Emys camperi* du Musée de Bruxelles. *Bull. Mus. r. Hist. nat. Belg.*, Brussels, **9**, 5 : 1–13, 4 figs.

Buc'hoz, P. J. 1778–1791. *Centuries de planches enluminées et non enluminées, représentant au naturel ce qui se trouve de plus intéressant de plus curieux parmi les animaux, les végétaux et les minéraux, pour servir d'intelligence à l'historie générale des trois règnes de la nature.* **2**, dec. 6, pl. I – X [+ 1p]. Amsterdam.

Burtin, F. X. 1784. *Oryctographie de Bruxelles, ou description des fossiles, tant naturels qu'accidentels, découverts jusqu'à ce jour dans les environs de cette ville.* 152 pp. 32 pls. Brussels.

Cope, E. D. 1870. Synopsis of the extinct Batrachia, Reptilia and Aves of North America. *Trans. Am. phil. Soc.*, Philadelphia, **14** : iv + 252 pp., 54 figs., 14 pls.

Curry, D. 1966. Problems of correlation in the Anglo–Paris–Belgium Basin. *Proc. Geol. Ass.*, London, **77** : 437–468, 5 figs.

Cuvier, G. 1812. *Recherches sur les ossemens fossiles.* 1st ed. **4** : 5 + 447, 38 pls. Paris.

—— 1824. *Recherches sur les ossemens fossiles.* 2nd ed. **5**, 2 : 1–547, 38 pls. Paris.

Dollo, M. L. 1886. Les chéloniens Landéniens (Éocène inférieur) de la Belgique. *Bull. Mus. r. Hist. nat. Belg.*, Brussels, **4**, 3 : 129–142, 4 figs.

—— 1887. On some Belgian fossil reptiles. *Geol. Mag.*, London, **3**, 4 : 392–396.

—— 1888. Sur le genre *Euclastes*. *Annls Soc. géol. N.*, Lille, **15** : 114–122. [Also in *Geol. Mag.* **3** : 519.]

—— 1909. The fossil vertebrates of Belgium. *Ann. N.Y. Acad. Sci.*, New York, **19**, 4 (1) : 99–119, pls. 4–10.

—— 1923. L'*Emys camperi* est une tortue marine. *Bull. Acad. r. Belg. Cl. Sci.*, Brussels, **9**, 10–11 : 416–427.

EDINGER, T. 1933. Die Foramina parietalia der Säugetiere. *A. ges. Anat. Entw. Gesch.*, Berlin, **102** : 266–289, 28 figs.

FAUJAS, B. ST FOND. 1799. *Histoire naturelle de la Montagne de Saint Pierre de Maestricht.* 2 vols. : 263 pp., 53 pls. Paris.

GAFFNEY, E. & ZANGERL, R. 1968. A revision of the chelonian genus *Bothremys* (Pleurodira: Pelomedusidae). *Fieldiana, Geol. Mem.*, Chicago, **16**, 7 : 193–239, 22 figs.

GALEOTTI, H. 1837. Mémoire sur la constitution géonostique de la province de Brabant. *Mém. cour. Acad. r. Sci. Belg.*, Brussels, **12** : 1–192, 2 maps, 4 pls.

GOODRICH, E. S. 1930. *Studies on the structure and development of vertebrates.* xxx + 837 pp., 754 figs. London.

GRAY, J. E. 1831. *Synopsis Reptilium ; or short descriptions of the species of reptiles.* Part 1 : Cataphracta. Tortoises, Crocodiles and Enaliosaurians. viii + 85 pp., 11 pls. London.

HOFFSTETTER, R. & GASC, J. 1969. Vertebrae and ribs of modern reptiles. *In* Gans, C. (Ed.) *Biology of the Reptilia.* xv + 373 pp. Ch. 5 : 201–310, 82 figs. London.

LAGLER, K. F. 1943. Food habits and economic relations of the turtles of Michigan. *Am. Midl. Nat.*, Notre Dame, **29** : 257–312, 9 figs.

LYDEKKER, R. 1889*a*. On the remains of Eocene and Mesozoic chelonia and a tooth of (?) *Ornithopsis. Q. Jl geol. Soc. Lond.* **45** : 227–246, 7 figs., pl. 8.

—— 1889*b*. *Catalogue of fossil Reptilia and Amphibia in the British Museum* (*Natural History*). **3** (Chelonia) : xviii + 239 pp., 53 figs. London.

MOODY, R. T. J. 1968. A turtle, *Eochelys crassicostata* (Owen), from the London Clay of the Isle of Sheppey. *Proc. Geol. Ass.*, London, **79**, 2 : 129–140, 4 figs., 2 pls.

—— 1970. A revision of the taxonomy and morphology of certain Eocene Cheloniidae. Thesis (unpublished), University of London.

OWEN, R. 1841. Description of the remains of six species of marine turtles (Chelones) from the London Clay of Sheppey and Harwich. *Proc. geol. Soc. Lond.*, **3**, 2, 83 : 565–578

—— 1842. Report on British fossil reptiles. *Rep. Br. Ass. Advmt Sci.*, London, **11**, 2 : 60–204.

—— 1849. *A history of British fossil reptiles.* Part 1 : Chelonia. 79 pp., 43 pls., 6 figs.

—— 1850. Description of the remains of the fossil reptiles from the Tertiary deposits of Bracklesham and Bognor, in the Museum of Frederick Dixon, Esq., or figured in the present work. *In* Dixon, F., *Geology of Sussex.* 1st ed. xvi + 408 pp., 40 pls. London.

—— & BELL, T. 1849. The fossil Reptilia of the London Clay, and of the Bracklesham and other Tertiary beds. *Palaeontogr. Soc.* (*Monogr.*), London, **1** : 1–79, 6 figs., pls. 1–28.

PARKINSON, J. 1811. *Organic remains of a former world.* **3** : xv + 479 pp., 22 pls. London.

PARSONS, T. S. & WILLIAMS, E. E. 1961. Two Jurassic turtle skulls : A morphological study. *Bull. Mus. comp. Zool. Harv.*, Cambridge, Mass., **125**, 3 : 40–107, 6 pls., 11 figs.

POELMAN, C. 1868. *Catalogue des collections d'anatomie comparée, y compris les ossements fossiles, de l'Université de Gand.* 120 pp., 4 pls. Ghent.

SCHMIDT, K. P. 1944. Two new thalassemyd turtles from the Cretaceous of Arkansas. *Fieldiana, Geol. Mem.*, Chicago, **8**, 11 : 63–74, figs. 21–24.

SMETS, G. 1886. *Chelone vanbenedenii. Annls Soc. scient. Brussels,* **10** : 109–128, 2 figs.

VALLOIS, H. V. 1922. Les transformations de la musculature de l'épisome chez les vertébrés. *Arch. Morph. gén. exp.*, Paris, **13** : 1–538, figs.

VÖLKER, H. 1913. Über das Stamm-, Gliedmassen- und Hautskelett von *Dermochelys coriacea* L. *Zool. Jb.*, Jena, **33** : 431–552, 3 figs., pls. 30–33.

WILLIAMS, E. E. 1950. Variation and selection in the cervical central articulations of living turtles. *Bull. Am. Mus. nat. Hist.*, New York, **74**, 9 : 505–562, 20 figs., 10 tabs.

WINKLER, T. C. 1869. *Des tortues fossiles conservées dans le Musée Teyler et dans quelques autres musées.* 146 pp., 33 pls. Haarlem.

ZANGERL, R. 1953. The vertebrate fauna of the Selma Formation of Alabama. Part 4 : The turtles of the family Toxochelyidae. *Fieldiana, Geol. Mem.*, Chicago, **3**, 4 : 136–288, pls. 9–29, figs. 60–124.

Zangerl, R. 1957. A parietal foramen in the skull of a Recent turtle. *Proc. zool. Soc. Calcutta* Mookerjee Memorial vol. : 269–273, pl. 12.

—— 1958. Die oligozänen Meerschildkröten von Glarus. *Schweiz. palaeont. Abh.*, Basel, **73** : 1–56, 31 figs., 15 pls.

—— 1960. The vertebrate fauna of the Selma Formation of Alabama. Part 5 : An advanced cheloniid sea turtle. *Fieldiana, Geol. Mem.*, Chicago, **3**, 5 : 283–312, figs. 125–145, pls. 30–33.

—— 1969. The turtle shell. *In* Gans, C. (Ed.), *Biology of the Reptilia.* xv + 373 pp. Ch. 6 : 311–340, 15 figs. London.

—— & Sloan, R. E. 1960. A new specimen of *Desmatochelys lowi* Williston. (A primitive cheloniid sea turtle from the Cretaceous of South Dakota.) *Fieldiana, Geol. Mem.*, Chicago, **14**, 2 : 7–40, figs. 2–23, 2 pls.

INDEX

The page numbers of the principal references are printed in **bold** type ; an asterisk (*) denotes a figure.

All anatomical terms refer to the species *Puppigerus camperi* (Gray).

Argillochelys, 161–3, 168, 170, 174, 182
  antiqua, 179
  cuneiceps, 168, 174 ; plate 6
atlas, elements of, pl. 5, fig. A
axillo-inguinal width, 159–60

Barton Beds, 158
basioccipital depression, 161, 165
Bracklesham Beds, 158, 165
braincase, 165, **170–2** ; see also under the separate bones
Bruxelles, Sables de, 158, 165

carapace, 161–2, 165, **179–80**, 179*, 180*, 181* ; pl. 5, fig. B ; plate 7
Caretta, 174
Carettinae, 161
Catapleura, 163, 165, 182
caudal vertebrae, **175–6**
ceratobranchial arch, first, 173*
cervical vertebrae, 161, **174** ; plate 4
  of *Argillochelys cuneiceps*, plate. 6
  joints between, 162
Chelone anticeps, 163
  crassicostata, 165, 168
  longiceps, 155–6, **157**, 160, 163, 165
  trigoniceps, 155, **157–8**, 163
  'vanbenedeni', 177
Chelonia, 162, 171, 178
  mydas, 156, 163, 170–1, 176–7, 182
Cheloniidae, **161**, 175–7
Cheloniinae, 161
Chelydra, 178*
  serpentina, 182
choanae, 168
comparative table of turtle genera, 162
copula, 173* ; pl. 2, fig. B
coracoid, 176 ; pl. 5, fig. E
Corsochelys, 174
  haliniches, 172, 174, 177

dermal elements, 161
Dermochelys, 174
Desmatochelys lowi, 177
diagnosis, emended, of *Puppigerus camperi*, 165
dorsal vertebrae, **174–5** ; pl. 5, fig. B

ectopterygoid processes, 161, 165
Émydes de Bruxelles, de Sheppey, 163
Emys camperi, 155, **156**, 157, 163, 165
  cuvieri, 163
  parkinsonii, 157, 163
endocranial cast, **172**, 172*
entoplastron, 165
Eochelone, 161, 182
  brabantica, 177, 182
Eochelyinae, **161**, 165, 176–7, 183
Eochelys, 156–7, 160–1
  longiceps, 155–7, 160, 163
epidermal elements, 161, 180
  mosaic, 161
  shields, 162
epiplastra, 161, 163, 165, 182
Eretmochelys, 163, 177, 178*, 178
  imbricata, 177–8
Erquelinnesia, 157
Euclastes, 157

femur, pl. 5, fig. H

foramen, midline, 169
fontanelles, 161
  central, 163, 165, 182
  costo-peripheral, 162, 165, 180

Glarichelys knorri, 179

humeral : femoral ratio, 161
humerus, 177 ; pl. 5, fig. D
hyo-hypoplastral suture, 160, 163
hyoid apparatus, 172–3, 173*
hypoplastron, 182

Idiochelys, 162
ilium, pl. 5, fig. G
interorbital bar, 159
ischium, 177–8 ; pl. 5, fig. G

jaw, lower, **172–4**, 173* ; see mandible
jugal, 165, 168

Lepidochelys, 156, 162
  kempi, 176
  olivacea^2, 182
limbs, 161–2, **176–9** ; see also under the separate bones
London Clay, 158, 165
Lytoloma, 155–8, 160, 162
  'bruxelliensis', 158, 164, 182
  camperi, 155, 158–60, 163, 182
  crassicostatum, 158, 163
  longiceps, 156–60, 163, 182
  trigoniceps, 155, 157–9, 163, 175*, 182
  'wemelliensis', 158, 164

mandible, 161, 173* ; pl. 2, fig. B ; see also jaw, lower
marginal shields, 162
maxilla, 165, 168
metatarsals, 178–9

nares, external, 161
  internal, 158, 161, 165
    variation in position with size, 168
neurals, 161, 165
neural plates, 159, 161–2
  shields, 159

occipital shield, 161
orbit, 159, 161

Pachyrhynchus, 157
  longiceps, 163
  trigoniceps, 163

palate, 158
  secondary, 161–2, 165
palatine, 161, 165
parasitic lesions, 183
parietal foramen, 169 ; pl. 3, fig. A
pectoral girdle, **176–9**
pelvic girdle, **176–9**, 178*
peripheral plates, 162
plastral indices, 159–60, 165, 182
plastron, 159–63, 165, 179, 179*, **182** ; plate 8
Plesiochelidae, 161
Plesiochelys, 162
pleural shields, 162
premaxilla, 161, 165, 168
Pseudemys ornata, 175
pterygoid, 161, 165
pubis, 178 ; pl. 5, figs. F, G
Puppigerus, 155–7, 160, **161**, 162, **163**
  camperi, 153–86 *passim*, **163–83** ; plates 1–5, 7, 8
    description, 165–82
    diagnosis, 165
    historical review, 156–61
    lectotype, 155, 164*
    measurements and indices, 158–60
    occurrence, 165
    referred specimens, 164
    type material, 155, 163
  crassicostatus, 168
  longiceps, 155, 161, 163, 179
  trigoniceps, 155
pygals, 165

quadrato-jugal, 165, 168

radius, 177

sacral vertebrae, **175–6**
sacrum, 175*
scapula, 176 ; pl. 5, figs. C
sea-turtle, Eocene, of N. Europe, 153–86
skeleton, 162, 165
skull, 165–75, 166*, 167*, 169*, 170* ; pl. 2, figs. A, C, D, E, F ; plate 3
  compared with *Testudo denticulata*, table 169
  measurements and indices, 168
snout, 158, 161, 165
Stegochelys, 171
suprapygal plates, 162

tarsals, 178–9
Testudo corticata, 156, 163

  denticulata, 169, 170*
Thalassemydidae, 161
Thalassemys, 162
'Tortue Franche', 163
Toxochelyidae, 161, 176–7
Toxochelys, 162, 171, 177, 178*
  latimeris, 176–7
  moorevillensis, 177–8
turtle, marine, Eocene, of N. Europe, 153–86

ulna, 177

vertebrae, cervical, 161, **174**; plate 4
    joints between, 162
  dorsal, **174–5**; pl. 5, fig. B
  sacral and caudal, **175–6**
vertebral column, 161
  scutes, 161–2
vomer, 161, 165

Wemmel, Sables de, 158, 165

xiphiplastral index, 160
  tip, 160
xiphiplastron, 160, 162–3, 165, 182

Richard Thomas Jones Moody, Ph.D.
Kingston Polytechnic
Penrhyn Road
Kingston-upon-Thames
Surrey
England

PLATE 1

Puppigerus camperi (Gray)

A. I.R.S.N.B. R.14. From below × ¼

B. I.R.S.N.B. R.15. From below × ¼

A

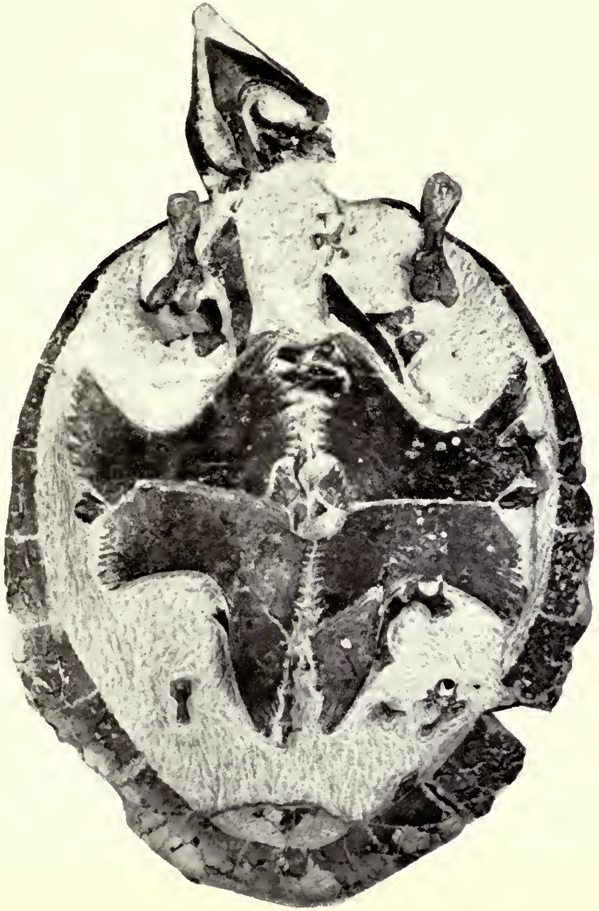

B

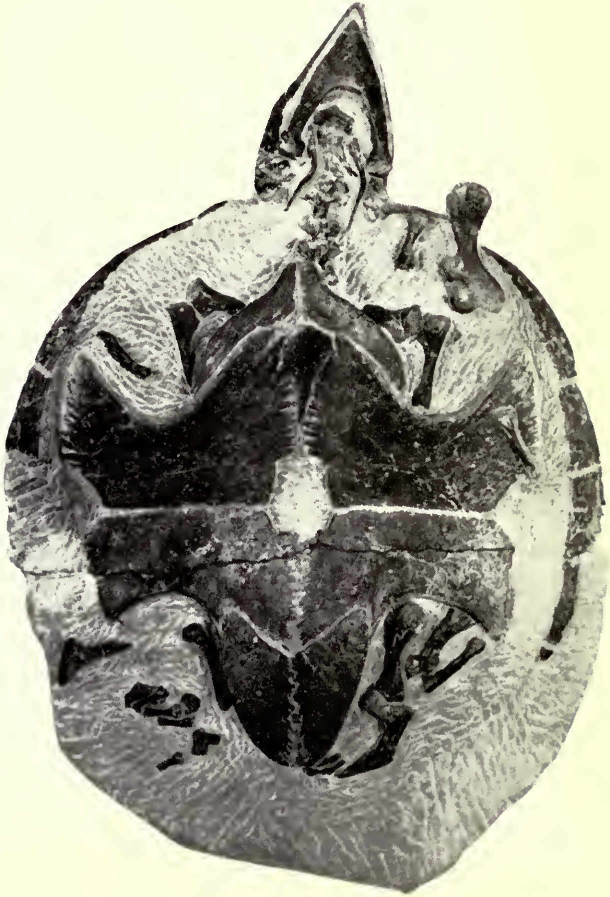

PLATE 2

Puppigerus camperi (Gray)

I.R.S.N.B. IG.8402

A.	Skull, from above × $\frac{2}{3}$
B.	Mandible and copula × $\frac{1}{2}$
C.	Skull from below × $\frac{2}{3}$
D.	Skull from left side × $\frac{2}{3}$
E, F.	Skull in section × $\frac{2}{3}$

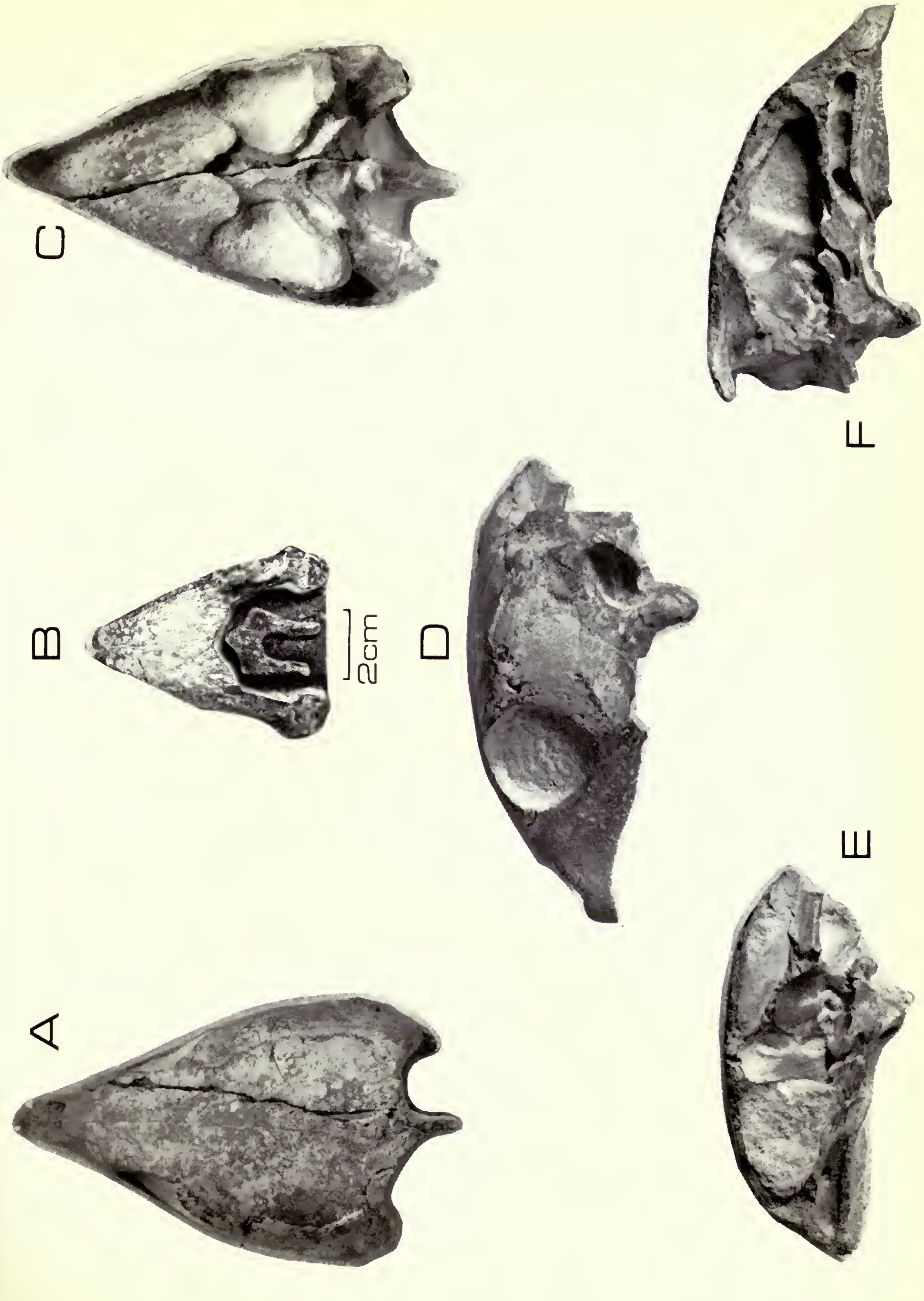
A
B
2cm
C
D
E
F

PLATE 3

Puppigerus camperi (Gray)

Skulls, from above

A. I.R.S.N.B. R.19 showing parietal foramen
B. I.R.S.N.B. R.18
C. I.R.S.N.B. R.16

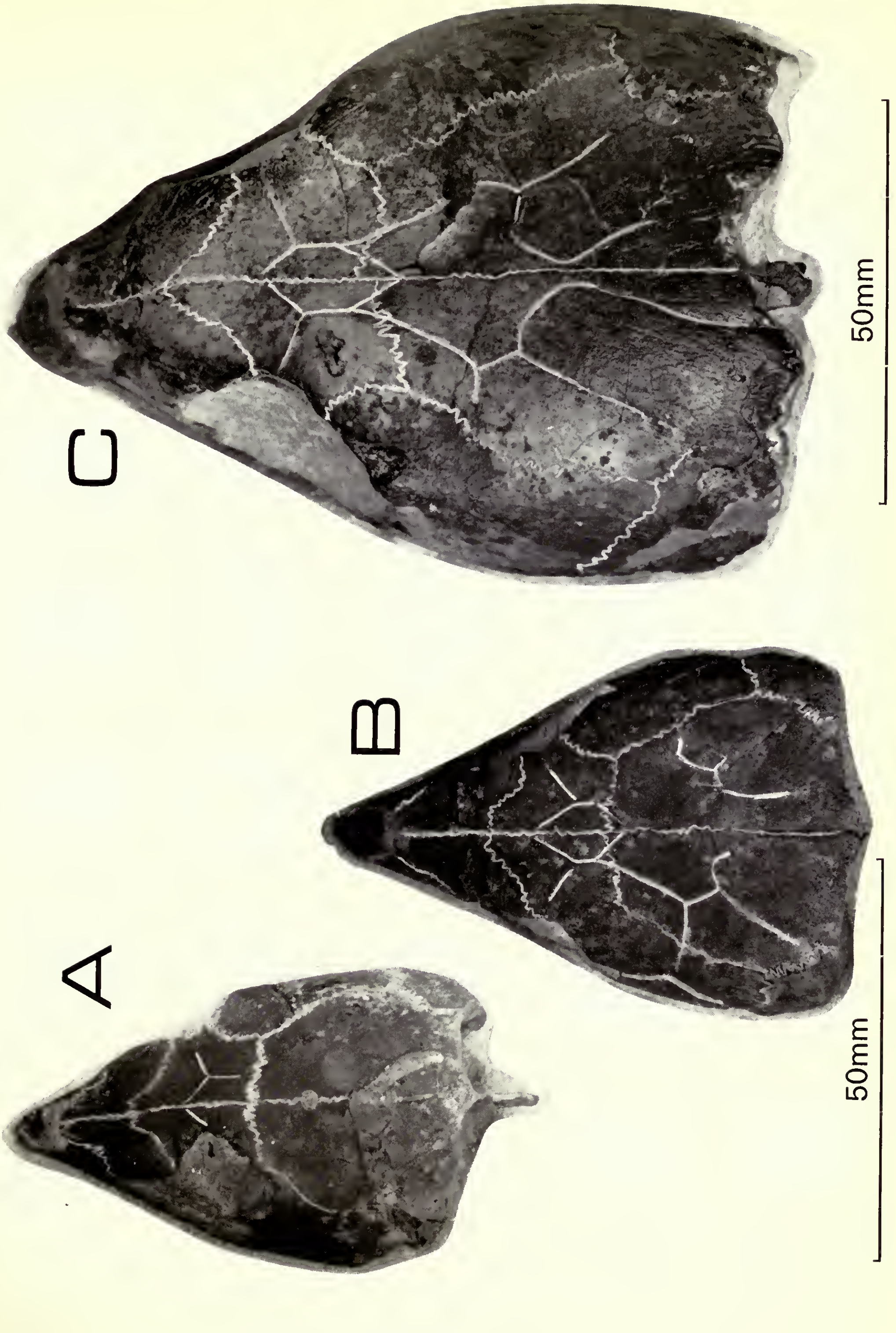
C
50mm
B
A
50mm

PLATE 4

Puppigerus camperi (Gray)

B.M.(N.H.) 28853
Cervical vertebrae 2–8
A. From right side
B. From in front
C. From behind
D. From above
E. From below

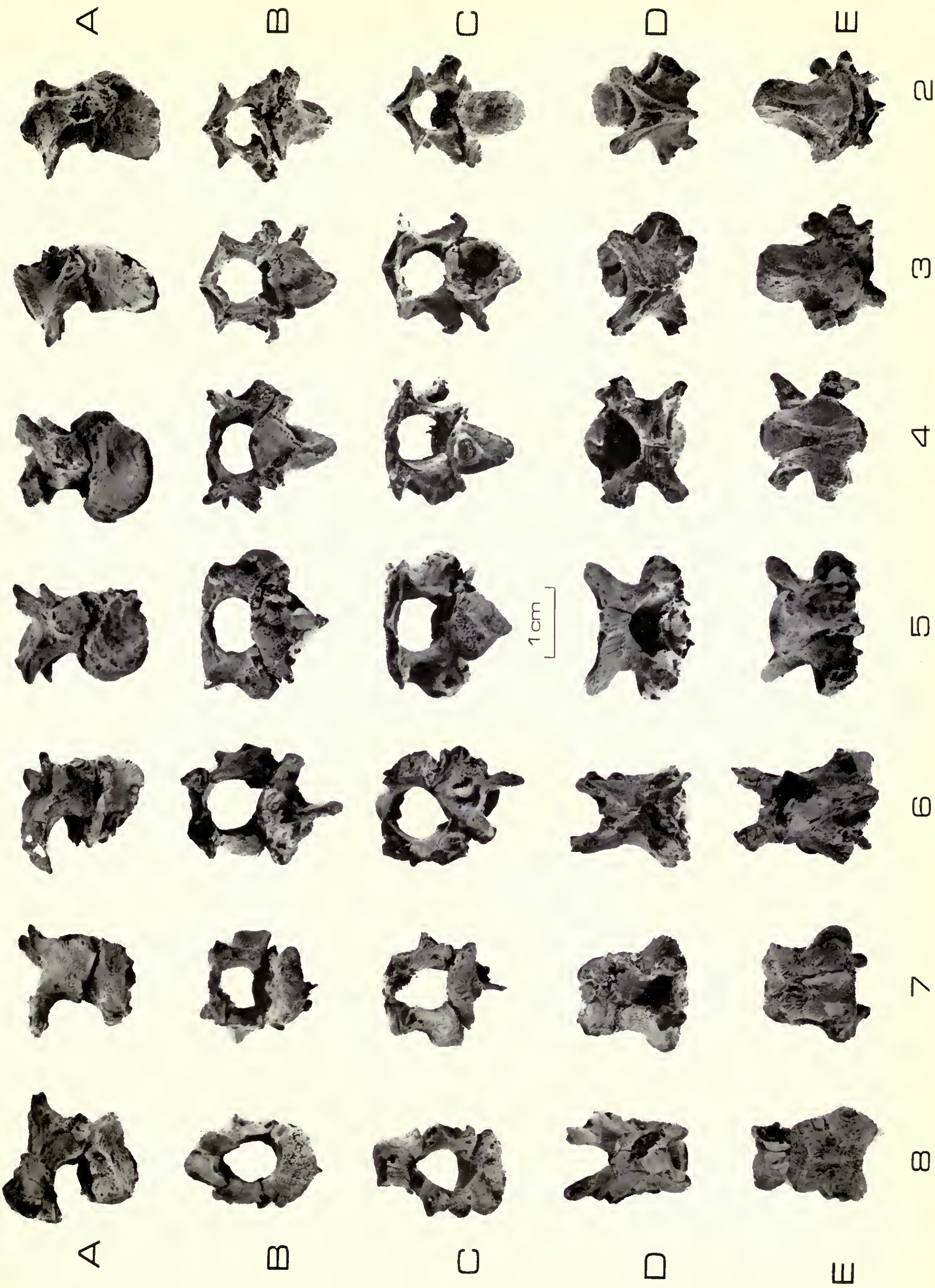
A
B
C
D
E
2
3
4
5
6
7
8
1 cm

PLATE 5

Puppigerus camperi (Gray)

B.M.(N.H.) 28853

A. Elements of atlas × 2
B. Carapace and dorsal vertebrae from below × 1
C. Scapulae
D. Right humerus
E. Right coracoid
F. Right pubis
G. Left pubis, ilium and ischium
H. Left femur
(C – H, × 1½)

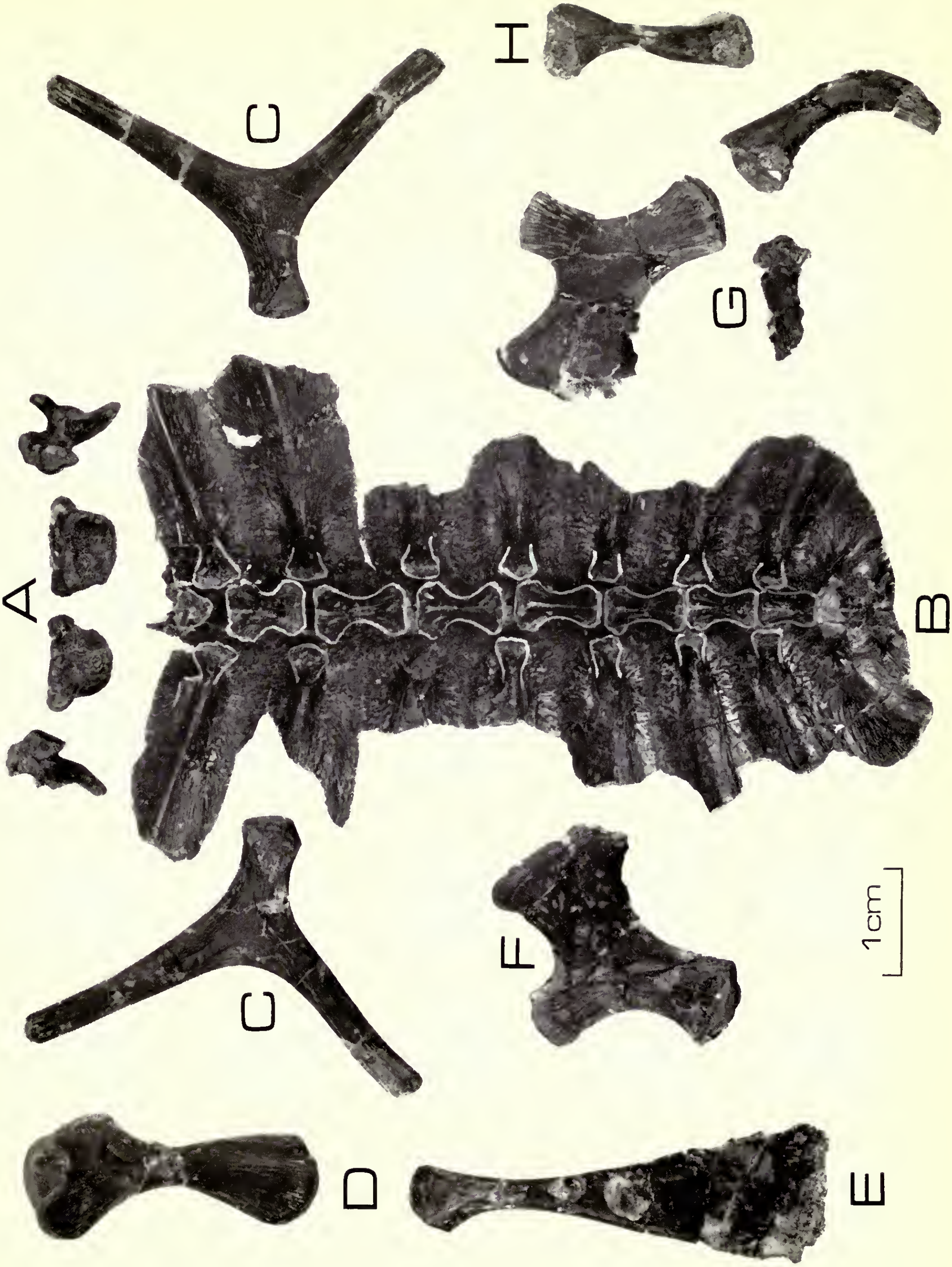
H
C
G
A
B
C
F
1cm
D
E

PLATE 6

Argillochelys cuneiceps (Owen)

S.M.C. 20937

Cervical vertebrae 1–8

A. From right side
B. From in front
C. From behind
D. From above
E. From below

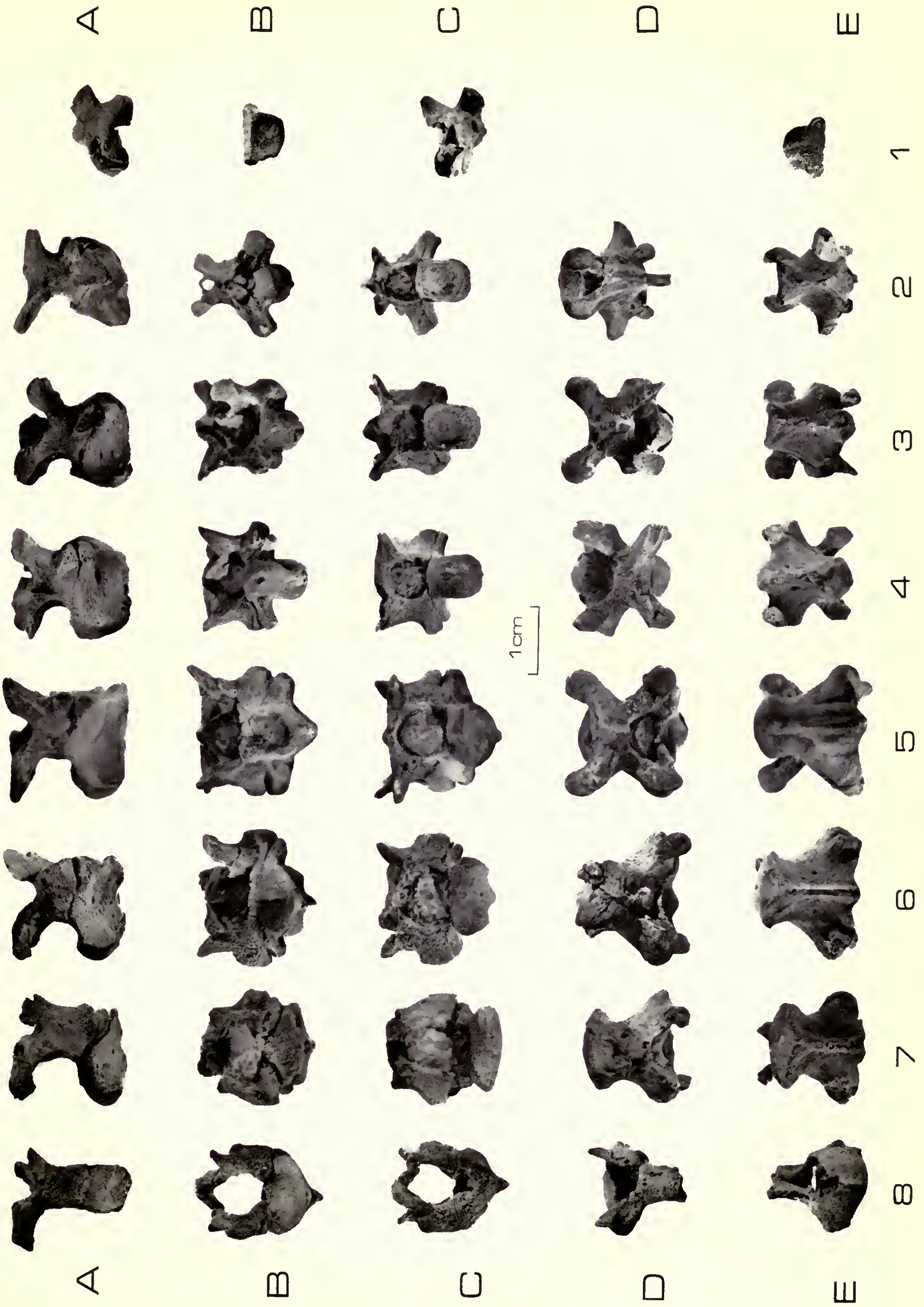
A
B
C
D
E
1
2
3
4
5
6
7
8
1cm

PLATE 7

Puppigerus camperi (Gray)

Carapaces from above

A. I.R.S.N.B. R.13

B. I.R.S.N.B. IG.9544

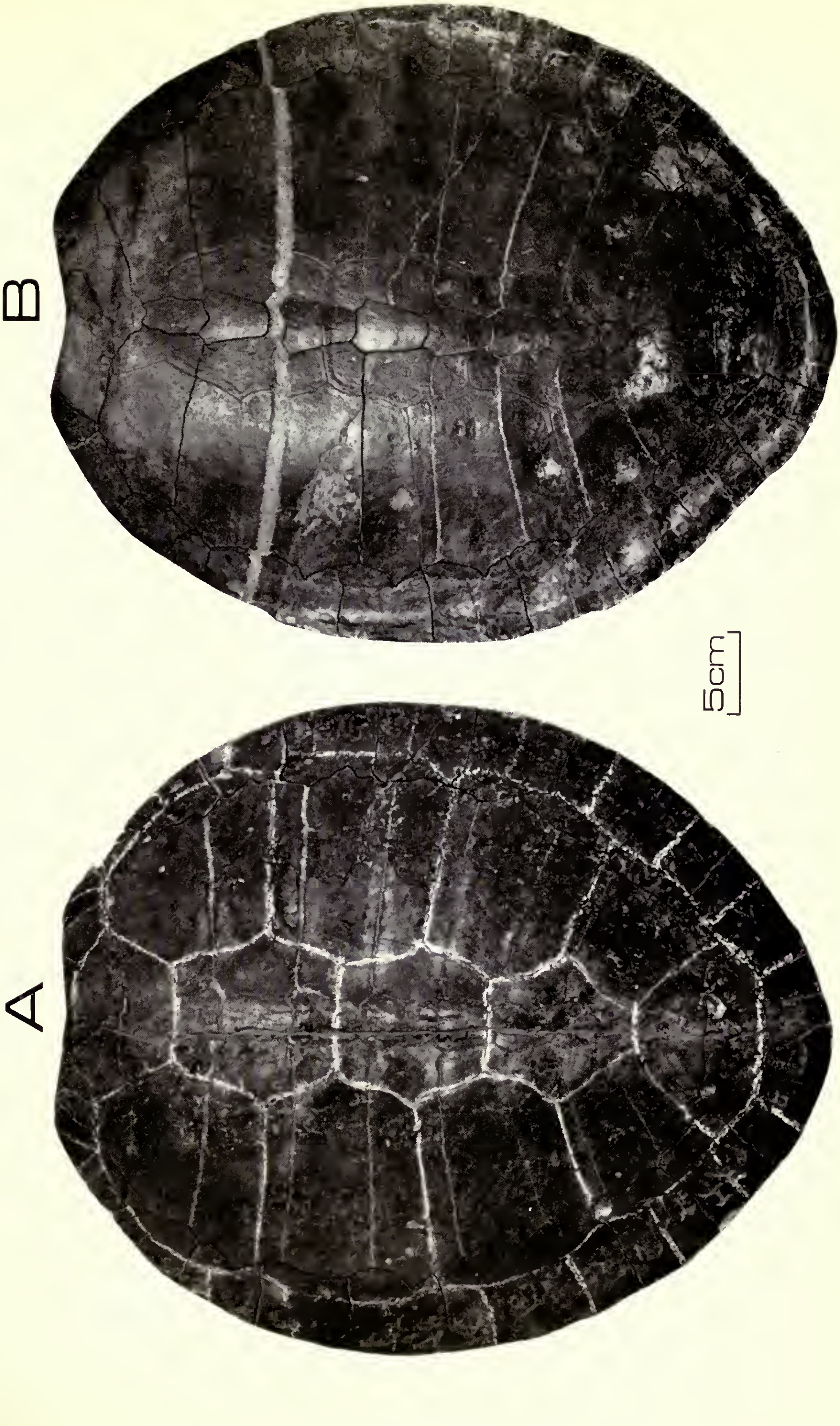
B
5cm
A

PLATE 8

Puppigerus camperi (Gray)

Plastra from below
A. I.R.S.N.B. IG.8632
B. B.M.(N.H.) 38951

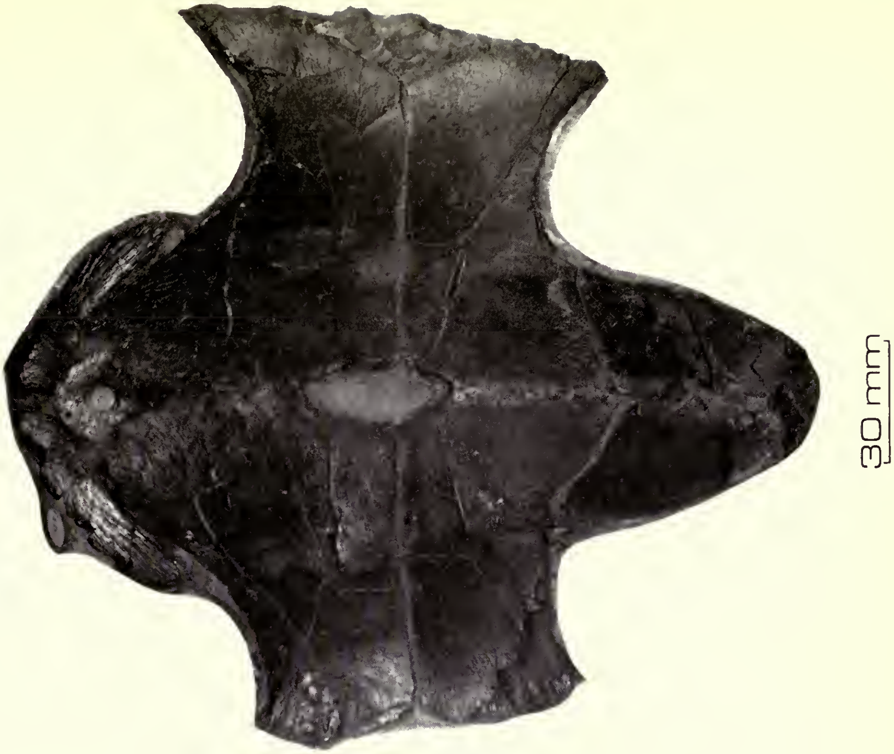
B
30 mm

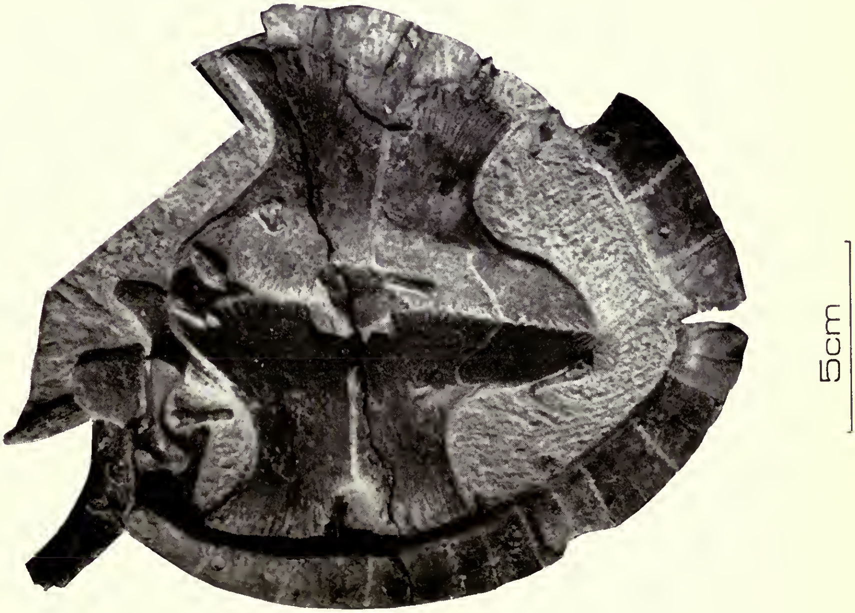
A
5cm

A LIST OF SUPPLEMENTS TO THE GEOLOGICAL SERIES OF THE BULLETIN OF THE BRITISH MUSEUM (NATURAL HISTORY)

---

1. Cox, L. R. Jurassic Bivalvia and Gastropoda from Tanganyika and Kenya. Pp. 213; 30 Plates; 2 Text-figures. 1965. £6.
2. El-Naggar, Z. R. Stratigraphy and Planktonic Foraminifera of the Upper Cretaceous—Lower Tertiary Succession in the Esna-Idfu Region, Nile Valley, Egypt, U.A.R. Pp. 291; 23 Plates; 18 Text-figures. 1966. £10.
3. Davey, R. J., Downie, C., Sarjeant, W. A. S. & Williams, G. L. Studies on Mesozoic and Cainozoic Dinoflagellate Cysts. Pp. 248; 28 Plates; 64 Text-figures. 1966. £7.
3. Appendix. Davey, R. J., Downie, C., Sarjeant, W. A. S. & Williams, G. L. Appendix to Studies on Mesozoic and Cainozoic Dinoflagellate Cysts. Pp. 24. 1969. 80p.
4. Elliott, G. F. Permian to Palaeocene Calcareous Algae (Dasycladaceae) of the Middle East. Pp. 111; 24 Plates; 17 Text-figures. 1968. £5.12½.
5. Rhodes, F. H. T., Austin, R. L. & Druce, E. C. British Avonian (Carboniferous) Conodont faunas, and their value in local and continental correlation. Pp. 315; 31 Plates; 92 Text-figures. 1969. £11.
6. Childs, A. Upper Jurassic Rhynchonellid Brachiopods from Northwestern Europe. Pp. 119; 12 Plates; 40 Text-figures. 1969. £4.75.
7. Goody, P. C. The relationships of certain Upper Cretaceous Teleosts with special reference to the Myctophoids. Pp. 255; 102 Text-figures. 1969. £6.50.
8. Owen, H. G. Middle Albian Stratigraphy in the Anglo-Paris Basin. Pp. 164; 3 Plates; 52 Text-figures. 1971. £6.
9. Siddiqui, Q. A. Early Tertiary Ostracoda of the family Trachyleberididae from West Pakistan. Pp. 98; 42 Plates; 7 Text-figures. 1971. £8.
10. Forey, P. L. A revision of the elopiform fishes, fossil and Recent. Pp. 222; 92 Text-figures. 1973. £9.45.

Printed in Great Britain by John Wright and Sons Ltd. at The Stonebridge Press, Bristol BS4 5NU

22 AUG 197
NATURAL HISTO

THE SHELL STRUCTURE OF SPIRIFERIDE BRACHIOPODA

D. I. MacKINNON

BULLETIN OF
THE BRITISH MUSEUM (NATURAL HISTORY)
GEOLOGY Vol. 25 No. 3
LONDON : 1974

BRITISH MU
22 AUG
NATURAL H

THE SHELL STRUCTURE OF SPIRIFERIDE BRACHIOPODA

BY
DAVID IRONSIDE MacKINNON
Department of Geology University of Canterbury
Christchurch New Zealand

Pp 187–261 ; 32 *Plates* ; 27 *Text-figures*

BULLETIN OF
THE BRITISH MUSEUM (NATURAL HISTORY)
GEOLOGY Vol. 25 No. 3
LONDON: 1974

THE BULLETIN OF THE BRITISH MUSEUM (NATURAL HISTORY), *instituted in* 1949, *is issued in five series corresponding to the Departments of the Museum, and an Historical series.*

Parts will appear at irregular intervals as they become ready. Volumes will contain about three or four hundred pages, and will not necessarily be completed within one calendar year.

In 1965 *a separate supplementary series of longer papers was instituted, numbered serially for each Department.*

This paper is Vol. 25, *No.* 3, *of the Geological (Palaeontological) series. The abbreviated titles of periodicals cited follow those of the World List of Scientific Periodicals.*

World List abbreviation :
Bull. Br. Mus. nat. Hist. (Geol.)

© Trustees of the British Museum (Natural History), 1974

TRUSTEES OF
THE BRITISH MUSEUM (NATURAL HISTORY)

Issued 26 *July*, 1974 *Price* £6.70

THE SHELL STRUCTURE OF SPIRIFERIDE BRACHIOPODA

By DAVID IRONSIDE MACKINNON

CONTENTS

Page

Synopsis . . . 189

I. Introduction . . . 190

II. Technique of specimen preparation . . . 191

III. Shell structure of *Spiriferina walcotti* (Sowerby) . . . 191

- (a) The shell succession . . . 192
  - (i) Periostracum . . . 192
  - (ii) Primary layer . . . 193
  - (iii) Secondary layer . . . 195
- (b) Punctation . . . 196
- (c) Hollow spines . . . 196
- (d) Concentric growth lines and mantle retraction . . . 198
- (e) Muscle attachment areas . . . 201
  - (i) Pedicle valve . . . 201
  - (ii) Brachial valve . . . 203
  - (iii) Functional considerations . . . 205
- (f) The brachidium . . . 206
- (g) Articulation . . . 210

IV. Shell structure of other Spiriferida . . . 212

- (a) Atrypidina . . . 212
  - (i) Atrypacea . . . 212
  - (ii) Dayiacea . . . 218
- (b) Retziidina . . . 220
- (c) Athyrididina . . . 221
  - (i) Athyridacea . . . 221
  - (ii) Koninckinacea . . . 225
- (d) Spiriferidina . . . 229
  - (i) Cyrtiacea . . . 229
  - (ii) Suessiacea . . . 230
  - (iii) Spiriferacea . . . 232
  - (iv) Spiriferinacea . . . 238
  - (v) Reticulariacea . . . 239
- (e) *Thecospira* . . . 240

V. Structure of the brachidium and inferred dispositions of the lophophore in Spiriferida . . . 243

- (a) Structure of spiralia . . . 243
- (b) Inferred dispositions of the spiriferide lophophore . . . 251

VI. Conclusions . . . 254

VII. Acknowledgements . . . 256

VIII. References . . . 256

Index . . . 258

SYNOPSIS

By studying the growth and structure of the shell of *Spiriferina walcotti* (Sowerby), a standard for the skeletal fabric of the order Spiriferida has been erected. Apart from the development of the spiral brachidium, shell growth involving deposition of primary and secondary calcareous layers (and also, presumably, a periostracum) in *Spiriferina* appears to have been little different from that of living Terebratulida. In many stocks, however, including the Atrypacea, Dayiacea, Reticulariacea, Koninckinacea and some Athyridacea and Spiriferacea, a tertiary layer similar to that deposited in the living terebratulacean *Gryphus vitreus* (Born) has been identified. Apart from the development of peripheral tubercles in Thecospiridae and some Koninckinacea (which are both assigned to the Spiriferida) the shell structure of all remaining spire-bearers does not differ markedly from that of living Rhynchonellida or Terebratulida.

The ultrastructure of the spiral brachidia of a number of genera has been examined and two distinct growth patterns have been recognized. 'Single-sided' growth is characteristic of the athyrididine spiralium whereas 'double-sided' growth is characteristic of all other spiriferides examined. Consideration is given to the disposition of the spiriferide lophophore.

I. INTRODUCTION

THE advent of the electron microscope has led to an upsurge in studies relating to the shell structure of living and fossil Brachiopoda. The most significant contribution to date, with respect to articulate Brachiopoda, has been that of Williams (1968a) in which it was shown that a triple division of the shell into periostracum, and primary and secondary calcareous layers, is characteristic of most members of this major class. By studying the soft tissues as well as the calcareous exoskeleton of living Rhynchonellida and Terebratulida, Williams was able to rationalize shell growth in terms of the secretory behaviour of individual outer epithelial cells. In dealing with the Spiriferida Williams (1968a : 31–34) referred briefly to the skeletal fabrics of a number of atrypidines, athyridines, retziidines and spiriferidines, showing that in general they possessed a shell ultrastructure similar in many ways to that found in Recent Rhynchonellida and Terebratulida, but it was outside the scope of that report to include a more detailed survey of the order. This paper is intended as a contribution towards a greater understanding of the processes of shell deposition within the phylum from both a functional and evolutionary standpoint.

To make sense of a comparative study of the shell fabrics of fossil Spiriferida, investigations must be based on a workable classification. In this exploratory survey the *Treatise* classification, as erected by Boucot, Johnson, Pitrat and Staton (1965) has been followed but only down to the rank of superfamily. As will be shown, below this level of classification trends in ultramicroscopic shell variation, as well as gross morphological distinctions, become less clearly defined.

The fact that no spiriferide genera (as far as is known) survive to the present day has necessitated the selection of a suitable fossil representative as a standard model for the skeletal fabric of the order. *Spiriferina walcotti* (Sowerby) fits this role well for, apart from being a member of the last surviving spiriferide stock, its mode of preservation is normally very good and adequate numbers of complete specimens may be readily collected and prepared for study. Consequently a complete section of this paper is devoted to a description of the shell structure of *Spiriferina walcotti* prior to consideration of the skeletal fabrics of the order as a whole.

One aspect of spiriferide morphology which has excited some interest in recent years has been the problem of establishing the nature and disposition of the lophophore which must have been supported by the calcareous spiralia. With this thought in mind, the structure of the spiralia of as many genera as possible has been studied and compared with the structure of the calcareous supports in living Terebratulida. Since the orientation of the lophophore in living Terebratulida can be determined in relation to the disposition of the ascending and descending branches of the calcareous loop, the possibilities of applying these findings to the Spiriferida have been investigated.

II. TECHNIQUE OF SPECIMEN PREPARATION

Both surfaces and sections of calcareous shells were examined under a Cambridge 'Stereoscan' scanning electron microscope. Initially specimens were embedded in Epon Araldite resin then cut and ground, first on a diamond grinder and then on fine grade (C600) silicon carbide paper. A relatively scratch-free finish was obtained by using a paste of Aloxite optical smoothing powder along with the silicon carbide paper. Surfaces prepared in this manner were finally polished on a cloth-covered disc which was impregnated with stannic oxide or slow-cutting polishing alumina. Before mounting, the embedded specimens were cut to a convenient area and thickness and ultrasonically cleaned for a few minutes in a mild detergent solution, then in acetone. Fragments of internal or external shell surfaces requiring investigation were cleaned in the same way. Once dry, specimens were mounted on aluminium stubs using a conductive adhesive (Lo-Kitt) then fixed on a rotatable table in a vacuum evaporator and coated with a thin deposit (about 0·03–0·05 μm in thickness) of gold/palladium alloy. A thin metallic coating of this nature is necessary when examining calcareous shell fragments in order to render the specimens conductive and prevent charge build-up.

All important 'Stereoscan' observations were recorded photographically. In certain cases it was found that the size of skeletal components, in particular secondary layer fibres, was such that individual 10 × 10 cm prints did not provide a sufficiently detailed overall view of the area under investigation. To overcome this lack of structural detail a montage of overlapping prints, which had been photographed at higher magnifications, was constructed. In general, a 20 per cent overlap was required to produce a reasonable match-up of corresponding features in adjacent prints.

All mounted specimens used in this study have been presented to the British Museum (Natural History) and retain the registered numbers BB 58878 to BB 59009.

III. SHELL STRUCTURE OF *SPIRIFERINA WALCOTTI* (SOWERBY)

Spiriferina walcotti (Sowerby) occurs within the British Lias and is especially common in the highly attenuated sequence of Lower Liassic rocks around Radstock and Bath. In this area, commonly referred to as the 'Radstock Shelf', the state of preservation of the shell is normally very good and complete specimens, with fully articulated valves, are abundant. It is convenient, therefore, to consider this species of the last surviving spiriferide genus as a model for the skeletal fabric of the order and, by studying the ultrastructure of its shell, reconstruct the morphology and disposition of its mantle. The restored species may then be used as a standard with which all other Spiriferida may be compared.

Tutcher & Trueman (1925 : 595) have given a detailed description of many fossiliferous localities within the Radstock area, though regrettably a number of sections and quarries listed by them are now overgrown with thick vegetation or filled in with earth and rubble. Fortunately Bowlditch Quarry (ST 668559) north of Radstock and Hodder's Quarry (ST 674584), Timsbury, both sources in the past of some of the finest specimens of *S. walcotti*, are still accessible. All specimens examined during the present investigation came from either one or other locality.

Before considering the microstructure of the shell of *S. walcotti*, it seems appropriate to describe the morphology of the shell because, as far as is known, no up-to-date account of the species is available. Certainly a knowledge of the morphology of exoskeletal outgrowths and their relationship with the shell is essential before the microstructure of critical sections can be fully understood. The following diagnosis supplements the descriptions given by Davidson (1852 : 25) and Hall & Clarke (1894 : 51) :

Shell moderately transverse in outline, with rounded cardinal extremities ; biconvex in profile, anterior commissure uniplicate, distinct fold and sulcus ; lateral slopes with distinct, rounded, simple costae ranging from 2 to 5 (modally 4) on each slope. Ventral interarea gently curved, dorsal interarea low ; both traversed by growth lines, fine striae intermittently developed normal to transverse growth lines. Triangular delthyrium, partly restricted by a pair of dental ridges (cf. Dunlop 1962 : 491) ; low triangular notothyrium. Surface further ornamented by concentric growth lines and numerous fine, tubular spines ; shell endopunctate.

Interior of pedicle valve with high, dorsally pointed median septum extending for almost half the length of the valve and bearing broad, well-defined adductor muscle scars ; diductor and ventral adjustor muscle scars impressed on valve floor on either side of median septum. Teeth prominent ; dental plates short, diverging from umbo and terminating on the valve floor just postero-laterally to the diductor muscle scars.

Interior of brachial valve with triangular cardinal process, usually striated parallel to the median plane, bounded laterally by posterior walls of inner socket ridges ; dorsal adjustor scars deeply impressed on the crural bases, situated just antero-laterally to the cardinal process and each bounded by an inner socket ridge. Crura broad, supporting laterally directed spires with as many as 15 convolutions ; primary lamellae united by single jugum ; anteriorly facing edges of spiral lamellae spinose ; two pairs of dorsal adductor muscle scars with the anterior pair more prominently inserted on floor of valve.

(a) The shell succession

(i) *Periostracum*

The chances of finding traces of the organic constituent of the shell of *Spiriferina* that are identifiable under the electron microscope are very small. However, amino-acids have been recovered by Jope (1965 : H161) from several spiriferide shells and it is highly likely that the organic parts of the exoskeletal succession were similar to those found in living species. In particular, a periostracum would have been necessary as a seeding sheet for the mineral part of the shell, and membranes must also have ensheathed the fibres of the secondary shell. Both constituents must have played a decisive part in determining the ultrastructure of the primary and secondary calcareous shell.

(ii) *Primary layer*

Although the external surface of the primary layer is finely granular a distinct lineation is visible with the long axes of the particles radially aligned (Pl. 1, fig. 1). At intervals of about 20 μm, fine concentric growth lines are superimposed on this fabric (Pl. 1, fig. 2) so that, whilst no remnant periostracal covering remains, an impression of its basal membrane is preserved. Anterior to the base of each spine the surface of the shell is dissected by a prominent longitudinal groove (Pl. 1, fig. 3) whilst several more conspicuous grooves, also aligned parallel to the long axis of the shell and spaced from 4 to 6 μm apart, are deflected around the posterior of the spine base (Pl. 1, fig. 4). If the dimensions of terminal faces of fibres situated around the periphery of the valve margins can be taken as a guide to the size of outer epithelial cells located close to the edge of the outer mantle lobe (about 5 μm wide), then it is reasonable to assume that the longitudinal grooves posterior to each spine base, being similarly spaced, correspond to the lateral boundaries of rows of cuboidal epithelium.

In mature specimens of *Spiriferina*, the thickness of the primary layer can vary from about 30 μm, close to the umbo, to 100 μm or more at the anterior commissure (Text-fig. 1). Since deposition of the primary layer is restricted to a narrow zone of outer epithelial cells located around the shell edge, the observed thickening of the primary layer can be interpreted as a progressive widening of this zone with age.

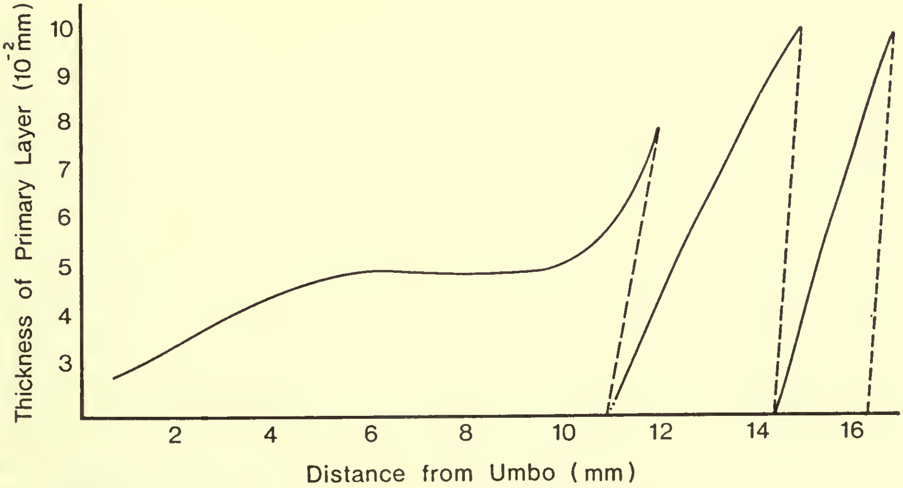

FIG. 1. Graph showing the increase in the thickness of the primary layer from umbo to anterior commissure in a brachial valve of *Spiriferina*. Broken lines denote regression planes of overlapping growth lamellae.

Unless the dimensions of newly proliferated cells increase drastically as the brachiopod approaches maturity, a widening of the zone of primary shell deposition must be accompanied by an overall increase in the number of cells involved in secreting that layer. If such is the case, the widening of the primary shell secretory zone must also reflect an increasing delay with age in the change-over to secondary shell deposition (cf. Williams 1971a : 58). Alternatively, primary layer thickening may be related to an increase in the marginal angle of the shell which may result from a reduction in the migration rate of cells in the conveyor-belt system of the outer mantle lobe.

In section, a twofold division of the primary layer is recognizable (Pl. 1, fig. 5). It is possible to distinguish between an outer, finely granular, porous part which gradually merges into a more compact inner portion composed of crystallites (averaging less than 10 μm in length) orientated with their long axes normal or posteriorly inclined to the isotopic boundary (Westbroek 1967 : 23) defining the junction between the primary and secondary shell layers. Electron micrographs of random, oblique sections of *Spiriferina* show that grain boundaries of primary layer crystallites are regularly found in continuity with the first-formed, inwardly convex boundaries of secondary layer fibres so that organic membranes, known to ensheath the latter, could also have extended deep within the primary layer. In radial sections, a faint banding is occasionally seen which runs posteriorly at a low angle from the external surface to the internal boundary with the secondary layer. The banding is considered to be depositional, and thus merits recognition as a superficial (isochronous) shell unit boundary, as defined by Westbroek. Such radial sections serve to establish the relationship between these surfaces and the calcareous skeletal constituents when the first formed fibres occur as long rods dipping gently towards the anterior shell edge. In addition, the crystallites of the primary layer are, in general, posteriorly inclined to the isotopic surfaces between the primary and secondary layers, but normal to the observed depositional banding.

As this twofold division of the primary layer is not characteristic of Recent Rhynchonellida and Terebratulida, it is possible that the textural variation is secondary in origin. If, for some unknown reason, the primary layer of *Spiriferina* were especially prone to recrystallization, the process would be confined within a space bounded externally by compacted grains of enclosing sediment and internally by the fibres of the secondary shell. Recrystallization normal to these two interfaces might then have given rise to two contrasting crystalline textures growing towards one another. However, specimens of the terebratulacean *Lobothyris punctata* (Sowerby), collected from the same localities as *Spiriferina*, exhibit a primary layer texture closely resembling that of living Terebratulida, whilst the fibres of the secondary shell of both species are in an identical state of preservation. Such evidence suggests that textural differences in the primary layer of *Spiriferina* are original.

The twofold nature of the primary shell is not unique to *Spiriferina*. Armstrong (1968a : 184), in describing the microstructure of the shell of the spiriferide *Subansiria* sp. from the Permian rocks of Queensland, Eastern Australia, distinguished within its primary layer an identical granular outer part and finely crystalline inner portion. Armstrong maintained that the boundaries between the primary layer components of *Subansiria* sp. are as distinctive as the inter-fibre junctions in the secondary shell.

Such a comparison prompted him to postulate the deposition of organic membranes around the crystals of the primary layer. The outer granular portion of the primary layer, he suggested, may have been the product of a transitional phase of organic–mineral deposition following the secretion of the periostracum and preceding formation of the more regular crystals.

Growth of the primary layer in Recent Rhynchonellida and Terebratulida, as described by Williams (1968a), could not account for the twofold structure of that layer in *Spiriferina.* In living articulates, the first formed seeds of calcite are secreted by cells situated at the tip of the outer mantle lobe onto an embedding protein cement comprising the innermost surface of the periostracum. Initially the seeds tend to be concentrated in zones separated by inwardly directed bars of periostracum and isolated from one another by membranous projections of the cells (microvilli) attached to the periostracum. As deposition continues, the crystallites grow and overlap one another across intercellular boundaries, but microvilli continue to permeate the primary layer to give its inner surface a highly porous appearance. However, observations recorded above suggest that, although growth of the primary layer of *Spiriferina* started in similar fashion with deposition of the first calcite crystallites onto an embedding protein sheet forming the internal surface of the periostracum, the crystallites did not quickly coalesce. Instead they were kept isolated from one another by a fine membranous web extending inwards from the periostracum and deposited simultaneously with the crystallites by the outer epithelial cells. As an increasingly thick wedge of primary layer was deposited, organic secretion became less prevalent and many connecting membranes became pinched out. Hence crystallites amalgamated with one another and imparted to the inner half of the layer a more homogeneous appearance. Finally at a certain distance from the shell edge, organic secretion became restricted to an arcuate sector of the secreting plasmalemma and deposition of the secondary layer began.

(iii) *Secondary layer*

The secondary shell layer is built up from orthodoxly stacked fibres. On the internal surface of the shell, the terminal faces of the overlapping fibres produce the standard secondary shell mosaic pattern (Pl. 1, fig. 6). Whilst secondary generative zones are known to occur in certain areas of the outer epithelium, the main zone of cell proliferation and fibre formation is located around the shell edge. In this area, the young fibres of *Spiriferina* with terminal faces no more than 5 μm wide grew normal to the commissure. The consistency of this initial growth direction is verified by examination of the external surface of specimens from which the primary layer has broken off during removal from the enclosing sediment. In such specimens, the freshly exposed trails of the secondary layer fibres are radially disposed over the entire shell surface. When young fibres of *Spiriferina* come to occupy a position up to about 100 μm behind the leading edge of the secondary shell mosaic, they become reorientated, broadly speaking, in a sub-parallel arc ; clockwise in the right half of the valve, anti-clockwise in the left.

Terminal faces of mature fibres are spatulate, normally 30 μm long and 15 μm at maximum width. However, on some parts of the inner shell surface, they may become elongate with long exposed trails. Other more drastic changes take place in those fibres underlying the muscle attachment areas, but these will be considered separately. Small localized convolutions in the form of spiral arcs and tight S-shaped patterns may be found in most parts of the shell. Similar minor modifications occur in the shells of a number of Recent articulates (Williams 1968a : 9) and are considered simply to reflect small epithelial adjustments in adjacent zones of the internal surface.

In gerontic forms, radial fibre growth around the commissure becomes less prevalent since the normal secretory regime in this area is disrupted by repeated mantle retractions. This particular aspect of mantle behaviour and shell deposition will, however, be dealt with separately.

(b) Punctation

The shell of *Spiriferina* is endopunctate. As in living Terebratulida, perfectly interlocking fibres of the secondary layer fashion and preserve the cylindroid shape of the canals which measure, on average, 30–40 μm in diameter. This is well displayed on the internal surfaces of *Spiriferina* where the advancing fibres are momentarily deflected from their paths of growth so as to sweep around the puncta, but thereafter continue on their previous course (Pl. 2, fig. 1). In some cases where a fibre trail lies directly in line with a caecum, the fibre may terminate on one side of the cavity and reappear, without any noticeable change in size or shape, on the side directly opposite. In section, the fibres on either side of the puncta arch outwards towards the primary layer (see Pl. 3). The puncta so defined do not run quite normal to the shell layers but slope anteriorly from the shell exterior at a steep angle of about 80 degrees. Within the umbonal region of the pedicle valve, groups of branching puncta are found. Towards the interior of the shell up to five discrete canals may merge into one central canal. Such branched puncta are considered to have formed as a result of the coalescence of originally discrete puncta due to extensive deposition of calcite in that part of the shell.

When viewed from the exterior, the puncta of *Spiriferina* usually break the surface of the primary layer, but in several cases fragmentary distal coverings, about 1 μm thick, were observed *in situ* (Pl. 2, fig. 2). This thin layer of primary shell material is perforated by densely distributed canals, each measuring approximately 500 nm in diameter (Pl. 2, fig. 3).

Since the perforate canopies covering the distal ends of puncta in *Spiriferina* are so unmistakably like those in living Terebratulida (MacKinnon 1971a), it seems certain that the puncta of *Spiriferina* must have accommodated caeca virtually identical in ultrastructure with those in living endopunctate brachiopods.

(c) Hollow spines

The micro-ornament visible on the exterior surface of *Spiriferina* consists of a variably dense concentration of hollow spines, on average 80 μm in diameter at their bases and tapering distally to about 35 μm, which project at low angles towards the commissure (Pl. 1, fig. 2). They are usually broken, but a few may remain more or less intact between costae where stalks up to 2 mm in length have been found. All spinose outgrowths are composed solely of primary shell material, but the narrow canals running through the spines, on average 30–40 μm wide in mature specimens, do not terminate at the primary/secondary shell layer boundary. Starting from the shell exterior, a canal can be traced running posteriorly parallel to the length of a spine until it reaches the spine base, whereupon it bends sharply through 90 degrees before passing through the remainder of the secondary layer (Text-fig. 2). Throughout the secondary layer, the walls of the canals are fashioned by fibre trails which are deflected around one side or the other in a manner identical to that found in puncta. On the inner shell surface, the cylindroid hollows forming both puncta and spine canals are indistinguishable. Although the distal ends of spines are broken off, no blocking up of canals due to subsequent shell deposition has been observed in the surviving basal parts.

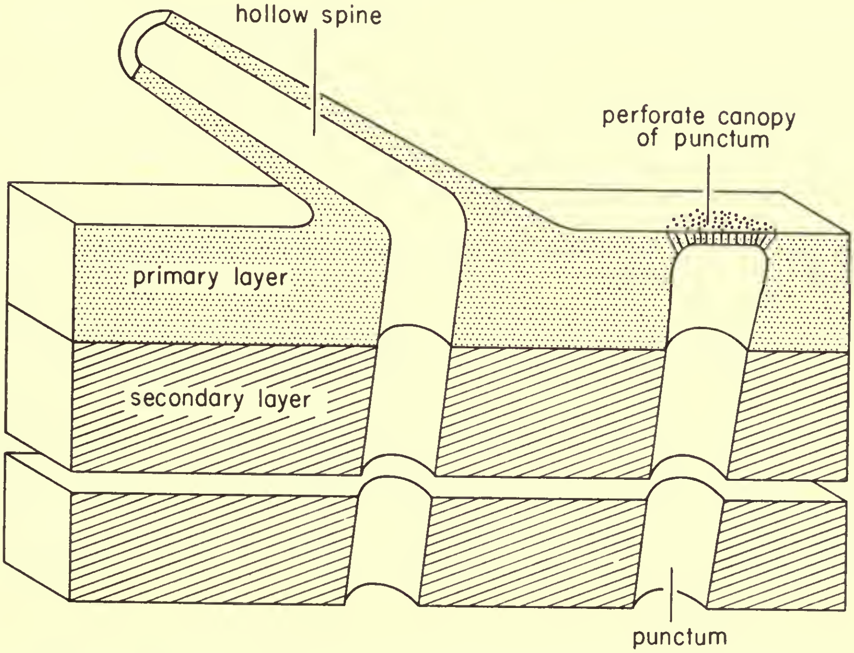

FIG. 2. Block diagram showing the relationship between a hollow spine, a punctum and the calcareous shell succession in *Spiriferina*. Anterior commissure of shell located beyond the left-hand margin of the diagram.

The density of distribution of spinose outgrowths is variable over the whole shell surface. Within 5 mm of the umbo, which incorporates the earliest formed parts of the shell, the surface density of hollow spines rarely exceeds 5 per mm^2. Around the commissure of mature specimens, however, the density is appreciably greater, rising to as much as 35 per mm^2. In general, the spines do not conform to any recognizable pattern on the shell exterior, but close to the anterior commissure of mature specimens where the concentration of spinose outgrowths is densest, localized groups of spines appear to be arranged 'in quincunx'. In such areas, a one-to-one correspondence exists between spine bases and puncta with the puncta set out in alternating rows between spine bases.

Clearly the spines were built up very quickly by the secretion of calcite in small circumferential generative zones of outer epithelium located close to the tip of the outer mantle lobe, but they did not continue to increase in length throughout life as happened in certain strophomenides. Whereas strophomenide spines continued to grow indefinitely with accretion of primary and secondary shell material (or were eventually sealed off), the spines of *Spiriferina* grew only during the period in which adjacent cells were employed in primary shell formation. Once the underlying epithelium changed to secreting the secondary layer, growth of the spines ceased.

The structure and distribution of the spines provide little indication of their function. Unlike the hollow spines of genera such as *Acanthothiris* (Rudwick 1965 : 610), and certain Siphonotretacea (Biernat and Williams 1971 : 429), the spines extending from the surface of *Spiriferina* were not long or large enough to have functioned efficiently as protective grilles. Even if the shell were closed, spines extending from both valves would not have intersected. Rudwick (1965 : 610) suggests that the hollow spines of *Acanthothiris* probably accommodated sensory organs which could have provided the brachiopod with effective 'early-warning' protection against potentially harmful agents in the environment. The tips of growing spines, however, would have been occupied by generative cells involved in the proliferation of new cells and the secretion of mucopolysaccharide and periostracum. Thus the presence of these external covers would surely have militated against any chemo-sensitivity of the tips of spines developed as extensions of the shells of any brachiopod, including *Spiriferina*. However, since the shell exterior is to a large extent free from boring organisms and any encrusting epifauna, it is possible that the function of the spines was protective. As Owen & Williams (1969 : 200) have pointed out, the typical brachiopod exterior seems frequently to attract a rich benthonic microfauna, consisting of bryozoans, sponges, algae etc. Obviously an irregular surface topography, broken up by spines, would tend to hinder and discourage the settlement of such organisms onto the surface of the periostracum.

(d) Concentric growth lines and mantle retraction

The presence of concentric growth lines on the outer surfaces of both valves is characteristic of a great number of Spiriferida. These are considered to be the result of a series of successive pauses or even complete breaks in deposition affecting the normal pattern of radial growth. In the past, palaeontologists have found sets of growth lines to be of great systematic value in recognizing a number of successive ontogenetic stages in many genera. Krans (1965 : 87), using a dry peel technique with carefully orientated sections, has made a study of the shell growth in a number of Devonian Spiriferida and has distinguished three main types of growth features. These are :

(1) *Slight flexures* where the shell layers are bent into a small kink due to a pause in radial growth whilst deposition of calcite continues.

(2) *Overlapping growth lamellae* where the primary and secondary shell layers are bent around to face posteriorly inwards before returning to normal radial growth.

(3) *Free growth lamellae* caused by a distinct break in deposition of calcite with a strip of mantle around the shell edge actually detaching itself from a part which it has already formed. In addition, the mantle undergoes an abrupt retraction before returning to the normal course of deposition.

Such observations are comparable with those made by Brunton (1969) and Williams (1971a) on Recent Rhynchonellida and Terebratulida, but the signs of depositional pauses or breaks described for *Spiriferina*, though similar, are not identical.

Minor fluctuations in the rate of shell deposition, as well as more drastic physiological changes in the secretory role of outer epithelial cells situated around the mantle edge, contributed to the appearance of a variety of concentric growth lines over most of the shell exterior. The finest, which are microscopic growth lines normally no more than 20 μm apart, are surface features unaccompanied by any differential thickening of the primary layer (Pl. 1, figs. 1, 2). Where there are slight flexures in the shell layers, each producing a concentric ridge in the order of 100 μm in amplitude, the primary layer is warped in a manner analogous to monoclinal folding, whereas the underlying fibres of the secondary layer are crowded together and display cross-sectional outlines different from those either in front of or behind the modified zone (Pl. 2, fig. 5). Most of the major overlapping shell units are found around the commissures of mature specimens. In radial section (Pl. 3), normal secondary layer fibres are bent sharply backwards against a line, posteriorly inclined, and running from the primary/secondary layer interface inwards towards the shell interior. Below this line, a series of lamellae, composed of primary shell material, are stacked one below the other so that their posterior ends are in continuity with the line of 'unconformity'. The lamellae are flat or slightly convex inwards and vary between 5 μm and 10 μm in thickness. Finally the lamellae pass inwards to a normal primary and secondary layer succession which extends anteriorly to the next major concentric growth line. Secondary layer fibres associated with major overlapping shell units are generally stacked with long axes parallel, and not at right angles, to the valve margins.

The frequency and spacing of the microscopic concentric growth lines suggest that they are remnants of the linear junctions between successive rows of outer epithelial cells as each in turn changed over from organic to mineral secretion. The slight flexures in the shell layers are produced by a change from radial to tangential growth which results in the radial growth vector being reduced to zero, whilst the growth vector normal to the shell edge is greatly increased. Calcite secretion does not stop and there is no retraction of the mantle, but the fibres located around the periphery of the shell tend to grow parallel and not at right angles to the shell edge. The major overlapping shell units which are found around the periphery of most mature individuals appear similar to the free growth lamellae of Krans (1965 : 88). When

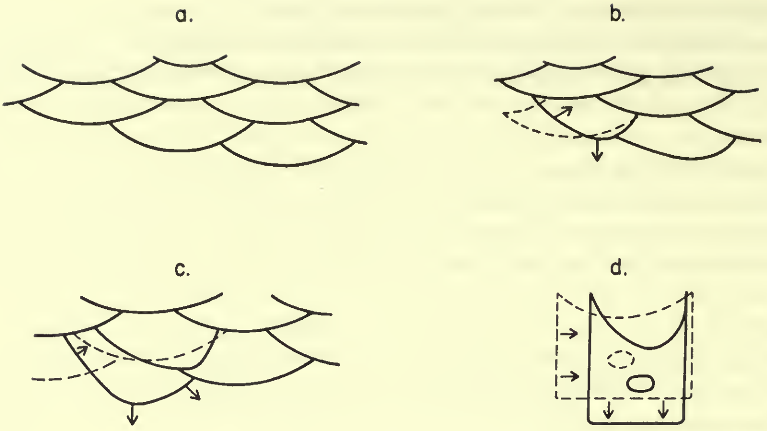

FIG. 3. a–c. Stylized drawings of transverse sections through secondary layer fibres showing how a series of slight changes in profile may produce a substantial overall displacement. d. Section through an outer epithelial cell showing how a lateral contraction will produce greater concavity in the secreting plasmalemma.

examined in greater detail, however, they are found to be the culmination of a series of minor mantle readjustments. The first stage in the formation of a new shell unit around the edge is brought about by a breakdown in the secretory regime of the underlying outer epithelium. This may be preceded by a slight posterior withdrawal of the outer mantle lobe, giving rise to a narrow zone of fibres which are bent round sharply on one another. It is remarkable how the gradual change in shape of a cell, and in particular its secreting plasmalemma, when combined with similar changes in adjacent cells, can give rise to macroscopic variations in the shell layers. A lateral contraction produces greater concavity in the secreting plasmalemma, hence the terminal face of the fibre secreted by it will become narrower and more highly convex (Text-fig. 3). The gross effect is to produce a lateral foreshortening and vertical thickening within the shell layer. The first major break in the secretory regime of the outer epithelium corresponds to a halt in the 'conveyor belt' system of cell proliferation and hence to a lapse in radial growth. Deposition continues normal to the plane of regression but the organic membranes secreted by arcuate strips of each outer epithelial cell are often pinched out. A gradual regression of the mantle edge follows with deposition of successive horizontal lamellae composed of primary shell. The lamellae are not stacked vertically one above the other, but are stepped progressively backwards. Between each regression plane there is a thin wedge of micritic material. Very probably the interlamellar spaces were occupied by organic material secreted by the mantle to assist in its backward slide. On the other hand, if deposition of periostracum were continuous at the mantle edge (as is highly likely) the spaces between the lamellae may have been occupied by folds of that protective outer cover which would have functioned as an ideal seeding sheet for each consecutive calcite lamina.

To produce a thickening of the shell in this manner, it is clear that the same outer epithelial cells must have undergone cyclical changes in secretory regime (Text-fig. 4). Initially involved in secreting the primary, then secondary, shell layers, they must have continually fluctuated between organic and inorganic episodes of deposition until the stage was reached where mantle retraction stopped and normal growth of the shell layers resumed.

(e) Muscle attachment areas

The areas of muscle attachment in *Spiriferina* are distributed similarly to those found in living articulates, except for the ventral adductor muscle fields which are situated on both sides of a large, pointed, ventral, median septum and not on the floor of the valve.

(i) *Pedicle valve*

The ventral diductor and adjustor muscle bases leave strong impressions on the valve floor, so that the ventral muscle scars are well defined (Pl. 2, fig. 4). Around the anterior margins of each scar, there is a prominent, anteriorly arcuate ridge (Pl. 2, fig. 4 ; Pl. 4, fig. 1) like that found around the anterior border of the ventral muscle scars of the Recent rhynchonellide *Notosaria nigricans* (Sowerby). It is built up from secondary layer fibres. Although the effects of fossilization tend to obscure the finer details of textural variations in the shell fabric, it is evident that the exposed parts of fibres on the posterior facing side of the ridge exhibit longer, more ragged trails than those comprising the crest of the ridge. Traced posteriorly from the ridge crest the exposed fibre trails are overlapped by fibres whose terminal faces exhibit a fairly well-developed mosaic pattern. The difference in growth direction of both sets of fibres is striking, which suggests that the zone of fibres overlapping the ridge grew quite independently of those which actually composed the ridge. Indeed, a significant lowering of the level of the valve floor behind the ridge and the existence of long, ragged, exposed trails on its posteriorly sloping side suggest that the outer epithelium in contact with that part of the ridge was resorbing and not depositing shell material. About 500 μm behind the ridge, the inner shell surface is cut up by a series of deeply impressed furrows, each measuring between 75–100 μm in width (Pl. 4, fig. 2). Within the ventral adjustor muscle field, the furrows run longitudinally and are generally separated from one another by narrow ridges of fibres exhibiting a fairly well-developed secondary shell mosaic (Pl. 4, fig. 3). Within the diductor muscle field, however, the anterior parts of the furrows bend round to face the median septum. In addition, groups of neighbouring furrows tend to merge together, unlike the adjustor scar, so that the outlines of the impressions appear flabellate.

The occurrence of a well-developed mosaic pattern within a muscle scar is unusual and has not been observed within the muscle scars of any Recent articulate. Generally a myotest shell fabric is quite distinct from the normal secondary shell mosaic pattern. The fact that fibres occurring within the elongate furrows of the muscle

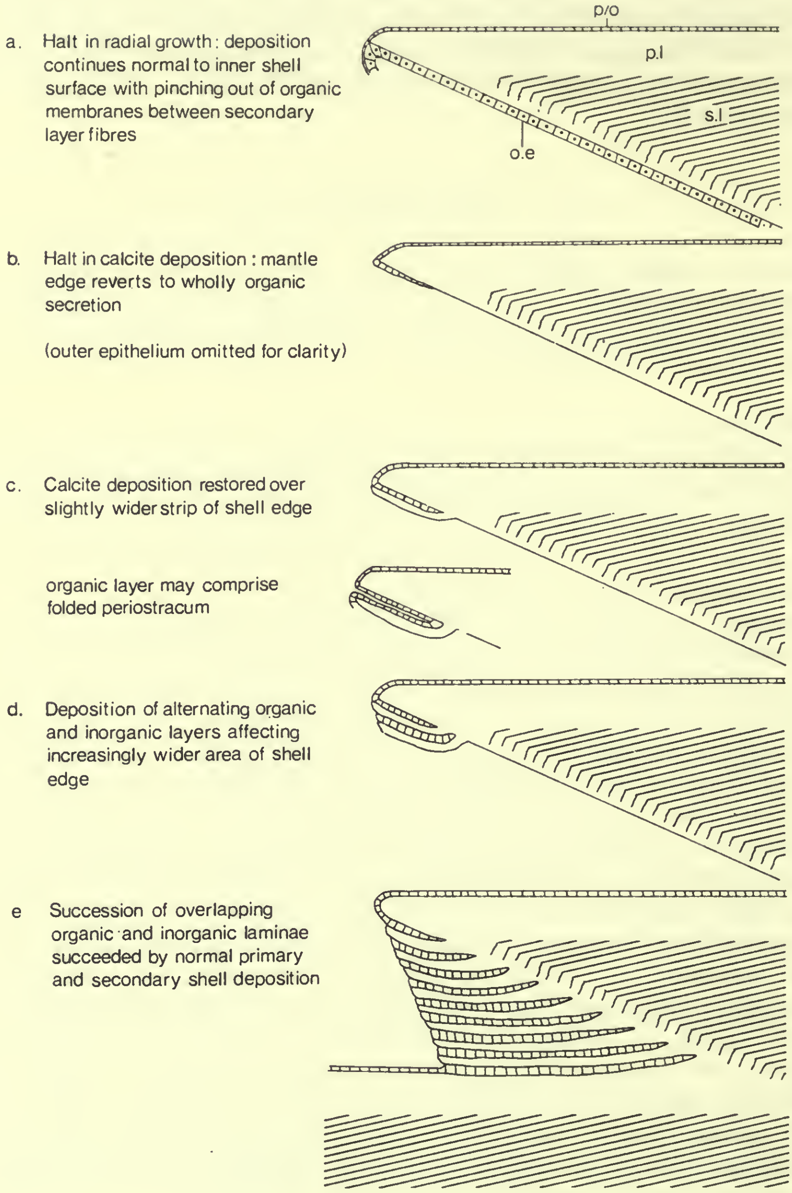
a. Halt in radial growth: deposition continues normal to inner shell surface with pinching out of organic membranes between secondary layer fibres
p/o
p.l
s.l
o.e
b. Halt in calcite deposition: mantle edge reverts to wholly organic secretion
(outer epithelium omitted for clarity)
c. Calcite deposition restored over slightly wider strip of shell edge
organic layer may comprise folded periostracum
d. Deposition of alternating organic and inorganic layers affecting increasingly wider area of shell edge
e Succession of overlapping organic and inorganic laminae succeeded by normal primary and secondary shell deposition

FIG. 4. a–e. Diagrammatic sections to illustrate the formation of a major overlapping shell unit by progressive mantle retractions at a valve margin of *Spiriferina* (p/o – periostracum, p.l – primary layer, s.l – secondary layer, o.e – outer epithelium).

scar are considerably more irregular in outline suggests that the terminal parts of the muscle base, which overlay the associated outer epithelium responsible for secreting myotest, were not evenly distributed. Since the presence of muscles in the vicinity of outer epithelial cells in Recent Brachiopoda has been shown to promote the formation of tonofibrils within each cell body, as well as drastically affecting its secretory behaviour (Williams 1968a : 14), it is reasonable to assume that the outer epithelial cells underlying the muscle bases of *Spiriferina* must have been similarly affected. The linear arrangement of the furrows within the ventral muscle field of *Spiriferina* is consistent with an overlying muscle base which has been segregated into distinct bundles of contractile tissue. Since the furrows, in general, run parallel to the median plane, as do the corrugated grooves on the cardinal process, it is reasonable to assume that the sheet-like bundles of muscle tissue must have run lengthwise in the same direction.

The ventral adductor scars are large in comparison with those of Recent Rhynchonellida and Terebratulida. They are impressed upon both sides of the median septum and consist of a number of furrows which run dorso-ventrally. These furrows are similar to the ones occupying the adjustor and diductor scars and represent the areas of emplacement of the terminal parts of the ventral adductor muscle bases. The median septum is built up of secondary layer fibres, where, in general, the fibres grow from base to apex. Within the dorso-ventrally aligned furrows, however, the shell structure is more irregular and typical of a myotest shell fabric. The contrast between modified and standard secondary layer fibres is well seen in transverse sections through the median septum where the myotest stands out as a zone of small, gnarled, irregularly stacked fibres which lies sandwiched between two layers of more orthodoxly stacked fibres (Pl. 4, figs. 4, 5). The stacking is most unorthodox and there is evidence of fusion of adjacent trails.

Growth of the ventral median septum takes place by the addition of secondary shell material along its anterior facing edge. As the septum expands in size, however, its posterior, earlier-formed parts are gradually overlapped by more secondary shell material deposited subsequently in the umbonal region. This later deposit spreads evenly over the older shell surface and so produces what appears, in transverse section, to be a sharp line of unconformity (Pl. 4, fig. 6).

Around the posterior ends of the ventral adjustor and diductor scars the muscle impressions are very deep. Behind the muscle scars, the shell is considerably thickened by an overlapping accumulation of secondary layer fibres which piled up behind the muscle base. In this area, although some groups of fibres grow anteriorly and antero-laterally, the great majority appear to be directed posteriorly. In radial section, fibres around the posterior part of the muscle scars, showing good cross-sectional outlines, are seen suddenly to change growth directions.

(ii) *Brachial valve*

The quadripartite dorsal adductor scars are situated symmetrically on both sides of a slight median rise, with the anterior pair more closely spaced together than the posterior pair. Viewed at low magnifications, the surface textures of the scars are distinctive and unlike those of the ventral scars. The surface topography of the

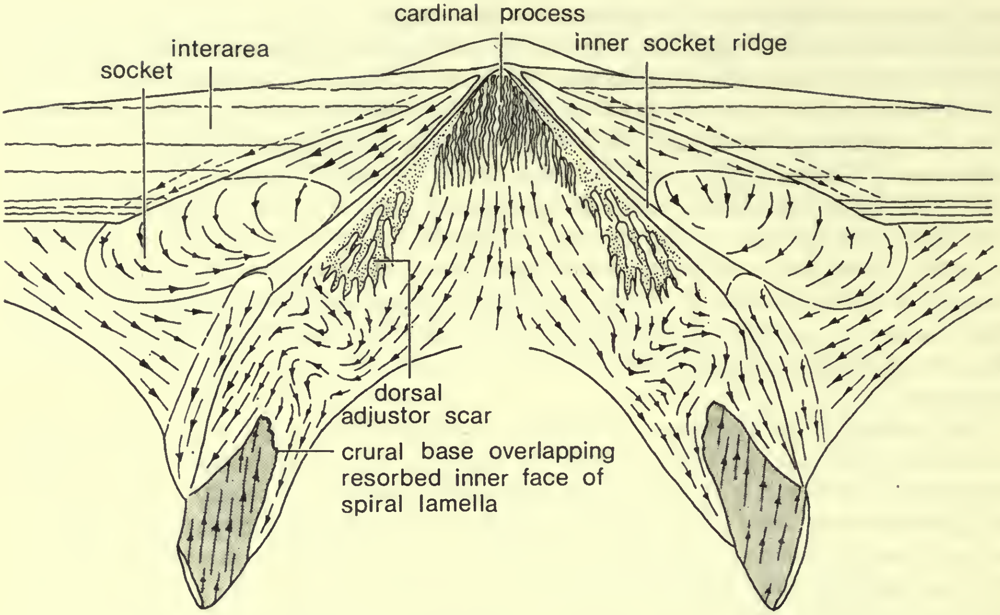

Fig. 5. Stylized drawing of the cardinalia of *Spiriferina* showing the growth vectors of the regular mosaic and the distribution of resorbed (stippled) irregular mosaic.

anterior scars is undulating with puncta occupying hollows between irregularly distributed mounds (Pl. 5, fig. 1). The surface of the posterior scar is, on the other hand, relatively flat. However, both sets of scars appear to be coated with a micritic crust so that the detailed shell ultrastructure cannot readily be discerned. On some parts of the surface, where the sedimentary coating is thin, it would appear that the under-surface is fibrous. However, the skeletal fabric is certainly unusual, for on broken parts of the shell myotest deposits bear little resemblance to the smooth regular outlines of fibres comprising the underlying shell succession (Pl. 5, fig. 2).

The cardinal process and the dorsal adjustor muscle scars are situated close to one another in the umbonal region of the brachial valve (Text-fig. 5). The striate cardinal process of *Spiriferina* closely resembles that of the terebratellacean *Terebratalia transversa* (Sowerby), in that it comprises a series of radially disposed, corrugated ridges, between 50 μm and 100 μm wide, made up of tightly interlocking secondary layer fibres (Pl. 5, fig. 3). The ridges extend from the posterior shell edge to terminate anteriorly as a series of buttresses which rise steeply from the valve floor. Antero-lateral to the cardinal process lie the dorsal adjustor scars which are inserted upon the crural bases. Both the cardinal process and each dorsal adjustor scar are themselves enclosed postero-laterally by an inner socket ridge. The adjustor scars are very deeply impressed upon the shell and, within each scar, a number of narrow stalks composed of secondary shell material project posteriorly at a low angle towards the umbo (Pl. 5, fig. 4). Since the surrounding parts of the shell surface are at a much higher level than that within the scars, it is obvious that the deep impressions of the adjustor scars have been fashioned as a result of strong resorption by the overlying outer epithelial cells which were attached to both dorsal adjustor muscle bases. The narrow stalks protruding from the floor of each scar are therefore not outgrowths of the shell. They are merely remnants of earlier-formed parts of the shell succession which have escaped resorption.

(iii) *Functional considerations*

In examining the surface topographies as well as the shell ultrastructure within the areas of muscle attachment in *Spiriferina*, some attempt has been made to reconstruct the morphology and disposition of its muscle system. The longitudinal 'striation' of the cardinal process and the flabellate pattern of the ventral diductor scars suggest that the diductor muscle fibres were segregated into a number of discrete bundles or sheets whose bases were accommodated within the various depressions of the shell. If the curiously ridged topography of the anterior dorsal adductor scars can be taken as a guide to the nature of the contractile tissue associated with them, then it seems likely that the adductor muscles consisted of a large number of spindle-shaped strands. Each strand was composed of a number of muscle fibres and corresponded to a ridge or hollow on the surface of the scar. However, it is possible that the posterior adductor muscles, like those in a number of Recent articulates (Rudwick 1961 : 1021), were striated. A variation in muscle composition between anterior and posterior adductors might explain the observed differences in surface texture within each pair of scars.

The close proximity of the inner arms of the spiralia and its transverse support, the jugum joining the distal ends of the crura, must have restricted the passage and emplacement of the muscle systems in *Spiriferina* to within relatively narrow limits. However, the size and distribution of the scars points to *Spiriferina* having had a rather strong and efficient muscle system. Mechanically it can be shown that muscles situated closest to the median line are most effective, since it is in such a position that the greatest proportion of the force is used either to open or to close the shell (Armstrong 1968b : 646).

Comparison of the myotest ultrastructures of *Spiriferina* with those of living brachiopods is not easy, for the muscle scar surfaces on which modified mosaic patterns might be displayed are usually badly affected by diagenesis. Either the surface may be covered by a thin micritic layer (as in the dorsal adductor scars) or, when this coating has been removed, the skeletal fabric may appear cracked and pitted (as in the ventral diductor scars). Since terminal faces located well outside the muscle scars of many other fossil genera, as well as *Spiriferina*, are found to be similarly affected, the existence of such ultrastructural irregularities on fibres incorporated within the muscle scars cannot be taken for certain as characteristic of any myotest shell fabric. Even though the detailed morphology of myotest fibres is obscured on the shell surface, some idea as to their overall shape and stacking can be obtained from a study of appropriately sliced radial and transverse sections. On carefully etched surfaces, the myotest fibres can be picked out readily on account of their distinctive size, shape and stacking.

(f) The brachidium

The brachidial apparatus of *Spiriferina* consists of a pair of calcareous spires which extend from the distal ends of the crura and are drawn out laterally away from the median plane. When viewed along the axis of coiling from base to apex, the left-hand spire is coiled clockwise and *vice-versa* for the right-hand spire. Just anterior to the distal ends of the crura, the innermost lamellae of each spire are connected by a curved jugum which is flattened dorso-ventrally (Text-fig. 6).

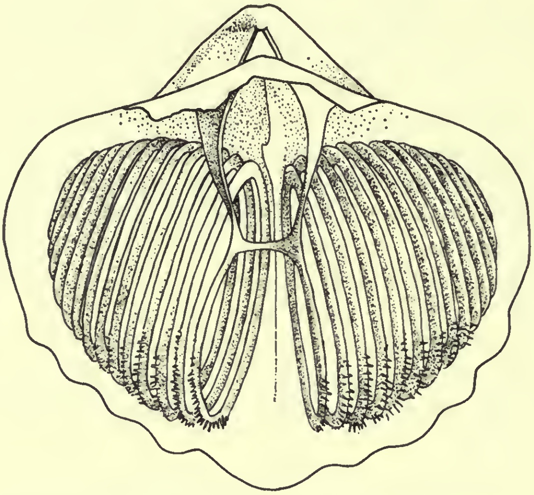

Fig. 6. View of the spiral brachidium of *Spiriferina walcotti* (Sowerby).

Davidson (1852 : 23–24) has given an accurate description of the spires belonging to the closely related species *Spiriferina rostrata* (Schlotheim) which possesses a spiral brachidium virtually identical to that found in *S. walcotti*. In describing the shape of a lamella, Davidson notes that it 'is neither smooth nor of equal thickness on all its width, differing on each side and variable, but always thicker on the inner side of the circumference than on the other which tapers out into an acute edge, and . . . the thickest part of the spire is towards its middle, where it forms a circular elevation, diminishing again towards the outer edge'.

As will be shown, the attitude and outline of the lamellae are important clues to the relationship between lophophore and spiralia. In this study, no set of spires completely free from matrix was available and observations were carried out on carefully selected horizontal and vertical transverse sections of intact spiralia entombed in rock matrix. However, a few fragments were extracted manually, so that it was possible to examine localized parts of the surface mosaic.

The spires are composed of secondary layer fibres which exhibit a distinctive and well-defined pattern of growth. Trails of fibres, exposed on the freshly broken surfaces of fragmentary pieces of spiral lamellae, are found to follow a crescentic path, convex towards the exterior, which runs from the inner to the outer edge of the

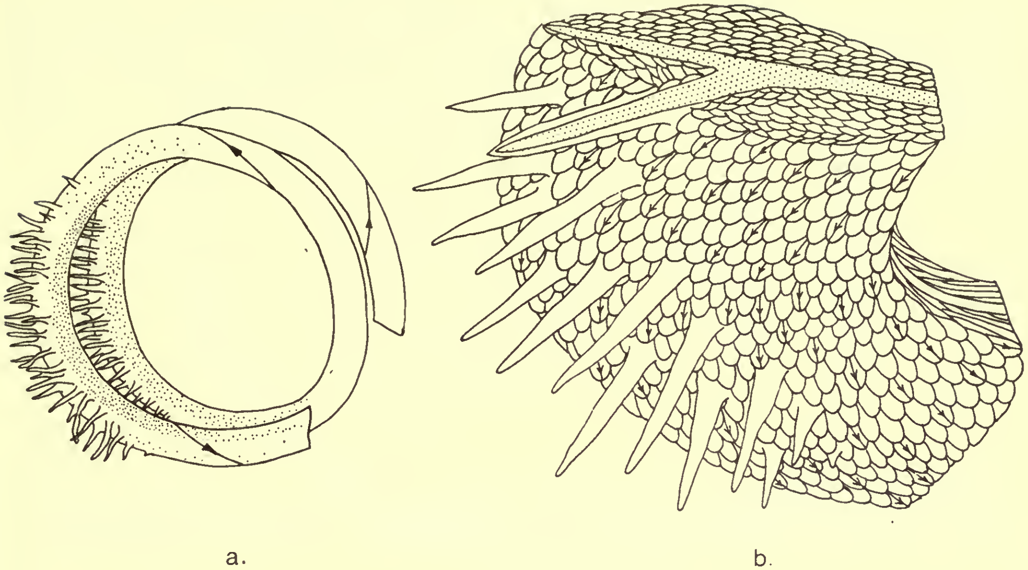

Fig. 7. a. Fragment of a spiral lamella showing the anterior projection of fine spines from the median-facing side. The orientation of fibre trails is shown by growth vectors. b. Schematic diagram of part of a spiral lamella showing the direction of growth of fibres. A mosaic is developed on both sides of the lamella so that, in section, fibres appear to arch outwards in both directions from a median plane. In sections through the innermost whorls, as shown here, a thin layer of non-fibrous calcite (stippled) is interposed between the two sets of fibres and is continuous with spine bases. The blunt inner edge of the lamella is undergoing constant resorption.

lamellae (Text-fig. 7a, b). In *Spiriferina,* shell deposition occurs on both the apical side (facing towards the apex of the spiralium) and basal side (facing towards the base of the spiralium) of the lamellae, so that in transverse cross-sections the convex faces of fibres are seen to arch outwards in both directions from a median plane. In effect, the path followed by each outer epithelial cell responsible for secreting the spiralia appears to be that of an equiangular (or logarithmic) spiral (Text-fig. 8). As the spiralium increases in size, the outer epithelial cells gradually migrate around the lamellae and so contribute to the growth of parts of the spiralium which are progressively more distant from its apex. In addition, if a tangential cut is made on a spiral lamella, the observed overlapping disposition of the long axes of secondary layer fibres (Text-fig. 9) indicates that, for the spiral lamella to expand continuously to fill the brachial cavity, new cells (and hence new fibres) must be proliferated continuously in a linear generative zone along the sharp leading edge of the lamella.

On certain parts of the spiralia there are surfaces of resorption. An area of resorption is readily recognized by the absence of a surface mosaic which is usually replaced by long exposed trails of fibres possessing no recognizable terminal faces. In transverse cross section, provided the surface of resorption is not coplanar with a growth surface, the distinction is clear-cut. The distinctive mode of stacking of fibres provides a convenient 'way-up criterion' (Williams 1968a : 8). The profile of the keel, which is convex towards the growing surface, serves to indicate the precise attitude of the depositional surface in that part of the shell at that moment in time. If groups of fibres, stacked in rows one above the other, are truncated by the existing surface profile, then resorption must have taken place.

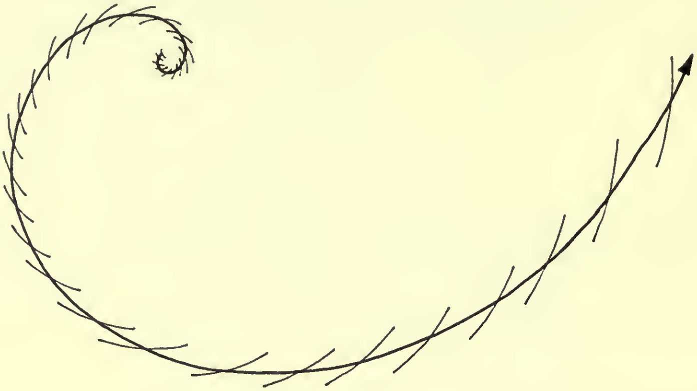

FIG. 8. Reconstruction of the growth path of a single fibre contributing to the growth of a spiral lamella. Only a small segment of the spiral is present at any one time since the inner edge of a lamella is constantly being resorbed.

Around the blunt inner edges of the lamellae fibres are resorbed. Some resorption also occurs on the basal sides of lamellae, especially on the posterior facing halves of the spires. Towards the dorsal and ventral extremities of each lamella, the zone of resorption gradually decreases until practically all outer epithelial cells on the basal side are actively secreting. As previously mentioned, the outer epithelial cells responsible for secreting each spiralium continually migrate backwards along the curved lamellae towards the median plane. This process does not continue indefinitely, however, for on the dorsal surface of the innermost lamellae of both spiralia, lateral to the jugum, resorption takes place.

On the anterior facing parts of the lamellae a considerable number of small spines project outwards at an oblique angle (Text-fig. 7a, b). As a rule, the spines always project from the basal sides of the lamellae whilst on the apical side the surface is devoid of any unusual outgrowths. Structurally they resemble the calcareous rods (taleolae) which permeate the shells of Plectambonitacea such as *Sowerbyella* (Williams 1970 : 339), in that the secondary layer fibres, deflected around the obliquely inclined cylindroid bodies, arch outwards towards their distal extremities. If the anterior facing part of a spiral lamella which bears the spinose projections is sectioned horizontally, the mode of formation of the spines becomes apparent from an examination of the newly exposed shell succession. Such sections of the innermost whorls of the spiralia expose a thin layer of non-fibrous calcite, about 10 μm wide, which runs from the blunt inner edge to the sharp outer edge of each lamella

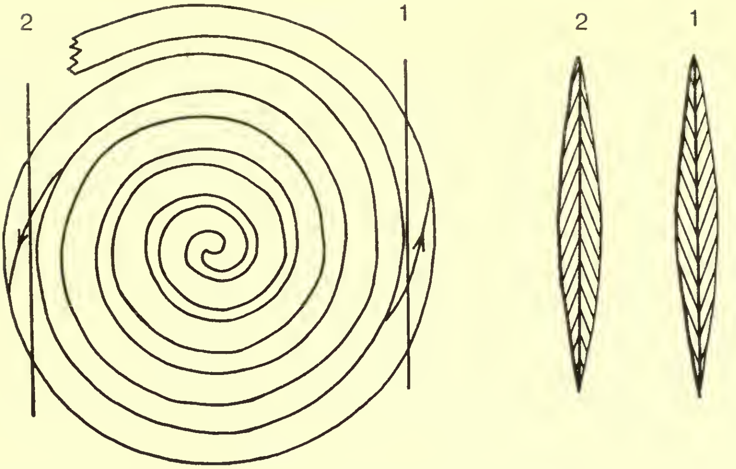

FIG. 9. Lateral view of a spire of *Spiriferina* showing lines of tangential section and the growth direction of fibres. In the anterior section (1), fibres diverge upwards from a median plane whereas in the posterior section (2), the fibres diverge downwards.

(Text-fig. 7b). At infrequent intervals, cylindroid bodies up to 60 μm in diameter swell out from this layer (on only the basal side of the lamella) and cause the surrounding secondary layer fibres to be deflected around them on all sides. Judging from the morphological differences between spines and fibres, and the sharpness of boundaries between them, there is every indication that each was deposited by a different type of cell. The manner in which the bases of spines are submerged in secondary layer fibres points to each spine having first been secreted by a small tubular evagination of specialized epithelium situated around the sharp, outer edge of the spiral lamella. As the diameter of each spiral whorl increased, the bases of spines were gradually overlapped by successive secondary layer fibres until finally they became engulfed in the resorbing epithelium situated at the blunt inner edge of the lamella. As well as forming the cores of the innermost whorls of the spiralia, the homogeneous calcite layer is also present within the jugum where it forms a prominent inner layer in transverse section. On the outer whorls of the spiralia, however, the layer is no longer present but spine bases continue to disrupt the shell succession. Evidently the specialized epithelium which gave rise to the subsidiary layer occupied the outer edges of the innermost spiralia and the jugum, but on the outer whorls was concentrated only in small circumgenerative zones which gave rise to isolated spinose outgrowths that did not otherwise affect the shell succession. The fact that the spines are situated only on that part of the spiralia facing the commissure tends to suggest that they may have served some protective function. The spines may have acted either as a prickly deterrent to predators seeking to devour the soft parts of the animal, or as a grille preventing coarse particles of sediment from entering the brachial cavity (assuming a lophophore current system which filtered food and water inwards through the arms of the spiralia).

(g) Articulation

The articulation provided by the teeth and sockets of *Spiriferina* is highly effective. Each is composed of secondary layer fibres, and by plotting the long axes of exposed trails as growth vectors, growth maps can be constructed for both structures. Since each fibre is a record of the path taken by each corresponding outer epithelial cell, growth maps can be used to interpret the nature of the build-up of both exoskeletal outgrowths in terms of bulk epithelial movements.

The dental sockets extend along the inner margins of the notothyrium from the umbo to the hingeline. On the median-facing side, each socket is bounded by a stout inner socket ridge whilst the overhanging edge of the interarea functions as an outer socket ridge (Text-fig. 5). Each socket can be divided into two regions with the anterior part forming a much deeper depression than the posterior part. In the anterior part, which accomodates the distal end of the tooth, the fibres grew across the socket from the overhanging edge of the interarea towards the inner socket ridge. In the posterior part, which was no longer involved in articulation and does not now come into contact with the point of the tooth, the fibres grew along the floor of the socket from the umbo outwards. As the outer surface of the dorsal interarea is composed of primary shell material, the directions of growth of the underlying secondary layer fibres are normally obscured. However, in specimens where the primary layer has been removed, the secondary layer fibres are seen to be directed outwards from the umbo parallel to the edge of the notothyrium.

The teeth and dental plates stand out as prominent features in the umbonal region of the pedicle valve. As well as functioning as part of the hinge mechanism, lateral outgrowths of the teeth also serve to restrict partially the triangular delthyrial opening. What appear, at first sight, to be a pair of disjunct deltidial plates are structures composed solely of secondary shell material. Each structure arises from that part of the tooth bordering the delthyrium and is fashioned into a laterally projecting ridge which runs from the apex of the delthyrium to the hinge line (Text-fig. 10). As similar ridged outgrowths of the teeth have been found bordering the delthyrium of *Spirifer trigonalis* (Dunlop 1962 : 491) and given the name *dental ridges*, it seems reasonable to apply the same terminology to the corresponding ridges in *Spiriferina*. The fibres comprising each dental ridge in *Spiriferina* grew along the length of the ridge from the delthyrial apex to the hinge line. Over the greater part of each tooth, fibres grew towards the distal end. However, on the side facing into the delthyrial cavity the pattern is more complex.

From the hinge line, part of the shell swells into a large bulbous ridge which is situated on the median-facing side of the tooth and just inside the dental ridge (Pl. 6, fig. 1 ; Text-fig. 10). This unusual outgrowth, which has been observed in every specimen so far examined, cannot be involved in articulation as it is situated on the opposite side of the hinge line from the distal end of the tooth. At its widest part the ridge is flattened and appears abraded. This observation is confirmed by a closer inspection of the surface which shows the exposed parts of fibres comprising that part of the ridge to be ragged and misshapen (Pl. 6, fig. 2). Due to the absence of any exoskeletal outgrowths on the brachial valve in the immediate vicinity, which

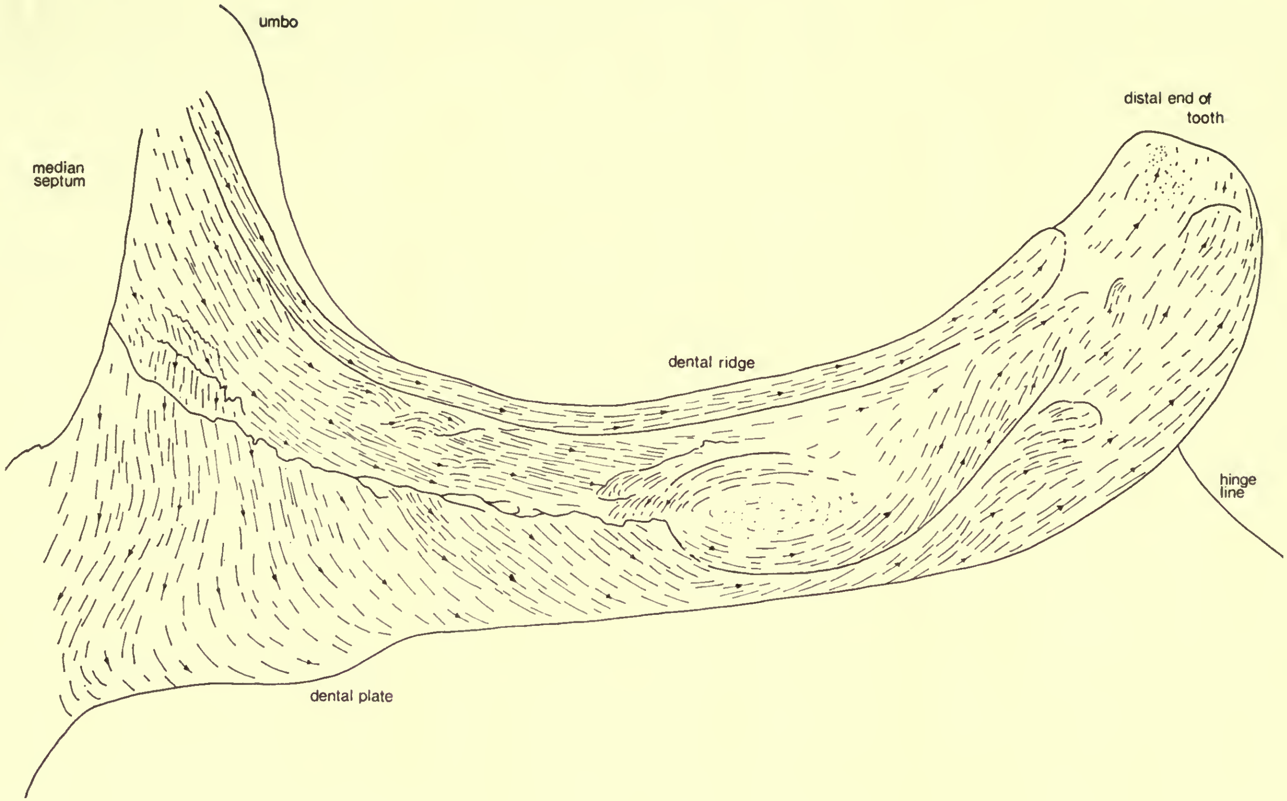
umbo
median septum
distal end of tooth
dental ridge
hinge line
dental plate

Fig. 10. Sketch of a tooth and associated structures of *Spiriferina* showing growth vectors of the secondary shell mosaic.

as a result of rubbing against the ridge could have given rise to such a shell fabric, it seems likely that the abrasion must have been caused by pressure and possible movement around the proximal end of the pedicle.

Both teeth fit snugly into the sockets of the brachial valve, but despite having to grow in a partially confined space, the distal extremities are still the main areas of growth on the teeth. In radial section, the cross-sectional outlines of fibres comprising the distal ends of the teeth show a rhythmic variation in direction of growth (Pl. 6, figs. 3, 4). At the point of the tooth the epithelium appeared to move in four consecutive directions – dorsally, laterally, ventrally, laterally – and then the sequence is repeated. If the two lateral movements of the cycle were in opposing directions, as seems likely, then the motion would be helical.

IV. SHELL STRUCTURE OF OTHER SPIRIFERIDA

(a) Atrypidina

According to Boucot *et al.* (1965 : H632), the Atrypidina are divided into two superfamilies based on the attitude of the spiralia. The Atrypacea bear spiralia with apices directed medially or dorso-medially, whereas the spiralia of the Dayiacea are directed laterally or ventrally. From an evolutionary standpoint, the Atrypidina are important since they include the earliest forms of spire-bearing brachiopods. Cooper (1956 : 136) cites a small undescribed form from the Row Park Formation of Maryland and another, possibly the same species, from the Crown Point Formation of New York (both Middle Ordovician) as stratigraphically the oldest yet recorded, but interior details of neither are known. They both appear to have '*Protozyga*-like' shells, and on this basis Cooper regards the slightly younger *Protozyga* s.s. as the most primitive of all Spiriferida. By late Ordovician times several stocks of spire-bearing brachiopods had become established. These include the small costate or multiplicate atrypaceans *Protozyga*, *Zygospira*, *Hallina* and *Catazyga*.

(i) *Atrypacea*

Though impunctate, the calcareous shell succession of *Protozyga elongata* Cooper from the Lower Bromide Formation (Upper Ordovician) of Oklahoma is broadly comparable with that of *Spiriferina walcotti* (Sowerby). *P. elongata* is small, seldom more than 5 mm in length, and thin-shelled. Its primary layer, measuring up to 10 μm in thickness, is composed of narrow crystallites with long axes disposed normal to the isotopic primary/secondary layer boundary. The secondary layer is also comparatively thin and has not been found to exceed 50 μm. Transverse sections across the widest part of the shell reveal a succession of small, flattened fibres which although irregular in profile are stacked in a very compact fashion (Pl. 6, fig. 5). Close to the valve margins fibres measure between 4 μm and 6 μm in width, but towards the postero-median regions of the same specimen lateral boundaries of individual fibres tend to amalgamate and produce a more massive skeletal fabric. In view of the irregular nature of the remainder of the skeletal succession, which may in any case have been diagenetically induced, it would be hazardous to guess as to the physiological significance of such a variation in fabric. However, if the overall irregularity in fibre profile is a primary feature, then the welding together of adjacent parts of fibres may reflect deposition by outer epithelial cells whose normal secretory processes were disrupted due to the encroachment of a muscle base. Were it not that *Protozyga* possessed a rudimentary spiralium of generally less than one convolution, it might easily be mistaken for a small, mildly plicate rhynchonellid.

Compared with *Protozyga, Zygospira* is further advanced along the spiriferid line of descent, in that it possesses a more fully developed spiralium of up to four convolutions with apices directed medially. Specimens of *Zygospira modesta* (Say), collected from beds assigned to the Richmond Group (Upper Ordovician) exposed near Nashville, Tennessee, reveal a secondary shell fabric which is more regular than that of *Protozyga elongata*. Although the shell exterior of *Zygospira* is markedly costate, the undulations of the costae are not preserved on the inner surface of the valves. When traced any great distance from the shell margins, the secondary layer fibres tend to fill out and eliminate the undulations so that both valves are thickened below the ribs and correspondingly reduced below the intervening grooves. Cross-sectional outlines of mature secondary layer fibres generally conform to a flattened diamond shape and measure about 10 μm to 12 μm in width (Pl. 6, fig. 6). As shown below, the outlines of sectioned secondary fibres are important in providing a means of deducing the pattern of the internal secondary shell mosaic. On this basis, the terminal faces of *Zygospira* are clearly rhomb-shaped (as opposed to smoothly curved in *Spiriferina*) with the longer diagonal of each rhombohedron coincident with the long axis of each corresponding fibre trail. The regular diamond-shaped outlines of fibres, though present over the greater part of both valves, are disrupted within the vicinity of the dorsal and ventral muscle scars ; but such localized modifications in the secretory regime do not lead to any great thickening of the shell succession in either valve.

In the related *Catazyga headi* Billings from the Richmond Group of Adana County, near Winchester, Ohio, the pedicle valve in particular is greatly thickened around its posterior regions. Anteriorly the shell thickening is confined to a median platform, probably a muscle platform, but towards the umbonal region deposition becomes more pronounced in the areas laterally adjacent to the scars. As a result of this postero-lateral shift in the main zone of calcification the level of the ventral muscle scar surface changes from being an area which anteriorly was above that of the surrounding floor to that of a deep impression. In cross-section, a primary layer about 20 μm thick is succeeded by secondary layer fibres which are diamond-shaped, like those of *Zygospira* (Pl. 7, fig. 1). Fibres comprising the lateral and anterior regions of both valves usually measure between 10 μm and 12 μm in width, but away from the margins there is an increase in fibre size with widths of 20 μm to 25 μm becoming common. Within the areas of maximum shell deposition, the secondary fibres give way to a coarse tertiary prismatic layer (Pl. 7, fig. 2). Compared with the uniformly stacked 'columns' of the Recent terebratulide *Gryphus vitreus* (Born) (MacKinnon 1971b : 41), the tertiary layer of *Catazyga* is rather irregular. This is due mainly to the impersistent nature of adjacent crystal boundaries which, though generally aligned normal to the inner shell surface in true 'prismatic' fashion, tend to migrate laterally from time to time. The whole of the tertiary layer appears to take on a 'jigsaw-puzzle' type of shell fabric which is considered to be transitional between that of an orthodoxly stacked secondary layer and the more conventional 'columnar' tertiary layering which is typical of certain later spiriferide genera. In places, the prismatic shell material gives way both laterally and vertically to normal fibrous outlines, so that the outer epithelial cells responsible for secreting the tertiary layer were obviously capable of reverting to secondary shell deposition. The probability is high that such a distinctive tertiary layer fabric is original, for gently etched sections of *Catazyga* are, in places, traversed by a fine depositional banding. The banding, which persists across numerous adjacent crystalline boundaries, is similar to that found in sections of living *Gryphus*.

Around the shell margins of *Catazyga* there is evidence that the mantle became detached periodically or, at least, reverted to primary shell deposition. From a point near the outer shell edge, a wedge of primary shell material, about 35 μm at maximum thickness, dips posteriorly inwards to terminate a short distance from the inner shell surface (Pl. 7, fig. 3). This wedge is bounded on either side by orthodoxly stacked secondary layer fibres. Unlike similar wedges occurring in some Recent Brachiopoda, the primary shell material is not massive but is composed of a series of regularly stacked crystallites between 8 μm and 12 μm in width which stand at right angles to the earlier-formed parts of the secondary shell succession. As the boundaries between primary and secondary deposits are indistinct, it is not known for certain whether a clear break in deposition did occur before the changeover. However, if the fabric of the primary shell wedge is original, it is possible that organic membranes, continuous with those in the preceding secondary layer, ensheathed the primary layer crystallites. For such to be the case would not require complete mantle detachment, but merely a temporary reversal from secondary to primary shell deposition.

Contemporaneous with the ribbed zygospirid stock, but less common, are certain smooth-shelled Atrypacea, including *Idiospira*, which are assigned to the family Lissatrypidae. In transverse sections of *Idiospira thomsoni* (Davidson), from the Craighead Limestones (Caradoc) of the Girvan district, the outlines of secondary layer fibres are variable. Some sections show neatly stacked fibres with smooth curved outlines (Pl. 7, fig. 4), which contrast with the sharp, angular outlines of fibres comprising the shells of *Zygospira* and *Catazyga*, whereas other parts of the shell succession (Pl. 7, fig. 5), exhibit irregular outlines which resemble those of *Protozyga*. Judging from the way in which, in *Idiospira*, these fibres with smooth symmetrical outlines are seen to merge with neighbouring groups of irregularly stacked fibres, it seems highly likely that the latter are the product of secondary recrystallization across adjacent fibre boundaries. If this is the case, then the original secondary shell mosaic of *Idiospira* consisted of alternating rows of smooth spatulate terminal faces and not diamond-shaped outlines as in other Atrypacea. No tertiary layer has been found in *Idiospira*.

In Silurian and Devonian Atrypacea the external (and internal) morphology of both valves became highly diverse, yet much of this variety of form can be rationalized into two main components. These are a radial pattern of ribs and a concentric pattern of overlapping growth lamellae (Copper 1967 : 123) ; both components are usually built up from primary and secondary shell material. Complete specimens of five Siluro-Devonian forms were available for study. These were *Atrypa reticularis* (Linné) from the Wenlock Limestone of Shropshire, *Atrypa* sp. from the Upper Hamilton Group (Middle Devonian) of New York, *Atrypina hami* Amsden from the Haragan Formation (Lower Devonian) at White Mound, Murray County, Oklahoma, *Spinatrypa* sp. from the Hackberry Stage (Upper Devonian) of Rockford, Iowa, and *Desquamatia subzonata* Biernat from the Givetian shales of Skaly in the Holy Cross Mountains, Poland.

In all five stocks, the primary layer is well developed and usually attains a maximum thickness of up to 40 μm below the rims of overlapping growth lamellae where it is best protected from abrasion. As well as revealing a porous texture, sections of this thin outer layer (e.g. Pl. 7, fig. 6) show it to be traversed by a fine lineation which is orientated either at a steep inclination or normal to the outer shell surface.

The shape and stacking of secondary layer fibres are also remarkably uniform and compare well with those of *Catazyga* and *Zygospira* (but not *Idiospira*). In sections of the Middle Devonian species of *Atrypa* the outlines of secondary layer fibres are well defined (Pl. 8, fig. 1). Diamond-shaped profiles of sectioned fibres which measure, on average, about 25 μm in width are characteristic not only of this genus but also of all other representatives examined. Since even the early zygospirid stocks exhibit similar fibre outlines, it seems reasonable to assume that this feature was common to the family Atrypidae as a whole. In this respect, representatives of the Lissatrypidae (the smooth-shelled Atrypacea) have still to be investigated.

Copper (1967 : 127) has examined optically the shell structure of a number of Devonian Atrypacea by means of cellulose acetate peels. In more 'advanced' and 'complex' atrypids like *Gruenewaldtia*, *Mimatrypa*, *Spinatrypa* and *Atryparia*, he reports that secondary layer fibres are consistently larger than those of other related genera.

At regular intervals in the shell succession, groups of secondary layer fibres are outwardly deflected towards the primary layer in a manner reminiscent of punctation, but at the centre of such deflections no hollow canals are found. Instead, the clear-cut diamond-shaped outlines of fibres degenerate into a central nucleus of irregularly interwoven accretions (Pl. 8, fig. 2) which resemble in appearance the myotest shell fabric of certain living articulates, such as *Notosaria*. Since the outer epithelial cells responsible for the deposition of the latter are known to be permeated by dense concentrations of tonofibrils associated with muscle attachment, it is reasonable to assume that the cells responsible for the outward deflections of the *Atrypa* shell must have been affected to a similar degree. Over the greater part of the inner shell surface, excluding muscle areas and exoskeletal outgrowths, these outward deflections of the secondary layer find expression as a series of pits which have been recognized, in the past, as gonadal markings (Pl. 8, fig. 3). Presumably the gonads were attached to the outer epithelium and caused it to bulge outwards at points represented by the pitting on the shell surface. Modifications in the shell surface can thus be attributed to a breakdown in the normal processes of deposition such as are found under muscle attachment areas with a localized spread in the organic secretory phase and a corresponding reduction in mineral exudation.

The concentric overlapping growth lamellae adorning the surfaces of so many Atrypacea were deposited by the marginal parts of both mantle lobes, which were subject to periodic fluctuations in secretory behaviour (Pl. 8, figs. 4, 5). Both primary and secondary shell layers are affected but not in the manner described for *Spiriferina*. The structural relationships between overlapping shell units are, however, closely comparable with those described for Recent articulates by Brunton (1969 : 192) and Williams (1971a : 61). Each planar surface, along which the normal sequence of shell deposition was interrupted, dips posteriorly at a low angle towards the shell interior. In all genera examined, such regression planes invariably interrupt the secondary shell succession and none was found which could be considered to have affected only the primary layer. Sandwiched between the regression plane and the immediately younger parts of the shell succession is a wedge of primary shell material which thins posteriorly. Where the wedge thins out, the regression plane is marked by a narrow zone of sharply flexed fibres which can be traced running posteriorly for a short distance before becoming lost in the remainder of the secondary shell succession.

In the coarsely plicate form *Spinatrypa*, tubular prolongations of the ribs extend outwards from the inner edge of each prominent overlapping growth lamella. The spines grew in such a way that their development was complete before the onset of the succeeding mantle regression. Initially a spine was merely a gently curved extension of a rib-crest but gradually, due to peripheral accretion, the opposing edges grew round towards one another and met on the underside (Text-fig. 11). Where the two edges have come together a seam is preserved. The spines are built up from primary and secondary shell material.

Since each concentric row of spines is succeeded by a plane of regression, it is evident that no sooner had a row of spines grown to maturity than its outer epithelial lining became detached due to mantle retraction. If the regression was slow, the inner surfaces of spines may have been covered by a periostracal deposit, but in any case they could not have been functional for any length of time. With the onset of shell deposition after the mantle regression the base of the spine was overlapped by subsequent primary and secondary shell layers so that no further contact with the mantle was possible.

In addition to possessing a well-developed primary and secondary shell succession, Silurian and Devonian Atrypidae are characterized by an inner tertiary layer deposit which may be massive or interdigitate with parts of the secondary layer (Pl. 8, fig. 6). The tertiary layer attains maximum thickness in the postero-median region of both valves, but around the valve margins only primary and secondary shell deposition occurs. The nature of the tertiary layer is variable, even within a single specimen, and may either consist of a series of vertically disposed crystals with well-defined boundaries or be massive. When clear-cut crystal boundaries are present they are commonly in structural continuity with the outlines of underlying secondary layer fibres.

Tertiary layer deposits are also found within muscle scars. In *Atrypa*, the areas of muscle attachment are deeply impressed on the inner surfaces of both valves. In

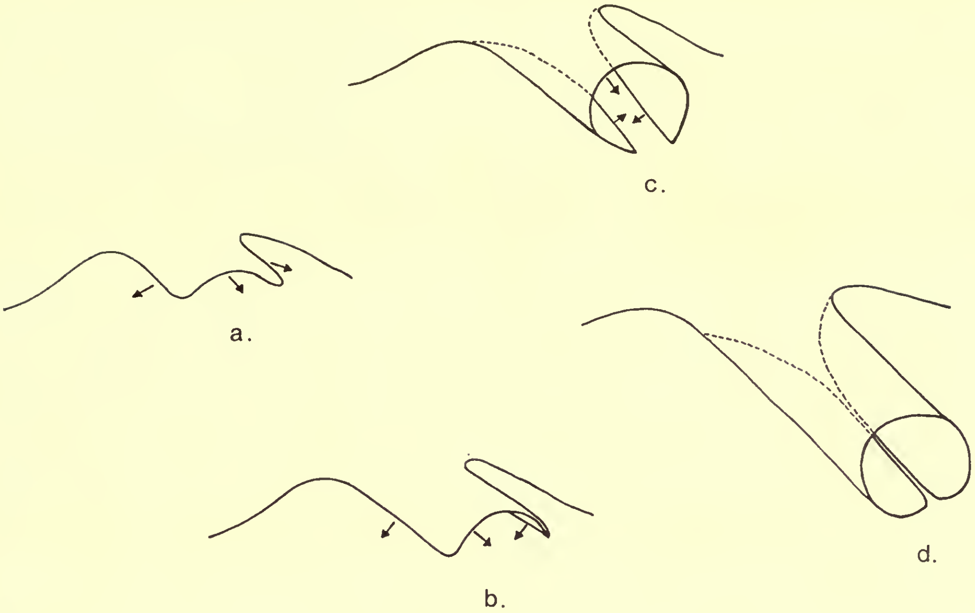

FIG. 11. a–d. Progressive stages in the formation of a tubular spine at the anterior edge of an overlapping growth lamella in *Spinatrypa*. Opposing edges grow round towards one another (see arrows) to meet on the underside.

transverse sections through the ventral muscle scars, a succession of secondary and tertiary layers in alternation is unconformably overstepped by a thick tertiary prismatic myotest (Text-fig. 12). The junction between myotest and underlying shell layers is sharp (Pl. 9, fig. 1) and, judging from the way in which successive secondary and tertiary layers are overlapped, it is evident that earlier-formed parts of the shell succession which lay in the path of the advancing muscle base were resorbed. An examination of ultrasonically cleaned ventral adductor and diductor muscle scar surfaces reveals a fabric very similar to that found in *Gryphus*. The outlines of individual crystals are highly irregular and lateral margins of adjacent ones interdigitate (Pl. 9, fig. 2). These terminal faces of tertiary layer crystals, upon which deposition took place, are rough and undulating and although some of this unevenness may be due to secondary diagenetic effects, it is probably for the most part original. Outside the muscle scars the terminal faces of tertiary layer crystals are virtually the same as those inside, and no clear-cut distinction between them at the submicroscopic level can be made.

Deposition of the atrypid tertiary layer must have taken place in a manner very similar to that occurring in living *Gryphus*. Instead of depositing obliquely disposed fibres ensheathed by protein membranes, the tertiary layer epithelium reverted to deposition in a plane normal to the inner shell surface. As Copper has shown (1967 : 129), there are some differences in the size and distribution of the secondary and tertiary layers within the atrypid group as a whole. Both *Atrypa* and *Desquamatia* examined by 'Stereoscan' show generous interlayering, but in later *Desquamatia*, according to Copper, the interlayering decreases. The disappearance of numerous interlayers and the thickening of the tertiary layer are also typical of *Spinatrypa, Spinatrypina, Atryparia* and *Kerpina.* In *Gruenewaldtia* and *Mimatrypa* the tertiary layer thickening becomes extreme and adjacent crystals merge to produce a more massive deposit.

(ii) *Dayiacea*

The Dayiacea include both smooth and plicate forms which bear spiralia with laterally or ventrally directed apices. In the earliest known genus *Cyclospira,* however, the spiral lamellae are coiled more or less in a plane parallel to the median plane of the valves. Although *Cyclospira* is reported to be ajugate, it closely resembles *Dayia* in morphology. Both have smooth, unequally biconvex shells with their pedicle valves more convex, and Schuchert and Cooper (1932 : 27) drew attention to the close similarity in their ventral muscle scars. The only other representative of the Dayiacea examined was *Coelospira,* which differs from the other two mainly in being plicate.

Although much of the shell material of *Cyclospira* sp. from the Upper Ordovician (Ashgillian) of Pomeroy, Co. Tyrone, Northern Ireland, was altered by recrystallization, it was possible to recognize parts of the secondary and tertiary succession. No primary layer was preserved. Secondary layer fibres which are diamond-shaped in transverse section measure about 12 μm in width (Pl. 9, fig. 3). The best preserved parts of the tertiary shell succession were located below parts of the ventral muscle scars. In those areas, the boundaries between tertiary layer crystals are impersistent but a prominent depositional banding delineates former cell boundaries (Pl. 9, fig. 4). The thickness of individual growth increments varied between 0·2 μm and 0·8 μm and prominent bands could be traced running across several adjacent crystal boundaries. The banding is closely comparable with that observed in sections of the tertiary layer of *Gryphus.*

A specimen of *Dayia navicula* (Sowerby) from the Dayia Shales (Ludlovian) of Shropshire provided the history of exoskeletal secretion in that genus. Both valves had been largely stripped of their thin outer primary layer but secondary layer fibres up to 20 μm wide showed good diamond-shaped outlines in transverse section (Pl. 9, fig. 5). As far as is known, tertiary layer deposits (Pl. 9, fig. 6) are restricted to the posterior regions of the pedicle valve, for no such deposit has been found in the brachial valve. The median septum which adds thickness to the brachial valve is composed solely of secondary shell material. Vertically stacked tertiary layer crystals have clearly defined outlines which measure, on average, 18 μm in thickness. These outlines are initially in continuity with the outlines of underlying secondary layer fibres. The overall pattern of tertiary layer deposition resembles that of *Catazyga* in that individual crystals are laterally deflected either one way or the other at fairly regular intervals to produce a 'jigsaw-puzzle' type of shell fabric. No interlayering of secondary and tertiary layer deposits was noted.

Although the only specimen of *Coelospira* available for study (*Coelospira saffordi* (Foerste) from the Brownsport Formation of Western Tennessee) was found to be

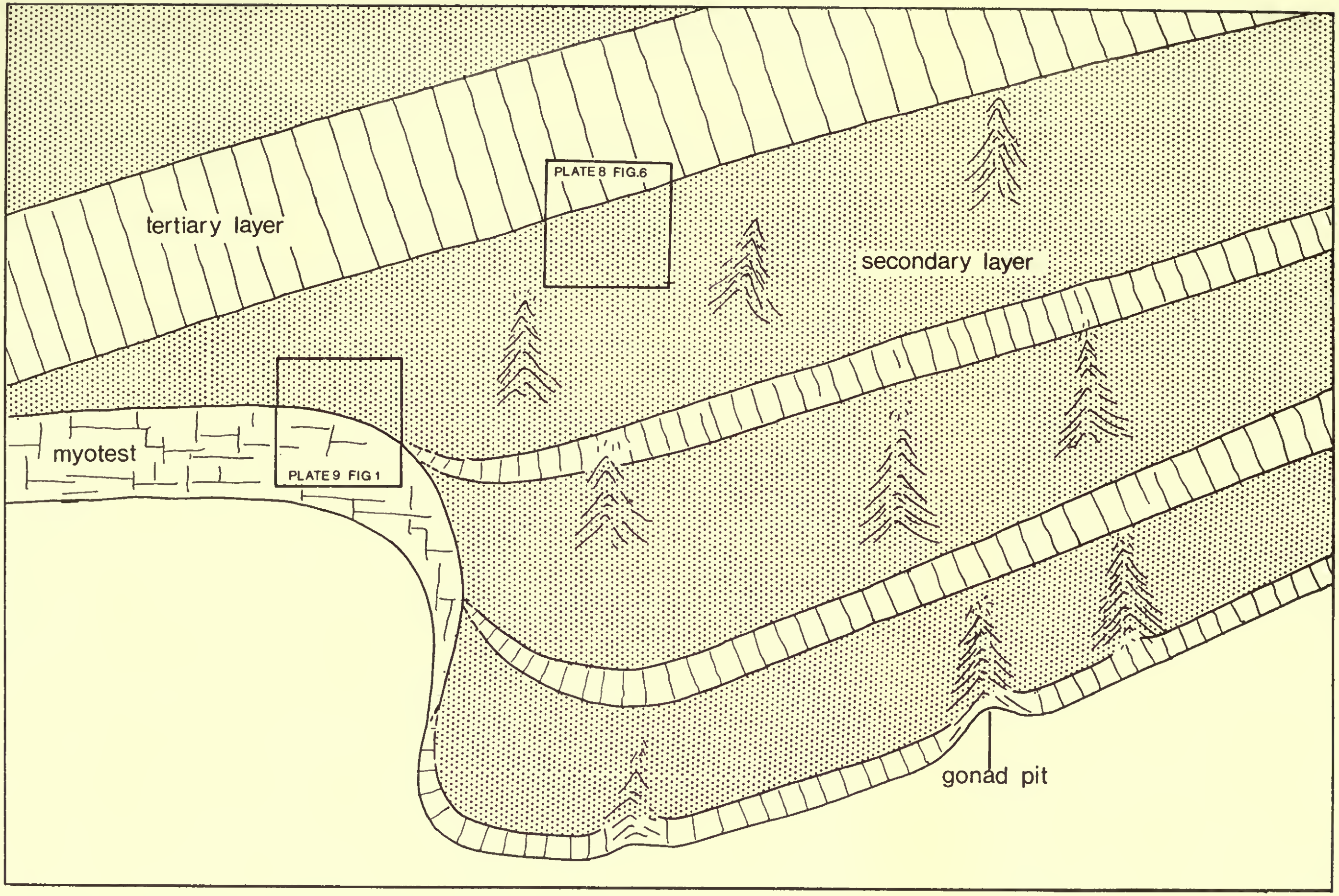
tertiary layer
PLATE 8 FIG.6
secondary layer
myotest
PLATE 9 FIG 1
gonad pit

Fig. 12. Stylized section through part of a pedicle valve of *Atrypa* showing the distribution of secondary and tertiary layers. The ventral myotest is situated at a lower level than the surrounding floor of the valve and 'oversteps' earlier-formed parts of the shell succession. The locations of Plate 8, fig. 6 and Plate 9, fig. 1 are shown.

partially silicified, remnants of three calcareous shell layers were recognized. The primary layer, which attains a thickness of about 12 μm, is composed of narrow crystallites stacked normal to the outer shell surface. The outlines of secondary layer fibres tend to be more rounded than those of other Dayiacea or Atrypacea, apart from *Idiospira*, and cross-sections reveal orthodoxly stacked groups with gently curved keels and saddles (Pl. 10, fig. 1). Shell deposition in the postero-median region of the pedicle valve was about three times as great as that in the corresponding part of the brachial valve. A thick tertiary layer, which has no counterpart in the brachial valve, augments the pedicle valve succession (Pl. 10, fig. 2). As in *Catazyga*, secondary layer fibres comprising the flanks of the pedicle valve pass laterally into a more massive tertiary layer which coincides roughly with the areas of ventral muscle attachment. The fabric of the tertiary layer in *Coelospira* is similar to that found in *Dayia*.

(b) Retziidina

The suborder Retziidina comprises costate and multiplicate rhynchonelliform Spiriferida with a medially directed V-shaped jugum and laterally directed spiralia. On the basis of presence or absence of shell punctation, the suborder is split into two superfamilies, respectively the Retziacea and Athyrisinacea (Boucot *et al.* 1964 : 813). Specimens of only four punctate genera were available for study. These were *Homeospira evax* (Hall) from the Waldron Formation (Upper Silurian) of Indiana, *Rhynchospirina maxwelli* Amsden from beds of the Haragan Formation (Lower Devonian) at White Mound, Murray County, Oklahoma, *Hustedia radialis* (Phillips) from the Arden Limestone (Lower Carboniferous), Arden, Lanarkshire, and *Retzia* sp. from the St Cassian Beds (Triassic) of Northern Italy.

A well-developed primary layer, on average 25 μm thick, is characteristic of all four genera. In the *Rhynchospirina* (Pl. 10, fig. 3) and *Homeospira* (Pl. 10, fig. 4) it was found to be partially recrystallized, but in *Hustedia* (Pl. 10, fig. 5) and especially *Retzia* (Pl. 10, fig. 6) features such as the porous texture and fine lineations disposed normal to the shell layers were seen, reminiscent of the primary layer fabric of Recent articulates. In *Retzia* sp. a fine depositional banding with an average periodicity of 0·8 μm has been recognized (Pl. 11, fig. 1). This banding, which is considered to be diurnal, dips posteriorly at a low angle from the outer shell surface to the inner primary/secondary shell layer interface.

Fibres comprising the secondary layer of the Retziidina are consistently small. Indeed, in none of the genera examined were any found which had grown to a width much in excess of 10 μm. Secondary layer fibres of *Homeospira* and *Rhynchospirina* are generally rather irregular in outline although this unevenness is probably of secondary diagenetic origin. However, in *Retzia* and *Hustedia* transverse sections reveal orthodoxly stacked fibres which possess smoothly rounded keels and saddles. The shape and stacking of the fibres indicate a regular internal secondary shell mosaic pattern made up of alternating rows of smooth, spatulate terminal faces like those in *Spiriferina*. Depositional banding with a periodicity of between 0·15 μm and 0·4 μm was recognized in sectioned fibres of *Retzia* sp. (Pl. 11, fig. 2).

The endopunctate condition of the Retziidina closely resembles that of Recent Terebratulida. In *Homeospira* and *Rhynchospirina* puncta measure about 10 μm in diameter, whereas in *Hustedia* and *Retzia* (Triassic) they measure up to 25 μm. Normally the puncta are unbranched, but with continuing deposition below the crests of ribs, several discrete puncta may gradually encroach upon one another to unite, eventually, as one central canal (Pl. 10, fig. 6). As well as being deflected laterally, secondary layer fibres forming puncta also arch outwards towards the shell exterior. Within the primary layer, the slightly bulbous distal ends of puncta are separated from the shell exterior by a thin canopy of calcite between 2 μm and 4 μm thick (Pl. 11, figs. 3, 4). Although such canopies are grossly recrystallized or broken, it seems reasonable to assume that they were perforated by minute canals such as are found in Recent Terebratulida (Owen and Williams 1969) and *Spiriferina* (MacKinnon 1971a).

(c) Athyrididina

The Athyrididina are divided into two superfamilies, the Athyridacea and Koninckinacea, to include smooth or plicate, short hinged forms with spiralia directed laterally and ventrally respectively. The two superfamilies are easily distinguishable, since Athyridacea are generally biconvex in profile whereas the Koninckinacea include only concavo-convex forms.

(i) *Athyridacea*

The shell structure of early Athyridacea is closely comparable to that of contemporary Atrypacea in that three calcareous shell layers are recognizable. In *Meristella atoka* Girty, from the Haragan Formation at White Mound, Oklahoma, a well-developed primary layer measuring up to 20 μm in thickness can be identified (Pl. 11, fig. 5) and traces of fine transverse banding, which are indicative of periodic deposition, are occasionally preserved. Transverse sections through the shell layers reveal a succession of secondary layer fibres which measure up to 25 μm in width. Judging from the regular stacking of secondary layer fibres which display smoothly curved keels and saddles, it is evident that the internal mosaic comprises alternating rows of terminal faces with arcuate anterior margins. The tertiary layer is exceptionally thick, especially in the pedicle valve (Pl. 11, fig. 6). In sections through the pedicle valve of *Meristina tumida* (Dalman) from the Silurian (Wenlock) of Gotland, tertiary layer crystals stacked normal to the shell surface were found to constitute over 80 per cent of the calcareous shell succession. Traced inwards from the secondary/tertiary layer interface, vertical intercrystalline boundaries are fairly persistent but some appear to die out as a result of amalgamation of adjacent crystals (Pl. 12, fig. 1).

The ventral muscle scars of *Meristella* and *Meristina* are deeply impressed in the postero-median region of the pedicle valve. Transverse sections across the muscle scars reveal that, apart from causing a localized depression on the inner shell surface, the tertiary layer fabric is unaffected. It is evident, however, that shell deposition within muscle scars did not proceed at the same rate as in laterally adjacent areas. The fact that the shell succession is thinner under muscle scars may be attributable to a partial reversal in the secretory behaviour of the outer epithelium from mineral to organic exudation as a means of maintaining adhesion between shell and tissue. In the brachial valve of *Meristella* the dorsal adductor scars are impressed on secondary shell material The myotest fabric produced by the breakdown in secondary shell deposition is very irregular (Pl. 12, fig. 2) and can be traced running posteriorly within the shell succession, and diminishing in extent, towards the umbo.

Many Athyridacea are characterized by the development of a cardinal plate extending across the apical region of the brachial valve. Such a structure, which may be perforated posteriorly, is built up laterally of outer hinge plates and medially of either conjunct inner hinge plates or one single plate. In *Meristella atoka* Girty the cardinal plate is depressed medially and is supported by a median septum which extends forward for half to two-thirds the length of the valve. When sectioned transversely, the structure is Y-shaped, with the base of the letter Y corresponding to the base of the median septum and the crural bases situated at points represented by the other two extremities (Pl. 12, fig. 3). Both the cardinal plate and supporting septum must have grown as one unit in the same way as that described for the *spondylium simplex* of *Skenidioides* by Williams and Rowell (1965 : H114), for the convex faces of secondary layer fibres (keels) are invariably directed away from the median plane of the septum. Growth on the underside of the cardinal plate was continuous with that on the flanks of the median septum and on the upper surface of the cardinal plate which faces toward the pedicle valve. However, as might be expected, part of the shell fabric on the upper side of the cardinal plate, which would be deposited by outer epithelial cells in contact with the dorsal region of the pedicle base, is grossly modified. In a deposit up to 50 μm thick, which coats the upper surface of most of the cardinal plate, the outlines of individual fibres are destroyed and replaced by a highly porous fabric (Pl. 12, fig. 4) which is roughly lineated normal to the shell surface in a manner reminiscent of a primary layer fabric. Apart from the sporadic lineations, it may also be compared with the fabric of the neighbouring dorsal adductor myotest. Presumably the cardinal plate served as the area of attachment for the dorsal ends of the dorsal pedicle adjustor muscles. Indeed, within the brachial valve of *Waltonia inconspicua* (Sowerby), the inner hinge plates unite medially with a septum in a manner identical to that described for *Meristella*; and on the upper surface of its cardinal plate the secondary mosaic is considerably modified though not as much as in *Meristella*.

In most younger Athyridacea, such as *Athyris* and *Composita*, deposition of a tertiary layer did not occur, and the structure of their primary and secondary layers is unexceptional. The primary layer of *Athyris spiriferoides* (Eaton) from the Upper Hamilton Group (Middle Devonian) of New York measures up to 30 μm in thickness and is composed of vertically stacked crystallites (Pl. 12, fig. 5). It is succeeded by a thick secondary layer composed of orthodoxly stacked fibres with smoothly convex keels and saddles (Pl. 12, fig. 6). Mature fibres measure up to 25 μm in width. The fabric of the primary layer of *Composita ambigua* (Sowerby) from the Calmy Limestone (Lower Carboniferous) of Carluke, Lanarkshire, is the same as that of *Athyris spiriferoides*, and measures up to 20 μm in thickness (Pl. 13, fig. 1). Fibres of the secondary layer are indistinguishable in size and disposition from those of *Athyris.*

Cleiothyridina deroissii (Leveille) from the Blackbyre Limestone (Lower Carboniferous) at Brockley, Lesmahagow, Lanarkshire, excited more interest. It was found to possess a primary layer of up to 25 μm thickness which was succeeded by orthodoxly stacked secondary layer fibres and, like the profiles of secondary layer fibres composing the shells of other Athyridacea, those of *Cleiothyridina* possess smoothly convex keels and saddles (Pl. 13, fig. 2). However, over much of the interior of both valves, secondary layer fibres are succeeded by a thick tertiary layer deposit composed of tall crystals whose basal parts are continuous with the outlines of secondary fibres, as in *Gryphus vitreus* (Born). Of particular interest is the discovery, in sections through the tertiary layer, of a prominent transverse depositional banding which is traceable across adjacent crystal boundaries (Pl. 13, fig. 3). In general the prominence and periodicity of the banding varies greatly. A fairly regular banding with an average periodicity of 900 nm was recognized and taken to reflect diurnal deposition, but even this banding could be subdivided in places into units no more than 200 nm thick.

It is evident from a study of the distribution of the shell layers in *Cleiothyridina* that deposition of all three calcareous shell layers took place simultaneously. However, adjacent parts of the mantle must have been subject to temporary reversals in secretory behaviour, for secondary and tertiary layers interdigitate (Pl. 13, fig. 4), as do primary and secondary layers closer to the contemporaneous valve margins. The fluctuations in primary and secondary shell deposition are more intense than those affecting the tertiary layer and may give rise to a series of frill-like overlapping lamellae which characterize a number of late Palaeozoic Athyridacea. In *Cleiothyridina* the extremities of lamellae are fashioned into long, flat, spinose projections which generally break off when the fossils are extracted from the surrounding rock matrix. Fine spines may also develop upon the frilly edges of overlapping lamellae in *Athyris.*

In certain of the youngest athyridaceans, such as *Diplospirella*, bifurcations of the jugal stem gave rise to a pair of accessory spiral lamellae which grew in such a way as to become intercoiled with the arms of the primary spiralia. Specimens of *Diplospirella wissmani* (Münster) and *Anisactinella quadriplecta* (Münster) from the St Cassian Beds (Triassic) of Northern Italy were examined with a view to determining the skeletal ultrastructure of this stock. In most cases, specimens were small enough for complete valves to be comfortably accommodated on 1·3 cm diameter 'Stereoscan' stubs. In this way, it was possible to view whole shell interiors and thereby interpret the growth of particular areas of interest in relation to the overall fabric.

In sections of *Diplospirella wissmani* (Münster) the primary layer was found to be well preserved (Pl. 13, fig. 5). It is normally about 25 μm thick and exhibits a fine lineation disposed roughly normal to the outer shell surface. In the development of this lineation and its generally porous texture, the primary layer of *Diplospirella* is comparable with that found in living articulates. Transverse growth bands are only sporadically developed. The most striking aspect of the shell structure of *Diplospirella* is the size of secondary layer fibres (Pl. 13, fig. 6 ; Pl. 14, figs. 1, 2).

Compared with the fibres of *Athyris* or *Composita*, for example, the fibres of *Diplospirella* are exceptionally large and spatulate terminal faces up to 60 μm in width can be discerned even when the valve interiors are viewed under a conventional light microscope. Evidently the outer epithelial cells responsible for secreting the secondary layer of *Diplospirella* were much less mobile than those of most other articulates, for fibres newly proliferated at the valve margins appear to grow radially outwards but those located some distance from the commissure are only slightly reorientated with long axes disposed in such a way as to indicate growth in an anterior direction only. No exceptional twists, spirals or S-shaped convolutions have been observed. The only appreciable modification in the secondary shell mosaic occurs within muscle scars.

Around the anterior margins of scars, the standard secondary shell mosaic breaks down and is replaced posteriorly by a succession of very long exposed trails of fibres bearing no recognizable terminal faces (Pl. 14, fig. 3). Outlines of rather ragged, asymmetrical trails may extend along the scar for more than half its length. This breakdown in the normal process of shell deposition is also recognizable in sections through muscle scars where orthodoxly stacked secondary layer fibres are succeeded inwardly by a succession of fibres with very irregular, though closely interlocking outlines (Pl. 14, fig. 4). In most respects this breakdown in secondary shell deposition within the muscle scars of *Diplospirella* is similar to that which has been observed in young *Notosaria*, except that no arcuate zones of fibres with large terminal faces occur. At the posterior margins of each muscle scar, the long, exposed trails are overlapped by a cluster of very small fibres with terminal faces averaging less than 10 μm in width (Pl. 15, fig. 1). Within a relatively short distance however, the terminal faces of fibres attain dimensions more typical of the secondary layer mosaic pattern which occurs elsewhere on the shell surface. The occurrence of a zone of small fibres around the posterior margins of a muscle scar is important since it provides an indication of the size of outer epithelial cells which must have been located in that part of the shell. Since terminal faces less than 10 μm in width overlap trails which may exceed 60 μm in width, it is evident that a substantial size differential existed between cells located anterior and posterior to the muscle scars. Judging from the way in which the surface level drops around the anterior margins of muscle scars, it would appear that parts of the secondary mosaic which lay in the path of the encroaching muscle base were, to some extent, resorbed. The long exposed trails within muscle scars are interpreted as being remnants of fibres which were involved in resorption when formerly located around the anterior periphery of the scar. Within the muscle scar it is probable that organic membranes completely ensheathed exposed fibre trails, so that the main function of outer epithelial cells underlying muscle bases is likely to have been adhesion and not secretion. Since it is known from a study of living material that the optimum size range for outer epithelial cells underlying muscle bases is substantially less than that outside, it is not surprising to find that the first-formed fibres around the posterior margins of scars are of small dimensions.

The shell structure of *Anisactinella quadriplecta* (Münster) is essentially the same as that recorded for *Diplospirella*. In the only specimen of *Anisactinella* available for study, a thin primary layer consisting of vertically stacked crystals about 8 μm high is preserved (Pl. 15, fig. 2). The secondary layer fibres are large and attain widths of more than 60 μm. Unlike *Diplospirella* the exterior of *Anisactinella* is coarsely plicate, but on the inner shell surface the deposition of secondary layer material within the radially disposed hollows tends to fill out these external irregularities with the formation of a relatively smooth surface.

(ii) *Koninckinacea*

The Koninckinacea as presently constituted comprise six genera of small to medium-sized articulate brachiopods with smooth concavo-convex shells which enclose a double pair of ventrally directed spires. Despite the distinctive external shell morphology and an unusual brachidium, the superfamily has received little attention since the end of the nineteenth century. With the exception of *Cadomella*, the genera are perhaps best known as representatives of the Triassic St Cassian fauna of the Italian Dolomites so extensively collected and figured by Bittner (1890 : 304–309). It was not until Cowen and Rudwick (1966 : 403–406) discovered a spiral brachidium in *Cadomella davidsoni* (Eudes-Deslongchamps) that this Lower Jurassic genus was recognized as a member of the Koninckinacea.

In the *Treatise* (1965 : H666) Boucot *et al.* assign the Koninckinacea and Athyridacea to the suborder Athyrididina and the spiriferide affinities of the koninckinaceans were not questioned until Cowen and Rudwick proposed a rearrangement of this existing classification, based on general shell morphology, with the transference of the superfamily, amended to include *Cadomella*, from the Spiriferida to the Strophomenida. However, the strongly concavo-convex shell profile and the morphology of the apical region, though reminiscent of many Strophomenida, are not diagnostic features. In addition, the statement made by Cowen and Rudwick (1966 : 404) that the pedicle foramina of *Koninckella liassina* Bouchard, *K. triassina* Bittner and *Amphiclina suessi* Laube 'are definitely supra-apical' is not supported by recent observations on *K. triassina* Bittner, *Amphiclina amoena* Bittner, *Cadomella davidsoni* (Eudes-Deslongchamps) and *C. moorei* (Davidson) made by Brunton and MacKinnon (1972 : 410). As will be shown presently, the nature of the calcareous shell succession in Koninckinacea is comparable with that of a number of Spiriferida, but quite unlike that of any Chonetidina (Williams 1968a : 46) ; therefore, in the absence of any morphological detail, macroscopic or microscopic, that would serve to establish strophomenide identity, there now appears to be no valid reason for removing the Koninckinacea from the Spiriferida.

This account of the shell ultrastructure of the Koninckinacea is based on an examination of specimens belonging to three genera : *Koninckina leonhardi* (Wissman) and *Amphiclina amoena* Bittner from the St Cassian Beds (Triassic) of Northern Italy, and *Cadomella davidsoni* (Eudes-Deslongchamps) and *C. moorei* (Davidson) from Liassic clays near Caen, France.

The primary layer of *Koninckina* is about 10 to 12 μm thick. In transverse section it is usually discernible as a series of closely packed crystallites between 0·5 μm and 2·0 μm in width which are stacked normal to the isotopic boundary between the primary and secondary shell layers (Pl. 15, fig. 3). On the outer shell surface, faint concentric growth lines cut across a fine radial lineation (Pl. 15, fig. 4) which appears at higher magnifications to be a series of narrow troughs and ridges. The ridges are comparable in width and stacking to that of the crystallites observed in thin section, and because of their consistency and regular spacing are considered to be an original feature of the outer shell surface. Presumably the inner bounding membrane of the periostracum, which must have provided an outer organic cover to both valves, was moulded by crystal growth into a series of radial grooves and fine ridges corresponding in negative to the undulations on the shell surface. Possibly organic strands or membranes extended through the primary layer by way of the spaces between crystallites to join up with the organic components of the secondary shell layer. Apart from being slightly thicker, the primary layer of *Amphiclina* is little different from that of *Koninckina*.

Williams (1968a : 34) noted that the secondary layer of *Koninckina* is composed of fibres which grow to an unusually large size in comparison with the secondary layer fibres of most other articulates. On the internal surfaces of both valves the terminal faces of secondary layer fibres are rhomb-shaped (Pl. 15, fig. 5) and not spatulate as is common in Recent Terebratulida, Rhynchonellida and some Spiriferida. This distinctive secondary shell mosaic pattern has the general appearance of diagonally intersecting rows of rhomb-shaped faces but such rows are not perfectly

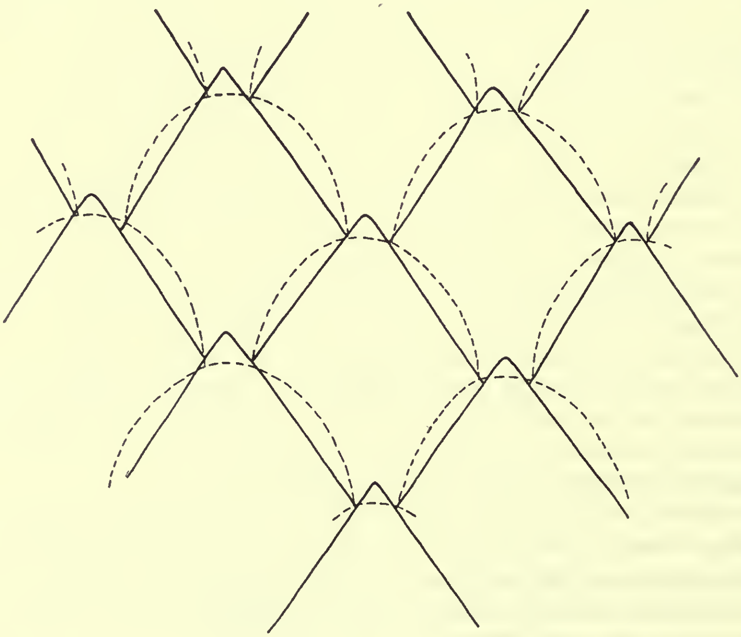

FIG. 13. Plan of the secondary shell mosaic on the internal surface of a valve of *Koninckina*, showing the diamond-shaped outlines of terminal faces. The more normal, smoothly curved mosaic, such as is found in Recent Rhynchonellida and Terebratulida, is shown by broken lines for comparison.

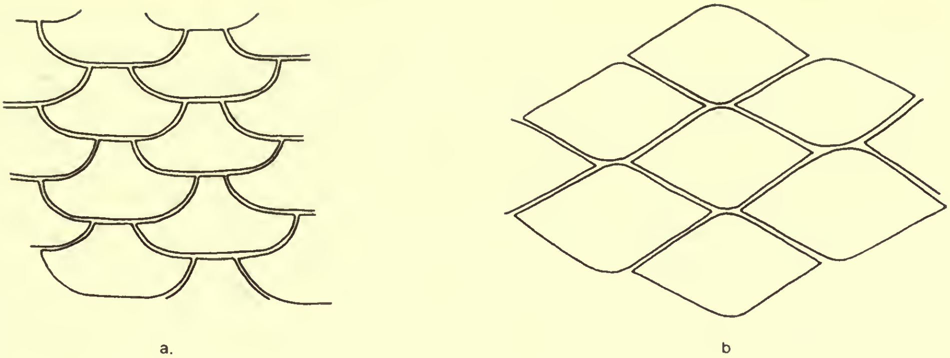

Fig. 14. a. Stylized transverse section of the secondary shell of a Recent rhynchonellide or terebratulide showing the characteristic shape and stacking of fibres. b. Stylized transverse section of the secondary shell of *Koninckina* showing the characteristic diamond-shaped outlines of fibres.

linear, as the outline of each terminal face is displaced fractionally from its neighbours. To derive this internal surface pattern from the more typical spatulate mosaic requires only a sharpening of the arcuate junction between the calcite and protein secretory zones in the overlying outer epithelium (Text-fig. 13). Diamond-shaped terminal faces with diagonal lengths and widths measuring up to 45 μm and 30 μm respectively have been observed in both *Koninckina* and *Amphiclina* (Pl. 15, fig. 6).

The shape and stacking of secondary layer fibres in transverse section are dependent initially on the slope and spatial relationships of the corresponding outer epithelial cells on the inner shell surface. For example, in a Recent rhynchonellide or terebratulide, cross sections of a typical fibre show that it is bounded by an inwardly curved surface (the keel) which is truncated by an outer one made up of two curved lateral areas and one median depression (the saddle) (Text-fig. 14a). The profile of the inner and outer surfaces of a fibre correspond to the foreshortened outlines of the anterior and posterior boundaries of the terminal face. Since both the anterior as well as the posterior boundaries on the terminal face of the koninckinacean secondary layer fibre are angular, the cross-sectional outline of the fibre is correspondingly modified. Transverse sections of *Koninckina* and *Amphiclina* reveal that the fibres are roughly diamond-shaped with inner and outer surfaces variably truncated (Text-fig. 14b).

In some, if not all, specimens of *Koninckina* recovered from the St Cassian beds, the secondary shell fabric is almost certainly original because fibres in longitudinal and transverse sections exhibit a fine depositional banding (Pl. 16, figs. 1, 2) of variable periodicity, which probably represents slight fluctuations in the physiological behaviour of the corresponding outer epithelial cells. The mean periodicity of 37 bands measured from cross-sections of six adjacent fibres was 0·89 μm (range 0·58 μm to 1·54 μm). However, until more is known of the factors controlling mineral secretion in living brachiopods, such as the effects of temperature, light and salinity of the local environment, feeding habits, availability of food, tidal conditions, etc., the precise significance of such depositional features must remain in some doubt.

Some distance in from the shell edge of *Koninckina* and *Amphiclina*, the secondary layer fibres are succeeded by a tertiary layer deposit which thickens towards the centre of both valves. The change-over from secondary to tertiary deposition corresponds with the anterior extremities of the primary lamellae which comprise the first and broadest convolution of the spiral brachidium. Posterior to this line, the narrow shell cavity is moulded to the shape of the two shallow, ventrally directed coils, thus producing a dome-shaped swelling (Pl. 16, fig. 3) on either side of the brachial valve mid-line and a pair of depressions in the pedicle valve. Superimposed on each outgrowth (or depression) is a spiral groove along which are channelled the arms of the spiralia. In addition, the shell surface is pock-marked by a number of shallow pits which appear in some parts to be distributed along the spiral grooves. However, it seems unlikely that the pits are related to any part of the brachial structure, and an interpretation favouring some form of gonadal markings (such as are commonly found in *Atrypa*) seems more plausible. Impressions related to brachidia (and gonads) have been observed in both *Koninckina* and *Amphiclina*.

An examination of the tertiary layer in *Koninckina*, in plan as well as in section, reveals a shell fabric closely comparable with that observed in living *Gryphus*. The secondary shell mosaic, with its distinctive diamond-shaped terminal faces, breaks down into a grossly modified surface pattern which appears as an irregularly anastomosing network of intercrystalline boundaries (Pl. 16, fig. 4). The rough undulating topography of each growing face contrasts with the smoothness of the secondary layer terminal faces. Dimensions of faces are difficult to measure, because of their irregularity in outline, and a better estimate of their dimensions can be made from sections cut at right angles to the plane of growth. Seen in depth, the tertiary layer is composed of vertically stacked and tightly interlocking columns of calcite, separated from one another by clear-cut boundaries (Pl. 16, fig. 5). Although the isotopic boundary between the secondary and tertiary layers is well defined, it is evident that the vertically stacked columns grew in continuity with the underlying secondary fibres. There is a one-to-one correspondence between tertiary layer columns and secondary layer fibres for, in longitudinal sections showing the secondary/tertiary layer junction, each rod-like fibre of the secondary layer gives rise to a single vertical column (Pl. 16, fig. 6).

The mode of formation of the tertiary layer in *Koninckina* must have been very similar to that occurring in living *Gryphus*. At a certain distance from the shell edge, the outer epithelial cells ceased to migrate in the horizontal plane but continued to secrete calcite, so that a thick deposit was laid down normal to the shell surface. Over certain parts of the inner shell surface of *Koninckina*, notably the posteromedian region behind muscle scars, there is a regrowth of the secondary layer fibres on top of the tertiary layer. Generally one tertiary layer column will be succeeded by one fibre but sometimes two or rarely three branches emerge at this inner isotopic boundary.

(d) Spiriferidina

The Spiriferidina constitute the largest and most diverse suborder of all spire-bearing brachiopods. In general the spiriferidine shell is broadly strophic and possesses a well-developed ventral interarea. The spiralia are directed laterally or postero-laterally.

The problems of spiriferid classification are well summed up by George (1933 : 423–456) who recognized the lack of reliable morphological criteria on which a workable and satisfactory scheme could be founded. In the *Treatise* classification, Pitrat (1965 : H667) considered the existence of longitudinal striations on the cardinal process to be a feature of critical importance. Using this fact as his main basis for suprageneric classification, he separated the 'non-striate' Cyrtiacea (impunctate) and Suessiacea (punctate) from the 'striate' Spiriferacea (generally impunctate, plicate), Reticularacea (impunctate, smooth) and Spiriferinacea (punctate).

(i) *Cyrtiacea*

The Cyrtiacea as defined in the *Treatise* (1965 : H667) include the Eospiriferinae and their impunctate derivatives, the Cyrtiinae and the Ambocoeliidae. Specimens of *Eospirifer*, the earliest cyrtiacean, were unavailable for study but sections of the related genus *Cyrtia exporrecta* (Wahlenberg) from the Silurian of Coalbrookdale, Shropshire, reveal a thin, recrystallized primary layer measuring up to 10 μm in thickness. Fibres of the secondary layer are unlike those of contemporary Atrypidina in that they exhibit symmetrical profiles with rounded keels and saddles instead of being diamond-shaped (Pl. 17, fig. 1). From the regular stacking of fibres and their smooth outlines, it can be deduced that the internal mosaic consists of alternating rows of broadly spatulate terminal faces. On average, fibres measure about 12 μm in width.

The Eospiriferinae and the Cyrtiinae are thought to be very closely related, since the two groups are substantially the same except for overall shell shape and modifications of the delthyrium (Pitrat 1965 : H667). The smooth-shelled, generally plano-convex Ambocoeliidae are less emphatically related to the other two subfamilies, but are grouped with them mainly on account of their possession of a non-striate cardinal process.

Ambocoelia umbonata (Conrad) from the Hamilton Group (Middle Devonian) of New York possesses a well-developed primary layer up to 40 μm thick which is best preserved around the commissures of mature specimens. In this area, primary and secondary shell layers interdigitate as the two major components of overlapping growth lamellae (Pl. 17, fig. 2). The curved outlines of secondary layer fibres in section indicate an orthodox secondary shell mosaic pattern with terminal faces about 20 μm wide (Pl. 17, fig. 3). In the vicinity of muscle scars the regular stacking of fibres breaks down and outlines of adjacent fibres become ragged and impersistently welded together. The interior of a brachial valve of the related genus, *Crurithyris* sp. from the Finis Shale (Pennsylvanian) of Texas, was sufficiently free from enclosing rock matrix to allow examination of the surface mosaic. As might be expected, the surface was badly etched and pitted but the outlines of individual secondary layer terminal faces, on average 20 μm wide, were still recognizable (Pl. 17, fig. 4). In the umbonal region of the brachial valve a narrow cardinal process lies between two prominent, inwardly convex inner socket ridges (Pl. 17, fig. 5). The base of the cardinal process is cylindroid and rises posteriorly to become densely tuberculate (Pl. 17, fig. 6), but no longitudinal striation, such as was found in *Spiriferina*, could be detected.

(ii) *Suessiacea*

Apart from the monotypic genus *Suessia* which constitutes the family Suessidae, the Suessiacea includes representatives of the family Cyrtinidae. Most genera are punctate and characterized by a weakly convex brachial valve and hemipyramidal pedicle valve. Although resembling most Cyrtiacea in the possession of a non-striate cardinal process as well as in external morphology they differ mainly in the development of a ventral median septum and dental plates which may merge to form a spondylium-like structure.

Two species of *Cyrtina* were examined in order to help determine the skeletal fabric of the superfamily. Specimens of *Cyrtina alpenensis* Hall and Clarke, from the Middle Devonian of Rockport, Alpena County, Michigan, possess well-developed primary and secondary shell layers. The primary layer, on average about 20 μm thick, has a spongy appearance and is traversed by a faint lineation disposed normal to the shell exterior (Pl. 18, fig. 1). Fibres of the secondary layer are small, presenting a mean width of 10 μm. In both valves the secondary layer fibres are outwardly deflected around puncta which may measure up to 25 μm in diameter. The puncta appear to penetrate the primary layer, but due to the homogeneity of the sedimentary infilling of puncta with the fabric of the primary layer, it was impossible to distinguish any distal coverings. Branching puncta may occur sporadically in both valves.

On the interior of the pedicle valve, the dental plates are strongly developed and converge rapidly to unite with a high, blade-like median septum. The septum of *Cyrtina* is unusual in that it supports a narrow medially partitioned chamber along its posterior facing edge. This chamber, the tichorhinum, extends from the umbo to the dorsal edge of the median septum and is subtended laterally by the inner surface of the dental plates. In some species of *Cyrtina* the tichorhinum is reported to be incompletely partitioned (Amsden 1958 : 135). In transverse sections of *Cyrtina* sp. from the Upper Devonian of Rockford, Iowa, the tichorhinum is seen to originate as a bulbous triple-branched extension of the median septum comprising one median partition and two lateral, curved walls (Pl. 18, fig. 2). Judging from the disposition of secondary layer fibres which tend to run parallel to the long axis of the tube, it is evident that the tichorhinum was fashioned as a result of the localized evagination of outer epithelium situated on both sides of the postero-dorsal edge of the median septum. The reasons for evagination having occurred in the first place are not clear, but it is evident that the greater part of the median septum served as a muscle attachment area. Two discrete myotest shell fabrics are recognizable in transverse sections through the median septum (Text-fig. 15). The first is situated close to the median plane of the septum and is overlapped by a subsequent deposit of

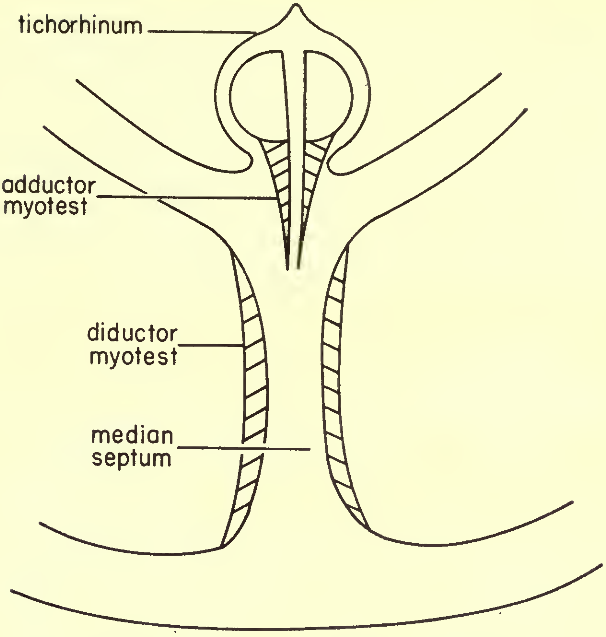

FIG. 15. Stylized transverse section through the ventral median septum and tichorhinum of *Cyrtina*, showing the distribution of myotest.

secondary shell material. Above the level of the fused dental plates this myotest can be traced running into the tichorhinum. The second myotest is situated on either side of the septum below its junction with the dental plates and extends as far as the floor of the valve (Pl. 18, fig. 3). Since the first myotest is unaffected by the union of the dental plates, it is evident that its former position of growth was located forwards (and dorsal) of the point where the dental plates join with the septum. This would correspond to a position on the septum which is situated at its postero-dorsal extremity close to the hinge line. Since the second myotest is located on the flanks of the septum below the dental plates, it must comprise part of a muscle scar which is impressed further back on the septum at a lower level within the hemi-pyramidal pedicle valve.

Despite its unusual pedicle valve morphology, the musculature of *Cyrtina* was probably no different from that of other articulate brachiopods. Certainly the emplacement of muscles in the brachial valve was quite orthodox. On the floor of the brachial valve are two pairs of adductor scars with a bilobed cardinal process situated in the umbonal region (Hall and Clarke, 1894 : 763). The muscle scar layout in the pedicle valve of *Cyrtina* can best be understood by making direct comparison with the pedicle valve musculature in Recent genera (Text-fig. 16a, b). In *Notosaria*, for example, two small adductor scars are bordered antero-laterally by the ventral diductor and adjustor scars. Extending this arrangement to *Cyrtina*, it seems most likely that the ventral ends of the adductors were inserted within the tichorhinum as well as being attached to the postero-dorsal part of the septum, and that the diductors ran obliquely forward from the cardinal process to attach to the antero-lateral parts of the median septum (Text-fig. 16c). The ventral adjustor muscles were probably attached to the antero-lateral surface of the dental plates.

The transference of the areas of ventral muscle attachment to a median septum was accompanied by an adjustment in the structure of the spiral brachidium. The innermost coils of both calcareous spires of *Cyrtina* are situated very close to one another and joined by a sharply pointed, anteriorly directed jugum (Text-fig. 17a, b). The apices of the spiralia are directed obliquely posterior and extend well within the lateral cavities of the hemipyramidal pedicle valve.

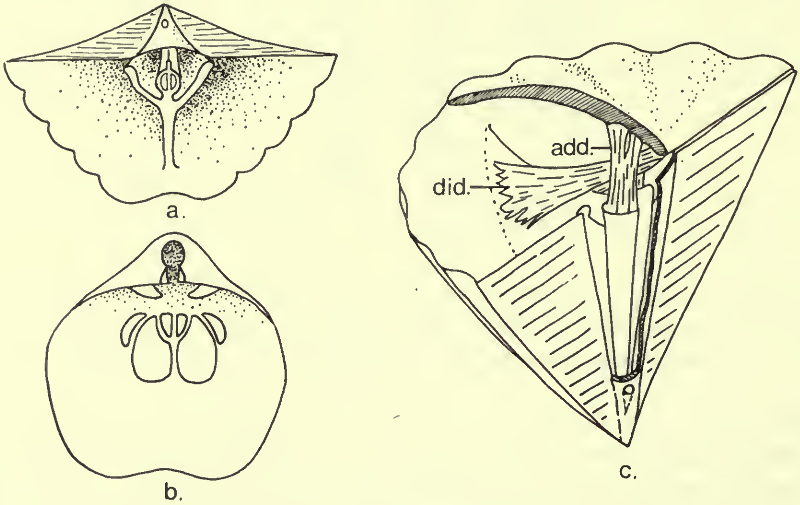

FIG. 16. a, b. Views of the interiors of the pedicle valves of *Cyrtina* (a) and a more conventional articulate such as *Notosaria* (b), showing the relative location of muscle attachment areas. c. Cut-away diagram of *Cyrtina* showing the inferred restoration of the adductor and diductor muscle systems.

(iii) *Spiriferacea*

The Spiriferacea is by far the largest of the five superfamilies comprising the Spiriferidina. Their shell form is variable but in general it tends to be rather transverse with either angular or slightly rounded cardinal extremities. In most cases maximum width is attained across the hinge line, but in some forms, such as the Brachythyrididae, the hinge line is substantially short of maximum width. The earliest Spiriferacea such as *Delthyris* and *Howellella* appeared at much the same time (Lower Silurian) as the first cyrtiaceans *Cyrtia* and *Eospirifer*. In such early genera, lateral plications are few and the fold and sulcus are generally smooth; however, in later Spiriferacea costation became more intense and varied as did the nature of concentric growth lamellae. In addition, there was considerable variation in the development of the finer elements of the surface ornament, such as spines, granules and capillae.

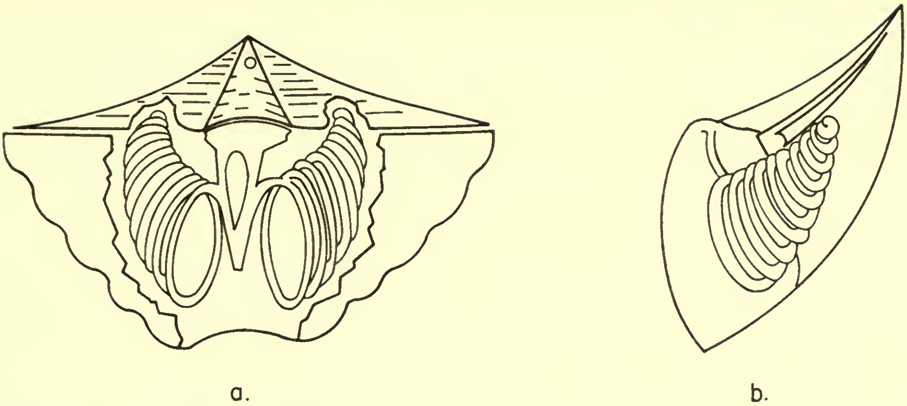

FIG. 17. Dorsal (a) and lateral (b) views of *Cyrtina* showing the disposition of the spiral brachidium.

The shell structures of two genera assigned to the Delthyridae were investigated. These were *Delthyris saffordi* (Hall) from the Brownsport Formation (Upper Silurian) of Western Tennessee and *Kozlowskiellina velata* (Amsden) from the Haragan Formation (Lower Devonian) at White Mound, Murray County, Oklahoma. No recognizable primary layer was preserved in *Delthyris*, but the fibres of the secondary layer, measuring up to 25 μm in width, displayed smoothly curved outlines of keels and saddles (Pl. 18, fig. 4). The regular stacking of fibres as seen in transverse section indicates the development of an internal surface mosaic comparable with that observed in *Spiriferina*. Some sections through fibres reveal traces of a transverse banding with an average periodicity of about 0·4 μm, which is considered to be depositional. In *Kozlowskiellina* a primary layer measuring up to 10 μm in thickness is preserved (Pl. 18, fig. 5). The shape and stacking of transversely sectioned secondary layer fibres, which measure on average 20 μm in width, point to an internal secondary shell mosaic pattern consisting of alternating rows of terminal faces with smooth spatulate outlines (Pl. 18, fig. 6). In the posterior parts of both valves, in particular the pedicle valve, the secondary layer attains considerable thickness. In some instances earlier-formed parts of exoskeletal outgrowths such as the crura and ventral median septum may be identified by the distinctive stacking of their fibres. Transverse sections through a crus of *Kozlowskiellina* reveal that it grew in much the same way as that described for the same structure in Recent Terebratulida and Rhynchonellida, with the growth of fibres along its length (Pl. 19, figs. 1, 2, 3). The fibres are so arranged as to indicate deposition on the ventro-lateral side of the crus only, with the dorso-median facing side exposing long trails without terminal faces (cf. Williams 1968a : text-fig. 12, p. 17). In both the brachial and pedicle valves of *Kozlowskiellina* a myotest shell fabric could be recognized. For example, within the ventral diductor myotest there is a sudden breakdown in normal secondary shell deposition with the replacement of orthodoxly stacked fibres by an irregular, semi-granular accretion of calcite forming a layer about 50 μm thick (Pl. 19, fig. 4). The first few rows of secondary layer fibres which succeed the myotest deposit are noticeably small, being less than 10 μm in width. In this respect they are comparable with the narrow zone of small fibres which overlap the posterior margins of muscle scars in *Notosaria*. Normal secondary shell growth does not become fully re-established behind the ventral diductor myotest, for transverse sections reveal the subsequent deposition of a semiprismatic layer of considerable thickness. This deposit resembles, in places, the 'jigsaw-puzzle' type of shell fabric that characterizes the tertiary layer of *Dayia navicula* (Sowerby).

While not showing the widespread development or regularity of the tertiary layer of living *Gryphus*, this localized deposit in *Kozlowskiellina* is quite distinct from the secondary layer which incorporates all exoskeletal outgrowths as well as adjacent parts of the valve floor. The location of the deposit may provide some clue as to its origin. Outer epithelial cells which secrete secondary layer fibres are known to migrate laterally across the floors of valves leaving trails of calcite marking the routes along which they proceed. It is possible that those outer epithelial cells situated behind the ventral muscle bases of *Kozlowskiellina* were unable to migrate forwards or laterally fast enough and thus contributed to the build-up of shell material which was deposited in a plane roughly normal to the inner shell surface. This hypothesis, however, can only be used in an attempt to explain the development of a tertiary shell fabric behind muscle scars in forms such as *Kozlowskiellina*, and not the widespread tertiary layer deposit as is found in other Spiriferida like *Cleiothyridina*.

The discovery of this incipient tertiary layer in *Kozlowskiellina* poses the question as to whether such a deposit is characteristic of other related genera. Unfortunately no other specimens were available for comparison under the scanning electron microscope, although Krans (1965) has examined the shell structure of a number of Delthyridae by means of cellulose acetate peels. In a study which included Devonian species of *Howellella, Howittia, Hysterolites, Spinella, Paraspirifer, Brachyspirifer* and *Euryspirifer*, Krans reports the growth and development of only two calcareous shell layers, the primary and secondary layers. From the primitive delthyrid stock are descended a large number of Spiriferacea which are subdivided, on the basis of differences on external and internal morphology, into eight other families.

The shell exterior of *Mucrospirifer* sp. from the Middle Devonian of Michigan is covered by a primary layer about 12 μm thick which is lineated normal to the isotopic boundary between the primary and secondary layers (Pl. 20, fig. 1). The first few rows of secondary layer fibres are small, measuring less than 8 μm in width, but when traced further inwards they show an increase in size to a maximum of 15 μm width. All fibres are orthodoxly stacked and display evenly curved keels and saddles (Pl. 20, fig. 2).

No specimens of *Fimbrispirifer* were available for study, but Krans (1965, pl. 9, figs. 3, 6) figures sections of two species from the Devonian of Spain which appear to possess a standard primary and secondary shell succession.

The shell structure of *Spinocyrtia* sp. from the Middle Devonian of Michigan is unexceptional. It possesses a recrystallized primary layer which measures about 12 μm in thickness (Pl. 20, fig. 3). Fibres of the secondary layer, although comparable in shape and stacking with those of *Mucrospirifer*, are generally smaller.

Young fibres which succeed the narrow zone of primary shell deposition located around the shell edge are generally about 4 μm wide, but mature fibres which are laid down well within the shell interior attain, on average, a width of 10 μm (Pl. 20, fig. 4).

Only fragments of a pedicle valve of *Syringothyris cuspidata* (Martin) from the Lower Carboniferous of Staffordshire were obtainable for the purpose of sectioning. Parts of fibrous secondary layer were recognizable (Pl. 20, fig. 5) but no primary layer was present. *Syringothyris* differs from all other Spiriferacea in being penetrated by puncta measuring up to 20 μm in diameter around which the secondary layer fibres are outwardly deflected (Pl. 20, fig. 6). Sass (1967 : 1244) has investigated the shell structure of six species of *Syringothyris* and found all of them to be punctate. In addition, he reports that the shell of *Syringothyris* comprises three calcareous layers, namely the primary, secondary and prismatic (tertiary) layers. Within the tertiary layer the puncta are traceable as irregular passageways which run along the boundaries of adjacent crystal faces (Sass 1967 : 1244). Certain generally impunctate spire-bearing brachiopods (Licharewiinae), which are found in beds of Upper Carboniferous and Permian age, are also assigned to the family Syringothyridae by Pitrat (1965 : H692). In most cases they appear to be morphologically indistinguishable from the Spinocyrtiidae but as the last surviving representatives of this family are considered to have become extinct during the late Devonian, direct descent of the Licharewiinae from such a stock is considered unlikely. Armstrong (1968a : 183) found only two calcareous shell layers in the punctate genus *Subansiria* from the Permian of Australia.

Investigations of the shell structure of the Devonian Costispiriferidae were confined to the finely ribbed form, *Theodossia hungerfordi* (Hall) from the Hackberry Stage (Upper Devonian) of Iowa. The primary layer, which may be up to 25 μm thick, is succeeded by regularly stacked secondary layer fibres which attain a width of about 10 μm. Exoskeletal outgrowths such as teeth and spiralia (Pl. 21, fig. 1) are built up from secondary layer fibres. In the postero-median parts of the shell a tertiary layer is developed. This thick inner layer consists of well-defined narrow crystals on average about 10 μm in width which are stacked normal to the inner shell surface (Pl. 21, fig. 2).

The shell structure of two representatives of the Costispiriferidae were investigated. These were *Tenticospirifer cyrtiniformis* (Hall and Whitfield) from the Hackberry Stage (Upper Devonian) of Iowa, and *Syringospira prima* Kindle from the Percha Formation (Upper Devonian) of New Mexico. In both valves of *Tenticospirifer* the calcareous shell succession was found to be in a particularly good state of preservation. The primary layer which may measure up to 45 μm in thickness has a porous texture and bears traces of a faint lineation disposed normal to the shell exterior (Pl. 21, fig. 3). Fibres of the secondary layer measure, on average, 10 μm in width but although outlines of fibres appear in transverse section to be flattened in the style of *Hemithiris* (Williams 1971b : pl. 1, fig. 3b), they are nonetheless orthodoxly stacked (Pl. 21, fig. 4). This levelling out of keels and saddles is considered to reflect a slight change in the profiles of terminal faces from spatulate to sub-rectangular in outline. Within the vicinity of muscle scars, the standard secondary layer fabric

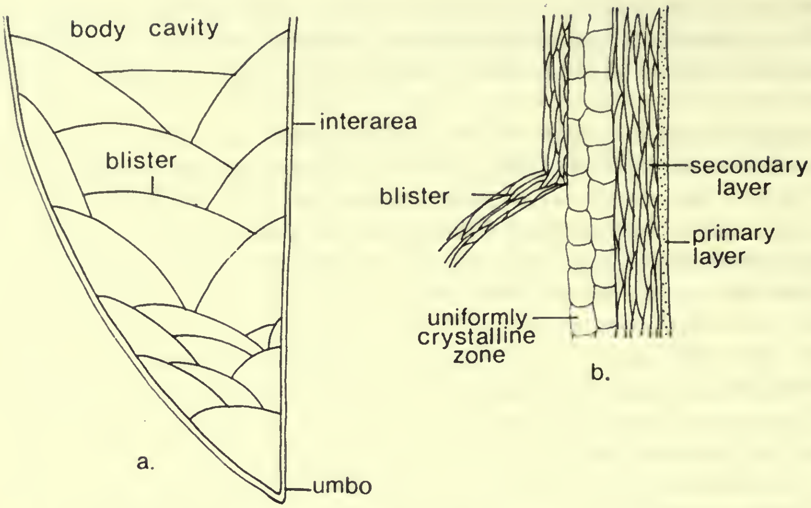

FIG. 18. a. Longitudinal section through a pedicle valve of *Syringospira* showing the development of a series of overlapping partitions. b. Stylized section through a partition and shell wall of *Syringospira* showing the intervening uniformly crystalline zone.

is grossly affected and the boundaries between myotest and earlier-formed parts of the shell succession are abrupt. The ultrastructure of the myotest is difficult to decipher but judging from its semigranular appearance in transverse section (Pl. 21, fig. 5) it is probably composed of small irregular fibres which are impersistently welded together in a manner reminiscent of the ventral myotest of *Notosaria*. *Syringospira*, like *Tenticospirifer*, possesses a well-developed primary layer which may measure up to 40 μm in thickness. Sections through the primary layer reveal a dense vertical striation on which there is superimposed a spongy fabric (Pl. 21, fig. 6). Secondary layer fibres are narrow and seldom exceed 10 μm in width. Shell growth in *Syringospira* was accompanied by the development of a succession of overlapping partitions (Text-fig. 18a) within the umbonal cavities of both valves (Cooper 1954 : 328). The ultrastructure and mode of formation of these blister-like plates have already been described by Williams (1971a : 66). Each blister is composed of conventional secondary layer fibres. Williams' view that secretion of an organic seeding shell preceded the deposition of fibres away from the valve floor is supported by the discovery of a uniformly crystallized zone, up to 35 μm wide, which lies sandwiched between the junction of two adjacent partitions (Pl. 22, fig. 1 ; Text-fig. 18b).

A temporary reversion to wholly organic exudation is by no means unlikely for similar changes in secretory behaviour are known to occur periodically in living Rhynchonellida and Terebratulida. Organic layers, believed to be composed of protein, have been found within the calcareous shell succession of *Hemithiris psittacea* (Gmelin). As such deposits tend to be exuded over the entire shell surface the optical properties of the total shell fabric become affected. Valves of *Hemithiris* which possess organic interlayers are invariably black in colour. In the terebratulide *Magasella sanguinea* (Leach) exudation of a thin organic layer facilitated the backward slide of the mantle edge during its periodic retractions (Williams 1971a : 64). A temporary reversal to organic deposition may have served much the same function in *Syringospira* as it does, at present, in *Magasella*. Just as the terebratulide mantle becomes detached from the adjacent shell surface (caeca included) so also is it likely that the mantle of *Syringospira* detached itself in part from the remainder of the valve floor. The space created by this movement may have become temporarily filled with fluid but in any case it is likely that exudation of a temporary organic covering followed in order to seal off the space and provide a convenient seeding sheet for the secretion of a more rigid partition composed of secondary layer fibres and their organic sheaths.

The shell structure of the family Spiriferidae, as represented by *Spirifer trigonalis* Martin from the Lower Carboniferous of Lanarkshire and *Neospirifer cameratus* (Morton) from the La Salle Limestone (Pennsylvanian) of Ohio, is variable. In *Neospirifer*, primary and secondary shell layers are clearly recognizable (Pl. 22, fig. 2). The primary layer which measures up to 40 μm in thickness is similar in texture to the primary layer of *Tenticospirifer*. It is rather porous and lineated normal to the outer shell surface. Fibres comprising the secondary layer are orthodoxly stacked and measure up to 15 μm in width. The calcareous shell succession of *S. trigonalis* differs from that of most other Spiriferacea in that it incorporates a well-developed tertiary layer. Three shell layers were first recognized in *S. trigonalis* by Dunlop (1962 : 483) who named them the lamellar (primary) layer, fibrous (secondary) layer and columnar (tertiary) layer. A 'Stereoscan' examination of both valves of *S. trigonalis* confirms most of Dunlop's findings. A primary layer about 15 μm thick is succeeded by a secondary layer of fibres, on average 20 μm wide, which are roughly diamond-shaped in profile (Pl. 22, fig. 3). Vertically stacked crystals comprising the tertiary layer of *S. trigonalis* occupy the greater part of the interior of both valves (Pl. 22, fig. 4). Towards the periphery of both valves secondary and tertiary layers may interdigitate (Pl. 22, fig. 5). Dunlop's view (1962 : 488) that the interlayering is due to fluctuations in the rate of shell growth is supported by my own observations. However, there are no sharp depositional breaks at any junction between secondary and tertiary layers, as Dunlop supposes, but occasionally slight variations in chemical composition of parts of the tertiary layer may produce, on etching, prominent growth lines which might be interpreted as such at lower magnifications. The tertiary layer fabric is grossly affected in the vicinity of muscle scars. Sections through a ventral muscle scar of one specimen of *S. trigonalis* reveal a myotest comprising narrow, irregular fibrous outlines, which in places almost tends to become finely granular (Pl. 22, fig. 6).

Representatives of the family Brachythyrididae differ from those of the family Spiriferidae mainly in being less transverse, with the width of the hinge line generally falling well short of maximum width. A well-preserved specimen of *Choristites mosquensis* Buckman from the Upper Carboniferous of the Moscow region, U.S.S.R., was used to determine the skeletal fabric of the family. The shell structure of *Choristites* is similar to that of *Spirifer trigonalis* in that three calcareous shell layers are present. The primary layer, measuring up to 25 μm thick, is normally recrystallized but it can still be recognized in sections as a uniform band of narrow, vertically stacked crystals which blanket the outer surface of both valves (Pl. 23, fig. 1). The secondary and tertiary layers, by contrast, are well preserved. In transverse sections, the secondary layer is seen to be built up of orthodoxly stacked fibres, averaging 10 μm in width, which display smoothly curved keels and saddles (Pl. 23, fig. 2). In both pedicle and brachial valves, the secondary layer is succeeded by a well-developed tertiary layer deposit (Pl. 23, fig. 3). The vertically stacked crystals of the tertiary layer may vary from 10 μm to more than 20 μm in width, due presumably to occasional localized breakdowns in the deposition of bounding organic membranes which may allow two or three adjacent crystals to merge as one. Nevertheless, the boundaries between crystals are normally upright, so it can be assumed that, during deposition of the tertiary layer, little or no lateral migration of outer epithelial cells took place. The tertiary layer of *Choristites* is characterized by a prominent transverse depositional banding with an average periodicity of 2 μm. Within each 2 μm-deep band, several more indistinct transverse bands may occur (Pl. 23, fig. 4). Approximately five minor bands may fit within one 2 μm band, giving an average periodicity for the minor banding of 0·4 μm. The latter value is consistent with measurements of fine depositional bandings recorded within the tertiary layers of other Spiriferida (and also *Gryphus*) and is thus considered to be diurnal. It is tempting, therefore, to rationalize the more prominent 2 μm bands in *Choristites* in terms of some other less frequent, yet still regular influence, such as fluctuating tidal behaviour. The secondary and tertiary layers of *Choristites* are seen to interdigitate frequently, as in *S. trigonalis* (Pl. 23, fig. 5). Muscle emplacement also gave rise to modifications in skeletal fabric similar to those observed in *S. trigonalis*. In the vicinity of muscle scars, the standard secondary or tertiary layers are disrupted and replaced by a deposit about 30 μm thick consisting of small, irregularly stacked fibres which may, in places, become more massive due to the welding together of adjacent margins (Pl. 23, fig. 6).

For comparison with *Choristites*, a specimen of *Brachythyris* sp. from the Lower Carboniferous of Kildare, Ireland, was sectioned. Although both valves proved to be badly altered, localized patches of secondary and tertiary layer deposits were positively recognized and allowed the calcareous shell succession for that genus to be established (Pl. 24, figs. 1, 2). In most respects, the calcareous shell succession of *Brachythyris* appears to be the same as that described for *Choristites*.

(iv) *Spiriferinacea*

The shell structures of three Carboniferous representatives of the Spiriferinacea were investigated with a view to making a general comparison with the standard shell succession of *Spiriferina walcotti*. These were *Crenispirifer* sp. from the La Salle Limestone (Pennsylvanian) of Ohio, and *Punctospirifer scabricosta* North and a specimen labelled as '*Spiriferina cristata* var. *octoplicata*' (tentatively referred to *Spiriferellina cristata* (Schlotheim)), both from Ashfell, Westmorland. Of these three, '*S. crista* var. *octoplicata*' was the least well preserved. A section through the pedicle valve of this specimen exposed a secondary layer built up of irregular fibres which measure, on average, 12 μm in width. The fibres are outwardly deflected to form cylindroid canals (puncta) which have a mean diameter of 20 μm (Pl. 24, fig. 3). No primary layer was preserved.

The shell of *Punctospirifer scabricosta* North was somewhat better preserved than that of the *S. cristata*, and a primary layer measuring 25 μm in thickness was clearly recognizable (Pl. 24, fig. 4). Fibres of the secondary layer are orthodoxly stacked and exhibit smoothly rounded keels and saddles like *S. walcotti* (Pl. 24, fig. 5). The puncta measure up to 30 μm diameter (Pl. 24, fig. 6).

The *Crenispirifer* sp. proved to be the most useful specimen for comparison with *S. walcotti*. Both primary and secondary shell layers are well preserved. The primary layer, which has a spongy texture, may measure up to 40 μm in thickness (Pl. 25, fig. 1). It is succeeded by an orthodoxly stacked secondary layer, composed of fibres on average 10 μm wide. Puncta up to 25 μm in diameter permeate both shell layers (Pl. 25, fig. 2), but no perforate canopies covering the distal ends of canals, as were found in *S. walcotti*, could be detected. The interior of the pedicle valve of *Crenispirifer* is divided medially by a high septum which like an identical structure in *S. walcotti* must have functioned as a muscle-attachment area. In transverse sections through the septum, narrow zones of small irregular myotest fibres can be traced running from base to apex on both sides to meet dorsally. The structure of the overlapping growth lamellae of *Crenispirifer*, which are formed as a result of periodic mantle retractions, differs in some respects from that of the overlapping growth lamellae described for *S. walcotti*. In *Spiriferina* the tip of the mantle lobe after the initial withdrawal began to deposit a series of horizontal, overlapping, organic and inorganic layers, but in *Crenispirifer* mantle regression was followed only by deposition roughly normal to the posteriorly inclined regression plane which preceded a return to normal primary and secondary shell deposition.

In summary, the shell structures of *Crenispirifer*, *Punctospirifer* and *Spiriferina cristata* are closely comparable with the standard shell succession of *Spiriferina walcotti*. No tertiary layer has been found in any Spiriferinacea.

(v) *Reticulariacea*

Unlike most forms assigned to the Spiriferidina, the Reticulariacea are generally recognized by being relatively smooth-shelled with rounded cardinal extremities and a short hinge line. Two species of *Phricodothyris* and one badly altered *Martinia* were available for study.

Transverse sections through both valves of *Phricodothyris* sp. from the Finis Shale (Pennsylvanian) of Texas reveal a remarkably well-preserved calcareous shell succession comprising three distinct layers. The primary layer, which measures up to 40 μm in thickness, is normally massive but in certain areas the texture may become porous, accompanied by the development of a fine lineation disposed normal to the outer shell surface (Pl. 25, figs. 3, 4). The surface micro-ornament of *Phricodothyris* is distinctive and involves some disruption of the primary layer. It consists of a series of regularly spaced concentric growth lamellae, each terminating anteriorly in a row of fine double-barrelled spines. Unlike the hollow spines of *Spiriferina walcotti* which connect with the shell interior by means of narrow canals, those of *Phricodothyris* terminate within the primary layer. Invariably the spines were broken, leaving only sunken bases which appear in longitudinal section as shallow, cigar-shaped hollows infilled with secondary material (Pl. 25, fig. 3). The general structure and possible function of the spines have already been discussed by George (1932 : 529) and need not be considered further. Clearly the spines of any one lamella were built up rapidly in localized patches of the circumferential generative zone of outer epithelium situated at the shell edge whilst neighbouring cells were still involved in the deposition of the primary layer. As George points out, the caecal prolongations of the mantle incorporated within the spines must have become wholly dead matter before the secretion of the next succeeding lamella.

Since a tertiary layer is deposited over the greater part of the shell interior, the secondary layer is comparatively thin, being about 25 μm in depth overall. Close to the valve margins, the secondary layer attains a thickness of nearer 40 μm which may indicate that the secondary layer secretory zone within the outer epithelium widened with age. Fibres are orthodoxly stacked and measure about 12 to 15 μm in width (Pl. 25, fig. 4). The tertiary layer consists of straight-sided, vertically stacked crystals which measure up to 15 μm in width (Pl. 25, figs. 4, 5). The fabric of the tertiary layer of *Phricodothyris* is strikingly similar to that of *Gryphus* even to the extent of exhibiting a regular transverse depositional banding. The banding in *Phricodothyris* sp. from the Finis Shale has an average periodicity of 1·5 μm.

From around the periphery of each concentric growth lamella, a plane dips posteriorly inwards to define the isochronous surface upon which the normal secretory processes were interrupted (Pl. 25, fig. 3). Such zones of mantle retraction must have been relatively narrow and confined to the outermost shell margins because regression planes, defining the extent of the disruption, terminate within the secondary layer. Although the zone of change-over from secondary to tertiary shell deposition is located very close to the valve margins, as in *Gryphus*, the tertiary layer is not affected by mantle regressions. As a result, there is no interdigitation of secondary and tertiary layers as, for example, in *Choristites*.

The shell structure of *Phricodothyris* sp. from the Carboniferous Limestone Series of Braidwood, Lanarkshire, was found to be identical to that of the American species. The transverse tertiary layer banding, in this case, had an average periodicity of 1·2 μm (Pl. 25, fig. 6).

The shell of the only specimen of *Martinia* that was available for study was badly altered, but parts of the original fabric could still be recognized. The primary layer had exfoliated, but parts of the secondary layer and a thick tertiary layer were identified (Pl. 26, figs. 1, 2).

(e) *Thecospira*

Thecospira is an unusual spire-bearing brachiopod, small but oyster-like in appearance, with a variably deep, cup-shaped pedicle valve and relatively flat, lid-like brachial valve. On the pedicle valve exterior there occurs a flattened cementation scar. In recent years there has been some debate as to the precise systematic position of *Thecospira*. Rudwick (1968 : 349) and Baker (1970 : 84) regarded it as an

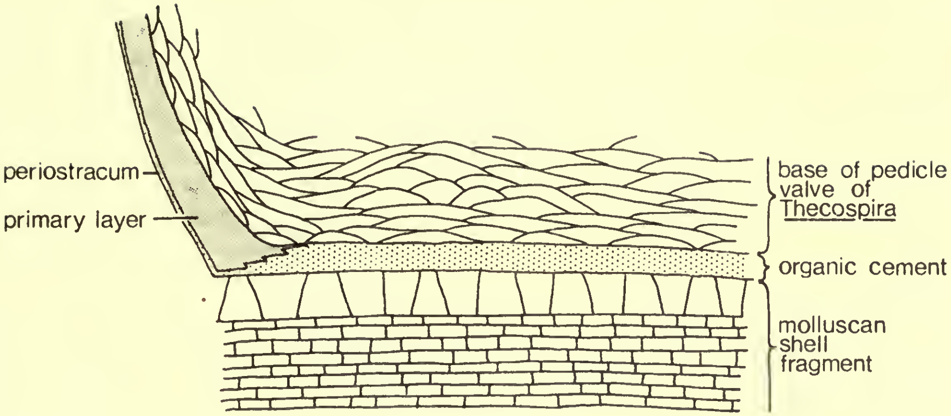

FIG. 19. Stylized section through part of the base of a pedicle valve of *Thecospira* cemented to a molluscan fragment, showing the inferred relationships between the organic cement, periostracum and primary layer.

aberrant strophomenide whereas Williams (1968a : 48 and 1972) argued convincingly in favour of a spiriferide identity for the genus. For precisely the same reasons as those put forward by Williams (1972) I regard *Thecospira* as a member of the Spiriferida.

The basic shell structure of *Thecospira* sp. collected from the St Cassian Beds (Triassic) of Northern Italy closely resembles that of *Spiriferina walcotti* (Sowerby) in that two calcareous shell layers are recognizable. An unusual aspect of growth of *Thecospira* is the absence of any recognizable primary layer within the cementation area of the pedicle valve. A complete specimen of *Thecospira* found cemented to a bivalve fragment was sectioned normal to the plane of attachment. In the brachial valve and in the convex, upstanding part of the pedicle valve, a primary layer measuring up to 25 μm in thickness was identified (Pl. 26, fig. 3), but below the attachment area a zone about 15 μm wide, infilled mainly with sediment, was found interposed between the flattened base of secondary layer fibres and the outer surface of the bivalve fragment (Pl. 26, fig. 5). Presumably this narrow zone was occupied during life by the organic adhesive which cemented the shell to the substrate (Text-fig. 19).

Since the initial secretory phase of newly proliferated cells comprising the outer mantle lobes of Recent brachiopods, both articulate and inarticulate, is known to involve the exudation of mucopolysaccharide, it is considered highly likely that a similar episode of organic deposition initiated the secretory regime of the thecospirid mantle. In the pedicle valve of *Crania anomala* Müller the cementing medium is the outer mucopolysaccharide layer (Williams and Wright 1970 : 18). The pedicle valves of living Thecideidina are presumably cemented to the substrate by a similar deposit, for mucopolysaccharide has been found as an impersistent external coating on the periostracum of *Thecidellina barretti* (Davidson) (Williams 1971b : 49). Since within the attachment area of the pedicle valve of *Thecospira* no primary layer is

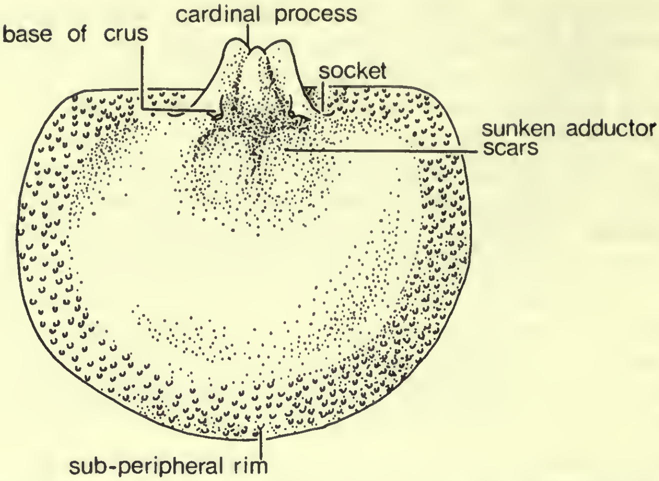

FIG. 20. View of the general morphology of the brachial valve interior of *Thecospira* (spiralium absent).

found, it seems likely that exudation of mucopolysaccharide and periostracum must have been sustained over a relatively broad zone of the outer mantle lobe. The suppression of the primary layer probably resulted from the persistent localized deposition of an organic pad internal to the periostracum which acted as a sufficiently rigid base and seeding sheet for the earliest-formed parts of secondary layer fibres.

Sections through both valves of *Thecospira* reveal that fibres of the secondary layer are orthodoxly stacked and measure, on average, 15 μm in width (Pl. 26, fig. 4). The interior of the brachial valve is not flat but sunken postero-medially in the vicinity of the dorsal adductor muscle scars and raised marginally as a tuberculate platform around the valve periphery (Text-fig. 20). A similar marginal tuberculate zone, forming a sub-peripheral rim, is known to occur in some thecideidines, including *Moorellina granulosa* (Moore) (Baker 1969 : 393). In radial sections through the brachial valve of *Thecospira*, each tubercle is found to comprise a cylindroid core of porous, non-fibrous calcite that protrudes above the surface of the rim and around which secondary layer fibres are deflected laterally and inwardly (Pl. 27, figs. 1, 2, 3, 4). Tubercles with solid cores of this sort measuring up to 60 μm in diameter closely resemble the pseudopuncta of certain Plectambonitacea and Gonambonitacea (Williams 1970 : 340). Pseudopunctation is also characteristic of the laminar shelled Strophomenida (Williams 1968a : 40), including all but the earliest Davidsoniacea. Yet the 'pseudopunctation' of *Thecospira* is much closer to that described for the spire-bearing *Cadomella*, the terebratulide *Megerlia* or more strikingly the Jurassic thecideidine *Moorellina* than it is for any of the earlier strophomenide or orthide stocks, for inwards of the sub-peripheral rim the tubercles are resorbed and overlapped by later secondary shell material. Submerged tubercles considered to have been functional peripherally are also found distributed sporadically within the secondary shell succession of the pedicle valve of *Thecospira*. The tubercles of both valves are not continuous with the primary layer as in *Moorellina* (Baker 1970 : 87), but arise as modifications of pre-existing secondary layer fibres.

Both punctate and impunctate specimens of *Thecospira* were collected from the same locality but whether or not they are variants of the same species has still to be established. The puncta occur as sediment-filled canals measuring up to 40 μm in diameter which permeate the primary and secondary shell layers (Pl. 27, figs. 4, 5). Whereas fibres are deflected towards the shell interior around tubercle cores, they are outwardly deflected around puncta.

In one punctate brachial valve of *Thecospira*, sections through the secondary layer revealed a series of at least six transverse micritic bands up to 10 μm thick which ran parallel with the inner shell surface and were outwardly deflected by puncta (Pl. 27, figs. 5, 6). The vertical spacing between bands is variable but generally measures about 10 μm to 20 μm. Since the bands are most prominent towards the inner surface and close to the valve periphery it is believed that they mark successive levels of organic layers which were sandwiched within the normal calcareous succession. Such periodic reversals to wholly organic exudation may have corresponded to temporary halts in shell growth, for fine overlapping growth lamellae do occur around the periphery of gerontic specimens. However, in the particular shell section which was found to exhibit a banded succession, individual growth lamellae could not be directly correlated with the micritic layers.

The dorsal and ventral myotests of *Thecospira* are composed of modified secondary layer fibres. The outlines of individual fibres are irregular and the lateral margins of adjacent fibres often occur welded together (Pl. 28, fig. 1). In the pedicle valve the arcuate anterior borders of the two ventral diductor scars are raised above the valve floor to form an anteriorly inclined overhang (Pl. 28, fig. 2). This semi-recumbent ridge is considered to have developed in response to the stresses placed on the overlying outer epithelium by the most anterior part of the ventral muscle base. It is evident that the angle between the shell surface and the estimated disposition of the long axes of muscle fibres in that region would approach more closely the most efficient maximum of 90 degrees (Text-fig. 21).

V. STRUCTURE OF THE BRACHIDIUM AND INFERRED DISPOSITIONS OF THE LOPHOPHORE IN SPIRIFERIDA

(a) Structure of spiralia

Within the order Spiriferida, the size, shape and disposition of the spiral brachidium that, in all probability, supported the lophophore are highly variable. In one of the earliest-known spiriferides, *Protozyga elongata* Cooper, support for the lophophore is rudimentary and consists simply of a pair of short prongs which extend anteriorly from a median connecting band, the jugum (Williams & Wright 1961 : 158, fig. 4g). When sectioned transversely close to the jugum, the calcareous outgrowths of *P. elongata* are found to be extremely slender. Sections through either branch reveal

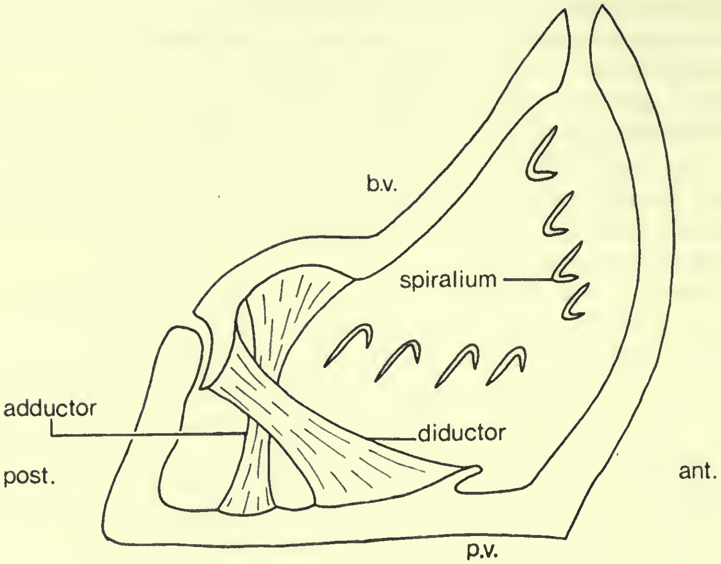

FIG. 21. Stylized longitudinal section through both valves of *Thecospira* showing the inferred dispositions of adductor and diductor muscles, and the U-shaped profiles of the spiral lamellae (b.v. – brachial valve, p.v. – pedicle valve).

outlines of only 25 to 30 secondary layer fibres stacked orthodoxly in rows up to five deep (Pl. 28, fig. 3). This compares with well over 1000 individual fibre outlines arranged in rows up to about 40 fibres deep occurring in any one transverse section through a spiral lamella of a mature *Spiriferina*. Due to secondary recrystallization, the precise attitude of the fibres comprising the brachidium of *P. elongata* could not be established with any degree of certainty.

In slightly younger representatives of the same stock, such as *Protozyga exigua* Hall which appeared in the late Ordovician (Rockland Formation), the anterior prolongations of the jugum extend further as a pair of narrow ribbons each coiling for up to one convolution, as a planispire aligned parallel to the median plane. Planispiral coiling of the brachidium in a plane parallel to the median plane is repeated and increased to 3 or 4 convolutions in the smooth Dayiacean, *Cyclospira*, although it is reported to be ajugate.

A number of late Ordovician and early Silurian genera characterized by the development of spiralia with medially directed apices are considered to have evolved from the primitive protozygid stock. These include *Catazyga, Zygospira, Idiospira* and *Glassia*. However in the majority of later Atrypacea, including *Atrypa*, the spiralia became reorientated dorso-medially with apices directed towards the midline of the brachial valve.

In almost all remaining Spiriferida, the apices of spiralia are directed laterally but in some genera, such as *Koninckina, Thecospira* and *Cyrtina*, the spiralia were directed ventrally or postero-ventrally. In a number of athyrididines, postero-median growth and bifurcation of the jugum resulted in the development of a pair of recurved arms (accessory lamellae) which were positioned adjacent to the innermost lamellae of the primary coils of the spiralia. In *Diplospirella* and certain allied genera continued growth of the accessory lamellae gave rise to a pair of intercoiled accessory spires which extended as far as the apices of the primary ones.

The structure and growth of the spiralia of *Spiriferina walcotti*, which may be considered as typical of many Spiriferida, have already been described (see p. 206). Secondary layer fibres which are generated in a zone running around the sharp outer edges of the spiralium are secreted on both sides of the spiral lamella and each fibre is seen to follow an arcuate path away from the apex of the spire which, it is believed, corresponds to a segment of a logarithmic spiral. In cross section, the convex keels of fibres arch outwards in both directions from a median plane (Text-fig. 7b). Similar double-sided spiral lamellae have been identified in the early atrypaceans *Catazyga headi* (Billings) (Pl. 28, fig. 4), *Idiospira thomsoni* Davidson (Pl. 28, figs. 5, 6), the dayiacean *Dayia navicula* (Sowerby) (Pl. 29, fig. 1), the early retziidine *Rhynchospirina maxwelli* Amsden (Pl. 29, fig. 2), the cyrtiacean *Ambocoelia umbonata* (Conrad) (Pl. 29, figs. 3, 4) and the spiriferaceans *Theodossia hungerfordi* (Hall) (Pl. 29, fig. 5), and *Spirifer trigonalis* Martin (Pl. 29, fig. 6). Spiralia belonging to the aforementioned genera, when sectioned, present a similar profile to that described for *Spiriferina*. The outward edge of each lamella is pointed whereas the inner edge is generally truncated. The thickest part of the lamella is around its mid-region. On either side of a line running from roughly the middle of the blunt inner edge to the fine outer edge, the convex keels of small regularly stacked secondary layer fibres, generally less than 10 μm in width, arch outwards. Narrow spines, which outwardly deflect localized groups of fibres, project from the median-facing side of the spiralia of *Idiospira* (Pl. 28, figs. 5, 6). Presumably these spines performed a similar function, and were deposited in a similar manner, to those projecting from parts of the spiralia of *Spiriferina*.

The structure of the spiralia of certain Athyrididina differs markedly from the structure of those previously described. Instead of exhibiting a double-sided growth pattern, sections through the athyrididine spiralia reveal deposition of secondary layer fibres on only the median-facing side of each lamella. As spiralia were generally embedded in rock matrix enclosed within both valves of each specimen, it was not possible to view surfaces of lamellae directly to establish the precise orientation of fibres. However, this could be deduced by preparing two vertical transverse sections which cut tangentially through the edges of the spiralia (Text-fig. 22a), once on its anterior side and once on its posterior side, and then noting the relative disposition of fibres in each section (Text-fig. 22b). In the anterior section, fibres are directed dorsally whereas in the posterior section they are directed ventrally. Progressive changes in the cross-sectional outlines of fibres between the dorsal and ventral extremities of each sectioned lamella are considered to reflect corresponding changes in the orientation of fibres from one end to the other. The observed pattern of sectioned fibres corresponds to that occurring in one half of a sectioned 'double-sided' spiral, such as in *Spiriferina*, and clearly reflects for each individual skeletal unit a

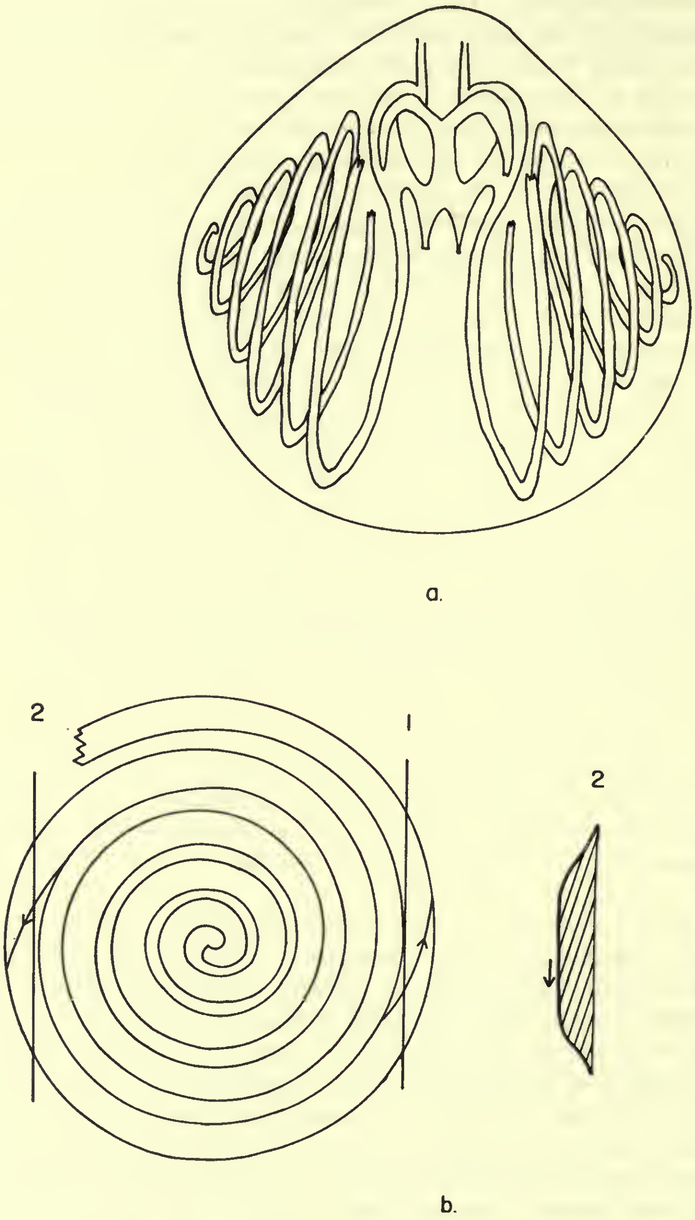

FIG. 22. a. Generalized plan view of an athyrid spiralium. The two lines of section are located on either side of the axis of the spiralium. Consecutive coils of each spire are not planar but curved so as to appear outwardly concave. b. Lateral view of a spire showing the lines of section and the growth direction of fibres. In the anterior section (1) fibres are directed dorsally whereas in the posterior section (2) fibres are directed ventrally.

similar pattern of fibre growth. Since each spiral lamella grew by accretion of secondary layer material on only the median-facing side, it is evident that resorptive processes must have operated on the apical side. Although the arrangement of growth and resorption faces is contrary to what might be expected, a steady overall increase in the size of the spiralia can still be achieved dependent on the attitude of the lamellae. Consecutive coils of the spiralia of many athyrididines are not planar but curved so as to appear outwardly concave. In consequence the terminal faces of fibres deposited on the median-facing side of both spires are directed outwards away from the median plane.

'Single-sided' spiral lamellae have been identified in the athyridaceans *Composita ambigua* (Sowerby) (Pl. 30, figs. 1, 2), *Athyris spiriferoides* (Eaton) (Pl. 30, fig. 3), *Diplospirella wissmani* (Münster) (Pl. 30, fig. 4) and *Anisactinella quadriplecta* (Münster) (Pl. 30, fig. 5), as well as other more distantly related forms including *Koninckina leonhardi* (Wissman) (Pl. 30, fig. 6 ; Pl. 31, fig. 1), *Amphiclina amoena* Bittner (Pl. 31, fig. 2) and *Thecospira* sp. (Pl. 31, fig. 3).

Compared with secondary layer fibres found elsewhere in the brachial valve, those comprising the spiralia of *Diplospirella* and *Anisactinella* are abnormally small. On both primary and accessory lamellae fibres measure, on average, 12 μm in width as opposed to 60 μm width on the floor of each brachial and pedicle valve. The accessory lamellae as well as the primary lamellae of *Diplospirella* and *Anisactinella* are characterized by one-sided growth, although the convex keels of fibres arch outwards towards the apices of the spiralia and not medially as on the main spires (Text-fig. 23). Since each coil of the accessory lamellae is situated lateral to the corresponding coils of the primary lamellae it is evident that two non-depositional faces are in opposition to one another throughout. Both primary and accessory lamellae are fimbriate but as yet it has not been established whether the fimbriae occur on only the anterior-facing edges of the spires, as in *Spiriferina*. Nevertheless, presumably they served a similar purpose. The spinous outgrowths are found to project from only the median-facing side of primary lamellae and the apical side of accessory lamellae. On the opposite sides of both sets of lamellae, spine bases are resorbed along with the long exposed trails of fibres comprising the rest of that surface.

Although parts of the calcareous lophophore supports of some living Terebratulida are known to be fimbriate, the relationships between fimbriae and adjacent soft tissues, as well as modes of secretion, have yet to be established. At high magnifications, the distal extremities of spines projecting from the spiralia of *Diplospirella* are noticeably jagged, resembling in shape the thorns of a rosebush. Such products of mineral deposition are totally foreign to mature outer epithelial cells which are normally involved in the build-up of more conventional secondary shell material, but some elements of spicular skeletons, known to be secreted within the lophophore and mantle of a number of living Terebratulida, bear resemblance to the jagged parts of spines. Spicules, however, are found only within the inner epithelium and connective tissue where, according to Williams (1968b : 280), they develop within scleroblasts. Assuming that the primary and accessory spiralia of *Diplospirella* were ensheathed by connective tissue and inner epithelium of the lophophore, the 'raw materials' for spicule formation were certainly available. However, to become embedded within the secondary shell succession of the spiralia, spines secreted by mesoderm or endoderm must first have pierced the outer epithelial lining, which seems unlikely. More probably, the spines were secreted by specialized outer epithelial cells reminiscent in structure and function of those which must have contributed to the formation of solid tubercle cores or taleolae in other genera.

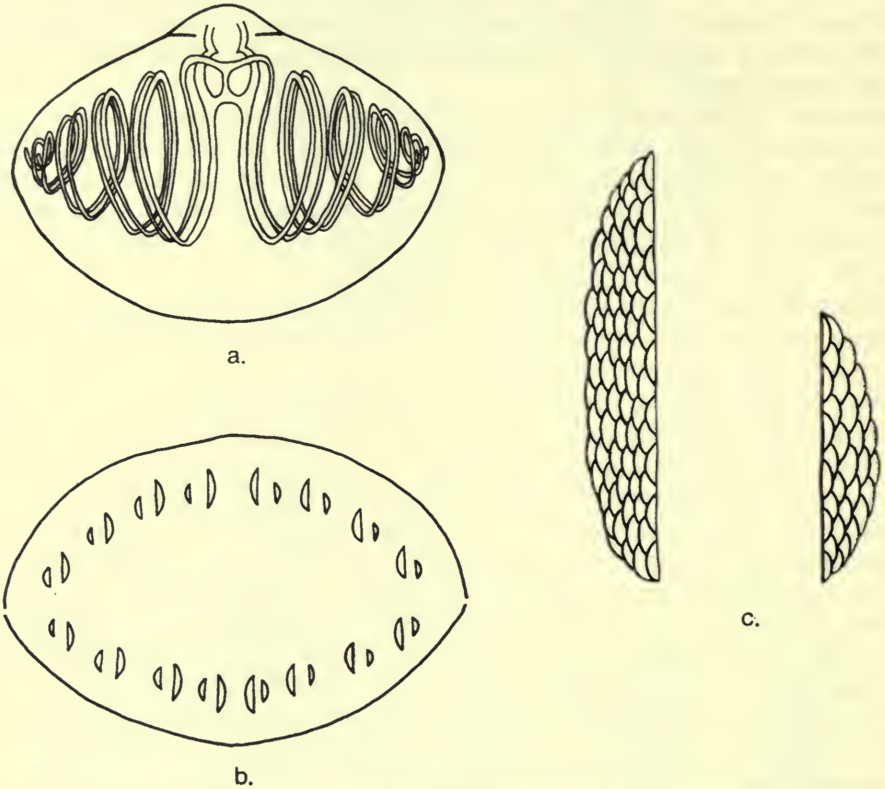

Fig. 23. a. View of the spiral brachidium of *Diplospirella wissmani* showing the disposition of the primary and accessory lamellae. b. Transverse section through both valves and spiralium of *Diplospirella*. c. More detailed view of a transverse section through a primary (left) and accessory (right) lamella of *Diplospirella* showing the shape and stacking of secondary layer fibres.

In Koninckinacea, the brachidium consists of a pair of double spires with the principal pair arising on a simple crural process from which they diverge at a sharp angle. A jugum is formed by the anterior extension and union of the crural processes, and the accessory spires which originate on this connecting band lie ventral to the main pair and are co-extensive with them. The apices of both pairs of spiralia are directed towards the lateral slopes of the pedicle valve (Text-fig. 24a, b).

By comparison with the giant-sized fibres which make up the general shell succession of *Koninckina*, the fibres composing the spiral brachidia are small (on average

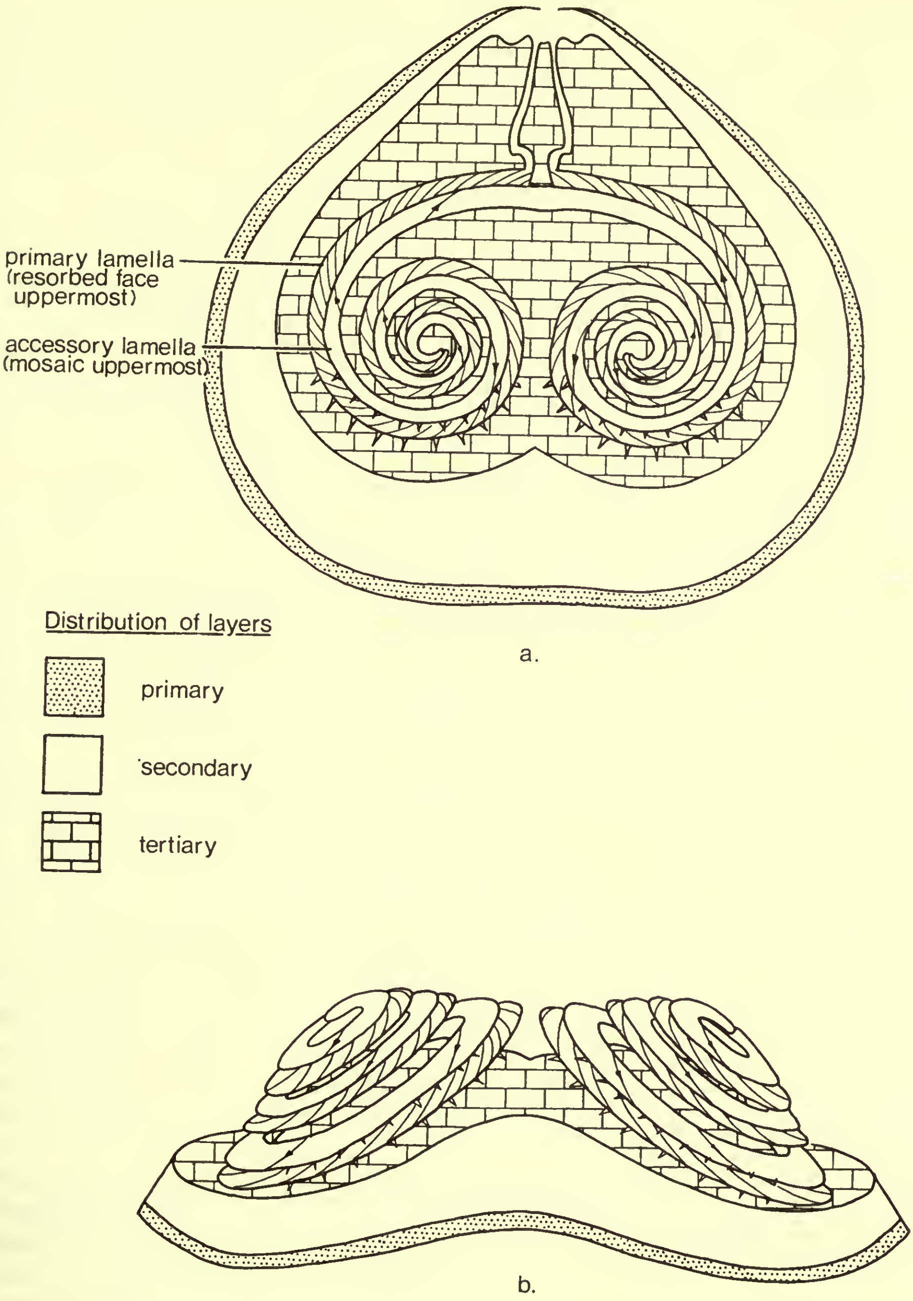
primary lamella
(resorbed face
uppermost)
accessory lamella
(mosaic uppermost)
Distribution of layers
a.
primary
secondary
tertiary
b.

FIG. 24. Plan view (a) and anterior view (b) of a generalized koninckinacean brachial valve interior showing the disposition of the spiralium (including growth vectors of fibres) and the distribution of shell layers.

about 7 μm wide). The size range of those fibres in the brachial structures, however, compares more favourably with that of fibres occurring in other articulates such as *Retzia* sp., even from the same horizon, in which mature secondary layer fibres are about 10 μm wide. As previously mentioned, fibres composing the spiralia of *Diplospirella* and related genera are about a fifth the size of those occurring elsewhere in both valves.

Transverse sections through the arms of the koninckinacean spiralium reveal something of the size, shape and stacking of its constituent fibres (Pl. 30, fig. 6 ; Pl. 31, fig. 1). Fibre outlines associated with such structures appear much more conventional than those of the rest of the shell in that they display easily recognizable keels and saddles. This configuration provides a convenient means of recognizing growth surfaces, since the convex surfaces of keels always face towards a depositional surface. In *Koninckina* the regular overlapping habit of fibres in sections through spires indicate that deposition took place on the dorsal surface of the primary lamellae and on the ventral surface of the accessory lamellae. The two inner opposing faces of the primary and accessory lamellae were thus surfaces of resorption.

Whilst examining specimens of *Amphiclina*, a disarticulated pedicle valve was found which retained part of a primary lamella still located in almost the exact position of growth (see Pl. 16, fig. 3). The ventral-facing (resorbed) side was uppermost. Nevertheless, despite the lack of any recognizable mosaic, it was possible to plot the long axes of exposed trails of fibres, and by using them as growth vectors, thereby reconstruct an overall brachidial growth pattern. The fibres comprising each spiral lamella curve obliquely across its surface (Pl. 31, fig. 2 ; Text-fig. 24), from inner to outer edge, like those of *Spiriferina*, in such a way that their trails inscribe a spiral curve (probably logarithmic) on which the terminal parts of fibres are directed progressively further away from the apex of the spire to produce a gradual peripheral expansion along the outer edge of every whorl. On the outer half of the ventral side of the primary lamella, the oblique outlines of exposed trails are replaced by a much finer lineation aligned at right angles to the outer edge of the lamella. At high magnification (Pl. 31, fig. 4), the lineation appears as a series of narrow troughs and ridges, on average 4 μm wide. No comparable features have, as yet, been recognized on any other articulate brachiopod so that the mode of formation and function of such lineations are problematical. However, it seems likely that they may be the product of some unusual resorptive process. Both primary and accessory lamellae of koninckinaceans are fimbriate, in the sense that fine spines project obliquely from their depositional surfaces and cause the trails of surrounding fibres to be gently deflected around them.

The form of spiral brachidium that is characteristic of *Thecospira* differs markedly from that found in all other Spiriferida. A comprehensive description of the macroscopic morphology of the thecospirid brachidium has been given by Rudwick (1968 : 337) and needs only to be referred to briefly. From the base of the cardinal process, a pair of short crura extends anteriorly to join with, and support, the ventrally directed spiralia. According to Rudwick, a simple transverse jugum connects the proximal ends of the crura. Each lamella is U-shaped in section (Text-fig. 21) with the dorsal branch being thicker and about twice as long as the ventral one. The two branches close inwardly on the side closest to the spiral axis, so that the groove faces laterally outwards.

At the microscopic level, the dorsal limb of the U is found to comprise small, orthodox secondary layer fibres which measure, on average, 8 μm in width, but the lower limb is essentially non-fibrous (Pl. 32). The convex keels of fibres in the upper limb face ventrally into the groove and towards the lower limb. In cross section the profile of the lower limb is undulating in such a manner as to suggest, in three dimensions, that it is fluted parallel or subparallel to the length of the spire. This interpretation is further supported by the occurrence of a series of concentrically banded zones, each about 20 μm wide, which coincide with the undulations (Pl. 31, fig. 5). The narrowest diameters of the concentric bands are so fine that it seems most likely that the zones terminate distally as sharp points. If this is the case, then the undulations may be considered as sections through laterally fused spinose outgrowths which project obliquely outwards from the lower limb of the U-shaped groove.

At the junction of the upper and lower limbs the secondary layer fibres are bent round through 180 degrees so that their curved saddles come to rest against the inner surface of the lower limb. At the opposite, outer edge of the upper lamella, fibres are deflected around spine bases. Since peripheral spine bases have been recognized in every section through the spiralia of *Thecospira* that has been examined, they must be densely distributed in that area. Fibres of the upper limb are also disturbed within a variably wide non-fibrous zone which runs from midway along the ventral surface, obliquely inwards, and terminates on the dorsal surface just above the junction of the upper and lower limbs of the U. In some sections, the enclosed accretions are fairly massive, but in others they are much less prominent. Small concentrically banded zones have been recognized within some of these, and may represent parts of embedded spines (Pl. 31, fig. 6). Since no similar deposits have been recognized within the brachidia of other fossil or Recent brachiopods, they are extremely difficult to interpret mainly because any sediment-free fragments of spires on which a three-dimensional reconstruction could be based are lacking. Once suitable specimens are found a more enlightened explanation may be forthcoming. At present, the only objects that can be considered as likely to give rise in section to such amorphous shapes are forms of spicules such as are found within the lophophore and mantle of some living Terebratulida.

Sections cut through the middle of spiral coils reveal transverse outlines of fibres but tangential sections show successions of long trails of fibres. If the shape of sectioned fibres can be taken as a rough guide to their orientation, then it is evident that the fibres comprising the upper limbs of the grooved spiral lamellae are aligned sub-parallel to the curved edges of the spiralia. This is essentially the same pattern as that observed in more conventional spiralia (equiangular spiral growth), thus it is assumed that the spiral lamellae of *Thecospira* grew in the same way.

(b) Inferred dispositions of the spiriferide lophophore

The relationships between skeletal supports and brachial appendages have been investigated in living Terebratulida with a view to establishing the most likely dispositions of the lophophore in extinct Spiriferida. In living long-looped forms, such as *Macandrevia*, the lateral arms of the plectolophous lophophore are supported by the ascending and descending branches of the calcareous loop (Text-fig. 25).

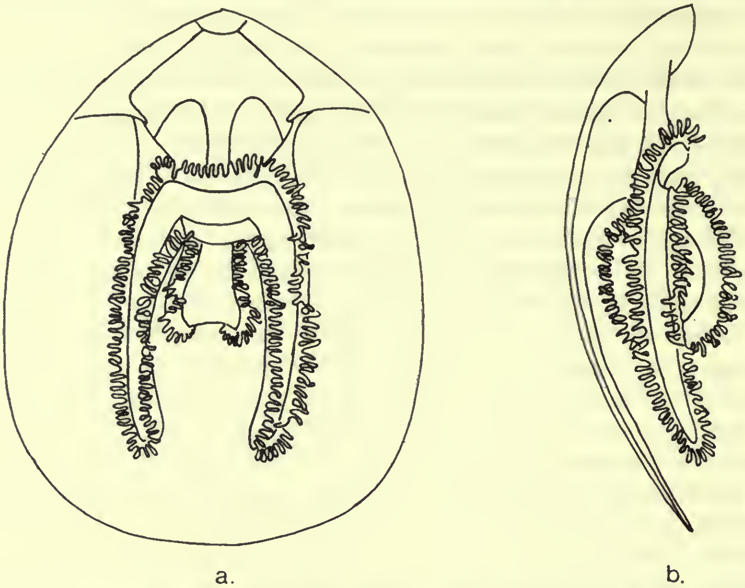

FIG. 25. Ventral (a) and lateral (b) views of the plectolophe of *Macandrevia* and its calcareous supports.

They bear a double brachial fold, two rows of paired filaments, and are served by two brachial canals (Williams 1956 : 263). As both canals are tucked in between the ascending and descending branches of the loop, it is of interest to note that opposing faces of the calcareous support of each side-arm bear surfaces of resorption while those on outward-facing sides bear surfaces of growth which exhibit a well-developed secondary shell mosaic. When viewed in section, the convex keels of fibres comprising the ascending and descending branches are seen to arch outwards away from each other (Text-fig. 26). Since exactly the same relationship exists between fibres comprising the primary and accessory lamellae of *Diplospirella* and *Koninckina* it seems reasonable to assume that the brachial canals of these extinct genera must also have occupied a median position between the two lamellae. Thus in more normal athyrididines in which the accessory lamellae are greatly reduced or non-existent, the brachial canals of the lophophore must have been situated on the apical sides of the primary lamellae. By using the one-sided distribution of spinose outgrowths (fimbriae) as a means of determining the position of the lophophore, Rudwick (1960a : 375) arrived at the same conclusion. Since the double-sided spiral lamellae of most other Spiriferida also bear spines on their median-facing sides, Rudwick considered that they too possessed brachial systems orientated with the main body of the lophophore situated on the apical sides of lamellae. Certainly in those forms which

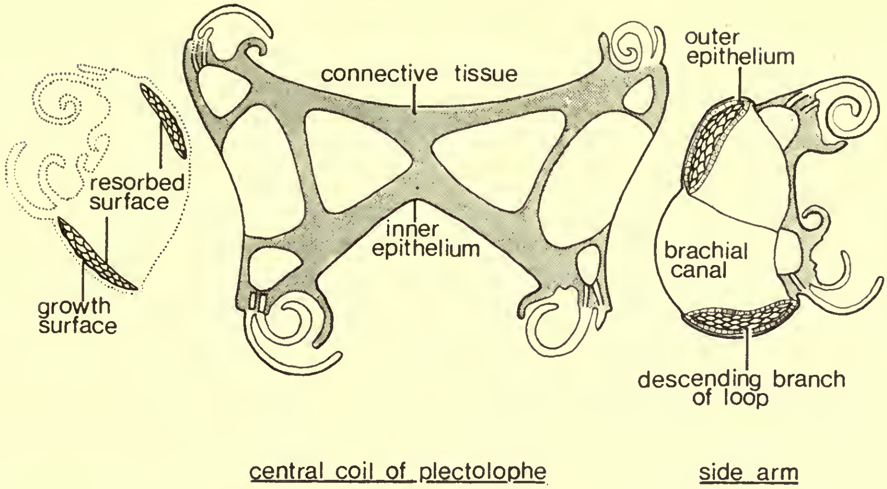

FIG. 26. Stylized transverse section through part of the plectolophe of *Macandrevia* showing the relationship of soft parts to the growth and resorbed surfaces of the ascending and descending branches of the loop. (After Williams, 1956 : text-fig. 4.)

show the greatest swelling in the median regions of lamellae, such as *Spirifer trigonalis*, the greater part of the swelling is on the apical side. In addition, since the width of the lamella is greatly reduced in its inner half, behind the swelling, partial resorption must have operated on some parts of that side. Thus the disposition of the brachial canals can still be correlated with areas of resorption on double-sided lamellae. In *Thecospira*, the inferred disposition of the lophophore, as deduced by this method, contradicts the hitherto perfectly plausible views expressed by previous authors (e.g. Rudwick 1968 : 335, fig. 3B). Placed against the surface undergoing resorption the main body (or brachial axis) of the lophophore would have rested on the dorsal surface of the broad fibrous limb of the U-shaped lamellae, and not within the groove. The precise orientations of the brachial groove(s) and filaments which comprised the food-gathering apparatus of the lophophore are less easy to decipher and, regrettably, ultrastructural studies relating to brachidial structure shed little new light on this tantalizing problem. Whether the spiriferid brachidium supported a simple spirolophe (Rudwick 1960a, b) with only a single set of filaments and one food groove, or a doubled set of appendages, the deuterolophe (Williams 1956 : 270, 1960 : 515 ; Williams & Wright 1961 : 149-176) is still open to discussion. However, since spiral brachidia may be divided into two separate groups based principally on the recognition of single or double-sided growth patterns, it may well have been that a genuine diversity in brachial structure existed. By analogy with the side-arms of long-looped terebratulides, the twin coils of spiralia belonging to forms such as *Diplospirella* and *Koninckina* may have supported a double row of paired filaments. If so, the single spiral coils of other athyrididines may also have provided a lesser support for the same system. On the other hand, spiral brachidia exhibiting double-sided growth may have supported single spirolophes, especially in those forms which appear to be without a jugum as in a number of cases.

VI. CONCLUSIONS

Recent research has shown that, in all probability, the secretory regime of articulate and inarticulate brachiopods has always involved at least three fundamental operations. Certainly in all forms of living brachiopods yet studied at the ultrastructural level (including Craniacea, Rhynchonellida, Terebratulida and Thecideidina) deposition of an outer mucopolysaccharide cover and an inner fibrillar triple-layered membrane has preceded secretion of the predominantly mineralized part of the exoskeleton. Presumably these two organic constituents comprised part, if not all, of the periostracal covering to the calcareous exoskeleton of the primitive *Protozyga*-like stock which is considered as ancestral to all Spiriferida (Text-fig. 27). If similarities in shell structure between *Protozyga* and contemporary Rhynchonellida are of any significance in indicating a common ancestor, then the earliest representatives of the Spiriferida almost certainly had only two calcareous shell layers. By the beginning of Silurian times, however, the secretory regime of most Spiriferida had developed further giving rise to three main types of skeletal fabric. The first, which includes the Atrypacea, Dayiacea, early Athyridacea and some early Spiriferacea, was characterized by being impunctate and possessing a variably thick tertiary prismatic layer in addition to the standard primary and secondary layers. The second group, including the Retziacea and Suessiacea, which were both punctate, possessed only primary and secondary shell layers. The third group, including the Cyrtiacea and remaining Spiriferacea, was the most conservative and secreted impunctate shells consisting only of primary and secondary layers.

Throughout the remainder of spiriferide evolution such clear-cut distinctions were not maintained. As far as is known all Atrypidina possessed three calcareous shell layers, but, unlike the Meristellidae, few later Athyridacea appear to have secreted a tertiary layer. *Cleiothyridina* is the only known Carboniferous athyrid to have done so. The Triassic Diplospirellinae are characterized by an exceedingly coarse fibrous secondary layer, but no additional tertiary layer deposit like that found in contemporary and younger Koninckinacea is present. The exoskeletal succession of the Retziacea was remarkably stable from Silurian to Triassic times. The impunctate Cyrtiacea and punctate Suessiacea were equally conservative. Considerable variation is shown, however, within the remainder of the Spiriferidina. As far as is known, nearly all Devonian Spiriferacea possessed only primary and secondary layers but later stocks show greater diversity. Punctation was developed in at least two stocks, the Spiriferinacea and Syringothyridae, and tertiary prismatic layers are found in some Carboniferous Spiriferidae and Brachythyrididae. In the Reticulariacea, too, a tertiary layer was deposited. Tubercles with non-fibrous cores grew peripherally in punctate and impunctate Thecospiridae and some Koninckinacea, but away from the shell edge they ceased to become functional and were submerged within later-formed parts of the calcareous succession. In this respect, such rod-like bodies differ from the pseudopuncta of Strophomenida with which they have, in the past, been compared and no special phylogenetic significance is attached to their appearance.

From the foregoing account, it is evident that despite the great diversity of form that has accompanied spiriferide evolution, there were few radical changes in

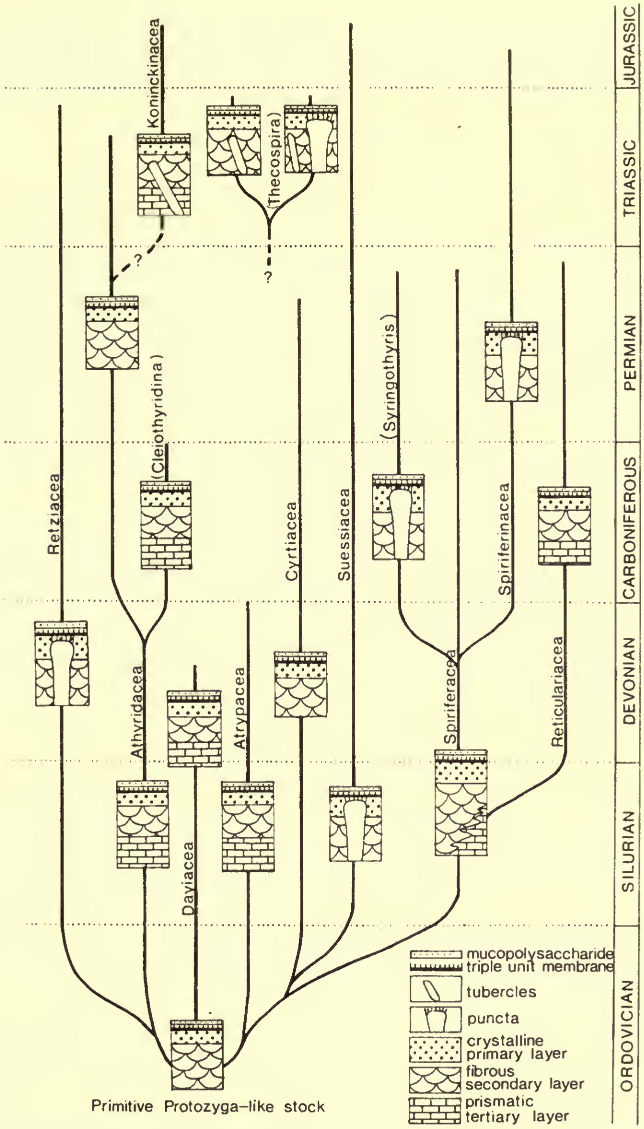
JURASSIC
TRIASSIC
PERMIAN
CARBONIFEROUS
DEVONIAN
SILURIAN
ORDOVICIAN
Koninckinacea
(Thecospira)
?
?
Retziacea
(Cleiothyridina)
Athyridacea
Daviacea
Atrypacea
Cyrtiacea
Suessiacea
(Syringothyris)
Spiriferacea
Spiriferinacea
Reticulariacea
Primitive Protozyga–like stock
mucopolysaccharide
triple unit membrane
tubercles
puncta
crystalline primary layer
fibrous secondary layer
prismatic tertiary layer

FIG. 27. Inferred phylogeny of the skeletal successions of the Spiriferida.

secretory regime. In *Spiriferina walcotti* (Sowerby), which has been selected as a standard model for spiriferide shell deposition, and in living Terebratulida, the structure of the primary and secondary layers and the finer details of shell punctation are very similar. Clearly the spiriferide outer epithelium was little different from that found in most living articulates. Even in forms possessing a tertiary layer, the nature of the outer epithelium may be reasonably inferred on account of a similar layer occurring in the living terebratulide *Gryphus vitreus* (Born). Indeed, all basic mantle secretory processes that are known to have operated in spire-bearing Brachiopoda, from their appearance in the Ordovician to their extinction in the Jurassic, were successful enough to have been retained by living articulate brachiopods of one form or another.

VII. ACKNOWLEDGEMENTS

I am greatly indebted to Professor Alwyn Williams, Queen's University of Belfast, for his guidance and encouragement whilst this work was in progress, for critically reading the manuscript and for his willingness to discuss the subject at all times. Additional discussion on many aspects of the work with Dr C. H. C. Brunton of the British Museum (Natural History) was invaluable and rewarding.

To Mr R. Reed and the technical staff of the Faculty of Science Electron Microscopy Unit, Queen's University of Belfast, I am most grateful for instruction in the preparation and examination of the material referred to in this publication, and for the production of electron micrographs figured herein.

For the loan or gift of fossil material I am most grateful to Dr W. D. I. Rolfe of the Hunterian Museum, University of Glasgow, Professor Alwyn Williams, Dr A. D. Wright and Mr Ian Mitchell of the Department of Geology, Queen's University of Belfast, and Dr C. H. C. Brunton.

Finally, I gratefully acknowledge the award of a research studentship from the Natural Environment Research Council.

VIII. REFERENCES

AMSDEN, T. W. 1958. Haragan articulate brachiopods; supplement to the Henryhouse brachiopods. *In* Amsden, T. W. & Boucot, A. J. Stratigraphy and paleontology of the Hunton Group in the Arbuckle Mountain region. *Bull. Okla. geol. Surv.*, Norman, **78**: 9–157, pls. 1–14.

ARMSTRONG, J. D. 1968a. Microstructure of the shell of a Permian spiriferid brachiopod. *J. geol. Soc. Aust.*, Adelaide, **15**: 183–188, pls. 15–18.

—— 1968b. Analysis of the function of the diductor muscles in articulate brachiopods. *Neues Jb. Geol. Paläont. Mh.*, Stuttgart, **11**: 641–654.

BAKER, P. G. 1969. The ontogeny of the thecideacean brachiopod *Moorellina granulosa* (Moore) from the Middle Jurassic of England. *Palaeontology*, London, **12**: 388–399, pls. 73, 74.

—— 1970. The growth and shell microstructure of the thecideacean brachiopod *Moorellina granulosa* (Moore) from the Middle Jurassic of England. *Palaeontology*, London, **13**: 76–99, pls. 18–21.

BIERNAT, G. & WILLIAMS, A. 1971. Shell structure of the siphonotretacean brachiopods. *Palaeontology*, London, **14**: 423–430, pls. 75, 76.

BITTNER, A. 1890. Brachiopoden der Alpinen Trias. *Abh. K.-K. geol. Reichsanst.*, Wien, **14**: 1–325, pls. 1–41.

BOUCOT, A. J., JOHNSTON, J. G. & STATON, R. D. 1964. On some atrypoid, retzioid and athyridoid brachiopods. *J. Paleont.*, Tulsa, **38**: 805–822, pls. 125–128.

—— —— —— 1965. Order Spiriferida, suborders Atrypidina, Retziidina, Athyrididina. *In* Moore, R. C. (Ed.), *Treatise on Invertebrate Paleontology*, **H**: 632–668. Lawrence, Kansas.

BRUNTON, C. H. C. 1969. Electron microscopic studies on growth margins of articulate brachiopods. *Z. Zellforsch. mikrosk. Anat.*, Berlin, &c., **100**: 189–200, 13 figs.

Brunton, C. H. C. & MacKinnon, D. I. 1972. The systematic position of the Jurassic brachiopod *Cadomella*. *Palaeontology*, London, **15** : 405–411, pls. 76–78.

Cooper, G. A. 1954. Unusual Devonian brachiopods. *J. Paleont.*, Tulsa, **28** : 325–332, pls. 36, 37.

—— 1956. Chazyan and related brachiopods. *Smithson. misc. Collns*, Washington, **127** : 1–1245, pls. 1–269.

Copper, P. 1967. The shell of Devonian Atrypida (Brachiopoda). *Geol. Mag.*, London, **104** : 123–131, pls. 5, 6.

Cowen, R. & Rudwick, M. J. S. 1966. A spiral brachidium in the Jurassic chonetoid brachiopod *Cadomella*. *Geol. Mag.*, London, **103** : 403–406.

Davidson, T. 1852. Oolitic and Liasic Brachiopoda. *In* A monograph of the British fossil Brachiopoda. *Palaeontogr. Soc.* (*Monogr.*), London, **1**, (3) : 1–100, pls. 1–18.

Dunlop, G. M. 1962. Shell development in *Spirifer trigonalis* from the Carboniferous of Scotland. *Palaeontology*, London, **4** : 477–506, pls. 64, 65.

George, T. N. 1932. The British Carboniferous reticulate Spiriferidae. *Q. Jl geol. Soc. Lond.*, **88** : 516–575, pls. 31–35.

—— 1933. Principles in the classification of Spiriferidae. *Ann. Mag. nat. Hist.*, London, (10) **11** : 423–456.

Hall, J. & Clarke, J. M. 1894. An introduction to the study of the Brachiopoda. *Rep. St. Geol. N.Y.*, Albany, **13**, (2) : 751–943, pls. 23–54.

—— —— 1894. An introduction to the study of the genera of Palaeozoic Brachiopoda. *Paleontology of New York*, **8** : 1–394, pls. 21–84.

Jope, H. M. 1965. Composition of brachiopod shell. *In* Moore, R. C. (Ed.), *Treatise on Invertebrate Paleontology*, **H** : 156-164. Lawrence, Kansas.

—— 1969. The protein of brachiopod shell – III. Comparison with structural protein of soft tissue. *Comp. Biochem. Physiol.*, London, **30** : 209–224.

Krans, T. F. 1965. Études morphologiques de quelques spirifères Dévoniens de la Chaîne Cantabrique (Espagne). *Leid. geol. Meded.*, Leiden, **33** : 73–184, pls. 1–16.

MacKinnon, D. I. 1971a. Perforate canopies to canals in the shells of fossil Brachiopoda. *Lethaia*, Oslo, **4** : 321–325.

—— 1971b. Studies in shell growth in living articulate and spiriferide Brachiopoda. Ph.D. thesis (unpubl.), Queen's University of Belfast.

Owen, G. & Williams, A. 1969. The caecum of articulate Brachiopoda. *Proc. R. Soc.*, London, **127**, (B) : 187–201, pls. 55–62.

Pitrat, C. W. 1965. Order Spiriferida, suborder Spiriferidina. *In* Moore, R. C. (Ed.), *Treatise on Invertebrate Paleontology*, **H** : 668–727. Lawrence, Kansas.

Rudwick, M. J. S. 1960a. The feeding mechanisms of spire-bearing fossil brachiopods. *Geol. Mag.*, London, **97** : 369–383.

—— 1960b. Correspondence. *Ibid.* **97** : 516–518.

—— 1961. 'Quick' and 'catch' adductor muscles in brachiopods. *Nature, Lond.* **191** : 1021.

—— 1965. Sensory spines in the Jurassic brachiopod *Acanthothiris*. *Palaeontology*, London, **8** : 604–617, pls. 84–87.

—— 1968. The feeding mechanisms and affinities of the Triassic brachiopods *Thecospira* Zugmayer and *Bactrynium* Emmrich. *Palaeontology*, London, **11** : 329–360, pls. 65–68.

Sass, D. B. 1967. Electron microscopy, punctae, and the brachiopod genus *Syringothyris* Winchell, 1863. *J. Paleont.*, Tulsa, **41** : 1242–1246, pls. 167–169.

Schuchert, C. & Cooper, G. A. 1932. Brachiopod genera of the suborders Orthoidea and Pentameroidea. *Mem. Peabody Mus. Yale*, New Haven, **4**, (1) : 1–270, pls. A and 1–29.

Tutcher, J. W. & Trueman, A. E. 1925. The Liassic rocks of the Radstock district. *Q. Jl geol. Soc. Lond.*, **81** : 595–666, pls. 38–41.

Westbroek, P. 1967. Morphological observations with systematic implications on some Paleozoic Rhynchonellida from Europe with special emphasis on the Uncinulidae. *Leid. geol. Meded.*, Leiden, **41** : 1–82, pls. 1–14.

Williams, A. 1956. The calcareous shell of the Brachiopoda and its importance to their classification. *Biol. Rev.*, Cambridge, **31** : 243–287.

—— 1960. Correspondence (The feeding mechanisms of spire bearing fossil brachiopods). *Geol. Mag.*, London, **97** : 514–516.

—— 1968a. Evolution of the shell structure of articulate brachiopods. *Spec. Pap. Palaeont.*, London. **2** : 1–55, 24 pls.

—— 1968b. A history of skeletal secretion among articulate brachiopods. *Lethaia*, Oslo, **1** : 268–287.

—— 1970. Origin of laminar shelled articulate brachiopods. *Lethaia*, Oslo, **3** : 329–342.

—— 1971a. Comments on the growth of the shell of articulate brachiopods. *In* Dutro, J. T., jr (Ed.), Paleozoic perspectives : a paleontological tribute to G. Arthur Cooper. *Smithson. Contr. Paleobiol.*, Washington, **3** : 47–67, pls. 1–3.

—— 1971b. Scanning electron microscopy of the calcareous skeleton of fossil and living Brachiopoda. *In* Heywood, V. H. (Ed.), *Scanning Electron Microscopy: Systematic and Evolutionary Applications*, London (Academic Press, for the Systematics Association) : 37–66, pls. 1–5.

—— 1972. The secretion and structure of evolution of the shell of Thecideidine brachiopods. *Phil. Trans. R. Soc.*, London, **264** (B) : 439–478, pls. 40–53.

—— & Rowell, A. J. 1965. Brachiopod anatomy, morphology. *In* Moore, R. C. (Ed.), *Treatise on Invertebrate Paleontology*, **H** : 6–155. Lawrence, Kansas.

—— & Wright, A. D. 1961. The origin of the loop in articulate brachiopods. *Palaeontology*, London, **4** : 149–176.

—— —— 1970. Shell structure of the Craniacea and other calcareous inarticulate Brachiopoda. *Spec. Pap. Palaeont.*, London, **7** : 1–51, pls. 1–15.

INDEX

An asterisk (*) denotes a figure.

Acanthothiris, 197
accessory lamellae, 245
adductor scars, dorsal, 203
  ventral, 201–3
Aloxite, 191
Ambocoelia umbonata, 229, 245 ; pl. 17, figs 2, 3 ; pl. 29, figs 3, 4
Ambocoeliidae, 229
amino-acids, 193
Amphiclina, 226–8, 250
  amoena, 225, 247 ; pl. 15, fig. 6 ; pl. 16, fig. 3 ; pl. 31, figs 2, 4
  suessi, 225
Anisactinella, 224–5, 247
  quadriplecta, 223–4, 247 ; pl. 15, fig. 2 ; pl. 30, fig. 5
articulation, 210–2
Athyridacea 190, 221–5, 254
Athyrididina 190, 221–8, 245, 247
  spiralium 246*
Athyris 222–4
  spiriferoides 222, 247 ; pl. 12, figs 5, 6 ; pl. 30, fig. 3
Athyrisinacea, 220
Atrypa, 215–7, 219*, 228, 244
  reticularis, 215 ; pl. 7, fig. 6
  sp. 215 ; pl. 8 ; pl. 9, figs 1, 2
Atrypacea, 190, 212–8, 220, 244, 254
Atryparia, 215, 218
Atrypidina, 212–20, 229, 254
Atrypina hami, 215

Bowlditch Quarry, 192
brachial valve, 203–5
brachidium, 190, 206–9
  structure of, 190, 243–51, 248*
Brachyspirifer, 234
Brachythyrididae, 237, 254
Brachythyris sp., 238 ; pl. 24, figs 1, 2

Cadomella, 225, 242
  davidsoni, 225
  moorei, 225
caecum, 196
cardinalia, 204*
Catazyga, 212, 214–5, 218, 220, 244
  headi, 213, 245 ; pl. 7, figs 1–3 ; pl. 28, fig. 4

Chonetidina, 225
Choristites, 237–8, 240
  mosquensis, 237 ; pl. 23
classification of Spiriferida, 190
Cleiothyridina, 223, 234, 254
  deroissii, 223 ; pl. 13, figs 2–4
Coelospira saffordi, 218, 220 ; pl. 10, figs 1, 2
Composita, 222, 224
  ambigua, 222–3, 247 ; pl. 13, fig. 1 ; pl. 30, figs 1, 2
Costispiriferidae, 235
Crania anomala, 241
Craniacea, 254
Crenispirifer sp., 238–9 ; pl. 25, figs 1, 2
Crurithyris sp., 229–30 ; pl. 17, figs 4–6
  cardinal process, 230
Cyclospira sp., 218, 244 ; pl. 9, figs 3, 4
Cyrtia, 232
  exporrecta, 229 ; pl. 17, fig. 1
Cyrtiacea, 229–30, 254
Cyrtiinae, 229
Cyrtina, 230–2, 232*, 233*, 244
    ventral median septum and tichorhinum, 231*
  alpenensis, 230 ; pl. 18, fig. 1
  sp., 230–1 ; pl. 18, figs 2, 3
Cyrtinidae, 230

Davidsoniacea, 242
Dayia, 218, 220
  navicula, 218, 234, 245 ; pl. 9, figs 5, 6 ; pl. 29, fig. 1
Dayiacea, 190, 212, 218–20, 254
Delthyridae, 233
Delthyris, 232–3
  saffordi, 233 ; pl. 18, fig. 4
dental ridges, 210
depositional banding, transverse, 223
Desquamatia, 218
  subzonata, 215
Diplospirella, 223–5, 245, 247–8, 250, 252–3
  wissmanni, 223, 247, 248* ; pl. 13, figs 5, 6 ; pl. 14 ; pl. 15, fig. 1 ; pl. 30, fig. 4
Diplospirellinae, 254
diurnal banding, 220
'double-sided' growth of spiralia, 190, 245–7

electron microscope, 190–1
endopunctate brachiopoda, 196
Eospirifer, 229, 232
Eospiriferinae, 229
Epon Araldite, 191
Euryspirifer, 234
Fimbrispirifer, 234
functional considerations, muscle attachment areas, 205

gerontic forms, 196
Glassia, 244
Gonambonitacea, 242
growth lamellae, 199
growth lines, concentric, 198–201
Gruenewaldtia, 215, 218
Gryphus, 214, 217–8, 223, 228, 234, 238, 240
  vitreus, 190, 213, 255

Hallina, 212
Hemithiris psittacea, 235–7
Hodder's Quarry, Timsbury, 192
hollow spines, 196–8
Homeospira evax, 220–1 ; pl. 10, fig. 4
Howellella, 232, 234
Howittia, 234
Hustedia radialis, 220–1 ; pl. 10, fig. 5 ; pl. 11, figs 3, 4
Hysterolites, 234

Idiospira, 214–5, 220, 244–5
  thomsoni, 214, 245 ; pl. 7, figs 4, 5 ; pl. 28, figs 5, 6

'jigsaw-puzzle' shell fabric, 214, 218, 234
jugum, 206, 209, 243, 248, 250, 253

keel, 227, 227*, 250
Kerpina, 218
Koninckella liassina, 225
  triassina, 225
Koninckina, 225–8, 226*, 227*, 244, 248, 250, 253
  leonhardi, 225, 247 ; pl. 15, figs 3–5 ; pl. 16, figs 1, 2, 4–6 ; pl. 30, fig. 6 ; pl. 31, fig. 1
Koninckinacea, 190, 221, 225–8, 248–50, 249*, 254
Kozlowskiellina velata, 233–4 ; pl. 18, figs 5, 6 ; pl. 19

lamellae, spiral, 206–7, 207*, 208* ; *see* spiralia
Licharewiinae, 235
lineation, 250
Lissatrypidae, 214–5
Lobothyris punctata, 194
Lo-Kitt, 191
lophophore, 190–1, 206, 243 ; *see* plectolophe
  inferred dispositions of, 190, 209, 251–3

Macandrevia, 252, 252*, 253*
Magasella sanguinea, 237
mantle retraction, 198–201, 202*
Martinia sp., 239–40 ; pl. 26, figs 1, 2
median septum, 201, 203
Megerlia, 242
Meristella atoka, 221–2 ; pl. 11, figs 5, 6 ; pl. 12, figs 2–4
Meristellidae, 254
Meristina tumida, 221–2 ; pl. 12, fig. 1
microscope, electron, 190–1 ; *see* Stereoscan
microvilli, 195
Mimatrypa, 215, 218
Moorellina granulosa, 242–3
morphology of shell, 192
mucopolysaccharide, 241–2, 254
Mucrospirifer sp., 234 ; pl. 20, figs 1, 2
muscle attachment areas, 196, 201–5
muscle system, 205, 244*
myotest, 203

Neospirifer camaratus, 237 ; pl. 22, fig. 2
Notosaria, 215, 224, 231, 232*, 234, 236
  nigricans, 201

orthide stocks, 242

Paraspirifer, 234
pedicle valve, 201–3
perforate canopies of puncta, 196
periostracum, 190, 192–3, 195, 200, 241–2
Phricodothyris sp., 239–40 ; pl. 25, figs 3–6
phylogeny of skeletal successions, 255*
plasmalemma, 195, 200*
Plectambonitacea, 208, 242
plectolophe, 252, 253*
preparation of specimens, technique, 191
primary layer, 190, 193–5
  thickness of, 193*
Protozyga, 212, 214, 243, 254
  elongata, 212–3, 243–4 ; pl. 6, fig. 5 ; pl. 28, fig. 3
  exigua, 244
'*Protozyga*-like' shells of Middle Ordovician, 212, 254
pseudopunctation, 242
punctation, puncta, 196–7, 197*
Punctospirifer scabricosta, 238–9 ; pl. 24, figs 4–6

Queensland, Permian of, 194

Radstock Shelf, 191–2
resorption, surfaces of, 207–8
Reticulariacea, 190, 229, 239–40, 254
Retzia sp., 220–1, 250 ; pl. 10, fig. 6 ; pl. 11, figs 1, 2
Retziacea, 220, 254
Retziidina, 220–1
Rhynchonellida, 190, 194–5, 199, 203, 226–7, 227*, 233, 236, 254
Rhynchospirina maxwelli, 220–1, 245 ; pl. 10, fig. 3 ; pl. 29, fig. 2

saddle, 227, 227*, 250
scleroblasts, 247
secondary layer, 190, 195–6, 200*, 210
shell layers, calcareous, in brachiopods, 190
  flexures in, 199
  fluctuations in deposition of, 201, 202*
shell structure of Spiriferide brachiopoda, 187–258
  of *Spiriferina walcotti*, 191–212
  of other spiriferida, 212–43
shell succession, 192–6, 197*
' single-sided ' growth of spiralium, 190, 247
Siphonotretacea, 198
skeletal fabric, 189
Skenidioides, 222
sockets, 210, 212
Sowerbyella, 208
specimen preparation, technique of, 191
Spinatrypa sp., 215, 218
  tubular spines of, 216, 217*
Spinatrypina, 218
spine canals, 197*
spines, hollow, 196–8, 197*, 216, 217*
  on spiral lamellae, 247–8
Spinella, 234
Spinocyrtia sp., 234–5 ; pl. 20, figs 3, 4
Spinocyrtiidae, 235
spiralia, 190–1, 206, 209*, 244*, 249*
  spines on, 209
  structure of, 243–51
Spirifer trigonalis, 210, 237–8, 245, 253 ; pl. 22, figs 3–6 ; pl. 29, fig. 6
Spiriferacea, 190, 229, 232–8, 254
Spiriferida, 187–258
Spiriferidae, 254
Spiriferide brachiopoda, shell structure, 187–258
Spiriferidina, 229–40
  classification, 229
Spiriferina, 190, 212–3, 216, 220–1, 233, 239, 244–5, 247, 250
  '*cristata* var. *octoplicata*', 238–9 ; pl. 24, fig. 3
  rostrata, 206

walcotti, 189–90, **191–212,** 238–9, 241, 255 ; pls 1–5 ; pl. 6, figs 1–4
  articulation, 210–2
  brachial valve, 203–5
  brachidium, 206–9
  diagnosis, 191
  functional considerations of muscle attachment areas, 205
  growth lines, concentric, 198–201
  hollow spines, 196–8
  mantle retraction, 198–201
  morphology of shell, 192
  muscle attachment areas, 201–5
  pedicle valve, 201–3
  periostracum, 192–3
  primary layer, 193–5
  punctation, 196
  secondary layer, 195–6
  shell succession, 192–6
  spines, hollow, 196–8
  spiralia, 206–9, 245
Spiriferinacea, 229, 238–9, 254
Spiriferinella cristata, 238 ; see " *Spiriferina cristata* var. *octoplicata* "
spondylium simplex, 222
' Stereoscan ', 191, 218, 223, 237
Strophomenida, 225, 254
  spines, 198
Subansiria, 235
  sp., 194
Suessia, 230
Suessiacea, 229–32, 254
Suessidae, 230
Syringospira, 236*, 236–7
  prima, 235 ; pl. 21, fig. 6 ; pl. 22, fig. 1
Syringothyridae, 235, 254
Syringothyris cuspidata, 235 ; pl. 20, figs 5, 6

taleolae, 207*, 208
teeth, 210, 211*, 212
Tenticospirifer cyrtiniformis, 235–7 ; pl. 21, figs 3–5
Terebratalia transversa, 204
Terebratulida, 190–1, 194–5, 199, 203, 221, 226–7, 227*, 233, 236, 247, 251, 254–5
tertiary layer, 190, 234, 238, 255
Thecideidina, 241–2, 254
Thecidellina barretti, 241
Thecospira, 240–4, 241*, 242*, 244*, 250–1, 253
  sp., 247 ; pl. 26, figs 3–5 ; pl. 27 ; pl. 28, figs 1, 2 ; pl. 31, figs 3, 5, 6 ; pl. 32
Thecospiridae, 190, 254
Theodossia hungerfordi, 235, 245 ; pl. 21, figs 1, 2 ; pl. 29, fig. 5
tichorhinum, 230–1
Timsbury, 192
tonofibrils, 203
tubercles, peripheral, 190

ventral adductor muscle fields, 201–3

Waltonia inconspicua, 222

Zygospira, 212–5, 244
  modesta, 213 ; pl. 6, fig. 6

DAVID I. MACKINNON
Department of Geology
UNIVERSITY OF CANTERBURY
CHRISTCHURCH
NEW ZEALAND

Accepted for publication 18 September 1973

PLATE 1

All figures are scanning electron micrographs of the shell.

Spiriferina walcotti (Sowerby)

Lower Lias, Bowlditch Quarry, Radstock, Somerset

FIG. 1. View of the external surface of a valve showing the fine radial lineations (running obliquely from bottom to top) on which are superimposed concentric growth lines (running obliquely from left to right). BB 58878. ×650. (pp. 193, 199)

FIG. 2. More general view of concentric growth lines on the external surface of a valve and a number of broken, anteriorly inclined, spine bases. Same specimen, BB 58878. ×60. (pp. 193, 197, 199)

FIG. 3. Detailed view of a prominent longitudinal groove which occurs directly in front of a spine base. The spine base would be located directly below the micrograph. BB 58884. ×1250. (p. 193)

FIG. 4. Detailed view of parallel grooves situated behind and deflected around a spine base. The spine base would be located directly above the micrograph. Same specimen, BB 58884. ×1200. (p. 193)

FIG. 5. Section through the primary layer showing the twofold division into outer granular (top) and inner, more massive (bottom) parts. Secondary layer fibres are just visible at the bottom of the micrograph. Same specimen as Pl. 2, fig. 5, BB 58887. ×1450. (p. 194)

FIG. 6. View of the secondary shell mosaic on a valve interior showing the smooth, spatulate outlines of terminal faces. Same specimen as Pl. 2, fig. 1, BB 58885. ×1200. (p. 195)

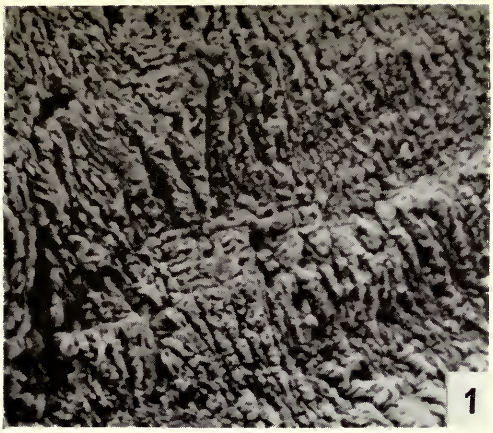
1

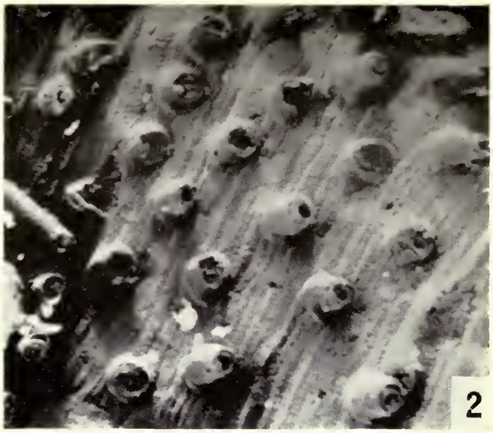
2

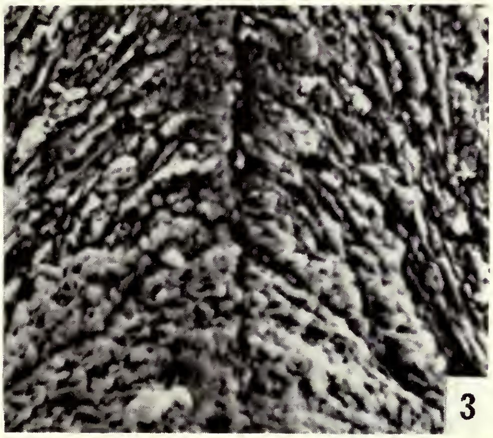
3

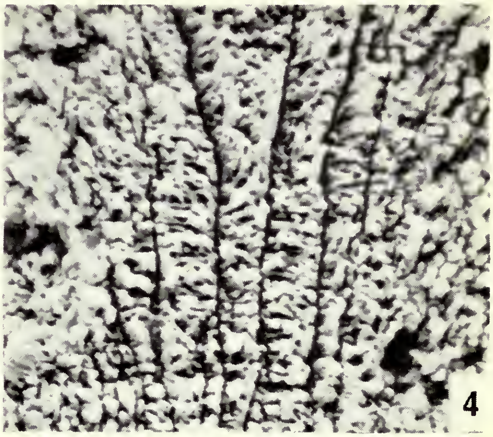
4

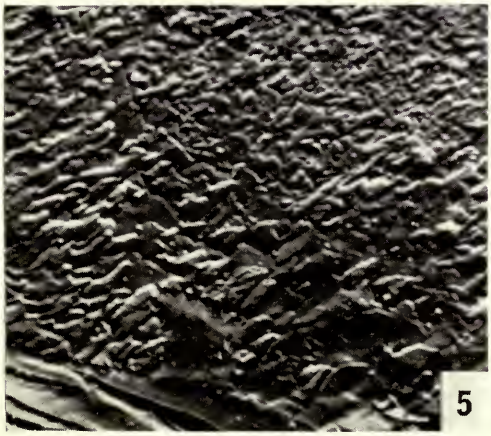
5

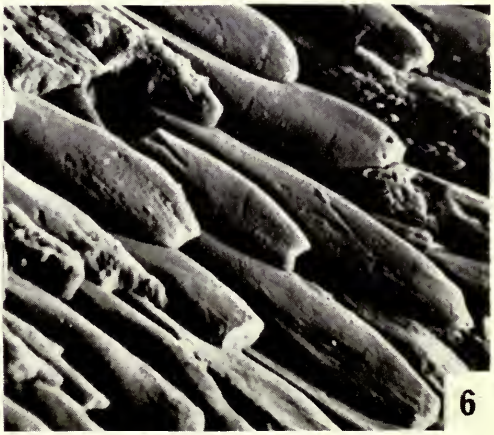
6

PLATE 2

All figures are scanning electron micrographs of the shell.

Spiriferina walcotti (Sowerby)
Lower Lias, Bowlditch Quarry, Radstock, Somerset

FIG. 1. View of the internal surface of a valve showing a punctum formed by the deflection of secondary layer fibres. Same specimen as Pl. 1, fig. 6, BB 58885. ×700. (p. 196)

FIG. 2. General view of the external surface of a valve showing a punctum with damaged perforate canopy. BB 58880. ×1200. (p. 196)

FIG. 3. More detailed view of the perforate canopy in fig. 2, showing canals. BB 58880. ×6000. (p. 196)

FIG. 4. General view of a ventral muscle scar showing straight grooves of the adjustor area (left) and the more flabellate impression of the diductor area (top). Anterior ridge at the bottom. Same specimen as Pl. 4, figs. 1-3, BB 58896. ×c. 60. (p. 201)

FIG. 5. Radial section through primary and secondary layers showing a slight flexure. Although secondary layer fibres close to the primary layer (top left) exhibit long trails, those caught up within the flexure are transversely sectioned. Same specimen as Pl. 1, fig. 5, BB 58887. ×1350. (p. 199)

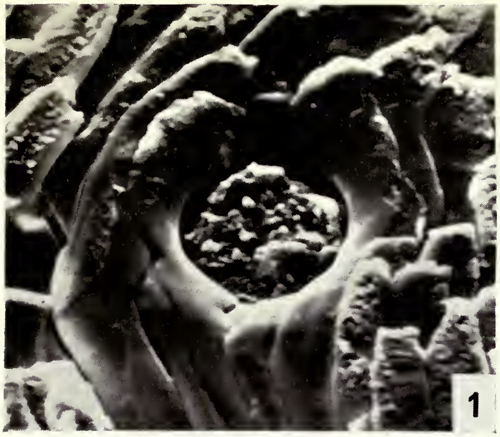
1

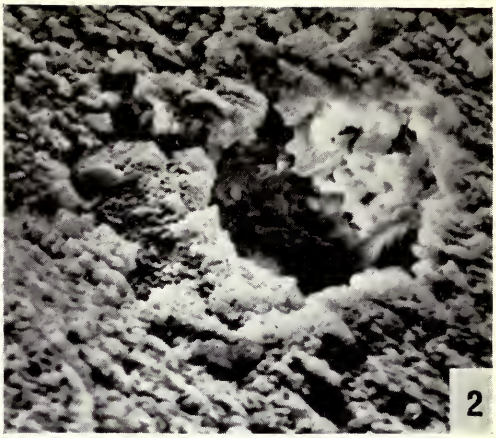
2

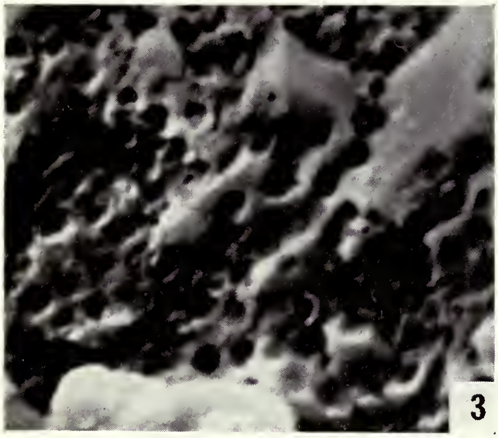
3

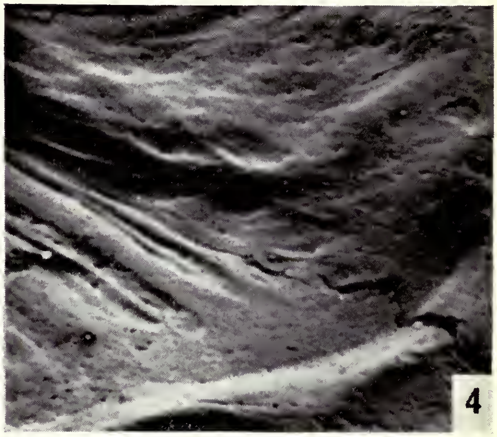
4

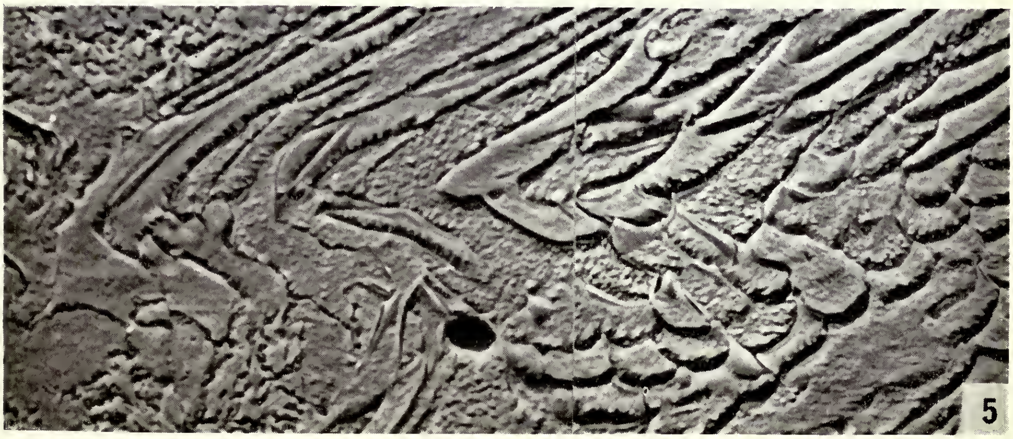
5

PLATE 3

Spiriferina walcotti (Sowerby)

Scanning electron micrograph montage of a shell from the Lower Lias, Hodder's Quarry, Timsbury, Somerset. Radial section through a brachial valve margin showing two major overlapping shell units. The regression planes are directed posteriorly inwards from the primary layer and separate the bulk of the secondary layer fibres from the series of vertically stacked, flat or gently curved lamellae of primary shell material which mark consecutive stages in the retreat of the mantle edge. The second and most recent overlapping unit (bottom of micrograph) is located right at the periphery of the valve. BB 58890. ×250. (pp. 196, 199)

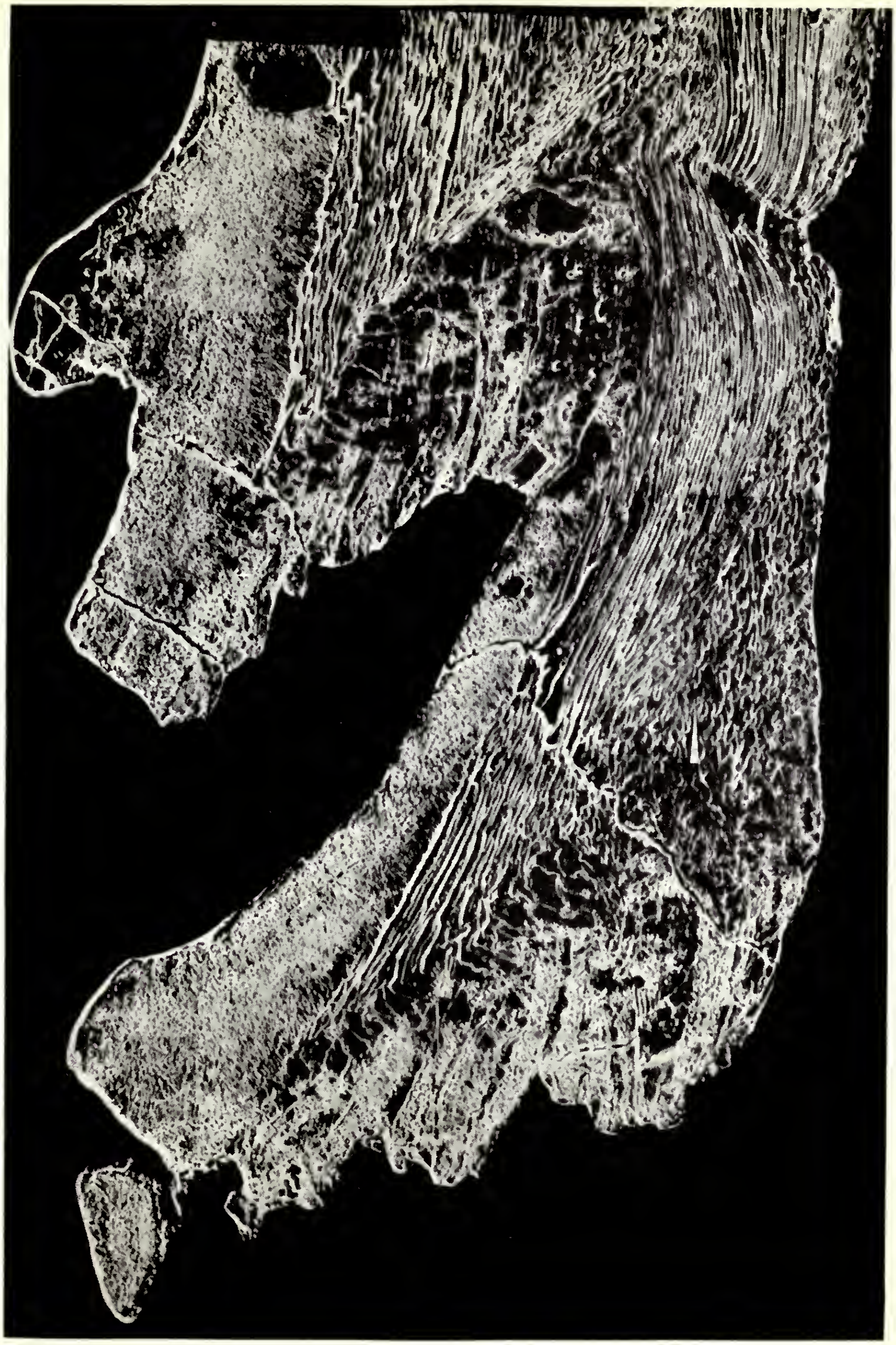

PLATE 4

All figures are scanning electron micrographs of the shell.

Spiriferina walcotti (Sowerby)

Lower Lias, Bowlditch Quarry, Radstock, Somerset

FIG. 1. Detail of the posteriorly inclined slope of an anterior ridge around a ventral muscle scar showing the development of long exposed trails and the encroachment of myotest (bottom left). Same specimen as Pl. 2, fig. 4, BB 58896. ×240. (p. 201)

FIG. 2. General view of the anterior part of a ventral muscle scar showing the deeply impressed furrows. Same specimen, BB 58896. ×65. (p. 201)

FIG. 3. Detailed view of a deeply impressed furrow within a ventral adjustor scar and surrounding fibres which are orthodoxly stacked. Same specimen, BB5 8896. ×220. (p. 201)

FIG. 4. Section through the ventral median septum showing a zone of small, gnarled, irregularly stacked fibres comprising part of the ventral adductor myotest. BB 58901. ×850. (p. 203)

FIG. 5. More detailed view from the centre of fig. 4. BB 58901. ×3400. (p. 203)

FIG. 6. Section through the ventral median septum cut close to the umbo showing the overlap of a later secondary layer deposit upon a postero-dorsal edge. BB 58902. ×750. (p. 203)

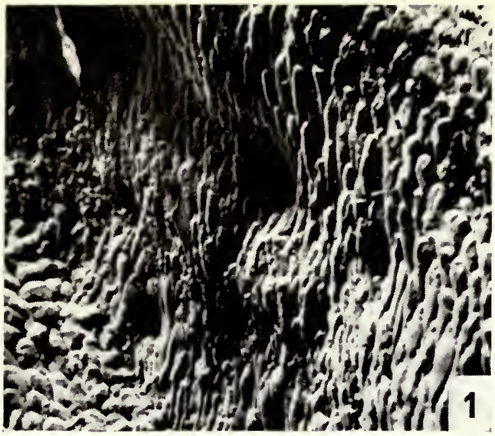
1

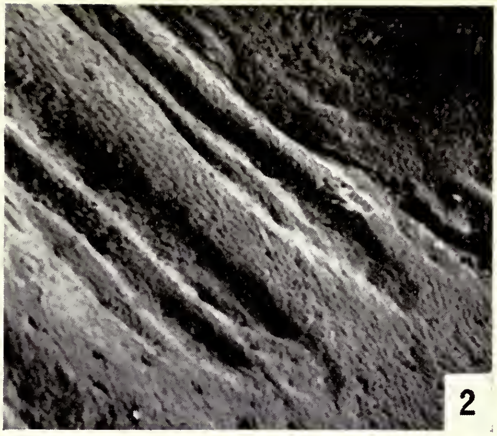
2

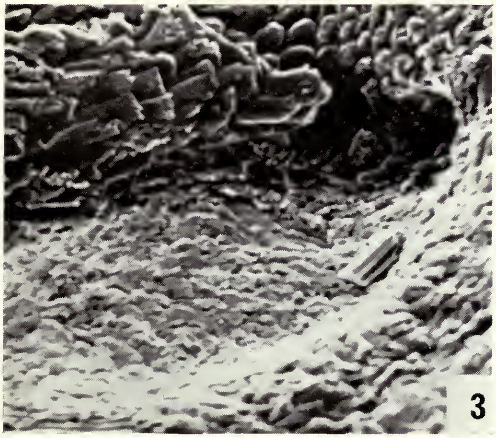
3

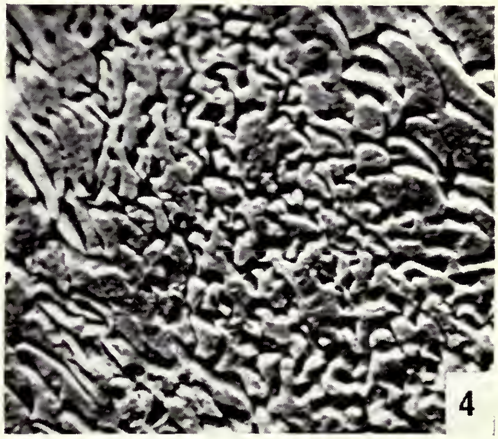
4

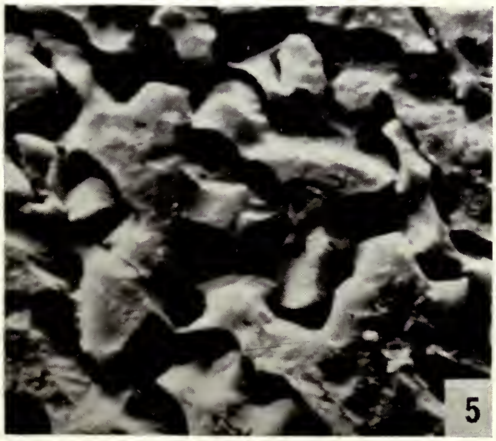
5

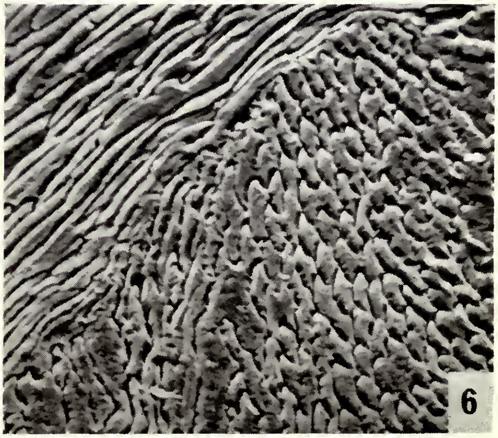
6

PLATE 5

All figures are scanning electron micrographs of the shell.

Spiriferina walcotti (Sowerby)

Lower Lias, Bowlditch Quarry, Radstock, Somerset

FIG. 1. General view of anterior (right) and posterior (left) dorsal adductor scars. Anterior to the top of the micrograph. BB 58898. × 25. (p. 204)

FIG. 2. View of a fracture surface within an anterior dorsal adductor scar showing the finely granular myotest underlain by conventional secondary layer fibres. Same specimen, BB 58898. × 130. (p. 204)

FIG. 3. View of two corrugated ridges comprising the cardinal process. Each ridge is composed of tightly interlocking secondary layer fibres. BB 58903. × 690. (p. 204)

FIG. 4. View of the deeply impressed dorsal adductor muscle scar showing a series of narrow stalks which project towards the umbo. Same specimen, BB 58903. × 130. (p. 204)

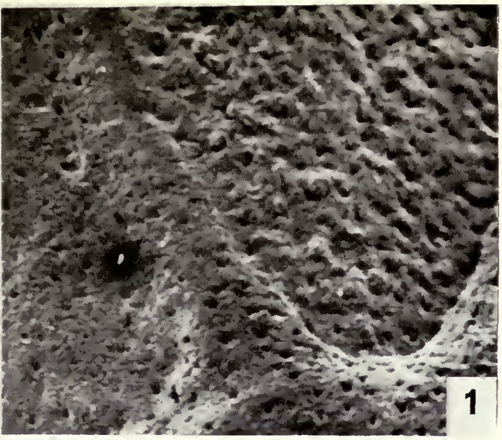
1

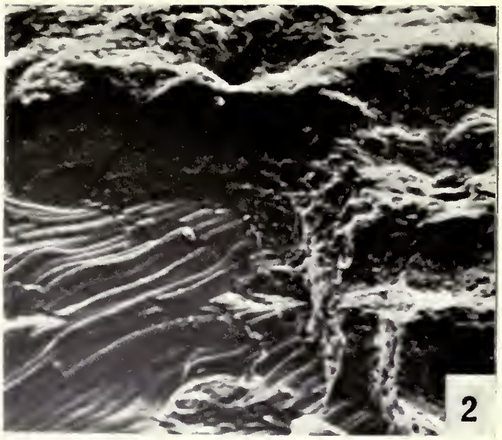
2

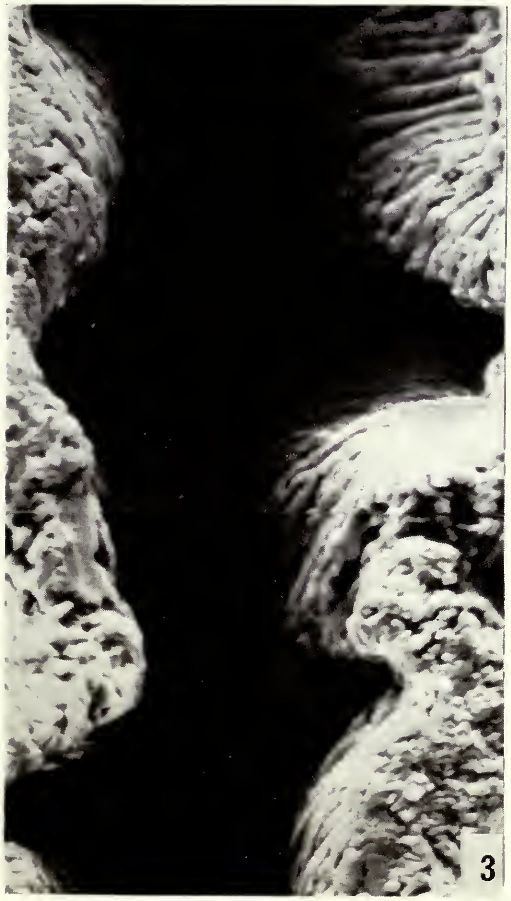
3

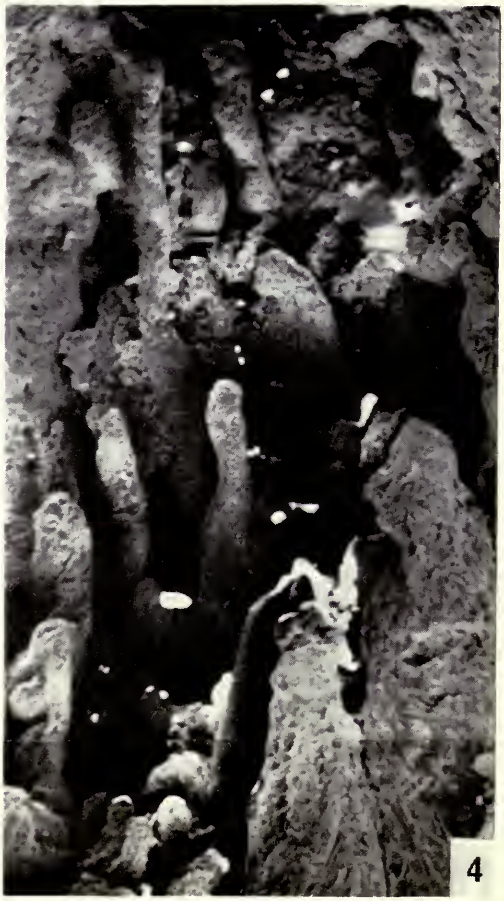
4

PLATE 6

All figures are scanning electron micrographs of the shell.

Spiriferina walcotti (Sowerby)

Lower Lias, Bowlditch Quarry, Radstock, Somerset

FIG. 1. General view of a tooth showing a dental ridge projecting within the delthyrial cavity (bottom) and a large bulbous swelling. BB 58906. ×25. (p. 210)

FIG. 2. Detailed view of the abraded ends of secondary layer fibres comprising the bulbous ridge. Same specimen, BB 58906. ×1200. (p. 210)

FIG. 3. Section through the distal end of a tooth showing the regular variation in the disposition of secondary layer fibres. Same specimen, BB 58906. ×300. (p. 212)

FIG. 4. More detailed view of part of fig. 3. BB 58906. ×750. (p. 212)

Protozyga elongata Cooper

FIG. 5. Ordovician (Lower Bromide Formation), 1 mile west of Dolese Brothers Crusher, Bromide, Oklahoma. Transverse section through the secondary layer showing irregular outlines of fibres; exterior of valve towards the bottom. Same specimen as Pl. 28, fig. 3, BB 58918. ×2600. (p. 212)

Zygospira modesta (Say)

FIG. 6. Ordovician (Richmond Group), road cutting 0·3 mile north of Vaughan's Gap, US 100, near Nashville, Tennessee. Transverse section through the secondary layer in the pedicle valve showing diamond-shaped profiles of fibres; exterior of valve towards the bottom right corner. BB 58920. ×1300. (p. 213)

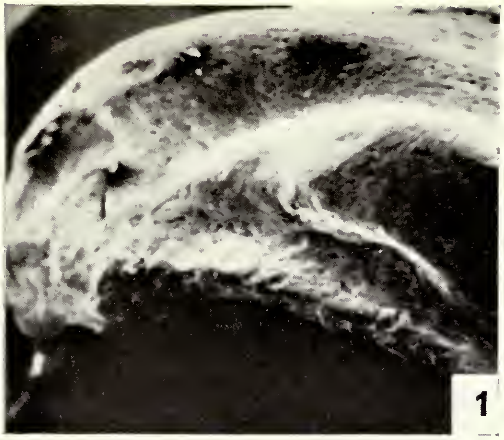
1

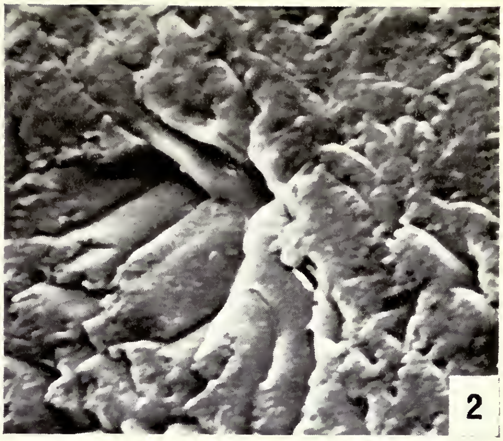
2

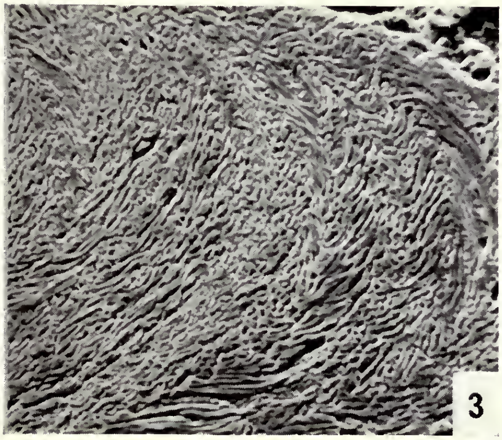
3

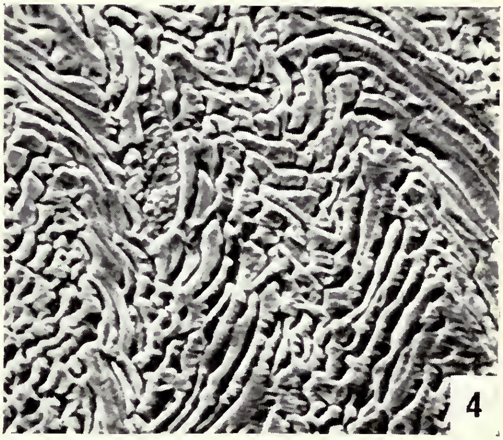
4

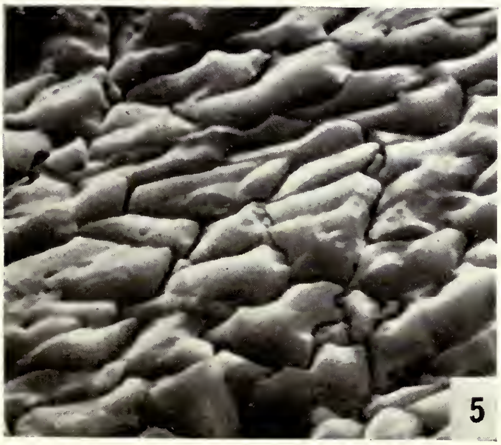
5

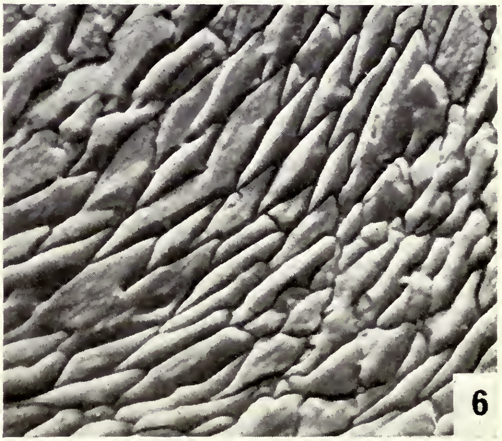
6

PLATE 7

All figures are scanning electron micrographs of the shell.

Catazyga headi Billings

Ordovician (Richmond Group), Adana Co., near Winchester, Ohio.
Same specimen as Pl. 28, fig. 4, BB 58921

Fig. 1. Section of the secondary layer showing the characteristic diamond-shaped outlines of fibres. × 1400. (p. 213)

Fig. 2. Section showing the junction of the secondary (bottom) and tertiary (top) layers in a pedicle valve; exterior of valve towards the bottom. × 1300. (p. 213)

Fig. 3. Section close to a valve margin showing the development of a wedge of primary shell sandwiched between earlier and later secondary shell deposits. × 630. (p. 214)

Idiospira thomsoni (Davidson)

Ordovician (Craighead Limestone), Girvan, Ayrshire.
Same specimen as Pl. 28, figs. 5–6, BB 58922

Fig. 4. Detail of sectioned secondary layer fibres showing well-developed keels and saddles. × 5600. (p. 214)

Fig. 5. Section through a secondary layer showing partial fusion of adjacent fibres due to secondary recrystallization. × 2400. (p. 214)

Atrypa reticularis (Linné)

Fig. 6. Silurian (Wenlock Limestone), Much Wenlock Railway, Shropshire. Section through the primary and secondary shell layers; primary layer located at top left corner. BB 58923. × 2450. (p. 215)

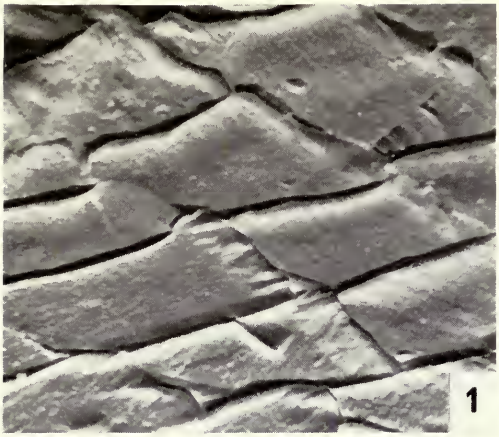
1

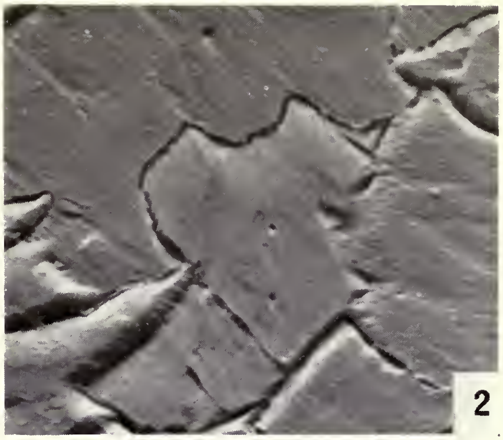
2

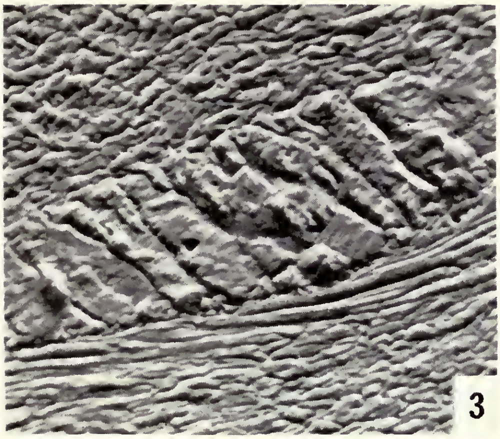
3

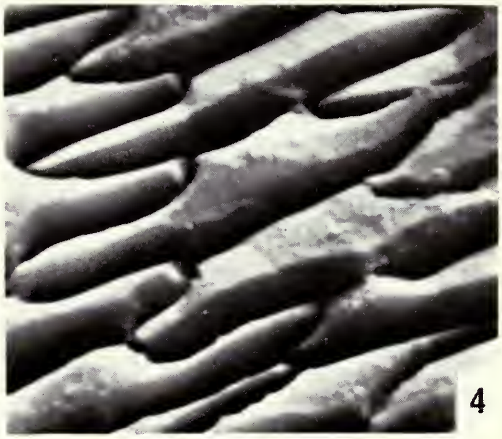
4

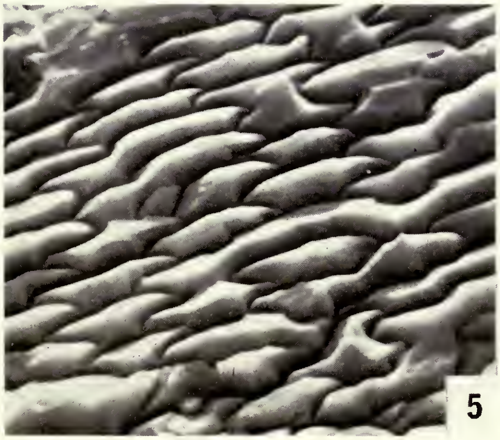
5

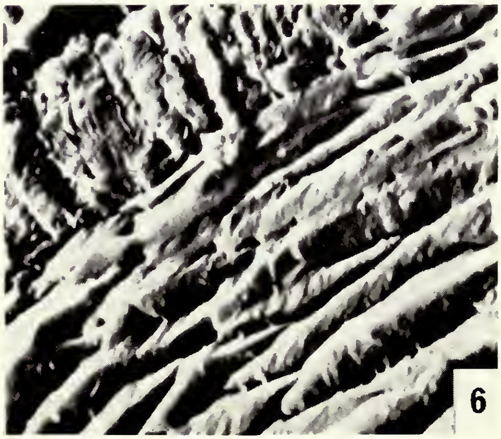
6

PLATE 8

All figures are scanning electron micrographs of the shell.

Atrypa sp.

Devonian (Hamilton Group), New York

FIG. 1. Transverse section through the pedicle valve showing the characteristic outlines and mode of stacking of secondary layer fibres. Same specimen as Pl. 9, fig. 1, BB 58924. × 280. (p. 215)

FIG. 2. Transverse section through the pedicle valve showing the outward deflection of secondary layer fibres around a (submerged) gonadal pit ; exterior of valve towards the top. Same specimen, BB 58924. × 280. (p. 215)

FIG. 4. General view of section through a valve margin showing a series of overlapping growth lamellae. Same specimen, BB 58924. × 70. (p. 216)

FIG. 5. More detailed view of part of fig. 4, showing the interdigitation of primary and secondary layers in the vicinity of overlapping growth lamellae ; shell exterior towards the top. Same specimen, BB 58924. × 270. (p. 216)

FIG. 6. Transverse section through a pedicle valve showing the development of a tertiary layer which is succeeded inwardly (bottom) by a later secondary shell deposit. Same specimen, BB 58924. × 280. (See also Text-fig. 12.) (p. 216)

FIG. 3. General view of part of the inner surface of a ventral valve showing the development of gonadal pits ; lateral shell edge situated towards the right. BB 58928. × 30. (p. 215)

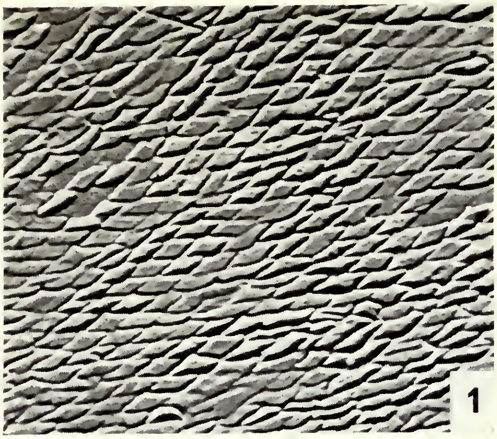
1

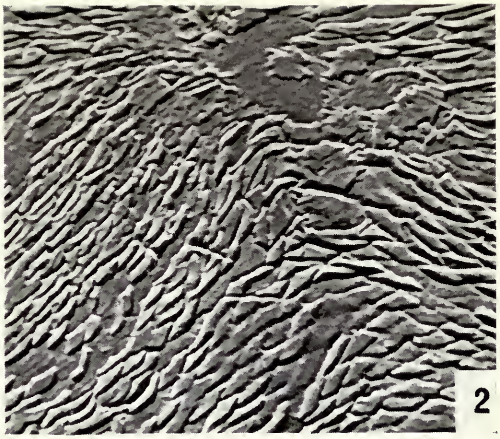
2

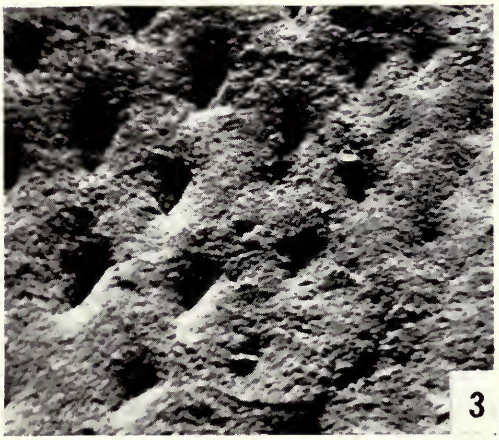
3

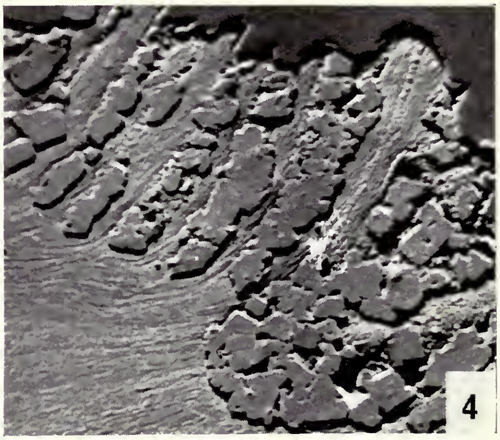
4

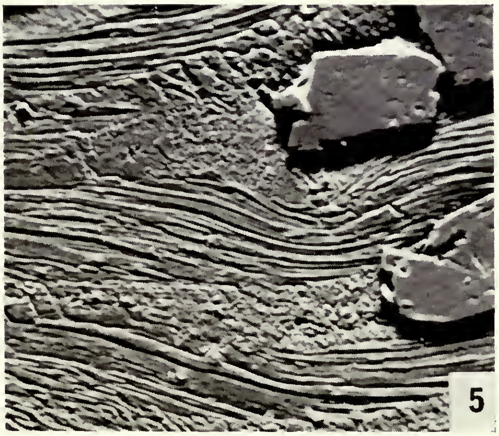
5

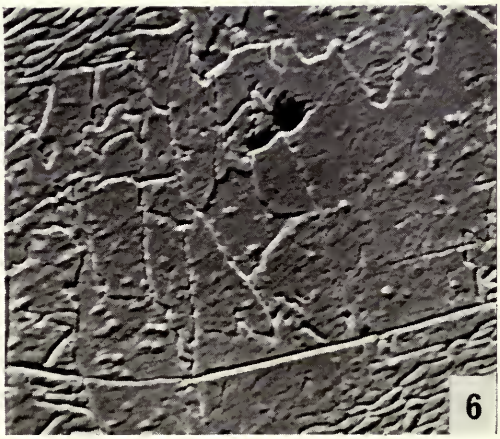
6

PLATE 9

All figures are scanning electron micrographs of the shell.

Atrypa sp.

Devonian (Hamilton Group), New York

FIG. 1. Section through a pedicle valve showing the junction between the secondary layer and the ventral myotest (bottom). Same specimen as Pl. 8, figs. 1–2, 4–6, BB 58924. × 280. (See also Text-fig. 12.) (p. 217)

FIG. 2. View of the surface topography within the ventral adductor muscle scar showing the irregular outlines of individual crystals. BB 58925. × 1400. (p. 217)

Cyclospira sp.

Ashgillian (Killey Bridge beds), exposed in the bank of Little River,
200 yards east of Slate Quarry Bridge, 2¼ miles ENE of Pomeroy,
Co. Tyrone, Northern Ireland. BB 58931

FIG. 3. Section through a pedicle valve showing diamond-shaped outlines of secondary layer fibres. × 1200. (p. 218)

FIG. 4. Section through a pedicle valve showing depositional banding within the tertiary layer below a ventral muscle scar. × 2400. (p. 218)

Dayia navicula (Sowerby)

Ludlovian (Dayia Shales), Park Farm Quarry, Onibury, Shropshire.
BB 58933. (See also Pl. 29, fig. 1)

FIG. 5. Section through a pedicle valve showing the junction between the secondary (top left) and tertiary (bottom right) layers. × 1200. (p. 218)

FIG. 6. Section through a pedicle valve showing a more general view of the secondary layer and part of the tertiary layer. × 600. (p. 218)

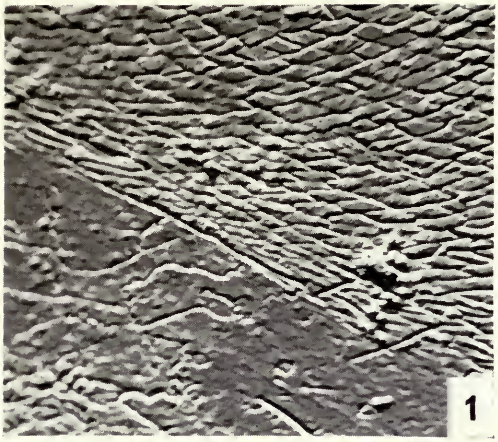
1

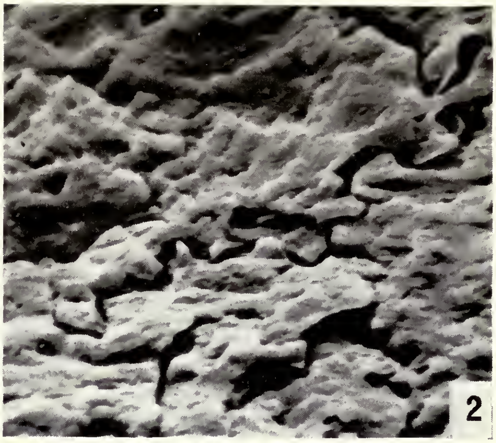
2

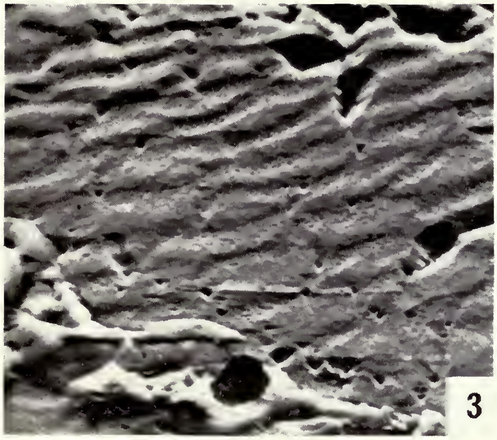
3

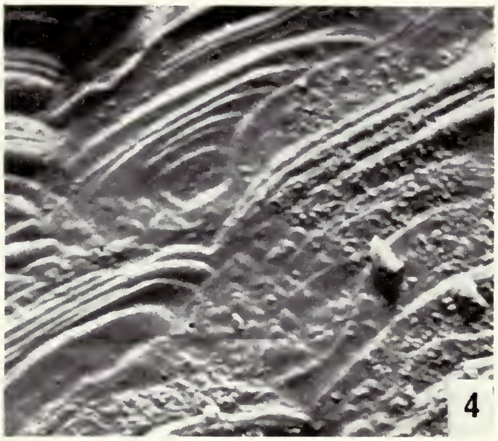
4

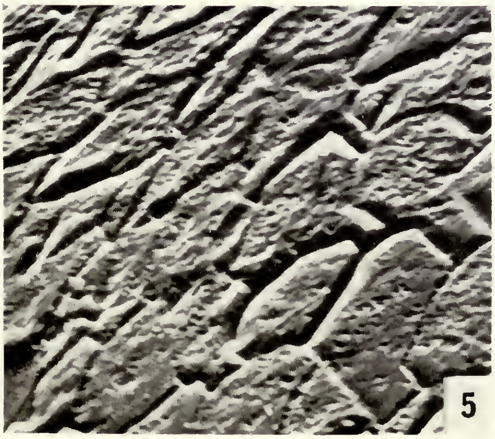
5

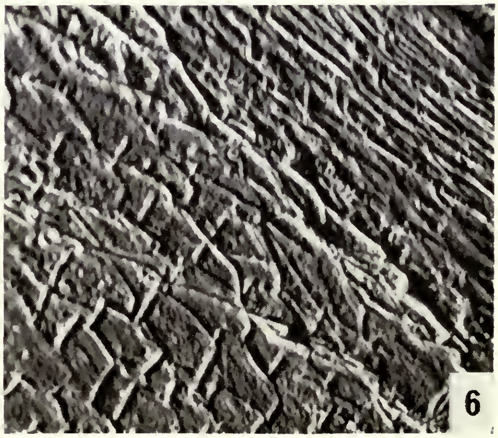
6

PLATE 10

All figures are scanning electron micrographs of the shell.

Coelospira saffordi (Foerste)

Silurian, Brownsport Formation, Western Tennessee. BB 58932

FIG. 1. Section through a pedicle valve showing the shape and stacking of secondary layer fibres. ×1200. (p. 220)

FIG. 2. Section through a pedicle valve showing the development of a tertiary layer. Silicified parts of the shell stand out. ×250. (p. 220)

Rhynchospirina maxwelli Amsden

FIG. 3. Devonian (Haragan Formation), White Mound, Murray County, Oklahoma. Section through a valve showing the distribution of the primary and secondary layers. Secondary layer fibres arch outwards around a punctum. Same specimen as Pl. 29, fig. 2, BB 58936. ×650. (p. 220)

Homeospira evax (Hall)

FIG. 4. Silurian (Waldron Formation), Waldron, Indiana. Section through a valve showing the disposition of the primary and secondary layers. Secondary layer fibres arch outwards around a punctum. BB 58935. ×1200. (p. 220)

Hustedia radialis (Phillips)

FIG. 5. Carboniferous (Arden Limestone), Arden, Lanarkshire. Section through the primary and secondary shell layers. The primary layer is strongly lineated normal to the primary/secondary layer boundary. Secondary layer fibres arch outwards around a punctum. Same specimen as Pl. 11, figs. 3–4, BB 58937. ×1200. (p. 220)

Retzia sp.

FIG. 6. Triassic (St Cassian beds), 1 km east of Rif. Pralongia-Htt. (Pralongia Refuge Chalet), Pralongia Ridge, 4·5 km ESE of Corvara in Badia, Italy. Section through the primary and secondary layers showing two puncta which coalesce inwardly within the secondary layer. Same specimen as Pl. 11, figs. 1–2, BB 58939. ×1200. (pp. 220, 221)

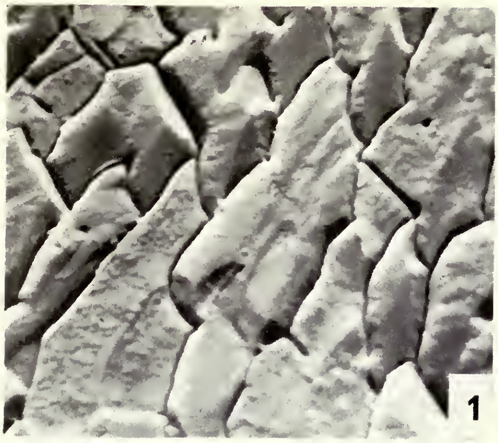
1

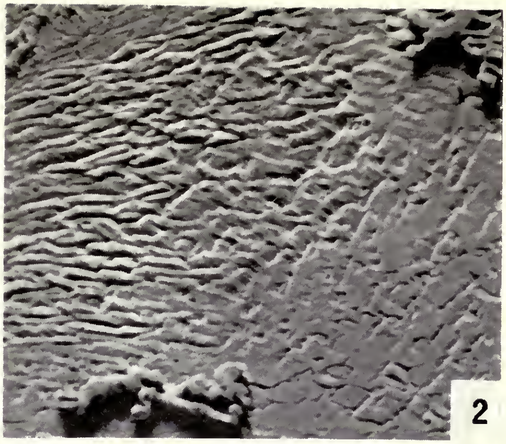
2

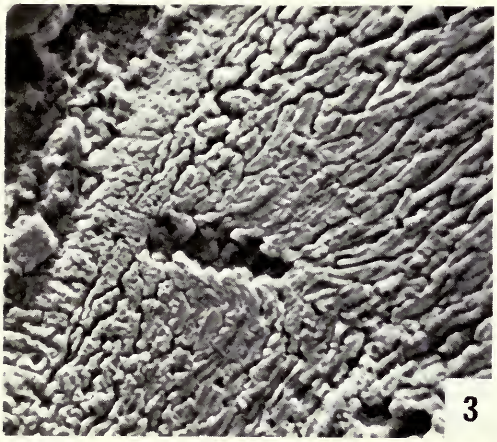
3

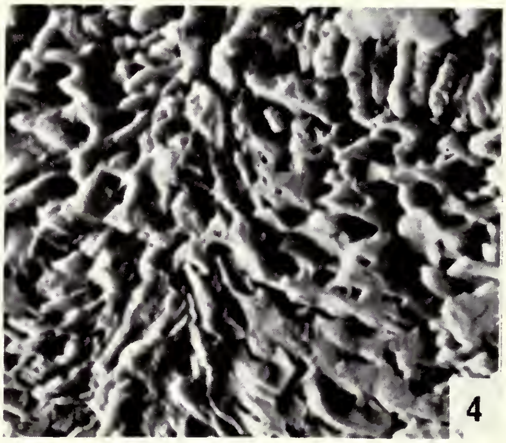
4

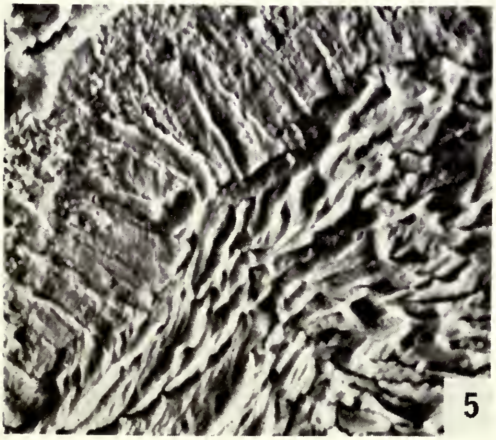
5

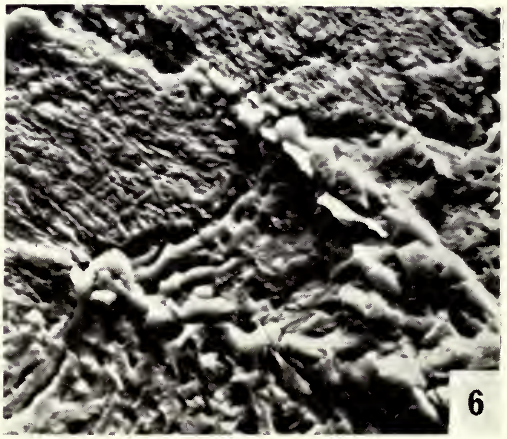
6

PLATE 11

All figures are scanning electron micrographs of the shell.

Retzia sp.

Triassic (St Cassian beds), 1 km east of Rif. Pralongia-Htt. (Pralongia Refuge Chalet),
Pralongia Ridge, 4·5 km ESE of Corvara in Badia, Italy.
Same specimen as Pl. 10, fig. 6, BB 58939

FIG. 1. Section through the primary layer showing a fine transverse depositional banding. The shell exterior is located beyond the top right corner. ×2400. (p. 220)

FIG. 2. Section through secondary layer fibres showing their general outlines and mode of stacking. Some depositional banding can be recognized. ×6200. (p. 220)

Hustedia radialis (Phillips)

Carboniferous (Arden Limestone), Arden, Lanarkshire.
Same specimen as Pl. 10, fig. 5, BB 58937

FIG. 3. Section through the primary and secondary layers showing the bulbous distal end of an infilled punctum, which is separated from the outer sedimentary coating by a uniformly narrow zone. Presumably this space was occupied by a calcite canopy. ×1200. (p. 221)

FIG. 4. Detailed view of a distal end of a punctum infilled by small crystals of iron pyrites in the form of pyritohedra. The space above the distal end of the punctum was, presumably, occupied by a calcite canopy. ×2400. (p. 221)

Meristella atoka Girty

Devonian (Haragan Formation), White Mound, Murray County, Oklahoma. BB 58940

FIG. 5. Section through the primary and secondary shell layers. ×2300. (p. 221)

FIG. 6. Section through the secondary and tertiary shell layers. ×650. (p. 221)

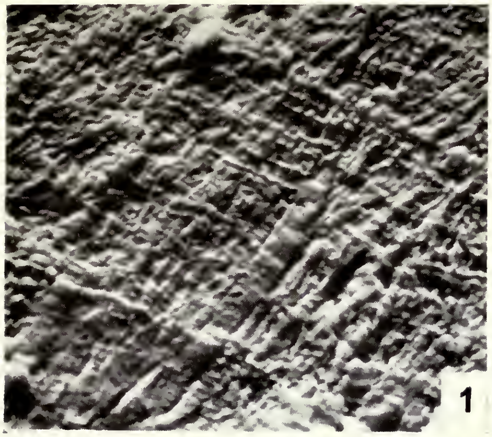
1

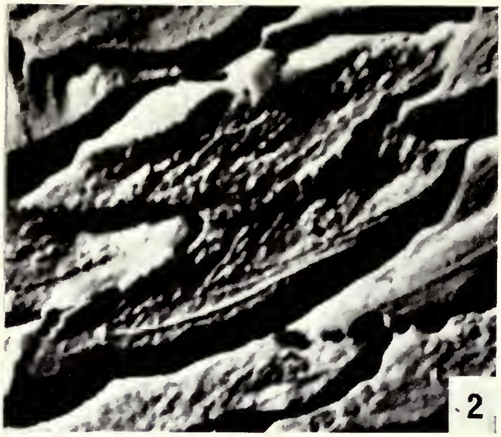
2

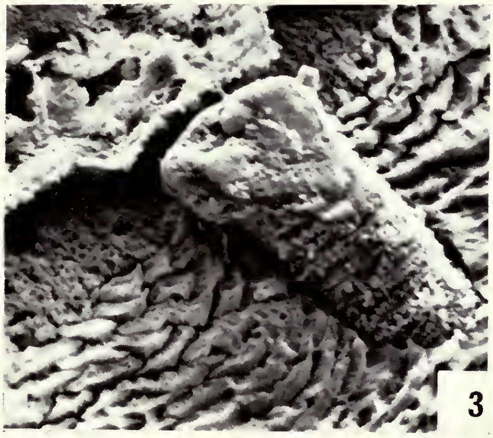
3

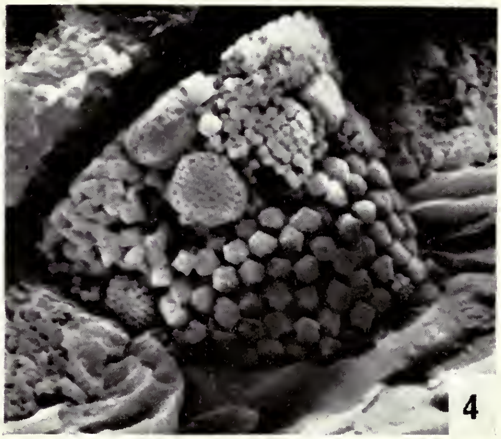
4

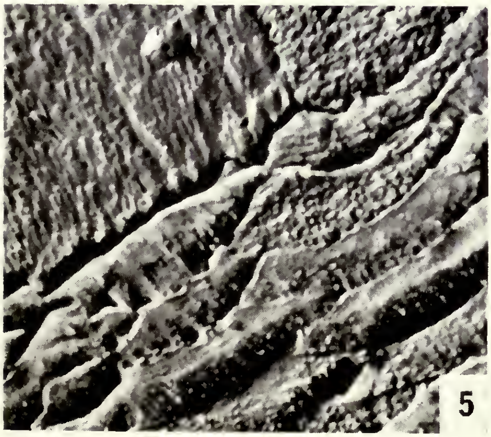
5

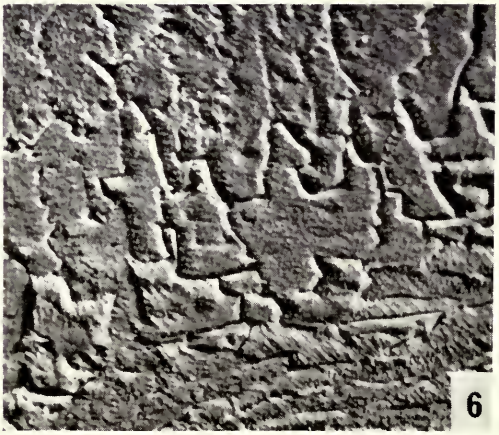
6

PLATE 12

All figures are scanning electron micrographs of the shell.

Meristina tumida (Dalman)

FIG. 1. Silurian, Gotland. Section through the secondary layer (bottom right) and very thick tertiary layer. BB 58944. ×68. (p. 221)

Meristella atoka Girty

Devonian (Haragan Formation), White Mound, Murray County, Oklahoma. BB 58943

FIG. 2. Transverse section through brachial valve showing the irregular skeletal fabric of an adductor myotest. ×1350. (p. 222)

FIG. 3. General view of a transverse section through the cardinal plate (top) and supporting median septum. ×58. (p. 222)

FIG. 4. Transverse section through the cardinal plate showing the development of a highly porous skeletal fabric on top of the normal secondary layer succession. It is probably a dorsal adjustor myotest. ×1170. (p. 222)

Athyris spiriferoides (Eaton)

Devonian (Wanakah Shale), Canandaiga Lake, New York State.
BB 58948. (See also Pl. 30, fig. 3)

FIG. 5. Section through the primary and secondary shell layers. ×1100. (p. 222)

FIG. 6. More detailed view of a section through the secondary layer showing the regular shape and stacking of constituent fibres. ×2200. (p. 222)

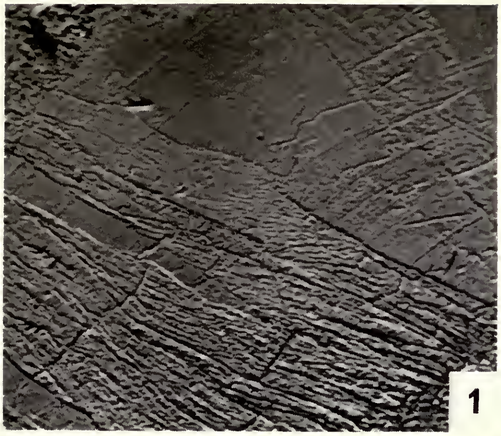
1

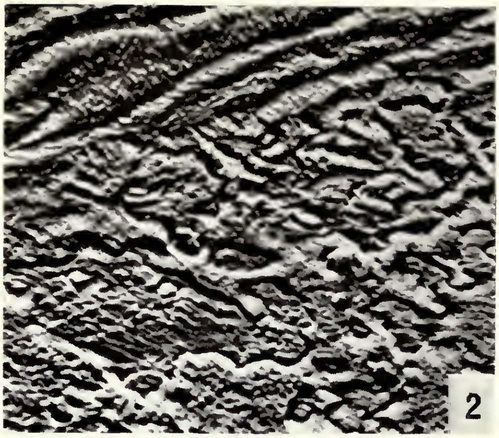
2

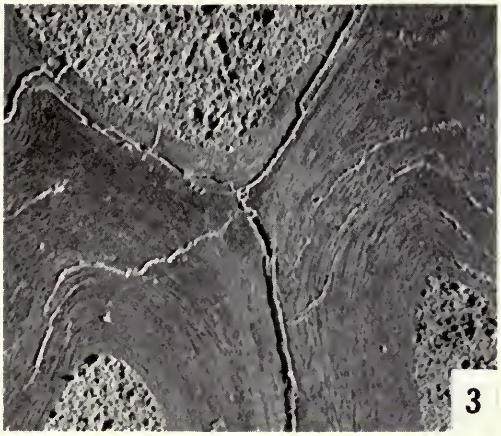
3

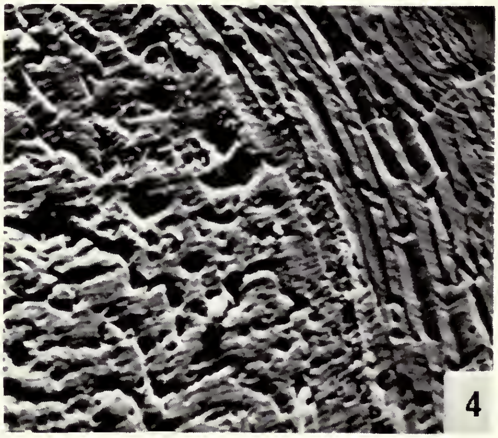
4

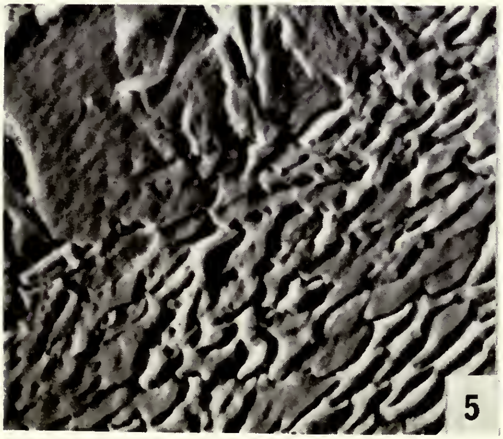
5

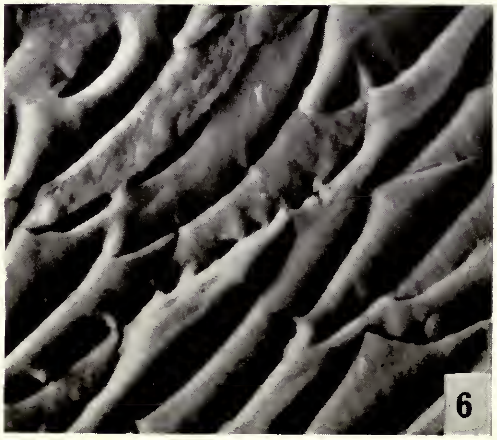
6

PLATE 13

All figures are scanning electron micrographs of the shell.

Composita ambigua (Sowerby)

FIG. 1. Carboniferous (Calmy Limestone), Carluke, Lanarkshire. Section through the primary and secondary shell layers. BB 58951. ×1250. (pp. 222, 223) (See also Pl. 30, figs. 1–2.)

Cleiothyridina deroissii (Leveille)

Carboniferous (Blackbyre Limestone), Brockley, Lesmahagow, Lanarkshire. BB 58952

FIG. 2. Section through the secondary layer showing the general shape and stacking of constituent fibres. ×6500. (p. 223)

FIG. 3. Section through the tertiary layer showing prominent transverse depositional banding. ×2500. (p. 223)

FIG. 4. Section through valve showing an alternation of secondary and tertiary layers. Shell interior beyond the top left corner. ×625. (p. 223)

Diplospirella wissmani (Münster)

Triassic (St Cassian beds), Alpe de Specie (formerly Seelandalpe),
2·5 km NW of Carbonin (formerly Schluderbach), 11 km NE of Cortina
d'Ampezzo, Trentino, Italy

FIG. 5. Transverse section through the primary and secondary shell layers. Same specimen as Pl. 30, fig. 4, BB 58956. ×1300. (p. 223)

FIG. 6. View of the secondary shell mosaic on the internal surface of the brachial valve. Same specimen as Pl. 14, figs. 1–3 and Pl. 15, fig. 1, BB 58959. ×650. (p. 223)

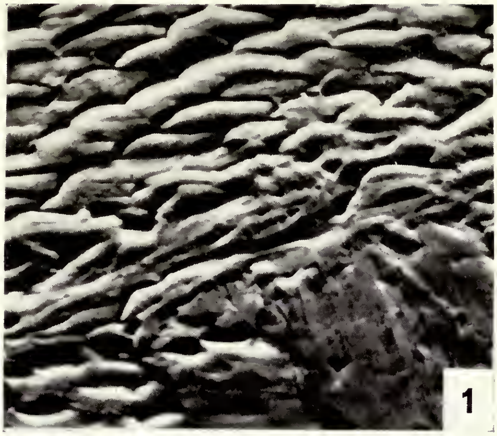
1

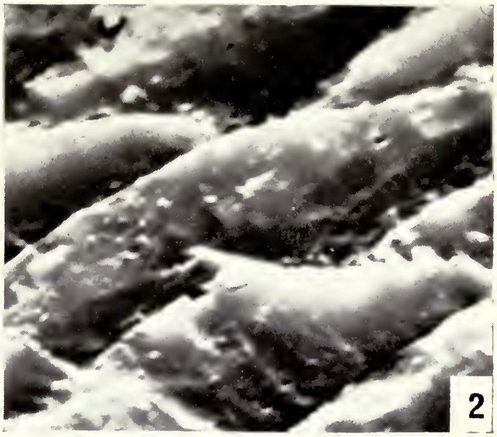
2

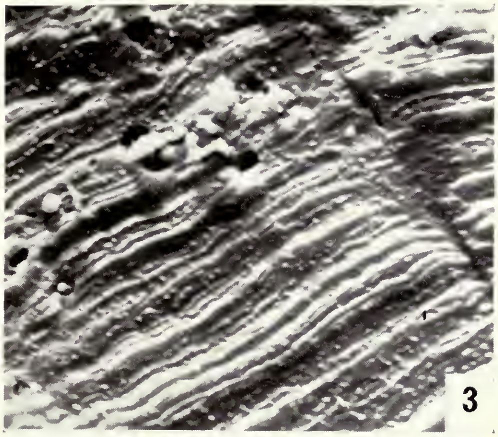
3

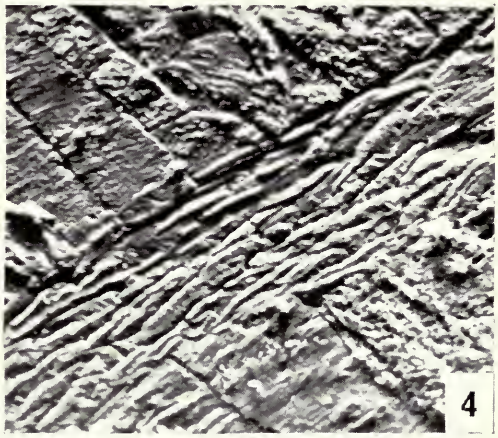
4

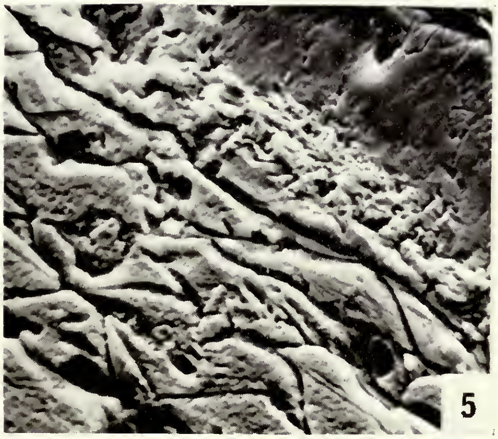
5

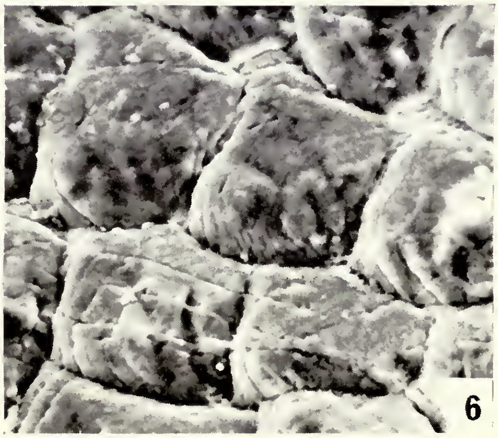
6

PLATE 14

All figures are scanning electron micrographs of the shell.

Diplospirella wissmani (Münster)

Triassic (St Cassian beds), Alpe de Specie (formerly Seelandalpe),
2·5 km NW of Carbonin (formerly Schluderbach), 11 km NE of
Cortina d'Ampezzo, Trentino, Italy

FIG. 1. General view of the secondary shell mosaic located in front of the dorsal median septum. Anterior shell edge located beyond the top left corner. Same specimen as Pl. 13, fig. 6 and Pl. 15, fig. 1, BB 58959. ×65. (p. 223)

FIG. 2. General view of the interior of a brachial valve in which the secondary shell mosaic can still be discerned. Same specimen, BB 58959. ×27. (p. 223)

FIG. 3. View of anterior margin of a dorsal adductor myotest showing the breakdown of the secondary shell mosaic. Anterior shell edge located beyond the bottom left corner. Same specimen, BB 58959. ×280. (p. 224)

FIG. 4. Transverse section through a dorsal adductor myotest showing the irregular outline of fibres. The shell interior is located at the bottom of the micrograph. BB 58957. ×650. (p. 224)

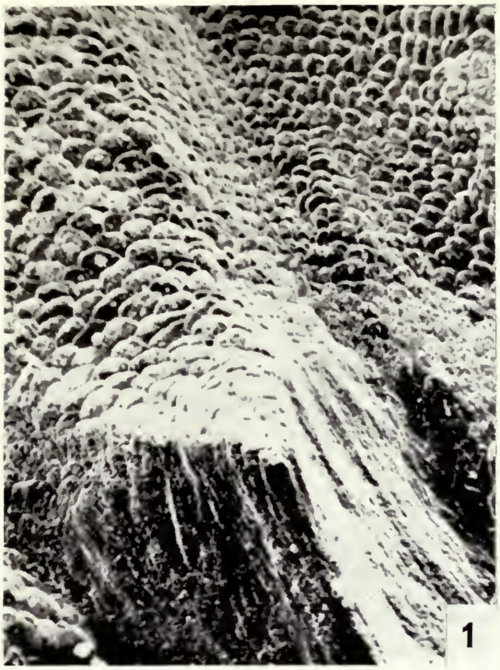

1

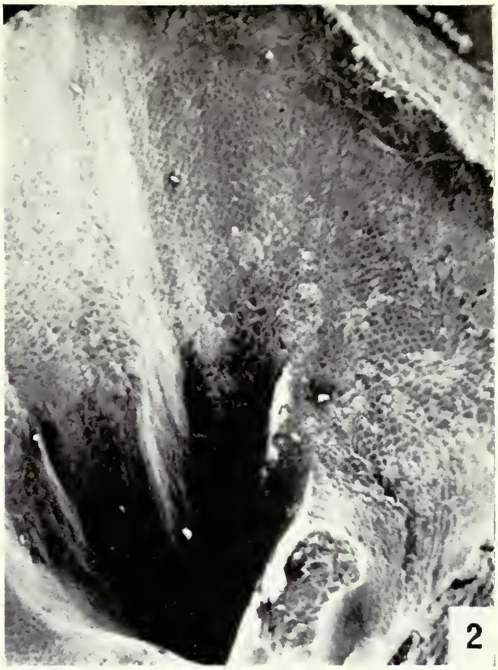

2

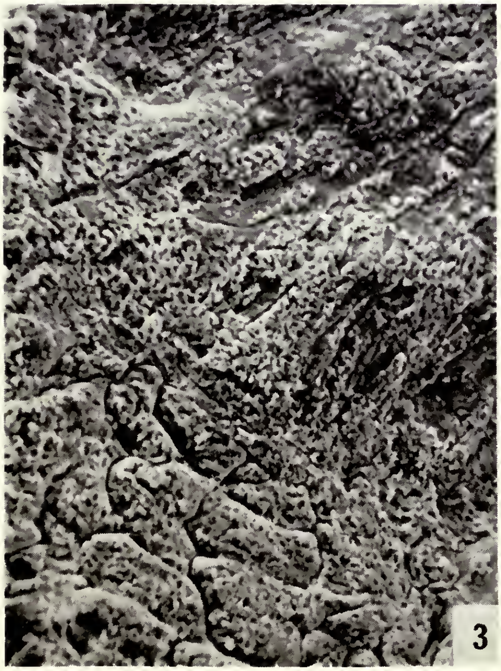

3

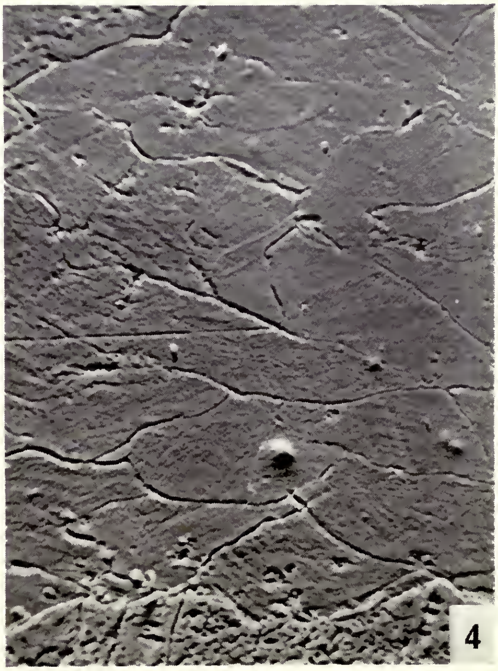

4

PLATE 15

All figures are scanning electron micrographs of the shell.

Diplospirella wissmani (Münster)

FIG. 1. Triassic (St Cassian beds), locality as Pl. 14. View of the posterior margin of a dorsal adductor myotest showing the overlap of long-exposed trails by a cluster of very small fibres. Anterior shell edge located beyond the bottom left corner. Same specimen as Pl. 13, fig. 6 and Pl. 14, figs. 1-3, BB 58959. ×280. (p. 224)

Anisactinella quadriplecta (Münster)

FIG. 2. Triassic (St Cassian beds), 1 km east of Rif. Pralongia-Htt. (Pralongia Refuge Chalet), Pralongia Ridge, 4·5 km ESE of Covara in Badia, Italy. Section through the primary and secondary shell layers. Same specimen as Pl. 30, fig. 5, BB 58960. ×1250. (p. 225)

Koninckina leonhardi (Wissman)

Triassic (St Cassian beds), 0·5 km SE of Rif. Pralongia-Htt. (Pralongia Refuge Chalet), 4 km SE of Corvara in Badia, Italy

FIG. 3. Transverse section through the primary and secondary shell layers. BB 58962. ×2600. (p. 225)

FIG. 4. General view of the outer shell surface showing a fine radial striation (running from bottom to top) with a few fine concentric growth lines (running from left to right). BB 58966. ×240. (p. 226)

FIG. 5. General view of the diamond-shaped terminal faces comprising the secondary shell mosaic. Anterior shell edge located beyond the left edge of the micrograph. Same specimen as Pl. 16, fig. 4, BB 58963. ×280. (p. 226)

Amphiclina amoena Bittner

FIG. 6. Triassic (St Cassian beds), Alpe de Specie (formerly Seelandalpe), 2·5 km NW of Carbonin (formerly Schluderbach), 11 km NE of Cortina d'Ampezzo, Trentino, Italy. View of diamond-shaped terminal faces comprising the secondary shell mosaic on the brachial valve interior. Same specimen as Pl. 16, fig. 3, BB 58967. ×660. (p. 227) (See also Pl. 31, figs. 2, 4.)

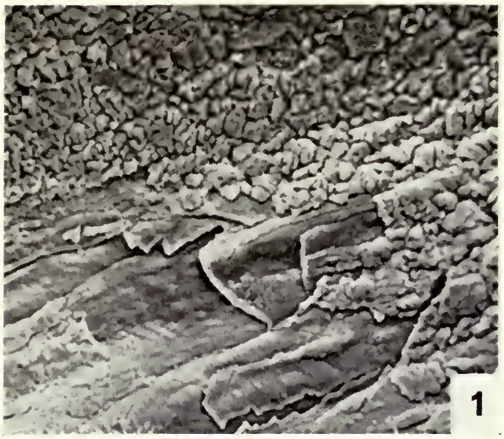
1

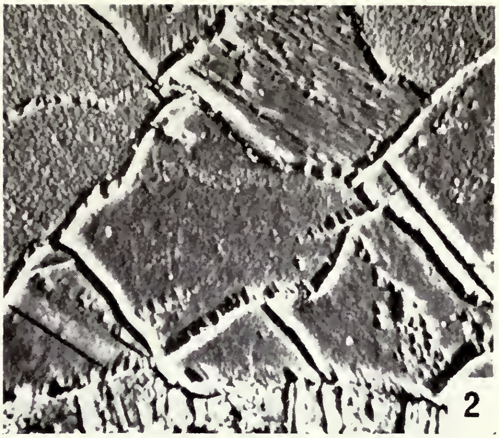
2

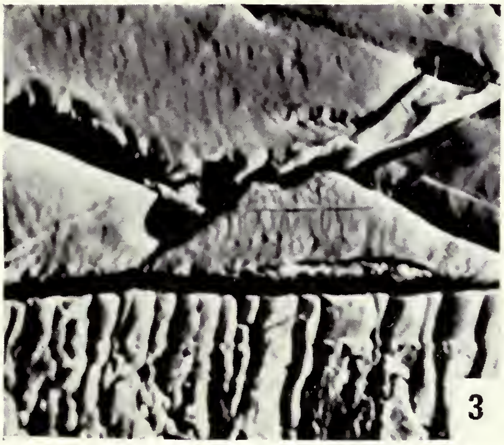
3

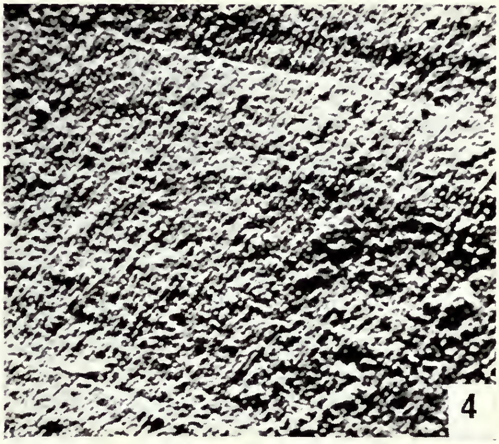
4

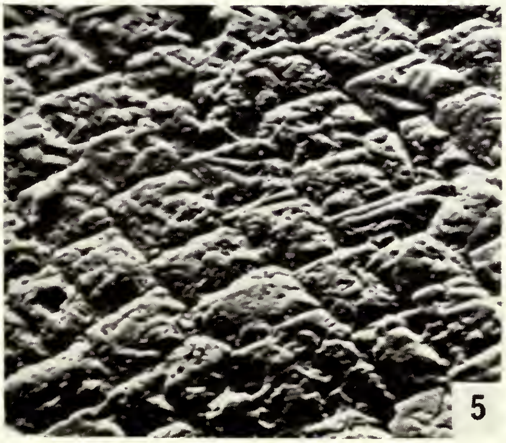
5

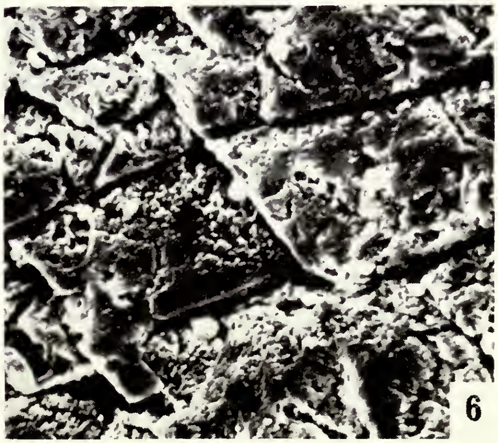
6

PLATE 16

All figures are scanning electron micrographs of the shell.

Koninckina leonhardi (Wissman)

Triassic (St Cassian beds), 0·5 km SE of Rif. Pralongia-Htt. (Pralongia Refuge Chalet), 4 km SE of Corvara in Badia, Italy

FIG. 1. Longitudinal section through secondary layer fibres showing a prominent depositional banding. Same specimen as Pl. 30, fig. 6 and Pl. 31, fig. 1, BB 58961. ×1300. (p. 227)

FIG. 6. Longitudinal section through a brachial valve showing a regrowth of some secondary layer fibres upon a tertiary layer deposit. Shell interior at the top; anterior shell edge beyond the left edge of the micrograph. Same specimen, BB 58961. ×270. (p. 228)

FIG. 2. Oblique section through the secondary layer showing depositional banding. BB 58965. ×1300. (p. 227)

FIG. 4. View of the tertiary layer fabric on top of a dome-shaped swelling on the interior surface of a brachial valve. Same specimen as Pl. 15, fig. 5, BB 58963. ×750. (p. 228)

FIG. 5. Transverse section through a brachial valve showing secondary and tertiary layers. BB 58964. ×650. (p. 228)

Amphiclina amoena Bittner

FIG. 3. Triassic (St Cassian beds), Alpe de Specie (formerly Seelandalpe), 2·5 km NW of Carbonin (formerly Schluderbach), 11 km NE of Cortina d'Ampezzo, Trentino, Italy. General view of dome-shaped swelling on the interior of the brachial valve showing spiral grooves and gonadal pits. A fragment of a primary lamella of the spiralium can be seen adhering to the surface in the foreground. Same specimen as Pl. 15, fig. 6, BB 58967. ×c. 80. (pp. 227, 250) (See also Pl. 31, figs. 2, 4.)

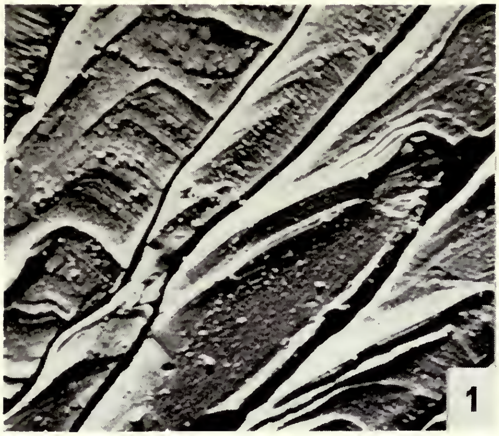

1

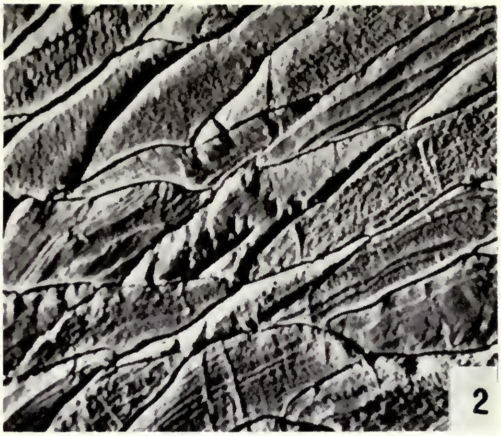

2

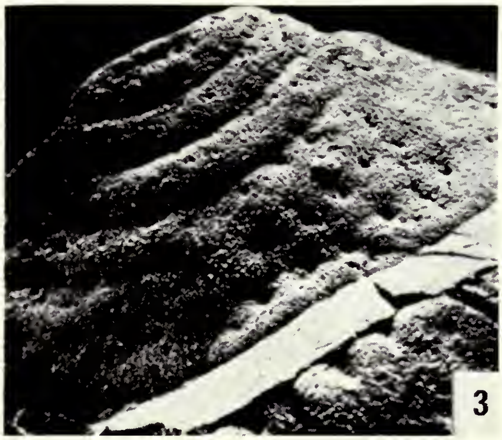

3

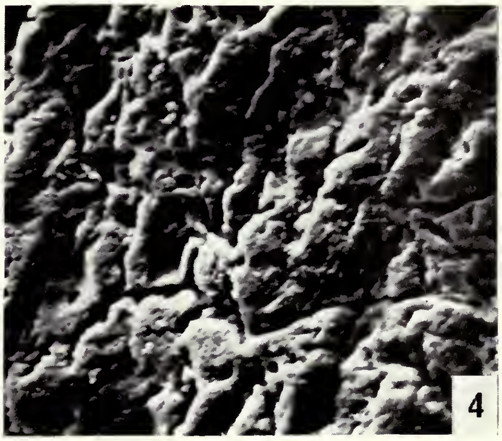

4

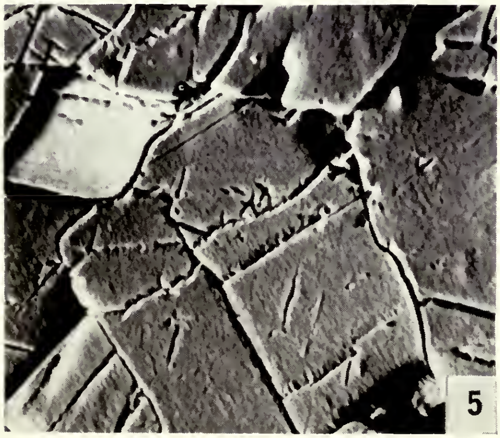

5

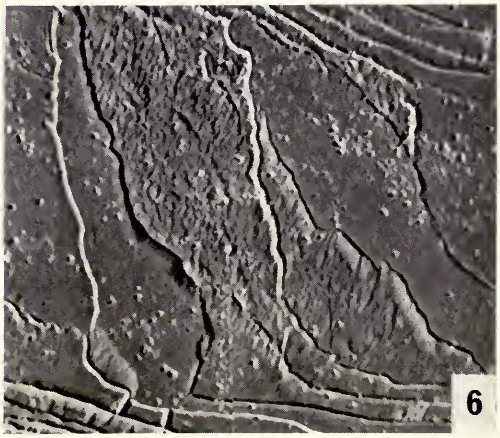

6

PLATE 17

All figures are scanning electron micrographs of the shell.

Cyrtia exporrecta (Wahlenberg)

Fig. 1. Silurian, Coalbrookdale, Shropshire. View of a section through the secondary layer showing the shape and stacking of constituent fibres. BB 58970. ×5800. (p. 229)

Ambocoelia umbonata (Conrad)

Devonian (Wanakah Shale), Canandaiga Lake, New York State.
Same specimen as Pl. 29, figs. 3, 4, BB 58971

Fig. 2. Section through a valve periphery showing a series of overlapping growth lamellae with interdigitation of primary and secondary shell layers. ×600. (p. 229)

Fig. 3. Section through the secondary layer showing the characteristic shape and stacking of fibres. ×2400. (p. 229)

Crurithyris sp.

Carboniferous (Finis Shale), Texas. BB 58972

Fig. 4. View of the interior of a brachial valve showing the standard secondary shell mosaic. ×550. (p. 230)

Fig. 5. General view of the umbonal region of a brachial valve showing cardinal process, crura, sockets and faint adductor muscle scars. ×26. (p. 230)

Fig. 6. More detailed view of part of fig. 5, showing the tuberculate nature of the cardinal process. ×64. (p. 230)

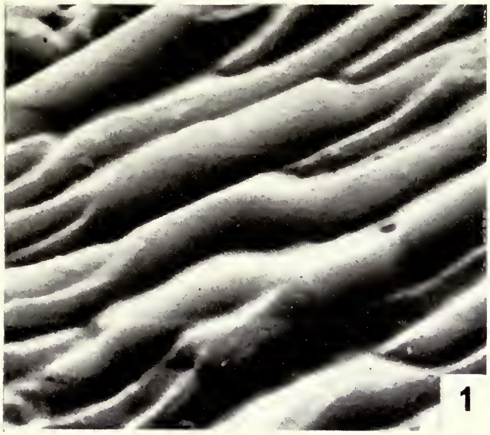
1

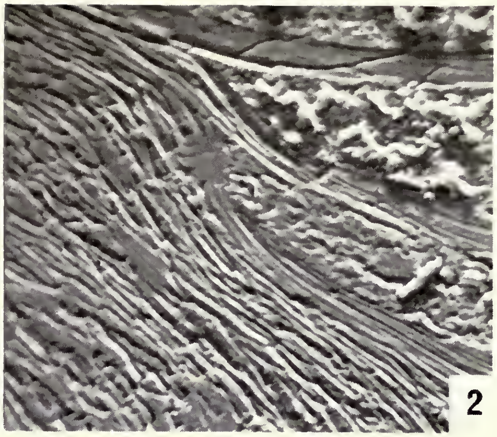
2

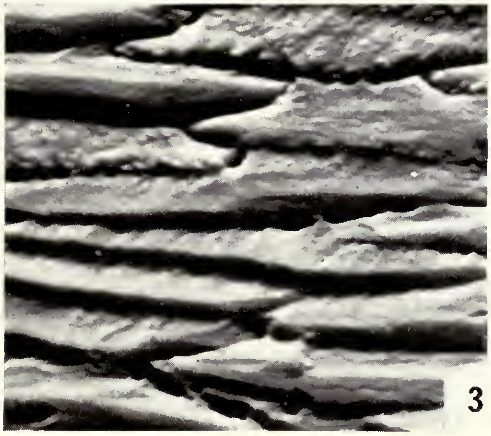
3

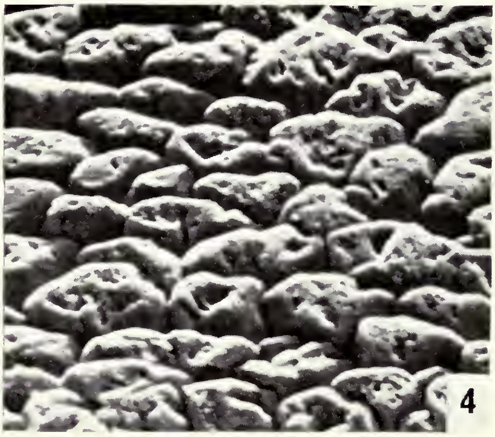
4

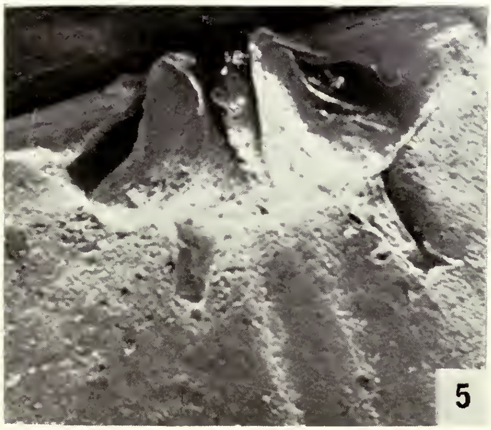
5

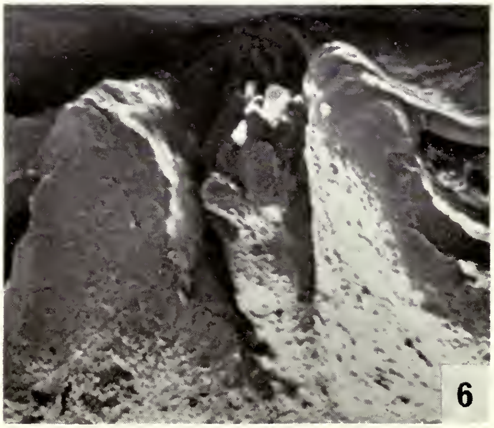
6

PLATE 18

All figures are scanning electron micrographs of the shell.

Cyrtina alpenensis Hall & Clarke

FIG. 1. Devonian, Rockport, Alpena County, Michigan. Section through the primary and secondary shell layers. Puncta penetrate both layers. BB 58973. × 1300. (p. 230)

Cyrtina sp.

Devonian (Hackberry Stage), Bird Hill, 5 miles WSW of Rockford, Iowa

FIG. 2. Transverse section through a pedicle valve showing the median septum with partitioned tichorhinum (outlined for clarity). Part of one dental plate is visible in the bottom right corner. BB 58975. × 115. (p. 230)

FIG. 3. Transverse section through a pedicle valve showing the development of a myotest (diductor) on the lower flanks of the median septum. BB 58976. × 1200. (p. 231)

Delthyris saffordi (Hall)

FIG. 4. Silurian (Brownsport Formation), western Tennessee. Section through the secondary layer showing the characteristic shape and stacking of fibres. BB 58977. × 2500. (p. 233)

Kozlowskiellina velata (Amsden)

Devonian (Haragan Formation), White Mound, Murray County, Oklahoma.
Same specimen as Pl. 19, figs. 1–4, BB 58978

FIG. 5. Section through the primary and secondary shell layers. × 2600. (p. 233)

FIG. 6. Section through the secondary layer showing the shape and stacking of constituent fibres. Shell interior located beyond the top of the micrograph. × 1400. (p. 233)

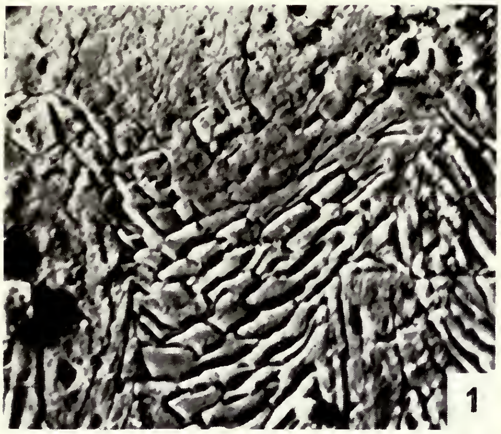
1

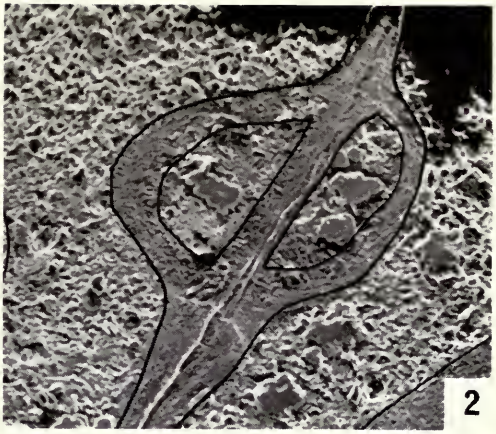
2

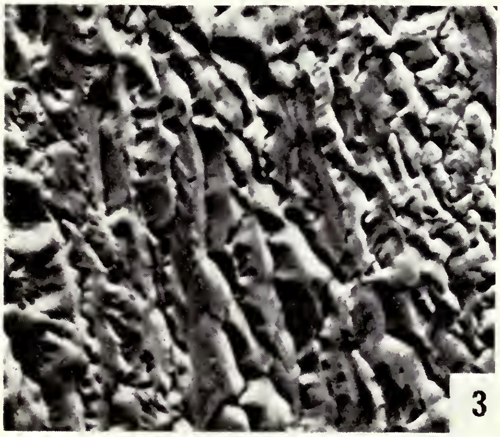
3

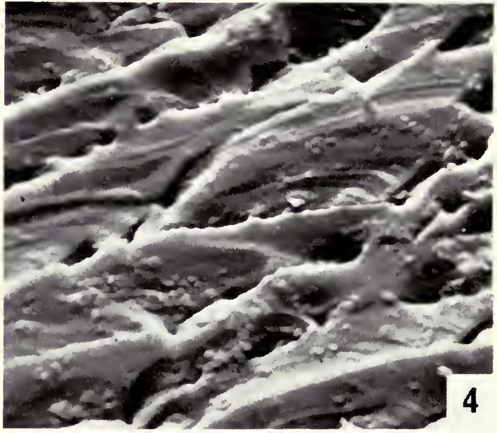
4

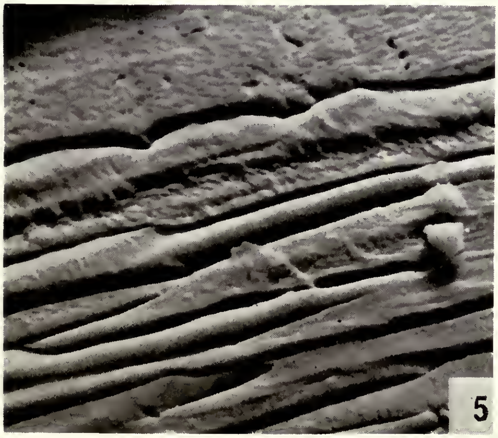
5

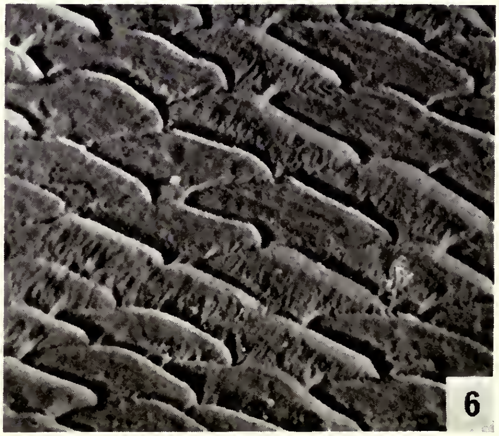
6

PLATE 19

All figures are scanning electron micrographs of the shell.

Kozlowskiellina velata (Amsden)
Devonian (Haragan Formation), White Mound, Murray County, Oklahoma.
Same specimen as Pl. 18, figs. 5, 6, BB 58978

FIG. 1. General view of a transverse section through both valves. The area squared off within the brachial valve (top) is shown in fig. 2. × c. 75. (p. 233)

FIG. 2. Transverse section through part of a brachial valve. The squared-off area, taking in a submerged crus, is reproduced in fig. 3. × 130. (p. 233)

FIG. 3. Detailed view of a section through a submerged crus showing the shape and stacking of secondary layer fibres. × 1300. (p. 233)

FIG. 4. Transverse section through a pedicle valve showing part of the ventral diductor myotest (lower middle) which is succeeded (upwards) by small orthodoxly stacked secondary layer fibres. The interior is located beyond the top of the micrograph. × 720. (p. 233)

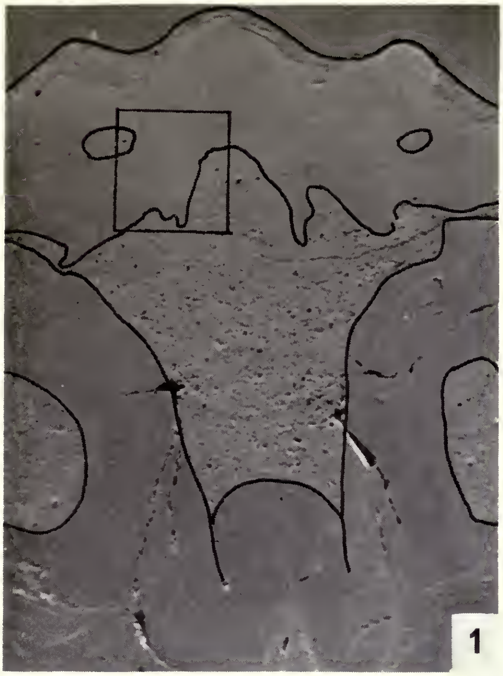
1

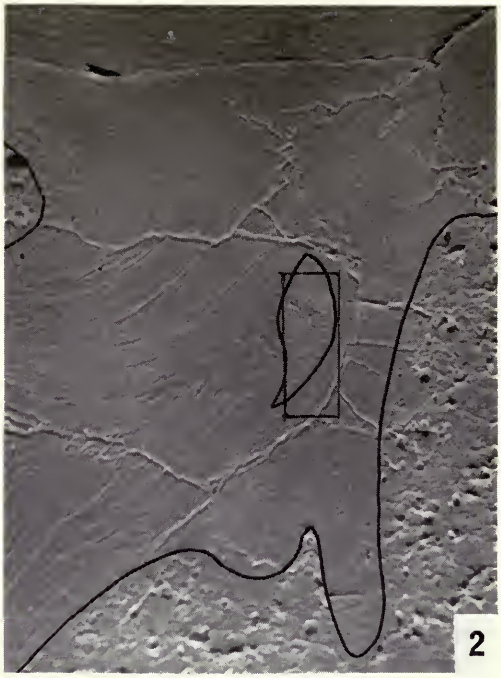
2

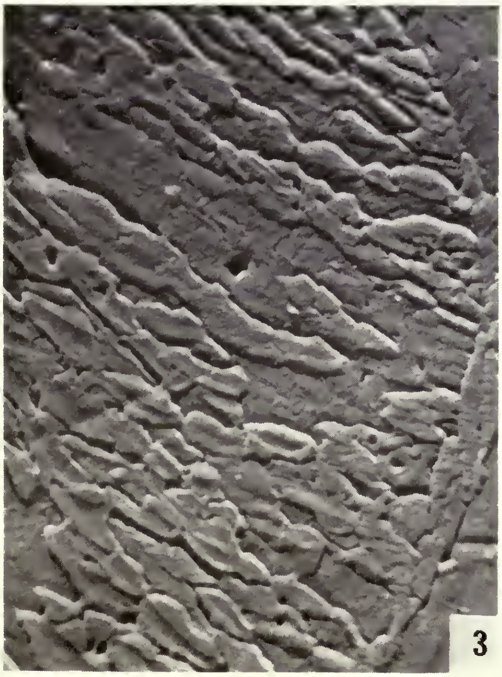
3

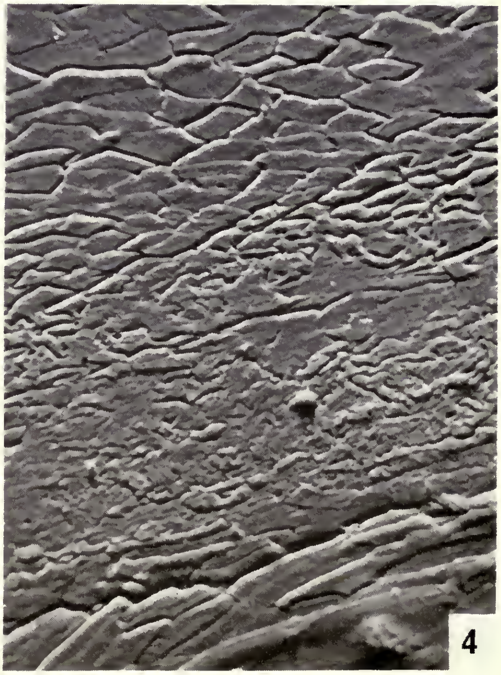
4

PLATE 20

All figures are scanning electron micrographs of the shell.

Mucrospirifer sp.

Devonian, Killians, Presque Isle Co., Road 634, 0·2 miles north of Presque/Alpena County line, Michigan. BB 58979

FIG. 1. Section through the primary and secondary shell layers. ×3000. (p. 234)

FIG. 2. Section through the secondary layer showing the shape and stacking of fibres. ×2800. (p. 234)

Spinocyrtia sp.

Devonian, Killians, Presque Isle Co., 1·3 miles west of Leroy, Michigan. BB 58984

FIG. 3. Section through the primary and secondary shell layers. ×2200. (p. 234)

FIG. 4. Section through the secondary layer showing the shape and stacking of fibres. ×6000. (p. 235)

Syringothyris cuspidata (Martin)

Carboniferous (Upper Viséan), Staffordshire. BB 58985

FIG. 5. Section through a partially recrystallized secondary layer with fibres outwardly deflected (bottom right) around a punctum. ×2400. (p. 235)

FIG. 6. More general view of fig. 5. Shell exterior is located beyond the bottom of the micrograph. ×1170. (p. 235)

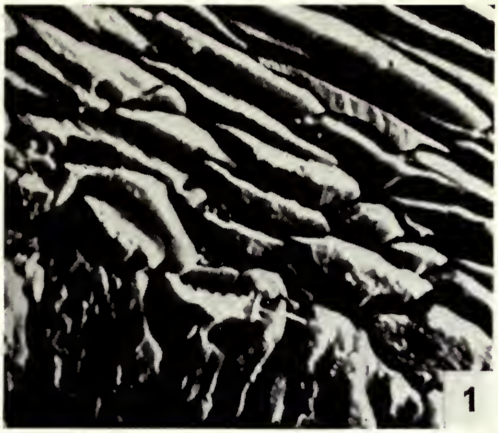
1

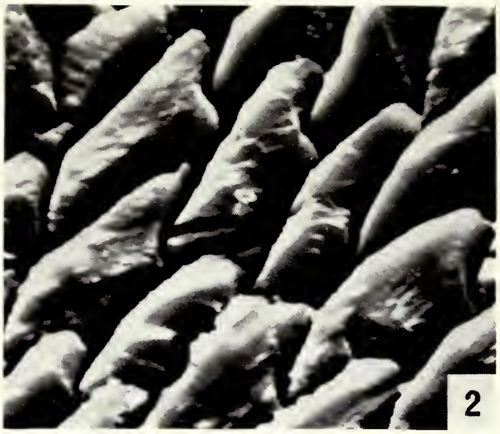
2

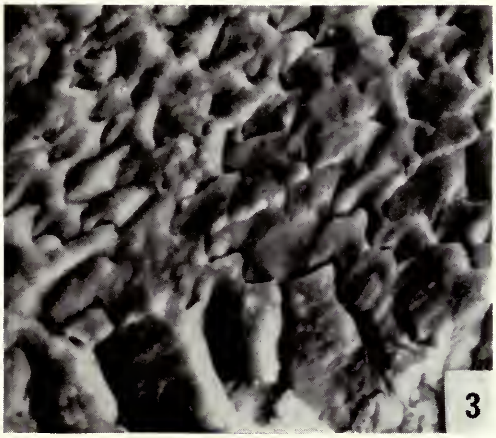
3

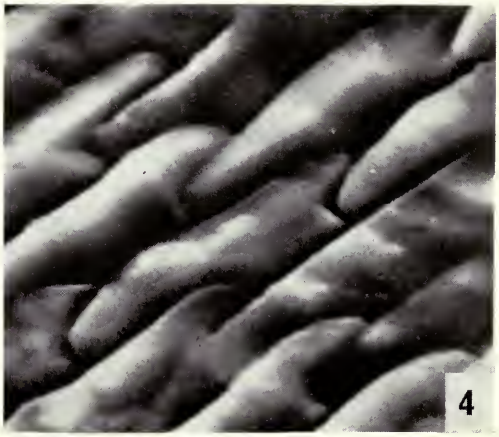
4

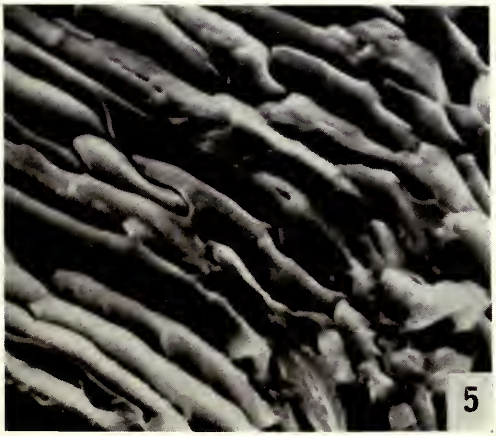
5

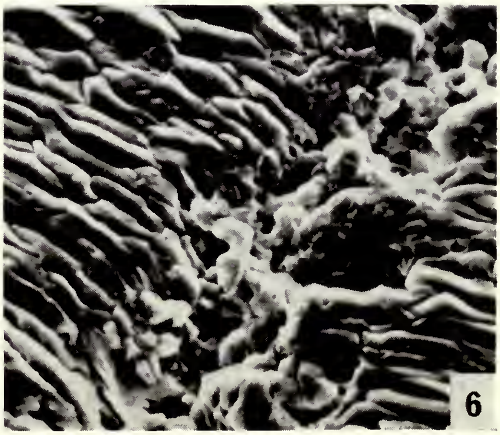
6

PLATE 21

All figures are scanning electron micrographs of the shell.

Theodossia hungerfordi (Hall)
Devonian (Hackberry Stage), Tile Yard, Rockford, Iowa.
Same specimen as Pl. 29, fig. 5, BB 58986

FIG. 1. Section through secondary layer fibres comprising a spiral lamella, showing their characteristic shape and stacking. ×2600. (p. 235)

FIG. 2. Section through part of the tertiary layer. ×640. (p. 235)

Tenticospirifer cyrtiniformis (Hall & Whitfield)
Devonian (Hackberry Stage), Tile Yard, Rockford, Iowa. BB 58987

FIG. 3. Section through the primary and secondary shell layers. ×1400. (p. 235)

FIG. 4. Section through the secondary layer showing the characteristic shape and stacking of fibres. ×2500. (p. 235)

FIG. 5. Section through a ventral myotest of a pedicle valve showing the grossly modified skeletal fabric. ×1500. (p. 236)

Syringospira prima Kindle

FIG. 6. Devonian (Percha Formation), New Mexico. Section through the primary and secondary shell layers. Same specimen as Pl. 22, fig. 1, BB 58988. ×600. (p. 236)

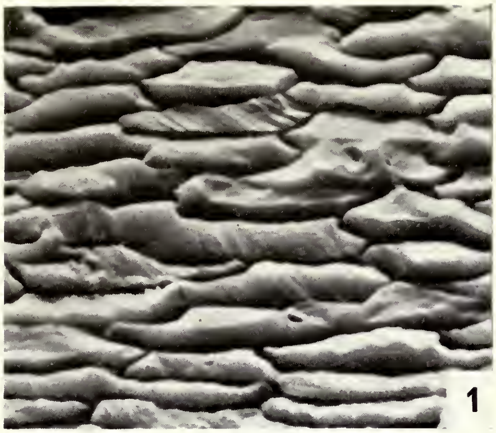
1

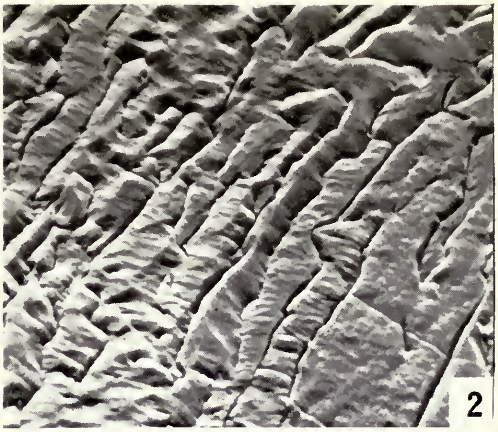
2

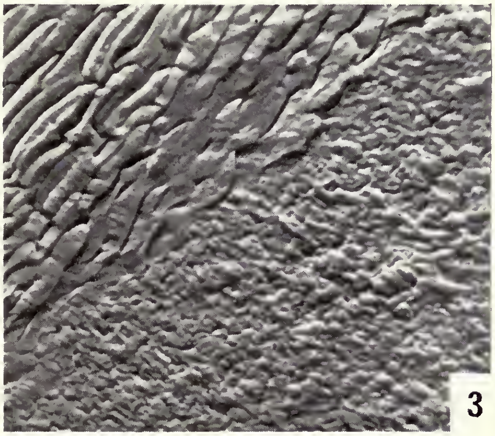
3

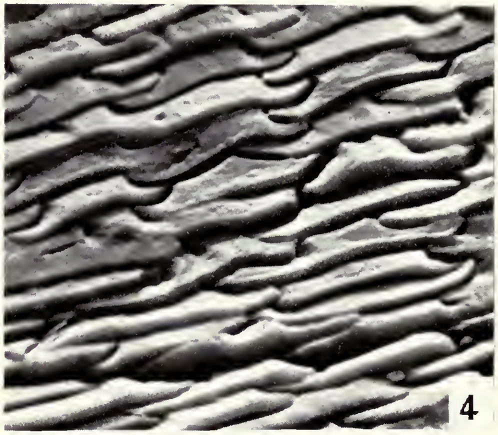
4

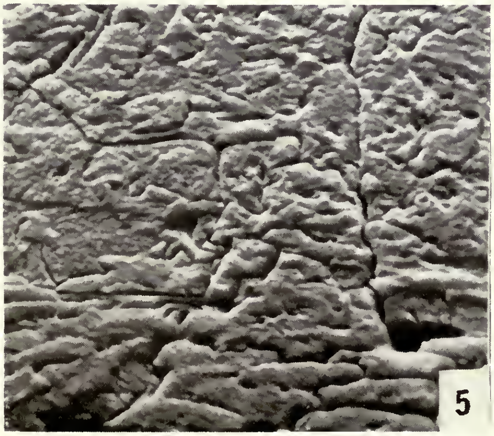
5

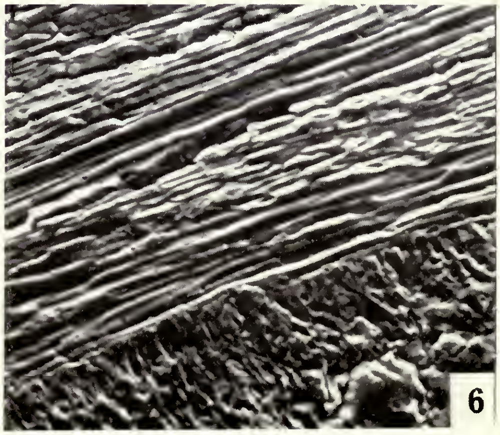
6

PLATE 22

All figures are scanning electron micrographs of the shell.

Syringospira prima Kindle

FIG. 1. Devonian (Percha Formation), New Mexico. Section through the junction of 'blisters' showing a uniformly crystalline zone between partitions composed of secondary layer fibres. Same specimen as Pl. 21, fig. 6, BB 58988. ×640. (p. 236)

Neospirifer cameratus (Morton)

FIG. 2. Pennsylvanian (La Salle Limestone), quarry south of U.S. Highway 6, 1·1 miles east of La Salle, Ohio. Section through the primary and secondary shell layers. BB 58994. ×1300. (p. 237)

Spirifer trigonalis Martin

Carboniferous (Douglas Main Limestone), Lower Limestone Group, Brockley, Lanarkshire

FIG. 3. Section through a brachial valve of a young specimen showing thin primary, secondary, and tertiary layers. Same specimen as Pl. 29, fig. 6, BB 58992. ×1300. (p. 237)

FIG. 5. Section through a brachial valve showing an alternating sequence of secondary and tertiary layers. Same specimen, BB 58992. ×280. (p. 237)

FIG. 4. Section through a thick tertiary layer showing some interdigitation with secondary layer material. BB 58991. ×145. (p. 237)

FIG. 6. Section through a ventral myotest showing narrow irregular fibrous outlines which inwardly succeed a tertiary layer (top). Same specimen, BB 58991. ×1200. (p. 237)

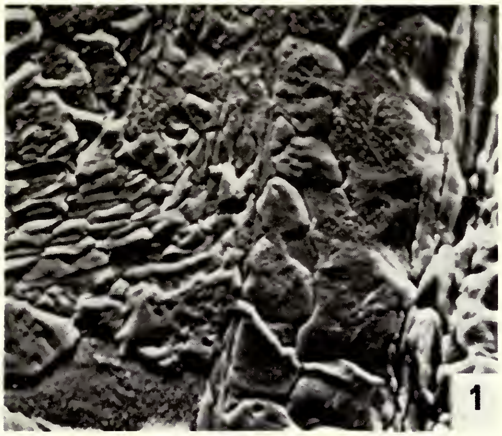
1

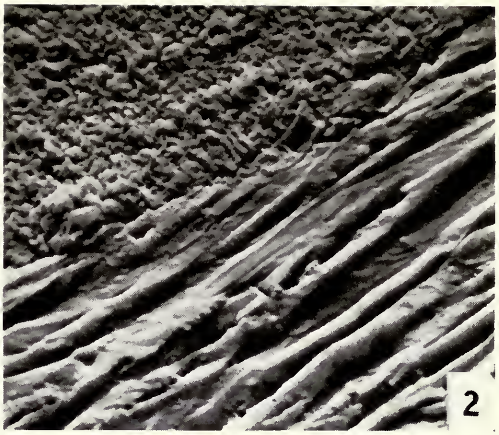
2

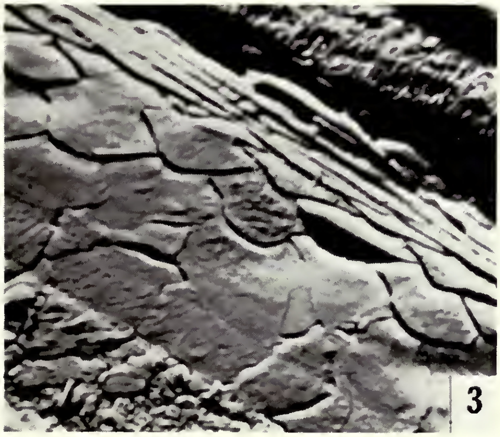
3

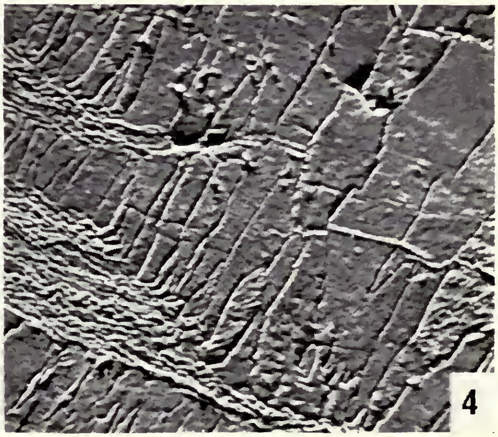
4

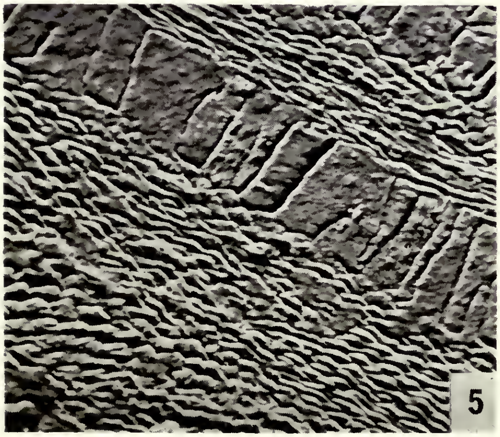
5

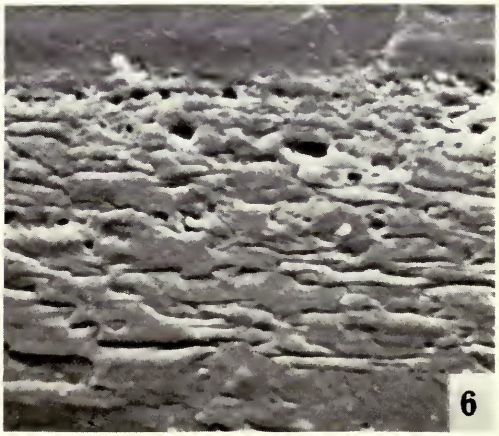
6

PLATE 23

All figures are scanning electron micrographs of the shell.

Choristites mosquensis Buckman
Carboniferous, Moscow. BB 58995

FIG. 1. Section through the primary and secondary shell layers. × 2550. (p. 238)

FIG. 2. Section through the secondary layer showing the characteristic shape and stacking of fibres. × 2500. (p. 238)

FIG. 3. Section through the tertiary layer showing the prominent transverse depositional banding. The shell interior is located beyond the top of the micrograph. × 2500. (p. 238)

FIG. 4. More detailed view of the prominent transverse depositional banding within the tertiary layer showing the development of several finer bands within each major one. × 6200. (p. 238)

FIG. 5. Section showing interdigitation of secondary and tertiary layers. × 260. (p. 238)

FIG. 6. Section through a ventral myotest showing the irregular outlines of fibres which succeed the normal secondary layer succession. × 1250. (p. 238)

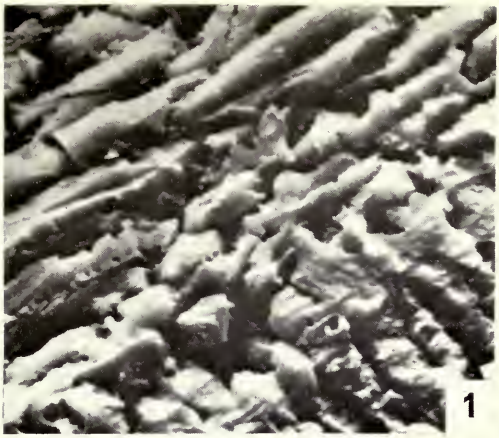
1

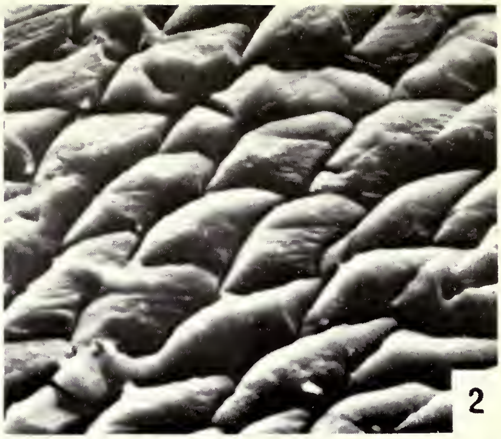
2

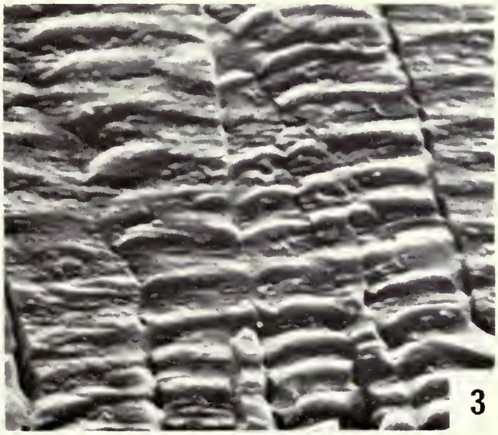
3

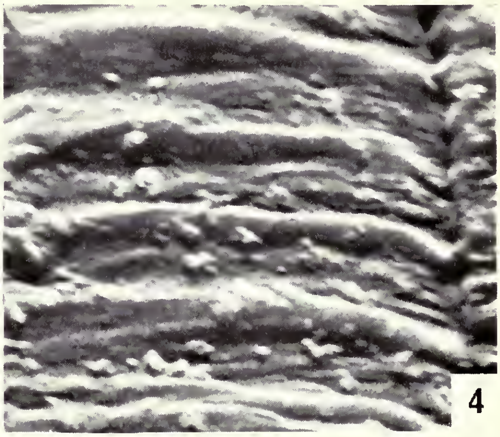
4

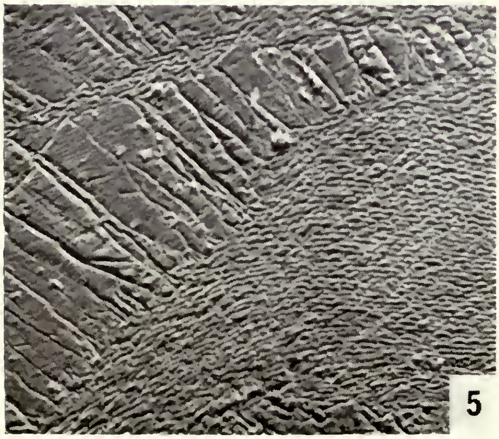
5

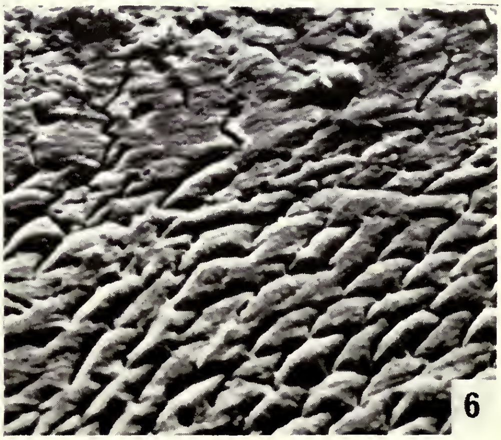
6

PLATE 24

All figures are scanning electron micrographs of the shell.

Brachythyris sp.

Carboniferous, Kildare, Ireland. BB 58997

FIG. 1. Section through the secondary layer. ×2400. (p. 238)

FIG. 2. Section through the tertiary layer showing several vertically stacked crystals. Shell interior located beyond the top left corner. ×1200. (p. 238)

'*Spiriferina cristata,* var. ***octoplicata*'**

FIG. 3. Carboniferous (Carboniferous Limestone Series), Ashfell, England. Section through the secondary layer showing the outward deflection of fibres around a punctum. BB 59001. ×1250. (p. 239)

Punctospirifer scabricosta North

Carboniferous (Carboniferous Limestone Series), England. BB 58999

FIG. 4. Section through the primary and secondary shell layers. ×1200. (p. 239)

FIG. 5. Section through the secondary layer showing the characteristic shape and stacking of fibres. ×2600. (p. 239)

FIG. 6. Section through the secondary layer showing the outward deflection of fibres around a punctum. ×1300. (p. 239)

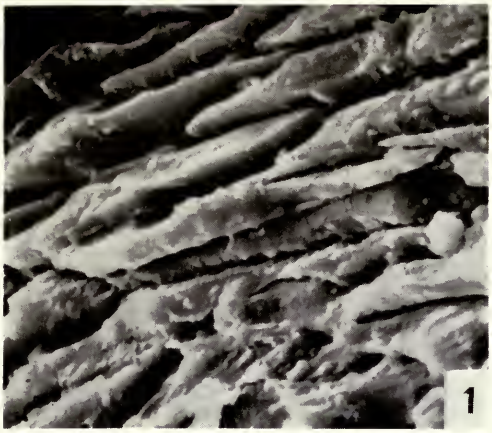
1

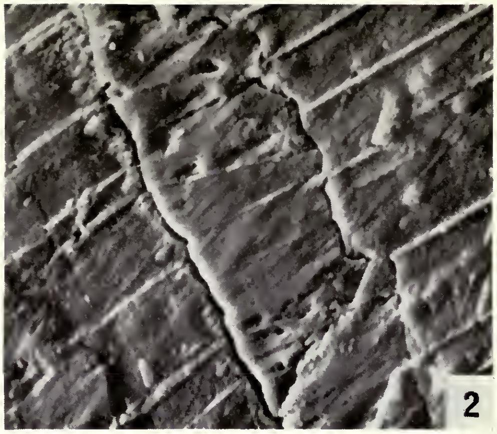
2

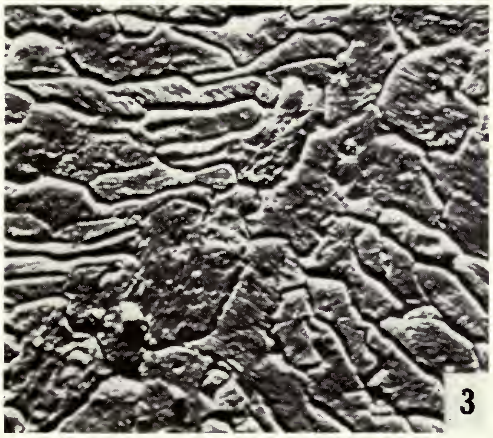
3

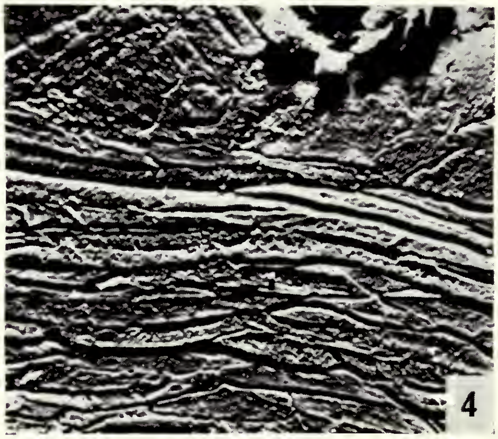
4

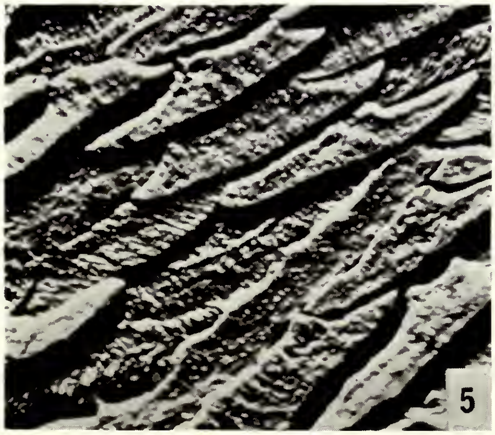
5

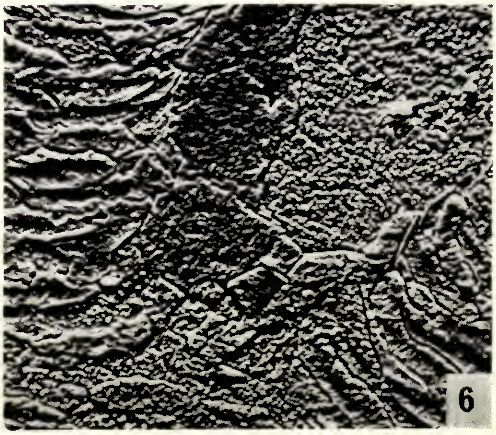
6

PLATE 25

All figures are scanning electron micrographs of the shell.

Crenispirifer sp.

Pennsylvanian (La Salle Limestone), quarry south of U.S. Highway 6, 1·1 miles east of La Salle, Ohio. BB 58998

FIG. 1. Section through the primary and secondary shell layers. × 1350. (p. 239)

FIG. 2. Section through the secondary layer showing the outward deflection of fibres around a punctum. × 620. (p. 239)

Phricodothyris sp.

Carboniferous (Finis Shale), Texas. BB 59002

FIG. 3. Section through the primary (bottom), secondary and tertiary (top left) shell layers. The primary layer accommodates a hollow spine base (now infilled) which is located upon an overlapping growth lamella. A wedge of primary shell material extends within the secondary layer but does not affect the tertiary layer. × 600. (pp. 239, 240)

FIG. 4. Section through the primary (bottom), secondary, and tertiary (top) layers, showing a transverse depositional banding within the tertiary layer. × 550. (pp. 239, 240)

FIG. 5. Section through the secondary and tertiary layers showing a prominent transverse depositional banding within the tertiary layer. × 2200. (p. 240)

FIG. 6. Carboniferous (Carboniferous Limestone Series), Braidwood, Lanarkshire. Section through the tertiary layer showing depositional banding identical to that found in the American species of *Phricodothyris*. BB 59003. × 1400. (p. 240)

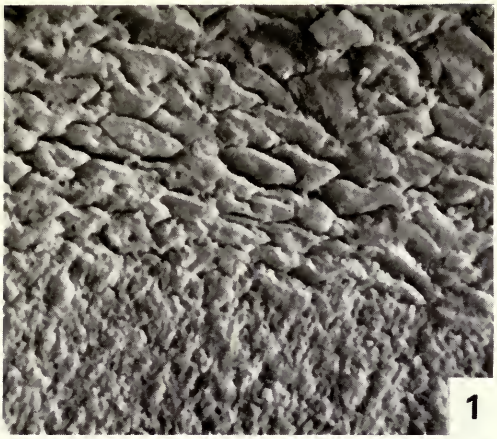
1

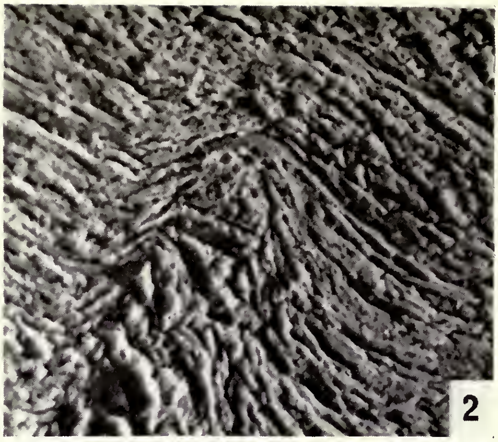
2

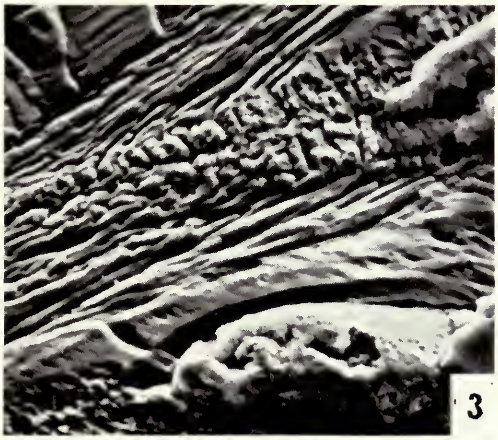
3

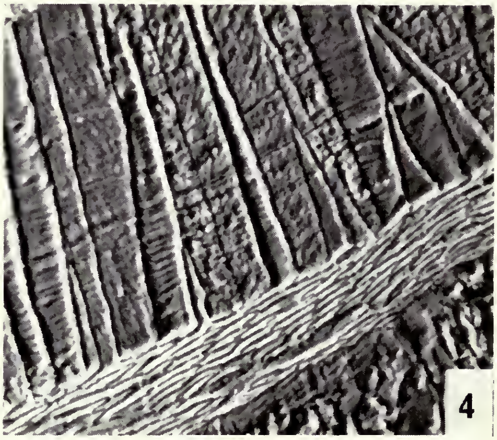
4

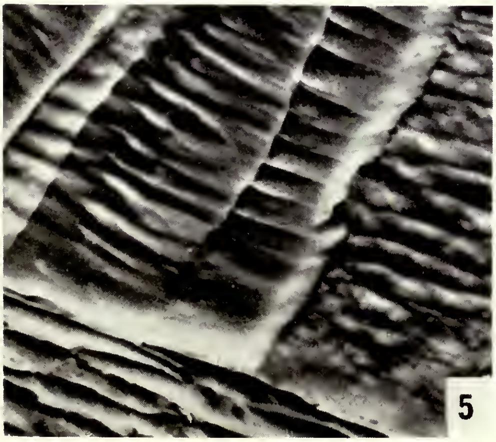
5

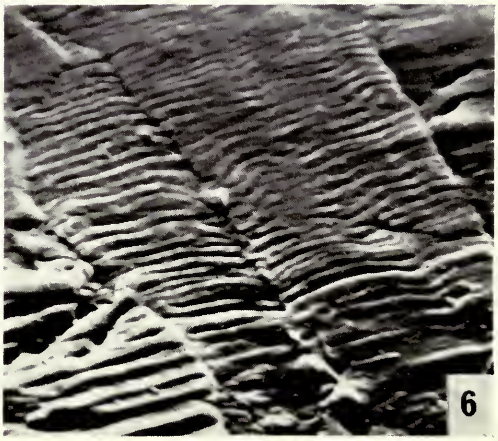
6

PLATE 26

All figures are scanning electron micrographs of the shell.

Martinia sp.

Carboniferous, Kildare, Ireland. BB 59004

FIG. 1. Section through the secondary layer showing indistinct outlines of fibres. ×2400. (p. 240)

FIG. 2. Section through part of the tertiary layer. Shell interior located beyond top left corner. ×650. (p. 240)

Thecospira sp.

Triassic (St Cassian beds), Alpe de Specie (formerly Seelandalpe), 2·5 km NW of Carbonin (formerly Schluderbach), 11 km NE of Cortina d'Ampezzo, Trentino, Italy

FIG. 3. Section through a brachial valve showing primary and secondary shell layers. BB 59007. ×1400. (p. 241)

FIG. 4. Section through the secondary layer showing the characteristic shape and stacking of fibres. Same specimen, BB 59007. ×2800. (p. 242)

FIG. 5. Section through the cementation area of a pedicle valve. A narrow zone, mainly infilled with sediment, separates the secondary layer fibres of *Thecospira* (top) from the prismatic layers of a molluscan shell fragment (bottom) to which the brachiopod is attached. Same specimen as Pl. 31, figs. 3, 5–6, BB 59005. ×700. (p. 241) (See also Text-fig. 19.)

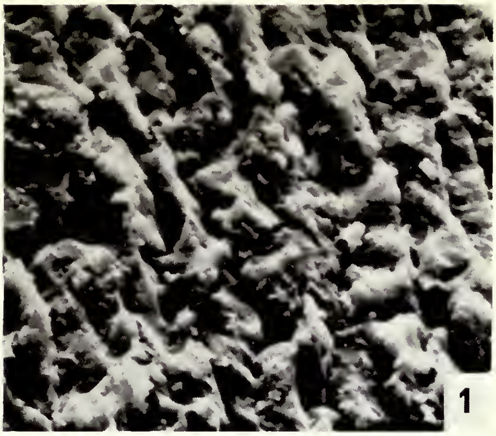
1

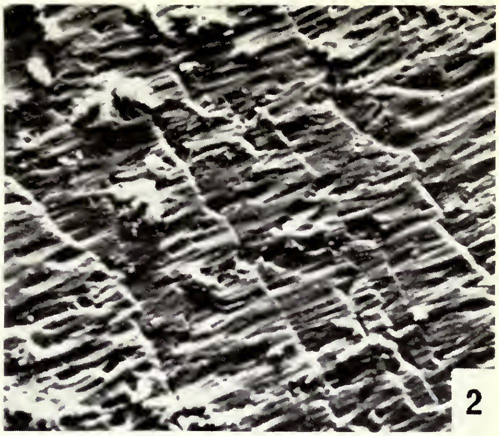
2

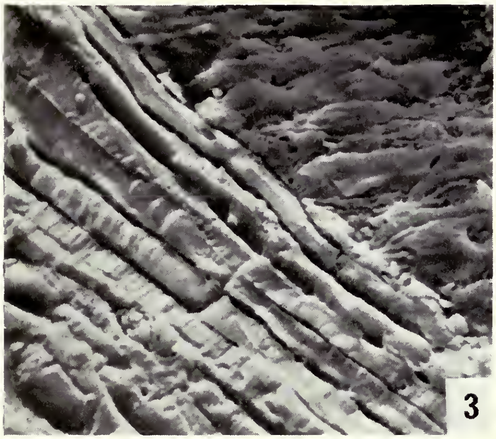
3

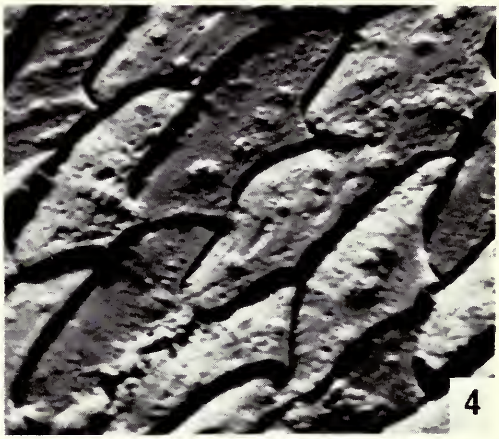
4

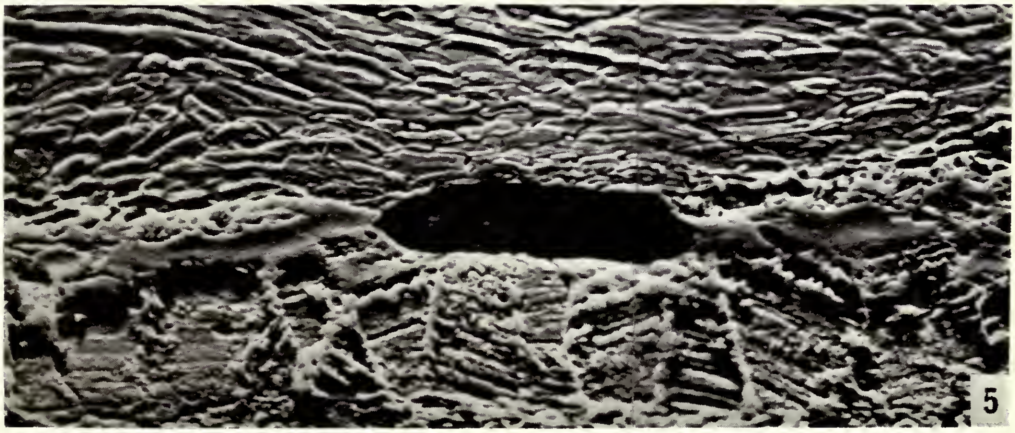
5

PLATE 27

All figures are scanning electron micrographs of the shell.

Thecospira sp.

Triassic (St Cassian beds), Alpe de Specie (formerly Seelandalpe), 2·5 km NW of Carbonin (formerly Schluderbach), 11 km NE of Cortina d'Ampezzo, Trentino, Italy.
Same specimen as Pl. 28, figs. 1–2, BB 59008

FIG. 1. Oblique section of a tubercle core within the secondary layer showing the deflection of fibres. ×1400. (p. 242)

FIG. 2. Section through a tubercle submerged within the secondary layer showing the inward deflection of fibres. ×670. (p. 242)

FIG. 3. Section through a submerged tubercle showing some transverse depositional banding and the inward deflection of secondary layer fibres. ×1350. (p. 242)

FIG. 4. More general view of fig. 3, showing primary (top right) and secondary layers. Tubercle cores can be recognized within the secondary layer which is also penetrated by puncta. ×270. (pp. 242, 243)

FIG. 5. Section through the secondary layer showing the outward deflection of fibres around a punctum. Several transverse micritic bands are also outwardly deflected around the punctum. ×650. (p. 243)

FIG. 6. More detailed view of a section through the secondary layer showing a porous, micritic band. ×2650. (p. 243)

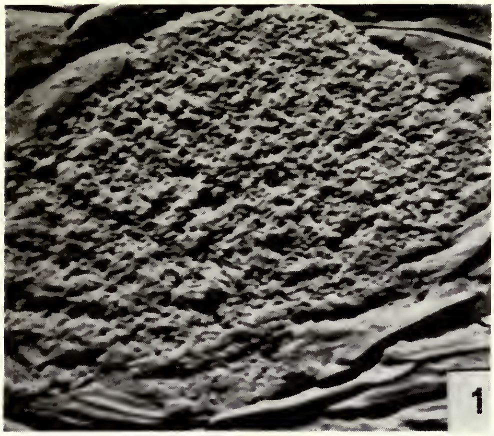
1

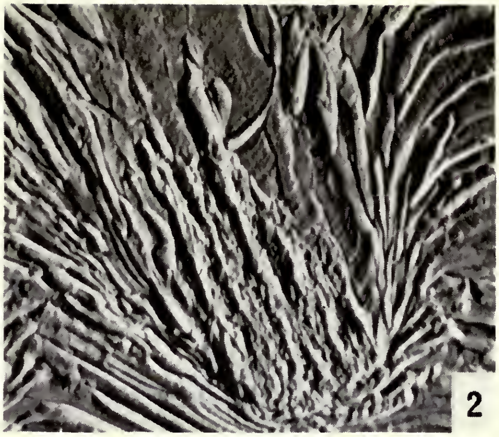
2

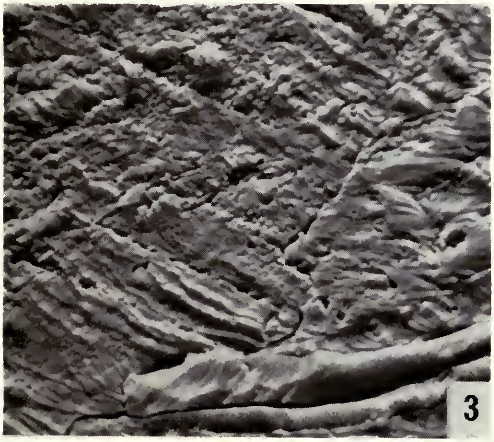
3

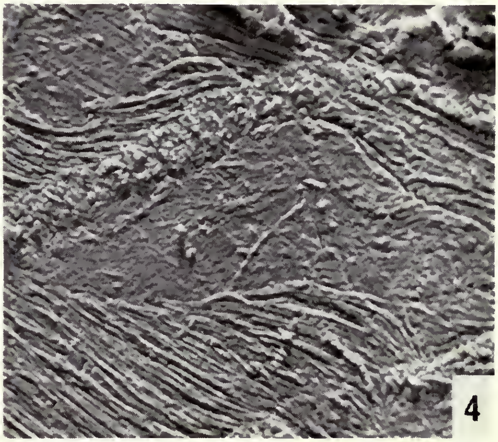
4

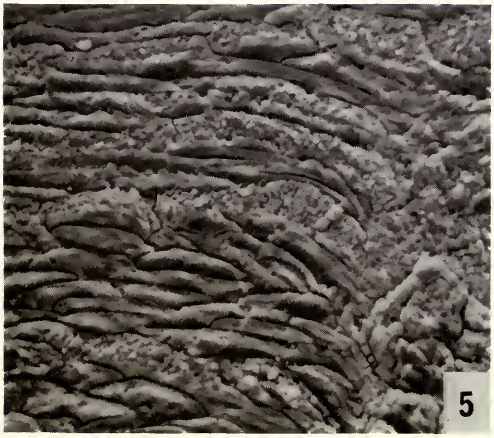
5

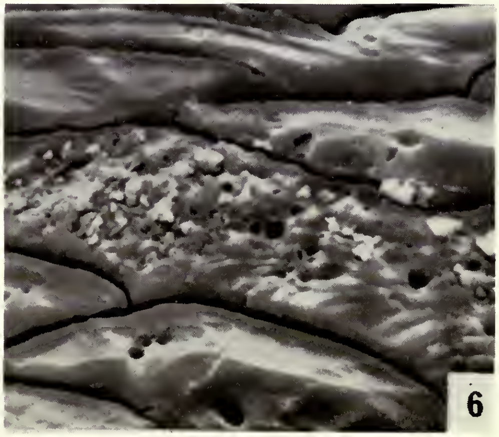
6

PLATE 28

All figures are scanning electron micrographs of the shell (figs. 1, 2) or spiralium (figs. 3-6).

Thecospira sp.

Triassic (St Cassian beds), Alpe de Specie (formerly Seelandalpe), 2·5 km NW of Carbonin (formerly Schluderbach), 11 km NE of Cortina d'Ampezzo, Trentino, Italy.
Same specimen as Pl. 27, BB 59008

Fig. 1. Section through a brachial valve showing part of a dorsal adductor myotest. × 1250. (p. 243)

Fig. 2. General view of a section through the overhanging ridge located at the anterior margin of the ventral diductor muscle scar. × 140. (p. 243)

Protozyga elongata Cooper

Fig. 3. Ordovician (Lower Bromide Formation), 1 mile west of Dolese Brothers Crusher, Bromide, Oklahoma. Transverse section through one prong of the rudimentary spiralium. Same specimen as Pl. 6, fig. 5, BB 58918. × 2800. (p. 244)

Catazyga headi (Billings)

Fig. 4. Ordovician (Richmond Group), Adana Co., near Winchester, Ohio. Transverse section through a spiral lamella showing the double-sided distribution of secondary layer fibres. Same specimen as Pl. 7, figs. 1-3, BB 58921. × 1350. (p. 245)

Idiospira thomsoni (Davidson)

Ordovician (Craighead Limestone), Girvan, Ayrshire.
Same specimen as Pl. 7, figs. 4-5, BB 58922

Fig. 5. Transverse section through a spiral lamella showing the double-sided distribution of secondary layer fibres. × 610. (p. 245)

Fig. 6. More detailed view of part of fig. 5, showing the deflection of fibres around a spine base which projects from the median-facing side of the lamella. × 2400. (p. 245)

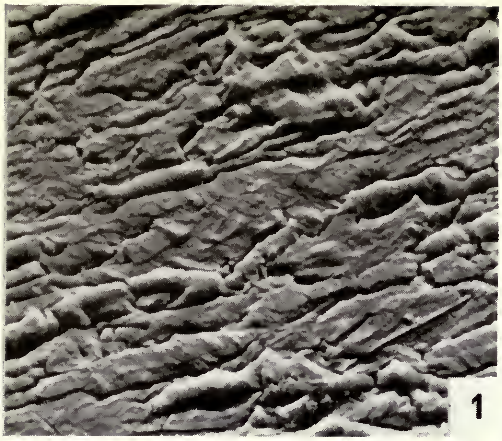
1

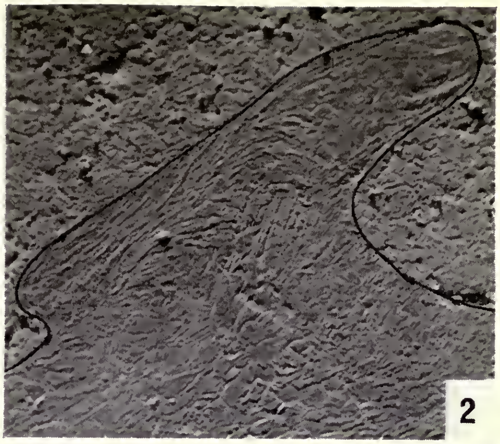
2

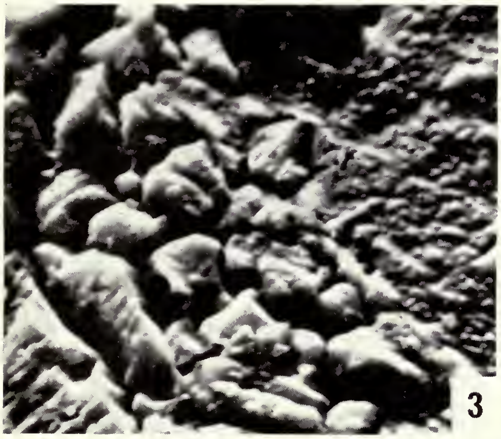
3

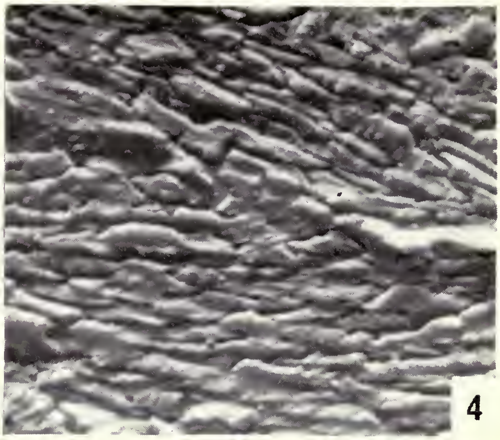
4

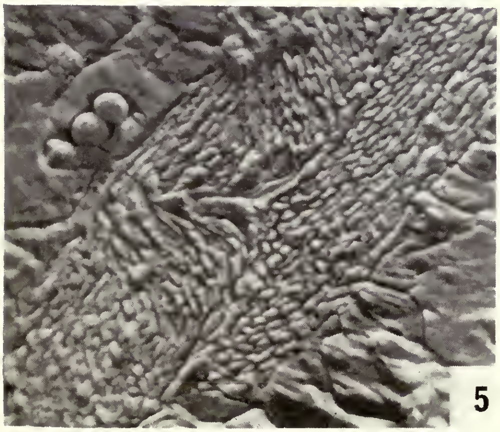
5

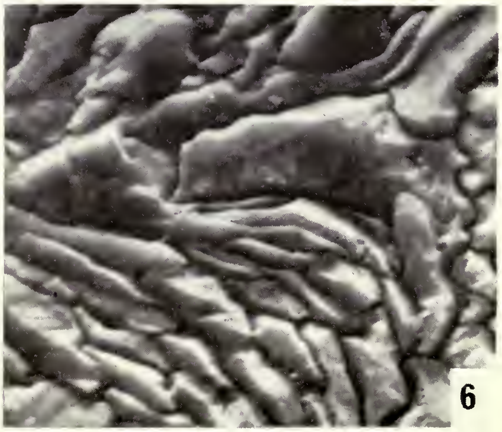
6

PLATE 29

All figures are scanning electron micrographs of the spiralium.

Dayia navicula (Sowerby)

Fig. 1. Ludlovian (Dayia Shales), Park Farm Quarry, Onibury, Shropshire. Transverse section through a spiral lamella showing the double-sided distribution of secondary layer fibres. BB 58934. ×1200. (p. 245) (See also Pl. 9, figs. 5–6.)

Rhynchospirina maxwelli Amsden

Fig. 2. Devonian (Haragan Formation), White Mound, Murray County, Oklahoma. Transverse section through a spiral lamella showing the double-sided distribution of secondary layer fibres. Same specimen as Pl. 10, fig. 3, BB 58936. ×700. (p. 245)

Ambocoelia umbonata (Conrad)

Figs. 3, 4. Devonian (Wanakah Shale), Canandaiga Lake, New York State. Transverse section through a spiral lamella showing the double-sided distribution of secondary layer fibres. Same specimen as Pl. 17, figs. 2, 3, BB 58971. ×600, ×2600. (p. 245)

Theodossia hungerfordi (Hall)

Fig. 5. Devonian (Hackberry Stage), Tile Yard, Rockford, Iowa. Transverse section through a spiral lamella showing the double-sided distribution of secondary layer fibres. Same specimen as Pl. 21, figs. 1–2, BB 58986. ×630. (p. 245)

Spirifer trigonalis Martin

Fig. 6. Carboniferous (Douglas Main Limestone), Lower Limestone Group, Brockley, Lanarkshire. Transverse section through a spiral lamella showing the double-sided distribution of secondary layer fibres. Same specimen as Pl. 22, figs. 3, 5, BB 58992. ×650. (p. 245)

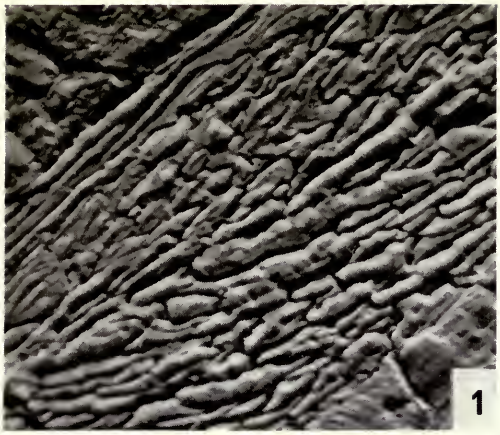
1

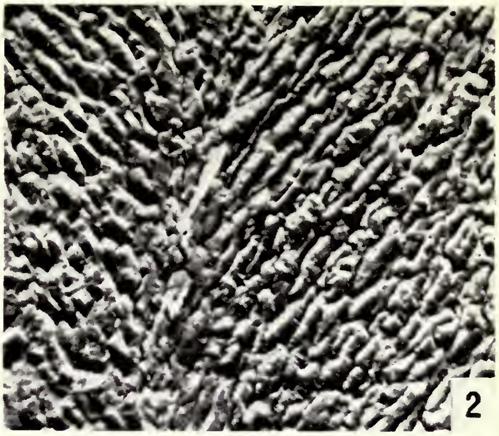
2

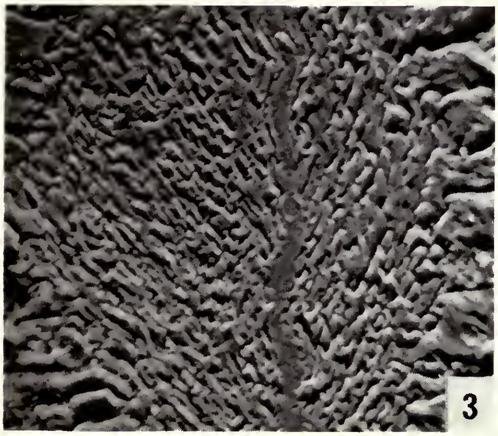
3

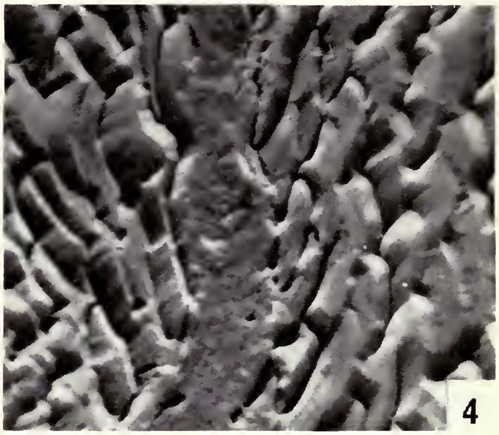
4

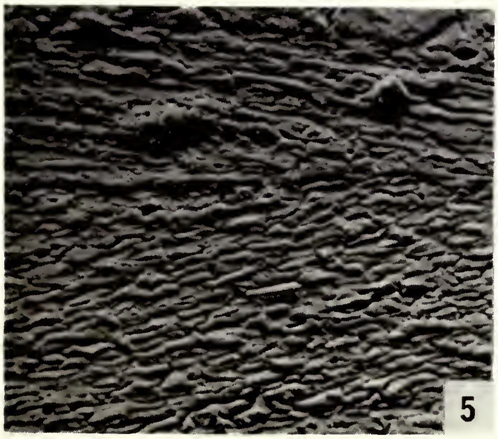
5

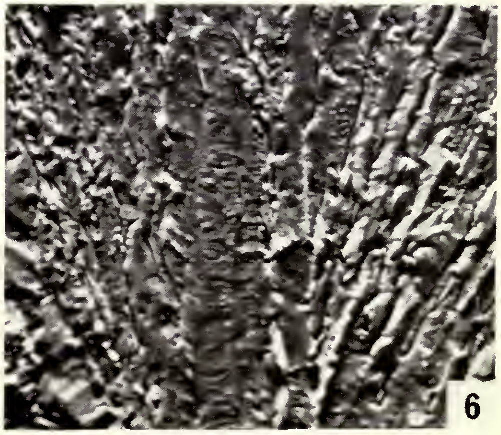
6

PLATE 30

All figures are scanning electron micrographs of the spiralium.

Composita ambigua (Sowerby)
Carboniferous (Calmy Limestone), Carluke, Lanarkshire.
BB 58950. (See also Pl. 13, fig. 1)

FIG. 1. Section through a spiral lamella showing the flat apical-facing side (bottom left corner). Growth is one-sided. × 280. (p. 247)

FIG. 2. More detailed view of part of fig. 1, showing the regular shape and stacking of fibres. × 2800. (p. 247)

Athyris spiriferoides (Eaton)

FIG. 3. Devonian (Wanakah Shale), Canandaiga Lake, New York State. Transverse section through a spiral lamella showing the disposition of fibres. The curved keels are convex towards the median-facing side (bottom). BB 58949. × 1150. (p. 247) (See also Pl. 12, figs. 5–6.)

Diplospirella wissmani (Münster)

FIG. 4. Triassic (St Cassian beds), Alpe de Specie (formerly Seelandalpe), 2·5 km NW of Carbonin (formerly Schluderbach), 11 km NE of Cortina d'Ampezzo, Trentino, Italy. Section through a primary lamella showing the disposition of secondary layer fibres. Growth is one-sided. Same specimen as Pl. 13, fig. 5, BB 58956. × 1300. (p. 247)

Anisactinella quadriplecta (Münster)

FIG. 5. Triassic (St Cassian beds), 1 km E of Rif. Pralongia-Htt. (Pralongia Refuge Chalet), Pralongia Ridge, 4·5 km ESE of Corvara in Badia, Italy. Transverse section through a primary lamella showing the disposition of secondary layer fibres. A spine base (right) projects from the median-facing side. Same specimen as Pl. 15, fig. 2, BB 58960. × 2500. (p. 247)

Koninckina leonhardi (Wissman)

FIG. 6. Triassic (St Cassian beds), 0·5 km SE of Rif. Pralongia-Htt. (Pralongia Refuge Chalet), 4 km SE of Corvara in Badia, Italy. Transverse section through a primary lamella showing the shape and stacking of constituent secondary layer fibres. Same specimen as Pl. 16, figs. 1, 6 and Pl. 31, fig. 1, BB 58961. × 1400. (pp. 247, 250)

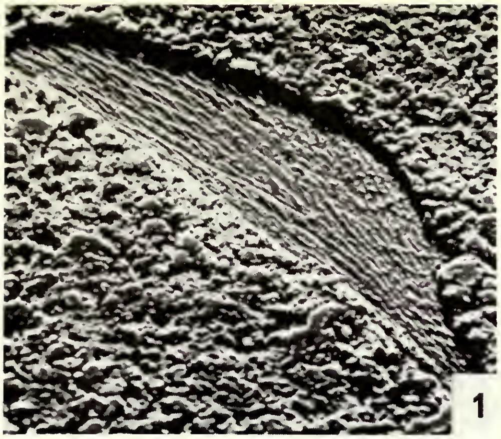
1

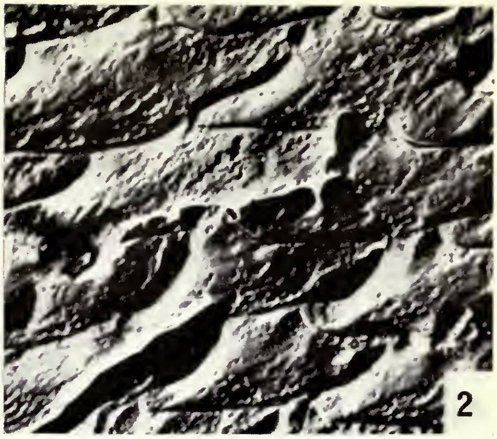
2

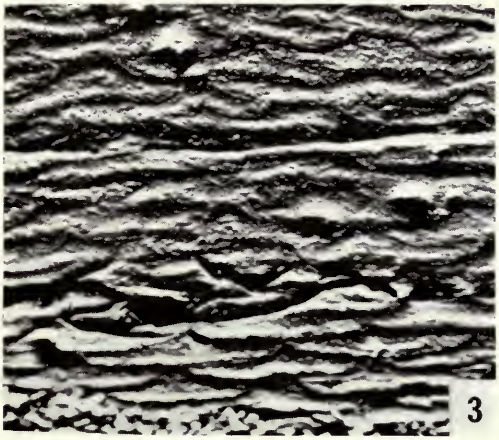
3

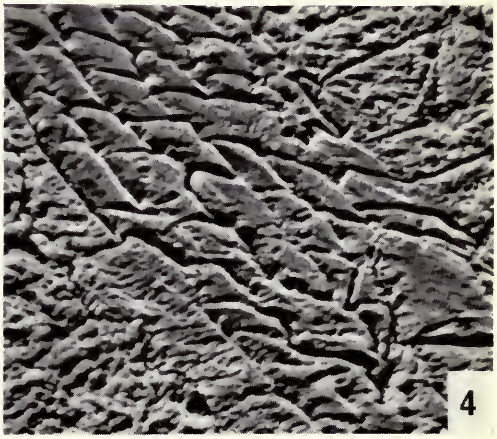
4

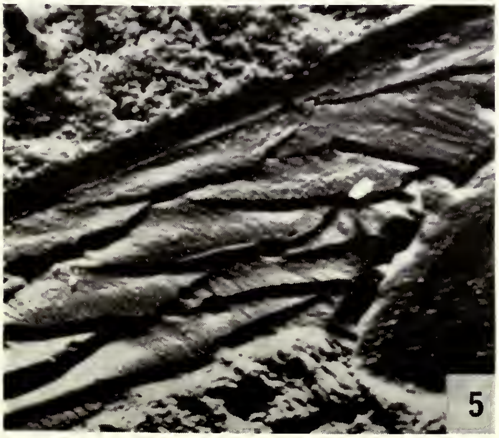
5

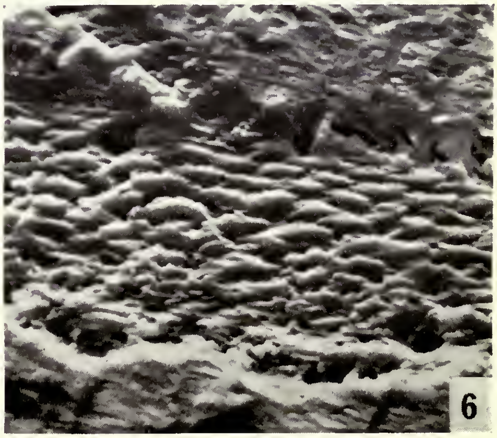
6

PLATE 31

All figures are scanning electron micrographs of the spiralium.

Koninckina leonhardi (Wissman)

FIG. 1. Triassic (St Cassian beds), 0·5 km SE of Rif. Pralongia-Htt. (Pralongia Refuge Chalet), 4 km SE of Corvara in Badia, Italy. Transverse section through a primary (top) and accessory (bottom) lamella seen in attitudes of growth relative to one another. Same specimen as Pl. 16, figs. 1, 6, and Pl. 30, fig. 6, BB 58961. ×670. (pp. 247, 250)

Amphiclina amoena Bittner

Triassic (St Cassian beds), Alpe de Specie (formerly Seelandalpe), 2·5 km NW of Carbonin (formerly Schluderbach), 11 km NE of Cortina d'Ampezzo, Trentino, Italy. BB 58968. (See also Pl. 15, fig. 6 and Pl. 16, fig. 3)

FIG. 2. View of the resorbed face of a primary lamella showing the trails of fibres disposed obliquely across its surface. ×130. (pp. 247, 250)

FIG. 4. More detailed view of part of fig. 2, showing the series of narrow troughs and ridges aligned at right angles to the outer edge of the primary lamella. ×1200. (p. 250)

Thecospira sp.

Triassic (St Cassian beds), Alpe de Specie (formerly Seelandalpe), 2·5 km NW of Carbonin (formerly Schluderbach), 11 km NE of Cortina d'Ampezzo, Trentino, Italy. Same specimen as Pl. 26, fig. 5, BB 59005

FIG. 3. Transverse section through part of the dorsal limb of a spiral lamella showing the stacking of secondary layer fibres. ×670. (p. 247)

FIG. 5. Transverse section through part of the ventral non-fibrous limb of a U-shaped spiral lamella showing a series of concentric bands which are probably depositional. ×2800. (p. 251)

FIG. 6. Transverse section through part of the dorsal limb of a U-shaped spiral lamella showing non-fibrous, concentrically banded zones. ×1350. (p. 251)

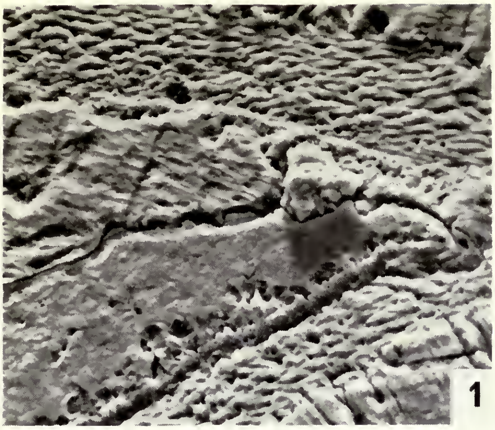
1

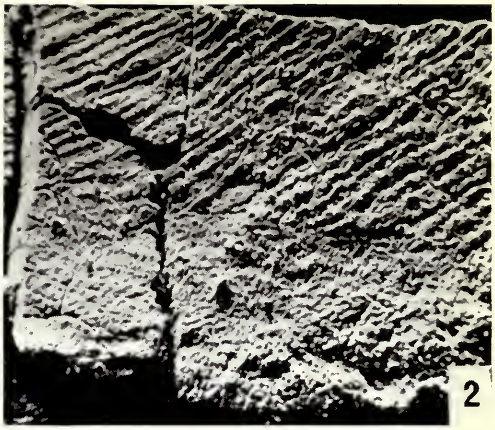
2

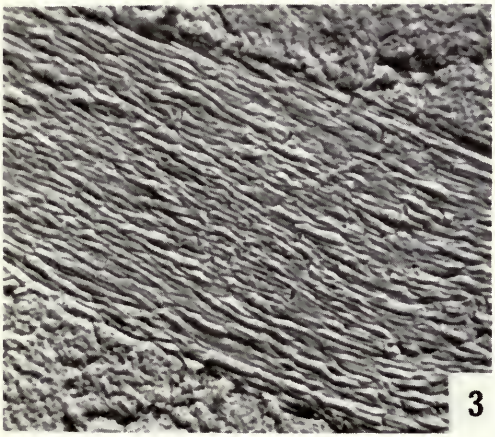
3

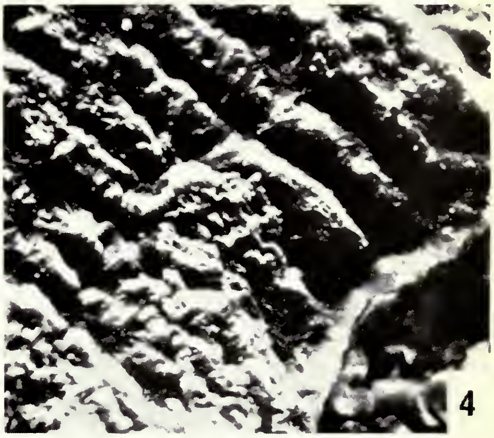
4

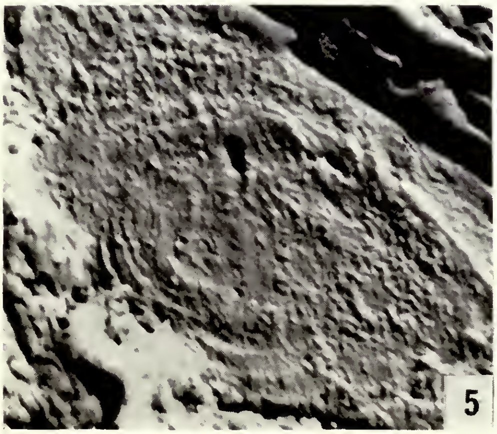
5

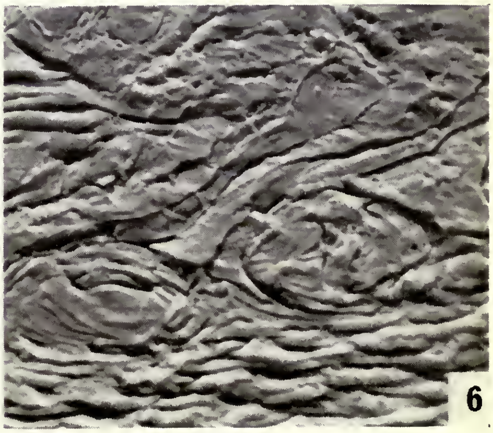
6

PLATE 32

Thecospira sp.

Scanning electron micrograph montage of the spiralium of a specimen from the Triassic (St Cassian beds), Alpe de Specie (formerly Seelandalpe), 2·5 km NW of Carbonin (formerly Schluderbach), 11 km NE of Corvara d'Ampezzo, Trentino, Italy. Transverse section through a spiral lamella showing the general U-shaped profile. Longer, dorsal limb to left, shorter ventral limb to right. BB 59006. × 300. (p. 251)

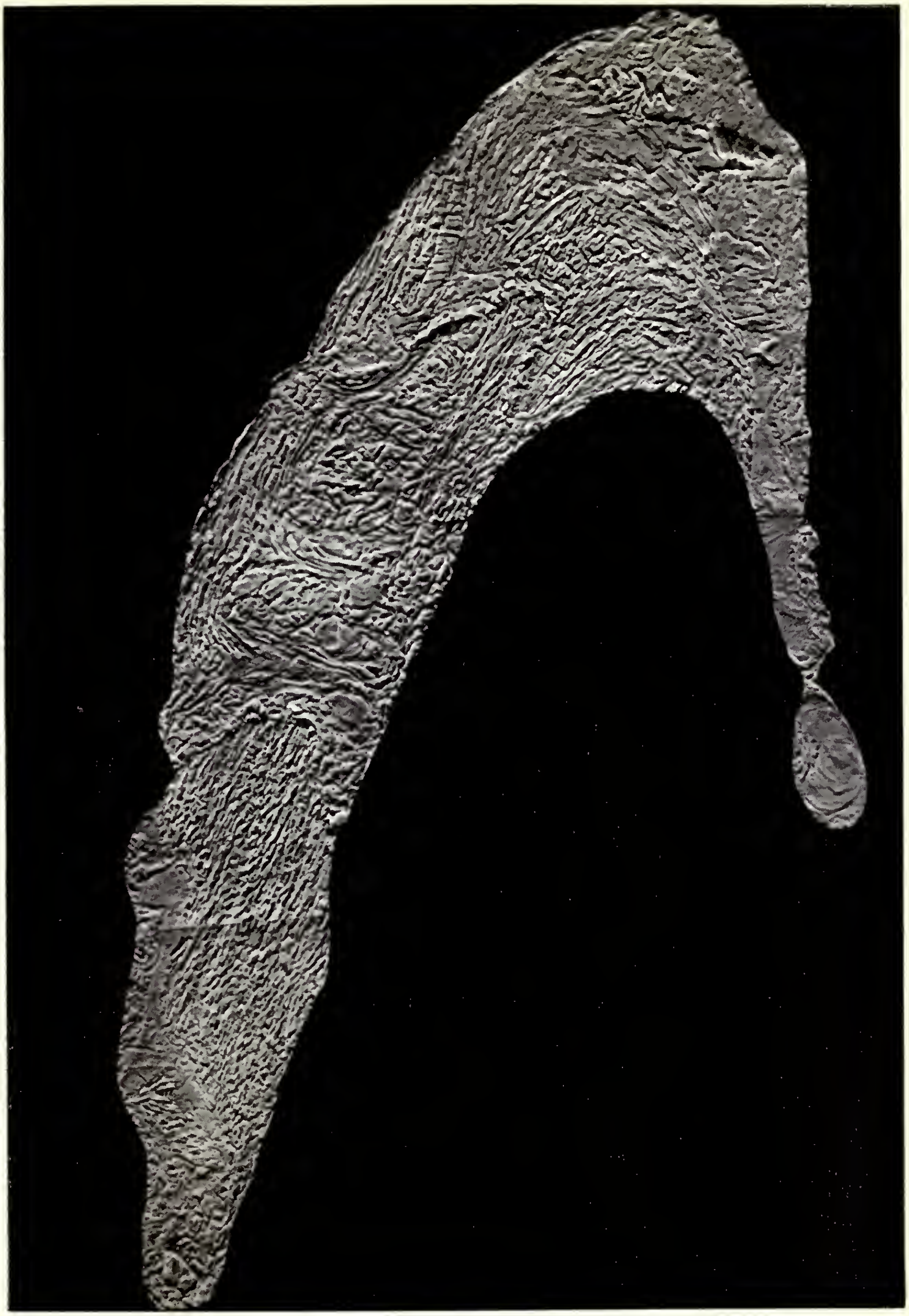

A LIST OF SUPPLEMENTS TO THE GEOLOGICAL SERIES OF THE BULLETIN OF THE BRITISH MUSEUM (NATURAL HISTORY)

---

1. Cox, L. R. Jurassic Bivalvia and Gastropoda from Tanganyika and Kenya. Pp. 213; 30 Plates; 2 Text-figures. 1965. £6.
2. El-Naggar, Z. R. Stratigraphy and Planktonic Foraminifera of the Upper Cretaceous—Lower Tertiary Succession in the Esna-Idfu Region, Nile Valley, Egypt, U.A.R. Pp. 291; 23 Plates; 18 Text-figures. 1966. £10.
3. Davey, R. J., Downie, C., Sargeant, W. A. S. & Williams, G. L. Studies on Mesozoic and Cainozoic Dinoflagellate Cysts. Pp. 248; 28 Plates; 64 Text-figures. 1966. £7.
3. Appendix. Davey, R. J., Downie, C., Sargeant, W. A. S. & Williams, G. L. Appendix to Studies on Mesozoic and Cainozoic Dinoflagellate Cysts. Pp. 24. 1969. 80p.
4. Elliott, G. F. Permian to Palaeocene Calcareous Algae (Dasycladaceae) of the Middle East. Pp. 111; 24 Plates; 17 Text-figures. 1968. £5.12½.
5. Rhodes, F. H. T., Austin, R. L. & Druce, E. C. British Avonian (Carboniferous) Conodont faunas, and their value in local and continental correlation. Pp. 315; 31 Plates; 92 Text-figures. 1969. £11.
6. Childs, A. Upper Jurassic Rhynchonellid Brachiopods from Northwestern Europe. Pp. 119; 12 Plates; 40 Text-figures. 1969. £4.75.
7. Goody, P. C. The relationships of certain Upper Cretaceous Teleosts with special reference to the Myctophoids. Pp. 255; 102 Text-figures. 1969. £6.50.
8. Owen, H. G. Middle Albian Stratigraphy in the Anglo-Paris Basin. Pp. 164; 3 Plates; 52 Text-figures. 1971. £6.
9. Siddiqui, Q. A. Early Tertiary Ostracoda of the family Trachyleberididae from West Pakistan. Pp. 98; 42 Plates; 7 Text-figures. 1971. £8.
10. Forey, P. L. A revision of the elopiform fishes, fossil and recent. Pp. 222; 92 Text-figures. 1973. £9.45.
11. Williams, A. Ordovician Brachiopoda from the Shelve District, Shropshire. 28 Plates. *In press*, expected 1974.

Printed in Great Britain by John Wright and Sons Ltd. at The Stonebridge Press, Bristol BS4 5NU

GENERAL
LIBRARY

CRETACEOUS FAUNAS FROM ZULULAND AND NATAL, SOUTH AFRICA

INTRODUCTION, STRATIGRAPHY

W. J. KENNEDY
AND
H. C. KLINGER

BULLETIN OF
THE BRITISH MUSEUM (NATURAL HISTORY)
GEOLOGY Vol. 25 No. 4
LONDON: 1975

BRITISH MUSEUM
GENERAL
28 JAN 1975
LIBRARY
NATURAL HISTORY

CRETACEOUS FAUNAS FROM ZULULAND AND NATAL, SOUTH AFRICA

INTRODUCTION, STRATIGRAPHY

BY
WILLIAM JAMES KENNEDY
AND
HERBERT CHRISTIAN KLINGER

Pp. 263–315 ; 1 *Plate* ; 12 *Text-figures*

BULLETIN OF
THE BRITISH MUSEUM (NATURAL HISTORY)
GEOLOGY Vol. 25 No. 4
LONDON: 1975

THE BULLETIN OF THE BRITISH MUSEUM (NATURAL HISTORY), *instituted in* 1949, *is issued in five series corresponding to the Departments of the Museum, and an Historical series.*

Parts will appear at irregular intervals as they become ready. Volumes will contain about three or four hundred pages, and will not necessarily be completed within one calendar year.

In 1965 *a separate supplementary series of longer papers was instituted, numbered serially for each Department.*

This paper is Vol. 25, *No.* 4 *of the Geological (Palaeontological) series. The abbreviated titles of periodicals cited follow those of the World List of Scientific Periodicals.*

World List abbreviation :
Bull. Br. Mus. nat. Hist. (Geol.)

© Trustees of the British Museum (Natural History), 1975

TRUSTEES OF
THE BRITISH MUSEUM (NATURAL HISTORY)

Issued 3 *January* 1975 *Price* £3·75

CRETACEOUS FAUNAS FROM ZULULAND AND NATAL, SOUTH AFRICA

INTRODUCTION, STRATIGRAPHY

By WILLIAM J. KENNEDY AND HERBERT C. KLINGER

CONTENTS

		Page
I.	Introduction	266
II.	Place names	267
III.	Stratigraphic synthesis	267
IV.	History of research	269
V.	Stratigraphic nomenclature	272
VI.	Stage limits and subdivisions	273
	Barremian	273
	Aptian	274
	Albian	275
	Cenomanian	276
	Turonian	277
	Coniacian	278
	Santonian	279
	Campanian	280
	Maastrichtian	281
VII.	Locality details	281
	A. Pondoland	281
	B. Durban	282
	C. Kwa-Mbonambi, Zululand	282
	D. Mfolozi and Umkwelane Hill, Zululand	282
	E. The Nyalazi River, south of Hluhluwe, Zululand	283
	F. Glenpark Estate, Zululand	284
	G. The Mzinene River and its tributaries, Zululand	285
	(i) Upper reaches	285
	(ii) The Skoenberg region	288
	(iii) Sections along the Munywana	289
	(iv) Lower reaches	292
	H. Sections around False Bay and Lake St Lucia, Zululand	292
	(i) Western False Bay	292
	(ii) The Hluhluwe flood plain	294
	(a) Western side	294
	(b) Eastern side	295
	(iii) False Bay: SE shores	295
	(iv) The Nibela Peninsula	296
	(v) The Southern Peninsula	296
	(vi) Lake St Lucia	298
	J. The Mkuze River and its tributaries	298
	(i) Southern part of Mkuze Game Reserve	299
	(ii) The Morrisvale Area	299
	(iii) Mantuma Rest Camp Area	300

K. NORTHERN ZULULAND 300
(i) Mayezela Spruit 301
(ii) Mfongosi Spruit 301
(iii) Mlambongwenya Spruit 302
(iv) Ndumu 302
VIII. DISCUSSION 304
IX. ACKNOWLEDGEMENTS 306
X. REFERENCES 306
XI. INDEX 312

SYNOPSIS

Cretaceous sediments outcrop in two main areas in eastern South Africa, north of Durban, from the Mfolozi River to the Mozambique border, and to the south, between the Itongazi and Mpenjati Rivers.

The term *Zululand Group* is proposed for the succession in the northern area, subdivided into : (1) The Makatini Formation (Upper Barremian to Aptian) ; (2) The Mzinene Formation (Albian to Cenomanian) ; (3) The St Lucia Formation (Coniacian to Maastrichtian). The term 'Umzamba Formation' is retained for the Coniacian to Campanian sequences south of Durban.

Sedimentation began in Lower Cretaceous (pre-Upper Barremian) times, with deposition of piedmont fan and fluviatile sands and conglomerates in northern Zululand. Transgression, beginning during the Upper Barremian, extended through at least into Albian, and probably Cenomanian, times, depositing first sands and conglomerates, followed by glauconitic silts. During late Cenomanian or early Turonian times, regression was under way, accompanied by widespread penecontemporaneous erosion. The highest Cenomanian and all the Turonian are thus absent on land. Renewed transgression during the early Coniacian extended through into at least the Campanian, and the base of the Senonian is diachronous. In northern Zululand, Coniacian silts rest on lithologically similar Upper Cenomanian deposits. Along the Mfolozi River, slightly higher horizons in the Coniacian rest first on Lower Cretaceous conglomerates and, to the south, overstep onto Stormberg Basalts and Basement rocks. South of Durban, yet higher horizons in the Coniacian rest on formations down to the Table Mountain Sandstone.

Preliminary work on the ammonite faunas allows subdivision of the Barremian to Lower Maastrichtian stages into 31 widely recognizable units and points to the development of a refined biostratigraphy when systematic work is complete. Apart from ammonites, the Cretaceous sequences described yield a rich fauna. Bivalves, gastropods and nautiloids are abundant, with scarcer echinoids, brachiopods, bryozoans and corals. Locality details of 185 sections in the area are given as a basis for subsequent taxonomic work.

I. INTRODUCTION

DURING the summers of 1970–71 we collected from and measured the sections at over 150 localities in the Cretaceous successions of Zululand, Natal, and the Northern Transkei. Many of the fossils collected have been added to the collections of the British Museum (Natural History), which already contain classic South African material described by Daniel Sharpe, G. C. Crick, R. B. Newton, R. Etheridge, L. F. Spath and others, examined by us.

In addition, we have studied important collections in the Geological Survey of South Africa at Pretoria, including material collected by one of us (H. C. K.), by E. C. N. van Hoepen, S. H. Haughton and others. We have also been able to study the collections of the Transvaal Museum, the National Museum Bloemfontein, the South African Museum, Cape Town, the Durban Museum, and the University Collections at Durban and Pretoria.

The present publication is the first of a series in which we intend to describe the invertebrate faunas collected in this region. This work will need many years of study, for the South African Cretaceous yields diverse faunas which, in spite of an extensive literature (Haughton, 1959, provides the most complete bibliography), remain largely unknown in contemporary terms, whilst an acceptable stratigraphic framework is still lacking. Detailed biostratigraphy must await the results of further research, as must palaeoecological and palaeoenvironmental syntheses ; we present here an outline of the geological history of the area, a provisional biostratigraphy upon which to base our systematic work, and locality information of relevant sections.

II. PLACE NAMES

Over most of the area described in this paper, place names are taken from the Second Edition of the 1 : 50 000 and the 1 : 250 000 topographic maps of South Africa. Standardization of spelling of Zulu names leads to the alteration of the names of many classic localities. Thus the Umsinene becomes the Mzinene, Manuan becomes Munywana, and so on.

III. STRATIGRAPHIC SYNTHESIS

Cretaceous sediments outcrop in two main areas in eastern South Africa (Fig. 1) ; in Zululand, from the Mozambique border south to Umkwelane Hill on the Mfolozi River, and south of Durban, as reefs exposed only at low tide as between the Itongazi and Mpenjati Rivers, or in low cliffs, as at the mouth of the Umzamba River. There are small but important outcrops at Enseleni Reserve, and subsurface Cretaceous is recorded at Durban and Richards Bay.

Exposures are poor in the region studied, whilst dips are low and difficult to measure. The probable thickness of the Cretaceous in the St Lucia area is of the order of 1000 m, but the sequence quite clearly thickens northwards and eastwards, suggesting the presence of a substantial wedge of sediment out to sea.

In northern Zululand, coarse clastic pre-Upper Barremian fluviatile Cretaceous sediments rest on Jurassic Lebombo Volcanics. The lowest marine horizons known consist of Upper Barremian silts, sandstones and conglomerates. The succeeding Aptian has a similar facies, and in the area around Hluhluwe, this too rests on the Lebombos. The Albian/Aptian boundary is an important non-sequence marked by a horizon of hiatus concretions (Kennedy & Klinger 1972) which can be traced for 175 km, from Ndumu to 12 km north of Mtubatuba. Lowermost Albian sediments seem to be wholly absent in Zululand. Locally, the Albian may overlap onto Lebombo Volcanics. In general, however, the Albian forms an expanded sequence of shallow marine silts and sands, sometimes glauconitic, with shelly concretionary

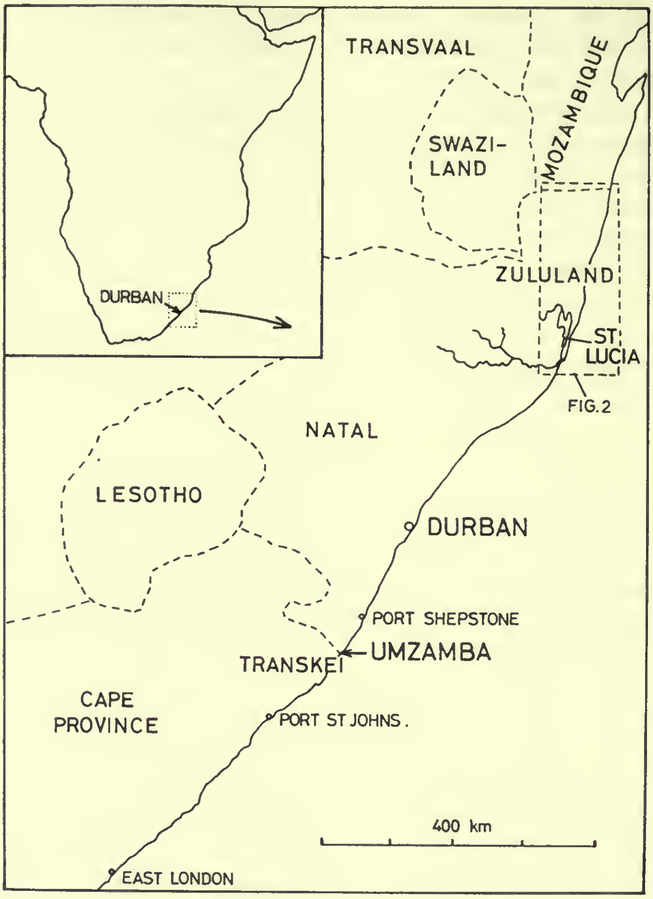
TRANSVAAL
MOZAMBIQUE
SWAZI-LAND
ZULULAND
ST LUCIA
FIG. 2
DURBAN
NATAL
LESOTHO
DURBAN
PORT SHEPSTONE
UMZAMBA
TRANSKEI
CAPE PROVINCE
PORT ST JOHNS.
400 km
EAST LONDON

FIG. 1. Locations of the areas studied.

horizons and small-scale sedimentary cycles. Locally a more marginal basal conglomeratic facies may be developed. Horizons up to and including the *Stoliczkaia dispar* Zone have been recognized, followed by a conformable Lower, Middle and Upper Cenomanian sequence, again in a silty glauconitic facies, and with a rich marine fauna.

Turonian rocks are absent on land in Zululand, and along the Mzinene River a Coniacian basal conglomerate rests on Cenomanian silts, with a horizon of hiatus concretions at the contact (Kennedy & Klinger 1972). Along the Mzinene, Hluhluwe and Nyalazi Rivers, around False Bay and Lake St Lucia, a succession from Coniacian through to Lower Maastrichtian can be traced; the sequence is, throughout, one of shelly, sometimes glauconitic, silts, with concretionary horizons.

The next extensive outcrops of Cretaceous sediments appear along the Mfolozi River and at Umkwelane Hill (Fig. 1). At Riverview, Lower Coniacian sediments rest on Lower Cretaceous non-marine fluviatile conglomerates, and to the south, at

Umkwelane Hill, overstep onto Stormberg Basalts and granitic basement rocks within a distance of only a few kilometres. The basal Coniacian is a thin conglomerate; fossils from just above the base of the sequence at Umkwelane Hill suggest a horizon higher than that seen in the basal Coniacian along the Mzinene. Above, there is a succession of silts and shelly limestones extending up to the Lower Campanian. Probable Upper Campanian silts occur to the east, and around Monzi horizons up to the Lower Maastrichtian are present.

Cretaceous silts and shell beds are known beneath Durban, and sparse faunas indicate the presence of horizons in the Campanian and high in the Santonian. South of Durban, the deposits of the Upper Cretaceous transgression rest on horizons down to the Table Mountain Sandstone. The age of these, the Umzamba Beds, has long been disputed (p. 270), but a high Coniacian (?) to Campanian age seems most likely.

Available evidence thus indicates that sedimentation began in Lower Cretaceous (pre-Upper Barremian) times, with deposition of piedmont fan and fluviatile sands and conglomerates. Transgression, beginning during the Upper Barremian, extended through at least into Albian, and probably Cenomanian, times, but during late Cenomanian or early Turonian times regression was under way, accompanied by widespread penecontemporaneous erosion. Renewed transgression during the early Coniacian extended through into the Campanian at least, and the base of the Senonian is diachronous from Zululand, 600 km to the south, into the Northern Transkei.

IV. HISTORY OF RESEARCH

The Cretaceous rocks of eastern South Africa were first discovered by H. F. Fynn in 1824, although they were not described until three decades later. Thus Captain R. J. Garden (1855 : 453–454) gave as graphic and accurate a picture of the Umzamba Beds as any during the following century:

> '. . . the lowest rock visible is a hard shelly rock with pebbles; above it is a brownish-red sandstone, traversed in every direction by white veins, which are the broken edges of colossal bivalve shells (*Inoceramus*). The shells are thin, and too easily broken to be extracted from the rock . . . alternate layers of the above mentioned two rocks occur to the height of about eighteen feet, above which are hard bluish-black, brown and greenish argillaceous and sandy beds. Shells were found in all these clay beds, and Ammonites at different heights, and in certain of the strata . . . Fossil trees are seen at low water on a reef of flat rocks (nearby).'

The fossils collected by Garden were described by W. H. Bailey in the succeeding pages of the *Quarterly Journal of the Geological Society of London.*

This section passed into the literature as the Umtamvuna or Umtamfuna Cretaceous (Tate 1867, Griesbach 1871, Gottsche 1887, Etheridge 1904, Crick 1907b, 1907d, and others), on the basis of the misconception that they outcrop at the mouth of the Umtamvuna River, although Griesbach (1871) refers to them as the Izindhluzabalungu Deposits. Latterly, they have become known as the Umzamba Beds, and in addition to the type section, outcrops have been described at several localities along the coast of southern Natal (Pondoland), in particular between the Itongazi and Umkandandhlouvu Rivers (Griesbach 1871, Rogers & Schwartz 1901, 1902, Crick 1907b, Plows 1921, Gevers & Little 1956, du Toit 1920, 1954, Haughton 1969). The most satisfactory description of the type section is that of Plows (1921). Faunas and floras have been described by Griesbach (1871), Chapman (1904, 1923), Lang (1906), Woods (1906), Rennie (1930, 1935), Spath (1921b, 1922a), van Hoepen (1920, 1921, 1966a), Broom (1907), Crick (1907b), Little (1957), Smitter (1956), Mandel (1960), Muller-Stoll & Mandel (1962), and Dingle (1969).

The age suggested for the Umzamba Beds has varied from Albian or Cenomanian to Maastrichtian, and the view long accepted that but a single faunal horizon is represented (Woods 1906, Rennie 1930, du Toit 1954). The most recent appraisal of the ammonites by Spath (1953) led him to suggest a Campanian to Lower Maastrichtian age for the fauna, and the latest microfaunal study led Dingle (1969) to a similar conclusion.

In fact, the base of the Umzamba Beds in the type section has yielded a Coniacian collignoniceratid: *Subprionotropis cricki* (Spath) (= *Barroisiceras umzambiensis* van Hoepen), whilst inoceramids and ammonites from higher in the section are of Santonian/Campanian age. There is no evidence for the Lower Maastrichtian. The outcrops between the Itongazi and Mpenjati Rivers yield Santonian inoceramids and ammonites.

The presence of Cretaceous rocks beneath Durban was first noted by Anderson (1906 : 48), whilst faunas have been recorded by Krige (1932) and King & Maud (1964), all of whom equate the sequence with the Umzamba Beds. Material from recent excavations indicate the presence of horizons within both the Santonian and the Campanian stages.

North of Durban, Cretaceous sediments in the Lake St Lucia region were first recorded by Griesbach (1871). The principal work in this area was, however, by William Anderson, the one-man Geological Survey of Zululand and Natal. Anderson noted possible subsurface Cretaceous occurrences in the region of what he called the Umlatuzi Lagoon, and described important sections in two areas: along the Mfolozi River and Umkwelane Hill, and along the Mzinene River and its tributaries. He also noted the occurrence of Cretaceous deposits as far north as the junction of the Ingwavuma and Pongola Rivers (1907 : 60–61), whilst Kilian had recorded Aptian sediments across the border in southern Mozambique a few years previously (Kilian 1902a–c; see also Krenkel 1910a–c, 1911a–b).

Faunas from Umkwelane Hill were described by Etheridge (1904), who compared them with those of the Umzamba Beds of Pondoland (see also Woods 1906 : 337) and the Arialoor and Trichinopoly Groups of Southern India (then regarded as Turonian and Senonian respectively). Crick (1907a : 228) recorded a further ammonite, *Mortoniceras umkwelanense* Crick, and confirmed an Upper Cretaceous age for the deposits; additional fossils were recorded by R. B. Newton in 1909. No further work was published until Spath (1921a) described a large collection of ammonites made by A. L. du Toit from exposures at and near Umkwelane Hill. On the basis of this material Spath identified the Campanian and Maastrichtian stages as being present in the area. This region was visited during excursion C18 of the 1929

International Geological Congress (du Toit & van Hoepen 1929), and a series of papers describing and discussing the region resulted (Heinz 1930, Besaire 1930, Venzo 1936, Dietrich 1938, Socin 1939, Montanaro & Lang 1937).

Heinz, Besaire and van Hoepen all claimed to recognize Turonian rocks at the base of the sequence, followed by horizons from Coniacian through to Campanian. Rennie (1930) returned to the view that the sequence was equivalent to the Umzamba Beds, accounting for peculiarities in ammonite fauna on the basis of facies differences. Du Toit (1954) suggested a Lower Santonian age for the sequence, whilst Frankel suggested Coniacian to Upper Santonian or Campanian. Our own collecting indicates that horizons from Lower Coniacian to well up into the Campanian are represented, and that Upper Campanian and Maastrichtian sediments are present to the east, beneath the Tertiary and Recent deposits around Monzi.

Early work on the Lake St Lucia and Mzinene region centre around collections made by Anderson (1902–07) and their description by Etheridge (1907) and Crick (1907a, c). Etheridge gave no date to the material he described (although it is undoubtedly an Albian assemblage), but Crick recognized a Cenomanian fauna from the 'north end of False Bay' (later corrected to the junction of the Munywana and Mzinene Rivers), and recorded Upper Albian and Senonian fossils from the Munywana. Spath (1921a) added further records and in addition recognized supposed Coniacian and Campanian forms.

Van Hoepen (1926–66) described a vast number of ammonite species from this part of Zululand, suggested a classification of the succession, and recognized Aptian to Maastrichtian stages, as discussed below (p. 272). His basic views were supported in publications resulting from the 1929 Congress visit (Besaire 1930, Besaire & Lambert 1930, Heinz 1930, Venzo 1936, Socin 1939, Montanaro & Lang 1939). Van Hoepen's systematic work (1929 onwards) suffers from extensive splitting, and the majority of his taxa are synonyms of well-established classic genera and species (see, for instance, Haas 1942, Wright 1957).

Since van Hoepen's work, little has been published. Muir-Wood (1953) described a single brachiopod from the Mzinene whilst Foraminiferida are noted by Smitter (1957). As already described (Kennedy & Klinger 1971 ; see also p. 268 above), the section in this area is in fact incomplete, and the supposed Maastrichtian of van Hoepen and others is high Campanian.

North of the Mzinene, supposed Turonian sediments were described by van Hoepen *in* du Toit & van Hoepen (1929) from close to the junction of the Mkuze and Msunduzi Rivers, and apparently accepted as such by many other workers (e.g. Besaire 1930, Venzo 1936, Furon 1950, 1963). These beds, said to be characterized by large oysters, are of a Coniacian age, the oysters coming from the overlying Tertiary. Still further north, there are excellent accounts of sections along streams draining east from the Lebombos to the Pongola River by Haughton (1936a) and Boshoff (1945), and some molluscs from the area were described by Rennie (1936). Unfortunately, the rich ammonite faunas (Haughton 1936b, Spath 1953) were never described, although horizons from Upper Aptian to Upper Albian were recognized. Some additional information is provided by Spath (1925), Dietrich (1938), and Haughton (1969).

No horizons higher than the Lower Cenomanian are exposed at the surface in this northernmost part of Zululand, for east of the Pongola the country is a wilderness of drifted sand. Davey (1969) and Pienaar (1969) have, however, described Campanian to Palaeocene microfloras from a deep borehole in the Lake Sibayi region.

V. STRATIGRAPHIC NOMENCLATURE

Present nomenclature of the Cretaceous deposits of Zululand and Natal is in a far from satisfactory state. The term 'Umzamba Beds' is used for the Santonian and Campanian strata of Southern Natal, whilst to the north, the following terms have been used in the Mzinene–St Lucia region by van Hoepen (1926, 1929) and others :

Umzamba Beds	Upper Senonian
Itweba Beds	Middle Senonian
Peroniceras Beds	Lower Senonian
Munyuana Beds	Turonian
Skoenberg Beds	Cenomanian
Umsinene Beds	Albian
Ndabana Beds	Aptian/Albian

These divisons are variously described as 'Beds' or 'Zones' and it is quite clear from van Hoepen's original accounts (1926, 1929) that they are based upon faunal differences, and that, apart from the conglomerate and sandstone units of the Ndabana Beds and the sandy base of the Umsinene Beds, the sequence is of a uniform silt facies.

These divisions are thus neither wholly lithostratigraphic nor biostratigraphic units, nor are they precisely defined in terms of faunas or lithology. We see no need for a local biostratigraphic system, for the internationally recognized stages of the Cretaceous can be recognized in South Africa. We therefore propose the *lithostratigraphic* terminology outlined in Table 1.

TABLE 1

Lithostratigraphic and biostratigraphic subdivisions of the Zululand Cretaceous

VAN HOEPEN (1926, 1929)		KENNEDY & KLINGER (herein)	STAGES
Umzamba Beds Itweba Beds *Peroniceras* Beds Munyuana Beds	Zululand Group	St Lucia Formation	Lower Maastrichtian Campanian Santonian Coniacian
Skoenberg Beds Umsinene Beds		Mzinene Formation	Cenomanian Albian
Ndabana Beds		Makatini Formation	Aptian Upper Barremian
			(pre-Upper Barremian ?)

We further propose that the Cretaceous sediments developed in Zululand be termed the *Zululand Group*, and that the term 'Umzamba Formation' be retained for the Upper Cretaceous deposits of Pondoland.

Definitions of these lithostratigraphic units are as follows :

Zululand Group

1. *The Makatini Formation.* The type section extends along the Mfongosi Spruit, in northern Zululand, from where the base of the formation rests on Lebombo Volcanics to Loc. 169, 27° 21′ 38″ S, 32° 09′ 57″ E. The succession consists of sandstones, siltstones and conglomerates, with marine Upper Aptian fossils. Details of localities are given on pp. 301–302. To the north, along the Mlambongwenja, the same formation yields Upper Barremian and Aptian marine faunas.

2. *The Mzinene Formation.* The type section extends along the Mzinene River from Loc. 51, 27° 53′ 43″ S, 32° 19′ 22″ E, to Loc. 60, 27° 52′ 45″ S, 32° 20′ 55″ E. The base of the formation is taken at the minor non-sequence and bored concretion bed which separates the Aptian and Albian stages. A complete succession up to and including the lower part of the Upper Cenomanian is represented in this formation, which consists largely of silts with shelly and concretionary horizons. Details of localities are given on p. 288.

3. *The St Lucia Formation* has as its type locality river bank sections along the Mzinene from Loc. 60, 27° 52′ 45″ S, 32° 20′ 55″ E, to its entry into False Bay, and the cliff and foreshore sections around False Bay and Lake St Lucia. The base of the formation is taken at the base of the Coniacian conglomerate exposed at Loc. 60 on the Mzinene (p. 288) : locality details are given on pp. 288–298. The succession consists predominantly of siltstones, with concretionary and shelly horizons. The base of the formation is of Lower Coniacian age ; the highest horizons exposed at the surface yield Lower Maastrichtian ammonites and inoceramid bivalves.

The *Umzamba Formation* has as its type section the cliffs and foreshore exposures north of the mouth of the Umzamba River, 31° 06′ S, 30° 10′ E approximately. The type section ranges in age from high Coniacian to Campanian.

VI. STAGE LIMITS AND SUBDIVISIONS

All the stages of the Cretaceous present problems of definition, and almost without exception international usage is highly variable. For clarity, we outline here our working definitions of the Barremian to Maastrichtian stages. Since correlation with the European type areas is still not fully possible, and because the European stratotypes still present problems of interpretation, these are 'local' definitions only. We also present our working subdivisions of the stages, although again it must be stressed that all our systematic determinations are provisional. A far more detailed biostratigraphic system will be available when our taxonomic work is complete.

Barremian

'L'étage Barrémien' was introduced by Coquand in 1862. The type area for the stage is the environs of Barrême, near Digne, Basses-Alpes, France. Busnardo

(1965a) has designated the Angles section close by as stratotype : recent discussions of the stage in its type area are given by Sornay (1957), Busnardo (1965a, b), Guillame & Sigal (1965), Bouché (1965) and Fauré (1965) ; an English summary is given by Middlemiss & Moullade (1970 : 352–354).

We have recognized only Upper Barremian faunas in Zululand, so that the vexing problem of the base of the stage and the position of the *Pseudothurmannia anguli-costata* Zone is not relevant here. The Mesogean aspect of much of the fauna of the type Barremian makes direct correlation with our sequence difficult. More relevant is the work of Druzhchitz (1963a, b) on the revision of the Barremian sequence in Georgia, Dagestan and the Northern Caucasus, which clearly demonstrates the uppermost Barremian age of the classic 'Aptian' *Colchidites* faunas of the region described by Rouchadzé (1932), Eristavi (1955), Rengarten (1926) and others. These faunas closely resemble our Zululand material and are the basis for recognition of the Upper Barremian.

Barremian I

Characterized by an abundance of crioceratitids, including a variety of '*Emericiceras*' and '*Acrioceras*'-like forms, hemihoplitids, *Heteroceras*, abundant juvenile aconeceratids, together with large *Sanmartinoceras*-like body chambers, *Phylloceras serum* (Oppel), *Eulytoceras phestum* (Matheron) and occasional *Colchidites*.

Barremian II

Characterized by the occurrence of *Colchidites* (*Colchidites*) in vast numbers, with juvenile aconeceratids locally common. The only other forms recorded are occasional *Sanmartinoceras*, *Phylloceras*, crioceratid-like fragments and indeterminate ancyloceratids.

APTIAN

'L'étage Aptien' was first used by d'Orbigny in 1840 ; the type locality of the stage is around Apt, Vaucluse, in southern France. Sornay (1957) reviews early usage of the name ; the succession in the type area and adjoining regions is discussed by Taxy *et al.* (1965), Moullade (1965a, b) and Flandrin (1965). The most complete review of Aptian biostratigraphy is given by Casey (1961). The classic definition of the Aptian/Barremian boundary is at the appearance of primitive deshayesitids, *Pseudohaploceras matheroni* (d'Orbigny) and *Procheloniceras albrechti-austriae* (Hoehnneger *in* Uhlig). Of these forms, only early cheloniceratids are known from Zululand, and we have drawn the base of the Aptian below their first occurrence. Subdivisions of the stage are as follows :

Aptian I

Juvenile cheloniceratids, tentatively referred to *Procheloniceras*, are abundant. The only other ammonites known are *Tropaeum* sp., *Ancyloceras* sp. and other ancyloceratid fragments.

Aptian II

Cheloniceras s.s. becomes frequent, and includes forms resembling *Cheloniceras gottschei* (Krenkel) and *C.* aff. *proteus* Casey, together with larger specimens having *Procheloniceras*-like outer whorls. A desmoceratid (*Valdedorsella* or *Pseudohaploceras*) is not uncommon, as are large, poorly preserved ancyloceratids, e.g. *Ancyloceras, Tropaeum* and *Australiceras.*

Above this level there may be a non-sequence.

Aptian III

Characterized by an abundance of diverse *Acanthoplites* species, *Diadochoceras* ?, *Valdedorsella, Phylloceras,* diverse small heteromorphs including *Ancyloceras, Protanisoceras*-like and *Tonohamites*-like forms, and *Lytoceras.*

Aptian IV

Characterized by an abundance of giant *Tropaeum,* especially finely-ribbed forms. Large '*Lytoceras*' are common, together with *Tonohamites,* giant *Acanthoplites, Diadochoceras nodostocatum* (d'Orbigny) and related forms.

ALBIAN

'L'étage Albien' was introduced by d'Orbigny in 1842. The type area of the stage is Aube, Roman Alba, in southern France. Sornay has reviewed previous usage and interpretation of the stage (1957), whilst Lower Albian stratigraphy is revised by Casey (1961), the Middle Albian reviewed by Owen (1971) and sections in the type area and adjacent regions described by Larcher *et al.* (1965), Destombes & Destombes (1965), Marie (1965) and Collignon (1965).

The subdivision of much of the type Albian is based upon the typically boreal hoplitids, which did not range into southern Africa, and as a result correlation with Europe, especially during the Middle Albian, is difficult. We follow Breistroffer (1947) and Casey (1961) in placing the 'Clansayes' horizon in the Aptian, taking the base of the Albian as the base of the European *Leymeriella tardefurcata* Zone. In Zululand, as in Madagascar (Collignon 1965), this basal part of the Albian is missing, and the Aptian/Albian boundary is a non-sequence (Kennedy & Klinger 1972), the local base of the Albian being marked by the abundance of *Douvilleiceras.* Subdivisions of the stage are as follows :

Albian I – absent

Albian II

Abundant *Douvilleiceras,* including forms close to *D. orbignyi* Spath, *D. mammillatum* (Schlotheim) and varieties. Other ammonites are scarce, but include poorly preserved desmoceratids and lytoceratids.

Albian III

Douvilleiceras is abundant, but in contrast to Albian II, diverse other ammonites occur. A *Damesites* ? sp. nov. is common, whilst *Lyelliceras* species, including *L. lyelli* (d'Orbigny) and *L. pseudolyelli* (Parona & Bonarelli) are frequent, together with *'Neosilesites'*, *Phylloceras* (*Hypophylloceras*), *'Beaudanticeras'*, *'Cleoniceras'* and *'Sonneratia'* species, *Rossalites*, *Ammonoceratites*, abundant *Anagaudryceras sacya* (Forbes), *Eubrancoceras* aff. *aegoceratoides* (Steinmann) and *Oxytropidoceras* species.

Albian IV

Oxytropidoceras is common, including subgenera *O.* (*Oxytropidoceras*), *O.* (*Manuaniceras* and *O.* (*Androiavites*). Other ammonites include *Pseudhelicoceras*, *Mojsisovicsia*, *Phylloceras* (*Hypophylloceras*) *velledae* (Michelin) and desmoceratids.

Albian V

Characterized by the abundance of mortoniceratids, and the bulk of the faunas described by van Hoepen for his Umsinene Beds come from this broad division. Genera present are : *Hysteroceras* (including *Askoloboceras*, *Komeceras*, *Petinoceras* and *Terasceras* van Hoepen), *Oxytropidoceras* (including *Lophoceras* van Hoepen), *O.* (*Tarfayites*), *D.* (*Dipoloceras*) (including *Rhytidoceras*, *Cechenoceras*, *Ricnoceras* and *Euspectoceras* van Hoepen), *D.* (*Diplasioceras*), *M.* (*Mortoniceras*), *M.* (*Deiradoceras*), *Erioliceras*, *Arestoceras*, *Cainoceras*, *Puzosia*, *Bhimaites*, *Desmoceras*, *P.* (*Hypophylloceras*), *Anagaudryceras*, *Gaudryceras*, *Tetragonites*, *Hamites*, *Anisoceras*, *Labeceras* and *Myloceras*.

Albian VI

Characterized by the appearance of *Mortoniceras* (*Durnovarites*) species, together with *Stoliczkaia* species including *S. africana* (Pervinquière), *S. notha* (Seeley) and *S. dorsetensis* (Spath), together with abundant *Idiohamites*, *Hamites* and *Anisoceras* species, with scarcer *Lechites*, *Mariella*, *Hypengonoceras* and puzosiids.

Cenomanian

'L'étage Cenomanien' was introduced by d'Orbigny (1847, 1850, 1852) with the environs of Le Mans, Roman Cenomanum, as the type area. Sornay (1957) has reviewed the history of various usages of the term whilst Hancock (1959) lists the ammonite faunas of the type area and other localities in Sarthe. Kennedy & Hancock (1971) have discussed the problem of the supposed *martimpreyi* Zone at the base of the stage, whilst the higher parts of the stage are discussed by Juignet *et al.* (1973).

The base of the Cenomanian is drawn at the base of the classic *Mantelliceras mantelli* Zone of Hancock (1959), Kennedy (1969–71) and others. It is marked by the diversification of the Mantelliceratinae ; genera such as *Mantelliceras*, *Sharpeiceras*, *Graysonites*, *Utaturiceras* and *Acompsoceras* appear, as does *Hypoturrilites*, whilst *Schloenbachia* becomes abundant in the Boreal Realm. In South Africa, we draw the base of the stage at the incoming of abundant *Sharpeiceras* and *Mariella oehlerti* (Pervinquière). Subdivisions of the stage are as follows :

Cenomanian I

Characterized by abundant *Sharpeiceras* especially *S. florencae* Spath and *S. falloti* (Collignon), abundant *Mariella oehlerti*, together with scarcer *Desmoceras latidorsatum* (Michelin), *Sciponoceras roto* Cieśliński, *S.* (*Scaphites*) cf. *simplex* Jukes-Browne ?, *Mariella, Ostlingoceras, Hypoturrilites* and *Mantelliceras.*

Cenomanian II

Characterized by a rather more diverse assemblage, *Ostlingoceras rorayensis* (Collignon) is common with *Hypoturrilites carcitanensis* (Matheron), *H. gravesianus* (d'Orbigny), *H. tuberculatus* (Bosc), *H. nodiferus* (Crick), *Mariella* spp., *Sciponoceras roto* Cieśliński, *Scaphites* sp., *Desmoceras latidorsatum, Tetragonites subtimotheanus* Wiedmann, *Forbesiceras largilliertianum* (d'Orbigny), *Sharpeiceras laticlavium* (Sharpe) and *Mantelliceras* spp. including *M. spissum* Collignon, *M.* group of *cantianum* Spath, *M. patens* Collignon, *M. indianense* Hyatt and a number of desmoceratids.

Cenomanian III

Turrilites acutus Passy is abundant, with scarcer *T. costatus* Lamarck and *T. scheuchzerianus* Bosc. Abundant *Acanthoceras* spp., including the forms described by Crick (1907a) as *A. flexuosum* Crick, *A. crassiornatum* Crick, *A. munitum* Crick, *A. robustum* Crick, *A. quadratum* Crick, *A. hippocastanum* Crick (*non* Sowerby) and *A. latum* Crick, occur in the lower part of the division, being replaced above by abundant *Calycoceras* of the *choffati* (Kossmat) group, e.g. *C. newboldi newboldi* Crick (*non* Kossmat ?), *C. newboldi spinosum* Crick (*non* Kossmat ?), *C. newboldi planecostata* Crick (*non* Kossmat ?) and *C. laticostatum* Crick. Other ammonites are *Acanthoceras cornigerum* Crick, *Forbesiceras largilliertianum* d'Orbigny, *F. sculptum* Crick, *Calycoceras gentoni* (Brongniart) *paucinodatum* (Crick) and species of *Desmoceras, P.* (*Hypophylloceras*), *Borissiakoceras, Anisoceras, Stomohamites, Sciponoceras, Scaphites, Puzosia* and *Bhimaites.*

Cenomanian IV

Sparsely fossiliferous ; *Calycoceras* of the *choffati* group persists, whilst other ammonites are *Calycoceras nitidum* (Crick), *C.* group of *naviculare* (Mantell) and *Eucalycoceras* sp.

The highest parts of the Cenomanian are absent on land in South Africa.

TURONIAN

'L'étage Turonien' was introduced by d'Orbigny in 1842, and amended to its present limits by him in 1847 and 1850. The type area of the stage is Touraine, Roman Turonia, between Saumur and Montrichard, France.

Sornay (1957) has reviewed the history of the various usages of the stage, whilst the problems associated with the definition of the base of the Turonian are discussed by Juignet *et al.* (1973) and Kennedy & Juignet (1973). The base of the stage is taken as the base of the classic *Inoceramus labiatus/Mammites nodosoides* Zone for the purpose of discussion here, although no Turonian rocks are known on land in South Africa.

CONIACIAN

'L'étage Coniacien' was introduced by Coquand (1857) with the suburbs of the town of Cognac in Charente, France, as the type area. Here, the stage consists of rather poorly fossiliferous calcarenites (Séronie-Vivien 1959, Dalbiez 1959 : 862). The base of the stage is taken as being at the base of the classic *Barroisiceras haberfellneri* Zone of de Grossouvre (1901), the fauna of which is better known in the Craie de Villedieu of Touraine (de Grossouvre 1894, 1900), where *Barroisiceras, Tissotia, Peroniceras* and other early texanitids typify the Zone.

Barroisiceras, well known in the lowest Coniacian of Madagascar (e.g. Basse 1947, Collignon 1965), are absent in our faunas, and it may be that the lowermost Coniacian is absent in South Africa. Instead, our lowest Coniacian yields a sparse fauna of Collignon's (1965) Middle Coniacian *Kossmaticeras theobaldianum* and *Barroisiceras onilahyense* Zone whilst our higher faunas contain elements typical of this zone and his Lower Coniacian *Peroniceras dravidicum* Zone. Our provisional subdivisions of the stage are as follows :

Coniacian I

Proplacenticeras are abundant including forms named *P. kaffrarium* (Etheridge), *P. subkaffrarium* (Spath) and *P. umkwelanense* (Etheridge), all of which represent no more than a single variable species. Other ammonites are *Kossmaticeras theobaldianum* (Stoliczka), *Bostrychoceras indicum* (Stoliczka), *Pachydesmoceras denisonianum* (Stoliczka), and *P.* sp.

Coniacian II

Proplacenticeras are again abundant, with strongly ornamented *kaffrarium* and *subkaffrarium* more frequent than below. Evolute *Peroniceras* of the *tridorsatum* (Schlüter) group are common, e.g. forms named by van Hoepen as *P. besairei* van Hoepen (= *Fraudatoroceras besairei* van Hoepen) and *P. tenuis* van Hoepen. *Forresteria* are common, e.g. *F. alluaudi* (Boule, Lemoine & Thévenin), *F. razafiniparyi* Collignon, *F. vandenbergi* van Hoepen, *F. reymenti* van Hoepen and *F. hammersleyi* van Hoepen, all of which represent no more than a single variable species ; other ammonites are '*Eedenoceras*' *multicostatum* van Hoepen, *Forresteria itwebae* van Hoepen, *Basseoceras krameri* van Hoepen, *Kossmaticeras sparsicosta* (Kossmat), *K. sakondryense* Collignon, *Puzosia* spp., *Pachydesmoceras* sp., *Lewesiceras australe* van Hoepen, *L.* spp., *Yabeiceras* spp., *Pseudoxybeloceras matsumotoi* Collignon, *Hyphantoceras reussianum* (d'Orbigny), *Allocrioceras* spp., *Baculites bailyi* Woods, *Scaphites meslei* de Grossouvre and *S.* spp.

Coniacian III

Placenticeras are common, as below, as are coarsely ornamented peroniceratids, e.g. van Hoepen's *P.* (*Zuluiceras*) : *P.* (*Z.*) *zulu* van Hoepen, *P.* (*Z.*) *charlei* van Hoepen and their allies (perhaps no more than a single variable species) ; *Protexanites* (*Protexanites*), *P.* (*Miotexanites*) and *Paratexanites* (*Paratexanites*) species, *Baculites bailyi*, *Kossmaticeras* and *Praemuniericeras* ? sp.

Coniacian IV

Baculites of the *capensis* group are abundant, whilst compressed, finely ornamented peroniceratids, van Hoepen's *Peroniceras* (*Zuluites*) and robustly ornamented *Gauthiericeras* ?, e.g. *'Falsebayites' peregrinus* van Hoepen, *'Fluminites' albus* van Hoepen, *'Hluhluweoceras' fugitivum* van Hoepen and *'Andersonites' listeri* van Hoepen, are locally common.

Coniacian V

The highest Coniacian is not well exposed in Zululand. Above the rather distinctive association of Coniacian IV are beds with abundant *Baculites* ornamented only by growth striae, and also yielding ammonites resembling *Pseudoschloenbachia primitiva* Collignon, and *Scaphites*. This appears to be the horizon of *Subprionotropis cricki* (Spath).

SANTONIAN

'L'étage Santonien' was introduced by Coquand (1857). The type area is around the village of Saintes in the northern part of the Aquitaine Basin. The position of the base of the stage is disputed (see, for instance, Collignon 1959, Wiedmann 1959, 1964, Dalbiez 1959). The classic ammonite zonation of the stage (de Grossouvre 1894, 1901) is :

Placenticeras syrtale Zone
Eupachydiscus isculensis Zone
Texanites texanus Zone

This is based upon the Corbières succession in southern France ; typical forms of the *texanus* Zone in addition to the index species include *Parabehavites serratomarginatus* (Redtenbacher) and *Muniericeras lapparenti* de Grossouvre. In South Africa we have drawn the base of the stage at the level of the appearance of *Texanites* s.s. in numbers. Subdivisions are :

Santonian I

Texanites oliveti (Blanckenhorn), *T.* (*Plesiotexanites*) *stangeri* (Baily) *densicosta* (Spath), *T.* (*P.*) *stangeri sparcicosta* Spath, *Hauericeras gardeni* (Baily), *Pseudoschloenbachia* sp., *Pseudophyllites indra* (Forbes), *Karapadites* ? sp., *Eupachydiscus* ? sp., *Gaudryceras* spp., *Hyphantoceras* sp., and diplomoceratids.

Santonian II

Abundant *Texanites* (*Plesiotexanites*) *stangeri* and varieties, *T. soutoni* (Baily), *T.* spp., *Hauericeras* and *Pseudoschloenbachia* occur, as do *Eupachydiscus* ?, *Hyphantoceras* and diplomoceratids.

Santonian III

Hauericeras gardeni is abundant ; the remainder of the fauna is as in Santonian II and is relatively scarce.

CAMPANIAN

'L'étage Campanien' was first used by Coquand in 1857. The type area of the stage is in Grand Champagne, in the Aubeterre (Charente) region of Aquitaine. There are considerable problems associated with the succession in the type area, and the interpretation of the base of the stage used here is taken from de Grossouvre's (1901) synthesis of the French ammonite succession, e.g. at the base of the *Diplacmoceras bidorsatum* Zone. The correlation of the European sequence with South Africa is tenuous, and we have drawn the local base of the stage below the level of abundant *Submortoniceras*. Subdivisions are :

Campanian I

Submortoniceras woodsi (Spath) and related forms are common ; other ammonites include *Bevahites* and *Menabites*, *Hauericeras gardeni*, *Pseudoschloenbachia*, *Bostrychoceras* and diplomoceratids.

(There may be an unexposed interval in the lithological and faunal sequence at this level.)

Campanian II

The texanitid *Menabites* (*Australiella*) is abundant in the lower part of this division, but species including *M.* (*A.*) *australis* (Besaire) and *M.* (*A.*) *besairei* (Collignon) appear to range throughout, together with *Bevahites* species. *Baculites sulcatus* (Baily) (= *Baculites vagina* var. *Van Hoepeni* (Venzo)) is abundant throughout whilst pachydiscids become common in the higher part of the sequence, e.g. *Anapachydiscus subdulmensis* (Venzo), *A. wittekindi* (Schlüter), *A. arialoorensis* (Stoliczka), *Pachydiscus manambolensis* Basse. Other ammonites are *Hoplitoplacenticeras plasticum plasticum* Paulcke, *Maorites* sp., *Neogaudryceras* sp., *Gaudryceras* sp., *Bostrychoceras* sp.

Campanian III

Faunas are sparse, but highly distinctive. A feebly nodose *Baculites* is abundant, and giant (up to 1 m) pachydiscids (probably *Eupachydiscus*) are very common.

Campanian IV

Saghalinites cala (Forbes) and *P.* (*Pachydiscus*) are common. Other ammonites are : *Gunnarites antarticus* (Weller), *Nostoceras* ? sp., and *Pachydiscus* (*Neodesmoceras*) sp.

Campanian V

Giant *Bostrychoceras* are abundant, with scarcer *Saghalinites* and compressed pachydiscids.

MAASTRICHTIAN

The term 'Calcaire de Maastricht' was first used by Omalius d'Halloy in 1808, but stratigraphic definition of the stage dates from the work of Dumont (e.g. 1850). The concept of the stage has changed greatly subsequently, and Dumont's Maastrichtian is equivalent to what is now regarded as Upper Maastrichtian. We have thus followed current European practice, and taken the base of the stage as below the *Pachydiscus neubergicus* Zone. It is not at present possible to correlate directly between the classic European sequence and our South African one ; we have therefore drawn the local base of the Maastrichtian below the appearance of abundant *Eubaculites*. Our subdivisions of the stage are as follows :

Maastrichtian I

Feebly ornamented to smooth *Eubaculites* are abundant. Other ammonites are *Saghalinites*, *Pachydiscus* (*Neodesmoceras*), *Menuites*, '*Epiphylloceras*' and *Hoploscaphites*.

Maastrichtian II

Coarsely ornamented baculitids of *Eubaculites ootacodensis* (Stoliczka) type are abundant. Pachydiscids are also present.

Maastrichtian III

No ammonites. Inoceramid debris abundant.

VII. LOCALITY DETAILS

Detailed logs and stratigraphic accounts plus locality maps for sections studied are deposited in the Palaeontology Library of the British Museum (Natural History). Outline locality details only are given for all but the most important sections in the following pages. Latitude and longitude are given in every case.

A. PONDOLAND

LOC. 1. Cliff and foreshore exposures 1 km north of the mouth of the Umzamba River, Northern Transkei, 31° 05′ 50″ S, 30° 10′ 30″ E. Umzamba Formation.

AGE. The base of the formation is high in the Coniacian (Coniacian V ?) as indicated by the presence of *Subprionotropis cricki* (Spath) (= *Barroisiceras umzambiensis* van Hoepen) in the Basement Bed. The occurrence of abundant *Pseudoschloenbachia umbulazi*, *Hauericeras gardeni*, *Texanites soutoni*, *Texanites stangeri* and *Inoceramus expansus* (Baily) at various levels above this indicate that horizons up to at least Santonian III, and possibly Campanian I, are present.

Locs 2, 3. Reefs exposed at low water around Trafalgar Beach, between the Mhlangamkulu and Mpenjati Rivers, Southern Natal (Pondoland), 30° 57′ 50″ S, 30° 18′ 00″ E. Umzamba Formation.
AGE. Loc. 2 lies close to the base of the succession and yielded abundant Santonian *Sphenoceramus*. Loc. 3, higher in the succession, is probably Campanian, yielding *Kossmaticeras* (*Natalites*) and *Baculites sulcatus*. *Pseudoschloenbachia umbulazi* has been recorded from this area (Crick 1907b, Spath 1922a).

B. DURBAN

Loc. 4. Excavations for the new Magistrates' Court on Sometsu Road, Durban. Umzamba Formation.
AGE. Campanian II ? It seems likely that more than one horizon is represented in the collection.

Loc. 5. Excavations for the new sugar terminal at Maydon Wharf, Durban Bay. Umzamba Formation.
AGE. Santonian III and Campanian I ? Several horizons are clearly represented.

C. KWA-MBONAMBI, ZULULAND

Loc. 6. Excavations (1971) for new bridge over the Nyokaneni River, west of the Mtubatuba–Empangeni road, south of Empangeni, 28° 41′ 14″ S, 32° 01′ 22″ E. St Lucia Formation.
AGE. Santonian II–III, Campanian I.

D. MFOLOZI AND UMKWELANE HILL, ZULULAND

In this region (Fig. 2), Cretaceous sediments are largely obscured by Tertiary and Quaternary deposits (Fig. 3). Outcrops are limited to strips along the flanks of Lake Teza, followed by the railway (with most exposures in cuttings), and the north bank of the Mfolozi, below Riverview as far east as Monzi.

Locs 7, 8. Small cuttings alongside the track leading from the Mtubatuba Club towards Mains Farm (Frankel 1960 : 236, fig. 3), south of Mtubatuba, 28° 26′ 38″ S, 32° 10′ 20″ E and 28° 26′ 34″ S, 32° 10′ 22″ E respectively. Makatini and St Lucia Formations.
AGE. The Makatini conglomerates and sandstones at these localities cannot be dated more precisely than Lower Cretaceous. The base of the St Lucia Formation is Lower Coniacian, probably Coniacian II.

Loc. 9. Railway cutting 100 m north of Lake View siding, 28° 29′ 18″ S, 32° 08′ 45″ E, on the western side of Lake Teza, south of Mtubatuba. St Lucia Formation. These cuttings expose the contact between the Cretaceous and metamorphic and granitic Basement. The contact is sharp, with a basal Cretaceous conglomerate with boulders of granite and schist up to 30 cm long, set in a matrix of bioclastic limestone. Above are 3 m of hard shelly limestone with softer lenticles, both crowded with oysters, cidarid spines and plates.
AGE. Coniacian.

Loc. 10. Railway cutting 1·1 km north of Haig Halt, 28° 27′ 40″ S, 32° 09′ 58″ E on the eastern flank of Umkwelane Hill, south of Mtubatuba. St Lucia Formation. This is locality d of du Toit (*in* Spath 1921a), also mentioned by Besaire (1930 : 619) and others. The St Lucia Formation, dipping eastwards at 1° to 2°, rests on an undulating surface of deeply-weathered basalt dipping 70° S. The base of the sequence is a tough, buff, sandy and silty limestone, with scattered quartz and quartzite pebbles, abundant oysters, other molluscs and cidarid spines. Perhaps 20 m of alternations of deeply weathered silts and layers of intensely hard concretions with drifted shelly lenticles are exposed above this. There is a diverse molluscan fauna, dominated by bivalves and gastropods. Concretions 3 m above the base yielded *Proplacenticeras umkwelanense*, *Forresteria alluaudi* and a scaphitid. Besaire (1930 : 619, 634, pl. 26, fig. 4) described a *Peroniceras*

from this locality, and Spath records *Proplacenticeras subkaffrarium*, *Diaziceras tissotiaeforme* Spath and other species.
Age. The presence of *Proplacenticeras* suggests a Coniacian age for the base of the sequence.

Loc. 11. Road cut on the north side of the new road from road N 14 to Haig Halt, Umkwelane Hill, south of Mtubatuba, 20° 28′ 22″ S, 32° 09′ 32″ E. St Lucia Formation.
Age. The presence of *Proplacenticeras* suggests a Coniacian age for the sequence.

Loc. 12. A small quarry 300 m SSE of the previous section, south of the road and north of the railway near Haig Halt, Umkwelane Hill, south of Mtubatuba, 28° 28′ 31″ S, 32° 09′ 34″ E. St Lucia Formation.
Age. Coniacian.

Loc. 13. Hill slopes below Riverview Compound, 750 m north of the Cane Railway Bridge across the Mfolozi, south of Mtubatuba, 28° 26′ 52″ S, 32° 10′ 48″ E. St Lucia Formation.
Age. Coniacian II–III; as indicated by species of *Proplacenticeras*, *Peroniceras*, *Forresteria*, *Scaphites*, *Baculites*, kossmaticeratids, puzosiids and diplomoceratids.

Loc. 14. Road cuttings below the compound immediately south of the Msunduzi River, 2·1 km NNE of Mfolozi, south of Mtubatuba, 28° 28′ 24″ S, 32° 10′ 43″ E. St Lucia Formation.
Age. Santonian II and III, Campanian I.

Loc. 15. Small quarry east of track on lot 71 13567, 1200 m east of Riverview Sugar Mill, south of Mtubatuba, 28° 26′ 35″ S, 32° 11′ 24″ E. St Lucia Formation.
Age. Coniacian IV.

Loc. 16. Small quarry 175 m SSE of loc. 15; 28° 26′ 42″ S, 32° 11′ 25″ E. St Lucia Formation.
Age. Coniacian III ?

Loc. 17. Cuttings in cane road leading down to Peaston North Bank Drain on lot 72 13569, 350 m south of the farm Pasina, SE of Mtubatuba, 28° 26′ 04″ S, 32° 11′ 48″ E. St Lucia Formation.
Age. Coniacian V.

Loc. 18. Outcrops in cane road leading down to Peaston North Bank Drain on lot 47 12967, 1200 m SE of the farm Chelmsford, ESE of Mtubatuba, 28° 26′ 38″ S, 32° 12′ 38″ E. St Lucia Formation.
Age. Santonian.

Loc. 19. Road cutting west of Lake Mfuthululu on Shire Estate, leading down to Peaston North Bank Drain, ESE of Mtubatuba, 28° 25′ 39″ S, 32° 14′ 45″ E. St Lucia Formation.
Age. Campanian I.

Loc. 20. Section at junction of the old course of the Mfolozi, the present river and the unnamed stream draining south from Lake Mfuthululu, ESE of Mtubatuba, 28° 26′ 59″ S, 32° 16′ 36″ E. St Lucia Formation.
Age. Maastrichtian I–II.

Loc. 21. Roadside section 9 km north of Monzi, east of Mtubatuba, 28° 25′ 00″ S, 32° 18′ 35″ E. St Lucia Formation.
Age. Campanian V.

E. The Nyalazi River, south of Hluhluwe, Zululand

North of Mtubatuba, exposures are poor, due to an extensive cover of Tertiary and Recent deposits. Such sections as are visible are deeply decalcified and often barren of recognizable macrofossils. There are, however, a series of exposures along the Nyalazi River which give a discontinuous sequence from Karoo sediments and Lebombo Volcanics through to the St Lucia Formation.

LOC. 22. Cut on the north side of the Nyalazi River, east of the old Nyalazi road and railway bridge, 2 km north of the Nyalazi River Trading Store, 28° 12′ 23″ S, 32° 18′ 02″ E. St Lucia Formation.
AGE. Coniacian IV.

LOC. 23. Stream exposures 1·4 km NW of the old Nyalazi bridge, 28° 12′ 05″ S, 32° 17′ 01″ E. St Lucia Formation.
AGE. Coniacian III ?

LOC. 24. Cuttings and excavations at the new Nyalazi River bridge in Moroval 1884 section, 28° 14′ 27″ S, 32° 17′ 37″ E. St Lucia Formation.
AGE. Coniacian II–V.

LOC. 25. Cutting alongside new road 2·8 km ESE of Nyalazi River trading store, 28° 13′ 42″ S, 32° 16′ 48″ E. St Lucia Formation.
AGE. Coniacian II.

LOC. 26. River banks on NE side of the Nyalazi, 1 km ENE of the old combined road/rail bridge 28° 12′ 12″ S, 32° 18′ 42″ E. St Lucia Formation.
AGE. Santonian ?

LOC. 27. Trackside exposures leading down to the eastern bank of the Nyalazi 1·25 km SE of the old bridge, 28° 12′ 35″ S, 32° 18′ 44″ E. St Lucia Formation.
AGE. Campanian I.

LOC. 28. Abandoned quarry on southern side of Nyalazi River trading store–Charters Creek track 1·3 km east of the store, 28° 13′ 12″ S, 32° 19′ 10″ E. St Lucia Formation. Scattered exposures of Campanian silts occur for several kilometres along the Nyalazi downstream of this locality.
AGE. Campanian.

LOC. 29. Excavations by abandoned dam on Cekeni Estate 2·9 km ESE of Mfekayi Halt, 28° 10′ 54″ S, 32° 20′ 05″ E. St Lucia Formation.
AGE. Campanian I–II.

LOC. 30. Overgrown hill slopes on the western side of the Nyalazi River in Bantu Reserve No. 3, 5 km east of Glenpark Estate, 28° 07′ 52″ S, 32° 20′ 56″ E. St Lucia Formation.
AGE. Campanian I–II.

LOC. 31. Gullies and hill slopes on west bank of Nyalazi in Bantu Reserve No. 3, 6 km ENE of Glenpark Estate, 28° 07′ 12″ S, 32° 21′ 47″ E. St Lucia Formation.
AGE. Santonian.

F. GLENPARK ESTATE, ZULULAND

Sections along the lower Hluhluwe are poor, but exposures along the railway on Glenpark Estate prove definitely the presence of Albian sediments. Cenomanian faunas are unknown, but there is a very complete Coniacian sequence exposed to the NE (p. 295). Although not proven, the base of the St Lucia Formation may rest upon Upper Albian Mzinene Formation in this area.

LOC. 32. Cutting in acute bend of railway west of Glenpark Estate, 11 km south of Hluhluwe, 28° 07′ 55″ S, 32° 17′ 18″ E. Mzinene Formation.
AGE. Albian III.

LOC. 33. Railway cuttings west of Glenpark Estate, 11 km south of Hluhluwe, 28° 07′ 50″ S, 32° 17′ 39″ E. Mzinene Formation.
AGE. Albian IV.

G. The Mzinene River and its tributaries, Zululand

(i) Upper reaches

The Mzinene and its tributaries provide a discontinuous succession from the Lebombo Volcanics and pre-Upper Aptian clastics of the Makatini Formation to the Upper Coniacian and perhaps Lower Santonian St Lucia Formation. It is the type section of the Mzinene Formation and the base of the succeeding St Lucia Formation.

Sections along the tributary streams are poor, and those along the main river are usually below water, because of extensive damming. Bilharzia and crocodiles (see du Toit and van Hoepen 1929) render these sections rather inaccessible, but extensive droughts prior to our visit had reduced water levels and raised salinities so much that we were able to see far more of this section than is usually exposed, and collect important faunas from the lower parts of the Upper Albian.

Dips in this area are low, of the order of 2°–6°, and it is difficult to measure the thickness of the sequence when exposures are limited to the stream bed. Cliff exposures are available, but are often deeply weathered and choked by thorn and scrub. Some additional exposures are available in old river cliffs, as at the Skoenberg, and south of the kraal in Ndabana 13162 section, but these are deeply decalcified and the fossil fauna lies loose on hill slopes.

Loc. 34. Cliff and stream section 600 m north of the farm Amatis, just to NE of the confluence of the Mzinene and an un-named, eastward-flowing tributary, north of Hluhluwe, 27° 58′ 32″ S, 32° 18′ 02″ E. Makatini Formation.
Age. Aptian IV.

Loc. 35. Cliff and stream sections extending over several hundred metres along the Mzinene, approximately 1200 m NE of the farm Amatis, north of Hluhluwe, 27° 58′ 03″ S, 32° 18′ 31″ E. Mzinene Formation.
Age. Albian III.

Loc. 36. Degraded river cliff on the eastern bank of the Mzinene close to the boundary of lots H 84 14107 and H 85 14108, north of Hluhluwe, 27° 57′ 14″ S, 32° 18′ 34″ E. Mzinene Formation.
Age. Albian III.

Loc. 37. Discontinuous exposures in the bed of the Mzinene over a distance of some 600 m in lots H 86 13655 and H 87 13656, north of Hluhluwe, 27° 56′ 37″ S, 32° 18′ 08″ E. Makatini Formation.
Age. Aptian IV.

Locs 38–43. North of loc. 37, the Mzinene swings west in a long meander, crossed by the road running east from the National Road N 14, just north of Ngweni. In this region, there are a series of exposures in the Makatini Formation, with hills of Lebombo Volcanics rising to the east. Makatini Formation.

Loc. 38.	27° 56′ 09″ S, 32° 18′ 03″ E.	Loc. 41.	27° 55′ 42″ S, 32° 17′ 50″ E.
Loc. 39.	27° 55′ 57″ S, 32° 17′ 44″ E (Plate, Fig. 1).	Loc. 42.	27° 55′ 38″ S, 32° 17′ 02″ E.
Loc. 40.	27° 55′ 58″ S, 32° 17′ 58″ E.	Loc. 43.	27° 55′ 20″ S, 32° 18′ 10″ E.

Age. Pre-Upper Aptian. No ammonites or other diagnostic fossils are known.

Loc. 44. Stream section 900 m SE of Baboon's Krans, north of Hluhluwe, 27° 54′ 24″ S, 32° 17′ 48″ E.
Age. Pre-Upper Albian.

Locs 45–49. Stream and river cliff exposures extending downstream from the drift where the minor road leading north from the sisal factory to Monte Rosa crosses the Mzinene, 27° 53′ 59″ S, 32° 18′ 06″ E to 27° 53′ 50″ S, 32° 19′ 10″ E. Makatini Formation.
Age. Pre-Upper Aptian.

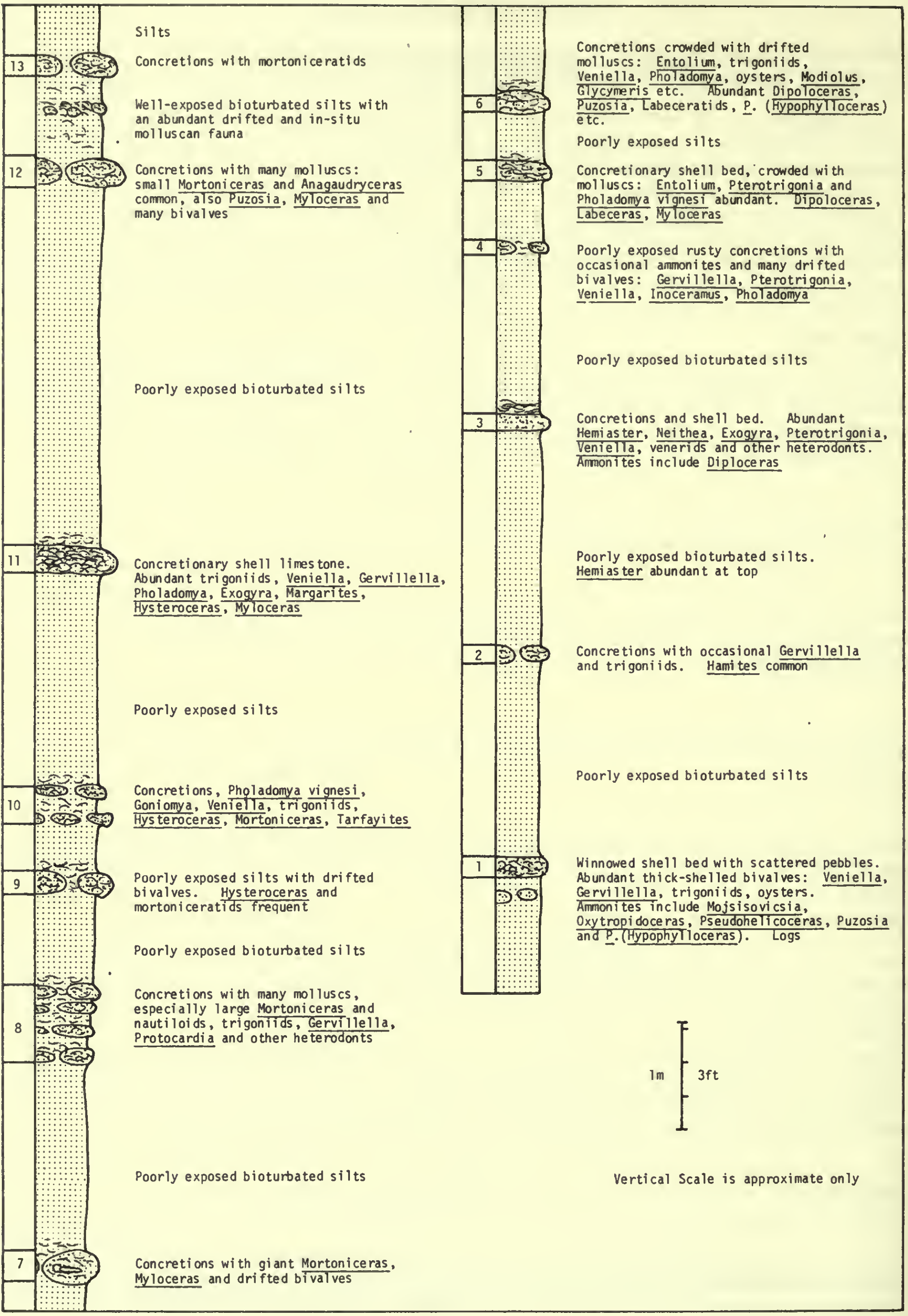

Silts

13 Concretions with mortoniceratids

Well-exposed bioturbated silts with an abundant drifted and in-situ molluscan fauna

12 Concretions with many molluscs: small *Mortoniceras* and *Anagaudryceras* common, also *Puzosia*, *Myloceras* and many bivalves

Poorly exposed bioturbated silts

11 Concretionary shell limestone. Abundant trigoniids, *Veniella*, *Gervillella*, *Pholadomya*, *Exogyra*, *Margarites*, *Hysteroceras*, *Myloceras*

Poorly exposed silts

10 Concretions, *Pholadomya vignesi*, *Goniomya*, *Veniella*, trigoniids, *Hysteroceras*, *Mortoniceras*, *Tarfayites*

9 Poorly exposed silts with drifted bivalves. *Hysteroceras* and mortoniceratids frequent

Poorly exposed bioturbated silts

8 Concretions with many molluscs, especially large *Mortoniceras* and nautiloids, trigoniids, *Gervillella*, *Protocardia* and other heterodonts

Poorly exposed bioturbated silts

7 Concretions with giant *Mortoniceras*, *Myloceras* and drifted bivalves

6 Concretions crowded with drifted molluscs: *Entolium*, trigoniids, *Veniella*, *Pholadomya*, oysters, *Modiolus*, *Glycymeris* etc. Abundant *Dipoloceras*, *Puzosia*, Labeceratids, *P.* (*Hypophylloceras*) etc.

Poorly exposed silts

5 Concretionary shell bed, crowded with molluscs: *Entolium*, *Pterotrigonia* and *Pholadomya vignesi* abundant. *Dipoloceras*, *Labeceras*, *Myloceras*

4 Poorly exposed rusty concretions with occasional ammonites and many drifted bivalves: *Gervillella*, *Pterotrigonia*, *Veniella*, *Inoceramus*, *Pholadomya*

Poorly exposed bioturbated silts

3 Concretions and shell bed. Abundant *Hemiaster*, *Neithea*, *Exogyra*, *Pterotrigonia*, *Veniella*, venerids and other heterodonts. Ammonites include *Diploceras*

Poorly exposed bioturbated silts. *Hemiaster* abundant at top

2 Concretions with occasional *Gervillella* and trigoniids. *Hamites* common

Poorly exposed bioturbated silts

1 Winnowed shell bed with scattered pebbles. Abundant thick-shelled bivalves: *Veniella*, *Gervillella*, trigoniids, oysters. Ammonites include *Mojsisovicsia*, *Oxytropidoceras*, *Pseudohelicoceras*, *Puzosia* and *P.* (*Hypophylloceras*). Logs

Vertical Scale is approximate only

FIG. 4. The sequence at loc. 51.

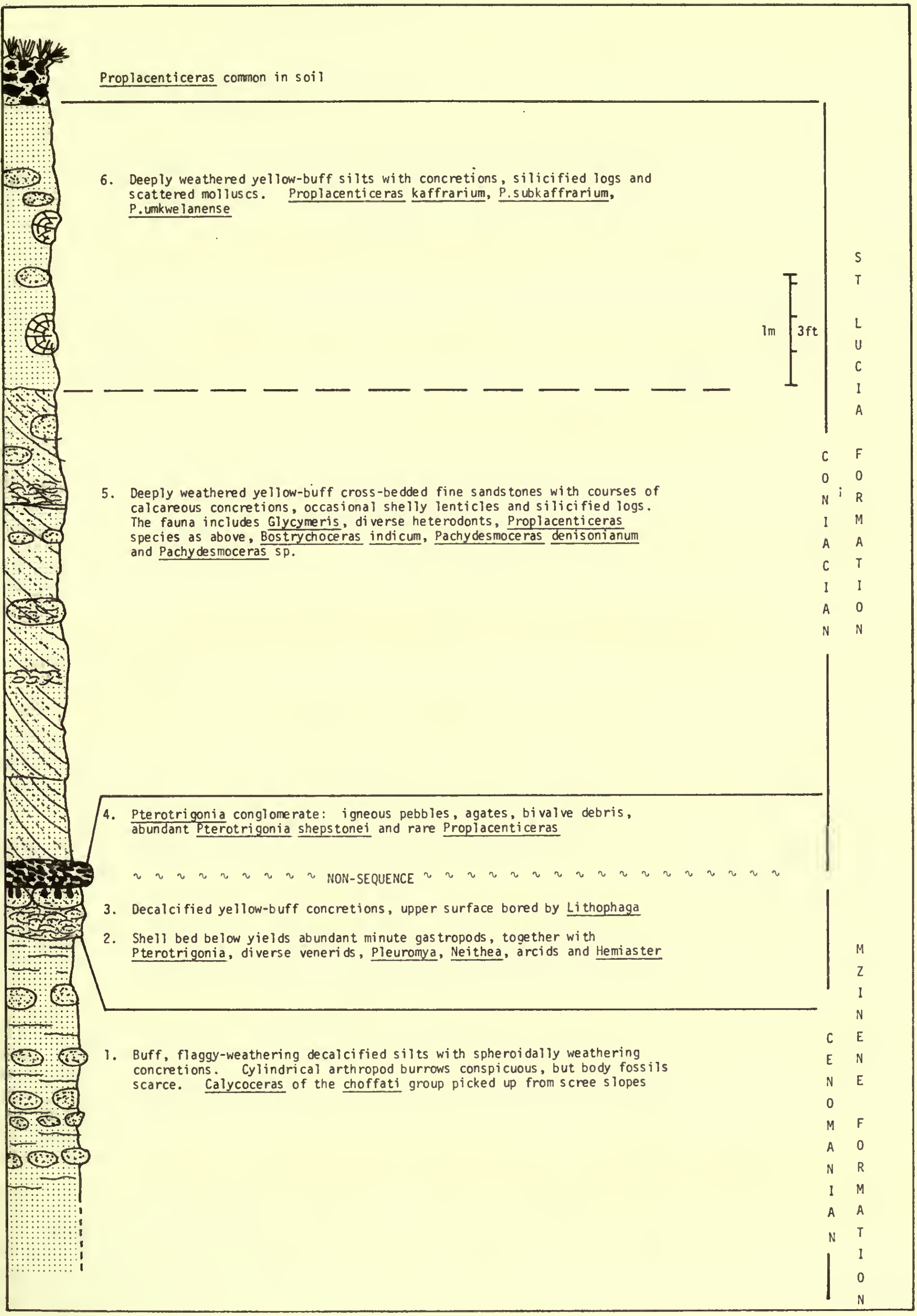
Proplacenticeras common in soil
6. Deeply weathered yellow-buff silts with concretions, silicified logs and scattered molluscs. Proplacenticeras kaffrarium, P.subkaffrarium, P.umkwelanense
1m
3ft
5. Deeply weathered yellow-buff cross-bedded fine sandstones with courses of calcareous concretions, occasional shelly lenticles and silicified logs. The fauna includes Glycymeris, diverse heterodonts, Proplacenticeras species as above, Bostrychoceras indicum, Pachydesmoceras denisonianum and Pachydesmoceras sp.
4. Pterotrigonia conglomerate: igneous pebbles, agates, bivalve debris, abundant Pterotrigonia shepstonei and rare Proplacenticeras
NON-SEQUENCE
3. Decalcified yellow-buff concretions, upper surface bored by Lithophaga
2. Shell bed below yields abundant minute gastropods, together with Pterotrigonia, diverse venerids, Pleuromya, Neithea, arcids and Hemiaster
1. Buff, flaggy-weathering decalcified silts with spheroidally weathering concretions. Cylindrical arthropod burrows conspicuous, but body fossils scarce. Calycoceras of the choffati group picked up from scree slopes
CONIACIAN
CENOMANIAN
ST LUCIA FORMATION
MZINENE FORMATION

FIG. 5. The sequence at loc. 60.

Loc. 50. Outcrops in the river bed north of the earth dam 1200 m ENE of the sisal factory, where the track to the farm Belvedere approaches the Mzinene, north of Hluhluwe, 25° 53′ 50″ S, 32° 19′ 10″ E. Makatini Formation.
Age. Aptian.

Loc. 51. Stream bed and bank exposures extending 100–600 m downstream from loc. 50, around the eastern limb of the broad meander ENE of the sisal factory, north of Hluhluwe, 27° 53′ 43″ S, 32° 19′ 22″ E (Fig. 4). Mzinene Formation.
Age. Albian IV–V.

Loc. 52. West bank of the Mzinene just north of a gully entering from the west in Indabana 13162 section, north Hluhluwe, 27° 53′ 04″ S, 32° 19′ 21″ E. Mzinene Formation.
Age. Albian V.

Loc. 53. Derelict dam site on Indabana 13162, 2·2 km south of the farm Izwehelia, north of Hluhluwe, 27° 52′ 24″ S, 32° 19′ 02″ E. Mzinene Formation.
Age. Albian III.

Loc. 54. Degraded river cliff 200–350 m west of south-trending gully which joins the Mzinene in Munywana 13161 section, close to where the river turns sharply eastwards north of Hluhluwe, 27° 52′ 46″ S, 32° 19′ 40″ E. Mzinene Formation.
Age. Albian V.

Loc. 55. Sections in the gully immediately east of the previous locality, 500 m north of its junction with the Mzinene in Munywana 13161 section, 27° 52′ 26″ S, 32° 19′ 42″ E. Mzinene Formation.
Age. Albian V.

Loc. 56. Degraded river cliffs immediately east of loc. 55, in Munywana 13161 section, 27° 52′ 30″ S, 32° 19′ 44″ E. Mzinene Formation.
Age. Albian V.

Loc. 57. Outcrops in the bed of the Mzinene at Beacon 624, where the river swings east in Munywana 13809 section, north of Hluhluwe, 27° 52′ 40″ S, 32° 19′ 58″ E. Mzinene Formation.
Age. Albian V.

Loc. 58. Degraded cliff on the north bank of the Mzinene in Iswelihle 13163 section WNW of the farm Belvedere, NNE of Hluhluwe, 27° 52′ 42″ S, 32° 20′ 36″ E. Mzinene Formation.
Age. Albian V.

Loc. 59. Section on eastern side of swamp at the mouth of a gully draining south to the Mzinene from the Skoenberg in Iswelihle 13163 section, 1200 m NNW of the farm Belvedere, NNE of Hluhluwe, 27° 52′ 41″ S, 32° 20′ 45″ E. Mzinene Formation.
Age. Cenomanian III.

Loc. 60. River cliff and river bed outcrops extending for several hundred metres along the north side of the Mzinene in Iswelihle 13163 section, 1000 m NNW of the farm Belvedere, north of Hluhluwe, 27° 52′ 45″ S, 32° 20′ 55″ E (Fig. 5). Mzinene and St Lucia Formations.
Age. Mzinene Formation: Cenomanian III–IV; St Lucia Formation: Coniacian I.

(ii) The Skoenberg region

The Skoenberg, in Iswelihle 13163, NNW of Hluhluwe, is a crescentic hill lying between the Mzinene and Munywana (Manuan of early workers). The steep NW face rises to over 30 m at the western end; to the east it falls to the level of the flood plain. It represents an abandoned river cliff of the Munywana, which now flows across the northern part of its flood plain at this point, 700 m from the old cliff.

This is the celebrated locality described by William Anderson in 1907 (p. 60) as situated near the junction of the Manuan and Mzinene Rivers. It is the source of the rich Cenomanian fauna described by G. C. Crick in 1907, and the type locality of van Hoepen's Skoenberg Beds.

The hill itself is capped by a veneer of Pleistocene debris, including dark brown, glazed rock fragments and derived Senonian fossils. The NW cusp of the hill is capped by the Coniacian *Pterotrigonia* conglomerate (Anderson's 1907 : 60 'hard calcareous sandstone full of broken shells'). This dips gently to the east, at first forming the rim to the north face of the Skoenberg, and then crossing down the face to disappear below the alluvium of the Munywana/Mzinene flood plain.

There are good exposures of the silts above and below the conglomerate along the main face of the Skoenberg, whilst to the west gullies and hill slopes provide a magnificent series of exposures, extending down to the Upper Albian. These correspond to localities 5-8 of van Hoepen (1966a, b).

Loc. 61. Hill slopes and gullies west of the western 'horn' of the Skoenberg, 27° 52′ 19″ S, 32° 20′ 19″ E (Fig. 6). Mzinene Formation.
Age. Albian VI-Cenomanian II.

Loc. 62. Hill slopes at, and extending west from, the western end of the Skoenberg, 27° 52′ 17″ S, 32° 20′ 26″ E (Fig. 7). Mzinene and St Lucia Formations.
Age. Mzinene Formation : Cenomanian II-IV ; St Lucia Formation : Coniacian I.

Loc. 63. The steep, northern face of the scarp of the Skoenberg, 27° 52′ 15″ S, 32° 20′ 30″ E. St Lucia Formation.
Age. Coniacian I.

(iii) Sections along the Munywana

In Munywana 13161 section, NNE of Hluhluwe, Zululand.

Loc. 64. River cliff on the south side of the main southern tributary of the Munywana, 1·5 km ESE of the farm Izwehelia, 27° 51′ 36″ S, 32° 19′ 41″ E. Mzinene Formation.
Age. Albian V.

Loc. 65. Dam site excavation and adjacent hillside 200-300 m west of the previous locality and 1300 m SW of the farm Izwehelia, 27° 51′ 38″ S, 32° 19′ 30″ E. Mzinene Formation.
Age. Albian V.

Loc. 66. River-bed and cliff sections extending for some 400-500 m along the northern branch of the Munywana north of a point 1·5 km east of the farm Izwehelia and just south of a group of native huts, 27° 51′ 16″ S, 32° 19′ 44″ E. Mzinene Formation.
Age. Albian V.

Loc. 67. Poor exposures in the north bank of the gully 600 m SSW of the farm Izwehelia, 27° 51′ 37″ S, 32° 19′ 01″ E. Mzinene Formation.
Age. Albian.

Loc. 68. North bank of gully 300 m SW of the farm Izwehelia, 27° 51′ 32″ S, 32° 19′ 03″ E. Mzinene Formation.
Age. Albian II.

Loc. 69. Densely vegetated outcrop in gully 600 m ESE of the farm Izwehelia, 27° 51′ 29″ S, 32° 19′ 11″ E. Mzinene Formation.
Age. Albian II.

Loc. 70. Excavations for a dam site 500 m east of the farm Izwehelia, 27° 51′ 20″ S, 32° 19′ 04″ E. Mzinene Formation.
Age. Albian II.

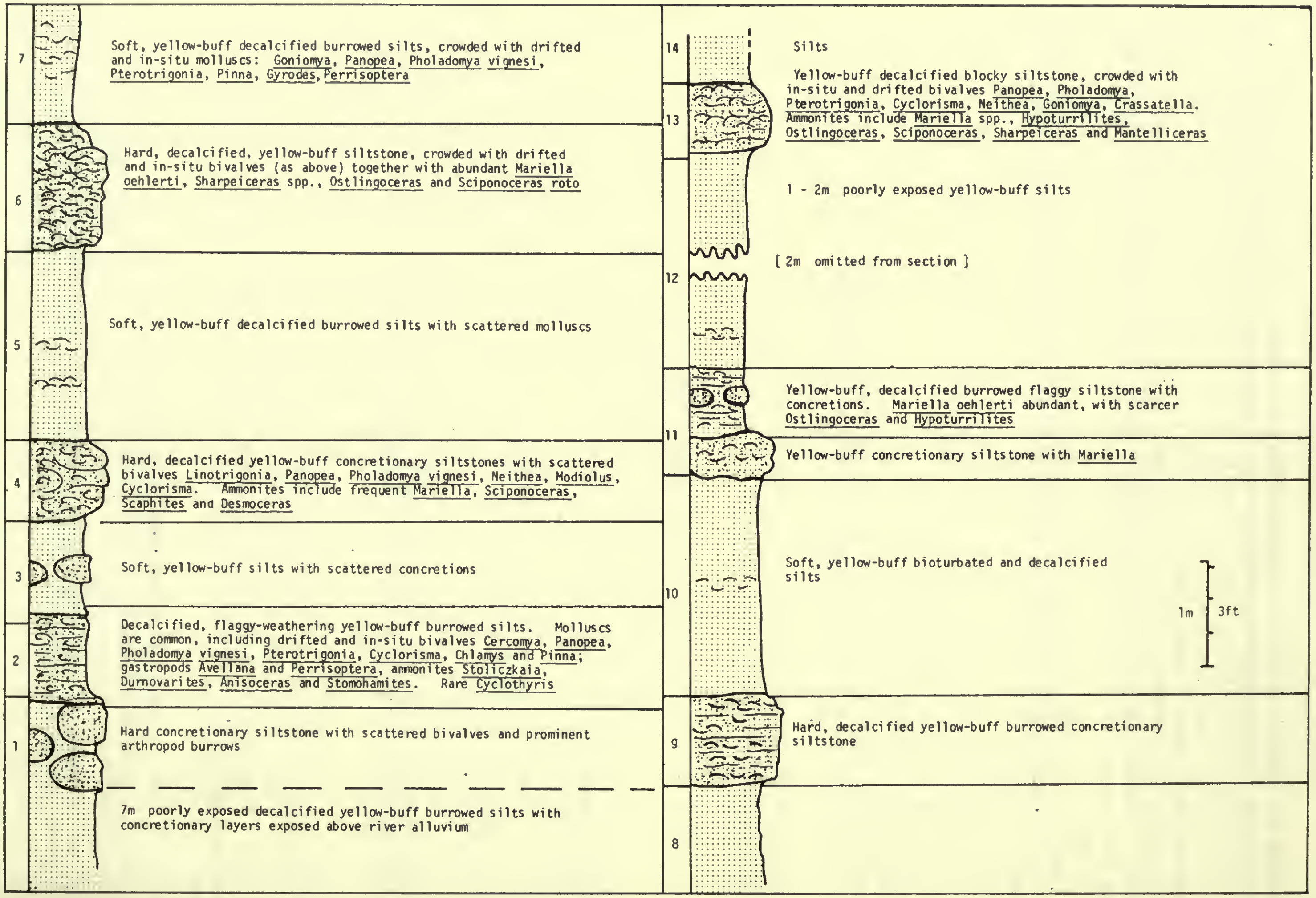
7
Soft, yellow-buff decalcified burrowed silts, crowded with drifted and in-situ molluscs: Goniomya, Panopea, Pholadomya vignesi, Pterotrigonia, Pinna, Gyrodes, Perrisoptera
6
Hard, decalcified, yellow-buff siltstone, crowded with drifted and in-situ bivalves (as above) together with abundant Mariella oehlerti, Sharpeiceras spp., Ostlingoceras and Sciponoceras roto
5
Soft, yellow-buff decalcified burrowed silts with scattered molluscs
4
Hard, decalcified yellow-buff concretionary siltstones with scattered bivalves Linotrigonia, Panopea, Pholadomya vignesi, Neithea, Modiolus, Cyclorisma. Ammonites include frequent Mariella, Sciponoceras, Scaphites and Desmoceras
3
Soft, yellow-buff silts with scattered concretions
2
Decalcified, flaggy-weathering yellow-buff burrowed silts. Molluscs are common, including drifted and in-situ bivalves Cercomya, Panopea, Pholadomya vignesi, Pterotrigonia, Cyclorisma, Chlamys and Pinna; gastropods Avellana and Perrisoptera, ammonites Stoliczkaia, Durnovarites, Anisoceras and Stomohamites. Rare Cyclothyris
1
Hard concretionary siltstone with scattered bivalves and prominent arthropod burrows
7m poorly exposed decalcified yellow-buff burrowed silts with concretionary layers exposed above river alluvium
14
Silts
13
Yellow-buff decalcified blocky siltstone, crowded with in-situ and drifted bivalves Panopea, Pholadomya, Pterotrigonia, Cyclorisma, Neithea, Goniomya, Crassatella. Ammonites include Mariella spp., Hypoturrilites, Ostlingoceras, Sciponoceras, Sharpeiceras and Mantelliceras
12
1 - 2m poorly exposed yellow-buff silts
[2m omitted from section]
11
Yellow-buff, decalcified burrowed flaggy siltstone with concretions. Mariella oehlerti abundant, with scarcer Ostlingoceras and Hypoturrilites
Yellow-buff concretionary siltstone with Mariella
10
Soft, yellow-buff bioturbated and decalcified silts
1m
3ft
9
Hard, decalcified yellow-buff burrowed concretionary siltstone
8

FIG. 6. The sequence at loc. 61.

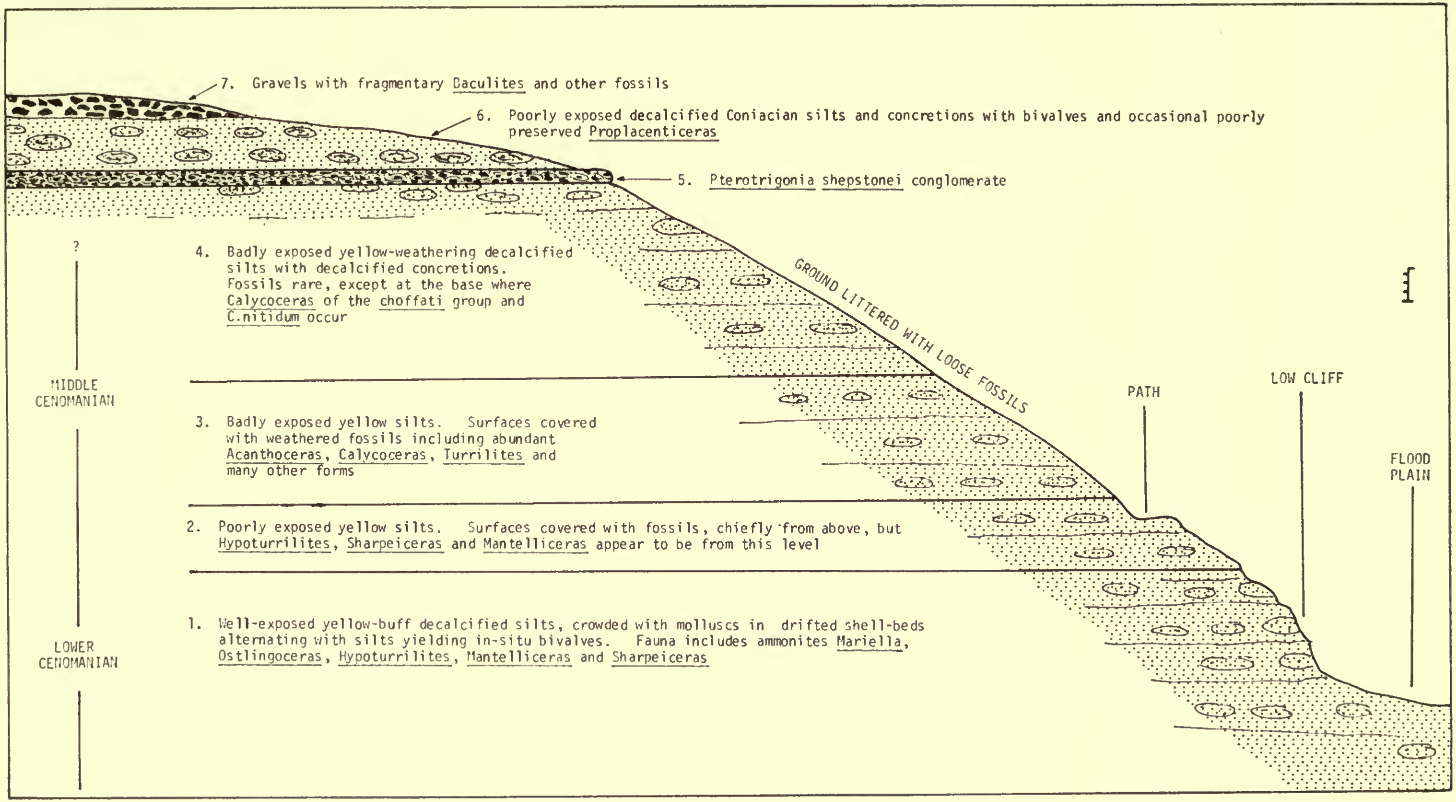
7. Gravels with fragmentary Baculites and other fossils
6. Poorly exposed decalcified Coniacian silts and concretions with bivalves and occasional poorly preserved Proplacenticeras
5. Pterotrigonia shepstonei conglomerate
4. Badly exposed yellow-weathering decalcified silts with decalcified concretions. Fossils rare, except at the base where Calycoceras of the choffati group and C.nitidum occur
3. Badly exposed yellow silts. Surfaces covered with weathered fossils including abundant Acanthoceras, Calycoceras, Turrilites and many other forms
2. Poorly exposed yellow silts. Surfaces covered with fossils, chiefly from above, but Hypoturrilites, Sharpeiceras and Mantelliceras appear to be from this level
1. Well-exposed yellow-buff decalcified silts, crowded with molluscs in drifted shell-beds alternating with silts yielding in-situ bivalves. Fauna includes ammonites Mariella, Ostlingoceras, Hypoturrilites, Mantelliceras and Sharpeiceras
?
MIDDLE CENOMANIAN
LOWER CENOMANIAN
GROUND LITTERED WITH LOOSE FOSSILS
PATH
LOW CLIFF
FLOOD PLAIN

FIG. 7. The sequence at loc. 62.

(iv) Lower reaches

In Umzigi 13809 section, NNE of Hluhluwe, Zululand.

Loc. 71. Degraded river cliffs on the north bank of the Munywana Creek, north of the Skoenberg, 3 km SW of the farm Insleep, and just west of the earth dam 400 m west of the causeway across the Mzinene just below the confluence with the Munywana, 27° 51′ 48″ S, 32° 21′ 08″ E. St Lucia Formation.
Age. Coniacian I.

Loc. 72. Degraded river cliff and alluvial flats on the north side of the Mzinene, 200–300 m east of the causeway across the river, downstream from its junction with the Munywana, 27° 51′ 52″ S, 32° 21′ 34″ E. St Lucia Formation.
Age. Coniacian IV-V, Santonian I ?

H. Sections around False Bay and Lake St Lucia, Zululand

The False Bay and Lake St Lucia Game Reserves form a lagoon 80 km long, separated from the sea by dunes up to 200 m high. The lake is nowhere more than a few metres deep and drains to the sea via the Narrows, 16 km to the south. During drought or when the entrance to the Narrows is blocked, the lake level falls and salinity rises steeply, accompanied by mass mortality of the bulk of the invertebrate fauna. During floods, the lake becomes temporarily freshwater.

Four principal rivers drain into the lake, the Mzinene, Mkuze, Hluhluwe and Nyalazi. Each has an associated swampy flood plain at its mouth, several miles across. The flood plains and the lake itself are flanked by cliffs up to 30 m high. These are, for the most part, degraded and heavily vegetated, but locally expose vertical sections of Cretaceous silts and concretionary horizons over stretches of several hundred metres. Foreshore platforms are cut in the Upper Cretaceous at many localities ; extreme drought during our visit exposed many normally submerged outcrops. Elsewhere, saltmarsh and saline pans extend from degraded cliffs to the lake shore, masking the Cretaceous.

The dip is low, perhaps 3° just south of east, and as a result many exposures approximate to strike sections.

We have been able to collect and measure sections along the western shores of False Bay, around the southern termination of the Nibela Peninsula, along the SW shores of Lake St Lucia, and around the southern peninsula.

(i) Western False Bay

Loc. 74. 1400 m stretch of cliff and foreshore section at Die Rooiwalle, 1·3 km east of the farm Mfomoto, northern part of False Bay, NNE of Hluhluwe, 27° 54′ 12″ S, 32° 23′ 47″ E to 24° 54′ 48″ S, 32° 23′ 15″ E (Fig. 8). St Lucia Formation.
Age. Santonian I–Campanian I.

Locs 75–77. Gullies in degraded cliffs 300 m, 1200 m and 1700 m respectively south of Die Rooiwalle, and inland of an extensive saline pool, NW shores of False Bay, NE of Hluhluwe. St Lucia Formation.
Loc. 75. 27° 54′ 57″ S, 32° 23′ 07″ E.
Loc. 76. 27° 55′ 19″ S, 32° 22′ 49″ E.
Loc. 77. 27° 55′ 04″ S, 32° 22′ 56″ E.
Age. Coniacian V.

Loc. 78. Foreshore platform 4 km north of Lister's Point and 3·1 km east of the farm Onderdeel, NW shores of False Bay, NE of Hluhluwe, 27° 56′ 02″ S, 32° 22′ 54″ S. St Lucia Formation.
Age. Santonian I–II.

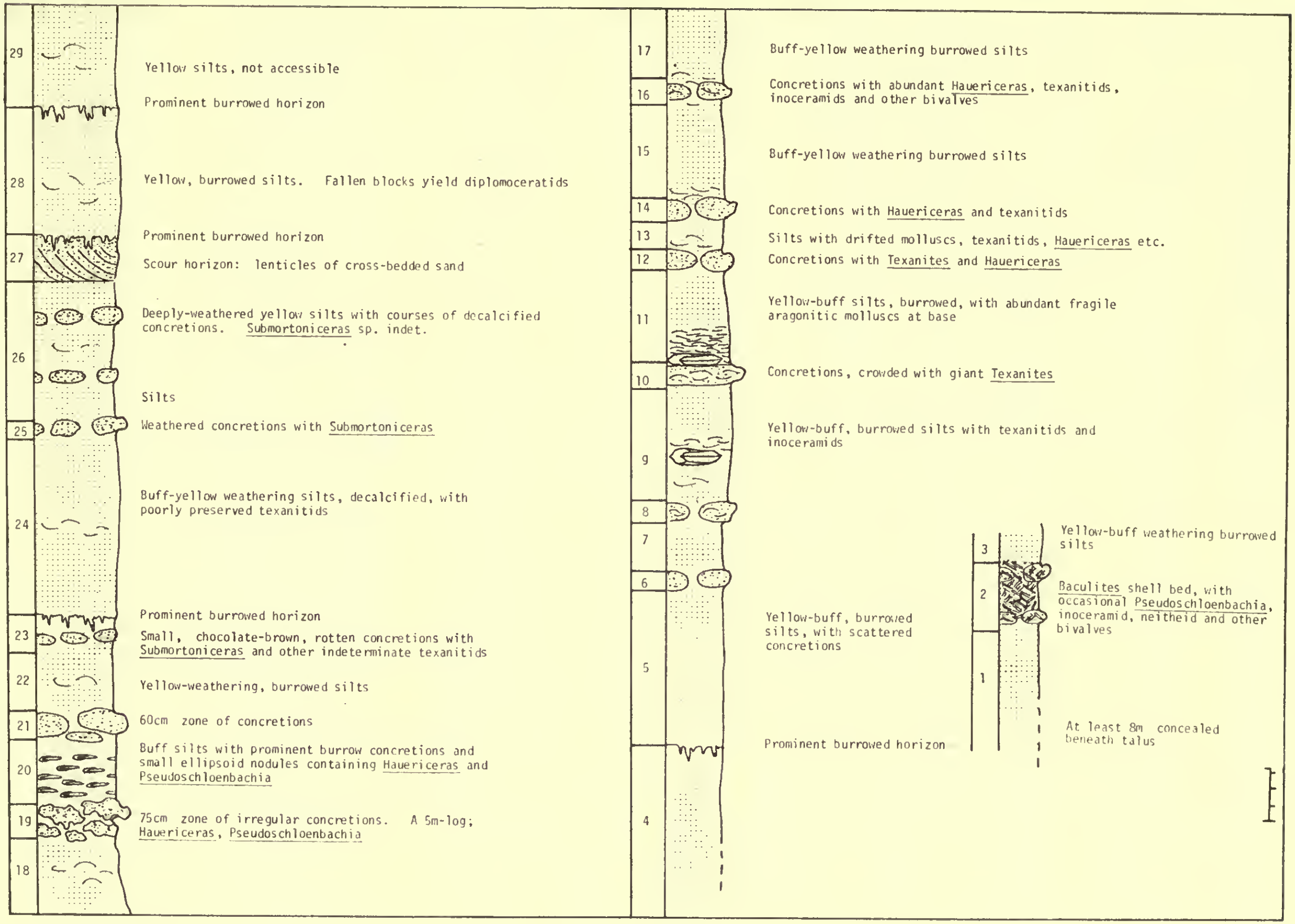
29
Yellow silts, not accessible
Prominent burrowed horizon
28
Yellow, burrowed silts. Fallen blocks yield diplomoceratids
Prominent burrowed horizon
27
Scour horizon: lenticles of cross-bedded sand
26
Deeply-weathered yellow silts with courses of decalcified concretions. Submortoniceras sp. indet.
Silts
25
Weathered concretions with Submortoniceras
24
Buff-yellow weathering silts, decalcified, with poorly preserved texanitids
Prominent burrowed horizon
23
Small, chocolate-brown, rotten concretions with Submortoniceras and other indeterminate texanitids
22
Yellow-weathering, burrowed silts
21
60cm zone of concretions
20
Buff silts with prominent burrow concretions and small ellipsoid nodules containing Hauericeras and Pseudoschloenbachia
19
75cm zone of irregular concretions. A 5m-log; Hauericeras, Pseudoschloenbachia
18
17
Buff-yellow weathering burrowed silts
16
Concretions with abundant Hauericeras, texanitids, inoceramids and other bivalves
15
Buff-yellow weathering burrowed silts
14
Concretions with Hauericeras and texanitids
13
Silts with drifted molluscs, texanitids, Hauericeras etc.
12
Concretions with Texanites and Hauericeras
11
Yellow-buff silts, burrowed, with abundant fragile aragonitic molluscs at base
10
Concretions, crowded with giant Texanites
9
Yellow-buff, burrowed silts with texanitids and inoceramids
8
7
6
Yellow-buff, burrowed silts, with scattered concretions
5
Prominent burrowed horizon
4
3
Yellow-buff weathering burrowed silts
2
Baculites shell bed, with occasional Pseudoschloenbachia, inoceramid, neitheid and other bivalves
1
At least 8m concealed beneath talus

FIG. 8. The sequence at loc. 74.

Loc. 79. Degraded cliff section at the northern end of the coastal track 1700 m north of Lister's Point, NW shores of False Bay, NE of Hluhluwe, 27° 57′ 09″ S, 32° 22′ 36″ E. St Lucia Formation.
Age. Coniacian V.

Loc. 80. Foreshore reefs alongside camp site, 600 m north of Lister's Point, western shores of False Bay, NE of Hluhluwe, 27° 57′ 43″ S, 32° 28′ 38″ E. St Lucia Formation.
Age. Coniacian V.

Loc. 81. Foreshore platforms west of Lister's Point, western shores of False Bay, NE of Hluhluwe, 27° 58′ 14″ S, 32° 27′ 26″ E. St Lucia Formation.
Age. This locality extends across the strike. Faunas from the western outcrops are undoubtedly Coniacian IV–V. To the east, higher horizons may be present.

Loc. 82. Foreshore platforms at the end of the small promontory 1·3 km SW of Lister's Point, western shores of False Bay, NE of Hluhluwe, 27° 58′ 38″ S, 32° 22′ 20″ E. St Lucia Formation.
Age. Coniacian IV.

Loc. 83. Foreshore exposures extending around the headland 3·5 km north of Picnic Point and known locally as Mason's Camp, western shores of False Bay ENE of Hluhluwe, 28° 00′ 18″ S, 32° 22′ 20″ E. St Lucia Formation.
Age. Coniacian IV.

Loc. 84. Beach exposures and low cliff 3·2 km north of Picnic Point, SW shores of False Bay, east of Hluhluwe, 28° 01′ 00″ S, 32° 22′ 08″ E. St Lucia Formation.
Age. Santonian I.

Loc. 85. Low cliff and foreshore exposures extending from 1200 to 1800 m north of Picnic Point, SW shores of False Bay, east of Hluhluwe, 20° 01′ 17″ S, 32° 22′ 08″ E. St Lucia Formation.
Age. Santonian I.

Loc. 86. Line of concretions striking across the foreshore 750 m north of Picnic Point, SW shores of False Bay, east of Hluhluwe, 28° 01′ 45″ S, 32° 22′ 03″ E. St Lucia Formation.
Age. Coniacian V–Santonian I or II.

(ii) The Hluhluwe flood plain

South of Picnic Point, the alluvial flats of the Hluhluwe extend out into False Bay, and there are no major exposures for several miles down the coast. Instead, outcrops are limited to poor sections and loose boulders along the river cliffs on the sides of the Hluhluwe. This area is of some importance, being the type locality of van Hoepen's (1926 onwards) *Peroniceras* Beds, and the source of many Coniacian ammonites described by him (1966a–c). The cliffs run oblique to the strike, and progressively lower horizons appear to the SW.

(a) *Western side*

Loc. 87. Boulders and concretions littering hill slopes just east of the point where the track to Picnic Point descends to the flood plain of the Hluhluwe, ESE of Hluhluwe Village, 28° 02′ 10″ S, 32° 21′ 55″ E. St Lucia Formation.
Age. Santonian I.

Loc. 88. Loose boulders and concretions littering slopes over a radius of 200 m from 150 m west of the point where the track to Picnic Point descends to the flood plain of the Hluhluwe, ESE of Hluhluwe Village, 28° 02′ 12″ S, 32° 21′ 40″ E. St Lucia Formation.
Age. Coniacian IV–V, perhaps also Santonian I ?

Locs 89, 90. Boulder- and concretion-strewn slopes east and west respectively of the gully 250 m east of the western boundary of the St Lucia Game Reserve, ESE of Hluhluwe Village, 28° 02′ 16″ S, 32° 21′ 19″ E to 28° 02′ 20″ S, 32° 21′ 11″ E. St Lucia Formation.
Age. Coniacian IV.

Loc. 91. Degraded river cliffs and artificial cut extending over 200 m west of the boundary fence of the St Lucia Game Reserve and lot H 103 13368, ESE of Hluhluwe Village, 28° 02′ 21″ S, 32° 21′ 02″ E. St Lucia Formation.
Age. Coniacian IV or V.

Loc. 92. Bulldozer scrapings and adjacent hill slopes around the pumping station at the southern end of the track leading south from the farm Panplaas, on lot H 102 13364, ESE of Hluhluwe Village, 28° 03′ 07″ S, 32° 20′ 10″ E. St Lucia Formation.
Age. Coniacian II and III.

Loc. 93. Hill slopes extending 200 m on either side of the boundary fence of lots H 102 13364 and H 101 3046, 1600 m SE of the farm Ncedomhlope, ESE of Hluhluwe Village, 28° 03′ 19″ S 32° 20′ 00″ E. St Lucia Formation.
Age. Coniacian II.

(b) *Eastern side*

Locs 94–96. Shore outcrops SE of the end of the track running north of Nkundusi, ESE of Hluhluwe, 28° 03′ 50″ S, 32° 21′ 46″ E. St Lucia Formation.
Age. Coniacian V and Santonian I.

Loc. 97. Cliff section 2 km NE of Nkundusi, SE of Hluhluwe, 28° 04′ 42″ S, 32° 22′ 32″ E. St Lucia Formation.
Age. Santonian.

Loc. 98. Hill slopes alongside track leading north from Nkundusi, 2·0–2·3 km north of the village, SE of Hluhluwe, 28° 04′ 12″ S, 32° 21′ 14″ E. St Lucia Formation.
Age. Coniacian V ?

Loc. 99. Hill slopes alongside the track running north from Nkundusi, 1·0–1·5 km north of the village, SE of Hluhluwe, 28° 04′ 37″ S, 32° 21′ 26″ E. St Lucia Formation.
Age. Coniacian V.

Loc. 100. Hill slopes alongside track leading north from Nkundusi, 1·3 km north of the village, SE of Hluhluwe, 28° 04′ 47″ S, 32° 21′ 27″ E. St Lucia Formation.
Age. Santonian I.

Loc. 101. Slopes 250 m south of loc. 100, 28° 04′ 57″ S, 32° 21′ 26″ E. St Lucia Formation.
Age. Santonian II or III.

(iii) False Bay: SE shores

Loc. 102. Cliff exposure at SE end of False Bay east of Nkundusi, and SE of Hluhluwe, 28° 05′ 18″ S, 32° 23′ 02″ E. St Lucia Formation.
Age. Campanian I or II ?

Loc. 103. Hill slopes 1·6 km NNE of the mouth of the Nyalazi, SE of Hluhluwe, 28° 04′ 42″ S, 32° 23′ 37″ E. St Lucia Formation.
Age. Campanian II ?

Loc. 104. Cliff and foreshore exposures 2·3–2·7 km NNE of the mouth of the Nyalazi, SE of Hluhluwe, 28° 04′ 12″ S, 32° 23′ 38″ E. St Lucia Formation.
Age. Santonian II.

Loc. 105. Cliff section 3·5 km north of the mouth of the Nyalazi, ESE of Hluhluwe, 28° 03′ 27″ S, 32° 23′ 08″ E. St Lucia Formation.
Age. Santonian III to Campanian I.

Loc. 106. Cliffs 4·2 km north of the mouth of the Nyalazi, ESE of Hluhluwe, 28° 03′ 06″ S, 32° 23′ 16″ E. St Lucia Formation.
Age. Campanian I.

Loc. 107. Loose concretions on shore 400 m north of loc. 106, ESE of Hluhluwe, 28° 02′ 45″ S, 32° 23′ 26″ E. St Lucia Formation.
Age. Campanian ?

Loc. 108. Foreshore exposures 6 km north of the mouth of the Nyalazi, east of Hluhluwe, 28° 02′ 21″ S, 32° 23′ 32″ E. St Lucia Formation.
Age. Campanian I.

(iv) The Nibela Peninsula

This area is a Native Reserve, access is restricted, and we have only visited the southern coast. For long stretches this is a dip section across interbedded silts and concretions dipping at approximately 3° just south of east. Exposures consist of vertical cliffs up to 25 m high, capped by Miocene(?) and Pleistocene sediments, and broad foreshore exposures.

From the SW corner of the peninsula, and running northwards, the cliffs are degraded. We have not examined this area, rather relying on material in the South African Survey (van Hoepen Collection), nor have we examined the eastern side.

Loc. 109. Foreshore exposures at the SW tip of the Nibela Peninsula, 27° 59′ 03″ S, 32° 24′ 36″ E. St Lucia Formation.
Age. Campanian II.

Loc. 110. 150 m stretch of cliff and foreshore section at the SW tip of the Nibela Peninsula, 27° 59′ 10″ S, 32° 24′ 34″ E (Fig. 9). St Lucia Formation.
Age. Campanian III.

Loc. 111. Cliff section just east of the southernmost tip of the Nibela Peninsula, 27° 59′ 30″ S, 32° 25′ 26″ E. St Lucia Formation.
Age. Campanian III.

Loc. 112. Foreshore exposures 1·4 km north of Hell's Gate, Nibela Peninsula, 27° 58′ 47″ S, 32° 25′ 49″ E. St Lucia Formation.
Age. Campanian III.

Loc. 113. Cliff section at the SE corner of the Nibela Peninsula, 27° 58′ 12″ S, 32° 26′ 57″ E. St Lucia Formation.
Age. Campanian IV–V.

(v) The Southern Peninsula

Loc. 114. Foreshore exposures at the NW tip of the peninsula, 28° 00′ 51″ S, 32° 24′ 44″ E. St Lucia Formation.
Age. Campanian II.

Loc. 115. Foreshore exposures NW of Lake Pisechene, 28° 01′ 03″ S, 32° 25′ 32″ E. St Lucia Formation.
Age. Campanian III.

Loc. 116. Cliff section NE of Lake Pisechene, 28° 01′ 06″ E, 32° 26′ 04″ E. St Lucia Formation.
Age. Campanian IV.

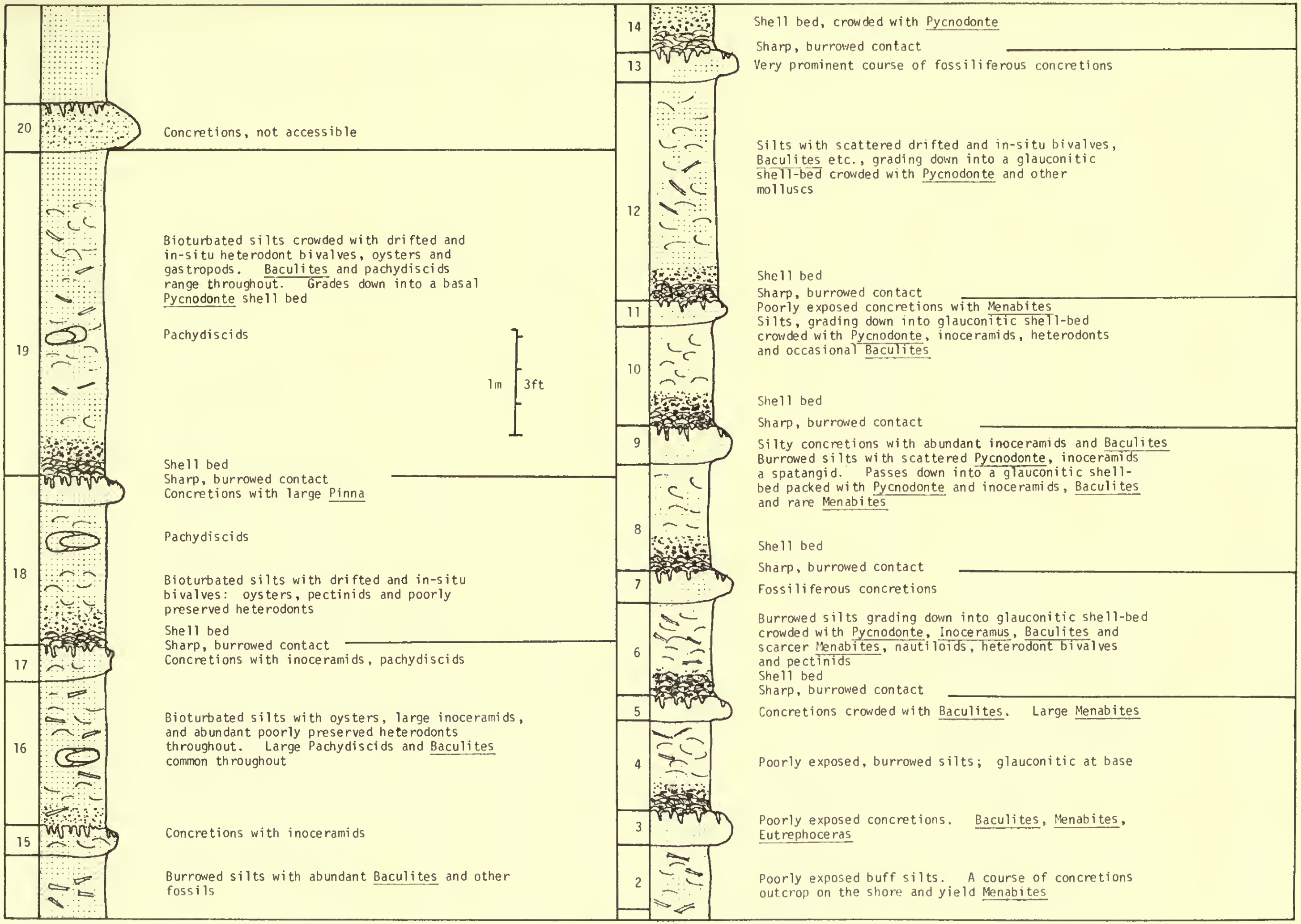
20
Concretions, not accessible
19
Bioturbated silts crowded with drifted and in-situ heterodont bivalves, oysters and gastropods. Baculites and pachydiscids range throughout. Grades down into a basal Pycnodonte shell bed
Pachydiscids
1m
3ft
Shell bed
Sharp, burrowed contact
Concretions with large Pinna
18
Pachydiscids
Bioturbated silts with drifted and in-situ bivalves: oysters, pectinids and poorly preserved heterodonts
Shell bed
Sharp, burrowed contact
17
Concretions with inoceramids, pachydiscids
16
Bioturbated silts with oysters, large inoceramids, and abundant poorly preserved heterodonts throughout. Large Pachydiscids and Baculites common throughout
15
Concretions with inoceramids
Burrowed silts with abundant Baculites and other fossils
14
Shell bed, crowded with Pycnodonte
Sharp, burrowed contact
13
Very prominent course of fossiliferous concretions
12
Silts with scattered drifted and in-situ bivalves, Baculites etc., grading down into a glauconitic shell-bed crowded with Pycnodonte and other molluscs
Shell bed
Sharp, burrowed contact
11
Poorly exposed concretions with Menabites
10
Silts, grading down into glauconitic shell-bed crowded with Pycnodonte, inoceramids, heterodonts and occasional Baculites
Shell bed
Sharp, burrowed contact
9
Silty concretions with abundant inoceramids and Baculites
8
Burrowed silts with scattered Pycnodonte, inoceramids a spatangid. Passes down into a glauconitic shell-bed packed with Pycnodonte and inoceramids, Baculites and rare Menabites
Shell bed
Sharp, burrowed contact
7
Fossiliferous concretions
6
Burrowed silts grading down into glauconitic shell-bed crowded with Pycnodonte, Inoceramus, Baculites and scarcer Menabites, nautiloids, heterodont bivalves and pectinids
Shell bed
Sharp, burrowed contact
5
Concretions crowded with Baculites. Large Menabites
4
Poorly exposed, burrowed silts; glauconitic at base
3
Poorly exposed concretions. Baculites, Menabites, Eutrephoceras
2
Poorly exposed buff silts. A course of concretions outcrop on the shore and yield Menabites

FIG. 9. The sequence at loc. 110.

Loc. 117. Beach exposures at Hell's Gate, the extreme NE tip of the peninsula, 28° 00′ 36″ S, 32° 26′ 48″ E. St Lucia Formation.
Age. Campanian IV.

(vi) Lake St Lucia

Locs 118–121. The Coves, and cliff sections for 2 km to the north and 3 km to the south, eastern shores of the Southern Peninsula. St Lucia Formation.

Loc. 118.	28° 00′ 58″ S, 32° 26′ 49″ E.	Loc. 120.	28° 03′ 23″ S, 32° 26′ 27″ E.
Loc. 119.	28° 02′ 48″ S, 32° 26′ 47″ E.	Loc. 121.	28° 03′ 57″ S, 32° 26′ 32″ E.

Age. Campanian III–IV.

Locs 122–125. Foreshore platforms 1200, 1600, 1900 and 2200 m north of Fanies Island Camp, eastern shores of the Southern Peninsula. St Lucia Formation.

Loc. 122.	28° 05′ 39″ S, 32° 26′ 22″ E.	Loc. 124.	28° 04′ 57″ S, 32° 26′ 25″ E.
Loc. 123.	28° 05′ 19″ S, 32° 26′ 25″ E.	Loc. 125.	28° 04′ 40″ S, 32° 26′ 30″ E.

Age. Campanian III–IV.

Loc. 126. Foreshore exposure 700 m south of the shore track leading south from Fanies Island Camp, 28° 07′ 27″ S, 32° 25′ 56″ E. St Lucia Formation.
Age. Maastrichtian II.

Loc. 127. Foreshore exposures 1·8 km south of Fanies Island Camp, 28° 07′ 40″ S, 32° 25′ 56″ E. St Lucia Formation.
Age. Maastrichtian.

Loc. 128. Cliff and foreshore exposures 2·7 km south of Fanies Island Camp, 28° 08′ 02″ S, 32° 25′ 58″ E. St Lucia Formation.
Age. Maastrichtian III.

Locs 129, 130. Cliff and shore sections from 4·4 to 5·2 km south of Fanies Island Camp, 28° 08′ 59″ S, 32° 25′ 47″ E to 28° 09′ 23″ S, 32° 25′ 41″ E. St Lucia Formation.
Age. Maastrichtian III.

Loc. 131. Low cliff and foreshore section 3·1 km north of Charter's Creek Rest Camp, 28° 09′ 53″ S, 32° 25′ 37″ E. St Lucia Formation.
Age. Maastrichtian II.

Loc. 132. Degraded cliff and shore platform 300 m NE of the northern jetty at Charter's Creek Rest Camp, 28° 11′ 32″ S, 32° 25′ 17″ E. St Lucia Formation.
Age. Maastrichtian I.

Loc. 133. Cliff section and beach platforms below Charter's Creek Rest Camp, 28° 12′ 38″ S, 32° 28′ 08″ E. St Lucia Formation.
Age. Maastrichtian I.

Loc. 134. Cliffs and foreshore 1·2 km south of Charter's Creek Rest Camp, 28° 12′ 59″ S, 32° 25′ 08″ E. St Lucia Formation.
Age. Maastrichtian I.

Loc. 135. Foreshore outcrops in Makakatana Bay, east of the village, 28° 13′ 51″ S, 32° 25′ 08″ E. St Lucia Formation.
Age. Maastrichtian I.

J. The Mkuze River and its tributaries

North of Lake St Lucia, the coastal plain east of the Lebombo Mountains is covered by Miocene to Pliocene marine sediments and Pleistocene to Recent dune sands. Exposures of the Cretaceous are very poor, and are restricted to cliffs and pans along the Mkuze and its tributaries.

Scattered exposures show Lebombo Volcanics overlain by conglomeratic Makatini Formation with marine Upper Aptian fossils at the summit. Above the Aptian/Albian non-sequence, Albian rocks are well exposed, and to the west there are isolated outcrops of Coniacian and Santonian sediments.

(i) Southern part of Mkuze Game Reserve

Loc. 136. Banks of rivulet west of the road leading to the mine, 27° 44′ 08″ S, 32° 16′ 50″ E. Makatini Formation.
Age. Pre-Aptian ?

Loc. 137. Trackside exposures 1·5 km NNW of the old Msunduze drift along the road leading to the mine, 27° 44′ 25″ S, 32° 16′ 54″ E. Makatini Formation.
Age. Aptian ?

Loc. 138. Rivulet 800 m NE of the landing strip on Nxala Estate, 27° 43′ 06″ S, 32° 16′ 38″ E. Makatini Formation.
Age. Aptian IV.

Loc. 139. Roadside section and hillside on Nxala Estate 2·3 km NNE of Mt Nxala, 27° 41′ 18″ S, 32° 15′ 30″ E. Makatini Formation.
Age. Aptian IV.

Loc. 140. Large working quarry south of road and west of Nsumu Pan, 27° 40′ 16″ S, 32° 15′ 18″ E. Makatini Formation.
Age. Aptian IV.

Loc. 141. Hill slopes 750 m NNE of the previous locality. 27° 39′ 52″ S, 32° 15′ 22″ E. Makatini Formation.
Age. Aptian IV.

Loc. 142. Hillside east of track leading to the mine, 27° 44′ 24″ S, 32° 17′ 12″ E. Makatini and Mzinene Formations.
Age. Aptian IV ? ; Albian III.

Loc. 143. Small outcrops east of road by unnamed pan 3 km north of drift over Msunduze, 27° 43′ 12″ S, 32° 17′ 20″ E. Mzinene Formation.
Age. Albian III.

Loc. 144. Low ridge on SW side of Nsumu Pan at mouth of unnamed northwards-flowing rivulet, 27° 41′ 19″ S, 32° 17′ 50″ E. Mzinene Formation.
Age. Albian V.

(ii) The Morrisvale Area

Loc. 145. Degraded cliffs on the eastern side of the Msunduzi, 3 km SW of the farm Morrisvale, north of Ngweni, 27° 42′ 28″ S, 32° 20′ 56″ E. St Lucia Formation. This locality extends for several hundred metres, with a few metres of silts and concretions sporadically exposed in the steep slopes between the flood plain and lowest terrace of the Msunduzi. The locality is of great importance, for it represents one of the sections which van Hoepen (1926, 1929) and others (e.g. Furon 1963) recognized as Turonian, and is said to be characterized by large oysters. In fact, the Cretaceous sequence is capped by a basal conglomerate and limestone rubble of Miocene(?) age, which yields the oysters, in turn capped by Pleistocene sands. The Cretaceous rocks are poorly exposed, but loose boulders and excavations reveal richly fossiliferous horizons, crowded with bivalves, both drifted and in life position. One level of concretions is crowded with ammonites, especially *Proplacenticeras*, together with scarcer *Yabeiceras*, *Forresteria*, *Peroniceras* and nautiloids.
Age. Coniacian II.

Loc. 146. Quarry 1·71 km NW of the farm Morrisvale, on the south bank of the Mkuze, east of its junction with the Msunduzi, 27° 40′ 36″ S, 32° 22′ 03″ E. St Lucia Formation.
Age. Santonian.

Loc. 147. Hill slopes in the Bantu area 4 km north of the confluence of the Mkuze and Msunduze, north of Ngweni, 27° 38′ 23″ S, 32° 22′ 22″ E. St Lucia Formation.
Age. Santonian.

(iii) Mantuma Rest Camp Area

Loc. 148. River cliff on west bank of Mkuze due east of Ndlelakufa Pan, 27° 34′ 55″ S, 32° 11′ 50″ E. Makatini Formation.
Age. Aptian or pre-Aptian.

Loc. 149. Southern cliffs of Nhlohlela Pan, 2 km west of Mantuma Camp, 27° 35′ 38″ S, 32° 12′ 05″ E. Makatini Formation.
Age. Aptian or pre-Aptian.

Loc. 150. Cliff section on southern side of Nhlohlela Pan, 1·3 km west of Mantuma Camp, 27° 35′ 48″ S, 32° 12′ 28″ E. Makatini Formation.
Age. Aptian III–IV.

Loc. 151. Hill slopes on eastern side of Nhlohlela Pan, 1 km WNW of Mantuma Camp, 27° 35′ 28″ S, 32° 12′ 53″ E. Makatini Formation.
Age. Aptian IV.

Loc. 152. Hill slopes south of road leading to Nhlohlela Pan from Denyer's Drift, 500 m west of Mantuma Camp, 27° 35′ 39″ S, 32° 12′ 53″ E. Makatini and Mzinene Formations.
Age. Aptian IV, Albian II–III.

Loc. 153. Site excavations for reservoir in Mantuma Camp, just east of Denyer's Drift, 27° 35′ 36″ S, 32° 13′ 10″ E. Mzinene Formation.
Age. Albian III, IV ?

Loc. 154. Abandoned road metal quarry south of track 500 m east of Mantuma Camp, 27° 35′ 33″ S, 32° 13′ 38″ E. Mzinene Formation.
Age. Albian III–IV ?

Loc. 155. Gully on south side of the Ndlamyane at Gujini, NE of the road leading NW from Mantuma Camp, 27° 32′ 54″ S, 32° 10′ 48″ E. Makatini Formation.
Age. Aptian.

Loc. 156. Bed of Ndlamyane, 600 m downstream from loc. 155, 27° 32′ 42″ S, 32° 11′ 20″ E. Mzinene Formation.
Age. Albian III.

K. Northern Zululand

This term covers the area from Jozini north to Ndumu, on the Mozambique border. In this region, the crest of the Lebombos rises to more than 600 m, the volcanics dipping east at 2°–3°. Dip slopes descend to the level of the coastal plain, with spurs extending eastwards into the littoral, west of the Pongola.

The coastal plain itself has an average elevation of less than 100 m, rising to 180 m in the Ndumu region. The Cretaceous succession has been truncated by a series of Tertiary transgressions, the deposits of which, together with Pleistocene and Recent dune sands, mask the whole area. Outcropping Cretaceous accounts for less than 1 per cent of the region. Sections are thus confined to areas where streams and gullies draining west from the Lebombos to join the Pongola cut through the Tertiary cover, and a few natural exposures and quarries, chiefly

in the high ground around Ndumu. We have seen no exposures on the littoral, east of the Pongola, nor have we been able to examine sections along the Usutu and in the Ndumu Game Reserve.

(i) Mayezela Spruit

This is Myesa Spruit of Haughton (1936a : 285) ; there are exposures both east and west of the drift on the dirt road from Jozini to Ndumu, 4·2 km NNE of the store at Otobotini.

To the west, platy rhyolites are well exposed, dipping in an easterly direction at about 10°. The base of the Cretaceous is not visible, but on the high ground east of the crossing on the northern branch, buff, coarse sandstones are well exposed.

Loc. 157. Gullies just east of the road, beyond the drift on the north branch of the Mayezela Spruit, 10 km NE of Jozini, 27° 22′ 45″ S, 32° 06′ 43″ E. Makatini Formation.
Age. Pre-Upper Aptian.

(ii) Mfongosi Spruit

Horizons from Lebombo Volcanics through conglomerates and up into marine Aptian and Albian are exposed along this section, which lies 8 km NNE of Otobotini. A valuable account and guide to this section is given by Haughton (1936a : 286), although it must be noted that the present dirt track crosses the spruit 1·5 km east of the track shown by him (1936a : fig. 2).

Cretaceous sediments are exposed in the bed and walls of the deep gully cut by the Mfongosi, and along degraded bluffs, capped by river gravels, both north and south of the present stream bed.

Loc. 158. Cliffs on the north side of the north branch of the Mfongosi, 800 m NW of the drift and 400 m from the junction with the main stream, 27° 21′ 20″ S, 32° 07′ 18″ E. Makatini Formation.
Age. Pre-Upper Aptian.

Loc. 159. Cliff on the south side of the Mfongosi, 100 m NW of the drift, 27° 21′ 30″ S, 32° 04′ 25″ E. Makatini Formation.
Age. Pre-Upper Aptian.

Loc. 160. Cliff on south side of stream, at bend 400 m SE of the drift, 27° 21′ 50″ S, 32° 07′ 45″ E. Makatini Formation.
Age. Pre-Upper Aptian.

Loc. 161. Sheer cliff at the bend of the stream 550 m east of the drift, 27° 21′ 38″ S, 32° 08′ 00″ E. Makatini Formation.
Age. Pre-Upper Aptian.

Loc. 162. Cliff on south side of the stream 1200 m SE of the drift, 27° 21′ 57″ S, 32° 08′ 15″ E. Makatini Formation.
Age. Aptian.

Loc. 163. Cliff on the north side of the stream, just east of the old drift, 27° 21′ 39″ S, 32° 08′ 30″ E. Makatini Formation.
Age. Haughton (1936a : 288) records *Acanthoplites* spp. from this section, which thus appears to be Aptian III.

Loc. 164. River cliff on the north side of the stream, 200 m NE of the old drift, 27° 21′ 36″ S, 32° 08′ 32″ E. Makatini Formation.
Age. Aptian III.

Loc. 165. Cliff and cliff-top exposure on the south side of the stream 450 m SE of the old drift, 27° 21′ 58″ S, 32° 08′ 43″ E. Makatini Formation.
Age. Aptian III.

Locs 166, 167. Bluffs on the north side of the spur running eastwards from loc. 165, 27° 22′ 02″ S, 32° 08′ 53″ E to 27° 22′ 04″ S, 32° 09′ 03″ E. Makatini Formation.
Age. Aptian III (loc. 166) ; Aptian III–IV (loc. 167).

Loc. 168. Bluffs along the ridge on the north side of the stream, 700–1200 m ESE of the old drift, 27° 21′ 43″ S, 32° 09′ 25″ E (Fig. 10). Makatini Formation.
Age. Aptian III–IV.

Loc. 169. Gully and adjacent hill slopes on the north side of the stream 2 km east of the old drift, 27° 31′ 38″ S, 32° 09′ 57″ E (Fig. 10). Makatini and Mzinene Formations.
Age. Aptian IV, Albian II, III.

(iii) Mlambongwenya Spruit

This stream section (Lombangwena Spruit of Haughton 1936a : 292) lies 20 km NNE of the Mfongosi sections. It is the most important section in Northern Zululand, for it provides the only known exposures of fossiliferous Barremian marine sediments, previously unknown in southern Africa. To the east, around Mlambongwenya Store, there are magnificent sections across the Aptian–Albian boundary.

Loc. 170. Cliff and gully sections 2 km NW of the store, on the north side of the stream, 27° 10′ 10″ S, 32° 10′ 13″ E (Fig. 11). Makatini Formation.
Age. Barremian I–II, Aptian I–II.

Loc. 171. River cliff north of the stream, and hill slopes above, 250 m WSW of the store, 27° 10′ 59″ S, 32° 11′ 08″ E. Makatini and Mzinene Formations.
Age. Aptian IV, Albian II–III.

Loc. 172. Cliff section on the south side of the stream, 100 m west of the drift, 27° 11′ 37″ S, 32° 11′ 25″ E. Makatini Formation.
Age. Aptian IV.

Loc. 173. Steep cliff on the south side of the creek 300 m below the drift, 27° 11′ 37″ S, 32° 11′ 45″ E. Makatini Formation.
Age. Albian II–III.

Loc. 174. Shallow excavations and road sections extending from the store south towards the drift, 27° 11′ 02″ S, 32° 11′ 21″ E. Mzinene Formation.
Age. Albian III.

(iv) Ndumu

The occurrence of Cretaceous outcrops in the Ndumu region was known already to Anderson (1907 : 61). The area was briefly described by Dietrich (1938), whilst Spath (1925) described a *Sharpeiceras* which we believe to be from this area. Exposures occur along the north bank of the Msunduzi, on hill slopes, south from Ndumu Store to the river, and around the police station ; horizons from low in the Albian to the Lower Cenomanian are exposed (Fig. 12).

Loc. 175. Exposures in and around gully west of the track leading SW from Ndumu, in Impala, 300 m south of Quotho Pan, 26° 56′ 22″ S, 32° 12′ 48″ E. Mzinene Formation.
Age. Albian II–III.

Loc. 176. Slopes south of track and north of Quotho Pan across the boundary of Impala and Wisteria 18122 locations, 26° 55′ 59″ S, 32° 18′ 04″ E. Mzinene Formation.
Age. Albian III.

Loc. 177. Field along the north side of the Msunduzi Pan in Wisteria 18122 location, 2 km SW of Ndumu Store, 26° 56′ 08″ S, 32° 13′ 57″ E. Mzinene Formation.
Age. Albian IV–V.

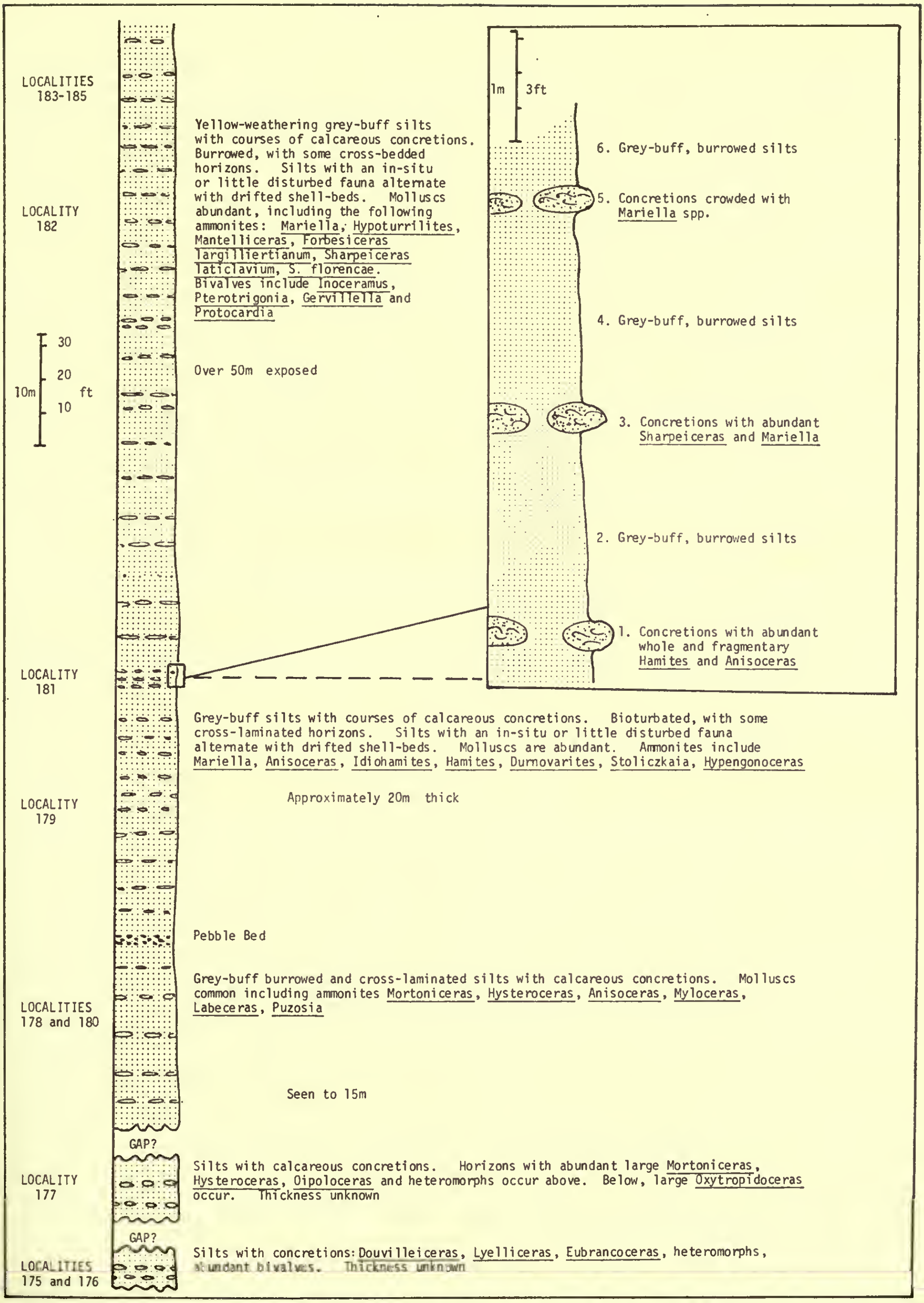

Yellow-weathering grey-buff silts with courses of calcareous concretions. Burrowed, with some cross-bedded horizons. Silts with an in-situ or little disturbed fauna alternate with drifted shell-beds. Molluscs abundant, including the following ammonites: Mariella, Hypoturrilites, Mantelliceras, Forbesiceras largilliertianum, Sharpeiceras laticlavium, S. florencae. Bivalves include Inoceramus, Pterotrigonia, Gervillella and Protocardia

Over 50m exposed

6. Grey-buff, burrowed silts

5. Concretions crowded with Mariella spp.

4. Grey-buff, burrowed silts

3. Concretions with abundant Sharpeiceras and Mariella

2. Grey-buff, burrowed silts

1. Concretions with abundant whole and fragmentary Hamites and Anisoceras

Grey-buff silts with courses of calcareous concretions. Bioturbated, with some cross-laminated horizons. Silts with an in-situ or little disturbed fauna alternate with drifted shell-beds. Molluscs are abundant. Ammonites include Mariella, Anisoceras, Idiohamites, Hamites, Durnovarites, Stoliczkaia, Hypengonoceras

Approximately 20m thick

Pebble Bed

Grey-buff burrowed and cross-laminated silts with calcareous concretions. Molluscs common including ammonites Mortoniceras, Hysteroceras, Anisoceras, Mylocеras, Labeceras, Puzosia

Seen to 15m

Silts with calcareous concretions. Horizons with abundant large Mortoniceras, Hysteroceras, Oipoloceras and heteromorphs occur above. Below, large Oxytropidoceras occur. Thickness unknown

Silts with concretions: Douvilleiceras, Lyelliceras, Eubrancoceras, heteromorphs, abundant bivalves. Thickness unknown

FIG. 12. The sequence around Ndumu, locs 175–185.

Loc. 178. Sisal field north of Msunduzi Pan, on Ndumu A location, 1400 m SW of Ndumu Store, 26° 56′ 14″ S, 32° 14′ 25″ E. Mzinene Formation.
Age. Albian V–VI.

Loc. 179. Sisal fields north of the Msunduzi around the pumping station 2100 m SSW of Ndumu Store, 26° 56′ 28″ S, 32° 14′ 55″ E. Mzinene Formation.
Age. Albian V–VI.

Loc. 180. Concretions in the bed of the Msunduzi by the bridge 1·8 km SSE of Ndumu Store, 26° 56′ 18″ S, 32° 15′ 25″ E. Mzinene Formation.
Age. Albian V.

Loc. 181. Hill slopes east of the road, 1 km SE of Ndumu Store, 26° 55′ 51″ S, 32° 18′ 29″ E. Mzinene Formation.
Age. Albian V, Cenomanian I–II.

Loc. 182. Ground surfaces over a radius of 300 m from Ndumu Store, 26° 55′ 38″ S, 32° 15′ 13″ E. Mzinene Formation.
Age. Cenomanian II.

Loc. 183. Degraded quarry east of the road and 300 m SW of Ndumu police post, 26° 55′ 10″ S, 32° 15′ 45″ E. Mzinene Formation.
Age. Cenomanian II.

Locs 184, 185. Hill slopes 600 m south and 500 m WSW of Ndumu police post, 26° 55′ 28″ S, 32° 15′ 57″ E and 26° 51′ 18″ S, 32° 16′ 10″ E. Mzinene Formation.
Age. Cenomanian II.

Loc. 186. Makaane's Drift, 7·7 km south of Ndumu, 26° 59′ 28″ S, 32° 16′ 13″ E. Mzinene Formation.
Age. Albian VI.

VIII. DISCUSSION

The review and detailed description of sections given above outlines in broad terms the history of eastern South Africa during the Cretaceous.

In Zululand, actual exposures account for less than 1 per cent of the area currently shown on the 1 : 5 000 000 Carte Géologique d'Afrique (AGSA/UNESCO 1963). In spite of this, we have been able to estimate a thickness of at least a kilometre for the succession in the Mzinene–St Lucia region. The succession thickens markedly north-eastwards, presumably towards the centre of the basin. The Lower Cenomanian, of the order of 10 m in thickness along the Mzinene, has thus thickened to 100 m at Ndumu. In the same direction, progressively lower marine horizons appear, including previously unsuspected Upper Barremian sediments. Offshore, we would infer that even lower marine horizons are present, and that there is a continuous marine succession through the whole of the Cretaceous. The non-sequences we have noted are thus probably features of the marginal areas of the basin only, and borehole data suggest that marine sedimentation extended continuously into the Palaeocene.

A number of striking features of the succession are worthy of note at this point. The bulk of the marine sequence consists of glauconitic silt–sand grade clastics; pure clays are rare. Conglomerates are confirmed to the basal parts of the sequence or to minor units associated with breaks in the succession. Throughout the sequence, small-scale faunal/sedimentary cycles are conspicuous. These frequently take the form of alternations of drifted shell-beds, and silts with an *in situ* fauna, or sequences in which the sediment becomes finer in grade upwards. The base of each sequence is crowded with pelletal glauconite and rests on a sharp sedimentary discontinuity.

Small-scale sedimentary structures are singularly lacking throughout much of the sequence, especially the Mzinene and St Lucia Formations. This is due mainly to intense biogenic reworking of the sediment. Diagnostic trace-fossils are rare, but arthropod burrows (especially *Thalassinoides*) and *Chondrites* are abundant.

At several levels, high energy episodes disinterred early diagenetic concretions, which were subsequently bored by lithodomous bivalves, and encrusted by oysters, serpulids and other epizoans (Kennedy & Klinger 1972). These horizons are present in the Aptian and Lower Albian, where they indicate minor breaks in sedimentation. The 'hardground' at the Aptian/Albian boundary, however, is a palaeontologically detectable non-sequence and can be traced from Ndumu Spruit to the Nyalazi River. The bored surfaces of the concretions below the *Pterotrigonia shepstoni* conglomerate of Skoenberg represents part of Cenomanian, all Turonian and some of Coniacian time.

Faunally, the Zululand Group is impressive. Our collection of ammonites is fairly complete, but the few thousand bivalves and gastropods collected represent only a fraction of the diverse fauna awaiting systematic and palaeoecological analysis. Macroinvertebrate groups other than the Bivalvia, Gastropoda and Cephalopoda form only a minority of the fauna. Belemnites occur in numbers only in the Aptian. Echinoids are scarce save for a few levels in the Albian and Cenomanian. Brachiopods are common at only two levels in the Albian, although they range from Aptian to Maastrichtian.

Ahermatypic corals are common only in the Cenomanian ; only one hermatype is known, and is of Aptian age. Arthropods range throughout but (except cirripede bores and ubiquitous burrows) are rare. Serpulids are frequent throughout ; bryozoans less so. We have seen no macroscopic sponge remains.

Vertebrates are not common. Other than fish fragments (largely teeth) we have noted occurrences of large reptilian remains only in the Lower Albian and the Santonian–Lower Campanian. In contrast, plant remains are incredibly abundant from the Barremian through to the Lower Campanian. Logs, up to several metres long and 60 cm in diameter, are common at many levels, and in the Barremian–Aptian there is a series of log beds. Lignite chips form an appreciable portion of the sediment at many levels up into the Campanian.

Many of the above comments can also be applied to the Umzamba Formation below and south of Durban. There, the bulk of the clastic material is sand–silt sized, although a coarser glauconite fraction is more conspicuous than to the north. Small-scale sedimentary rhythms are present and the sequence is bioturbated. The fauna of the Umzamba Formation is far better documented than that of the Zululand Series. It is predominantly molluscan ; we know of one coral, no brachiopods, belemnites, nor macroscopic sponge remains. Echinoids are scarce, save at one horizon ; arthropods (cirripede bores and burrows excepted) are absent. Serpulids and bryozoans range throughout. Wood, with logs several metres long, is abundant. Lignite chips form an appreciable part of the sediment. Vertebrates are relatively common at the base of the sequence; Broom (1907) records a large mosasaur, a plesiosaur and abundant chelonian debris. Woodward (1907) records elasmobranch and teleost teeth.

IX. ACKNOWLEDGEMENTS

The visit to South Africa by one of us (W. J. K.) was made possible by a grant from the Trustees of the Sir Henry Strakosch Bequest, which is gratefully acknowledged, as is the assistance of the staff of the Union Corporation (Johannesburg), the Natal Parks Board, and the South African Geological Survey. Mrs J. Hobday, Dr D. Hobday, Professor L. C. King, Dr N. M. Savage, Mr J. Mcarthy, Mr M. Cooper and Miss G. Lambert, all of Durban, assisted in many ways. Dr H. W. Ball, Dr M. K. Howarth, Dr N. J. Morris, Mr D. Phillips, Mr R. J. Cleevely and Mr C. P. Nuttall of the British Museum (Natural History) provided invaluable assistance in London.

We are both grateful to Mr P. J. Rossouw for his help and encouragement in ways too numerous to mention, to Mr Johannes Nonyane for his help in the field, and to the many farmers, land owners and others who rendered our fieldwork so profitable.

To the Director, South African Geological Survey, we are indebted for permission to publish the data contained herein.

X. REFERENCES

Anderson, W. 1902. Report on a reconnaissance Geological Survey of the eastern half of Zululand with a geological sketch map of the country traversed. *Rep. geol. Surv. Natal Zululand*, Pietermaritzburg, **1** : 37–66, pl. 19.

—— 1904. Further notes on the reconnaissance Geological Survey of Zululand. *Ibid.* **2** : 39–67.

—— 1906. On the geology of the Bluff Bore, Durban, Natal. *Trans. geol. Soc. S. Afr.*, Johannesburg, **9** : 111–113.

—— 1907. The Upper Cretaceous rocks of Natal and Zululand. *Rep. geol. Surv. Natal Zululand*, Pietermaritzburg, **3** : 47–64.

Basse, E. 1947. Paléontologie de Madagascar 26. Les peuplements Malgaches de *Barroisiceras*. Révision du genre *Barroisiceras* de Gross. *Annls Paléont.*, Paris, **33** : 100–190, 9 pls.

Besaire, H. 1930. Les rapports du Crétacé Malgache avec le Crétacé de l'Afrique australe. *Bull. Soc. géol. Fr.*, Paris, (4) **30** : 613–643, pls 64–67.

—— & Lambert, J. 1930. Note sur quelques échinides de Madagascar et du Zululand. *Bull. Soc. géol. Fr.*, Paris, **30** : 107–117, 2 pls.

Boshoff, J. C. 1945. *Stratigraphy of the Cretaceous System in the Nduma area of Northern Zululand* (unpublished M.Sc. Thesis, University of Pretoria).

Bouché, P. M. 1965. Nannofossiles calcaires. *Mém. Bur. Rech. géol. minièr.*, Paris, **34** : 131–138.

Broom, R. 1907. On some reptilian remains from the Cretaceous Beds at the mouth of the Umpenyati River. *Rep. geol. Surv. Natal Zululand*, Pietermaritzburg, **3** : 95.

—— 1912. On a species of *Tylosaurus* from the Upper Cretaceous Beds of Pondoland. *Ann. S. Afr. Mus.*, Cape Town, **7** : 332–333, pl. 22.

BUSNARDO, R. 1965a. Lithologie et macrofaune. *In* Le Stratotype du Barrémien. Colloque sur le Crétacé Inférieur. *Mém. Bur. Rech. géol. minièr.*, Paris, **34** : 101–116.

—— 1965b. Rapport sur l'étage Barremien. *Ibid.* : 161–169.

CASEY, R. 1961. The stratigraphical palaeontology of the Lower Greensand. *Palaeontology*, London, **3** : 487–621, pls 77–84.

CHAPMAN, F. 1904. Foraminifera and Ostracoda from the Cretaceous of East Pondoland, South Africa. *Ann. S. Afr. Mus.*, Cape Town, **4** : 221–237, pl. 29.

—— 1923. On some Foraminifera and Ostracoda from the Cretaceous of Umzamba River, Pondoland. *Trans. geol. Soc. S. Afr.*, Johannesburg, **26** : 1–6, pl. 1.

COLLIGNON, M. 1959. Corrélations sommaires entre les dépôts du Crétacé Supérieur de Madagascar et ceux de l'Europe occidentale, en particulier de la France. *In* Colloque sur le Crétacé Supérieur Français. *C. r. Congr. Socs sav. Paris Sect. Sci.* (Dijon), **1959** : 41–52.

—— 1965a. L'Albien à Madagascar. Ses subdivisions comparées à celles de l'Europe occidentale : essai de chronostratigraphie aussi générale que possible. *Mém. Bur. Rech. géol. minièr.*, Paris, **34** : 303–310.

—— 1965b. *Atlas des Fossiles Caractéristiques de Madagascar* (*Ammonites*) **13** (Coniacien). 88 pp., pls 415–454. Serv. Géol., Tananarive.

COQUAND, D. H. 1857. Sur le position des *Ostrea columba* et *biauriculata* dans le groupe de la Craie Inférieur. *Bull. Soc. géol. Fr.*, Paris, **14** : 745–770.

—— 1862. Sur la convenance d'établir dans le groupe inférieur de la formation crétacée un nouvel étage entre le néocomien proprement dit (couches à *Toxaster complanatus* et à *Ostrea couloni*) et le néocomien supérieur (étage urgonien d'Alc. d'Orbigny). *Bull. Soc. géol. Fr.*, Paris, (2) **19** : 531–541.

CRICK, G. C. 1907a. The Cephalopoda from the deposit at the North End of False Bay, Zululand. *Rep. geol. Surv. Natal Zululand*, Pietermaritzburg, **3** : 163–234, pls 10–15.

—— 1907b. The Cephalopoda from the tributaries of the Manuan Creek, Zululand. *Ibid.* : 235–249.

—— 1907c. Note on a Cretaceous ammonite from the mouth of the Umpenyati River, Natal. *Ibid.* : 250.

—— 1907d. The Cretaceous rocks of Natal and Zululand and their Cephalopod fauna. *Geol. Mag.*, London, **4** : 339–347.

DALBIEZ, M. F. 1959. Rapport V : Corrélations et résolutions. *In* Colloque sur le Crétacé Supérieur Français. *C. r. Congr. Socs sav. Paris Sect. Sci.* (Dijon), **1959** : 857–867.

DAVEY, R. J. 1969. Some dinoflagellate cysts from the Upper Cretaceous of northern Natal, South Africa. *Palaeont. afr.*, Johannesburg, **12** : 1–23, 4 pls.

DESTOMBES, P. & DESTOMBES, J. P. 1965. Distribution zonale des ammonites dans l'Albien du Bassin de Paris. *Mém. Bur. Rech. géol. minièr.*, Paris, **34** : 255–270.

DIETRICH, W. O. 1938. Zur Stratigraphie der Kreide im nordlichen Zululand. *Zentbl. Miner. Geol. Paläont.*, Stüttgart, (B) **1938** : 228–240.

DINGLE, R. V. 1969. Upper Senonian ostracods from the coast of Pondoland, South Africa. *Trans. R. Soc. S. Afr.*, Cape Town, **38** : 347–385, 21 figs.

DRUZHCHITZ, V. V. 1963a. Stratigraphic position of the *Colchidites* Beds, *Colchidites securiformis* Zone. *Dokl. Akad. Nauk. SSSR*, Leningrad, **147** : 115–117 (in Russian).

—— 1963b. The Hauterivian–Barremian boundary. *Ibid.* : 900–903 (in Russian).

DUMONT, A. 1850. Rapport sur la carte géologique du royaume. *Bull. Acad. r. Belg.*, Bruxelles, **16** : 351–373.

DU TOIT, A. L. 1920. *The Geology of Pondoland and portions of Alfred and Lower Umzimkulu Counties, Natal. An Explanation of Cape Sheet* **28** (*Pondoland*). 45 pp. Geological Survey, Pretoria.

—— 1954. *Geology of South Africa.* 3rd edition. 611 pp., 73 figs, 41 pls. Edinburgh.

—— & VAN HOEPEN, E. C. N. 1929. *Guide Book. Excursion C18, Durban–Zululand.* 20 pp. XV Int. geol. Congr. South Africa, Pretoria.

ERISTAVI, M. S. 1955. Fauna of the Lower Cretaceous of Georgia. *Monogr. Inst. Geol. Akad. Nauk Gruz. SSR*, Tiflis, **6** : 1–224, 8 pls (in Russian).

ETHERIDGE, R. 1904. Cretaceous fossils of Natal. 1. The Umkwelane Hill Deposit. *Rep. geol. Surv. Natal Zululand*, Pietermaritzburg, **2** : 71–93, pls 1–3.

—— 1907. Cretaceous fossils of Natal. 2. The Umzinene River Deposit, Zululand. *Ibid.* **3** : 67–90, pls 1–6.

FABRE-TAXY, S., MOULLADE, M. & THOMEL, G. 1965. Le Bédoulien dans sa région type, la Bédoule-Cassis (B.-du-R.). *In* Les Stratotypes de l'Aptien. *Mém. Bur. Rech. géol. minièr.*, Paris, **34** : 173–199.

FAURE, D. 1965. Le Barrémien du sud du couloir Rhodanien. *Mém. Bur. Rech. géol. minièr.*, Paris, **34** : 139–146.

FLANDRIN, J. 1965. Rapport sur l'étage Aptien. *Mém. Bur. Rech. géol. minièr.*, Paris, **34** : 227–234.

FRANKEL, J. J. 1960a. The geology along the Umfolozi River, south of Mtubatuba, Zululand. *Trans. geol. Soc. S. Afr.*, Johannesburg, **63** : 231–252, pls 33–36.

—— 1960b. Late Mesozoic and Cenozoic events in Natal, South Africa. *Trans. N. Y. Acad. Sci.*, **22** : 565–577.

FURON, R. 1950. *Géologie de l'Afrique.* 350 pp., 34 figs. Paris.

—— 1963. *Geology of Africa.* 377 pp. Edinburgh.

GARDEN, R. J. 1855. Notice of some Cretaceous rocks near Natal, South Africa. *Q. Jl geol. Soc. Lond.*, **11** : 453–454.

GEVERS, T. W. & LITTLE, J. DE V. 1946. Upper Cretaceous beds between Intongazi and Umkandandhlobu Rivers, Alfred Country, Natal. *Trans. geol. Soc. S. Afr.*, Johannesburg, **48** : 27–29.

GÖTTSCHE, C. 1887. Ueber die obere Kreide von Umtafuna (S. Natal). *Z. dt. geol. Ges.*, Berlin, **39** : 622–624.

GRIESBACH, C. L. 1871. On the geology of Natal in South Africa. *Q. Jl Geol. Soc. Lond.*, **27** : 53–72, pls 2, 3.

GROSSOUVRE, A. DE 1894. Recherches sur la Craie Supérieure. **2**, Paléontologie. Les ammonites de la Craie Supérieure. *Mém. Serv. Carte géol. dét. Fr.*, Paris, 264 pp., atlas of 39 pls.

—— 1900. Types du Turonien de Touraine et du Cénomanien du Mans. *Excursion guide, VIII Int. géol. Congr.*, Paris, **5** : 1–10.

—— 1901. Recherches sur la Craie Supérieure. **1**, Stratigraphie générale. *Mém. serv. Carte géol. dét. Fr.*, Paris, 1013 pp.

GUILLAME, S. & SIGAL, J. 1965. Les Foraminifères. *Mém. Bur. Rech. géol. minièr.*, Paris, **34** : 117–129.

HAAS, O. 1942. The Vernay collection of Cretaceous (Albian) ammonites from Angola. *Bull. Am. Mus. nat. Hist.*, New York, **81** : 1–224, pls 1–47.

HALLOY, O. DE 1808. Essai sur la géologie du Nord de la France. *J. Mines, Paris*, **52** : 271–318.

HANCOCK, J. M. 1959. Les ammonites du Cénomanien de la Sarthe. *In* Colloque sur le Crétacé Supérieur Français. *C. r. Congr. Socs sav. Paris Sect. Sci.* (Dijon), **1959** : 249–259.

HAUGHTON, S. H. 1936a. Account of the geology of the Cretaceous Beds of Northern Zululand. *Ann. S. Afr. Mus.*, Cape Town, **31** : 283–294.

—— 1936b. Preliminary analysis of the ammonite fauna of Northern Zululand. *Ibid.* : 295–297.

—— 1959. *Geological Bibliography of Africa south of the Sahara. Bibliography of the Jurassic and Cretaceous Systems.* Commission de co-opération technique en Afrique au sud du Sahara. iii + 83 pp. London.

—— 1963. *The Stratigraphic History of Africa south of the Sahara.* xii + 365 pp. Edinburgh and London.

—— 1969. *Geological History of Southern Africa.* Geol. Soc. S. Afr. 535 pp. Cape Town.

HEINZ, R. 1930. Ueber Kreide-Inoceramen der südafrikanischen Union. *C. r. XV Int. geol. Congr.*, Cape Town, **2** : 681–687.

JUIGNET, P., KENNEDY, W. J. & WRIGHT, C. W. 1973. Remarques sur la limite Cenomanien–Turonien dans la région du Mans (Sarthe). *Annls Paléont., Paris*, **59** (Invert. 2) : 207–250, pls 1–3.

KENNEDY, W. J. 1969. The correlation of the Lower Chalk of south-east England. *Proc. Geol. Ass.*, London, **80** : 459–560, pls 15–22.

—— 1970. The correlation of the Uppermost Albian and Cenomanian of south-west England. *Ibid.* **81** : 613–675.

—— 1971. Cenomanian ammonites from southern England. *Spec. Pap. Palaeont.*, London, **8** : 133 pp., 64 pls.

—— & HANCOCK, J. M. 1971. *Mantelliceras saxbii* (Sharpe) and the horizon of the Martimpreyi Zone in the Cenomanian of England. *Palaeontology*, London, **14** : 437–454, pls 79–82.

—— & JUIGNET, P. 1973. Observations on the lithostratigraphy and ammonite succession across the Cenomanian–Turonian boundary in the environs of Le Mans (Sarthe, N.W. France). *Newsl. Stratigr.*, Leiden, **2** (4) : 189–202.

—— & KLINGER, H. C. 1971. A major intra-Cretaceous unconformity in eastern South Africa. *Jl geol. Soc.*, London, **127** : 183–186.

—— —— 1972. Hiatus concretions and hardground horizons in the Cretaceous of Zululand, South Africa. *Palaeontology*, London, **15** : 539–549, pls 106–108.

KILIAN, W. 1902a. Sur la présence de l'étage Aptien dans le Sud-Est de l'Afrique. *C. r. hebd. Séanc. Acad. Sci., Paris*, **75** : 68.

—— 1902b. Sur quelques gisements de l'étage Aptien. *Bull. Soc. géol. Fr.*, Paris, **2** : 358.

—— 1902c. Ueber Aptien in Südafrika. *Zentbl. Miner. Geol. Paläont.*, Stuttgart, **1902** : 465–468.

KING, L. A. 1962. The post Karroo stratigraphy of Durban. *Trans. geol. Soc. S. Afr.*, Johannesburg, **65** (2) : 85–93.

KING, L. C. & MAUD, R. M. 1964. The geology of Durban. *Bull. geol. Surv. Rep. S. Afr.* **42** : 1–54.

KRENKEL, E. 1910a. Die untere Kreide von Deutsch Ost-Afrika. *Beitr. Paläont. Geol. Ost.-Ung.*, Vienna & Leipzig, **23** : 201–250, pls 20–23.

—— 1910b. Die Aptfossilien der Delagoa Bai. *Neues Jb. Miner. Geol. Paläont. Jahrg.*, Stüttgart, **1910** (1) : 142–168, fig. 17.

—— 1911a. Zur unteren Kreide von Deutsch Ost-Afrika. *Zentbl. Miner. Geol. Paläont.*, Stuttgart, **1911** : 285.

—— 1911b. Die Entwickelung der Kreideformation auf dem afrikanischen Kontinente. *Geol. Rdsch.*, Leipzig, **2** : 330–366.

KRIGE, L. J. 1932. The geology of Durban. *Trans. geol. Soc. S. Afr.*, Johannesburg, **35** : 37–67.

LANG, W. D. 1906. Polyzoa. *In* WOODS, H. The Cretaceous fauna of Pondoland. *Ann. S. Afr. Mus.*, Cape Town, **4** : 275–350, pls 33–45.

LARCHER, C., RAT, P. & MALPRIS, M. 1965. Documents paléontologiques et stratigraphiques sur l'Albien de l'Aube. *Mém. Bur. Rech. géol. minièr.*, Paris, **34** : 237–253.

LITTLE, J. DE V. 1957. A new species of *Trigonia* from Upper Cretaceous Beds near the Itongazi River, Natal. *Palaeont. afr.*, Johannesburg, **4** : 117–122.

MANDEL, E. 1960. Monimiacean-Hölzer aus der oberkretazischen Umzambaschichten von Ost-Pondoland, S. Afrika. *Senckenberg. leth.*, Frankfurt a.M., **41** : 331–391, 10 pls.

MARIE, P. 1965. Sur une échelle stratigraphique de l'Albien du Bassin Parisien basée sur les foraminifères. *Mém. Bur. Rech. géol. minièr.*, Paris, **34** : 271–288.

MIDDLEMISS, F. A. & MOULLADE, M. 1970. Summer Field Meeting in the south of France between Lyon and Avignon. *Proc. Geol. Ass.*, London, **81** : 303–362.

MONTANARO, E. & LANG, Z. 1937. Coelenterati, echinodermi, e brachiopodi del cretaceo medio-superiore dello Zululand. *Palaeontogr. ital.*, Pisa, **37** : 193–201, 1 pl.

MOULLADE, M. 1965a. Révision des stratotypes de l'Aptien : Gargos (Vaucluse). *Mém. Bur. Rech. géol. minièr.*, Paris, **34** : 201–214.

—— 1965b. Révision des stratotypes de l'Aptien Clansayes (Drôme). *Ibid.* : 303–310.

Muir-Wood, H. M. 1953. Description of a new species of "*Terebratula*" from the Cretaceous of Zululand. *Trans. geol. Soc. S. Afr.*, Johannesburg, **55** : 183–187, pl. 19.

Muller-Stoll, W. R. & Mandel, E. 1972. Fossil woods of Monimiacea and Euphorbiacea from the Upper Cretaceous Umzamba Beds of East Pondoland, C.P. *Trans. geol. Soc. S. Afr.*, Johannesburg, **65** : 93–104.

Newton, R. B. 1909. Cretaceous Gasteropoda and Pelecypoda from Zululand. *Trans. R. Soc. S. Afr.*, Cape Town, **1** : 1–106, pls 1–9.

Orbigny, A. d' 1840–42. *Paléontologie française. Terrains Crétacés I. Céphalopodes.* 662 pp., 148 pls. Paris.

—— 1848–51. *Paléontologie française. Terrains Crétacés IV. Brachiopodes.* 390 pp., 109 pls. Paris.

—— 1850. *Prodrome de Paléontologie stratigraphique universelle des animaux mollusques et rayonnés*, **2**. 427 pp. Paris.

—— 1852. *Cours élémentaire de Paléontologie et de Géologie stratigraphique*, **2** (2) : 383–847. Paris.

Owen, H. G. 1971. Middle Albian stratigraphy in the Anglo-Paris Basin. *Bull. Br. Mus. nat. Hist.* (Geol.), London, Suppl. **8** : 164 pp., 3 pls.

Pienaar, R. N. 1969. Upper Cretaceous calcareous nannoplankton from Zululand, South Africa. *Palaeont. afr.*, Johannesburg, **12** : 75–128, 11 pls.

Plows, W. J. 1921. The Cretaceous rocks of Pondoland. *Ann. Durban Mus.*, **3** : 58–66, pl. 8.

Renngarten, V. P. 1926. La faune des dépôts crétacés de la région d'Assakambiléevka, Caucase du Nord. *Trudy̆ geol. Kom.*, Leningrad, n.s. **147** : 132 pp., 9 pls (in Russian, French résumé).

Rennie, J. V. L. 1929. Cretaceous fossils from Angola (Lamellibranchia and Gastropoda). *Ann. S. Afr. Mus.*, Cape Town, **28** : 1–54, pls 1–5.

—— 1930. New Lamellibranchia and Gastropoda from the Upper Cretaceous of Pondoland (with an appendix on some species from the Cretaceous of Zululand). *Ibid.* : 159–260, pls 16–31.

—— 1935. On a new species of *Lysis* (Gastropoda) from the Cretaceous of Pondoland. *Rec. Albany Mus.*, Grahamstown, **4** : 244–247, pl. 24.

—— 1936. Lower Cretaceous Lamellibranchia from Northern Zululand. *Ann. S. Afr. Mus.*, Cape Town, **31** : 277–391, pls 37–55.

Rogers, A. W. & Schwarz, E. H. L. 1901. Report on parts of the Uitenhage and Port Elizabeth Divisions. *Rep. geol. Commn Cape Good Hope*, Cape Town, **1900** (1) : 3–18.

—— —— 1902. General survey of the rocks in the southern parts of the Transkei and Pondoland including a description of the Cretaceous rocks of eastern Pondoland. *Ibid.* **1901** (25) : 25–46.

Roniewicz, P. 1970. Borings and burrows in the Eocene littoral deposits of the Tatra Mountains, Poland. *Geol. J.*, Liverpool, Spec. Issue **3** : 439–446, 2 pls.

Rouchadzé, J. 1932. Les ammonites aptiennes de la Géorgie Occidentale. *Bull. Inst. géol. Géorgie*, Tiflis, **1** : 165–273, pls 1–23.

Schelpe, E. A. C. L. E. 1955. *Osmundites natalensis*—a new fossil fern from the Cretaceous of Zululand. *Ann. Mag. nat. Hist.*, London, (12) **8** : 652–656, pl. 17.

Sellwood, B. W. 1970. The relation of trace fossils to small scale sedimentary cycles in the British Lias. *Geol. J.*, Liverpool, Spec. Issue **3** : 489–504, 1 pl.

Séronie-Vivien, M. 1959. Les localités types du Sénonien dans les environs de Cognac et Barbezieux (Charente). *In* Colloque sur le Crétacé Supérieur Français. *C. r. Congr. Socs sav. Paris Sect. Sci.* (Dijon), **1959** : 579–589.

Smitter, Y. H. 1956. Foraminifera from the Upper Cretaceous beds occurring near the Itongazi River, Natal. *Palaeont. afr.*, Johannesburg, **3** : 103–107.

—— 1957. Upper Cretaceous Foraminifera from Sandy Point, St Lucia Bay, Zululand. *S. Afr. J. Sci.*, Cape Town, **53** : 195–201.

SOCIN, C. 1939. Gasteropodi e Lamellibranchi del Cretaceo medio-superiore dello Zululand. *Palaeontogr. ital.*, Pisa, **40** : 21–38, pls 5–6.

SORNAY, J. (Ed.) 1957. France, Belgique, Pays-Bas, Luxembourg. Crétacé. *In Lexique Stratigraphique International I (Europe)*, **4 a VI**, 403 pp. CNRS, Paris.

SPATH, L. F. 1921a. On Cretaceous Cephalopoda from Zululand. *Ann. S. Afr. Mus.*, Cape Town, **12** : 217–321, pls 19–26.

—— 1921b. On Upper Cretaceous Ammonoidea from Pondoland. *Ann. Durban Mus.*, **3** : 39–57, pls 6, 7.

—— 1922. On the Senonian ammonite fauna of Pondoland. *Trans. R. Soc. S. Afr.*, Cape Town, **10** : 113–147, pls 5–9.

—— 1923–43. A monograph of the Ammonoidea of the Gault. *Palaeontogr. Soc. (Monogr.)*, London, 787 pp., 72 pls.

—— 1925. On Upper Albian Ammonoidea from Portuguese East Africa. *Ann. Transv. Mus.*, Pretoria, **11** : 179–216, 10 pls.

—— 1953. The Upper Cretaceous Cephalopod fauna of Grahamland. *Scient. Rep. Falkld Isl. Depend. Surv.*, London, **3** : 60 pp., 13 pls.

TATE, R. 1867. On some secondary fossils from South Africa. *Q. Jl geol. Soc. Lond.*, **23** : 139–174, pls 3–9.

VAN HOEPEN, E. C. N. 1920. Description of some Cretaceous ammonites from Pondoland. *Ann. Transv. Mus.*, Pretoria, **7** : 142–147, pls 24–26.

—— 1921. Cretaceous Cephalopoda from Pondoland. *Ibid.* **8** : 1–48, pls 1–11.

—— 1926. Oor die Krytafsettinge van Soeloeland. *S. Afr. J. Sci.*, Cape Town, **23** : 216–222.

—— 1929. Die Krytfauna van Soeloeland. I. Trigoniidae. *Paleont. Navors. nas. Mus. Bloemfontein*, **1** : 1–38, pls 1–7.

—— 1931. Die Krytfauna van Soeloeland. 2. Voorlopige Beskrywing van enige Soeloelandse Ammoniete. 1. *Lophoceras*, *Rhytidoceras*, *Drepanoceras* en *Deiradoceras*. *Ibid.* : 39–54, 14 figs.

—— 1941. Die gekielde Ammoniete van die Suid-Afrikaanse Gault. I. Diploceratidae, Cechenoceratidae en Drepanoceratidae. *Ibid.* : 55–90, figs 1–55, pls 8–19.

—— 1942. Die gekielde Ammoniete van die Suid-Afrikaanse Gault. II. Drepanoceratidae, Pervinquieridae, Arestoceratidae, Cainoceratidae. *Ibid.* : 91–157, figs. 56–173.

—— 1944. Die gekielde Ammoniete van die Suid-Afrikaanse Gault. III. Pervinquieridae en Brancoceratidae. *Ibid.* : 159–198, pls 20–26.

—— 1946. Die gekielde Ammoniete van die Suid-Afrikaanse Gault. IV. Cechenoceratidae, Dipoloceratidae, Drepanoceratidae, Arestoceratidae. [and] V. Monophyletism or polyphyletism in connection with the ammonites of the South African Gault. *Ibid.* : 199–271, figs. 174–268.

—— 1951a. Die gekielde Ammoniete van die Suid-Afrikaanse Gault. VI. The so-called old mouth-edges of the ammonite shell. *Ibid.* : 273–284, figs 269–287.

—— 1951b. Die gekielde Ammoniete van die Suid-Afrikaanse Gault. VII. Pervinquieridae, Arestoceratidae, Cainoceratidae. *Ibid.* : 285–344, figs 288–442.

—— 1951c. A remarkable desmoceratid from the South African Albian. *Ibid.* : 345–349, 3 figs.

—— 1955a. New and little-known ammonites from the Albian of Zululand. *S. Afr. J. Sci.*, Cape Town, **51** : 355–377, figs 1–31.

—— 1955b. A new family of keeled ammonites from the Albian of Zululand. *Ibid.* : 377–382, figs 32–36.

—— 1963. An Albian astacurid from Zululand. *Ann. geol. Surv. Pretoria*, **1** : 253–255.

—— 1966a. New and little known Zululand and Pondoland ammonites. *Ann. geol. Surv. Pretoria*, **4** : 158–172, 12 pls.

—— 1966b. New ammonites from Zululand. *Ibid.* : 183–186, 7 pls.

—— 1966c. The Peroniceratidae and allied forms of Zululand. *Mem. geol. Surv. Rep. S. Afr.*, Pretoria, **55** : 70 pp., 27 pls.

Venzo, S. 1936. Cefalopodi del Cretacea medio-superiore dello Zululand. *Palaeontogr. ital.*, Pisa, **36** : 59–133, pls 5–12.

Wiedmann, J. 1959. La Crétacé supérieur de l'Espagne et du Portugal et ses céphalopodes. *In* Colloque sur le Crétacé Supérieur Français. *C. r. Congr. Socs sav. Paris Sect. Sci.* (Dijon), **1959** : 709–764, 7 pls.

—— 1964. Le Crétacé supérieur de l'Éspagne et du Portugal et ses Céphalopodes. *Estudios geol. Inst. geol. Lucas Mallada*, Madrid, **1964** : 107–148, 39 figs.

Woods, H. 1906. The Cretaceous fauna of Pondoland. *Ann. S. Afr. Mus.*, Cape Town, **4** : 275–350, pls 33–44.

Woodward, A. S. 1907. Notes on some Cretaceous fish teeth from the mouth of the Umpenyati River, Natal. *Rep. geol. Surv. Natal Zululand*, Pietermaritzburg, **3** : 99–101, pl. 10 (pars).

Wright, C. W. 1957. Mollusca 4. Cephalopoda, Ammonoidea. *In* Moore, R. C. (Ed.), *Treatise on Invertebrate Paleontology*, **L.** xxii + 400 pp. Lawrence, Kansas.

XI. INDEX

The page numbers of the principal references are printed in **bold** type; an asterisk (*) denotes a figure. Text-figs. 2 and 3 follow p. 280; text-figs. 10 and 11 follow p. 300.

Acanthoceras 277, 291
  cornigerum 277
  crassiornatum 277
  flexuosum 277
  hippocastanum Crick *non* Sow. 277
  latum 277
  munitum 277
  quadratum 277
  robustum 277
Acanthoplites 275, 301, fig. 10
Acompsoceras 276
Aconeceratidae 274, fig. 11
'*Acrioceras*' 274, fig. 11
Albian, 266–73, **275–6**
Allocrioceras spp. 278
alluvium, Recent fig. 3
Amatis farm 285
ammonites 269–70, 273
  faunas 266, 271
Ammonoceratites 276
Anagaudryceras 276, 286
  sacya 276
Anapachydiscus arialoorensis 280
  subdulmensis 280
  wittekindi 280
Ancyloceras 275, fig. 11
  sp. 274
Ancyloceratidae 274–5, fig. 11
Anderson, W. 270–1, 289
'*Andersonites*' *listeri* 279
Androiavites 276
Angles section (Basses-Alpes) 274
Anisoceras 276–7, 290, 303
Aptian 266–7, 270–3, **274–5**
  boundary with Barremian 274
Arcidae 287
Arestoceras 276
Arialoor Group (S. India) 270
arthropods 305
  burrows 287, 290, 305
Askoloboceras 276
Australiceras 275, fig. 11
Australiella 280
  australis 280
  besairei 280
Avellana 290

Baculites 279–80, 283, 291, 293, 297
  bailyi 278–9
  capensis group 279
  sulcatus 280, 282
  vagina Van Hoepeni 280
Bailey, W. H. 269
Bantu Reserve No. 3 284
Barremian 266–7, 269, 272, **273–4**
  boundary with Aptian 274
Barroisiceras 278
  haberfellneri zone 278
  onilahyense zone 278
  umzambiensis 270, 281
basement rocks 266, 269, fig. 3, 282
Basseoceras krameri 278
'*Beaudanticeras*' 276
Behavites 280
belemnites fig. 11, 305
Belvedere farm 288
Bhimaites 276–7
bilharzia 285
bivalves 266, 269, 282, 286–7, 290–1, 293, 297, 299, figs. 10–11, 303, 305; see also *Inoceramus*, Ostreidae, etc.
Borissiakoceras 277
Bostrychoceras 280–1
  indicum 278, 287
  sp. 280
brachiopods 266, 271, 305
British Museum (Natural History) 266, 306
bryozoans 266, 305–6
burrows, 293, 297; see also arthropods
Baboon's Krans 285

Cain Railway Bridge 283
Cainoceras 276
Calycoceras 291
  choffati group 277, 287, 291
  gentoni paucinodatum 277
  laticostatum 277
  naviculare group 277
  newboldi newboldi 277
    planecostata 277
    spinosum 277
  nitidum 277, 291
Campanian 266, 269–73, **280–1**
Cechenoceras 276
Cekeni Estate 284
Cenomanian 266, 268–73, **276–7**
Cercomya 290
Charter's Creek 284, 298
Chelmsford farm 283
chelonians 306
Cheloniceras 275, fig. 11
  gottschei 275
  aff. *proteus* 275
  spp. fig. 11
Cheloniceratidae 274
Chlamys 290
Chondrites 305
cidarid spines 282
cirripede bores 305
'Clansayes' horizon 275
'*Cleoniceras*' 276
Cognac 278
Colchidites 274, fig. 11
Collignonceratidae 270
Coniacian 266, 268–73, **278–9**
corals 266, 305
Corbières 279
Coves, the 298

Craie de Villedieu 278
Crassatella 290
Crick, G. C. 266, 289
Crioceratidae 274
'*Crioceratites*' fig. 11
crocodiles 285
Cyclorisma 290
Cyclothyris 290

Damesites fig. 10
  ? sp. nov. 276
Deiradoceras 276
Denyer's Drift 300
Deshayesitidae 274
Desmoceras 276–7, 290
  latidorsatum 277
Desmoceratidae 275–7
Diadochoceras 275, fig. 10
  nodostocatum 275
Diaziceras tissotiaeforme 283
Die Rooiwalle 292
Diplacmoceras bidorsatum zone, 280
Diplasioceras 276
Diploceras [sic] 286; see *Dipoloceras*
Diplomoceratidae 279–80, 283, 293
Dipoloceras (*Diplasioceras*) 276
  (*Dipoloceras*) 276, 286, 303
Douvilleiceras 275–6, fig. 10, 303
  mammillatum 275
  orbignyi 275
Durban 266–7, 269–70, **282**, 305
  Museum 267
  University Collection 267
Durnovarites 276, 290, 303
du Toit, A. L. 270

echinoids 266, 305
'*Eedenoceras*' *multicostatum* 278
'*Emericeras*' 274, fig. 11
Empangeni 282
Enseleni Reserve 267
Entolium 286
'*Epiphylloceras*' 281
epizoans 305
Erioliceras 276
Etheridge, R. 266
Eubaculites 281
  ootacodensis 281
Eubrancoceras 303
  aff. *aegoceratoides* 276
Eucalycoceras 277
Eupachydiscus 280
  isculensis zone 279
  ? sp. 279–80
Euspectoceras 276
Eutrephoceras 297
Eutyloceras fig. 11
  phestum 274
Exogyra 286, fig. 11

False Bay 268, 271, 273, fig. 3, **292–8**
'*Falsebayites*' *peregrinus* 279
Fanies Island Camp 298

fish teeth 305–6
'*Fluminites*' *albus* 279
Foraminiferida 271
Forbesiceras largilliertianum 277, 303
  sculptum 277
Forresteria 283, 299
  alluaudi 278, 282
  hammersleyi 278
  itwebae 278
  razafiniparyi 278
  reymenti 278
  vandenbergi 278
Fraudatoroceras besairei 278
Fynn, H. F. 269

Garden, R. J. 269
gastropods 266, 282, 287, 290, 297, fig. 10
Gaudryceras 276
  spp. 279–80
Gauthiericeras ? 279
Geological Survey of South Africa 266
Gervillella 286, figs. 10–11, 303
Glenpark Estate **284**
Glycymeris 286–7
Goniomya 286, 290
Grand Champagne 280
Graysonites 276
Gujini 300
Gunnarites antarticus 280
Gyrodes 290

Haig Halt 282–3
Hamites 276, 286, 303
Hauericeras 280, 293
  gardeni 279–81
Haughton, S. H. 266, 301
Hell's Gate 296, 298
Hemiaster 286–7
Hemihoplitidae 274, fig. 11
Heteroceras 274, fig. 11
heterodont bivalves 286–7, 297, figs. 10–11
heteromorph ammonites 275, fig. 10, 303
Hluhluwe 267–8, fig. 3, **283–4**, 285, 288, 292, 294–6
  River fig. 3, 284, 292, **294–5**
'*Hluhluweoceras*' *fugitivum* 279
Hoplitidae, boreal 275
Hoplitoplacenticeras plasticum[2] 280
Hoploscaphites 281
Hypengonoceras 276, 303
Hyphantoceras 280
  reussianum 278
  sp. 279
Hypophylloceras 276–7, 286
  velledae 276
Hypoturrilites 276–7, 290–1, 303
  carcitanensis 277
  gravesianus 277
  nodiferus 277
  tuberculatus 277
Hysteroceras 276, 286, 303

Idiohamites 276, 303
Impala 302
Indabana 288
Ingwavuma River 270
Inoceramidae 270, 273, 281, 293, 297; plate, fig. 2
Inoceramus 269, 286, 303
  expansus 281
  labiatus zone 278
Insleep 292
International Geological Congress, 1929 270–1
Iswelihle 288
Itongazi River 266–7, 270
Itweba Beds 272
Izindhluzabalungu Deposits 269
Izwehelia farm 288–9

Jozini 300–1

Karapadites ? sp. 279
Karoo formation 283
Komeceras 276
Kossmaticeras 279
  sakondryense 278
  sparcicosta 278
  theobaldianum 278; zone 278
  (*Natalita*) 282
Kossmaticeratidae 283
Kwa Mbonambi fig. 3, **282**

Labeceras 276, 286, 303
Labeceratidae 286
Lake View 282
Lebombo Mountains 271, 298, 300
  Volcanics 267, 273, 283, 285, 299–301
Lechites 276
Le Mans 276
Lewesiceras australe 278
  spp. 278
Leymeriella tardefurcata zone 275
Linotrigonia 290
Lister's Point 292, 294
lithodomous bivalves 305
Lithophaga 287, fig. 10
lithostratigraphic terminology 272
locality details 281–304
logs 286–7, 293, figs. 10–11, 305–6; see trees, fossil
Lombangwena Spruit 302
Lophoceras 276
Lyelliceras 276, 303
  lyelli 276
  pseudolyelli 276
Lytoceras 275
Lytoceratidae 275, fig. 10

Maastrichtian 266, 268–73, **281**
Madagascar 275, 278
Mains Farm 282
Makaane's Drift 304
Makakatana Bay 298
Makatini Formation 266, 272, **273**, fig. 3, 282, 285, 288, 299–302; plate, fig. 1
Mammites nodosoides zone 278

Mantelliceras 276–7, 290–1, 303
  cantianum group 277
  indianense 277
  mantelli zone 276
  patens 277
  spissum 277
Mantelliceratinae 276
Mantuma Rest Camp area **300**
Manuan 267, 288; see Munywana
Manuaniceras 276
Maorites sp. 280
Margarites 286
Mariella 276–7, 290–1, 303
  oehlerti 277, 290
  spp. 277, 290
martimpreyi zone 276
Mason's Camp 294
Maydon Wharf 282
Mayezela Spruit **301**
Megacucullaea fig. 11
Megatrigonia fig. 11
  shell bed plate, fig. 1
Menabites 280, 297
  australis 280
  besairei 280
  (*Australiella*) 280
Menuites 281
Mfekayi Halt 284
Mfolozi River 266–8, 270, fig. 3, **282–3**
Mfomoto farm 292
Mfongosi River 301
  Spruit 273, **301–2**, fig. 10
Mfuthululu, Lake 283
Mhlangamkulu River 282
microfloras 272
Miotexanites 279
Mkuze Game Reserve **299**
  River 271, 292, fig. 3, **298–300**
Mlambongwenja River 273
Mlambongwenya Spruit 302, fig. 11
Modiolus 286, 290
Mojsisovicsia 276, 286
molluscs 271, 282, 286–7, 290–1, 293, figs. 10–11, 303, 305; see also bivalves, gastropods, ammonites, etc.
Monte Rosa 285
Monzi 269, 271, 282–3
Monoval 284
Morrisvale area **299–300**
Mortoniceras (*Mortoniceras*) 276, 286, 303
  umkwelanense 270
  (*Deiradoceras*) 276
  (*Durnovarites*) 276
Mortoniceratidae 276, 286
mosasaur 306
Mozambique 266–7, 270
Mpenjati River 266–7, 270, 282
Msunduzi drift 299
  pan 304
  River 271, 283, 299–300, 302, 304
Mtubatuba 267, 282–3
Muniericeras lapparenti 279
Munyuana Beds 272; see Munywana
Munywana 267, 271, 288, **289**, 292
Myesa Spruit 301; see Mayezela Spruit
Myloceras 276, 286, 303
Mzinene Formation 266, 272, **273**, fig. 3, 284–5, 288–9, 299–300, 302, 304–5
  River 267–73, fig. 3, **285**, **292**, 304; plate, fig. 1
   lower reaches **292**
   upper reaches **285–8**

Narrows, the 292
Natal 272; see Pondoland
Natalita 282
National Museum, Bloemfontein 267
nautiloids 266, 286, 297, 299
Ncedomhlope farm 295
Ndabana 285
  Beds 272
Ndlamyane River 300
Ndlelakufa Pan 300
Ndumu 267, 300–1, **302–4**
  Spruit 305
Neithea 286–7, 290
Neitheidae 293
Neogaudryceras sp. 280
'*Neosilesites*'
Newton, R. B. 266
Ngweni 285, 299–300
Nhlohlela Pan 300
Nibela peninsula 292, **296**, 297*
Nkundusi 295
Nostoceras ? sp. 280
Nsumu Pan 299
Nxala Estate, Mt Nxala 299
Nyalazi River 268, fig. 3, **283–4**, 292, 295–6, 305
  trading store 284
Nyokaneni River 282

Onderdeel farm 292
Ostlingoceras 277, 290–1
  rorayensis 277
Ostreidae 271, 282, 286, 297, 299, figs. 10–11, 305
Otobotini 301
Oxytropidoceras 276, 286, 303
  (*Androiavites*) 276
  (*Manuaniceras*) 276
  (*Oxytropidoceras*) 276
  (*Tarfayites*) 276
oysters, see Ostreidae

Pachydesmoceras denisonianum 278, 287
  sp. 278, 287
Pachydiscidae 280–1, 297
Pachydiscus manambolensis 280
  neubergicus zone 281
  (*Neodesmoceras*) sp. 280–1
  (*Pachydiscus*) 280
Palaeocene 272
Panopea 290, fig. 11
Panplaas farm 295
Parabehavites serratomarginatus 279
Paratexanites (*Paratexanites*) 279
Pasina 283
Peaston North Bank Drain 283
Pectinidae 297
Peroniceras 278, 282–3, 299
  besairei 278
  dravidicum zone 278
  tenuis 278
  tridorsatum group 278
  (*Zuluiceras*) *charlei* 278
  (*Zuluites*) 279
Peroniceras Beds 272, 294
Peroniceratidae 279
Perrisoptera 290
Petinoceras 276
Pholadomya 286, 290
  vignesi 286, 290
Phylloceras 274–5, fig. 11
  serum 274, fig. 11
  (*Hypophylloceras*) 276–7, 286
   velledae 276
Picnic Point 294
Pinna 290, 297
Pisechene, Lake 296
Placenticeras 279
  syrtale zone 279
plant remains, see logs
Pleistocene sands fig. 3
plesiosaur 306
Plesiotexanites stangeri 279–80
Pleuromya 287, fig. 10
Pondoland 270, 273, **281–2**
Pongola River 270–2, 300–1
Praemuniericeras ? sp. 279
Pretoria University Collection 267
Protocheloniceras 274–5, fig. 11
  albrechtiaustriae 274
Proplacenticeras 283, 287, 291, 299
  kaffrarium 278, 283, 287
  subkaffrarium 278, 287
  umkwelanense 278, 282, 287
Protanisoceras 275, fig. 10
Protexanites (*Miotexanites*) 279
  (*Protexanites*) 279
Protocardia 286, 303
Pseudhelicoceras 276, 286
Pseudohaploceras 275
  matheroni 274
Pseudophyllites indra 279
Pseudoschloenbachia 280, 293
  primitiva 279
  umbulazi 281–2
  sp. 279
Pseudothurmannia angulicostata zone 274
Pseudoxybeloceras matsumotoi 278
Pterotrigonia 286–7, 290 fig. 10, 303
  shepstonei 287, 291
   conglomerate 287, 289, 291, 305

Puzosia 276–7, 286, 303
  spp. 278
Puzosiidae 276, 283
Pycnodonte 297

Quotho Pan 302

reptiles 305–6
research, history of 269–72
Rhytidoceras 276
Richards Bay 267, fig. 3
Ricnoceras 276
Riverview 268, 282
  sugar mill 283
Rossalites 276
Russia, S., Barremian sequence in 274

Saghalinites 281
  cala 280
St Lucia area 267, 268*, 270, 272, 304
  Game Reserve 295
  (Lake) 268, 271, 273, fig. 3, **292–8**; plate, fig. 2
St Lucia Formation 266, 272, **273**, fig. 3, 282–5, 288–9, 292, 294–6, 298–300, 305; plate, fig. 2
Saintes, Aquitaine 279
Sanmartinoceras 274, fig. 11
Santonian 266, 269–72, **279–80**
Sarthe 276
Scaphites (*Scaphites*) 277, 279, 290
    meslei 278
    cf. *simplex* 277
    spp. 277–8, 283
Scaphitidae 282
Schloenbachia 276
Sciponoceras 277, 290
  roto 277, 290
Senonian 269–72, 289; see also Coniacian, etc.
serpulids fig. 10, 305–6
Sharpe, Daniel 266
Sharpeiceras 276–7, 290–1, 302–3
  falloti 277
  florencae 277, 303
  laticlavium 277, 303
  spp. 290
Shire Estate 283
Sibayi, Lake 272
Skoenberg, the 288–92, 305
  Beds 272, 289
  region 285, **288–91**
Sometsu Road 282
'*Sonneratia*' 276
South African Museum, Cape Town 267
Southern peninsula, Lake St Lucia 292, **296–8**
Spatangidae 297
Spath, L. F. 266
sponges 305
Sphenoceramus 282
Sphenotrigonia fig. 10
stage limits and subdivisions, 273–81
Steinmanella henningi fig. 11
Stoliczkaia 276, 290, 303
  africana 276
  dispar zone 268
  dorsetensis 276
  notha 276
Stomohamites 277, 290
Stormberg Basalts 266, 269
stratigraphic nomenclature 272–273
  synthesis 267–9
Submortoniceras 280, 293
  woodsi 280
  sp. 293
Subprionotropis cricki 270, 281; horizon of 279

Table Mountain Sandstone 266, 269
Tarfayites 276, 286
Terasceras 276
Teredo figs. 10–11
Tertiary sands and limestones fig. 3
Tetragonites 276
  subtimotheanus 277
Texanites 279, 293
  oliveti 279
  soutoni 280–1
  texanus zone 279
  spp. 280
  (*Plesiotexanites*) *stangeri* 280–1
    densicosta 279
    sparcicosta 279
Texanitidae 278, 293
Teza, Lake 282
Thalassinoides 305; see arthropod burrows
Tissotia 278
Tonohamites 275
Trafalgar Beach 282
Transkei 268*, 269; see Umzamba River
Transvaal Museum 267
trees, fossil 269; see logs
Trichinopoly Group (S. India) 270
Trigoniidae 286, figs. 10–11
Tropaeum 275, figs. 10–11
  sp. 274
Turonian 266, 268–72, **277–8**
Turrilites 291
  acutus 277
  costatus 277
  scheuchzerianus 277

Umkandandhlouvu River 270
Umkwelane Hill 267–70, **282–3**
Umlatuzi Lagoon 270
Umsinene 267
  Beds 272, 276
Umtamvuna (Umtamfuna) Cretaceous 269
  River 269
Umzamba Formation, Beds 266, 269–72, **273**, 281–2, 305
  River 267, 268*, 273, 281
Umzigi 292
Utsutu River 301
Utaturiceras 276

Valdedorsella 275, fig. 11
van Hoepen, E. C. N. 266, 289, 294
Veneridae 286–7
Veniella 286, fig. 10
vertebrates 305–6

Wisteria 302
wood, fossil, see logs

Yabeiceras 299
  spp. 278

Zulu names 267
Zuluiceras charlei 278
Zuluites 279
Zululand 266–306 *passim*, 268*; see also Pondoland
    general locality map fig. 2
  Group 266, **272–3**, 305

W. J. KENNEDY
Dept of Geology & Mineralogy
PARKS ROAD
UNIVERSITY OF OXFORD
ENGLAND

H. C. KLINGER
GEOLOGICAL SURVEY OF SOUTH AFRICA
PRIVATE BAG X112
PRETORIA 0001
REPUBLIC OF SOUTH AFRICA

Accepted for publication 14 January 1974.

PLATE

Fig. 1. *Megatrigonia* shell bed, Makatini Formation (Aptian), loc. 39, Mzinene River, Zululand. Hammer-head is 15 cm long. (p. 285).

Fig. 2. Inoceramid fragments in Maastrichtian silts, St Lucia Formation, SE shores of Lake St Lucia, Zululand. Hammer-head is 15 cm long. (p. 298).

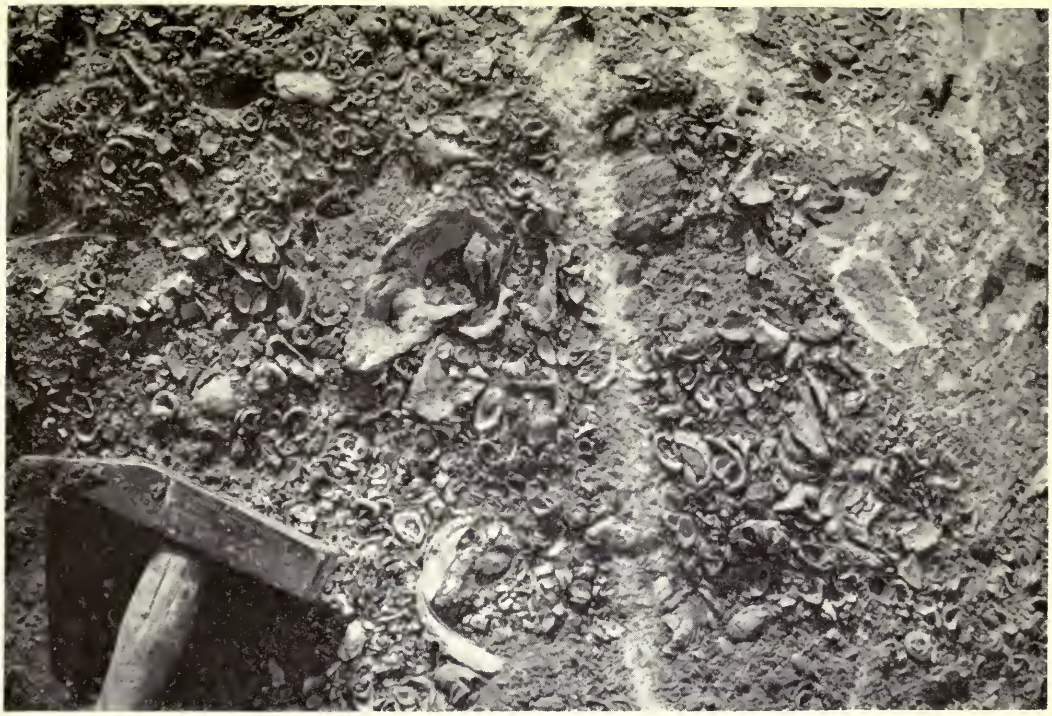

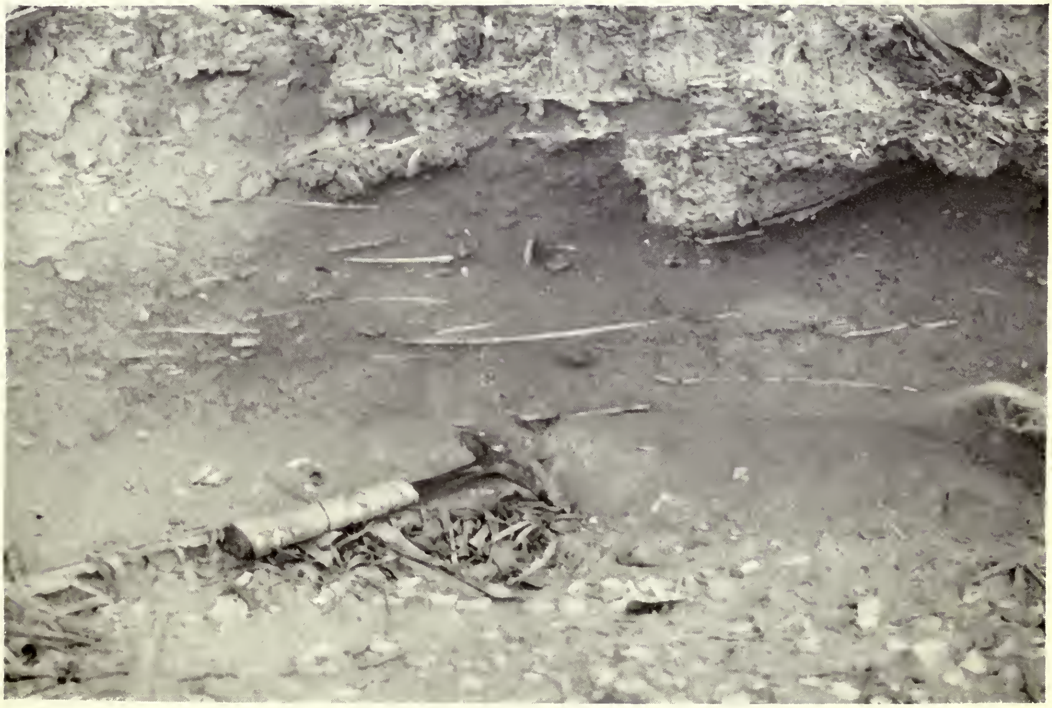

A LIST OF SUPPLEMENTS TO THE GEOLOGICAL SERIES OF THE BULLETIN OF THE BRITISH MUSEUM (NATURAL HISTORY)

---

1. Cox, L. R. Jurassic Bivalvia and Gastropoda from Tanganyika and Kenya. Pp. 213 ; 30 Plates ; 2 Text-figures. 1965. OUT OF PRINT.
2. El-Naggar, Z. R. Stratigraphy and Planktonic Foraminifera of the Upper Cretaceous—Lower Tertiary Succession in the Esna-Idfu Region, Nile Valley, Egypt, U.A.R. Pp. 291 ; 23 Plates ; 18 Text-figures. 1966. £11.
3. Davey, R. J., Downie, C., Sarjeant, W. A. S. & Williams, G. L. Studies on Mesozoic and Cainozoic Dinoflagellate Cysts. Pp. 248 ; 28 Plates ; 64 Text-figures. 1966. £8.20.
3. Appendix. Davey, R. J., Downie, C., Sarjeant, W. A. S. & Williams, G. L. Appendix to Studies on Mesozoic and Cainozoic Dinoflagellate Cysts. Pp. 24. 1969. 95p.
4. Elliott, G. F. Permian to Palaeocene Calcareous Algae (Dasycladaceae) of the Middle East. Pp. 111 ; 24 Plates ; 16 Text-figures. 1968. £6.10.
5. Rhodes, F. H. T., Austin, R. L. & Druce, E. C. British Avonian (Carboniferous) Conodont faunas, and their value in local and continental correlation. Pp. 313 ; 31 Plates ; 92 Text-figures. 1969. £13.10.
6. Childs, A. Upper Jurassic Rhynchonellid Brachiopods from Northwestern Europe. Pp. 119 ; 12 Plates ; 40 Text-figures. 1969. £5.25.
7. Goody, P. C. The relationships of certain Upper Cretaceous Teleosts with special reference to the Myctophoids. Pp. 255 ; 102 Text-figures. 1969. £7.70.
8. Owen, H. G. Middle Albian Stratigraphy in the Anglo-Paris Basin. Pp. 164 ; 3 Plates ; 52 Text-figures. 1971. £7.20.
9. Siddiqui, Q. A. Early Tertiary Ostracoda of the family Trachyleberididae from West Pakistan. Pp. 98 ; 42 Plates ; 7 Text-figures. 1971. £9.60.
10. Forey, P. L. A revision of the elopiform fishes, fossil and Recent. Pp. 222 ; 92 Text-figures. 1973. £11.35.
11. Williams, A. Ordovician Brachiopoda from the Shelve District, Shropshire. Pp. 163; 28 Plates; 11 Text-figures; 110 Tables 1974. £12.80.

Printed in Great Britain by John Wright and Sons Ltd. at The Stonebridge Press, Bristol BS4 5NU

BM.P.

A REVISION OF SAHNI'S TYPES OF THE BRACHIOPOD SUBFAMILY CARNEITHYRIDINAE

U. ASGAARD

BULLETIN OF
THE BRITISH MUSEUM (NATURAL HISTORY)
GEOLOGY Vol. 25 No. 5
LONDON: 1975

A REVISION OF SAHNI'S TYPES OF THE BRACHIOPOD SUBFAMILY CARNEITHYRIDINAE

BRITISH MUSEUM
GENERAL
27 MAY 1975
LIBRARY
NATURAL HISTORY

BY
ULLA ASGAARD
Institut for historisk Geologi og Palæontologi
Østervoldgade København Denmark

Pp. 317–365 ; 8 *Plates* ; 14 *Text-figures* ; 5 *Tables*

BULLETIN OF
THE BRITISH MUSEUM (NATURAL HISTORY)
GEOLOGY Vol. 25 No. 5
LONDON: 1975

THE BULLETIN OF THE BRITISH MUSEUM (NATURAL HISTORY), *instituted in* 1949, *is issued in five series corresponding to the Departments of the Museum, and an Historical series.*

Parts will appear at irregular intervals as they become ready. Volumes will contain about three or four hundred pages, and will not necessarily be completed within one calendar year.

In 1965 *a separate supplementary series of longer papers was instituted, numbered serially for each Department.*

This paper is Vol. 25, *No.* 5, *of the Geological (Palaeontological) series. The abbreviated titles of periodicals cited follow those of the World List of Scientific Periodicals.*

World List abbreviation:
Bull. Br. Mus. nat. Hist. (Geol.)

ISSN 0007-1471

© Trustees of the British Museum (Natural History), 1975

564.853

TRUSTEES OF
THE BRITISH MUSEUM (NATURAL HISTORY)

Issued 19 *May*, 1975 *Price* £4.50

A REVISION OF SAHNI'S TYPES OF THE BRACHIOPOD SUBFAMILY CARNEITHYRIDINAE

By ULLA ASGAARD

CONTENTS

		Page
	Synopsis	320
I.	Introduction	320
II.	Acknowledgements	320
III.	Historical review	321
IV.	The provenance of the type material	323
V.	Review of Sahni's material of carneithyridines	325
	Carneithyris carnea (J. Sowerby, 1812)	326
	C. elongata (J. de C. Sowerby, 1823)	327
	C. subpentagonalis Sahni, 1925	327
	C. circularis Sahni, 1925	328
	C. variabilis Sahni, 1925	328
	C. acuminata Sahni, 1925	329
	C. norvicensis Sahni, 1925	329
	C. subovalis Sahni, 1925a	330
	C. uniplicata Sahni, 1925a	330
	C. daviesi Sahni, 1925a	331
	C. ornata Sahni, 1929	331
	Pulchrithyris gracilis Sahni, 1925	332
	P. extensa Sahni, 1925	333
	Magnithyris magna Sahni, 1925	333
	M. truncata Sahni, 1929	334
	Piarothyris rotunda Sahni, 1925	334
	Ellipsothyris similis Sahni, 1925	334
	Ornithothyris carinata Sahni, 1925	335
	Chatwinothyris subcardinalis Sahni, 1925	335
	Ch. symphytica Sahni, 1925	336
	Ch. curiosa Sahni, 1925a	337
	Ch. gibbosa Sahni, 1925a	338
VI.	Discussion	338
	Material	339
	The phylogenetic tree of Sahni (1925a)	339
	Morphology of the cardinalia	341
	External morphology	343
	Statistical analyses	345
	Conclusions	359
VII.	Concluding remarks	360
VIII.	References	361
IX.	Index	362

SYNOPSIS

Sahni's type material of Upper Campanian and Lower Maastrichtian carneithyridine brachiopods is reviewed and the type specimens refigured. The present material of carneithyridines in English collections is discussed. It is concluded that only one genus, *Carneithyris*, is present and is represented by two species, *Carneithyris carnea* from the Upper Campanian and *Carneithyris subcardinalis* from the Lower Maastrichtian. The stratigraphical variation of the genus, its palaeoecology and relationship to different facies are examined.

I. INTRODUCTION

The Upper Campanian and Lower Maastrichtian terebratulids, formerly known under the names *Terebratula carnea* J. Sowerby (1812) and *T. elongata* J. de C. Sowerby (1823), were split up by Sahni (1925, 1925a, 1929) into seven genera represented by 22 species. In the course of work on Maastrichtian and Danian carneithyridine terebratulid material from Denmark (Asgaard 1963) I found it necessary to study the types of Sahni, and this led to many visits to the English museums housing the types and to fieldwork in the Norwich area in the years 1962 to 1972. This paper is a result of these investigations. A review of the types is followed by a discussion of the validity of the genera and species. It was found that Sahni's types have suffered much wear since they were figured.

The possibility that seven closely related genera represented by 22 species could have existed in the same area within the relatively short time-span covering the Upper Campanian and Lower Maastrichtian cannot be excluded. However, it can be shown that the premises on which these genera and species were founded are not tenable and that the phylogenetic tree created by Sahni (1925a) does not have a firm stratigraphical footing.

The conclusion of this paper is that the English material represents only one genus with two species, viz. *Carneithyris carnea* (J. Sowerby 1812) from the Upper Campanian and *Carneithyris subcardinalis* (Sahni 1925) from the Maastrichtian. The geographical and stratigraphical variation of these species is described. An attempt was made to demonstrate the variation statistically but this was not found to be possible with the present material.

The representatives of *Carneithyris* treated here are chiefly from the white chalk facies of Campanian and Maastrichtian age. However, the discussion is supplemented by reference to forms from other facies of the Upper Cretaceous and Lower Tertiary where these can shed light on the variation and phylogeny of the genus.

II. ACKNOWLEDGEMENTS

My sincere thanks are due to the following institutions and persons: Mr Ellis F. Owen of the British Museum (Natural History), Dr Brian McWilliams of the Norwich Castle Museum, and Mr Christopher J. Wood of the Institute of Geological Sciences, London. To Mr C. J. Wood and Mr Norman B. Peake of Norwich I am deeply indebted for valuable discussions on the stratigraphy of Norfolk and guidance in the field. Mr Walter Kegel Christensen of the Mineralogisk Museum, Copenhagen, kindly gave advice on statistical methods. I am grateful to Dr Finn Surlyk for many constructive discussions on brachiopods and their ecology, and to the late Professor Alfred Rosenkrantz who encouraged me to take up the study of the *Carneithyris* group. The text-figures are the work of Mr H. Egelund. Last but not least my thanks are due to Dr Richard G. Bromley who patiently took the many photographs of the types, often under trying conditions, and later, assisted by Dr John S. Peel, improved the English of the manuscript. My final visit to England for study in 1972 was supported by the Danish Science Council and the Royal Society of London.

III. HISTORICAL REVIEW

Terebratula carnea J. Sowerby 1812 and *Terebratula elongata* J. de C. Sowerby 1823 are among the species of terebratulids most quoted in the literature on the Upper Cretaceous White Chalk of northern Europe. Davidson (1854 : 67) placed *T. elongata* in synonymy with *T. carnea* and figured several specimens from the Upper Campanian of Norfolk.

The English Campanian–Maastrichtian terebratulids were treated comprehensively by Sahni (1925, 1925a, 1929, 1958). In 1925 he based his work on material in the Institute of Geological Sciences, London, and the Castle Museum, Norwich. Since he had seen the collections of neither Sowerby nor Davidson in the British Museum (Natural History), London, he found it impossible to identify any of the specimens available to him with the true *T. carnea* and *T. elongata*. Nevertheless, he erected four new genera to cover what different authors until then had called *T. carnea* and *T. elongata*, viz. *Pulchrithyris*, *Carneithyris*, *Chatwinothyris* and *Ellipsothyris*. In the same paper Sahni (1925) erected the following 13 species :

Pulchrithyris gracilis
P. extensa
Carneithyris subpentagonalis
C. circularis
C. variabilis
C. acuminata
C. norvicensis
Magnithyris magna
Chatwinothyris subcardinalis
Ch. symphytica
Piarothyris rotunda
Ellipsothyris similis
Ornithothyris carinata

Shortly after this he (1925a) added the following five new species to the list :

Carneithyris daviesi
C. subovalis
C. uniplicata
Chatwinothyris curiosa
Ch. gibbosa

and, concerning the evolution and ontogeny of the species of *Carneithyris*, he arrived at the following conclusions (1925a : 502) :

> 1. That the type of hinge-parts and cardinal process is of considerable importance in the study of Chalk Terebratulids.
> 2. That the cardinal process shows a distinct line of evolution in the genus *Carneithyris* expressed by :
> (a) Change in shape from pyramidal to globular.
> (b) Greater and greater development of its apophyses.
> (c) Change in position with respect to the surrounding hinge-parts.
> 3. That these changes are repeated in phylogeny as well as in ontogeny.

Sahni (1925a : pl. 25) arranged the following table to illustrate the changes in ontogeny and phylogeny :

	ontogeny	*phylogeny*
Stage IV	*Carneithyris subpentagonalis* (fig. 1)	
	C. subpentagonalis (fig. 7)	*C. variabilis* (fig. 2)
Stage III	*C. subpentagonalis* (fig. 8)	*C. daviesi* (fig. 3)
Stage II	*C. subpentagonalis* (figs 9, 10)	*C. subovalis* (fig. 4)
		C. subovalis (fig. 5)
Stage I	*C. subpentagonalis* (fig. 11)	*C. uniplicata* (fig. 6)

From this it must naturally follow that *C. uniplicata* is found in strata considerably older than those bearing *C. subpentagonalis* and *C. variabilis*.

In 1929 the species erected formally and correctly in 1925a Sahni again described as new and, in addition, the new species *Carneithyris ornata* and *Magnithyris truncata* were erected. In the same year he redescribed and refigured *Carneithyris carnea* and *C. elongata* for the first time.

In 1958 Sahni published a description of the Campanian and Maastrichtian terebratulids belonging to the *Carneithyris* group from A. W. Rowe's collection which, in about 1926, had come into the possession of the British Museum (Natural History). No new species were described, but more than 50 specimens of *Chatwinothyris subcardinalis* were examined and 17 specimens of *Carneithyris gracilis* and two of *C. carnea* from the Campanian of the Norwich area were also dealt with. Thus, by 1958, 19 species of carneithyridines from the Upper Campanian and three species from the Lower Maastrichtian of the Norwich area were known.

From the Maastrichtian Craie Phosphaté de Ciply, Belgium, Sahni (1929 : 41–2) erected the new species *Chatwinothyris ciplyensis* and placed some Danian specimens known under the name '*Terebratula lens*' Nilsson in *Chatwinothyris*.

Between 1925 and 1958 *Carneithyris* and *Chatwinothyris* were reported from the Campanian, Maastrichtian and Danian of Sweden (Hägg 1940, 1954), Denmark (Rosenkrantz 1945), Poland (Kongiel 1935) and Bulgaria (Tzankov 1940 ; Zakharieva-Kovaceva 1947). In 1965 Steinich monographed the Upper Lower Maastrichtian brachiopods from the island of Rügen, Germany, and gave an extremely comprehensive description of *Chatwinothyris subcardinalis*, including a first description of its ontogeny and variation.

Muir-Wood (1965 : 799) erected a new subfamily of terebratulids, the Carneithyridinae, represented only by the two genera *Carneithyris* and *Chatwinothyris*. Concerning *Pulchrithyris*, *Ellipsothyris*, *Magnithyris*, *Ornithothyris* and *Piarothyris* she wrote : 'These genera are considered to be variants of *Carneithyris* and not distinct genera.'

The Upper Cretaceous terebratulids of the Middle Vistula valley, Poland, were described by Popiel-Barczyk (1968). Among these were the carneithyridines *Carneithyris subpentagonalis*, *C. carnea* and *C. circularis* from the Campanian and Maastrichtian ; *C. elongata* from the Upper Maastrichtian ; and, in addition, *Chatwinothyris subcardinalis*, *Ch. curiosa* and *Ch. lens* from the Upper Maastrichtian. In her identification of the species she considered that external features were more dependable than internal ones, and (1968 : 23, 30) that the cardinalia in each species varied considerably, depending on the age of the individual specimen.

Asgaard (1970) discussed Sahni's specimens of *Chatwinothyris lens* and showed that they were not the true Upper Danian *Terebratula lens* of Nilsson (1827) but the slightly older *Terebratula incisa* Buch (1835) ; she considered furthermore that *Chatwinothyris* was a synonym of *Carneithyris*.

Surlyk (1972 : 24) also considered *Chatwinothyris* to be congeneric with *Carneithyris* and described the special adaptation of the Maastrichtian white chalk *C. subcardinalis* to a free-living mode of life as a 'self-righting tumbler'.

IV. THE PROVENANCE OF THE TYPE MATERIAL

During the period 1925–27, when Sahni wrote his first three papers, practically every carneithyridine in the collections of the British Museum (Natural History), the Geological Survey of Great Britain, now the Institute of Geological Sciences, London, and the Norwich Castle Museum was opened and dissected, and designated as a type, figured or identified. Later the British Museum (Natural History) came into the possession of A. W. Rowe's stratigraphically well-documented collection of brachiopods, part of which formed the basis of Sahni's latest paper (1958) on the British terebratulids, but these specimens were not dissected.

The classical 'Upper Chalk of Norwich, Zone of *Belemnitella mucronata*' was long considered a single stratigraphical unit and collectors and museum curators often considered it unimportant to state on the labels from which pits the specimens originated. However, the careful stratigraphical collections made by Rowe and Brydone showed that the Upper Chalk of Norwich could be split up into Campanian and Lower Maastrichtian parts (Brydone 1908, 1909, 1938). Mainly on the basis of Brydone's work Peake & Hancock (1961 : 297, fig. 3) divided the classical Norwich Chalk into six subdivisions :

	estimated thickness
Paramoudra Chalk	23 m
Beeston Chalk	23 m
Catton Sponge Bed (a complex of incipient hardgrounds at the top of :)	
Weybourne Chalk	23 m
Eaton Chalk	15 m
Basal *mucronata* Chalk	15 m

Thus the Upper Campanian (zone of *Belemnitella mucronata* s.l.) is about 100 m thick. Above this follows a Lower Maastrichtian series estimated to be about 33·5 m thick, which is only known well from glacially transported masses. The Campanian/Maastrichtian contact has not yet been observed with certainty in the Norfolk area (see p. 360). The subdivisions of Peake & Hancock (1961) will be used in this paper.

The specimens in Sahni's material which have labels with a locality name other than 'Upper Chalk, Norwich' originate from the following localities :

'Trowse.' According to the Sowerbys (1812, 1823) the types of *Terebratula carnea* and *T. elongata* came from this locality. Several pits in the Trowse area in high Beeston Chalk may have contributed towards what was called 'Trowse' on early 19th-century museum labels. Later on this designation might also have included *Whitlingham* (Crown Point Pit), which was opened in the late 19th century, exposing high Paramoudra Chalk.

'Thorpe.' Several types are labelled 'Thorpe'. This locality name also covers a number of pits which were found in the area stretching eastwards from near the centre of Norwich to Postwick. *Lollard's Pit* was in high Beeston Chalk ; it was the source of *Mosasaurus* remains and therefore might include some part of the hardground complex which is considered to separate the Beeston Chalk from the Paramoudra Chalk (Peake & Hancock 1970). The pit called *St James's Hollow* was in strata of approximately the same age. Two large pits known as *Thorpe Hamlets* were intensively worked in the early 19th century and much material collected by Fitch, King, S. Woodward and others may have come from here. These pits were also in high Beeston Chalk. Further east of these was the locality known as *Thorpe Limekiln* or *Thorpe Lunatic Asylum Pit.* The chalk in it was quite markedly yellow and a section about 2 m high could still be seen when I visited it in 1962. The pit is considered to have been in high Paramoudra Chalk. It was available to the early collectors, and later yielded much material to Rowe. The pit at *Thorpe Tollgate* also contained yellow chalk from high Paramoudra Chalk and was worked in the early 19th century. Further east was the *Postwick Grove* pit which exposed chalk of the same age as Thorpe Tollgate. These two pits exposed possibly the highest *in situ* Paramoudra Chalk in Norfolk.

Mousehold, earlier called *Magdalen Chapel.* From this pit Rowe collected many large carneithyridines and according to E. F. Owen, N. B. Peake and C. J. Wood (personal communications 1972) this was the pit which yielded most of Bayfield's collection of extremely large, often gerontic specimens. Now in the British Museum (Natural History), this formed an important part of Sahni's material ; it contains eight of his types, two possible types (one of which is figured), one figured specimen and three identified to species. The pit is considered to have been in Beeston Chalk and probably high in the lower half of it.

'Catton.' Some of Sahni's material originated from 'Catton by Norwich' (collected by H. M. Muir-Wood) and '? Norwich' (collected by Sahni). According to E. F. Owen (personal communication 1971) Sahni and Muir-Wood visited the Norwich area on one occasion guided by the late T. H. Withers, and collected in *Attoe's Pit,* Catton. At that time this pit exposed Weybourne Chalk at the bottom, with the Catton Sponge Bed complex at its summit, overlain by a considerable section in low Beeston Chalk.

Trimingham. These outcrops of glacially transported masses along the coast between Sidestrand and Mundesley have yielded much material to the old collections. The masses were mapped and described in detail by Brydone (1908). Brydone

(1938 : 7) concluded that the lower part of the Trimingham Chalk was of approximately the same age as the White Chalk of Rügen, Germany, and the upper part equivalent to the Tuffeau of Maastricht, Holland. The following subdivision by Brydone of the Trimingham Chalk has also been used by Peake & Hancock (1961, 1970) and Wood (1967) :

	estimated thickness	belemnite zones (Wood 1967)
Grey Beds	c. 6·7 m	base of *Belemnella occidentalis cimbrica* Zone
White Chalk with '*Ostrea lunata*'	c. 6·1 m	*B. occidentalis occidentalis* Zone
White Chalk without '*O. lunata*'	c. 2·7 m	
Sponge Beds	c. 3·7 m	restricted *B. lanceolata* Zone
Porosphaera Beds	c. 4·3 m	

According to Peake & Hancock (1961 : 323) the White Chalk with and without '*Ostrea lunata*' yielded most of the old material labelled 'Trimingham'. F. Surlyk (personal communication 1973) considers the Grey Chalk to belong to his Zone 5 on the basis of the brachiopods (Surlyk 1970) while the lower part of the Sponge Beds and the *Porosphaera* Beds predate brachiopod zones known from the Lower Maastrichtian of Denmark.

The old collection of Norwich Castle Museum. This collection was the basis for parts of Sahni's first paper (1925) and it contains ten types and two figured specimens of carneithyridines. It contains specimens from the Fitch, King and S. Woodward collections, but owing to inadequate curation at the beginning of this century the original labels were separated from the specimens. Apart from figured specimens and those marked with ink, it is impossible even to ascertain from which of the classical collections the brachiopods came and their exact localities are unknown (B. McWilliams, personal communication 1972).

For much of this section I am greatly indebted to Mr C. J. Wood, who has generously put at my disposal his extensive knowledge on the stratigraphical position of pits in the Norwich area, many of which are now obliterated.

V. REVIEW OF SAHNI'S MATERIAL OF CARNEITHYRIDINES

In this and the following sections the glossary of morphological terms used in the *Treatise on Invertebrate Paleontology*, **H** (1965) will be followed. Specimens treated in this chapter are housed in the British Museum (Natural History) (numbers with B), the Institute of Geological Sciences (GSM) and the Norwich Castle Museum old collections (CMN or KCN). A name in parentheses after the number of the specimen is that of the collector ; following this is the locality as originally given. In the plates no attempt has been made to retouch the photographs : the figures have been largely arranged according to the development of the cardinalia.

Carneithyris carnea (J. Sowerby, 1812)

Pl. 1, figs 1–3 ; Pl. 3, fig. 3 ; Pl. 5, fig. 9 ; Text-fig. 2B

Lectotype (sel. Sahni, 1929) : B 49836 (Sowerby) 'Trowse' (Pl. 1, fig. 1)
Sowerby, 1812 : 47 ; pl. 15, fig. 5
Sahni, 1929 : 31–2 ; pl. 4, fig. 34
The lectotype is here refigured.

Paralectotype ('Syntype' of Sahni) : B 49837 (Sowerby) 'Trowse' (Pl. 1, fig. 2)
Sowerby, 1812 : 47 ; pl. 15, fig. 6
Sahni, 1929 : pl. 9, fig. 26
The brachial valve of the 'syntype', last figured by Sahni, has since been lost and only the pedicle valve remains.

'Plesiotype'[1] of Sahni : B 45600 (Bayfield) 'Norwich' (Pl. 3, fig. 3)
Sahni, 1929 : pl. 9, fig. 25
This is practically identical in cardinalia and external features with the paratype B 45603 of *C. circularis* (Pl. 3, fig. 2), also from the Bayfield collection. It is also very similar to the holotypes of *C. subovalis*, *C. uniplicata* and *Ellipsothyris similis* (Pl. 4, figs 3, 9, 10).

Others : B 51289 (Rowe) 'Whitlingham'
Sahni, 1958 : 17 ; pl. 6, figs 8a–c
Of the three specimens from Rowe's collection, only this one has been returned to it.

B 51274 and B 51288 (Rowe), said to be from Norwich
Sahni, 1958 : pl. 6, figs 9a–c, 10a–b
These have not been found in the collection : the specimen now numbered B 51274 is clearly not that which Sahni figured under that number (see p. 330).

? B 49852 (Davidson) 'Trimingham' (Pl. 1, fig. 3)
Davidson, 1854 : pl. 8, fig. 1
This specimen was not mentioned by Sahni. Although it is said to be from Trimingham, its pink colour shows it to be Campanian.

26 KCN and 27 KCN 'Upper Chalk, Norwich' (Pl. 5, fig. 9 ; Text-fig. 2B)
Sahni, 1929 : pl. 4, figs 20–23 ; pl. 9, figs 17–18
Sahni called these *C.* cf. *carnea*, but they are not mentioned in the text. 27 KCN, here figured, has cardinalia of a type which very much resembles that of the holotypes of *Pulchrithyris gracilis* and *C. norvicensis* (Pl. 5, figs 7, 11). 26 KCN has never been dissected.

Terebratula carnea was the first carneithyridine brachiopod described and strictly should have been chosen as the type of the genus *Carneithyris*. (Instead, *C. subpentagonalis* was chosen.) The lectotype and 'syntype' are also from known localities, in contrast to the types of *C. subpentagonalis*. The three specimens of *C. carnea* with known localities are possibly from high Beeston Chalk (the types) and

---

[1] The use of the term 'Plesiotype' is to be discouraged. It has been used in a variety of senses (Frizzell 1933 : 662; Fernald 1939 : 699), all of them unnecessary. Sahni did not define his use of the term.

Paramoudra Chalk (B 51289); this agrees well with their rather small size and thin shells.

Carneithyris elongata (J. de C. Sowerby, 1823)

Pl. 2, figs 1–3; Pl. 4, fig. 5

Lectotype: B 49823 (Sowerby) 'Trowse' (Pl. 2, figs 1a–c)
Sowerby, 1823: 49; pl. 435, fig. 1
Sahni, 1929: 32; pl. 6, fig. 19
Paralectotype ('Syntype' of Sahni): B 49824 (Sowerby) 'Trowse' (Pl. 2, figs 2a–b)
Sowerby, 1823: pl. 435, fig. 2
Sahni, 1929: 32
'Plesiotype' of Sahni: B 45243 (Muir-Wood) 'Catton Pit, north of Norwich' (Pl. 4, fig. 5)
Sahni, 1929: pl. 4, figs 24–26; pl. 10, fig. 9
Others: B 6101 (Davidson *ex* Fitch) 'Upper Chalk, Norwich' (Pl. 2, figs 3a–c)
Davidson, 1854: pl. 8, fig. 3

The lectotype and syntype are both from Trowse, possibly the same locality which yielded the types of *C. carnea*. Both specimens are small and rather thin-shelled (Pl. 2, figs 1, 2). The 'plesiotype' might be from high Weybourne Chalk, the Catton Sponge Bed, or low Beeston Chalk. Sahni did not mention the specimen figured by Davidson which I have added here. Incidentally, Norwich Castle Museum also claims that its specimen no. 2072 is the one which Davidson figured; it is nearly identical to the London specimen but, according to Davidson's own label, there can be no doubt that B 6101 is the one which is figured. The cardinalia of the 'plesiotype' closely resemble those of the 'plesiotype' of *C. carnea* (Pl. 3, fig. 3) and of the paratype B 45604 of *C. circularis* (Pl. 4, fig. 7).

Carneithyris subpentagonalis Sahni, 1925

Pl. 7, figs 2, 3

Holotype: 8 KCN 'Upper Chalk, Norwich' (Pl. 7, fig. 2)
Sahni, 1925: 365; pl. 23, fig. 15; pl. 24, fig. 13; pl. 25, fig. 3
Sahni, 1925a: 498; pl. 25, fig. 1
Sahni, 1929: 31; pl. 5, figs 30, 31; pl. 9, figs 5, 6
Paratype: GSM 44491 'Norwich' (Pl. 7, fig. 3)
Sahni, 1925: pl. 24, fig. 2; pl. 26, fig. 3
Sahni, 1925a: pl. 25, fig. 7
Sahni, 1929: pl. 9, fig. 7
Others: Davidson, 1854: pl. 8, fig. 2 (Sahni (1925, 1929) considered this figure to represent the species, but the original specimen seems to be lost)
Sahni, 1925a: pl. 25, figs 3–5, 8 (not 9–11 as stated by Sahni)

When Sahni erected *Carneithyris* in 1925 he chose this species as type. In the collections today it is only represented by the two type specimens ; the specimens representing the ontogenetic Stages I–III of *C. subpentagonalis* (1925a : Pl. 25, figs 3–5, 8) have not been identified.

Carneithyris circularis Sahni, 1925

Pl. 3, figs 1, 2 ; Pl. 4, figs 6, 7

Holotype : 15 KCN 'Norwich' (Pl. 4, fig. 6)
  Sahni, 1925 : 365 ; pl. 24, fig. 14
  Sahni, 1929 : 33
Paratypes : B 49862 (Davidson) 'Norwich' (Pl. 3, fig. 1)
  Davidson, 1854 : pl. 8, fig. 5
  Sahni, 1929 : pl. 5, figs 11–13
    B 45602 (Bayfield) 'Norwich'
  Sahni, 1929 : pl. 5, figs 8–10
    B 45603 (Bayfield) 'Norwich' (Pl. 3, fig. 2)
  Sahni, 1929 : pl. 9, fig. 23
    B 45604 (Bayfield) 'Norwich' (Pl. 4, fig. 7)
  Sahni, 1929 : pl. 5, figs 6, 7 ; pl. 9, fig. 24

The cardinalia of the holotype have not been previously figured. They are very similar in morphology to those of the paratype of *C. variabilis* (Pl. 7, fig. 4) and somewhat like those of the paratype of *C. subpentagonalis* (Pl. 7, fig. 3).

Sahni (1929) stressed that this species differed from all other *Carneithyris* in its circular outline, but it shares this feature with the lectotype and the 'plesiotype' of *C. carnea* (p. 326), and the holotype of *Magnithyris magna* (p. 333).

Carneithyris variabilis Sahni, 1925

Pl. 5, fig. 1 ; Pl. 7, fig. 4

Holotype : 14 CMN 'Chalk near Norwich' (Pl. 5, fig. 1)
  Sahni, 1925 : 366
  Sahni, 1929 : 34
Paratype : 13 CMN 'Chalk near Norwich' (Pl. 7, fig. 4)
  Sahni, 1925 : pl. 25, fig. 4
  Sahni, 1925a : pl. 25, fig. 2
  Sahni, 1929 : pl. 4, fig. 27

The holotype shows the cardinalia which are not completely dissected out ; they are somewhat similar to those of the holotypes of *C. acuminata* (Pl. 5, fig. 3) and *C. daviesi* (Pl. 6, fig. 3), and of the two possible paratypes of *C. norvicensis*, B 52067 and B 45610 (Pl. 5, fig. 8 ; Pl. 6, fig. 5). The cardinalia of the paratype closely resemble those of the holotype of *C. circularis* (Pl. 4, fig. 6) and of the paratype of *C. subpentagonalis* (Pl. 7, fig. 3). While the outer shape of the paratype is very much like the holotype of *C. subpentagonalis*, Sahni (1925 : 366) stressed that *C. variabilis* had its symphytium hidden under the strongly incurved beak. He (1925a) considered *C. variabilis* as having reached a level of development between his Stages III and IV.

Carneithyris acuminata Sahni, 1925

Pl. 5, fig. 3

Holotype : 19 CMN 'Upper Chalk, Norwich'
Sahni, 1925 : 366 ; pl. 26, fig. 5
Sahni, 1929 : 33 ; pl. 5, figs 17–19 ; pl. 9, fig. 15

This species is represented by a single specimen. According to Sahni (1929 : 33) it is distinguished from *C. elongata* by having a 'very much more advanced' cardinal process. However, the only type-specimen of *C. elongata* in which the cardinal process is clearly visible is the 'plesiotype' (Pl. 4, fig. 5) and in this the process would appear to be at least as 'advanced' (in Sahni's terms) as that of *C. acuminata*. Furthermore, the cardinal process of *Ornithothyris carinata* (Pl. 5, fig. 2) is also comparable in morphology.

Carneithyris norvicensis Sahni, 1925

Pl. 5, figs 8, 11 ; Pl. 6, fig. 5 ; Text-fig. 2C

Holotype : GSM 44494 'Norwich' (Pl. 5, fig. 11)
Sahni, 1925 : 367 ; pl. 24, fig. 5 ; pl. 26, fig. 1
Sahni, 1929 : 34 ; pl. 4, fig. 29
It is not known from which pit the holotype was collected.

Paratypes : ? B 52067 'No information' (Pl. 5, fig. 8)
? B 45610 (Bayfield) 'Norwich' (Pl. 6, fig. 5 ; Text-fig. 2C)
? B 51636 and B 51637 (Sahni) '? Norwich'
Sahni, 1925 : pl. 26, fig. 14

Sahni (1925 : 367) considered this species distinct, with its vascular markings 'arising from in between the muscle-marks (instead of from their anterior apices), and forking as it were from the pseudoseptum'. Pl. 5, fig. 11 and Sahni (1925 ; pl. 24, fig. 5) show that what he interpreted as 'mantle impressions' are in reality slight depressions on either side of the ridges that form the anterior prolongation of Sahni's 'pseudoseptum' ; they represent a characteristic gerontic feature, like the pitted callus deposits round the bases of the inner socket ridges. It is now impossible to state which of the four specimens identified as *C. norvicensis* is the paratype figured, but not mentioned, in 1925. Both those here figured have large, swollen cardinal processes : the cardinalia of this nominal species are shown here for the first time. B 51636 and B 51637 are probably from Attoe's pit, Catton (see p. 324). The first of these two was originally about 42 mm long and has a somewhat thickened posterior end ; the other has very strong callus deposits in the posterior part of the valves, so much so that the cardinalia seem to sit astride a cushion.

Carneithyris subovalis Sahni, 1925a

Pl. 4, figs 3, 4; Text-fig. 2A

Holotype: B 15159 (Bayfield) 'Norwich' (Pl. 4, fig. 3; Text-fig. 2A)
? Sahni, 1925a: 500; pl. 25, fig. 10 (not 4 or 5 as stated by Sahni)
Sahni, 1929: 34; pl. 4, fig. 33; pl. 9, fig. 16

Paratype: Norwich Castle Museum (no number) 'Upper Chalk, Norwich' (Pl. 4, fig. 4)
Sahni, 1929: pl. 4, figs 31, 32; pl. 10, fig. 17
? Sahni, 1925a: pl. 25, fig. 11 (not 4 or 5 as stated by Sahni)

Others: B 45659 (C. Birley) 'Norwich' (identified and dissected by Sahni)
B 15157 (Bayfield) 'Norwich' (called 'young specimen' by Sahni)
B 45652 (Bayfield) 'Norwich' (called *C. subovalis* (?) by Sahni)
B 44182 (Rowe) 'Edward's Pit (now Campling's) Mousehold' (identified by Sahni)
B 51274 (Rowe) 'Mousehold' (identified by Sahni, *not* identical with the specimen figured in 1958 with the same number, see p. 326)

None of the three specimens which were opened and dissected by Sahni resemble either of the two specimens said to represent the species in his pl. 25, figs 4, 5. On the other hand, the holotype and the paratype look much more like his pl. 25, figs 10, 11, and it would seem that the figures have been mistakenly interchanged, as in pl. 25, fig. 9.

This species is considered to represent Stages I–II in the evolutionary tree. The two unopened specimens from Rowe's collection came from Mousehold Pit (= Magdalen Chapel) and the three specimens from Bayfield's collection might have come from the same. Thus, at least five of the specimens seem to have come from the upper low Beeston Chalk, which is known for its large brachiopods.

Carneithyris uniplicata Sahni, 1925a

Pl. 4, fig. 9

Holotype: GSM 48518 'Thorpe' (Pl. 4, fig. 9)
Sahni, 1925a: 500; pl. 25, fig. 6
Sahni, 1929: 35; pl. 4, fig. 30; pl. 10, fig. 18

Others: GSM 48514 and 48515 'Whitlingham' (brachial and pedicle valve of the same specimen identified by Sahni as *C.* cf. *uniplicata*)

In his original description of this species Sahni (1925a: 500) stressed 'the primordial character' of its cardinal process and made it the representative of his Stage I in his evolutionary tree of cardinal processes (see p. 322). This, however, does not fit very well with the provenance of the material, which is from late Beeston Chalk to Paramoudra Chalk. The incipient plication which is discussed on p. 361 also supports the late age.

Carneithyris daviesi Sahni, 1925a

Pl. 6, figs 1–4 ; Pl. 7, fig. 1 and Text-fig. 2D

Holotype : B 45599 (Bayfield) 'Norwich' (Pl. 6, fig. 3)
Sahni, 1925a : 500 ; pl. 25, fig. 9 (not 3 as stated by Sahni)
Sahni, 1929 : 36 ; pl. 9, fig. 10

Paratype : B 459 (Bayfield) 'Norwich' (Pl. 6, figs 1, 2 ; Pl. 7, fig. 1 ; Text-fig. 2D)
Sahni, 1929 : pl. 5, figs 4, 5 ; ? pl. 9, fig. 8 ; pl. 9, fig. 9

Others : B 45642 (C. F. Cockburn) 'Norwich' (identified and dissected by Sahni) (Pl. 6, fig. 4)

The two type specimens are the largest and most gerontic carneithyridines in the Bayfield collection. The paratype shows particularly extreme gerontic features : Pl. 6, fig. 1 and Pl. 7, fig. 1 show the swollen and protruding cardinal process and the thickened hinge region of the brachial valve in this specimen. The pedicle valve, moreover, shows the most gerontic features to be seen in any *Carneithyris* in the British collections (Pl. 6, figs 1, 2) ; the enormously thickened tooth bases overlap but have not fused and a tube is left open for the pedicle case and its muscles. There is a 'pearl' in the adductor muscle impression. The length of the pedicle valve is 43 mm. The 'drawing of the brachial valve of a large specimen with brachidium' (Sahni 1929 : pl. 9, fig. 8) has a remarkable resemblance to the paratype, when the brachial valve of this is tilted slightly.

The holotype (Pl. 6, fig. 3) also exhibits a swollen cardinal process and has some callus deposits in the posterior part of the valves. The length of the pedicle valve was c. 35·5 mm. The third specimen, B 45642, was not completely dissected by Sahni, but nevertheless shows a cardinal process very much like that of the holotype ; it is fairly thin-shelled and is only about 33 mm long.

C. daviesi was considered to represent Stage III in the evolution of cardinal processes (Sahni 1925a).

Carneithyris ornata Sahni, 1929

Pl. 4, figs 11, 12

Holotype : GSM 48498 'Thorpe'
Sahni, 1929 : 35 ; pl. 4, fig. 28 ; pl. 10, fig. 22

The nominal species is represented by a single specimen, in which, apart from the preserved original colour pattern, Sahni (1929 : 35) found 'a small septum in the pedicle valve' and unusually shaped vascular markings. There is a slight ridge between the ventral adjustor scars and the vascular markings are clear ; these, in connection with the pitted callus deposits in the posterior part of the valves (Pl. 4, fig. 12), are gerontic features of this particular specimen.

Pulchrithyris gracilis Sahni, 1925
Pl. 5, figs 4–7

Holotype : GSM 48487 'Magdalen Chapel, Norwich' (Pl. 5, fig. 7)
Sahni, 1925 : 362 ; pl. 23, fig. 6 ; pl. 24, fig. 12a
Sahni, 1929 : 36 ; pl. 5, figs 26–28 ; pl. 9, fig. 11

Paratype : GSM 48485 'Harford Bridges' (Pl. 5, fig. 6)
Sahni, 1925 : pl. 24, fig. 12
Sahni, 1929 : pl. 9, fig. 13

Others : B 46300 (Muir-Wood) 'Catton Pit, Norwich' (Pl. 5, fig. 5)
Sahni, 1929 : pl. 9, fig. 12
B 98123 (J. Brown) 'Charing, Kent' (Pl. 5, fig. 4)
Sahni, 1929 : pl. 9, fig. 14
B 51492 (Rowe) 'Thorpe, Limekiln Pit'
Sahni, 1958 : 16 ; pl. 6, figs 7a–c
B 51271–51273 (Rowe) 'Mousehold'
B 51275, 51276 (Rowe) 'Whitlingham'
B 51277 (Rowe) 'Mousehold'
B 51278 (Rowe) 'Whitlingham'
B 51279–51281 (Rowe) 'Mousehold'
B 51282 (Rowe) 'Whitlingham'
B 51283, 51284 (Rowe) 'Mousehold'
B 51285 (Rowe) 'Whitlingham'
B 51286, 51287 (Rowe) 'Mousehold'
Sahni 1958 : 16 (B 51271–3, B 51275–87 inclusive)
GSM 48484, 48486 (J. H. Blake) 'Trowse' (identified by Sahni)

When the species was first erected it was intended to cover what some authors had called *Terebratula elongata*. The genus *Pulchrithyris* was distinguished by having a loop which was 'exceptionally flat, bow-shaped with anteriorly directed apex (a very distinctive feature)' (1925 : 362). The peculiar loop can also clearly be seen on pl. 23, fig. 6. Later Sahni made *Pulchrithyris* a synonym of *Carneithyris* ; 'Owing to its delicate character I was unable to obtain the brachial apparatus of these two species without damaging the loop, and this led me into an error as to the orientation of this latter structure in relation to the crura' (Sahni 1929 : 31). The holotype was now figured with the loop glued on with the correct side up while the loop of the paratype remained upside down, as it does to this day (Pl. 5, fig. 6 ; see Sahni 1929 : pl. 9, fig. 13).

The holotype is from Magdalen Chapel (= Mousehold) ; the label of the paratype gives the locality erroneously as Lollard's pit, Thorpe (high Beeston Chalk), owing to an incorrect transcription of information from the old catalogue. The actual locality should be Harford Bridges which, according to C. J. Wood (personal communication 1973), comprised at least three pits in the upper third of the Weybourne Chalk.

Sahni (1929) figured two other specimens, one of which according to its label would be from Charing, Kent (Pl. 5, fig. 4). This must be an error, since from its characteristic features and pink colour there is no doubt that it came from an Upper Campanian locality in Norfolk. Later (1958) 17 specimens from Rowe's collection were dealt with. Of these, 11 are from Mousehold (the type locality), five from Whitlingham and one from Thorpe, Limekiln Pit (not Thorpe St Andrew's as stated on the label). Two specimens in the collections of the Institute of Geological Sciences, both from 'Trowse', have been identified by Sahni as belonging to this species. Thus the material of *C. gracilis* covers a stratigraphical range from high Weybourne Chalk to high Paramoudra Chalk. All specimens of the nominal species are rather small in comparison with many of the others, and none of the opened specimens shows extreme gerontic features.

Pulchrithyris extensa Sahni, 1925

Pl. 4, fig. 8

Holotype : 7 KCN 'Upper Chalk, Norwich'
Sahni, 1925 : 363 ; pl. 24, fig. 15 ; pl. 25, fig. 8 ; pl. 26, fig. 8
Sahni, 1929 : 36 ; pl. 6, figs 29–31

In its present condition the single specimen has no brachidium. Sahni neither figured nor described its cardinalia and brachidium, so it is difficult to see any reason for placing it in the genus *Pulchrithyris*. Sahni considered it distinct through its 'much elongate and pod-shaped character'. Its cardinal process is slightly asymmetrical but somewhat resembles that of *Carneithyris ornata* (Pl. 4, fig. 12).

Magnithyris magna Sahni, 1925

Pl. 4, fig. 1 ; Pl. 5, fig. 10

Holotype : GSM 48488 'Thorpe' (Pl. 4, fig. 1)
Sahni, 1925 : 367 ; pl. 23, fig. 1 ; pl. 24, fig. 1 ; pl. 25, fig. 1
Sahni, 1929 : 39 ; pl. 5, figs 1–3 ; pl. 10, fig. 7
Others : B 15149 (Bayfield) 'Norwich' (Pl. 5, fig. 10)
Sahni, 1929 : pl. 10, fig. 8
B 44680, 45609, 45611 (Bayfield) 'Norwich' (identified and dissected by Sahni)
B 45586 (Bayfield) 'Norwich' (called 'young' by Sahni)
B 45639 (C. F. Cockburn) 'Norwich' (identified and dissected by Sahni)

The genus *Magnithyris* is said to be distinct from *Carneithyris* in 'its peculiar obtuse beak, its distinctive cardinal process and brachidium. The foramen . . . is also much larger than in species of *Carneithyris*, and the socket-ridges very much thinner' (Sahni, 1929 : 39). Pl. 4, fig. 1 shows the cardinalia, which somewhat resemble those of *M. truncata* (Pl. 4, fig. 2).

The other figured specimen B 15149 has less feeble cardinalia than the holotype but the transverse band, which is broken off, is concealed in matrix and the left crus is glued on in the wrong position. The diameter of the pedicle foramen is 1·2 mm, but several of the types of *Carneithyris* spp. have foramina of this order of size, e.g. *C. circularis* (paratype B 49862), *C. daviesi* (paratype) and *Ellipsothyris similis* (holotype). Sahni (1929 : 38) erroneously called this specimen a paratype of *Ellipsothyris similis* (see p. 335).

B 44680, 45609, 45611 have been dissected ; none of them shows particularly thin socket ridges and the diameters of the pedicle foramina do not exceed 1·5 mm. B 45586 has not been opened ; its pedicle valve is 29 mm long and its foramen is 1·0 mm in diameter. B 45639 has cardinalia closely resembling those of *M. truncata* (Pl. 4, fig. 2). This type of *Carneithyris* is discussed further on p. 360.

Magnithyris truncata Sahni, 1929

Pl. 4, fig. 2

Holotype : B 45606 (Bayfield) 'Norwich'
Sahni, 1929 : 39 ; pl. 5, figs 14–16 ; pl. 10, fig. 6

This species is represented by a single specimen ; its shell is thin and transparent, the cardinalia are likewise very delicate and the foramen is large and labiate. For further discussion of this extreme variant of *Carneithyris* see p. 360.

Piarothyris rotunda Sahni, 1925

Pl. 3, fig. 4

Holotype : 18 KCN 'Upper Chalk Norwich'
Sahni, 1925 : 370 ; pl. 23, fig. 14 ; pl. 24, fig. 11 ; pl. 25, fig. 6 ; pl. 26, figs 6, 12
Sahni, 1929 : 37 ; pl. 5, figs 23–25 ; pl. 10, fig. 20

This single specimen, on which the genus *Piarothyris* was founded, was considered a *Carneithyris* by Muir-Wood (1965 : 799). However, it possesses all the characteristics of a *Gibbithyris*. The figure shows the feeble, transverse cardinal process, the ventrally convex hinge-plates and the dorsally directed crura bases. To judge from its external characters, the specimen may have come from a horizon rich in brachiopods in the upper part of the *Micraster coranguinum* Zone (Santonian) in south-east England (C. J. Wood, personal communication 1970). A tiny sample of chalk matrix was taken from the cardinalia, but an analysis of the coccoliths in it by Dr K. Perch-Nielsen of Copenhagen revealed only undiagnostic, long-ranged forms.

Ellipsothyris similis Sahni, 1925

Pl. 4, fig. 10 ; Pl. 7, fig. 5 and Text-fig. 2E

Holotype : 14 KCN 'Upper Chalk Norwich' (Pl. 4, fig. 10)
Sahni, 1925 : 371 ; pl. 23, fig. 13 ; pl. 24, fig. 8 ; pl. 25, fig. 9
Sahni, 1929 : 38 ; pl. 6, figs 12–15 ; pl. 9, fig. 22

? Paratype : B 45653 (Bayfield) 'Norwich' (Pl. 7, fig. 5 ; Text-fig. 2E)
Sahni 1929 : pl. 9, fig. 1 (in the text, p. 38, B 15149 is said to be a paratype, but this specimen is figured on pl. 10, fig. 8 as *Magnithyris magna*)
Others : B 45629 (J. F. Walker) 'Norwich' (identified and dissected by Sahni)

The genus *Ellipsothyris* is based on the cardinal process being 'ellipsoidal with flat dorsal surface, bearing two very incipient knobs postero-laterally and a median one' and the brachidium being 'narrow posteriorly, comparatively broad anteriorly'. The type of cardinal process (Pl. 4, fig. 10) is very similar to that of *Carneithyris circularis* (B 45604, Pl. 4, fig. 7). The brachidium of the holotype is only partly dissected out of the chalk matrix and is now detached from the valve ; its apparent shape in Sahni's illustration (1929 : pl. 9, fig. 22) is mainly due to retouching of the photograph. The presumed paratype differs markedly from the holotype, having completely fused *Chatwinothyris*-like cardinalia and a fairly parallel-sided brachidium (Pl. 7, fig. 5 and Text-fig. 2E). The third identified specimen has cardinalia of a more swollen type than those of the holotype.

Ornithothyris carinata Sahni, 1925

Pl. 5, fig. 2

Holotype : 17 KCN 'Upper Chalk Norwich'
Sahni, 1925 : 374 ; pl. 23, fig. 2 ; pl. 24, fig. 6 ; pl. 25, fig. 5
Sahni, 1929 : 44 ; pl. 6, figs 27, 28 ; pl. 10, fig. 19

The genus and species are represented by a single specimen. Sahni stressed the importance of the 'conspicuous carination of its ventral valve, which points to a sulcate ancestry' and of the transverse band of the brachidium which 'shows a sudden arching up in the middle, producing a slight break in the curve and forming as it were a sub-arch' (Sahni 1925 : 374 ; 1929 : 44). However, Sahni's illustration (1929 : pl. 6, fig. 28) does not show any conspicuous carination of the pedicle valve, and I was unable to see it on the remains of the specimen. The 'sub-arch' on the loop is no more accentuated than in other terebratulids, so far as can be seen, since the brachidium is partly covered by matrix (Pl. 5, fig. 2). In shape and preservation the cardinalia are practically identical with those of *C. acuminata* (Pl. 5, fig. 3).

Chatwinothyris subcardinalis Sahni, 1925

Pl. 8, figs 1–4

Holotype : GSM 44501 (C. Reid) 'Trimingham Foreshore, *O. vesicularis* Bed' (Pl. 8, fig. 1)
Sahni, 1925 : 369 ; pl. 23, fig. 9 ; pl. 24, fig. 4a ; pl. 26, fig. 4
Sahni, 1925a : 499 ; pl. 25, fig. 12
Sahni, 1929 : 40 ; pl. 5, figs 20–22 ; pl. 10, fig. 4
Paratype : B 46326 (A. Laur) 'Isle of Rügen, Germany' (Pl. 8, fig. 2)
Sahni, 1925 : pl. 24, fig. 4
Sahni, 1929 : pl. 6, figs 10–12 ; pl. 10, fig. 1

Others : B 46327 and B 21266 (A. Laur) 'Isle of Rügen, Germany' (Pl. 8, figs 3, 4)
Sahni, 1929 : pl. 10, figs 2, 3
B 51046, 51049 (Rowe) 'Trimingham, *lunata* reef'
Sahni, 1958 : 15 ; pl. 5, figs 1a–c, 2a–c
B 51087, 51058 (Rowe) 'Trimingham, "non-*lunata*" reef'
Sahni, 1958 : pl. 5, figs 3, 4
B 51060 (Rowe) 'Trimingham' (not present in the collection)
Sahni, 1958 : pl. 5, fig. 4x

The holotype is presumably from the lower part of the Grey Beds (C. J. Wood, personal communication 1972) while the paratype and the two other specimens figured in 1929 are from the Isle of Rügen, north Germany (*Belemnella occidentalis* Zone). Sahni (1958 : 15) mentioned that there were 'over fifty specimens' in Rowe's collection ; the specimens figured in 1958 were all from the Trimingham foreshore, from '*Ostrea lunata*' Beds and Grey Beds (see p. 325).

The genus *Chatwinothyris*, of which *Ch. subcardinalis* is the type, is distinguished from *Carneithyris* by having indistinct beak ridges and a pin-hole foramen. Furthermore, 'in *Carneithyris* there is no tendency towards fusion of cardinalia, which is an important feature of *Chatwinothyris*' (Sahni, 1929 : 40).

As can be seen from the figures, this species was permitted unusual freedom of variation in internal characters by its author. The cardinalia of the holotype and B 21266 (Pl. 8, figs 1, 4) show hardly any fusion (compare Popiel-Barczyk 1968 : pl. 9, fig. 1 ; pl. 3, fig. 5). The paratype (Pl. 8, fig. 2) has completely fused cardinalia and looks much like the specimens figured by Steinich (1965 : text-fig. 27(3)) from the Lower Maastrichtian of Rügen and by Popiel-Barczyk (1968 : pl. 8, fig. 7) from the Upper Maastrichtian of Poland. The paratype of *Ch. subcardinalis* is not quite as advanced in its fusion as the holotype of *Ch. curiosa* (Pl. 8, fig. 5). B 46327 (Pl. 8, fig. 3) has nearly completely fused cardinalia, though not to the degree of those of the paratype, and the flaps on the sides of the diductor muscle scars have united to form tubes which surrounded the posterior part of the diductor muscles. A similar development is shown by the specimen figured by Steinich (1965 : text-fig. 27(4)). Popiel-Barczyk (1968 : pl. 5, fig. 6) illustrated under the name *Carneithyris carnea* another specimen showing this development, and in pl. 9, fig. 3, a more gerontic specimen of *Ch. subcardinalis*, both from the Upper Maastrichtian of Poland.

Chatwinothyris symphytica Sahni, 1925

Pl. 2, fig. 4 and Text-fig. 2F

Holotype : GSM 47523 'Chalk near Norwich'
Sahni, 1925 : 369 ; pl. 23, fig. 7 ; pl. 24, fig. 7 ; pl. 26, fig. 9
Sahni, 1929 : 42 ; pl. 10, fig. 13 (called *Ch.* (?) *symphytica* in the text to the figure)

This single specimen shows no tendency to a fusion of the cardinalia, which should be the main feature separating *Chatwinothyris* from *Carneithyris*. Sahni (1925, 1929) himself mentioned this, but for reasons unknown preferred to retain this specimen in *Chatwinothyris*. The specimen is gerontic, with pitted callus deposits in the posterior part of the valves, and the extreme development of the cardinal process can be taken to be a result of old age as in the holotype and paratype of *Carneithyris daviesi* (Pl. 6, fig. 3 ; Pl. 7, fig. 1).

Chatwinothyris curiosa Sahni, 1925a

Pl. 8, fig. 5

Holotype : B 45669 (Savin) 'Trimingham, Zone of *Ostrea lunata*'
Sahni, 1925a : 499 ; pl. 25, fig. 13
Sahni, 1929 : 43 ; pl. 6, fig. 26 ; pl. 10, fig. 12
Sahni, 1958 : 15 ; text-fig. 3

The original description (1925a : 499) reads as follows : 'Here the socket-ridges and the crural bases are somewhat more developed and the process of fusion has gone a step further, so much so that no trace whatever is left of the cardinal process. Its position is now occupied by a narrow flat platform bounded laterally by the partially overhanging and fused crural bases and socket-ridges. Hence it follows that the diductor muscles, in this case, would be attached to this platform instead of directly to the cardinal process, and that the partial articulatory function of the latter has been assumed by the cardinalia.' The specimen figured in pl. 25, fig. 13 has no loop and apparently a gaping hole where the cardinal process should have been. In 1929 (pl. 10, fig. 12) a transverse band has curiously appeared which shows a striking colour difference from the cardinalia. The species was discussed again by Sahni (1958 : 15) under the genus *Chatwinothyris* : 'The cardinal process in such forms becomes atrophied and its function is relegated, partly at any rate, to the fused cardinalia. In extreme cases the cardinal process becomes almost completely resorbed, e.g. in *Chatw. curiosa*.'

An examination of the holotype showed that the gaping black hole on the 1925 illustration was in fact white chalk completely filling the space between the diductor muscle attachment area and the umbo of the valve. When this chalk was removed the diductor impressions could be seen (Pl. 8, figs 5a, b). The curious transverse band is glued onto the interior sides of the crura and thus does not fit this specimen, but must have been derived from a smaller one (Pl. 8, figs 5c, d). Furthermore, this transverse band has the pinkish colour typical of Campanian *Carneithyris* while the rest of the valve is of the greyish colour typical of beekitized Maastrichtian specimens. Specimens with completely fused cardinalia like the holotype are not uncommon in the Maastrichtian (e.g. Nielsen 1909 : pl. 2, figs 71, 75 ; Steinich 1965 : 43, figs 27(3), 32 ; Popiel-Barczyk 1968 : text-fig. 12, pl. 10, figs 1–5). Furthermore, both the paratype of *Chatwinothyris subcardinalis* and the paratype of *Ellipsothyris similis* belong to this type. The tendency towards a complete obliteration of the boundaries between the different elements in the cardinalia is very strong in the Maastrichtian specimens as a result of the general thickening of the posterior part of the shell. Growth studies (Steinich 1965 : text-figs 27 and 29–31) and cellulose peels of serial sections show that a gradual fusion of the cardinalia takes place and it is not a case of suppression or even resorption of the cardinal process as postulated by Sahni. (It is intended to publish serial sections of *Carneithyris* from the Danish Maastrichtian and Danian in a later study now under preparation.) I therefore see no reason to consider B 45669 as representing a separate species, but take it to be well within the variation of *Carneithyris subcardinalis*.

Chatwinothyris gibbosa Sahni, 1925a

Pl. 1, fig. 4

Holotype: B 45670 (Savin) 'Trimingham, Zone of *Ostrea lunata*'
Sahni, 1925a : 499 ; pl. 25, fig. 14
Sahni, 1929 : 43 ; pl. 5, figs 32, 33 ; pl. 10, fig. 21

In the original description (1925a : 499) Sahni pointed out that in *Ch. gibbosa* 'the degree of development and fusion reached by the hinge-parts is about the same as in *C. subcardinalis*, but the former species can be easily distinguished from the latter by its marked gibbous shell and mesothyrid foramen'. As can be seen from 1929 : pl. 5, fig. 33, the valves are gaping and this has added c. 1·5 mm to the thickness. In his generic diagnosis Sahni (1929 : 40) wrote 'beak-ridges feeble, so that it is impossible satisfactorily to define the position of the foramen with regard to these'. I consider that the position of a pin-hole foramen relative to beak ridges which are at best very indistinct and in most cases missing entirely is a character of no specific value.

The specimen is considered to fall well within the variation of *Carneithyris subcardinalis*.

V. DISCUSSION

Studies of living and fossil communities of brachiopods have shown that several species of the same genus can co-exist in the same environment. For example, in the Caribbean Sea off Barbados, three species of *Argyrotheca* can be found attached to the same sponge (unpublished observation). Similarly, three closely related genera of micromorphic cancellothyridines represented by five species adapted to the same mode of life occur in the Maastrichtian white chalk of Denmark (Surlyk 1972).

On the other hand, it is not easy to accept that six closely related genera represented by 18 species could have existed in the Upper Campanian sea of the Norwich area, of which at least nine species probably occur together at the same horizon in the Beeston Chalk. This high degree of apparent speciation in an environment offering a rather limited variety of ecological niches appears to be taxonomic rather than ecological and to be due to excessive 'splitting'.

The six genera of carneithyridines, represented by 18 species, were erected by Sahni on the basis of about 55 specimens in museum collections. Because of this limited material it is very difficult to identify any new material with the original type series. Sahni allowed single species little freedom of variation and his diagnoses were based on minor differences in outline of the shells, the size of the pedicle foramen, the curvature of the beak and the development of beak ridges. Small differences in the shape of the muscle impressions and cardinalia were also considered important.

Thus, with new material at hand, the student of carneithyridines has one of two courses open to him. Either he must continue to attempt to split the group up on the basis of Sahni's species characters, or he must combine some of the existing genera and species in order to create broader species which can be identified easily and so prove useful to the stratigrapher and field geologist. On the basis of a study of new material in the English collections and observations in the field I have chosen to follow the latter course.

Material

By 1929, Sahni's studies seem to have been based on about 55 specimens of Campanian carneithyridines. Since that time the British Museum (Natural History) has come into possession of A. W. Rowe's large collection of *Carneithyris* ; the Institute of Geological Sciences, London, has profited from C. J. Wood's intensive collecting in the extant exposures of Norfolk chalk ; and the Norwich Castle Museum has obtained R. M. Brydone's collection of Campanian carneithyridines, to which the collections of M. Leader and J. Goff have now been added.

The new material is stratigraphically well zoned. It has also the advantage that it consists not only of perfect but also of crushed and incomplete specimens, thus offering a good view over the internal and external features and their variation. This contrasts with the general attitude of collectors in the 19th century which led to the selection of very large, perfect specimens. There was consequently an unintentional bias towards the gerontic end of the spectrum of variation.

Fig. 1 shows the material used in this chapter. An attempt has been made to list the localities in stratigraphical order while the columns in mutual contact signify localities considered to be of the same age or with stratigraphical overlap. The figure also aims to give a visual impression of the quantitative distribution of the material. Altogether 214 specimens have been measured for a statistical analysis of the external characters.

Campanian carneithyridines so far have been found only in chalk ranging from the upper third of the Weybourne Chalk to the top of the Paramoudra Chalk ; according to Peake & Hancock (1961) this comprises about 55 m of chalk. The material from Bramerton is included here with the Campanian specimens because it has 'Campanian' cardinalia and colouration, in contrast to the Maastrichtian *Carneithyris subcardinalis*. But according to C. J. Wood (personal communication 1972), Bramerton is of Maastrichtian age although the small exposure in the river-bank has so far yielded only *Belemnitella* and no *Belemnella*.

The phylogenetic tree of Sahni (1925a)

According to Sahni (1925a : 498) this 'tree', in combination with Stages I to IV of the ontogeny of the cardinalia in *C. subpentagonalis*, 'confirms the dictum that Ontogeny repeats Phylogeny' (see p. 322). However, the provenance of the individual species of the tree suggests that the stratigraphical order in which they have been placed may be questioned.

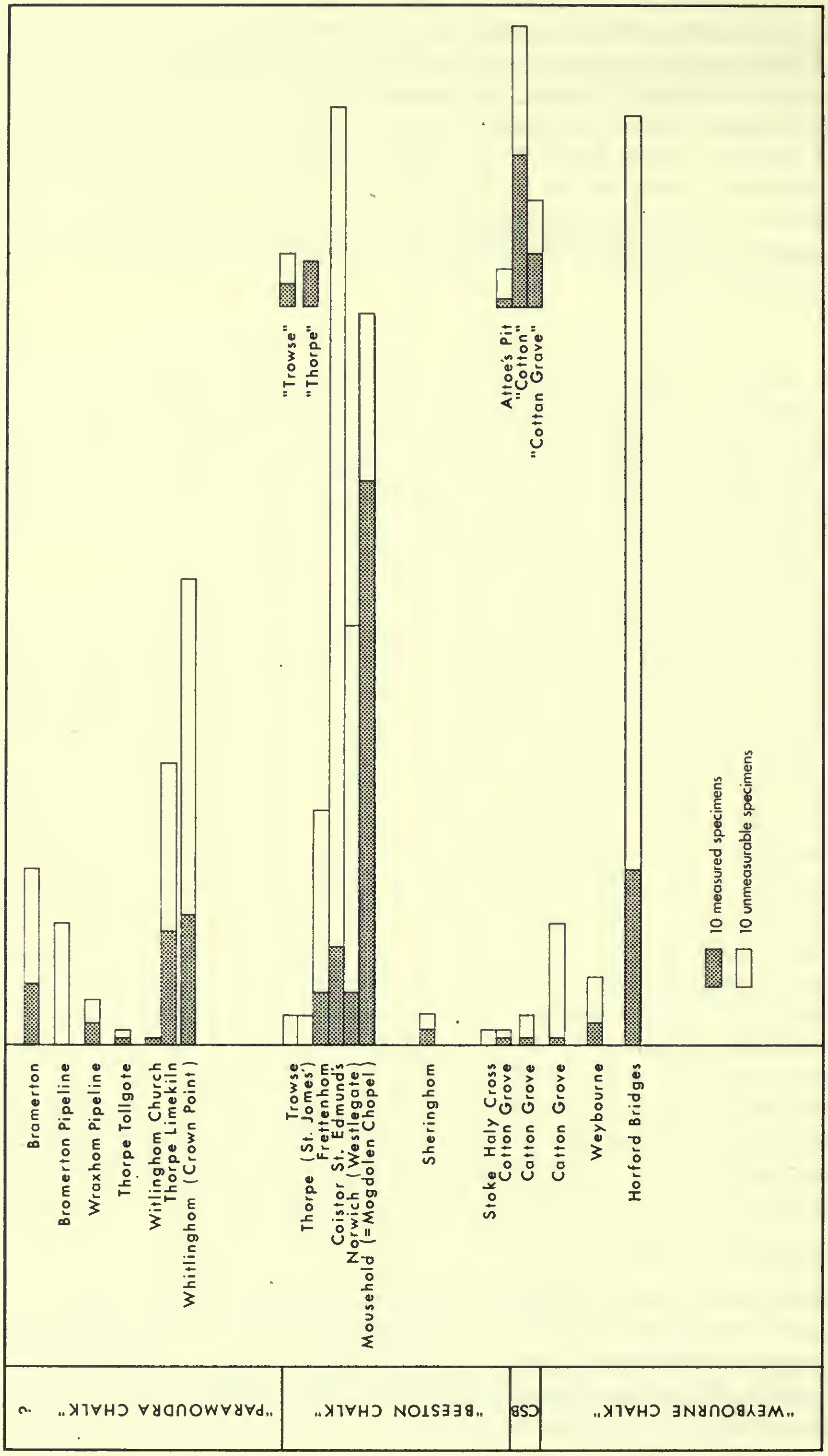

FIG. 1. Stratigraphical distribution of the material. Shaded columns represent measured specimens, white columns unmeasurable specimens. 5 mm = 10 specimens.

Carneithyris uniplicata was placed at the root of the tree. As mentioned on p. 330, however, the holotype is from high Beeston Chalk or high Paramoudra Chalk and the other specimen is from high Paramoudra Chalk. At least five of the seven known specimens of *C. subovalis* probably came from low Beeston Chalk. One of the three known specimens of *C. daviesi* is extremely gerontic and the two types are supposed to be from low Beeston Chalk. *C. variabilis* is represented by two specimens from the old collections of Norwich Castle Museum and are therefore unlocalized. The crown of the tree is *C. subpentagonalis* but it is not known from which horizons the two types came. The three unlocated specimens of this species figured by Sahni (1925a : pl. 25, figs 3–5 and 8) may be in his private collection and may therefore have come from Attoe's Pit, Catton (p. 324) ; they may thus be from highest Weybourne Chalk, the Catton Sponge Bed or low Beeston Chalk. It is thus clear that the species chosen by Sahni cannot represent a phylogenetic lineage.

Morphology of the cardinalia

Fig. 2 illustrates the six different types of cardinalia met with in the Upper Campanian carneithyridines. In Table 1, Sahni's figured specimens and those which he dissected and identified to species have been grouped according to type of

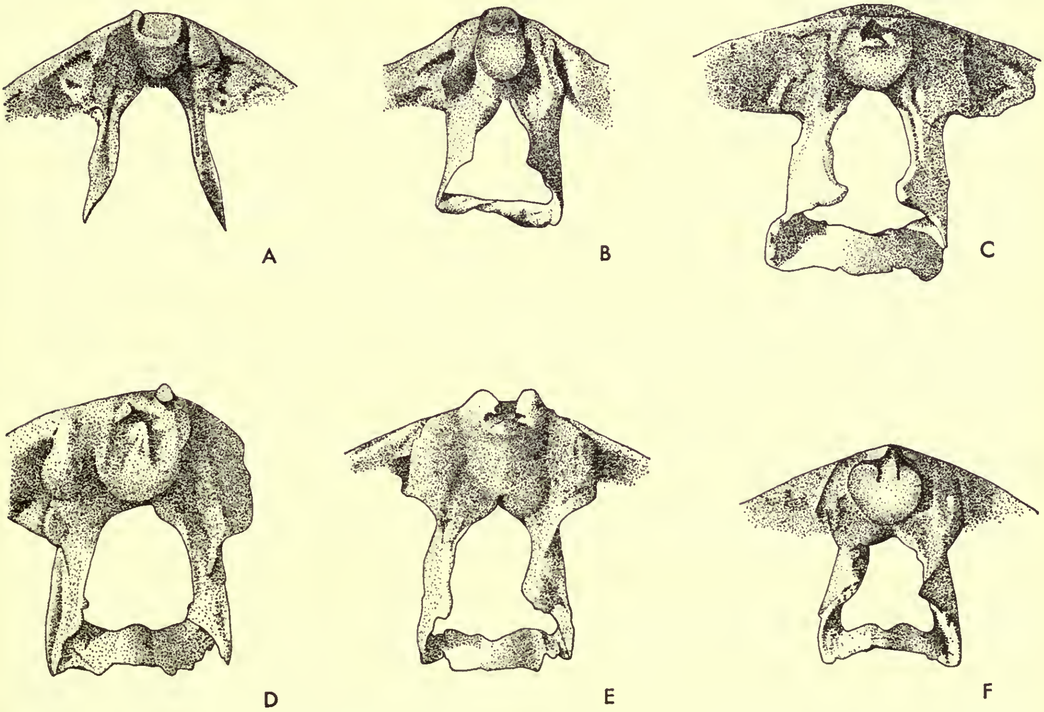

FIG. 2. Six different types of cardinalia in *Carneithyris*. A : *C. subovalis*, holotype ; B : *C.* cf. *carnea*, 27 KCN ; C : *C. norvicensis*, B 45610 ; D : *C. daviesi*, paratype ; E : *Ellipsothyris similis*, ? paratype ; F : *Chatwinothyris symphytica*, holotype.

Table 1

Sahni's specimens grouped according to the type of cardinalia

Type A: Slender, conical to hemispherical cardinal process with or without ridges or flaps between or around the diductor impressions; socket ridges and crural bases not thickened.

Carneithyris subovalis, holotype B 15159 (Fig. 2A; Pl. 4, fig. 3); unnumbered paratype (Pl. 4, fig. 4)
C. carnea, 'plesiotype' B 45600 (Pl. 3, fig. 3)
C. elongata, paralectotype B 49824 (Pl. 2, fig. 2); 'plesiotype' B 45243 (Pl. 4, fig. 5)
C. uniplicata, holotype GSM 48518 (Pl. 4, fig. 9)
C. circularis, holotype 15 KCN (Pl. 4, fig. 6); paratypes B 45603, B 45604 (Pl. 3, fig. 2; Pl. 4, fig. 7)
C. ornata, holotype GSM 48498 (Pl. 4, fig. 12)
Pulchrithyris extensa, holotype 7 KCN (Pl. 4, fig. 8)
Ellipsothyris similis, holotype 14 KCN (Pl. 4, fig. 10)
Magnithyris magna, holotype GSM 48488 (Pl. 4, fig. 1)
M. truncata, holotype B 45606 (Pl. 4, fig. 2)

Type B: Cardinal process more swollen and protruding than in type A; socket ridges and crural bases somewhat thickened.

Carneithyris cf. *carnea*, 27 KCN (Fig. 2B; Pl. 5, fig. 9)
C. variabilis, holotype 14 CMN (Pl. 5, fig. 1)
C. acuminata, holotype 19 CMN (Pl. 5, fig. 3)
C. norvicensis, holotype GSM 44494 (Pl. 5, fig. 11)
Pulchrithyris gracilis, holotype GSM 48487 (Pl. 5, fig. 7); paratype GSM 48485 (Pl. 5, fig. 6); B 46300 (Pl. 5, fig. 5)
Magnithyris magna, ? paratype B 15149 (Pl. 5, fig. 10)
Ornithothyris carinata, holotype 17 KCN (Pl. 5, fig. 2)

Type C: Cardinalia intermediate between types B and D; the specimens large and thick-shelled.

C. norvicensis, ? paratype B 45610 (Fig. 2C; Pl. 6, fig. 5); ? paratype B 52067 (Pl. 5, fig. 8); B 51636 (not figured)
C. daviesi, holotype B 45599 (Pl. 6, fig. 3); B 45642 (Pl. 6, fig. 4)
C. subpentagonalis, paratype GSM 44491 (Pl. 7, fig. 3)
C. variabilis, paratype 13 CMN (Pl. 7, fig. 4)
Pulchrithyris gracilis, B 98123 (Pl. 5, fig. 4)

Type D: Cardinalia strongly thickened with extremely swollen and protruding cardinal process with ridges and flaps.

C. daviesi, paratype B 459 (Fig. 2D; Pl. 7, fig. 1)
C. subpentagonalis, holotype 8 KCN (Pl. 7, fig. 2)

Type E: Swollen, completely fused cardinalia.

Ellipsothyris similis, ? paratype B 45653 (Fig. 2E; Pl. 7, fig. 5)

Type F: Cardinalia strongly thickened and completely dominated by the swollen cardinal process.

Chatwinothyris symphytica, holotype GSM 47523 (Fig. 2F; Pl. 2, fig. 4)
Carneithyris norvicensis, B 51637 (not figured)

cardinalia. Comparison of Sahni's material with the new, dissected material in the English collections clearly shows a general tendency in the development of the cardinalia. Types A and B are found in specimens showing no gerontic features. Type C appears in specimens which show incipiently gerontic features such as crowding of growth lines at the frontal margin and callus deposits around the teeth bases and the dental sockets. Type D is common in gerontic specimens while E and F are rarely met with and found only in specimens with extremely gerontic features (e.g. the paratypes of *Carneithyris daviesi* and *Ellipsothyris similis*).

It can furthermore be seen in Table 1 that in some of Sahni's species the specimens in the type series belong to different groups. In most cases, however, Sahni's diagnoses took account of the cardinalia of the holotypes only, as e.g. in *E. similis*.

The large numbers at hand demonstrate that the cardinalia of the carneithyridines are subject to great variation, which is dependent on the ontogenetic age of the single individual and not on its geological age. From the upper part of the Weybourne Chalk to the top of the Campanian (including Bramerton) there seems to be no trend in the development of the cardinalia towards any particular type. I agree here with Popiel-Barczyk (1968 : 23, 24) that the use of minute differences in the cardinalia for distinguishing between species is highly questionable when other features are not taken into account.

External morphology

Sahni (1925, 1929) stressed the importance of the external morphology in distinguishing between the different genera and species of carneithyridines. However, it is notoriously difficult to describe in words a terebratulid in which the two valves are equally biconvex and which has a rectimarginate frontal commissure, strongly incurved beak, indistinct to missing beak ridges, pinhole foramen and no ornament. It is even more difficult to word a differential diagnosis for such forms. As is seen in Sahni (1929 : 57), such short descriptions of the different species must have almost identical wording. It is clear that a statistical approach must be adopted.

In most cases Sahni (1925, 1929) only stated the dimensions of the holotypes and of these only the length of the brachial valve was given in mm while the width, thickness and total length were given as percentages. Most of these types have since been dissected and broken. For statistical purposes I have therefore had to recalculate their dimensions in mm from Sahni's percentages. But in some cases, where the specimen has survived undamaged, I have been able to check the measurements (e.g. the lectotypes of *C. carnea* and *C. elongata*, and the holotype of *C. ornata*). Some of the recalculated dimensions differ from corresponding direct measurements by as much as 5 mm.

The following statistical analyses are based on the length of brachial and pedicle valves, width and thickness. In addition, the diameter of the pedicle foramen and the curvature of the beak have been measured. These measurements are not used in the analyses since it is quite clear that there is no correlation between the curvature of the beak and the outline of the shell, though this was often stressed by Sahni in the diagnosis of a species. The diameter of the foramen is very variable, from

TABLE 2

Monovariate analyses of specimens of Carneithyridinae from different localities

Bramerton

	$\bar{X}$	SD	CV	OR	N
Lp in mm	20·2	2·50	12·38	16·5–23·4	8
Lb in mm	18·4	2·12	11·52	15·2–21·0	8
W in mm	17·3	2·18	12·6	14·4–20·4	8
T in mm	10·8	2·45	22·7	7·5–13·9	7

Wroxham Pipeline

	$\bar{X}$	SD	CV	OR	N
Lp in mm	17·6	2·04	11·6	15·3–19·1	3
Lb in mm	16·0	1·55	25·8	14·3–17·3	3
W in mm	15·4	1·27	8·3	14·4–16·8	3
T in mm	8·9	1·76	19·8	6·9–10·0	3

Thorpe Limekiln

	$\bar{X}$	SD	CV	OR	N
Lp in mm	25·6	4·60	18·0	17·6–33·0	15
Lb in mm	23·4	4·32	18·5	16·0–30·5	15
W in mm	22·2	3·92	17·7	15·8–30·1	15
T in mm	13·4	3·18	23·7	8·5–18·6	15

Whitlingham (Crown Point)

	$\bar{X}$	SD	CV	OR	N
Lp in mm	25·6	4·68	18·3	18·0–34·2	16
Lb in mm	23·4	4·30	18·4	16·3–31·5	16
W in mm	22·3	3·99	17·9	15·6–31·3	16
T in mm	14·1	3·25	23·1	8·4–19·4	16

'Trowse'

	$\bar{X}$	SD	CV	OR	N
Lp in mm	23·6	6·68	28·3	16·2–29·2	3
Lb in mm	21·3	6·09	28·6	14·6–26·5	3
W in mm	21·0	6·90	32·9	14·6–28·3	3
T in mm	13·2	4·69	35·5	8·0–17·1	3

'Thorpe'

	$\bar{X}$	SD	CV	OR	N
Lp in mm	31·5	5·86	18·6	22·6–38·0	6
Lb in mm	28·4	4·82	17·0	20·6–34·0	6
W in mm	27·6	5·45	19·7	21·0–36·0	6
T in mm	17·6	4·42	25·1	11·8–23·8	6

Frettenham

	$\bar{X}$	SD	CV	OR	N
Lp in mm	31·1	6·57	21·1	23·8–37·8	7
Lb in mm	28·3	4·72	16·7	21·7–34·3	7
W in mm	26·9	3·37	12·5	22·0–31·6	7
T in mm	17·4	3·72	21·4	13·4–21·8	7

TABLE 2 (Continued)

Westlegate

	X̄	SD	CV	OR	N
Lp in mm	27·5	5·05	18·4	21·0–35·0	7
Lb in mm	25·2	4·62	18·3	19·2–32·0	7
W in mm	24·6	4·79	19·5	18·8–30·4	7
T in mm	15·3	3·28	21·4	11·4–20·5	7

Caistor St Edmunds

	X̄	SD	CV	OR	N
Lp in mm	22·5	4·45	19·8	14·5–31·0	13
Lb in mm	20·6	4·22	20·5	13·0–28·5	13
W in mm	20·8	3·83	18·4	14·0–29·0	13
T in mm	11·7	2·96	25·3	6·3–17·0	13

Mousehold

	X̄	SD	CV	OR	N
Lp in mm	31·7	3·95	12·5	21·6–39·5	74
Lb in mm	28·7	3·55	12·4	20·0–36·0	74
W in mm	27·1	3·23	11·9	18·5–32·4	74
T in mm	18·1	3·01	16·6	10·6–26·0	74

Catton Grove + 'Catton'

	X̄	SD	CV	OR	N
Lp in mm	28·3	5·87	20·7	13·8–43·9	31
Lb in mm	25·8	5·40	20·9	13·0–40·2	31
W in mm	23·9	4·65	19·5	12·5–36·0	31
T in mm	16·0	4·16	26·0	6·3–26·0	31

Harford Bridges

	X̄	SD	CV	OR	N
Lp in mm	28·5	5·37	18·8	18·8–38·4	23
Lb in mm	26·0	4·94	19·0	16·8–35·5	23
W in mm	23·8	4·89	20·6	16·4–33·5	23
T in mm	16·8	3·76	22·4	10·0–22·0	23

Abbreviations. Lp: length of pedicle valve. Lb: length of brachial valve. W: width. T: thickness. N: number of specimens. X̄: computed mean value. SD: standard deviation. CV: coefficient of variation. OR: observed range.

0·1 mm to 2·0 mm, and cannot be connected with any particular shape of shell. However, there may be a connection with the thickness of the valves since mature specimens with large foramina tend to have thin valves.

Statistical analyses

The *t*-test was applied to the mean values of the lengths of the brachial valves for pairs of the localities represented in Table 2 after the *F*-test had shown that the variances can be considered equal (Simpson *et al.* 1960). The results are given in Table 3. They support the evidence of a decrease in size of mature specimens towards the top of the Campanian given by the histograms in Fig. 3. The only locality which shows an aberrant size distribution is Caistor St Edmunds which is of approximately the same stratigraphical age as Westlegate and Mousehold.

TABLE 3

Monovariate analyses: the *t*-test applied to the mean values of the lengths of the brachial valves, for pairs of the localities represented in Table 2

	t	df	< *P* <	
Bramerton versus Thorpe Limekiln	3·0718	21	0·1%	1%
Bramerton versus Mousehold	8·1580	80		0·1%
Bramerton versus Harford Bridges	*4·1889	29		0·1%
Thorpe Limekiln versus Whitlingham	0·003	29	90%	
Thorpe Limekiln versus 'Trowse'	0·7186	16	40%	50%
Thorpe Limekiln versus 'Thorpe'	2·3091	19	2%	5%
Whitlingham versus Mousehold	5·2807	88		0·1%
'Trowse' versus 'Thorpe'	1·9113	7	5%	10%
'Trowse' versus Mousehold	3·4916	75		0·1%
'Thorpe' versus Mousehold	0·2186	78	80%	90%
Frettenham versus Whitlingham	2·6160	24	1%	2%
Frettenham versus Westlegate	1·2590	12	20%	30%
Frettenham versus Caistor St Edmunds	4·5096	18		0·1%
Frettenham versus Mousehold	0·2491	79	80%	90%
Westlegate versus Caistor St Edmunds	2·2470	18	2%	5%
Caistor St Edmunds versus Whitlingham	1·7421	26	5%	10%
Caistor St Edmunds versus Mousehold	7·4508	85		0·1%
Mousehold versus Catton Grove + 'Catton'	*3·2905	103	0·1%	1%
Mousehold versus Harford Bridges	*2·8615	95	0·1%	1%
Catton Grove + 'Catton' versus Harford Bridges	0·1797	52	80%	90%

* In these cases the *F*-test gave a $P < 5\%$; nevertheless the *t*-test was made.
df: degrees of freedom.

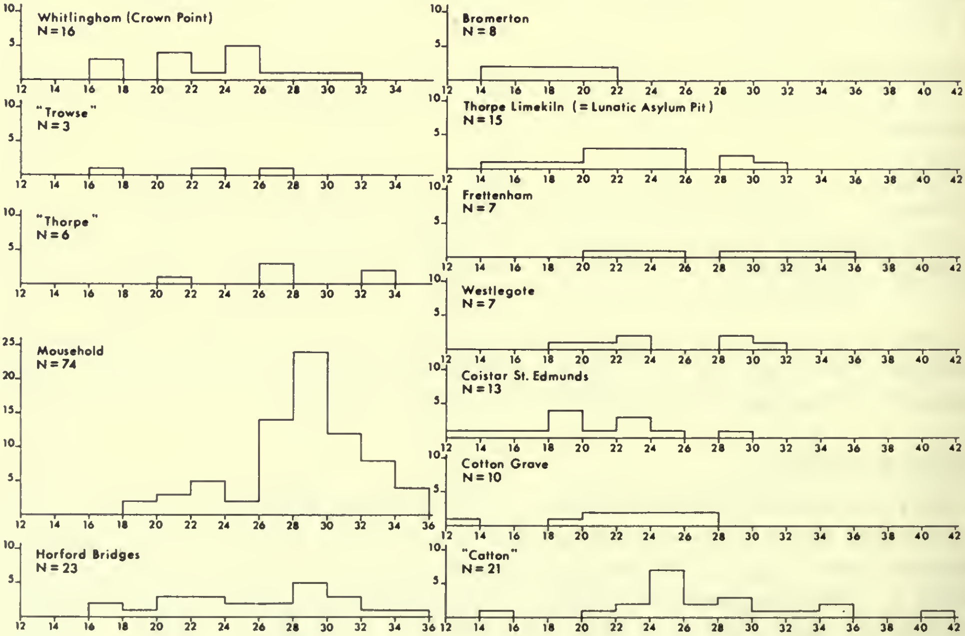

FIG. 3. Size-frequency histograms of the measurable specimens from 12 localities. Abscissa: length of brachial valve in mm; ordinate: number of specimens.

Figs 4–12 are length of brachial valve/width and thickness/width scatter diagrams from the 12 localities used in the monovariate analyses. Regression lines (least square method) are drawn for each graph and the equations for the lines are given in Table 4. For the calculation of the regression lines the original measurements have been used, since the scatter diagrams show a linear trend with an elliptical distribution of the plots, and not a fan-shape which would have necessitated use of logarithms (Christensen 1973, 1974).

TABLE 4

Equations for the regression lines of each graph shown in Figs 4–12

	Y = a + bX	sd	r	N
Bramerton	Lb = 2·1036 + 0·9405W	0·8441	0·9295	8
	T = −7·1429 + 1·0483W	0·8095	0·9533	7
Thorpe Limekiln	Lb = 0·2834 + 1·0407W	1·4610	0·9453	15
	T = −5·6774 + 0·6926W	1·7081	0·7712	15
Whitlingham (Crown Point)	Lb = 1·0461 + 1·0027W	1·6241	0·9309	16
	T = −0·4535 + 0·6527W	2·0052	0·8022	16
Frettenham	Lb = −8·2010 + 1·3587W	1·2821	0·9688	7
	T = −9·9033 + 1·0150W	1·5976	0·9198	7
Westlegate	Lb = 2·5293 + 0·9226W	1·4662	0·9572	7
	T = 1·5918 + 0·5588W	2·0793	0·8156	7
'Trowse' + 'Thorpe'	Lb = 3·4019 + 0·8893W	1·9497	0·9530	9
	T = −2·0128 + 0·7141W	1·2374	0·9699	9
Caistor St Edmunds	Lb = −1·6418 + 1·0713W	1·0104	0·9733	13
	T = −3·6525 + 0·7391W	0·9155	0·9565	13
Mousehold	Lb = 1·7163 + 0·9965W	1·3918	0·9187	74
	T = −1·9247 + 0·7399W	1·8529	0·7918	74
Catton Grove + 'Catton'	Lb = −1·2261 + 1·1296W	1·2518	0·9737	31
	T = −3·2015 + 0·8019W	1·8629	0·8977	31
Harford Bridges	Lb = 2·9904 + 0·9663W	1·5428	0·9530	23
	T = −0·1951 + 0·7124W	1·3599	0·9348	23

sd: standard deviation of the regression line. r: coefficient of correlation. Other abbreviations as in Table 2.

Though the regression lines were calculated on the bases of plots of mature and gerontic specimens they can to some extent be compared with the growth curves for the brachiopods. In order to test this, regression lines were calculated for most of the localities on the basis of growth line measurements on the specimens. The resulting regression lines were parallel to the straight middle part of the S-shaped growth curve for the specimens (not figured here). The regression lines based on growth line measurements were roughly parallel to the regression lines based on plots of mature and gerontic specimens, though the first mentioned sloped slightly

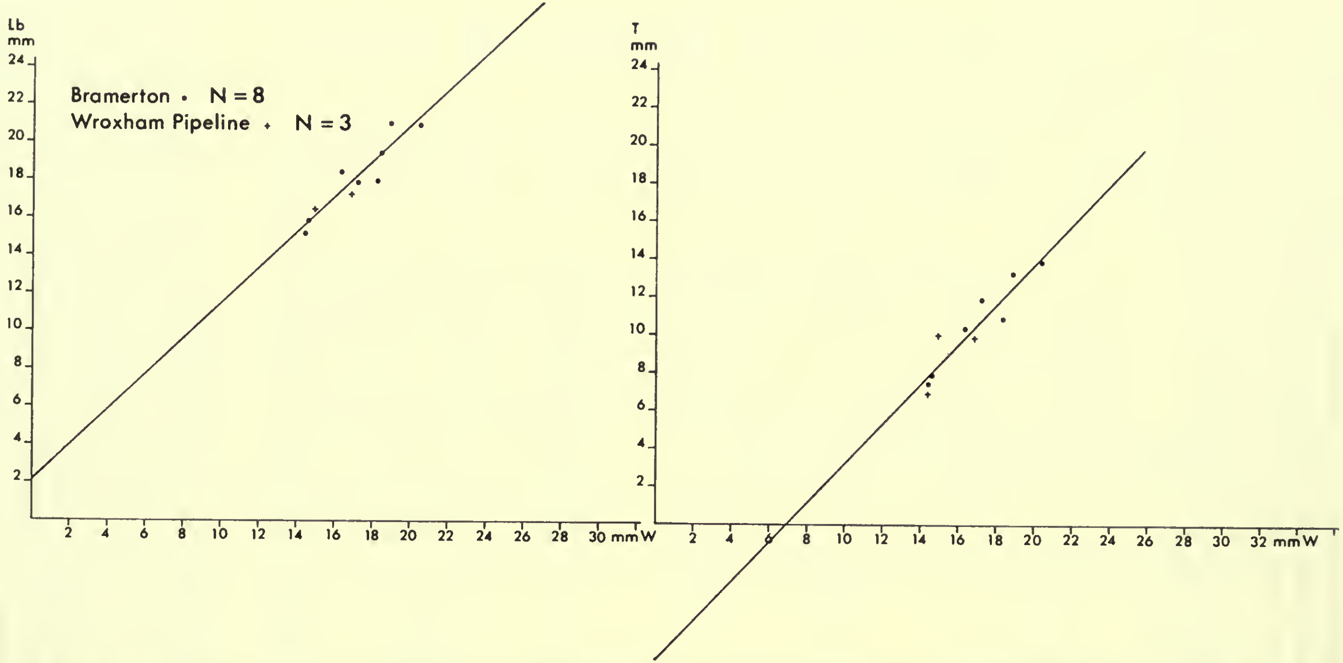

FIG. 4. Length of brachial valve/width and thickness/width scatter diagrams for Bramerton and Wroxham Pipeline localities. Equations for the regression lines, which are based on the Bramerton material only, are given in Table 4.

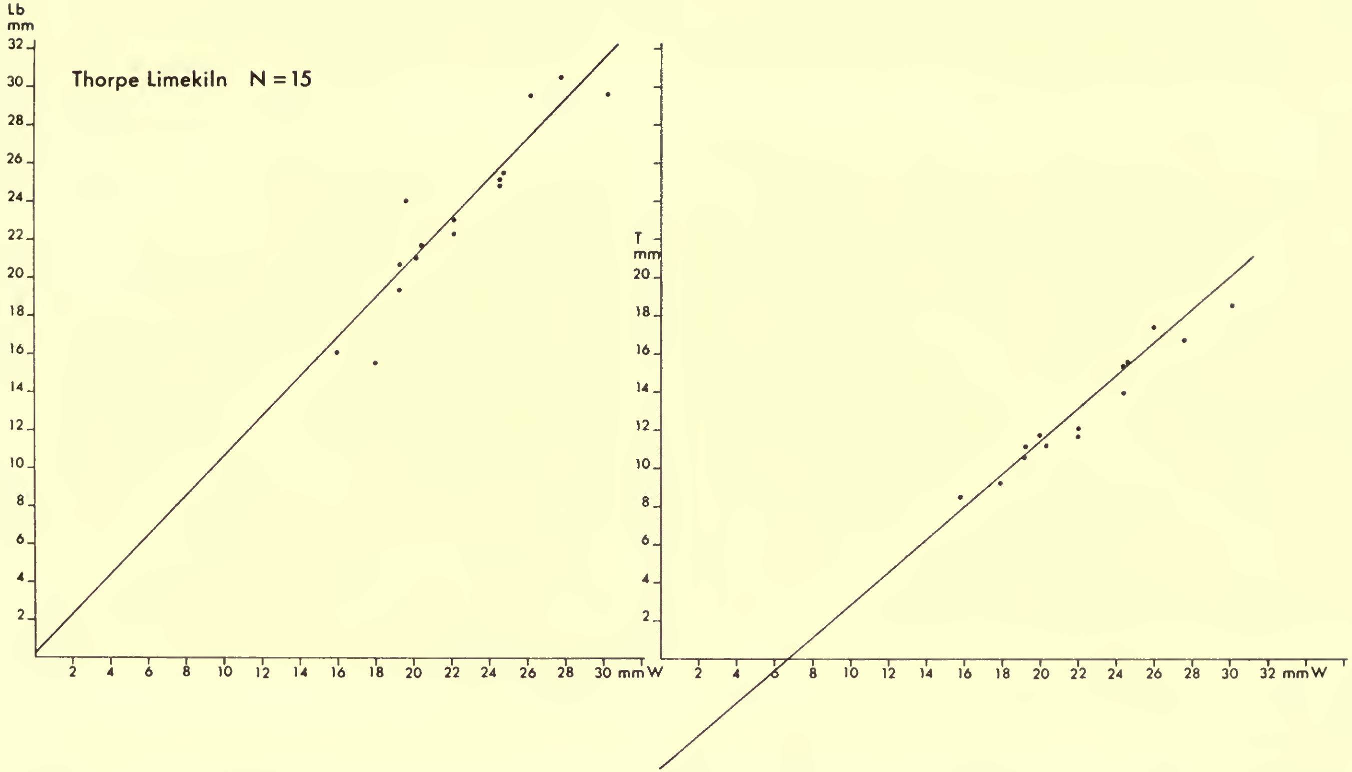

FIG. 5. Length of brachial valve/width and thickness/width scatter diagrams for Thorpe Limekiln locality. Equations for the regression lines are given in Table 4.

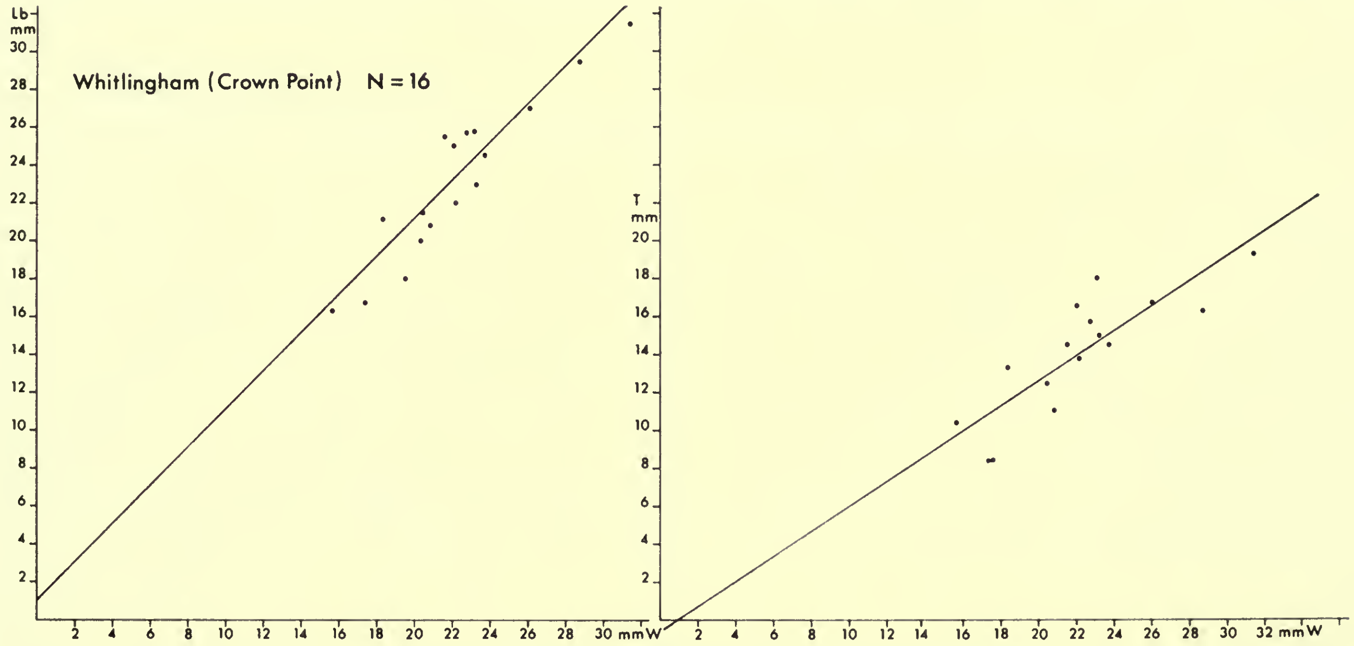

FIG. 6. Length of brachial valve/width and thickness/width scatter diagrams for Whitlingham (Crown Point) Pit locality. Equations for the regression lines are given in Table 4.

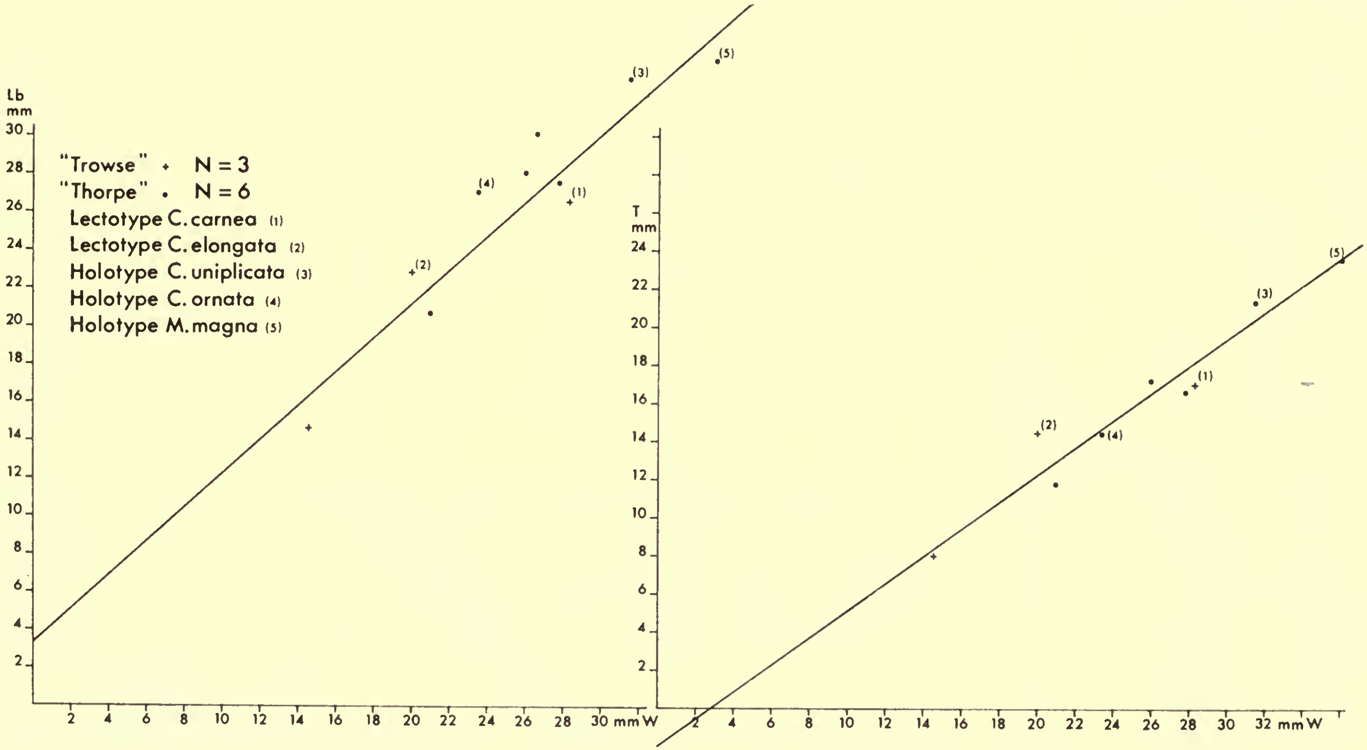

FIG. 7. Length of brachial valve/width and thickness/width composite scatter diagrams for specimens from 'Trowse' and 'Thorpe', including the lectotypes of *Carneithyris carnea* and *C. elongata* and the holotypes of *C. uniplicata*, *C. ornata* and *Magnithyris magna*. Though there is a difference in geological age between the localities covered by the names 'Trowse' and 'Thorpe', they have been combined as one in the bivariate statistical analyses. Equations for the regression lines are given in Table 4.

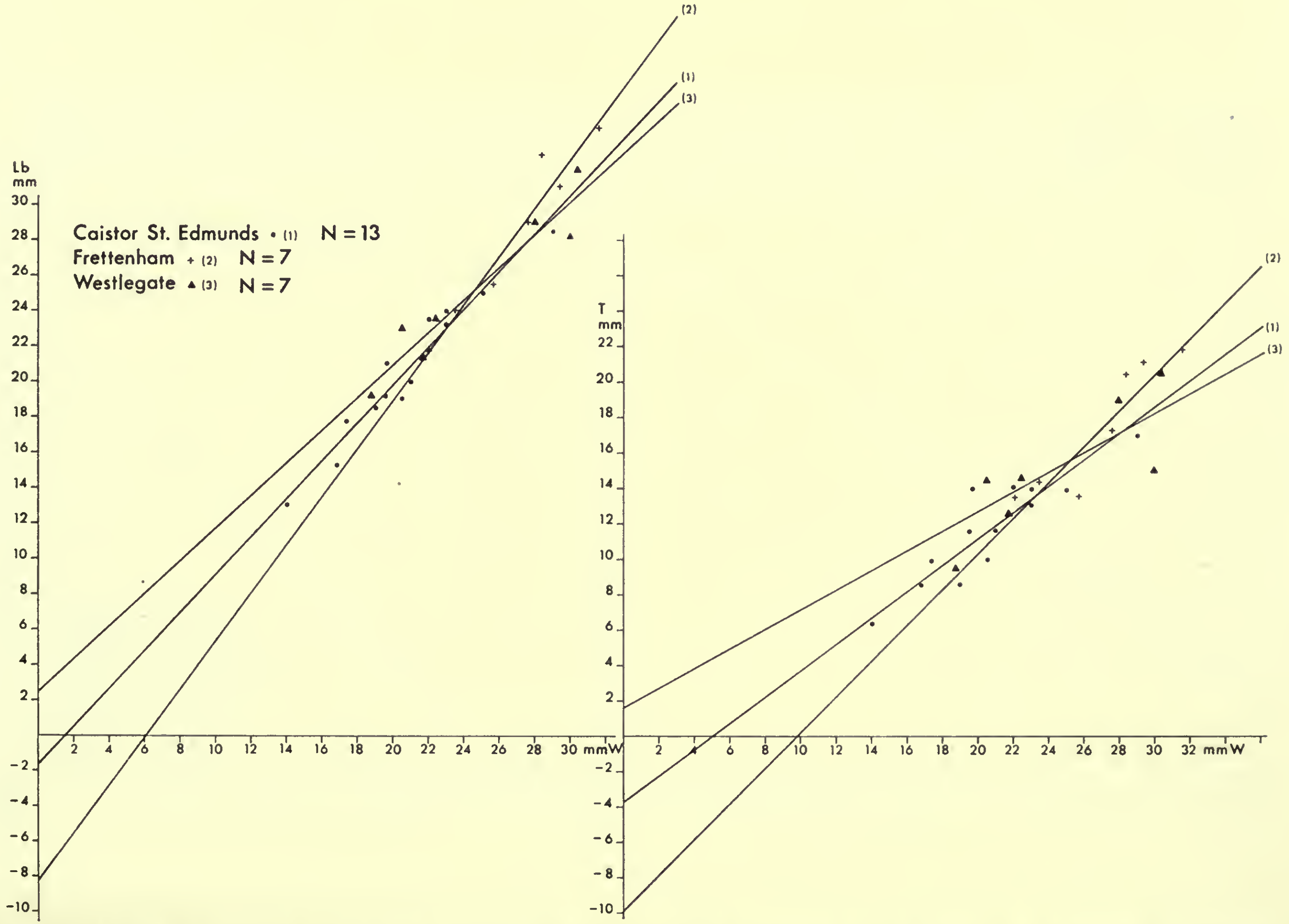

FIG. 8. Length of brachial valve/width and thickness/width scatter diagrams for the Caistor St Edmunds, Frettenham, and Westlegate localities.

more steeply and had a lower intercept on the ordinate. The two sets of regression lines were tested by the t-test and in all cases the differences in slopes were found to be insignificant ($P > 80\%$), and thus the regression lines in Figs 4–12 can roughly be considered to represent the straight middle part of the growth curves for the specimens from the different localities.

The t-test was applied to the slopes of the regression lines for pairs of localities after the F-test had shown that the variances can be considered equal. The results are given in Table 5. The differences in slope can nowhere be considered highly significant.

TABLE 5

Bivariate analyses. Test for differences in the slopes of regression lines for the pairs of localities shown in Table 3.

		t	df	$< P <$	
Bramerton versus Thorpe Limekiln	Lb/W	0·4000	19	70%	80%
	T/W	1·2017	18	20%	30%
Bramerton versus Whitlingham (Crown Point)	Lb/W	0·2260	20	80%	90%
	*T/W	1·1489	19	20%	30%
Bramerton versus 'Trowse' + 'Thorpe'	*Lb/W	0·1692	13	80%	90%
	T/W	1·6169	12	10%	20%
Bramerton versus Frettenham	Lb/W	1·5974	11	10%	20%
	T/W	0·1196	10	90%	
Bramerton versus Westlegate	Lb/W	0·0767	11	90%	
	*T/W	1·5342	10	10%	20%
Bramerton versus Caistor St Edmunds	Lb/W	0·7001	17	40%	50%
	T/W	1·7647	16	5%	10%
Bramerton versus Mousehold	Lb/W	0·0224	78	90%	
	*T/W	0·9147	77	30%	40%
Bramerton versus Catton Grove + 'Catton'	Lb/W	1·6147	35	10%	20%
	*T/W	0·7515	34	40%	50%
Bramerton versus Harford Bridges	Lb/W	0·0980	27	90%	
	T/W	1·4005	26	80%	90%
Thorpe Limekiln versus Whitlingham (Crown Point)	Lb/W	0·2612	27	70%	80%
	T/W	0·2272	27	80%	90%
Thorpe Limekiln versus Mousehold	Lb/W	0·4081	85	60%	70%
	T/W	0·3345	85	70%	80%
Whitlingham (Crown Point) versus Mousehold	Lb/W	0·0583	86	90%	
	T/W	0·6254	86	50%	60%
'Trowse' + 'Thorpe' versus Mousehold	Lb/W	1·1247	79	20%	30%
	T/W	0·2172	79	80%	90%
'Trowse' + 'Thorpe' versus Harford Bridges	Lb/W	0·6657	28	50%	60%
	T/W	0·0183	28	90%	

TABLE 5 (Continued)

		t	df	$< P <$	
Frettenham versus Westlegate	Lb/W	2·1371	10	5%	10%
	T/W	1·6606	10	20%	30%
Frettenham versus Caistor St Edmunds	Lb/W	1·8265	16	10%	20%
	T/W	1·6494	16	10%	20%
Frettenham versus Mousehold	Lb/W	2·0673	77	2%	5%
	T/W	1·1835	77	20%	30%
Frettenham versus Harford Bridges	Lb/W	2·0645	26	2%	5%
	T/W	1·6614	26	10%	20%
Westlegate versus Caistor St Edmunds	Lb/W	1·1150	16	20%	30%
	*T/W	1·1414	16	20%	30%
Westlegate versus Mousehold	Lb/W	0·5711	77	50%	60%
	T/W	1·0462	77	20%	30%

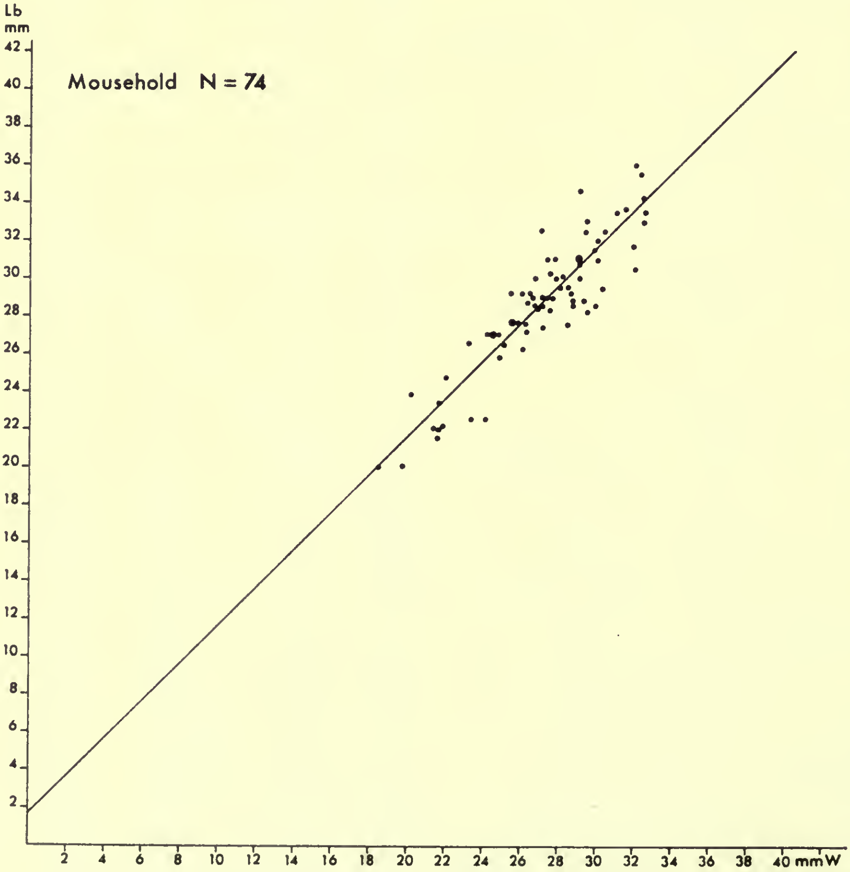

FIG. 9. Length of brachial valve/width scatter diagram for Mousehold locality.

TABLE 5 (Continued)

		t	df	$< P <$	
Caistor St Edmunds versus Mousehold	Lb/W	0·6636	83	50%	60%
	*T/W	0·0054	83	90%	
Mousehold versus Catton Grove + 'Catton'	Lb/W	1·8403	101	5%	10%
	T/W	0·6250	101	50%	60%
Mousehold versus Harford Bridges	Lb/W	0·3738	93	70%	80%
	T/W	0·2770	93	70%	80%
Catton Grove + 'Catton' versus Harford Bridges	Lb/W	2·0193	50	5%	10%
	T/W	0·9154	50	30%	40%

* In these cases the F-test gave a $P < 5\%$; nevertheless the t-test was made.
Abbreviations as in Tables 2 and 3.

In Figs 13 and 14 the regression lines for the different localities have been superimposed to give a visual impression of similarities of growth in the specimens; the only aberrant localities are Frettenham and Bramerton. The material from Frettenham shows a slightly more rapid growth in length of brachial valve than that of the other localities, while both Bramerton and Frettenham show a steeper increase in thickness with width than the other localities.

Twenty-seven specimens were plotted for length of brachial valve against width; these including the holotypes of *Carneithyris subpentagonalis*, *C. circularis*, *C.*

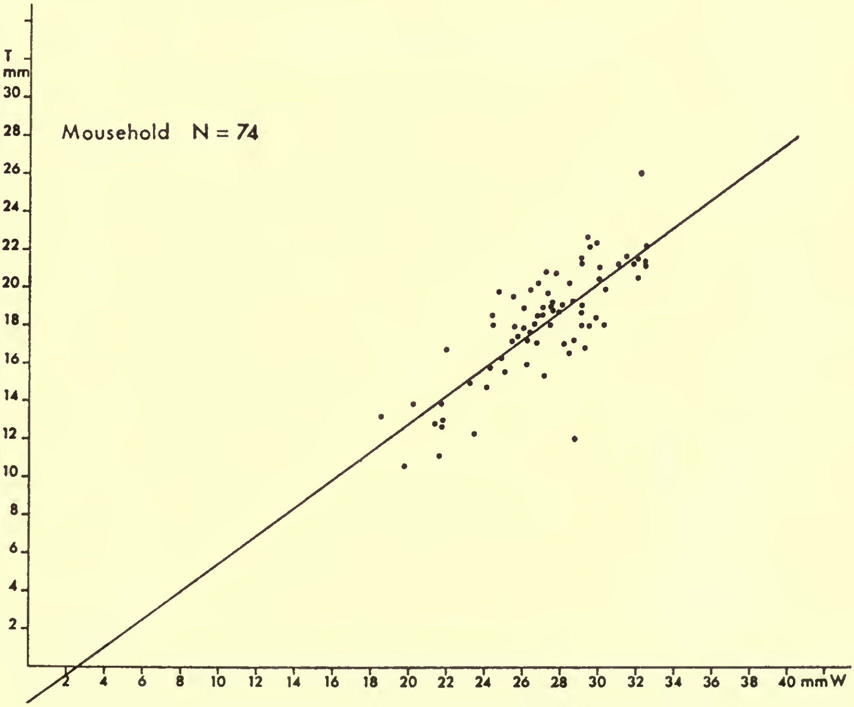

FIG. 10. Thickness/width scatter diagram for Mousehold locality.

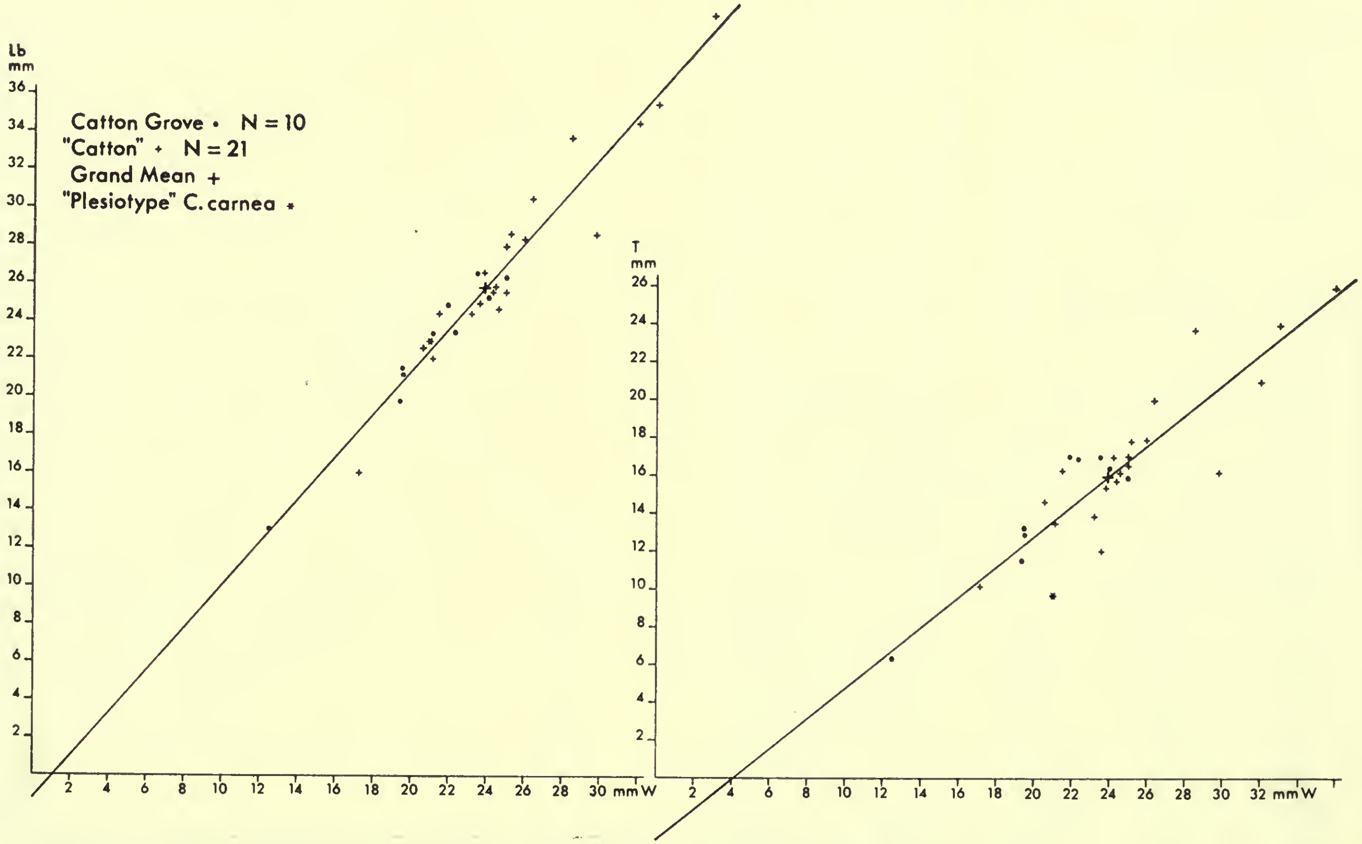

FIG. 11. Length of brachial valve/width and thickness/width scatter diagrams for Catton Grove + 'Catton' localities.

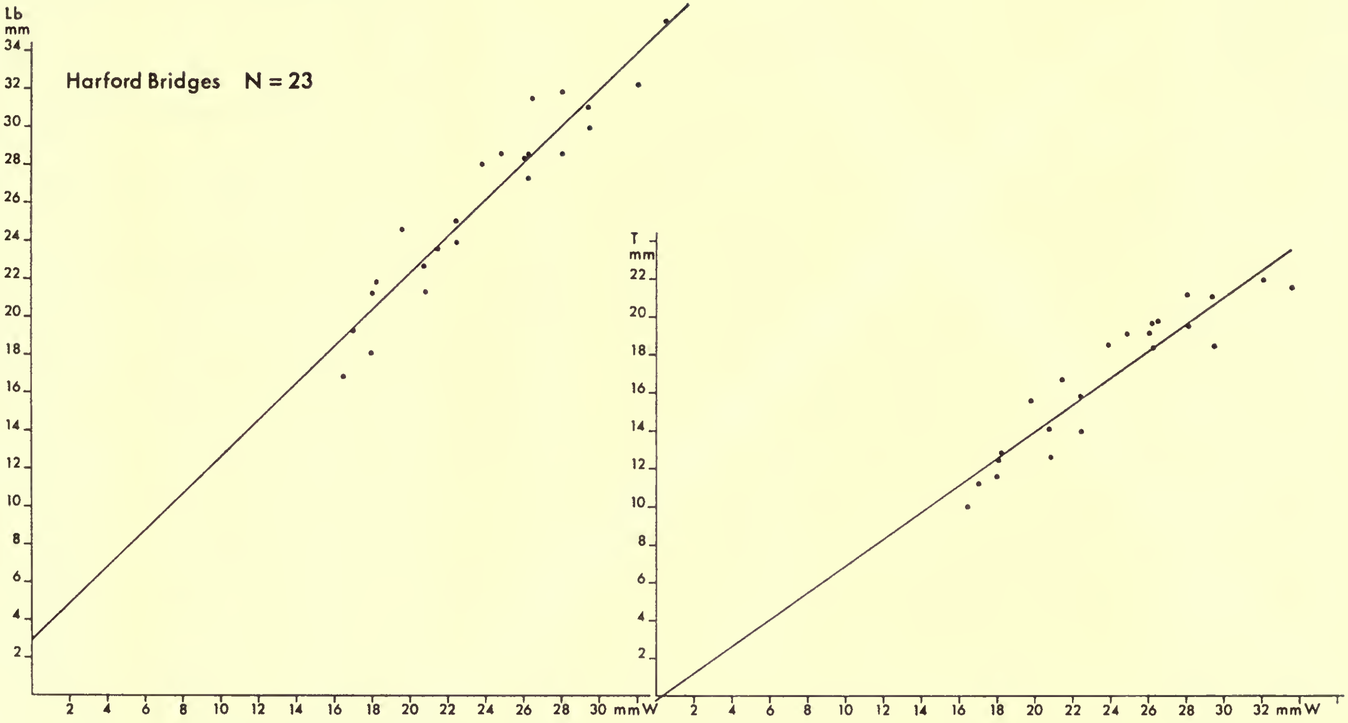

FIG. 12. Length of brachial valve/width and thickness/width scatter diagrams for Harford Bridges locality.

variabilis, *C. acuminata*, *C. norvicensis*, *C. subovalis*, *C. daviesi*, *Pulchrithyris extensa*, *Ellipsothyris similis*, *Chatwinothyris symphytica*, *Ornithothyris carinata*, *Magnithyris truncata* and paratypes of *Carneithyris subpentagonalis*, *C. circularis*, *C. variabilis*, *C. daviesi*, *Ellipsothyris similis* and *Magnithyris magna*. They are all from old collections with no locality specification and all were identified by Sahni. The regression line was computed (least square method) and gave the following result: Lb = 22·6890 + 0·3311W; sd = 3·8349; r = 0·4348. This regression line is

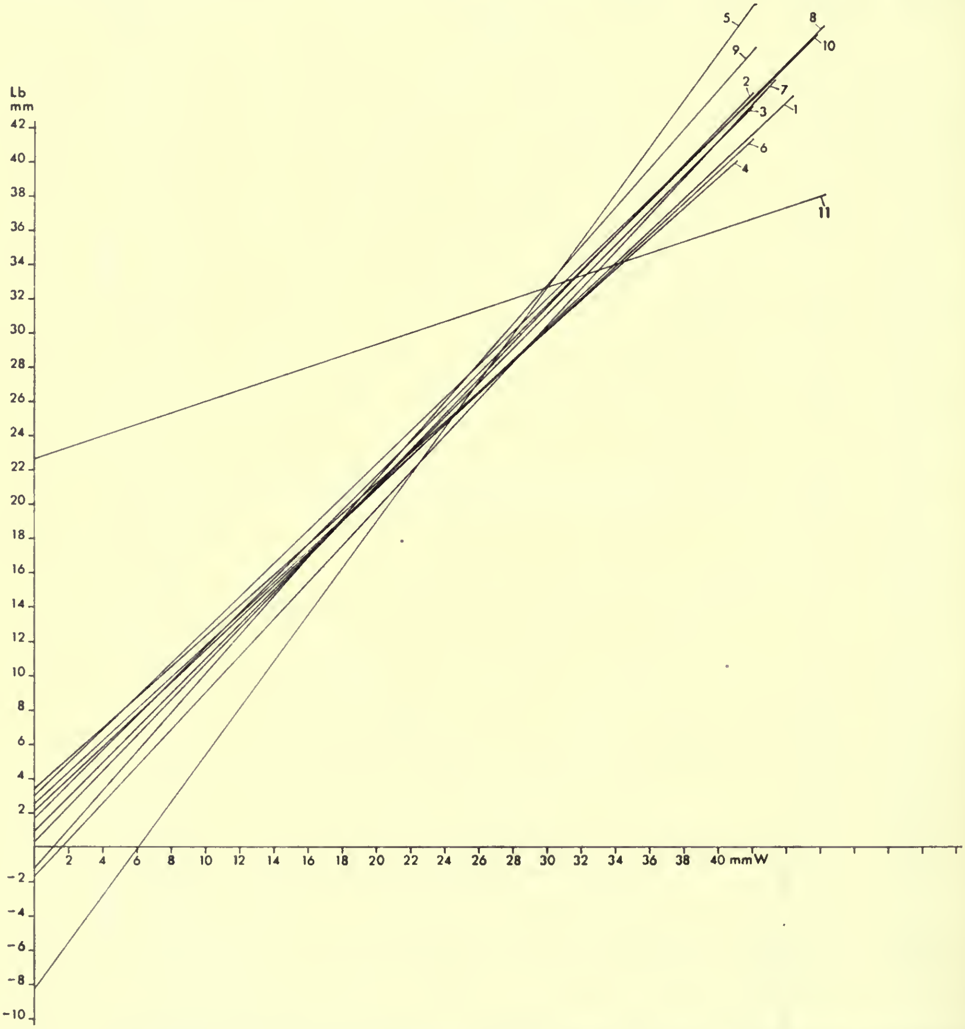

FIG. 13. Length of brachial valve/width. Superimposed regression lines for the material from the 10 localities used in the bivariate analyses. 1: Bramerton; 2: Thorpe Limekiln; 3: Whitlingham (Crown Point); 4: 'Trowse' + 'Thorpe'; 5: Frettenham (note the steep slope); 6: Westlegate; 7: Caistor St Edmunds; 8: Mousehold; 9: Catton Grove + 'Catton'; 10: Harford Bridges. 11: regression line based on the 27 merontic specimens discussed on p. 359.

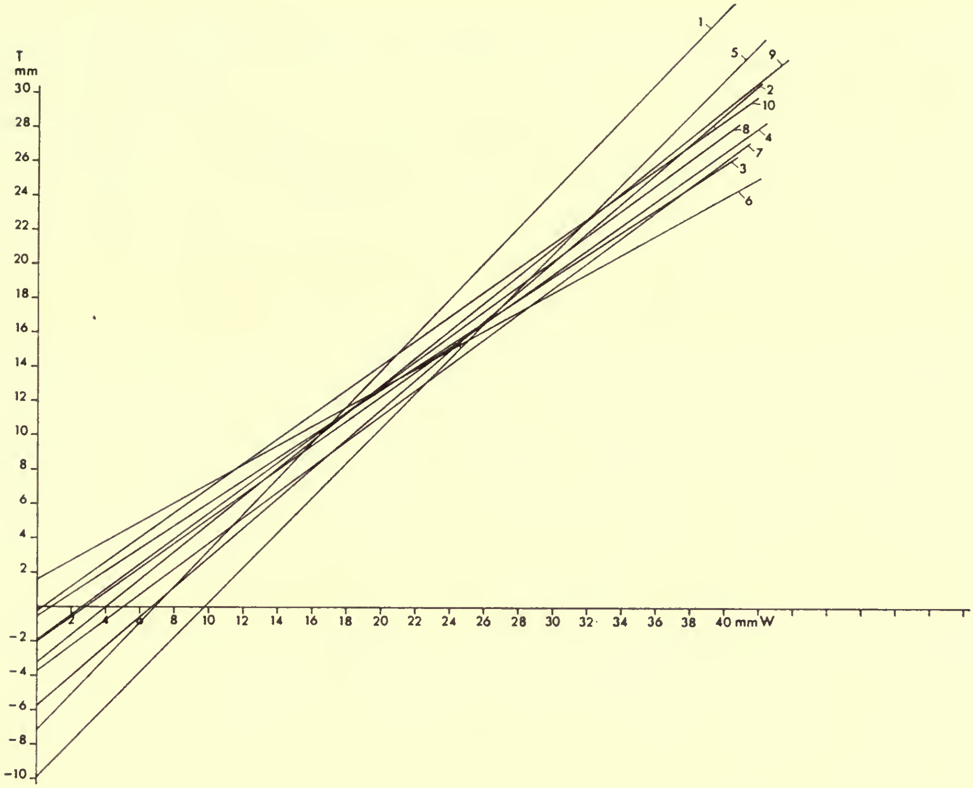

FIG. 14. Thickness/width. Superimposed regression lines for the same localities as in Fig. 13. Note the steep slopes for Bramerton and Frettenham; the two lines are approximately parallel.

included in Fig. 13 (no. 11) but shows a striking difference from the others. The slope of the line reflects the upper part of the S-shaped growth curve of the brachiopods in general, demonstrating the slow growth of senile specimens. It was partly on the basis of the differences in outline that Sahni established his many genera and species; the great variation in outline of these 27 senile specimens is well documented by the low correlation coefficient.

In contrast to the 27 senile specimens, however, the types from known localities fit well into the linear scatter plots, and the plots show high correlation, e.g. 'Trowse' and 'Thorpe' (Fig. 7).

Conclusions

It can be concluded from the statistical analyses here offered that the present material from known localities shows no significant differences in growth and outline that can be used for differentiating species. The 27 unlocated senile specimens on which 12 species were erected by Sahni demonstrate the wide variation in shape naturally to be found in gerontic material of any species, while localized type-specimens all fit into the scatter plot for their locality. It is also concluded that differences in the cardinalia demonstrated in the often gerontic types cannot be used to distinguish between species of *Carneithyris* in the English Campanian. Neither the growth of the specimens, their outline nor their cardinalia show any distinct trend which may be used for erecting species on a stratigraphical or geographical basis. In the available material I can recognize only one species of *Carneithyris* in the Upper Campanian of England, namely *C. carnea* (J. Sowerby).

VII. CONCLUDING REMARKS

On the basis of the present material I am unable to subdivide the Campanian carneithyridines into species which are visibly distinguishable or statistically valid. In the specimens from the Upper Campanian the only trend which I have detected is a tendency to develop smaller mature individuals towards the Campanian–Maastrichtian boundary. Single specimens, including those called *Magnithyris* and *Carneithyris circularis* by Sahni, seem to have retained to a great age certain juvenile characters such as thin shells, a circular outline, a beak which is not strongly incurved and a fairly large foramen. However, these and other external and internal features do not appear in any particular facies or horizon. On the contrary, they show a scattered occurrence throughout the Upper Campanian of Norfolk and can be considered to be due to peculiarities in the genetical composition of the individuals concerned. I thus consider that all the available carneithyridines from the Upper Campanian of Norfolk should be referred to the single species *Carneithyris carnea*.

In the Lower Maastrichtian chalk of Sidestrand and Trimingham, *C. carnea* is replaced by *C. subcardinalis* (Sahni), which is distinguishable from *C. carnea* on the basis of its internal features. Unfortunately the critical sediments at the Campanian–Maastrichtian boundary are not exposed in Norfolk and the replacement of the one species by the other, which would establish whether it is gradual, sharp or with overlap, cannot be studied in detail. *C. carnea* is still present at Bramerton and *C. subcardinalis* is found in the lowest exposed Maastrichtian at Sidestrand.

The subfamily Carneithyridinae thus contains only one genus, *Carneithyris*, the stratigraphical range of which is poorly known. Muir-Wood (1965) offered no suggestions as to the phyletic relationships of the subfamily ; its sudden appearance in the Upper Campanian of north-west Europe is, so far, an enigma. Some terebratulids from the Lower Campanian of the Hampshire Basin (R. M. Brydone collection, Institute of Geological Sciences, London) resemble carneithyridines externally but they have not been opened and dissected. Apart from these uncertain specimens, no carneithyridines are known of pre-Upper Campanian age. *Carneithyris* is known from the Maastrichtian and Danian of northern Europe (Asgaard 1963, 1970 ; Steinich 1965 ; Popiel-Barczyk 1968 ; Surlyk 1972).

Carneithyris probably invaded the chalk facies from a more coastal area, its ancestors having been 'normal' terebratulids with clearly distinguished cardinalia with ventrally concave outer hinge-plates (as seen in the specimen called *Magnithyris truncata*) and a stout functional pedicle. An experimental phase was passed through in the Upper Campanian chalk where the animals retained a thin, functional pedicle, possibly fastened to a small object as substrate used as a drag anchor, as seen in the Recent terebratellid *Laqueus californianus* on coarse sandy bottoms. During this phase a heavy posterior end with swollen and fused cardinalia was developed. In the Maastrichtian, *Carneithyris* increased the weight of the callus deposits in the posterior part of the valves and blocked the foramen, thereby becoming perfectly adapted for a free-living life habit as a 'self-righting tumbler' in the soft, fine-grained sea floor (Steinich 1965 ; Surlyk 1972). Stocks in the marginal calcarenite facies meanwhile retained a functional pedicle and had a less heavily weighted shell.

In Denmark and Sweden, *Carneithyris* disappeared with the introduction of calcarenite facies in the lowermost Tertiary and first migrated back into this area in the Middle Danian. In the calcarenite facies the genus developed a sulcate frontal commissure which was possibly a further development of the slightly sulcate to paraplicate commissure seen in some specimens from high Paramoudra Chalk and Bramerton, Norfolk. The Danian specimens furthermore have cardinalia very much like those of the Campanian *C. carnea* and in most cases they possessed a functional, though very slender pedicle (Asgaard 1963).

VIII. REFERENCES

ASGAARD, U. 1963. Slægterne *Chatwinothyris* og *Carneithyris* (Terebratulidae) i Danmarks Maastrichtien og Danien. Unpublished prize dissertation : 1–109, 41 pls. Univ. Copenhagen. (Reviewed in *Festskr. Københavns Univ. Årsfest*, 1963 : 241–247.)

—— 1970. The syntypes of *Carneithyris incisa* (Buch, 1835). *Meddr dansk geol. Foren.*, Copenhagen, **19** : 361–367, 2 pls.

BRYDONE, R. M. 1908. On the subdivisions of the Chalk of Trimingham (Norfolk). *Q. Jl geol. Soc. Lond.* **64** : 401–412, pls 17, 18.

—— 1909. The Trimingham Chalk-South Bluff. *Geol. Mag.*, London, **46** : 189–190.

—— 1938. *On correlation of some of the Norfolk exposures of Chalk with Belemnitella mucronata.* 16 pp. London.

CHRISTENSEN, W. K. 1973. The belemnites and their stratigraphical significance. *In*: Bergström, J., Christensen, W. K., Johansson, C. & Norling, E. An extension of Upper Cretaceous rocks to the Swedish west coast at Särdal. *Bull. geol. Soc. Denm.*, Copenhagen, **22** : 113–140, pls 9–11.

—— 1974. Morphometric analysis of *Actinocamax plenus* from England. *Bull. geol. Soc. Denm.*, Copenhagen, **23** : 1–26, pls 1–4.

DAVIDSON, T. 1854. A monograph of British Cretaceous Brachiopoda, 2. *Palaeontogr. Soc.* (*Monogr.*), London : 55–117, pls 6–12.

FERNALD, H. T. 1939. On type nomenclature. *Ann. ent. Soc. Am.* **32** (4) : 689–702.

FRIZZELL, D. L. 1933. Terminology of types. *Am. Midl. Nat.* **14** : 637–668.

HÄGG, R. 1940. Mollusken und Brachiopoden des Danien in Schweden. *Geol. För. Stockh. Förh.* **62** : 19–21.

—— 1954. Die Mollusken und Brachiopoden der Schwedischen Kreide. Die Schreibkreide (Mucronatenkreide). *Geol. För. Stockh. Förh.* **76** : 391–447.

KONGIEL, R. 1935. W sprawie wieku 'siwaka' w Puław. *Pr. Tow. Przyjac. Nauk Wilnie*, **9** (19) : 1–59, 8 pls.

MUIR-WOOD, H. M. 1965. Mesozoic Terebratulidina. *In* : R. C. Moore (Ed.), *Treatise on Invertebrate Paleontology*, **H** : 762–816. Lawrence, Kansas.

NIELSEN, K. B. 1909. Brachiopoderne i Danmarks Kridtaflejringer. *K. dansk. Vidensk. Selsk. Skr.*, Copenhagen (7, Naturvid. mat. Afd.), **6** : 128–178.

PEAKE, N. B. & HANCOCK, J. M. 1961. The Upper Cretaceous of Norfolk. *In*: Larwood, G. P. & Funnell, B. M. (Eds). The Geology of Norfolk. *Trans. Norfolk Norwich Nat. Soc.*, **19** (6) : 293–339, text-figs.

—— —— 1970. Addenda and Corrigenda. *In*: Larwood, G. P. & Funnell, B. M. (Eds). *The Geology of Norfolk*, reprinted edn : 339A–339J, map. Norwich.

POPIEL-BARCZYK, E. 1968. Upper Cretaceous terebratulids (Brachiopoda) from the middle Vistula gorge. *Pr. Muz. Ziemi*, Warsaw, **12** : 3–86, 20 pls.

ROSENKRANTZ, A. 1945. Slægten *Chatwinothyris* og andre Terebratler fra Danmarks Senon og Danien. *Meddr dansk geol. Foren.*, Copenhagen, **10** : 446–452.

SAHNI, M. R. 1925. Morphology and zonal distribution of some Chalk Terebratulids. *Ann. Mag. nat. Hist.*, London, (9) **15** : 353–385, pls 23–26.

—— 1925a. Diagnostic value of hinge-characters and evolution of cardinal process in the terebratulid genus *Carneithyris*, Sahni. *Ann. Mag. nat. Hist.*, London, (9) **16** : 497–501, pl. 25.

—— 1929. A monograph of the Terebratulidae of the British Chalk. *Palaeontogr. Soc.* (*Monogr.*), London. vi+62 pp., 10 pls.

—— 1958. Supplement to a monograph of the Terebratulidae of the British Chalk. *Monogr. palaeont. Soc. India*, Lucknow, **1** : 1–27, pls 1–6.

SIMPSON, G. G., ROE, A. & LEWONTIN, R. C. 1960. *Quantitative Zoology* (revised edn). vii+440 pp. New York.

SOWERBY, J. 1812–1815. *The Mineral Conchology of Great Britain*, **1** : i–vii, 9–234, pls 1–102. London.

SOWERBY, J. DE C. 1823–1825. *The Mineral Conchology of Great Britain*, **5** : 1–168, pls 408–503. London.

STEINICH, G. 1965. Die artikulaten Brachiopoden der Rügener Schreibkreide (Unter-Maastricht). *Paläont. Abh. Berl.* (A) **2** (1) : 1–220, 21 pls.

SURLYK, F. 1970. Two new brachiopods from the Danish white chalk (Maastrichtian). *Bull. geol. Soc. Denm.*, Copenhagen, **20** : 152–161, 2 pls.

—— 1972. Morphological adaptations and population structures of the Danish Chalk brachiopods (Maastrichtian, Upper Cretaceous). *Biol. Skr.*, Copenhagen, **19** (2) : 1–57, 5 pls.

TZANKOV, V. 1940. Études stratigrafiques et paléozoologiques du Danien de la Bulgarie du Nord. *Spis. bulg. geol. Druzh.*, Sofia, **11** : 455–514, pls 42–52.

WOOD, C. J. 1967. Some new observations on the Maestrichtian stage in the British Isles. *Bull. geol. Surv. Gt Br.*, London, **27** : 271–288, pls 20, 21.

ZAKHARIEVA-KOVACEVA, K. 1947. Les brachiopodes Supracrétaciques de la Bulgarie. *Spis. bulg. geol. Druzh.*, Sofia, **15–19** : 247–274.

IX. INDEX

An asterisk (*) denotes a figure; the page numbers of the principal references are printed in **bold** type.

Argyrotheca 338
Attoe's Pit, Catton 324, 329, 341

Bayfield collection 324, 326, 328–31, 333–5
Beeston Chalk 323–4, 327, 330, 332, 338, 340–1
Belemnella 339
  lanceolata Zone 325
  occidentalis cimbrica Zone 325
    occidentalis Zone 325, 336
Belemnitella 339
  mucronata Zone 323
Birley, C. 330
Blake, J. H. 332
Bramerton 339, 343–4, 346*, 347, 348*, 353, 355, 358–61, 358*
British Museum (Natural History) 321–5, 339
Bromley, Dr R. G. 321
Brown, J. 332

Brydone, R. M., collection 323–5, 339, 360
Bulgaria 322

Caistor St Edmunds 345–7, 346*, 352*, 353–5, 358–9, 358*
Campanian 320–3, 326, 333, 338–9, 341, 343, 360
Campling's Pit, see Edward's Pit
cancellothyridines 338
cardinalia, cardinal process 321, 323, **341–3**, 341*
Caribbean Sea 338
Carneithyridinae, carneithyridines 317–62; 322, 338
  English collections 320
  monovariate analyses 344–5
Carneithyris 320–3, 326, 328, 331, 333–4, 336–9, 360–1
  evolution and ontogeny 321–2
  stratigraphical range 360
  acuminata 321, 328, **329**, 335, 342, 358; pl. 5, fig. 3
  carnea 320, 322, **326–7**, 336, 341*, 342–3, 351, 356, 361; pl. 1, figs 1–3; pl. 3, fig. 3
  circularis 321–2, 326–7, **328**, 334–5, 342, 355, 358, 360; pl. 3, figs 1, 2; pl. 4, figs 6, 7
  daviesi 321–2, 328, **331**, 334, 337, 341–3, 341*, 358; pl. 6, figs 1–4; pl. 7, fig. 1
  elongata 322, **327**, 329, 342–3, 351; pl. 2, figs 1–3; pl. 4, fig. 5
  gracilis 322; see *Pulchrithyris*
  norvicensis 321, 326, 328, **329**, 341*, 342, 358; pl. 5, figs 8, 11; pl. 6, fig. 5
  ornata 322, **331**, 333, 342–3, 351; pl. 4, figs 11, 12
  subcardinalis 320, 323, 338–9, 360
  subovalis 321–2, 326, **330**, 341–2, 341*, 358; pl. 4, figs 3, 4
  subpentagonalis 321–2, 326, **327–8**, 329, 341–2, 355, 358; pl. 7, figs 2, 3
  uniplicata 321–2, 326, **330**, 341–2, 351; pl. 4, fig. 9
  variabilis 321–2, **328–9**, 341–2, 358; pl. 5, fig. 1; pl. 7, fig. 4
Catton Grove 345–7, 346*, 353, 355, 356*, 358–9, 358*
  Pit 332
  Sponge Bed 323–4, 327, 340–1
'Catton' **324**, 327, 345–7, 346*, 353, 355, 356*, 358–9, 358*
Chalk, white 321, 325, 338
  glacially transported 324
Charing, Kent 332–3
Chatwinothyris 321–3, 335–7
  ciplyensis 322
  curiosa 321–2, 336, **337–8**; pl. 8, fig. 5
  gibbosa 321, **338**; pl. 1, fig. 4
  lens 322–3
  subcardinalis 321–2, **335–6**, 337; pl. 8, figs 1–4
  symphytica 321, **336–7**, 341*, 342, 358; pl. 2, fig. 5
Christensen, W. K. 320
Ciply, Craie Phosphaté 322
coccoliths 334
Cockburn, C. F. 331, 333
colour pattern 331
Craie Phosphaté de Ciply 322
Cretaceous, Upper 321; see Campanian, Maastrichtian, etc.
Crown Point, see Whitlingham

Danian 320, 338, 360–1
Davidson collection 321, 326–8
Denmark 320, 322, 338, 361

Eaton Chalk 323
Edward's Pit 330
Egelund, H. 321
Ellipsothyris 321–2, 335
  similis 321, 326, **334–5**, 337, 341*, 342–3, 358; pl. 4, fig. 10; pl. 7, fig. 5

Fitch collection 324–5, 327
Frettenham 344, 346*, 347, 352*, 353–5, 358–9, 358*

Geological Survey of Great Britain, see Institute of Geological Sciences, London
Gibbithyris 334
Goff, J. 339
Grey Beds (Chalk) 325, 336

Hampshire Basin 360
Harford Bridges 332, 345–7, 346*, 353–5, 357*, 358–9, 358*
hinge-parts 321
historical review 321–3

Institute of Geological Sciences, London 320–1, 323, 325, 333, 339, 360

King collection 324–5

Laqueus californianus 361
Laur, A. 335–6
Leader, M. 339
Lollard's Pit 324, 332
lunata reef 336

Maastricht, Holland 325
Maastrichtian, Lower 320–3, 325, 336–8, 360
  Upper 336, 338
McWilliams, Dr B. 320, 325
Magdalen Chapel 324, 330, 332 ; see Mousehold
Magnithyris 322, 333, 360
  magna 321, **333–4**, 335, 342, 351, 358 ; pl. 4, fig. 1 ; pl. 5, fig. 10
  truncata 322, 333, **334**, 342, 358, 360 ; pl. 4, fig. 2
material 339
  stratigraphical distribution 340*
Micraster coranguinum Zone 334
morphology, external 343–5
Mosasaurus 324
Mousehold **324**, 330, 332–3, 345–7, 346*, 353–5, 354*, 355*, 358–9, 358*
mucronata Chalk, basal 323
Muir-Wood, H. M. 324, 327, 332
Mundesley 324

'non-*lunata*' reef 336
Norfolk 321, 339, 360 ; see also under localities
Norwich area 320, 322, 325–36, 338 ; see Norfolk
  Upper Chalk of 323–4
Norwich Castle Museum 320–1, 323, 327, 330, 339
  old collection of **325**, 341

Orinithothyris 322
  carinata 321, 329, **335**, 342, 358 ; pl. 5, fig. 2
'*Ostrea lunata*' 325, 336–8 ; see *lunata* reef, 'non-*lunata*' reef
  vesicularis Bed 335
Owen, E. F. 320, 324

Paramoudra Chalk 323–4, 327, 330, 333, 339–41, 361
Peake, N. B. 320, 324
'pearl' 331
Peel, Dr J. S. 321
Perch-Nielsen, Dr K. 334
Piarothyris 322, 334
  rotunda 321, **334** ; pl. 3, fig. 4
plesiotype, use of term 326 (footnote)
Poland 322, 336
Porosphaera beds 325
Postwick, Postwick Grove 324
Pulchrithyris 321–2, 332–3
  extensa 321, **333**, 342, 358 ; pl. 4, fig. 8
  gracilis 321–2, 326, **332–3**, 342 ; pl. 5, figs 4–7

regression lines 347–59
Reid, C. 335
Rosenkrantz, Professor A. 321
Rowe, A. W. 324
  collection 322–3, 326, 330, 332–3, 336, 339
Rügen, I. of, Germany 322, 324, 335–6

Sahni, M. R. 320–62 *passim*
  material of carneithyridines **325–38**
  phylogenetic tree and stages of 322, 330–1, 339–41
  specimens collected by 329
Savin 337
St James's Hollow 324
Santonian 334
'self-righting tumbler' 323, 361
senile specimens 355, 358–9, 358*
Sidestrand 324, 360
Sowerby collection 321, 326–7
'splitting' 338
Sponge Beds 325
statistical analyses 345–59
Surlyk, Dr F. 320, 325
Sweden, Cretaceous of 322, 361

Terebratula carnea 320–1, 324, 326 7
  elongata 320–1, 324, 332
  incisa 323
  lens 323
  '*lens*' 322–3
Terebratulidae 320–2, 360
Thorpe Hamlets 324
  Limekiln 324, 332–3, 344, 346*, 347, 349*, 353, 358–9, 358*
  Lunatic Asylum Pit 324, 346*
  St Andrew 333
  Tollgate 324

'Thorpe' **324**, 330–1, 333, 344, 346*, 347, 351*, 353, 358–9, 358*
Trimingham **324–5**, 326, 335–8, 360
  Chalk 325, 360
'Trowse' **324**, 326–7, 332–3, 344, 346*, 347, 351*, 353, 358–9, 358*
Tuffeau of Maastricht 325
type-material, provenance of 323–5

Vistula valley, Poland 322

Walker, J. F. 335
Westlegate 345–7, 346*, 352*, 353–4, 358–9, 358*
Weybourne Chalk 323–4, 327, 332–3, 339–41, 343
Whitlingham (Crown Point Pit) 324, 326, 330, 332–3, 344, 346*, 347, 350*, 353, 358–9, 358*
Withers, T. H. 324
Wood, C. J. 320, 324–5, 332, 334, 336, 339
Woodward, S., collection 324–5
Wroxham pipeline 344, 348*

U. Asgaard
Institut for historisk Geologi og Palæontologi
Østervoldgade 10
1350 København K
Denmark

Accepted for publication 1 April 1974

PLATE 1

Carneithyris carnea (J. Sowerby, 1812) (p. 326, see also Pl. 3, fig. 3)

FIG. 1a–c. Lectotype, B 49836, × 2.
FIG. 2. Paralectotype, B 49837, × 2.
FIG. 3a–c. Davidson's specimen, B 49852, × 2.

Chatwinothyris gibbosa Sahni, 1925a (p. 338)

FIG. 4a, b. Holotype, B 45670, ventral and posterior views of the cardinalia, × 4.

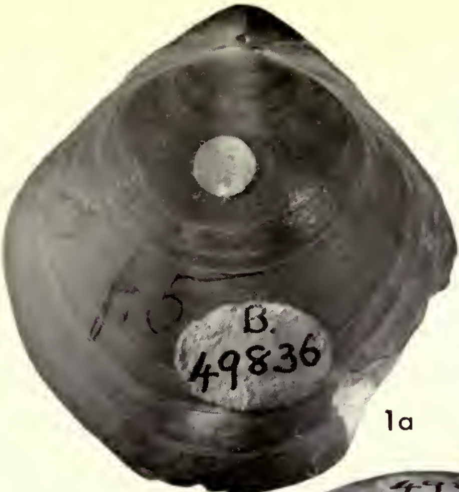

1a

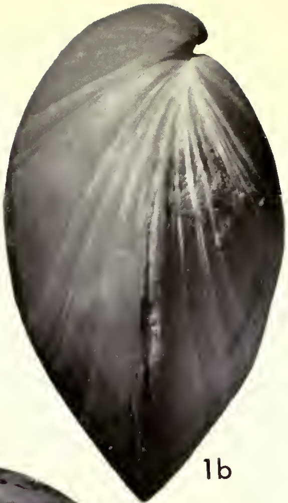
1b

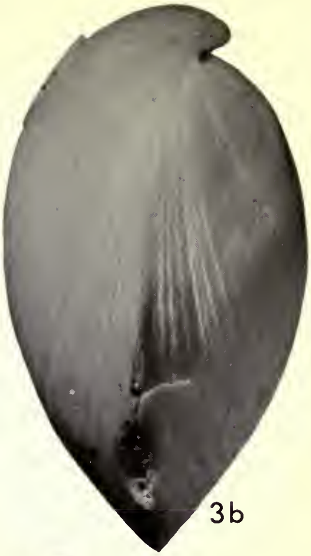
3b

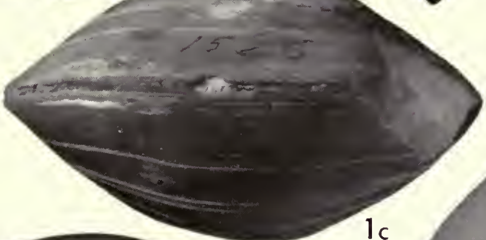

1c

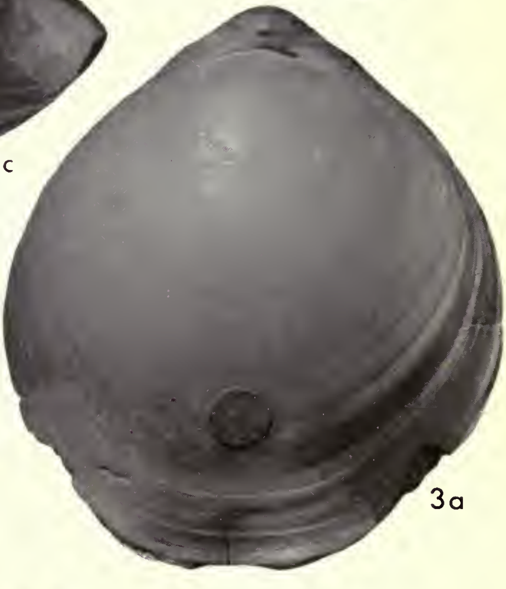
3a

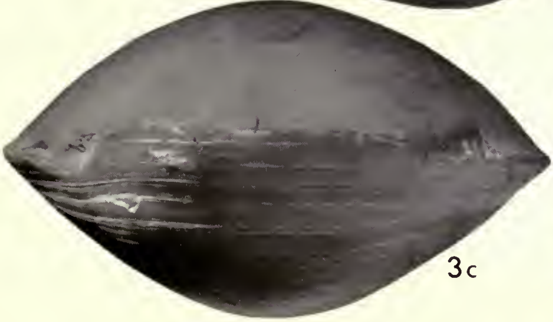
3c

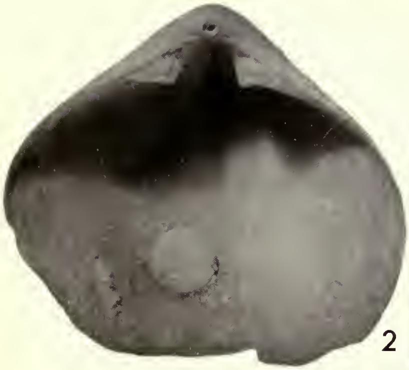
2

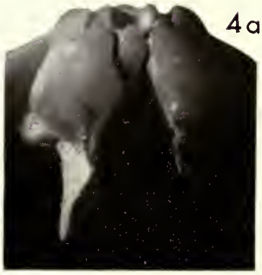
4a

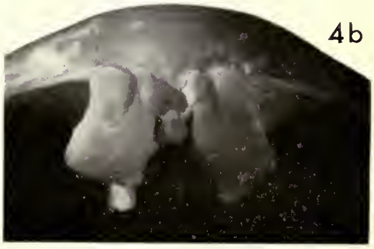
4b

PLATE 2

Carneithyris elongata (J. de C. Sowerby, 1823) (p. 327, see also Pl. 4, fig. 5)

FIG. 1a–c. Lectotype, B 49823, × 2.
FIG. 2a, b. Paralectotype, B 49824, dorsal and anterior-dorsal views, × 2.
FIG. 3a–c. Davidson's specimen, B 6101, × 2.

Chatwinothyris symphytica Sahni, 1925 (p. 336)

FIG. 4. Holotype, GSM 47523, detail of cardinalia, × 4. Note the pitted callus deposits and the extremely prominent cardinal process.

PLATE 2

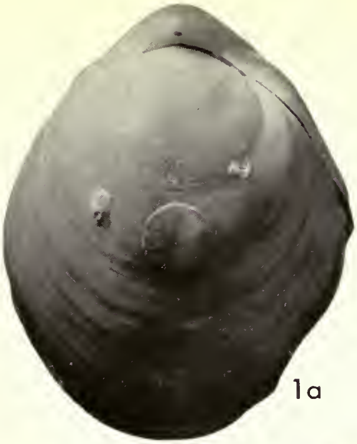
1a

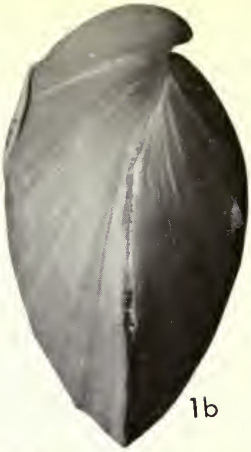
1b

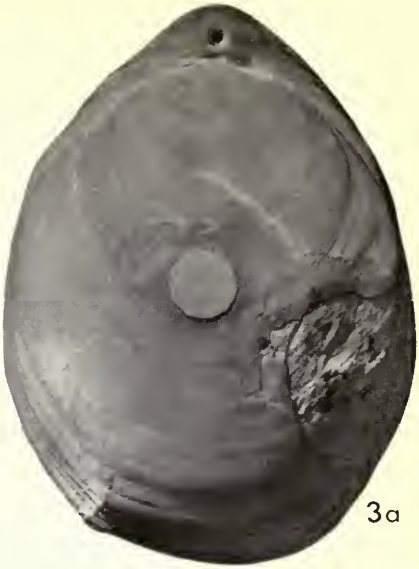
3a

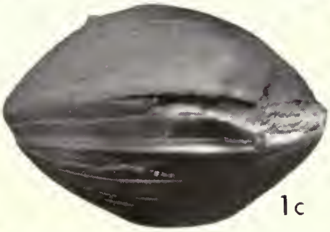
1c

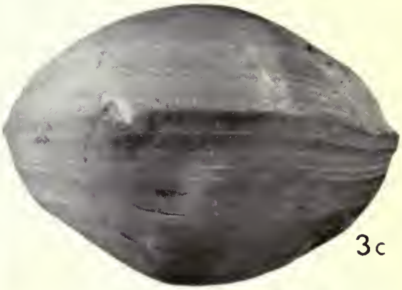
3c

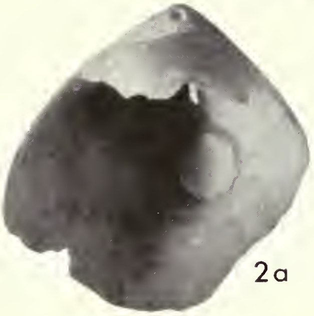
2a

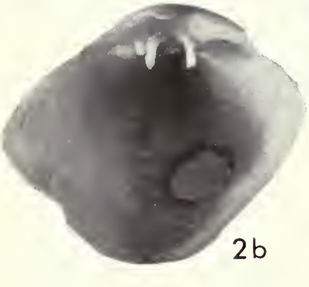
2b

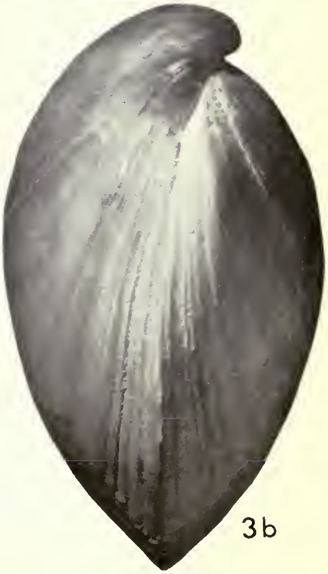
3b

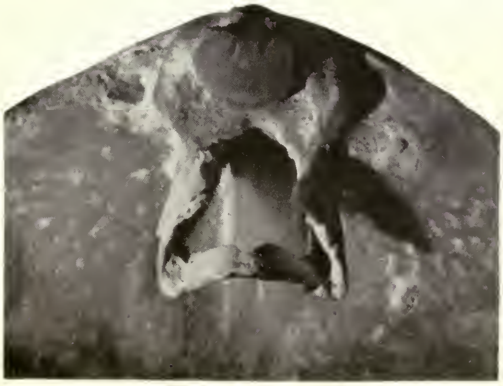
4

PLATE 3

Carneithyris circularis Sahni, 1925 (p. 328, see also Pl. 4, figs 6, 7)

Fig. 1a–c. Paratype, B 49862, × 2.
Fig. 2a, b. Paratype, B 45603, × 2 ; detail of cardinalia, × 4.

Carneithyris carnea (J. Sowerby, 1812) (p. 326, see also Pl. 1, figs 1–3)

Fig. 3a, b. 'Plesiotype', B 45600, × 2 ; detail of cardinalia, × 4.

Piarothyris rotunda Sahni, 1925 (p. 334)

Fig. 4. Holotype, 18 KCN, detail of cardinalia, × 4.

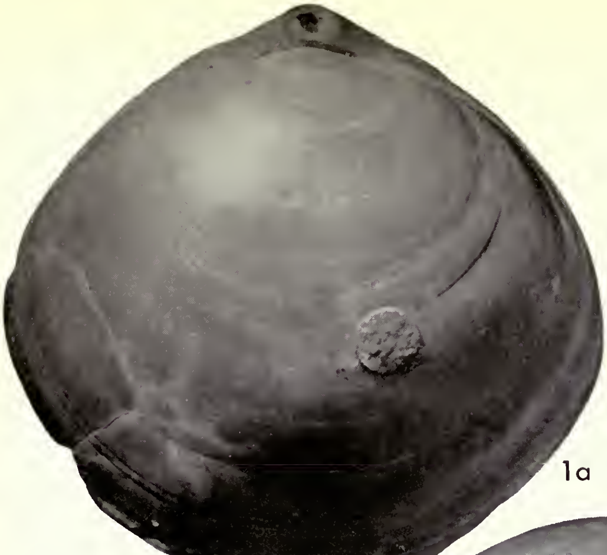
1a

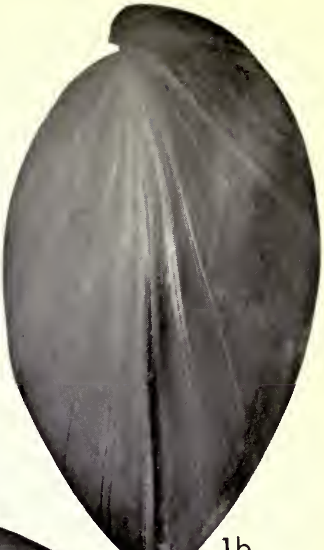
1b

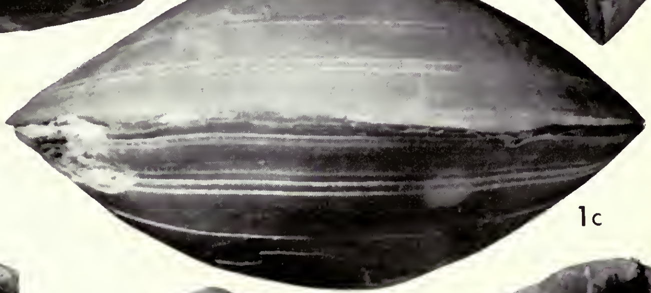
1c

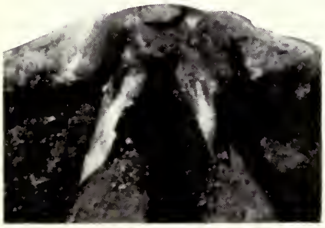
2b

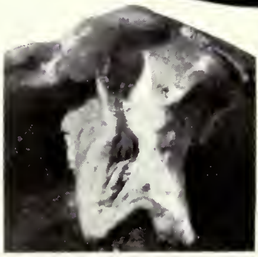
4

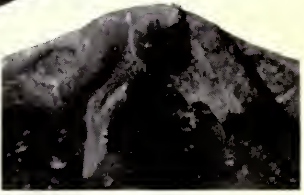
3b

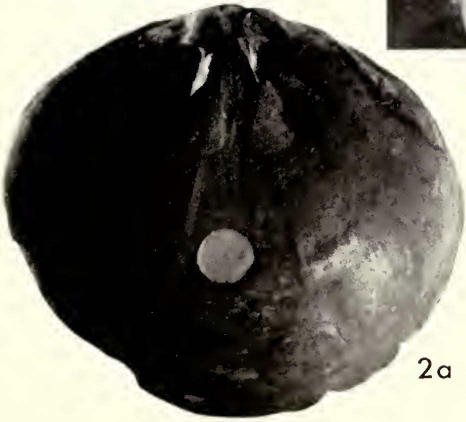
2a

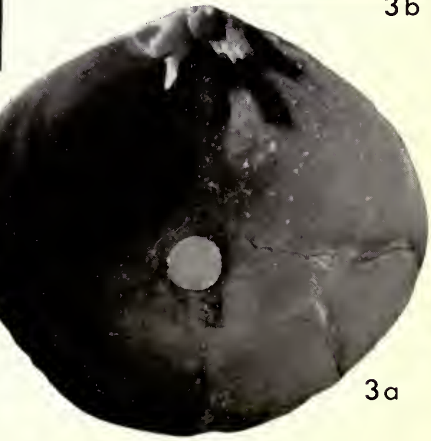
3a

PLATE 4

All figures except Fig. 11 show details of the cardinalia.

Magnithyris magna Sahni, 1925 (p. 333, see also Pl. 5, fig. 10)

Fig. 1. Holotype, GSM 48488, × 4.

Magnithyris truncata Sahni, 1929 (p. 334)

Fig. 2. Holotype, B 45606, × 4.

Carneithyris subovalis Sahni, 1925a (p. 330)

Fig. 3. Holotype, B 15159, × 4.
Fig. 4. Paratype, Norwich Castle Museum, no number, × 4.

Carneithyris elongata (J. de C. Sowerby, 1823) (p. 327, see also Pl. 2, figs 1–3)

Fig. 5. 'Plesiotype', B 45243, × 4.

Carneithyris circularis Sahni, 1925 (p. 328, see also Pl. 3, figs 1, 2)

Fig. 6. Holotype, 15 KCN, × 4.
Fig. 7. Paratype, B 45604, × 4.

Pulchrithyris extensa Sahni, 1925 (p. 333)

Fig. 8. Holotype, 7 KCN. Ventral view of the remains of the brachial valve, × 4.

Carneithyris uniplicata Sahni, 1925a (p. 330)

Fig. 9. Holotype, GSM 48518, × 4.

Ellipsothyris similis Sahni, 1925 (p. 334, see also Pl. 7, fig. 5)

Fig. 10. Holotype, 14 KCN, × 4.

Carneithyris ornata Sahni, 1929 (p. 331)

Fig. 11. Holotype, GSM 48498. Dorsal view of brachial valve, × 2.
Fig. 12. Same, ventral view of the posterior part of the brachial valve, showing cardinalia, very clear muscle impressions, and slightly pitted callus, × 4.

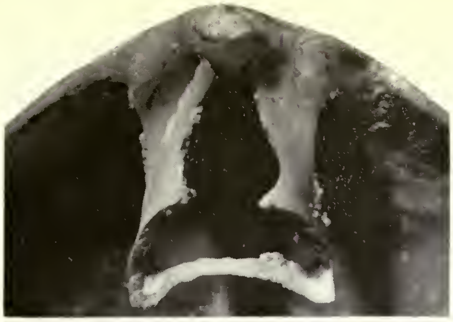
2

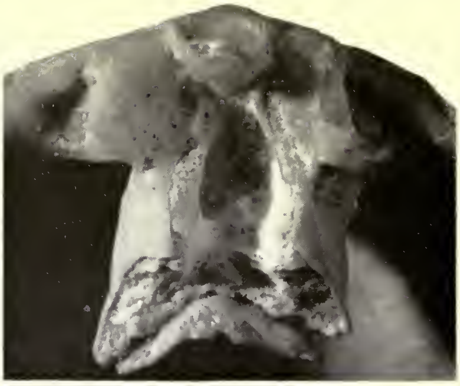
1

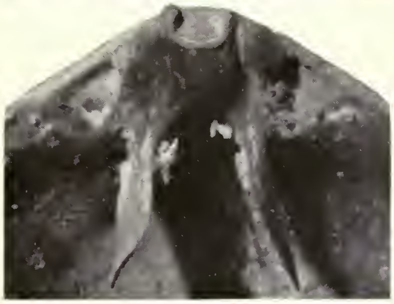
3

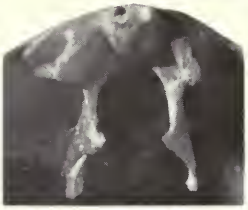
5

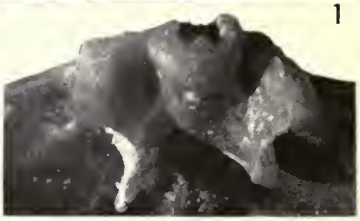
4

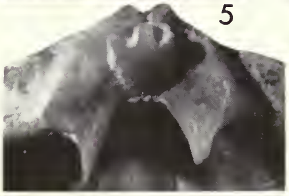
6

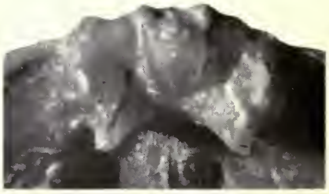
7

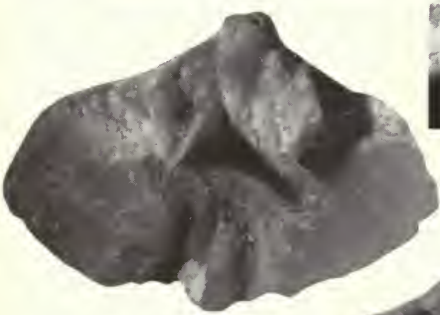
8

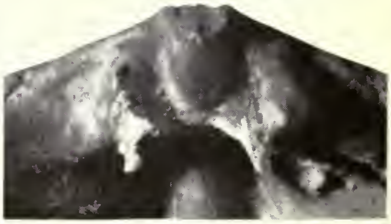
10

9

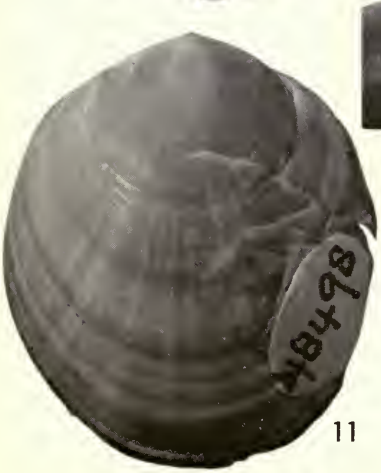

11

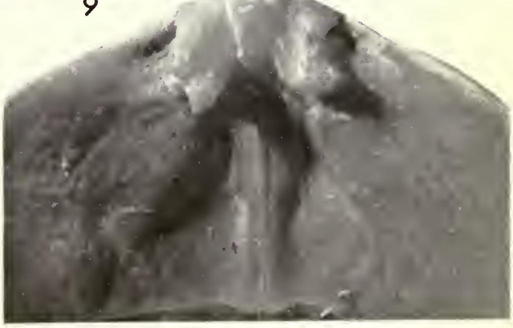
12

PLATE 5

All figures show details of the cardinalia.

Carneithyris variabilis Sahni, 1925 (p. 328, see also Pl. 7, fig. 4)

Fig. 1. Holotype, 14 CMN, × 4.

Ornithothyris carinata Sahni, 1925 (p. 335)

Fig. 2. Holotype, 17 KCN, × 4.

Carneithyris acuminata Sahni, 1925 (p. 329)

Fig. 3. Holotype, 19 CMN, × 4.

Pulchrithyris gracilis Sahni, 1925 (p. 332)

Fig. 4. B 98123, × 4.
Fig. 5. B 46300, × 4.
Fig. 6. Paratype, GSM 48485, × 4 ; the loop is glued on upside down.
Fig. 7. Holotype, GSM 48487, × 4.

Carneithyris norvicensis Sahni, 1925 (p. 329, see also Pl. 6, fig. 5)

Fig. 8. Possible paratype, B 52067, × 4.
Fig. 11. Holotype, GSM 44494, × 4.

Carneithyris cf. ***carnea*** (J. Sowerby) (p. 326)

Fig. 9. 27 KCN, × 4.

Magnithyris magna Sahni, 1925 (p. 333, see also Pl. 4, fig. 1)

Fig. 10. Presumed paratype, B 15149, × 4.

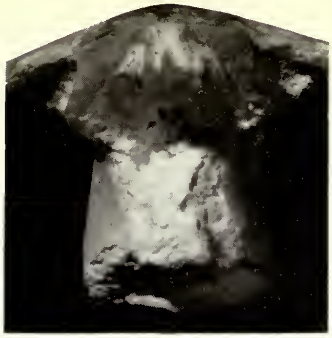

1

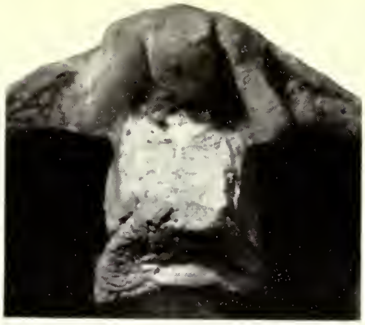

2

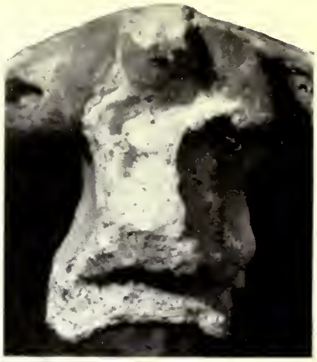

3

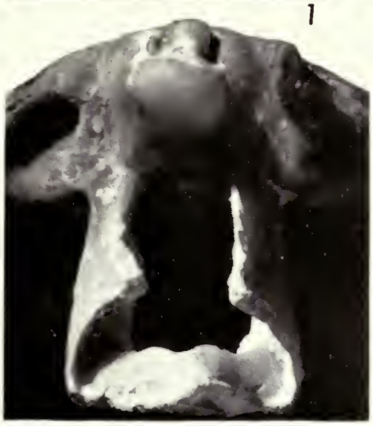

4

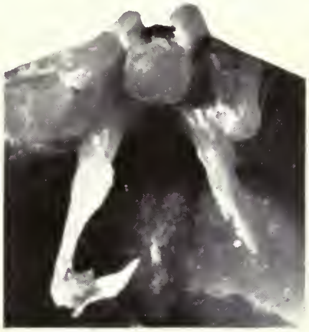

5

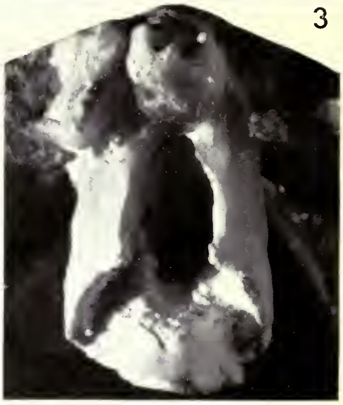

8

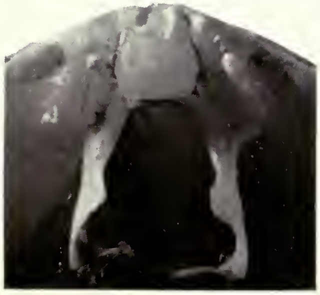

6

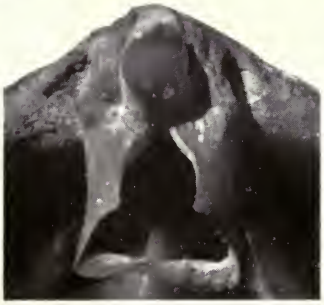

9

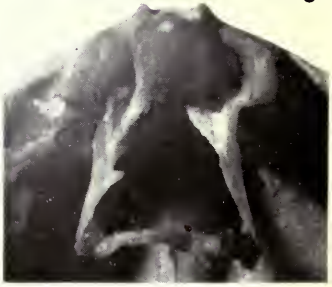

7

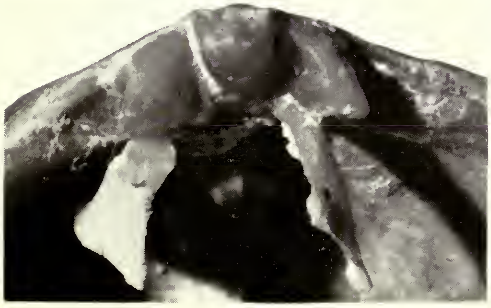

10

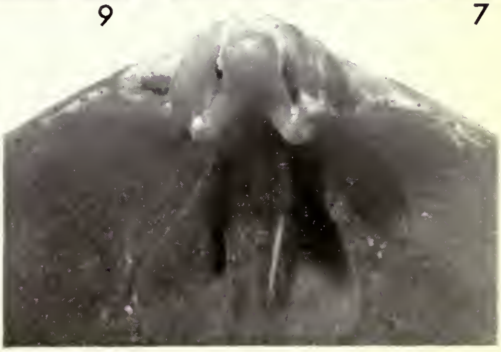

11

PLATE 6

All figures except Figs 1 and 2 show details of the cardinalia.

Carneithyris daviesi Sahni, 1925a (p. 331, see also Pl. 7, fig. 1)

FIG. 1a, b. Paratype, B 459, × 2.

FIG. 2a, b. Same, details of pedicle valve, oblique views to show the strongly swollen tooth bases, × 4.

FIG. 3. Holotype, B 45599, × 4.

FIG. 4. The third specimen, B 45642, × 4.

Carneithyris norvicensis Sahni, 1925 (p. 329, see also Pl. 5, figs 8, 11)

FIG. 5. Possible paratype, B 45610, × 4.

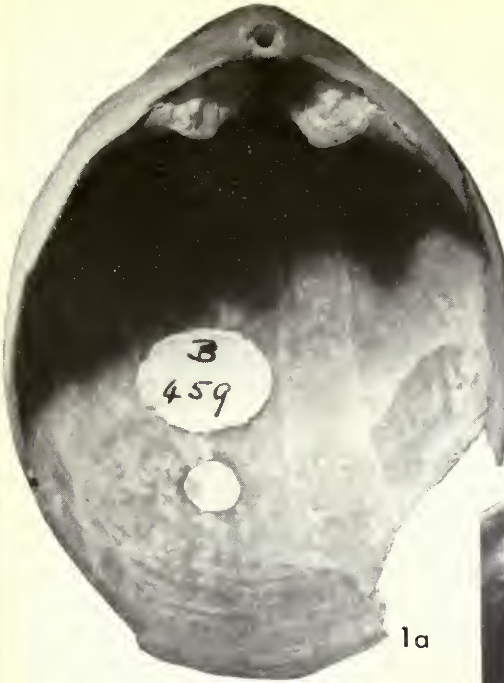

1a

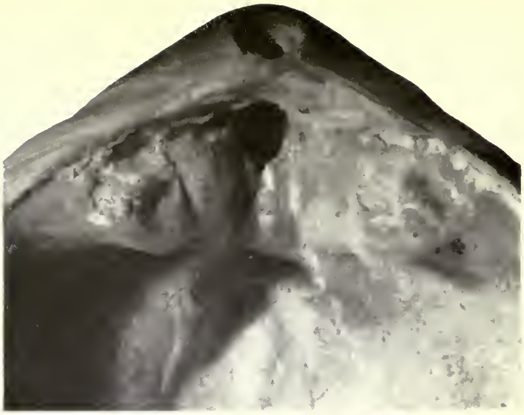
2a

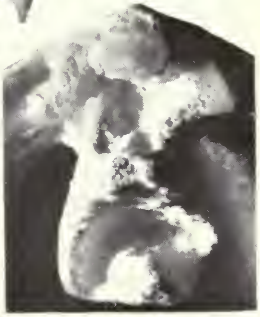
4

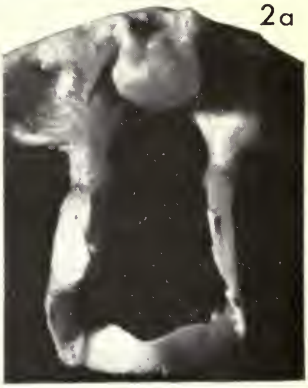
3

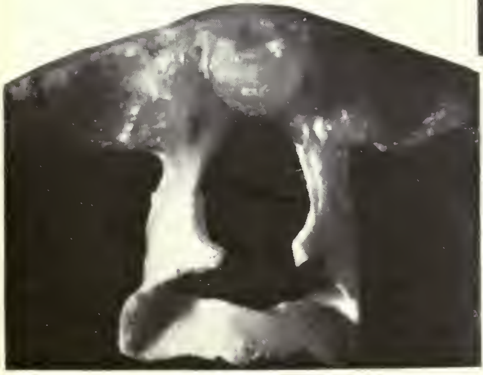
5

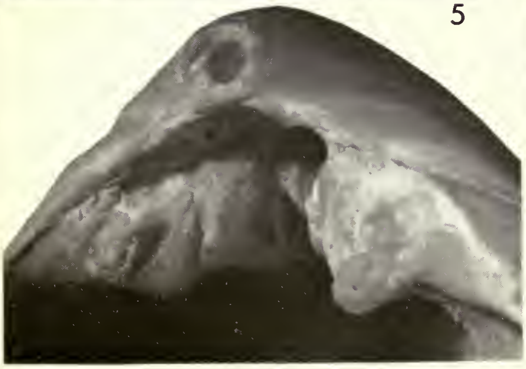
2b

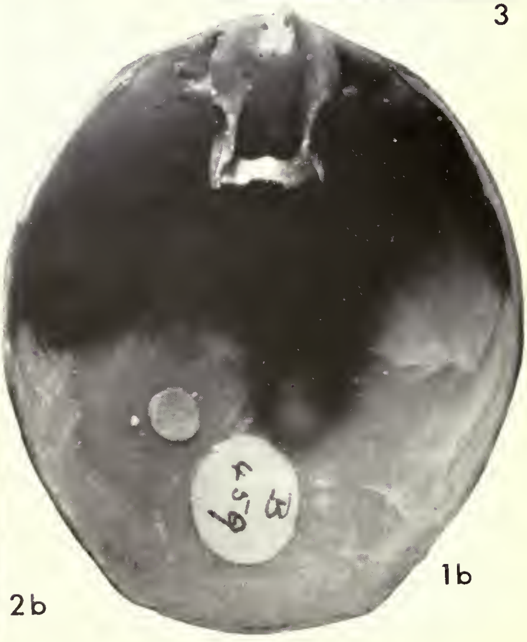

1b

PLATE 7

All figures show details of the cardinalia.

Carneithyris daviesi Sahni, 1925a (p. 331, see also Pl. 6, figs 1–4)

FIG. 1a–c. Paratype, B 459, ventro-lateral, ventral and ventro-posterior views, × 4.

Carneithyris subpentagonalis Sahni, 1925 (p. 327)

FIG. 2a, b. Holotype, 8 KCN, ventro-lateral and ventral views, × 4.
FIG. 3. Paratype, GSM 44491, ventral view, × 4.

Carneithyris variabilis Sahni, 1925 (p. 328, see also Pl. 5, fig. 1)

FIG. 4. Paratype, 13 CMN, ventral view, × 4.

Ellipsothyris similis Sahni, 1925 (p. 334, see also Pl. 4, fig. 10)

FIG. 5. ? Paratype, B 45653, ventral view, × 4.

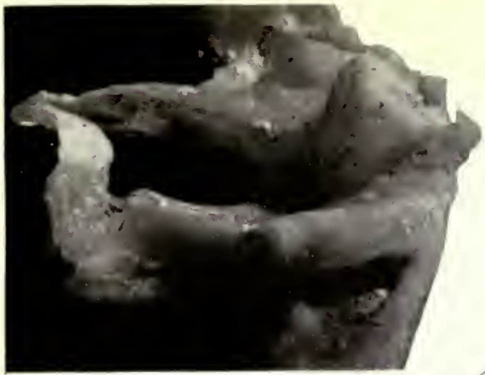
1a

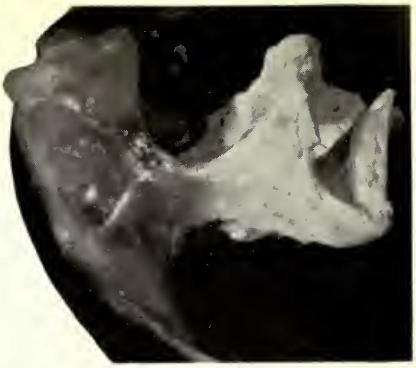
2a

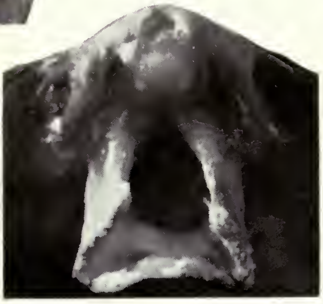
3

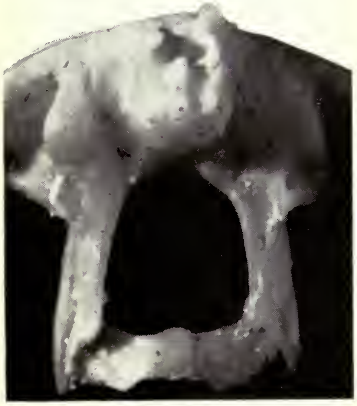
1b

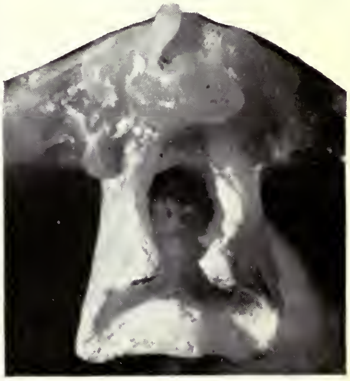
2b

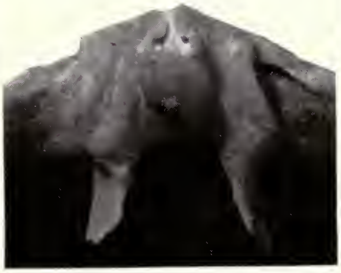
4

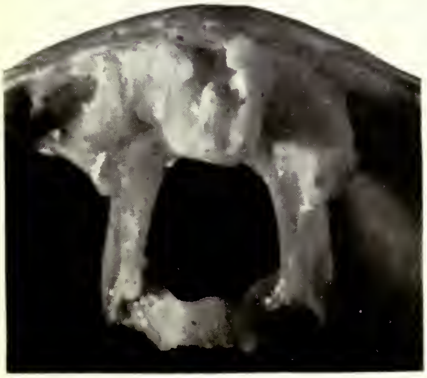
1c

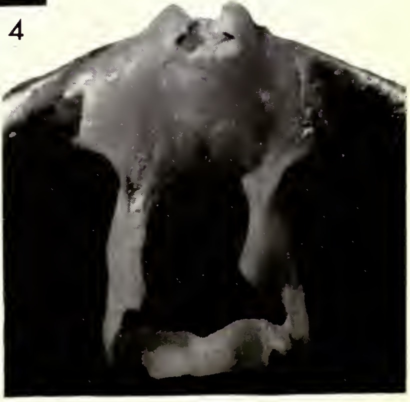
5

PLATE 8

All figures show details of the cardinalia.

Chatwinothyris subcardinalis Sahni, 1925 (p. 335)

FIG. 1a–c. Holotype, GSM 44501, ventral, ventro-posterior and posterior views, × 4.
FIG. 2a, b. Paratype, B 46326, ventral and ventro-posterior views, × 4.
FIG. 3a, b. Another specimen, B 46327, ventral and ventro-posterior views, × 4.
FIG. 4a, b. Another specimen, B 21266, ventral and ventro-posterior views, × 4.

Chatwinothyris curiosa Sahni, 1925a (p. 337)

FIG. 5a, b. Holotype, B 45669, ventral and ventro-posterior views, × 4.
FIG. 5c–e. Same, various oblique views of the cardinalia and brachidium showing the exotic loop, × 4.

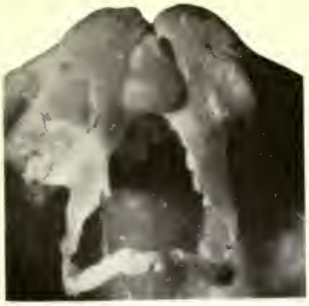

1a

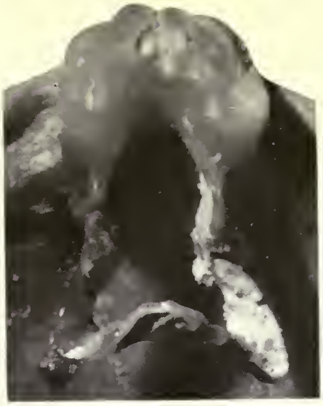

2a

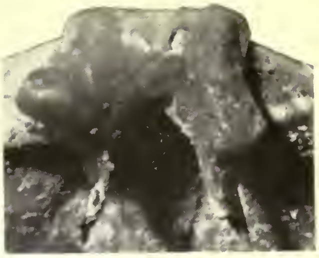

3a

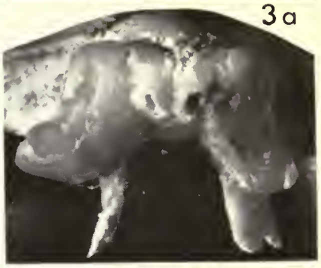

3b

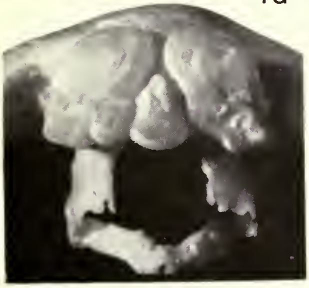

1b

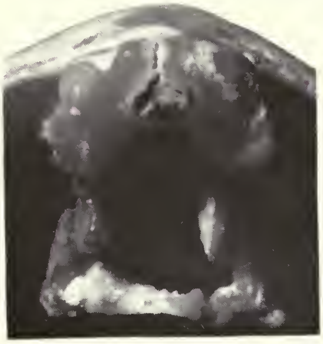

2b

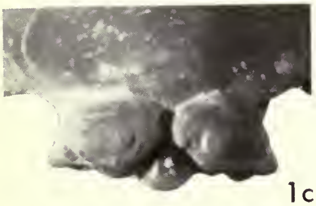

1c

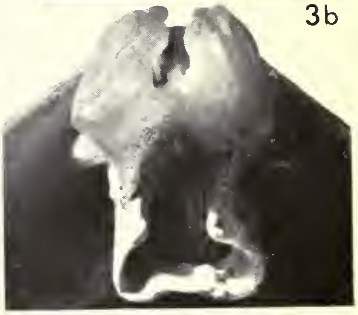

5a

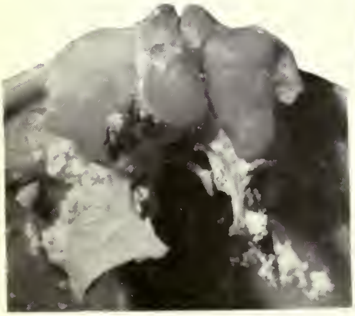

4a

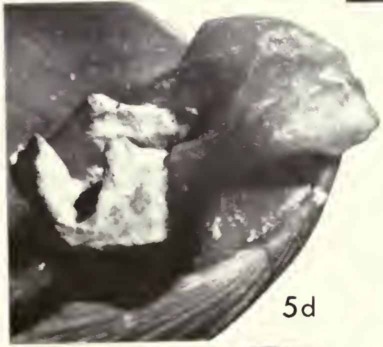

5d

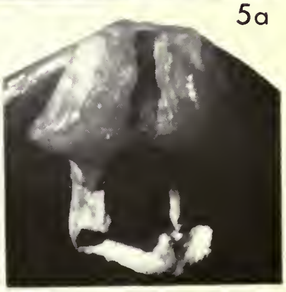

5b

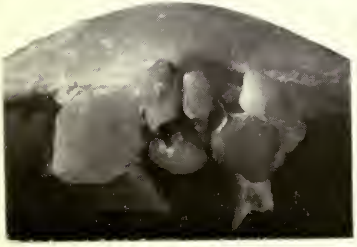

4b

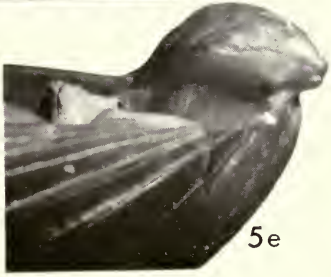

5e

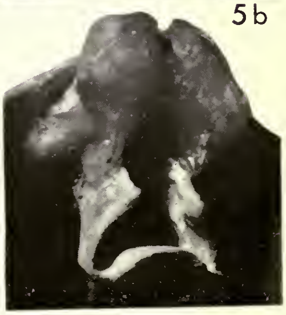

5c

A LIST OF SUPPLEMENTS TO THE GEOLOGICAL SERIES OF THE BULLETIN OF THE BRITISH MUSEUM (NATURAL HISTORY)

---

1. Cox, L. R. Jurassic Bivalvia and Gastropoda from Tanganyika and Kenya. Pp. 213 ; 30 Plates ; 2 Text-figures. 1965. OUT OF PRINT.
2. El-Naggar, Z. R. Stratigraphy and Planktonic Foraminifera of the Upper Cretaceous—Lower Tertiary Succession in the Esna-Idfu Region, Nile Valley, Egypt, U.A.R. Pp. 291 ; 23 Plates ; 18 Text-figures. 1966. £11.
3. Davey, R. J., Downie, C., Sarjeant, W. A. S. & Williams, G. L. Studies on Mesozoic and Cainozoic Dinoflagellate Cysts. Pp. 248 ; 28 Plates ; 64 Text-figures. 1966. £8.20.
3. Appendix. Davey, R. J., Downie, C., Sarjeant, W. A. S. & Williams, G. L. Appendix to Studies on Mesozoic and Cainozoic Dinoflagellate Cysts. Pp. 24. 1969. 95p.
4. Elliott, G. F. Permian to Palaeocene Calcareous Algae (Dasycladaceae) of the Middle East. Pp. 111 ; 24 Plates ; 16 Text-figures. 1968. £6.10.
5. Rhodes, F. H. T., Austin, R. L. & Druce, E. C. British Avonian (Carboniferous) Conodont faunas, and their value in local and continental correlation. Pp. 313 ; 31 Plates ; 92 Text-figures. 1969. £13.10.
6. Childs, A. Upper Jurassic Rhynchonellid Brachiopods from Northwestern Europe. Pp. 119 ; 12 Plates ; 40 Text-figures. 1969. £5.25.
7. Goody, P. C. The relationships of certain Upper Cretaceous Teleosts with special reference to the Myctophoids. Pp. 255 ; 102 Text-figures. 1969. £7.70.
8. Owen, H. G. Middle Albian Stratigraphy in the Anglo-Paris Basin. Pp. 164 ; 3 Plates ; 52 Text-figures. 1971. £7.20.
9. Siddiqui, Q. A. Early Tertiary Ostracoda of the family Trachyleberididae from West Pakistan. Pp. 98 ; 42 Plates ; 7 Text-figures. 1971. £9.60.
10. Forey, P. L. A revision of the elopiform fishes, fossil and Recent. Pp. 222 ; 92 Text-figures. 1973. £11.35.
11. Williams, A. Ordovician Brachiopoda from the Shelve District, Shropshire. Pp. 163 ; 28 Plates ; 11 Text-figures ; 110 Tables. 1974. £12.80.

Printed in Great Britain by John Wright and Sons Ltd. at The Stonebridge Press, Bristol BS4 5NU